



(51) International Patent Classification:

A61K 47/28 (2006.01) A61K 51/12 (2006.01)  
A61K 47/44 (2006.01)

(21) International Application Number:

PCT/DK2011/050479

(22) International Filing Date:

14 December 2011 (14.12.2011)

(25) Filing Language:

English

(26) Publication Language:

English

(30) Priority Data:

PA 2010 70542	14 December 2010 (14.12.2010)	DK
11151372.7	19 January 2011 (19.01.2011)	EP
61/434,070	19 January 2011 (19.01.2011)	US

(71) Applicants (for all designated States except US): **TECHNICAL UNIVERSITY OF DENMARK** [DK/DK]; Anker Engeldsvej 1, Bygning 101A, DK-2800 Kgs. Lyngby (DK). **RIGSHOSPITALET** [DK/DK]; Blegdamsvej 9, DK-2100 København Ø (DK).

(72) Inventors; and

(75) Inventors/Applicants (for US only): **PETERSEN, Anca-trine Luisa** [DK/DK]; Pilehøj 19, DK-2990 Nivå (DK). **HENRIKSEN, Jonas Rosager** [DK/DK]; Gravenstensevej 14, DK-3450 Allerød (DK). **RASMUSSEN, Palle Heden-gran** [DK/DK]; Kærmindevej 7, DK-2630 Taastrup (DK). **KJÆR, Andreas** [DK/DK]; Marielystvej 11, DK-2000

Frederiksberg (DK). **ANDRESEN, Thomas Lars** [DK/DK]; Krogebjerg 68, DK-2720 Vanløse (DK).

(74) Agent: **HØIBERG A/S**; St. Kongensgade 59 A, DK-1264 Copenhagen K (DK).

(81) Designated States (unless otherwise indicated, for every kind of national protection available): AE, AG, AL, AM, AO, AT, AU, AZ, BA, BB, BG, BH, BR, BW, BY, BZ, CA, CH, CL, CN, CO, CR, CU, CZ, DE, DK, DM, DO, DZ, EC, EE, EG, ES, FI, GB, GD, GE, GH, GM, GT, HN, HR, HU, ID, IL, IN, IS, JP, KE, KG, KM, KN, KP, KR, KZ, LA, LC, LK, LR, LS, LT, LU, LY, MA, MD, ME, MG, MK, MN, MW, MX, MY, MZ, NA, NG, NI, NO, NZ, OM, PE, PG, PH, PL, PT, QA, RO, RS, RU, RW, SC, SD, SE, SG, SK, SL, SM, ST, SV, SY, TH, TJ, TM, TN, TR, TT, TZ, UA, UG, US, UZ, VC, VN, ZA, ZM, ZW.

(84) Designated States (unless otherwise indicated, for every kind of regional protection available): ARIPO (BW, GH, GM, KE, LR, LS, MW, MZ, NA, RW, SD, SL, SZ, TZ, UG, ZM, ZW), Eurasian (AM, AZ, BY, KG, KZ, MD, RU, TJ, TM), European (AL, AT, BE, BG, CH, CY, CZ, DE, DK, EE, ES, FI, FR, GB, GR, HR, HU, IE, IS, IT, LT, LU, LV, MC, MK, MT, NL, NO, PL, PT, RO, RS, SE, SI, SK, SM, TR), OAPI (BF, BJ, CF, CG, CI, CM, GA, GN, GQ, GW, ML, MR, NE, SN, TD, TG).

Published:

— with international search report (Art. 21(3))

(54) Title: ENTRAPMENT OF RADIONUCLIDES IN NANOPARTICLE COMPOSITIONS

(57) Abstract: The present invention is directed to the technical field of imaging compositions useful for diagnosing cancer and other diseases in a subject. In particular, the invention relates to a class of diagnostic compounds comprising a novel liposome composition with encapsulated metal entities such as radionuclides, for example <sup>61</sup>Cu and <sup>64</sup>Cu copper isotopes. The invention further relates to a novel method for loading delivery systems, such as liposome compositions, with metal entities such as radionuclides, and the use of liposomes for targeted diagnosis and treatment of a target site, such as cancerous tissue and, in general, pathological conditions associated with leaky blood vessels. The present invention provides a new diagnostic tool for the utilization of positron emission tomography (PET) imaging technique.



WO 2012/079582 A1

## Entrapment of radionuclides in nanoparticle compositions

### Field of invention

5 The present invention is directed to the technical field of imaging compositions useful for diagnosing cancer and other diseases in a subject. In particular, the invention relates to a class of diagnostic compounds comprising a novel liposome composition with encapsulated radionuclides or metal entities, such as for example  $^{61}\text{Cu}$  and  $^{64}\text{Cu}$  copper isotopes. The invention further relates to a novel method for loading delivery systems, such as liposome compositions, with metal entities such as radionuclides and the use of liposomes comprising metal entities such as radionuclides for targeted 10 diagnosis and therapy of a target site, such as cancerous tissue and, in general, pathological conditions associated with leaky blood vessels. The present invention provides a new diagnostic tool for the utilization of positron emission tomography (PET) imaging technique.

15

### Background of invention

Liposomes can serve as vesicles to deliver a wide range of encapsulated and/or membrane-incorporated therapeutic or diagnostic entities. Liposomes are usually characterized as nano-scale vesicles consisting of an interior core separated from the 20 outer environment by a membrane of one or more bilayers. The bilayer membranes can be formed by amphiphilic molecules e.g. synthetic or natural lipids that comprise a hydrophobic and a hydrophilic domain [Lasic, Trends Biotechnol., 16: 307-321, 1998]. Bilayer membranes can also be formed by amphiphilic polymers constituting particles (e.g. polymersomes and polymerparticles).

25

Liposomes can serve as carriers of an entity such as, without limitation, a chemical compound, or a radionuclide, that is capable of having a useful property or provide a useful activity. For this purpose, the liposomes are prepared to contain the desired entity in a liposome-incorporated form. The liposome incorporated entity can be 30 associated with the exterior surface of the liposome membrane, located in the interior core of the liposome or within the bilayer of the liposome. Methods for the incorporation of radionuclides into liposomes are e.g. surface labeling after liposome preparation [Phillips, Adv Drug Deliv Rev., 37: 13-32, 1999], label incorporation into the lipid bilayer of preformed liposomes [Morgan et al., J Med Microbiol., 14: 213-217, 1981], surface 35 labeling of preformed liposomes by incorporating lipid chelator conjugate during

preparation [Goto et al., Chem harm Bull.(Tokyo), 37: 1351-1354, 1989; Seo et al., Bioconjugate Chem.,19: 2577-2584, 2008], and aqueous phase loading of preformed liposome [Hwang et al., Biochim Biophys Acta., 716: 101-109, 1982; Phillips et al., Int J Rad Appl Instrum B, 19: 539-547, 1992; Gabizon et al., J Liposome Res., 1: 123-125, 1988; Henriksen et al., Nucl Med Bio., 31: 441-449, 2004]. The incorporation of entities into liposomes by the aqueous phase loading of preformed liposome is also referred to as "loading" and thereby "encapsulating" or "entrapping" the entities.

Encapsulating entities into the interior of liposomes through aqueous phase loading seems to provide the greatest in vivo stability, because of the protected location of the entity inside the liposome. The purpose of encapsulating an entity into a liposome is often to protect the entity from the destructive environment and rapid excretion *in vivo*. The entrapment of the entity provides the opportunity for the encapsulated entity to apply the activity of the entity mostly at the site or in the environment where such activity is advantageous but less so at other sites where the activity may be useless or undesirable. It is known that liposomes having PEG chains attached to the outer surface have prolonged circulation time in the blood stream. These liposome compositions can effectively evade the immune system, which would otherwise attack the liposomes soon after injection causing fast clearance or rupture of the liposome and premature release of the agent entrapped inside. By increasing the blood circulation time, the agent entrapped in the liposome stays within the liposome until it reaches the target tissue. This phenomenon is referred to as passive targeting delivery, where an accumulation of long-circulating nanoparticles in tumor areas or inflammatory sites is due to leaky vasculature and lack of an effective lymphatic drainage system in these areas. For example, a radio-diagnostic entity entrapped within a long-circulating liposome can be delivered by passive targeting to a diseased site within a subject to facilitate a diagnosis thereof. Active- or ligand targeting delivery systems is referred to liposome compositions with ligands attached on the surface targeted against cell surface antigens or receptors [Allen, Science, 303: 1818-1822, 2004]. Combining the properties of targeted and long-circulating liposomes in one preparation comprising a radionuclide encapsulated liposome composition would significantly enhance the specificity and intensity of radioactivity localization in the target site e.g. a tumor. Ideally, such liposome compositions can be prepared to include the desired entity, e.g. a chemical compound or radionuclide, (i) with a high loading efficiency, i.e., high percentage of encapsulated entity relative to the total amount of the entity used in the

encapsulation process, and (ii) in a stable form, i.e., with minimal release (i.e. leakage) of the encapsulated entity upon storage or generally before the liposome reaches the site or the environment where the liposome entrapped entity is expected to apply its intended activity.

5

Entrapment of radionuclides into nanoparticles such as liposomes can be obtained through use of chemical compounds called ionophores capable of transporting metal ions across lipid membranes. Upon crossing the membrane barrier the radionuclide then binds preferably to a chelator, encapsulated in the interior of the liposome composition, due to its stronger affinity thereto, allowing the release of free ionophore, and the entrapment of the radionuclide in the liposome composition.

10

Copper isotopes are of great interest for use in diagnostic and/or therapeutic application. For diagnostic applications this relates to the positron-emitters  $^{61}\text{Cu}$  and  $^{64}\text{Cu}$ , which can be used in positron emission tomography (PET) diagnostic imaging.  $^{64}\text{Cu}$  is an interesting copper isotope possessing all decay modalities, and with a half-life of 12.7 h it is favorable for biological studies. A half-life of about 6-12 h appears to be ideal to allow for sufficient accumulation of liposome in inflammatory tissues or cancerous targets, yet providing enough background clearance to permit early identification of the target [Gabizon et al., Cancer Res., 50: 6371-6378, 1990]. Furthermore,  $^{64}\text{Cu}$  can be used as a model nuclide representing the chemical properties of all copper isotopes.

15

20

Ideal radioisotopes for therapeutic applications are those with low penetrating radiation, such as  $\beta^-$ ,  $\alpha^-$  and auger electron-emitters. Examples of such radioisotopes are  $^{67}\text{Cu}$ ,  $^{67}\text{Ga}$ ,  $^{225}\text{Ac}$ ,  $^{90}\text{Y}$ ,  $^{177}\text{Lu}$  and  $^{119}\text{Sb}$ . When the low energy emitting radioisotope in the form of a radiopharmaceutical reach the target site, the energy emitted is only deposited at the target site and nearby normal tissues are not irradiated. The energy of the emitted particles from the different radioisotopes and their ranges in tissues will vary, as well as their half-life, and the most appropriate radioisotope will be different depending on the application, the disease and the accessibility of the disease tissue.

25

30

Ideal radioisotopes for diagnostic applications are those with relatively short half-life, and those with high penetrating radiation to be detected by imaging techniques such as positron emission tomography (PET) and/or single photon emission computed

35

tomography (SPECT). The half-life of the radionuclide must also be long enough to carry out the desired chemistry to synthesize the radiopharmaceutical and long enough to allow accumulation in the target tissue in the patient while allowing clearance through the non-target organs. The radionuclide,  $^{64}\text{Cu}$ , has proven to be a versatile isotope with respect to its applications in both imaging [Dehdashti et al., J Nucl Med. 38: 103P, 1997] and therapy [Anderson et al., J Nucl Med., 36: 2315-2325, 1998]. Radiopharmaceuticals and for example radiolabeled liposome compositions consisting of radionuclides, such as  $^{61}\text{Cu}$  ( $T_{1/2} = 3.33$  h) and  $^{64}\text{Cu}$  ( $T_{1/2} = 12.7$  h) can be utilized for imaging by the positron emission tomography (PET) technique, with the main advantages over single photon emission computed tomography (SPECT) being: a) employing annihilation coincidence detection (ACD) technique whereby only photons detected simultaneously ( $< 10^{-9}$  sec) by a pair of scintillators opposite each other are registered, instead of collimator, the sensitivity is markedly improved ( $\times 30-40$ ) and the spatial resolution is enhanced by about a factor of two ( $< 5$  mm), since the detection field is (non-diverging) defined cylindrical volume and both the sensitivity and the resolution do not vary within the detection field [Kostarelos et al., J Liposome Res., 9: 429-460, 1999]; b) PET scanners provide all images in the unit of radioactivity concentrations (e.g. Bq/ml) after corrections for photon attenuation, scatters and randoms, thereby considering PET to be a more quantitative technique than SPECT [Seo, Curr. Radiopharm., 1: 17-21, 2008].

The patent applications WO/2001/060417, WO/2004/082627, WO/2004/082626 and US 20090081121, describe methods based on ionophoric loading of radionuclides into liposomes. Further, the disclosed radionuclides which are loaded into liposomes are heavy radionuclides and  $^{11}\text{C}$ ,  $^{18}\text{F}$ ,  $^{76}\text{Br}$ ,  $^{77}\text{Br}$ ,  $^{89}\text{Zr}$ ,  $^{67}\text{Ga}$ ,  $^{111}\text{In}$ ,  $^{177}\text{Lu}$ ,  $^{90}\text{Y}$  and  $^{225}\text{Ac}$ . From a diagnostic standpoint, these approaches are not useable for PET imaging applications, but only SPECT, because of the limited use of radionuclides.

Patent EP386 146 B1 describes a composition and method of use for liposome encapsulated compounds for neutron capture tumor therapy. However, these liposomes were loaded with stable elements (e.g. boron), that become radioactive only after activation.

In a theoretical study, Kostarelos et al., analyzed the therapeutic potential of liposomes labeled with one of the radionuclides  $^{131}\text{I}$ ,  $^{67}\text{Cu}$ ,  $^{188}\text{Re}$  or  $^{211}\text{At}$ , but chemical procedures

for the preparation of the labeled liposomes were not suggested [Kostarelos et al., J Liposome Res, 9:407-424, 1999].

5 Only a few radiopharmaceuticals based on radioactive copper isotopes are discovered and available today. Examples are  $^{60}\text{Cu}$ -ATSM as hypoxia marker, and  $^{64}\text{Cu}$ -ATSM and  $^{64}\text{Cu}$ -PTSM, which are suggested as potential agents for tumor therapy. Further classes of substances are copper-labeled peptides and antibodies in which the radioactive copper is linked to the biomolecule via a bifunctional chelator. There are no liposome compositions loaded with copper available for use as radiopharmaceuticals.

10 Several research groups have measured the permeability of anions and cations through lipid bilayers without the use of ionophores.

15 It is known in the field that the low ion permeability of phospholipid bilayers such as liposome compositions [Paula et al., Biophys. J., 74:319-327, 1998; Hauser et al., Nature, 239:342-344, 1972; Ceh et al., J. Phys. Chem. B, 102:3036-3043, 1998; Mills et al., Biochim. Biophys. Acta, 1716:77-96, 2005; Papahadjopoulos et al., Biochim. Biophys. Acta, 266:561-583, 1971; Puskin, J. Membrane Biol, 35:39-55, 1977] leads to highly unfavorable loading kinetics for charged ion species. Therefore it is common practice to use an ionophore to increase trans-bilayer diffusion rates, and thereby  
20 improve or increase the loading of monovalent, divalent and trivalent cations into nanoparticles such as liposomes.

25 The patent application WO2006/043083 describes a method for loading of radionuclides, which involves ionophores and chelators. It is mentioned in the application that a chelator may be an ionophore.

30 The patent application WO03/041682 discloses liposomes enclosing biological agents. It is disclosed in the application that ion-gradients, ionophores, pH gradients and metal complexation procedures can be used for active loading of liposomes with biological agents. The application does not disclose a method for loading of nanoparticles with metal entities wherein an osmotic gradient is used to increase the loading efficiency or loading rate.

There is a need in the technical field of diagnostic applications to provide various liposome compositions that are useful for delivery of a variety of compounds, for example radio-diagnostic and imaging entities useful for PET.

## 5 Summary of invention

The present invention relates to a novel and improved method for preparation of metal entities and/or radionuclides encapsulated within liposome compositions or nanoparticles. Contrary to what is common general knowledge in the field, the  
10 inventors have found that loading of metal entities and/or radionuclides is efficient without the use of ionophores. Thus, in the new and inventive methods according to the present invention, the metal entities or radionuclides are loaded into the nanoparticles without the use of an ionophore as a transporting molecule.

15 Further, the presence of an osmotic stress on the membrane of the nanoparticles of the present invention has been found by the inventors to improve the loading step of metal entities/radionuclides into the interior of the nanoparticles. The positron-emitter  $^{64}\text{Cu}$  is used as a model nuclide representing the chemical properties of all copper isotopes.

20 The methods for preparation of a nanoparticle composition loaded with metal entities wherein said methods do not involve the use of ionophore according to the present invention comprise steps of:

- a. Providing a nanoparticle composition comprising a vesicle forming component and an agent-entrapping component enclosed by said vesicle forming  
25 component;
- b. Entrapping (loading) the metal entities within the interior of the nanoparticle composition by enabling transfer of cation metal entities across a membrane formed by the vesicle forming component by incubation of the nanoparticle composition in a solution comprising the metal entities..

30

Wherein said entrapping step involving incubation is understood as the loading of metal entities into the nanoparticle, such as the liposome.

According to the present invention, the loading efficiency or entrapment of radionuclide is greater than 10%. Such a loading efficiency can be in the range of 10% to 100%, preferably 80% to 100%, more preferably in the range of 95% to 100%.

5 According to one embodiment of the present invention, the incubation temperature is lower than 100°C, such as for example in the range of 10°C to 80°C, such as 22°C to 80°C, or such as 30°C to 80°C.

The incubation time according to the present invention is a time period shorter than 48  
10 hours, such as between 1 min to 240 min, preferably between 1 min to 120 min and more preferably between 1 min to 60 min.

Metal entities according to the present invention may comprise or consist of one or  
15 more radionuclides selected from the group consisting of Copper (<sup>61</sup>Cu, <sup>64</sup>Cu, and <sup>67</sup>Cu), Indium (<sup>111</sup>In), Technetium (<sup>99m</sup>Tc), Rhenium (<sup>188</sup>Re), Gallium (<sup>67</sup>Ga, <sup>68</sup>Ga), Lutetium (<sup>177</sup>Lu), Actinium (<sup>225</sup>Ac), Yttrium (<sup>90</sup>Y), Antimony (<sup>119</sup>Sb), Tin (<sup>117</sup>Sn, <sup>113</sup>Sn), Dysprosium (<sup>159</sup>Dy), Cobalt (<sup>56</sup>Co), Iron (<sup>59</sup>Fe), Ruthenium (<sup>97</sup>Ru, <sup>103</sup>Ru), Palladium (<sup>103</sup>Pd), Cadmium (<sup>115</sup>Cd), Tellurium (<sup>118</sup>Te, <sup>123</sup>Te), Barium (<sup>131</sup>Ba, <sup>140</sup>Ba), Gadolinium (<sup>149</sup>Gd, <sup>151</sup>Gd), Terbium (<sup>160</sup>Tb), Gold (<sup>198</sup>Au, <sup>199</sup>Au), Lanthanum (<sup>140</sup>La), and Radium  
20 (<sup>223</sup>Ra, <sup>224</sup>Ra).

Metal entities according to the present invention may also comprise one or more metal  
entities selected from the group of Gd, Dy, Ti, Cr, Mn, Fe, Co, Ni including divalent or  
trivalent ions thereof.

25 In one embodiment of the present invention, the method for preparation of nanoparticles involves a step wherein there is a difference in osmotic pressure between the exterior of the nanoparticles and the interior of the nanoparticles during incubation, for example a difference of 5-800 mOsm/L, or preferably a difference of 5-  
30 100 mOsm/L.

The vesicle-forming component according to the present invention comprises one or more of the compounds selected from the group consisting of phospholipids, pegylated phospholipids and cholesterol, for example one or more amphiphatic compounds



selected from the group of HSPC, DSPC, DPPC, POPC, CHOL, DSPE-PEG-2000, DSPE-PEG-2000-RGD and DSPE-PEG-2000-TATE.

5 Agent-entrapping components according to the present invention are selected from the group consisting of chelators, reducing agents and agents that form low solubility salts with said radionuclides, for example chelators selected from the group consisting of 1,4,7,10-tetraazacyclododecane-1,4,7,10-tetraacetic acid (DOTA), 1,4,8,11-15 tetraazacyclotetradecane-1,4,8,11-tetraacetic acid (TETA), 1,4,7,10-tetraazacyclododecane-1,4,7,10-tetra(methanephosphonic acid) (DOTP), cyclam and  
10 cyclen.

The interior pH of the nanoparticles according to the present invention is within the range of 4 to 8.5, such as 4.0 to 4.5, for example 4.5 to 5.0, such as 5.0 to 5.5 for example 5.5 to 6.0, such as 6.0 to 6.5, for example 6.5 to 7.0, such as 7.0 to 7.5, for  
15 example 7.5 to 8.0, such as 8.0 to 8.5.

The stability of the radiolabeled nanoparticles provided by the present invention is such that less than 20% leakage of radioactivity is observed for example less than 15% leakage, such as less than 12% leakage, for example less than 10% leakage, such as  
20 less than 8% leakage, for example less than 6% leakage, such as less than 4% leakage, for example less than 3% leakage, such as less than 2% leakage, for example less than 1% leakage.

The present invention further provides kits of parts comprising:

- 25 a. A nanoparticle composition comprising i) a vesicle forming component, and ii) an agent-entrapping component enclosed by the vesicle forming component; and  
b. A composition containing a metal entity for loading into the nanoparticle,

30 Further, the present invention provides a nanoparticle composition loaded with metal entities comprising:

- i. a vesicle forming component,  
ii. an agent-entrapping component enclosed by said vesicle-forming component;

iii. a metal entity entrapped on the interior side of the nanoparticle composition.

5 In a particular embodiment of the present invention, the interior pH of the nanoparticle is within the range of 6 to 8.5, such as 6.0 to 6.5, for example 6.5 to 7.0, such as 7.0 to 7.5, for example 7.5 to 8.0, such as 8.0 to 8.5.

10 The present invention further provides nanoparticle compositions for use in a method for treating, monitoring or diagnosis in a subject in need, such as for example in an imaging method which may be selected from positron emission tomography (PET) scanning or single photon emission computed tomography (SPECT) scanning and magnetic resonance imaging (MRI).

15 The present invention further provides nanoparticle compositions prepared by the methods as disclosed by the invention.

### Description of Drawings

20 **Figure 1:** Separation of  $^{64}\text{Cu}$ -Liposomes and free un-entrapped  $^{64}\text{Cu}$  with size exclusion chromatography (SEC) using a Sephadex G-25 column. Preformed liposomes consisting of DSPC/CHOL/DSPE-PEG<sub>2000</sub> with DOTA pre-encapsulated were loaded with  $^{64}\text{Cu}$  using an incubation time of 60 min and an incubation temperature of 50-55°C achieving encapsulation efficiency as high as 96.7%.

25 **Figure 2:** Separation of  $^{177}\text{Lu}$ -Liposomes and free un-entrapped  $^{177}\text{Lu}$  with size exclusion chromatography (SEC) using a Sephadex G-25 column. Preformed liposomes consisting of DSPC/CHOL/DSPE-PEG<sub>2000</sub> with DOTA pre-encapsulated were loaded with  $^{177}\text{Lu}$  using an incubation time of 60 min and an incubation temperature of 50-55°C achieving encapsulation efficiency of 81.0%.

30 **Figure 3:** Loading efficiency of  $^{64}\text{Cu}$  into liposomes as function of incubation temperature without ionophore (dashed line) and with ionophore (2HQ) (solid line). The loading efficiency of  $^{64}\text{Cu}$  loaded into liposomes without ionophore at 50-55°C was 96.7%.

35

**Figure 4:** Plot of standard curve and obtained results from a remote loading experiment of Cu(II) into liposomes consisting of DSPC, CHOL and DSPE-PEG<sub>2000</sub>. The un-complexed Cu<sup>2+</sup> was measured via an Cu(II)-selective electrode and the achieved loading efficiency was  $\left(1 - \frac{1.2 \text{ ppm}}{25 \text{ ppm}}\right) \cdot 100\% > 95\%$ . Open squares denote Cu(II) standard curve in HEPES buffer, the cross denotes HEPES 10 mM, 150 mM NaNO<sub>3</sub>, pH 6.8, the open circle denotes unloaded liposomes and the closed circle denotes loaded liposomes.

**Figure 5:** Structure of 1,2-Di-O-Hexadecyl-sn-Glycero-3-phosphocholine (1,2-Di-O-DPPC).

**Figure 6:** Differential scanning calorimetry (DSC) scan of DSPC/CHOL/DSPE-PEG<sub>2000</sub> dispersion in HEPES buffer when mixtures containing 10 mol% DSPE-PEG<sub>2000</sub> and a) 20 mol% cholesterol and 70 mol% DSPC, b) 25 mol% cholesterol and 65 mol% DSPC c) 30 mol% cholesterol and 60 mol%, d) 35 mol% cholesterol and 55 mol% DSPC, e) 40 mol% cholesterol and 50 mol% DSPC, f) 50 mol% cholesterol and 40 mol% DSPC and g) Purified chelator-containing (10 mM DOTA) liposomes consisting of DSPC/CHOL/DSPE-PEG<sub>2000</sub> in the molar ratio 50:40:10.

**Figure 7:** <sup>64</sup>Cu<sup>2+</sup> loading efficiency into chelator containing liposomes without using ionophore as function of time at three different temperatures (50°C, 40°C and 30°C). The liposomes consist of DSPC/CHOL/DSPE-PEG<sub>2000</sub> in the molar ratio 50:40:10. The difference between the internal and external osmolarity of the liposomes was, Δ(mOsm/L) = +75 (higher internal osmolarity). The ratio between the interior <sup>64</sup>Cu-DOTA complex and the un-encapsulated or non-complexed free <sup>64</sup>Cu<sup>2+</sup> is measured as <sup>64</sup>Cu-loading efficiency (%) using radio-thin layer chromatography (radio-TLC).

**Figure 8:** <sup>64</sup>Cu<sup>2+</sup> loading efficiency into chelator-containing liposomes without using ionophore as function of time at three different temperatures (50°C, 40°C and 30°C). The liposomes consist of DSPC/CHOL/DSPE-PEG<sub>2000</sub> in the molar ratio 50:40:10 and with equal intra- and extra-liposomal osmolarties. The ratio between the interior <sup>64</sup>Cu-DOTA complex and the un-encapsulated or non-complexed free <sup>64</sup>Cu<sup>2+</sup> is measured as <sup>64</sup>Cu-loading efficiency (%) using radio-TLC.

35

## Definitions

5 With the term “vesicle”, as used herein, we refer to an entity which is characterized by the presence of an internal void. Preferred vesicles are formulated from lipids, including various amphiphatic components described herein.

10 In various aspects the term “nanoparticles”, as used herein, are liposomes, polymersomes or other lipid or polymer shell structures that constitute a membrane in its broadest term surrounding a hydrous core.

15 With the term “chelator” and “chelating-agent” as used herein interchangeably, we intend chemical moieties, agents, compounds, or molecules characterized by the presence of polar groups able to form a complex containing more than one coordinate bond with a transition metal or another entity. A chelator according to the present invention is a water soluble and/or non-lipophilic agent, and is thus not the same as a “lipophilic chelator” used for transportation of metal entities across lipophilic membranes such as vesicles formed by lipids.

20 With the term “metal entity” as used herein we intend a metal ion or a radionuclide, the latter used herein interchangeably with the term radioisotope.

With the term “phosphatide” we intend a phospholipid comprising a glycerol component.

25 With the term “amphiphatic” we intend a molecule which contains both polar and nonpolar regions.

30 With the term “binding affinity” and “affinity” as used herein interchangeably, we refer to the level of attraction between molecular entities. Affinity can be expressed quantitatively as the dissociation constant or its inverse, the association constant. In the context of this invention the affinity of a chelator or another agent-entrapping component can relate to the binding affinity of the chelator DOTA for a transition metal ion or another metal entity, for example, Cu(II) or Cu(I).

With the term “entrapped agent” we intend a metal isotope, which may be a radionuclide or a non-radioactive isotope, entrapped within a liposome composition or a nanoparticle composition as herein described.

5 With the term “agent-entrapping” as used herein, we refer to any compound, without limitation, capable of trapping a metal ion or a radionuclide inside a liposome composition. Preferred agent-entrapping components are chelating-agents, substances that have the ability to reduce other substances, referred to a reducing agent, or substances that form low solubility salts with radionuclides or metal entities.

10

With the terms “loading”, “encapsulation”, or “entrapment” as used herein, are referred to an incorporation of radionuclides or metal entities into the interior of nanoparticle compositions. In the methods of the present invention, this incorporation is done by incubation of nanoparticle compositions with a solution comprising radionuclides or metal entities.

15

With the terms “loading efficiency”, “entrapment efficiency” or “encapsulation efficiency” as used herein interchangeably, is referred to the fraction of incorporation of radionuclides or metal entities into the interior of nanoparticle compositions expressed as a percentage of the total amount of radionuclide or metal entity used in the preparation.

20

With the term “encapsulation stability”, “storage stability” or “serum stability” is referred to a stability test of the nanoparticle composition to measure the degree of leakage and/or release of the entrapped agent inside the nanoparticle composition.

25

With the term “radiolabeled complex” and the like, we refer to a chelating agent and a radionuclide that form a complex.

30

With the term “targeting moiety” as used herein we intend saccharides, oligosaccharides, vitamins, peptides, proteins, antibodies and affibodies and other receptor binding ligands characterized by being attached to the nanoparticle surface through a lipid or polymer component for delivering the nanoparticles to a higher degree to the target site or into target cells.

35

The terms "drug", "medicament", "agent", or "pharmaceutical compound" as used herein include, biologically, physiologically, or pharmacologically active substances that act locally or systemically in the human or animal body.

5 The terms "treating", "treatment" and "therapy" as used herein refer equally to curative therapy, prophylactic or preventative therapy and ameliorating therapy. The term includes an approach for obtaining beneficial or desired physiological results, which may be established clinically. For purposes of this invention, beneficial or desired  
10 clinical results include, but are not limited to, alleviation of symptoms, diminishment of extent of disease, stabilized (i.e., not worsening) condition, delay or slowing of progression or worsening of condition/symptoms, amelioration or palliation of the condition or symptoms, and remission (whether partial or total), whether detectable or undetectable. The term "palliation", and variations thereof, as used herein, means that  
15 the extent and/or undesirable manifestations of a physiological condition or symptom are lessened and/or time course of the progression is slowed or lengthened, as compared to not administering compositions of the present invention.

The term "osmolarity" as used herein refers to the measure of solute concentration, defined as the number of osmoles (Osm) of solute per liter (L) of solution (Osm/L).

20

#### **Detailed description of the invention**

The present invention relates to a novel and improved method for preparation of metal entities and/or radionuclides encapsulated within liposome compositions or  
25 nanoparticles which is based on an efficient loading temperature and favorable liposomal compositions. Further, the presence of an osmotic stress of the membrane of the nanoparticles of the present invention has been found by the inventors to improve the loading step of metal entities/radionuclides into the interior of the nanoparticles.

30

The inventors have surprisingly found a method for loading charged species (ions) into nanoparticles without adding ionophores to enhance trans-membrane diffusion rates. Thus, the present invention discloses a novel method for fast entrapment of radionuclides (e.g. monovalent, divalent and trivalent cations) into liposome  
35 compositions without adding any lipophilic ionophores or any other carrier.

During the last 40 years lipophilic ionophores or complexes have been used for enhancing the efficiency of encapsulating radionuclides (e.g.  $^{111}\text{In}^{3+}$ ,  $^{177}\text{Lu}^{3+}$ ,  $^{67/68}\text{Ga}^{2+}$ ,  $^{99\text{m}}\text{TcO}_4^-$ ) in nanoparticles for *in vivo* scintigraphic imaging and internal radiotherapeutic applications. The encapsulation (or loading) efficiencies using lipophilic ionophores have reached high levels as 90-95%. The present invention relates to a new method that does not use any lipophilic ionophores or other metal carriers and can obtain similar or even higher loading efficiencies of radionuclides into liposome compositions. A preparation method for loading metal entities and/or radionuclides into nanoparticles which does not involve the use of ionophore has several advantages. Ionophores may be toxic to mammals, in particular to human beings. Therefore, nanoparticles prepared with the use of an ionophore will need to undergo extensive toxicity testing prior to regulatory approval. Furthermore, such nanoparticles will need to be purified prior to use to remove as much ionophore as possible and the extent of such purification will need to be monitored to ensure that the level of ionophore is below a certain threshold.

Manufacture of nanoparticles of the present invention is done easily with few components and without the need for extensive purification. When the nanoparticles of the present invention are administered to patients, the risks of side-effects such as toxicity or other side-effects are reduced. Further, the novel preparation method allow for an interior pH range of the nanoparticles which improve the stability of the nanoparticles. In this way, the use of the nanoparticles, methods or kits of part of the present invention is facilitated since shelf-life, storage requirements and other aspects related to the use of the present invention is improved compared to the prior art.

Also, while lipophilic ionophores are finding their usefulness for enhancing the efficiency of encapsulation of radionuclides e.g. cations into liposomes, the very lipophilic ionophores can also facilitate the release of entrapped radionuclides from the liposomes. A release of entrapped materials prematurely can result in not only an erroneous estimation of distribution of liposomes *in vivo*, but also a loss of quality in the diagnostic images.

Further, the present invention solves a need in the technical field of diagnostic applications by providing nanoparticles for delivery of metal entities to tissues with

pathological conditions associated with leaky blood vessels such as inflammatory sites or cancerous tissues.

#### **Loading efficiency and loading rate**

5

The loading efficiency of loading methods for liposomes can be measured by use of conventional methods in the art including ion-exchange chromatography, radio thin layer chromatography (radio-TLC), dialysis, or size exclusion chromatography (SEC) which can separate free radioactive metal ions or free radiolabeled complexes from liposome encapsulated radionuclides. When using SEC, the amount of radioactivity retained in liposomes compared to the amount of free radioactive metal ions or free radiolabeled complexes can be determined by monitoring the elution profile during SEC and measuring the radioactivity with a radioactivity detector, or measuring the concentration of the metal entity using inductively coupled plasma mass spectrometry (ICP-MS), inductively coupled plasma atomic emission spectroscopy (ICP-AES) or inductively coupled plasma optical emission spectrometry (ICP-OES). The radioactivity measured in the eluted fractions containing liposomes compared to eluted fractions not containing liposomes can be used to determine the loading efficiency by calculating the percentage of radioactivity retained in liposomes. Likewise, the amount of radioactivity bound in liposomes can be compared to the amount of radioactivity not entrapped in liposomes to obtain a measure of the loading efficiency when using other conventional methods known in the art.

The methods of the present invention ensure that a high amount of the radionuclides used in preparation will be entrapped within the nanoparticle. In one embodiment of the present method the efficiency of loading is higher than 10%, such as in the range of 10%-100%, such as higher than 15%, such as higher than 20%, such as higher than 25%, such as higher than 30%, such as higher than 35%, for example higher than 40%, such as higher than 50%, for example higher than 60%, such as higher than 65%, for example higher than 70%, such as higher than 75%, for example higher than 80%, such as higher than 85%, for example higher than 90%, such as higher than 95%, or such as higher than 96%, or such as higher than 97%, or such as higher than 98%, or such as higher than 99% or such as higher than 99.5% or such as higher than 99.9%. In another embodiment of the present invention the efficiency of loading when using the methods of the present invention is higher than 30% when assayed using

35



size exclusion chromatography (SEC, described in examples), ion-exchange chromatography or dialysis, such as 30% to 100%, including 55% to 100% loading efficiency, 80% to 100% loading efficiency, and 95% to 100% loading efficiency.

5 Preferably, the efficiency of loading of the methods according to the present invention is in the range of 55% to 100% such as in the range of 80% to 100%, more preferably in the range of 95% to 100%, such as between 95% to 97%, or such as between 97% to 99.9% loading efficiency.

10 The loading rate:

The loading of metals ions into liposomes can be divided into several steps including: (i) binding/coordination/adsorption of the ion to the lipid membrane, (ii) trans-membrane ion diffusion and (iii) binding of ions to the chelator. In the methods of the present invention, the lipid and chelator may be in large excess compared to the metal entities  
 15 which may be for example, but not limited to,  $^{64}\text{Cu}^{2+}$ . In the example of  $^{64}\text{Cu}^{2+}$  the kinetics thus only depends on the  $^{64}\text{Cu}^{2+}$  concentration. The rate of coordination/binding of  $\text{Cu}^{2+}$  to the membrane is rapid (likely to be diffusion limited) and binding of  $\text{Cu}^{2+}$  to the chelator (for example DOTA) occurs on timescale of seconds and can be verified by radio-TLC, or other conventional methods of the art. Since binding of  
 20 metal entities to the membrane is fast, trans-membrane ion diffusion is the most probable rate limiting step.

In general, the rate of trans-membrane diffusion will depend on the concentration gradient of the transported entity (according to Ficks 1<sup>st</sup> law), the membrane phase  
 25 state (gel, fluid or liquid-ordered) and physicochemical (hydrophilicity vs. hydrophobicity) properties of the transported entity. These arguments substantiate the first order equation (equation 1) presented below, which is here shown for  $^{64}\text{Cu}^{2+}$ , but is usable for other metal entities as well. The loading kinetics (example shown in Fig. 7-8) can be characterized by the equation

30

$$\%load = \frac{A_{Cu-chelator}}{A_{Cu} + A_{Cu-chelator} + A_{Cu(ionophore)}} = a(1 - be^{-ct}) \quad (\text{equation 1})$$

where  $A_{Cu}$ ,  $A_{Cu-chelator}$  and  $A_{Cu(ionophore)}$  denote the TLC activity of the  $^{64}\text{Cu}^{2+}$ ,  $^{64}\text{Cu}$ -Chelator and  $^{64}\text{Cu}$ -ionophore specie. The fitting parameter  $a$ , describes the plateau

level ( $a \sim 100\%$  if loading proceeds according to 1<sup>st</sup> order kinetics),  $b$  describes offset and uncertainty in  $t$  ( $b = 1$  when offset and uncertainties in  $t$  are small) and  $c$  describes the loading rate. By fitting of equation 1, each loading profile can be characterized by:

(i) the initial velocity:

5 
$$v_{ini} = a \cdot b \cdot c \quad (\text{equation 2}),$$

(ii) the time required to reach 95% loading:

$$t_{(95\%)} = -\ln((1 - (95\%)/a)/b)/c \quad (\text{equation 3}),$$

and (iii) the degree of loading reached at 60 min ( $\%load_{1h}$ ). The latter is directly comparable to the loading degree achieved using the method based on SEC (see for example results in the examples and presented in Fig. 3 and Tables 1, 2, 6 and 7).

The first order rate constant ( $c$ ) depends on different parameters such as temperature and osmolarity (see Fig. 7-8) (see next section) at which the loading is conducted. The initial velocity ( $v_{ini}$ ),  $t_{(95\%)}$  and  $\%load_{1h}$  are given in Table 8 for a set of loading conditions.

15

The loading rate of methods of the present invention can also be described by the parameters initial velocity, the time required to reach 95% loading and the degree of loading reached at 60 min.

20

Thus in one embodiment of the present invention, the initial velocity is in the range of 0.5 %/min to 100%/min, preferably in the range of 3%/min to 100%/min and more preferably in the range of 23%/min to 100%/min.

25

In one embodiment of the present invention, the time required to reach 95% loading is in the range of 0 minutes to 360 minutes, such as 1 minutes to 240 minutes, preferably in the range of 5 minutes to 240 minutes, such as in 5 minutes to 20 minutes, or such as in the range of 9 minutes to 18 minutes.

30

In one embodiment of the present invention, the degree of loading reached after 60 minutes is in the range of 10% to 100%, more preferably in the range of 55% to 100%, such as the range of 80% to 100%, and even more preferably in the range of 95% to 100%, such as 95% to 99.9%.

35

Methods for loading of nanoparticles (such as liposomes) can be compared by measuring parameters such as loading efficiency and loading rates described by the

parameters initial velocity, the time required to reach 95% loading and the degree of loading reached at 60 min. Thus, the significance of the contribution of ionophores to the above mentioned loading efficiency or loading rate can be determined by the methods disclosed herein.

5

The present invention provides a method for preparation of nanoparticles (such as liposomes) loaded with metal entities, wherein ionophores are not used for loading of the nanoparticles, or wherein one or more ionophores are present in such small amounts that they do not contribute significantly to the loading rate or the loading efficiency of the loading, since such methods essentially use the same mechanisms for loading as provided by the present invention. Thus, such methods can include methods wherein one or more ionophores are present in such amounts that there is no significant increase in loading efficiency and/or loading rate as determined by the parameters selected from the group of initial velocity, time required to reach 95% loading, degree of loading reached at 60 min. Significance of differences in loading rate or loading efficiency can be calculated by using conventional statistical methods, such as for example Student t-test.

10

15

### **Nano-particles**

20

According to the embodiments of the invention, the liposome composition is a micro-sized or a nano-sized particle that comprises a vesicle forming component and an agent-entrapping component. The vesicle forming components form an enclosed barrier of the particle. The agent-entrapping component may have at least one chemical moiety that contains one or more negatively charged groups or is capable of trapping ions. The agent-entrapping component can furthermore be a reducing agent. The agent-entrapping component interacts with an encapsulated agent, such as a metal entity comprising radio-diagnostic or radio-therapeutic agent, by electrostatic interaction, to form a stable complex or low soluble salt, or by reduction to form a precipitate. The stabilization of the encapsulated agent, such as the radio-diagnostic or radio-therapeutic agent, prevents or minimizes the release of the agent from the vesicles in the blood circulation.

25

30

Agent entrapping components may further have at least one chemical moiety that contains one or more charged groups which may be negatively or positively charged or is capable of trapping ions.

35

**Metal entities**

Nanoparticles according to the present invention comprise metal entities. Metal entities according to the present invention may be selected from the metals known for a person skilled in the art and including any of the existing oxidation states for the metal, such as monovalent cations, divalent cations, trivalent cations, tetravalent cations, pentavalent cations, hexavalent cations and heptavalent cations.

In one embodiment of the present invention, the metal entities are cations selected from the group of monovalent cations, divalent cations, trivalent cations, tetravalent cations, pentavalent cations, hexavalent cations and heptavalent cations, wherein divalent and trivalent cations are preferred.

In one embodiment of the present invention, the metal entity is copper such as Cu(I) or Cu(II).

The nanoparticles of the present invention comprise entrapped metal entities, which may comprise or consist of metal radionuclides selected from the group of isotopes consisting of Copper ( $^{61}\text{Cu}$ ,  $^{64}\text{Cu}$ , and  $^{67}\text{Cu}$ ), Indium ( $^{111}\text{In}$ ), Technetium ( $^{99\text{m}}\text{Tc}$ ), Rhenium ( $^{188}\text{Re}$ ), Gallium ( $^{67}\text{Ga}$ ,  $^{68}\text{Ga}$ ), Lutetium ( $^{177}\text{Lu}$ ), Actinium ( $^{225}\text{Ac}$ ), Yttrium ( $^{90}\text{Y}$ ), Antimony ( $^{119}\text{Sb}$ ), Tin ( $^{117}\text{Sn}$ ,  $^{113}\text{Sn}$ ), Dysprosium ( $^{159}\text{Dy}$ ), Cobalt ( $^{56}\text{Co}$ ), Iron ( $^{59}\text{Fe}$ ), Ruthenium ( $^{97}\text{Ru}$ ,  $^{103}\text{Ru}$ ), Palladium ( $^{103}\text{Pd}$ ), Cadmium ( $^{115}\text{Cd}$ ), Tellurium ( $^{118}\text{Te}$ ,  $^{123}\text{Te}$ ), Barium ( $^{131}\text{Ba}$ ,  $^{140}\text{Ba}$ ), Gadolinium ( $^{149}\text{Gd}$ ,  $^{151}\text{Gd}$ ), Terbium ( $^{160}\text{Tb}$ ), Gold ( $^{198}\text{Au}$ ,  $^{199}\text{Au}$ ), Lanthanum ( $^{140}\text{La}$ ), and Radium ( $^{223}\text{Ra}$ ,  $^{224}\text{Ra}$ ), wherein said isotope of a metal radionuclide may appear in any of the existing oxidation states for the metal. These oxidation states include monovalent cations, divalent cations, trivalent cations, tetravalent cations, pentavalent cations, hexavalent cations and heptavalent cations.

In another embodiment, the entrapped metal entities comprise isotopes selected from the group of Rhenium ( $^{186}\text{Re}$ ), Strontium ( $^{89}\text{Sr}$ ), Samarium ( $^{153}\text{Sm}$ ), Ytterbium ( $^{169}\text{Yb}$ ), Thallium ( $^{201}\text{Tl}$ ), Astatine ( $^{211}\text{At}$ ), wherein said isotope of a metal radionuclide may appear in any of the existing oxidation states for the metal. These oxidation states include monovalent cations, divalent cations, trivalent cations, tetravalent cations, pentavalent cations, hexavalent cations and heptavalent cations.

35

In yet another embodiment, the entrapped metal entities comprise isotopes selected from the group of Copper ( $^{61}\text{Cu}$ ,  $^{64}\text{Cu}$ , and  $^{67}\text{Cu}$ ), Indium ( $^{111}\text{In}$ ), Technetium ( $^{99\text{m}}\text{Tc}$ ), Rhenium ( $^{188}\text{Re}$ ), Gallium ( $^{67}\text{Ga}$ ,  $^{68}\text{Ga}$ ), Actinium ( $^{225}\text{Ac}$ ), Yttrium ( $^{90}\text{Y}$ ), Antimony ( $^{119}\text{Sb}$ ), and Lutetium ( $^{177}\text{Lu}$ ), wherein said isotope of a metal radionuclide may appear in any of the existing oxidation states for the metal. These oxidation states include monovalent cations, divalent cations, trivalent cations, tetravalent cations, pentavalent cations, hexavalent cations and heptavalent cations.

In yet another embodiment of the present invention, one or more of the entrapped metal entities are selected from the group of metals which may be used for magnetic resonance imaging (MRI) selected from the group of consisting of Gd, Dy, Ti, Cr, Mn, Fe, Fe, Co, Ni. Said metal entity may appear in any of the existing oxidation states for the metal. These oxidation states include monovalent cations, divalent cations, trivalent cations, tetravalent cations, pentavalent cations, hexavalent cations and heptavalent cations.

In a preferred embodiment of the present invention, one or more of the entrapped metal entities are selected from the group of consisting of Gd(III), Dy(III), Ti(II), Cr(III), Mn(II), Fe(II), Fe(III), Co(II), Ni(II).

Combinations of radionuclides are useful for simultaneous monitoring/imaging and treatment of various diseases such as cancer, and/or for monitoring by use of several different imaging methods. Radionuclides and combinations of radionuclides may emit one or more types of radiation such as alpha particles, beta+ particles, beta- particles, auger electrons or gamma-rays. Combinations of radionuclides may further allow for one or more types of imaging and/or radiation therapy. Thus, in another embodiment, this invention relates to vesicles and methods for their preparation, wherein the vesicles comprise metal entities comprising two or more radionuclides, selected from the group of Copper ( $^{61}\text{Cu}$ ,  $^{64}\text{Cu}$ , and  $^{67}\text{Cu}$ ), Indium ( $^{111}\text{In}$ ), Technetium ( $^{99\text{m}}\text{Tc}$ ), Rhenium ( $^{186}\text{Re}$ ,  $^{188}\text{Re}$ ), Gallium ( $^{67}\text{Ga}$ ,  $^{68}\text{Ga}$ ), Strontium ( $^{89}\text{Sr}$ ), Samarium ( $^{153}\text{Sm}$ ), Ytterbium ( $^{169}\text{Yb}$ ), Thallium ( $^{201}\text{Tl}$ ), Astatine ( $^{211}\text{At}$ ), Lutetium ( $^{177}\text{Lu}$ ), Actinium ( $^{225}\text{Ac}$ ), Yttrium ( $^{90}\text{Y}$ ), Antimony ( $^{119}\text{Sb}$ ), Tin ( $^{117}\text{Sn}$ ,  $^{113}\text{Sn}$ ), Dysprosium ( $^{159}\text{Dy}$ ), Cobalt ( $^{56}\text{Co}$ ), Iron ( $^{59}\text{Fe}$ ), Ruthenium ( $^{97}\text{Ru}$ ,  $^{103}\text{Ru}$ ), Palladium ( $^{103}\text{Pd}$ ), Cadmium ( $^{115}\text{Cd}$ ), Tellurium ( $^{118}\text{Te}$ ,  $^{123}\text{Te}$ ), Barium ( $^{131}\text{Ba}$ ,  $^{140}\text{Ba}$ ), Gadolinium ( $^{149}\text{Gd}$ ,  $^{151}\text{Gd}$ ), Terbium ( $^{160}\text{Tb}$ ), Gold ( $^{198}\text{Au}$ ,  $^{199}\text{Au}$ ), Lanthanum ( $^{140}\text{La}$ ), and Radium ( $^{223}\text{Ra}$ ,  $^{224}\text{Ra}$ ), wherein said isotope of a

metal radionuclide may appear in any of the existing oxidation states for the metal. These oxidation states include monovalent cations, divalent cations, trivalent cations, tetravalent cations, pentavalent cations, hexavalent cations and heptavalent cations.

5 In a further embodiment, combinations of metal entities may include one or more metals and one or more radionuclides which further allow for one or more types of imaging and/or radiation therapy. Thus, in another embodiment, this invention relates to vesicles and methods for their preparation, wherein the vesicles comprise metal entities selected from the group of Gd, Dy, Ti, Cr, Mn, Fe, Fe, Co, Ni in any of the  
 10 existing oxidation states for the metal, with radionuclides selected from the group of the group of Copper ( $^{61}\text{Cu}$ ,  $^{64}\text{Cu}$ , and  $^{67}\text{Cu}$ ), Indium ( $^{111}\text{In}$ ), Technetium ( $^{99\text{m}}\text{Tc}$ ), Rhenium ( $^{186}\text{Re}$ ,  $^{188}\text{Re}$ ), Gallium ( $^{67}\text{Ga}$ ,  $^{68}\text{Ga}$ ), Strontium ( $^{89}\text{Sr}$ ), Samarium ( $^{153}\text{Sm}$ ), Ytterbium ( $^{169}\text{Yb}$ ), Thallium ( $^{201}\text{Tl}$ ), Astatine ( $^{211}\text{At}$ ), Lutetium ( $^{177}\text{Lu}$ ), Actinium ( $^{225}\text{Ac}$ ), Yttrium ( $^{90}\text{Y}$ ), Antimony ( $^{119}\text{Sb}$ ), Tin ( $^{117}\text{Sn}$ ,  $^{113}\text{Sn}$ ), Dysprosium ( $^{159}\text{Dy}$ ), Cobalt ( $^{56}\text{Co}$ ), Iron ( $^{59}\text{Fe}$ ),  
 15 Ruthenium ( $^{97}\text{Ru}$ ,  $^{103}\text{Ru}$ ), Palladium ( $^{103}\text{Pd}$ ), Cadmium ( $^{115}\text{Cd}$ ), Tellurium ( $^{118}\text{Te}$ ,  $^{123}\text{Te}$ ), Barium ( $^{131}\text{Ba}$ ,  $^{140}\text{Ba}$ ), Gadolinium ( $^{149}\text{Gd}$ ,  $^{151}\text{Gd}$ ), Terbium ( $^{160}\text{Tb}$ ), Gold ( $^{198}\text{Au}$ ,  $^{199}\text{Au}$ ), Lanthanum ( $^{140}\text{La}$ ), and Radium ( $^{223}\text{Ra}$ ,  $^{224}\text{Ra}$ ), wherein said isotope of a metal radionuclide may appear in any of the existing oxidation states for the metal. These oxidation states include monovalent cations, divalent cations, trivalent cations,  
 20 tetravalent cations, pentavalent cations, hexavalent cations and heptavalent cations.

Thus according to the present invention, nanoparticle compositions such as vesicles may comprise one or more combinations selected from the group of  $^{64}\text{Cu}$  and Gd(III),  $^{64}\text{Cu}$  and Dy(III),  $^{64}\text{Cu}$  and Ti(II),  $^{64}\text{Cu}$  and Cr(III),  $^{64}\text{Cu}$  and Mn(II),  $^{64}\text{Cu}$  and Fe(II),  $^{64}\text{Cu}$  and Fe(III),  $^{64}\text{Cu}$  and Co(II),  $^{64}\text{Cu}$  and Ni(II),  $^{68}\text{Ga}$  and Gd(III),  $^{68}\text{Ga}$  and Dy(III),  $^{68}\text{Ga}$  and Ti(II),  $^{68}\text{Ga}$  and Cr(III),  $^{68}\text{Ga}$  and Mn(II),  $^{68}\text{Ga}$  and Fe(II),  $^{68}\text{Ga}$  and Fe(III),  $^{68}\text{Ga}$  and Co(II),  $^{68}\text{Ga}$  and Ni(II),  $^{111}\text{In}$  and Gd(III),  $^{111}\text{In}$  and Dy(III),  $^{111}\text{In}$  and Ti(II),  $^{111}\text{In}$  and Cr(III),  $^{111}\text{In}$  and Mn(II),  $^{111}\text{In}$  and Fe(II),  $^{111}\text{In}$  and Fe(III),  $^{111}\text{In}$  and Co(II),  $^{111}\text{In}$  and Ni(II),  $^{99\text{m}}\text{Tc}$  and Gd(III),  $^{99\text{m}}\text{Tc}$  and Dy(III),  $^{99\text{m}}\text{Tc}$  and Ti(II),  $^{99\text{m}}\text{Tc}$  and Cr(III),  $^{99\text{m}}\text{Tc}$  and Mn(II),  
 25  $^{99\text{m}}\text{Tc}$  and Fe(II),  $^{99\text{m}}\text{Tc}$  and Fe(III),  $^{99\text{m}}\text{Tc}$  and Co(II),  $^{99\text{m}}\text{Tc}$  and Ni(II),  $^{177}\text{Lu}$  and Gd(III),  $^{177}\text{Lu}$  and Dy(III),  $^{177}\text{Lu}$  and Ti(II),  $^{177}\text{Lu}$  and Cr(III),  $^{177}\text{Lu}$  and Mn(II),  $^{177}\text{Lu}$  and Fe(II),  $^{177}\text{Lu}$  and Fe(III),  $^{177}\text{Lu}$  and Co(II),  $^{177}\text{Lu}$  and Ni(II),  $^{67}\text{Ga}$  and Gd(III),  $^{67}\text{Ga}$  and Dy(III),  $^{67}\text{Ga}$  and Ti(II),  $^{67}\text{Ga}$  and Cr(III),  $^{67}\text{Ga}$  and Mn(II),  $^{67}\text{Ga}$  and Fe(II),  $^{67}\text{Ga}$  and Fe(III),  $^{67}\text{Ga}$  and Co(II),  $^{67}\text{Ga}$  and Ni(II),  $^{201}\text{Tl}$  and Gd(III),  $^{201}\text{Tl}$  and Dy(III),  $^{201}\text{Tl}$  and Ti(II),  $^{201}\text{Tl}$  and Cr(III),  $^{201}\text{Tl}$  and Mn(II),  $^{201}\text{Tl}$  and Fe(II),  $^{201}\text{Tl}$  and Fe(III),  $^{201}\text{Tl}$  and Co(II),  $^{201}\text{Tl}$  and Ni(II),  
 30  
 35

<sup>90</sup>Y and Gd(III), <sup>90</sup>Y and Dy(III), <sup>90</sup>Y and Ti(II), <sup>90</sup>Y and Cr(III), <sup>90</sup>Y and Mn(II), <sup>90</sup>Y and Fe(II), <sup>90</sup>Y and Fe(III), <sup>90</sup>Y and Co(II) and <sup>90</sup>Y and Ni(II), wherein said isotope of a metal radionuclide may appear in any of the existing oxidation states for the metal. These oxidation states include monovalent cations, divalent cations, trivalent cations, 5 tetraivalent cations, pentavalent cations, hexavalent cations and heptavalent cations.

In a preferred embodiment, nanoparticle compositions such as vesicles may comprise one or more combinations of metal entities selected from the group consisting of <sup>64</sup>Cu and Gd(III), <sup>64</sup>Cu and Dy(III), <sup>64</sup>Cu and Ti(II), <sup>64</sup>Cu and Cr(III), <sup>64</sup>Cu and Mn(II), <sup>64</sup>Cu and 10 Fe(II), <sup>64</sup>Cu and Fe(III), <sup>64</sup>Cu and Co(II), <sup>64</sup>Cu and Ni(II), <sup>68</sup>Ga and Gd(III), <sup>68</sup>Ga and Dy(III), <sup>68</sup>Ga and Ti(II), <sup>68</sup>Ga and Cr(III), <sup>68</sup>Ga and Mn(II), <sup>68</sup>Ga and Fe(II), <sup>68</sup>Ga and Fe(III), <sup>68</sup>Ga and Co(II), <sup>68</sup>Ga and Ni(II), <sup>177</sup>Lu and Gd(III), <sup>177</sup>Lu and Dy(III), <sup>177</sup>Lu and Ti(II), <sup>177</sup>Lu and Cr(III), <sup>177</sup>Lu and Mn(II), <sup>177</sup>Lu and Fe(II), <sup>177</sup>Lu and Fe(III), <sup>177</sup>Lu and 15 Co(II), <sup>177</sup>Lu and Ni(II) wherein said isotope of a metal radionuclide may appear in any of the existing oxidation states for the metal. These oxidation states include monovalent cations, divalent cations, trivalent cations, tetraivalent cations, pentavalent cations, hexavalent cations and heptavalent cations,

In an even more preferred embodiment, the nanoparticle compositions such as 20 vesicles may comprise one or more combinations of metal entities selected from the group consisting of <sup>64</sup>Cu and Gd(III), <sup>68</sup>Ga and Gd(III), <sup>177</sup>Lu and Gd(III), <sup>111</sup>In and Gd(III), <sup>67</sup>Ga and Gd(III), <sup>90</sup>Y and Gd(III), wherein the combinations of <sup>64</sup>Cu and Gd(III) and <sup>68</sup>Ga and Gd(III) are most preferred.

25 Vesicles according to the present invention may comprise a combination of one or more radionuclides for imaging and one or more radionuclides for therapy. Radionuclides for imaging comprise radionuclides such as <sup>64</sup>Cu, <sup>61</sup>Cu, <sup>99m</sup>Tc, <sup>68</sup>Ga, <sup>89</sup>Zr and <sup>111</sup>In.

30 Radionuclides for therapy comprise radionuclides such as <sup>64</sup>Cu, <sup>67</sup>Cu, <sup>111</sup>In, <sup>67</sup>Ga, <sup>186</sup>Re, <sup>188</sup>Re, <sup>89</sup>Sr, <sup>153</sup>Sm, <sup>169</sup>Yb, <sup>201</sup>Tl, <sup>211</sup>At, <sup>177</sup>Lu, <sup>225</sup>Ac, <sup>90</sup>Y, <sup>119</sup>Sb, <sup>117</sup>Sn, <sup>113</sup>Sn, <sup>159</sup>Dy, <sup>56</sup>Co, <sup>59</sup>Fe, <sup>97</sup>Ru, <sup>103</sup>Ru, <sup>103</sup>Pd, <sup>115</sup>Cd, <sup>118</sup>Te, <sup>123</sup>Te, <sup>131</sup>Ba, <sup>140</sup>Ba, <sup>149</sup>Gd, <sup>151</sup>Gd, <sup>160</sup>Tb, <sup>198</sup>Au, <sup>199</sup>Au, <sup>140</sup>La, <sup>223</sup>Ra and <sup>224</sup>Ra.

In a preferred embodiment of the present invention, the vesicles or nanoparticles comprise two or more radionuclides selected from the group of  $^{61}\text{Cu}$ ,  $^{64}\text{Cu}$ ,  $^{67}\text{Cu}$ ,  $^{67}\text{Ga}$ ,  $^{68}\text{Ga}$ ,  $^{225}\text{Ac}$ ,  $^{90}\text{Y}$ ,  $^{177}\text{Lu}$ ,  $^{186}\text{Re}$ ,  $^{188}\text{Re}$  and  $^{119}\text{Sb}$ .

5 An even more preferred embodiment of the present invention relates to vesicles or nanoparticles comprising  $^{64}\text{Cu}$  and  $^{177}\text{Lu}$ , or  $^{64}\text{Cu}$  and  $^{67}\text{Cu}$ , or  $^{61}\text{Cu}$  and  $^{67}\text{Cu}$ , or  $^{64}\text{Cu}$  and  $^{90}\text{Y}$ , or  $^{64}\text{Cu}$  and  $^{119}\text{Sb}$ , or  $^{64}\text{Cu}$  and  $^{225}\text{Ac}$ , or  $^{64}\text{Cu}$  and  $^{188}\text{Re}$ , or  $^{64}\text{Cu}$  and  $^{186}\text{Re}$ , or  $^{64}\text{Cu}$  and  $^{211}\text{At}$ , or  $^{64}\text{Cu}$  and  $^{67}\text{Ga}$ , or  $^{61}\text{Cu}$  and  $^{177}\text{Lu}$ , or  $^{61}\text{Cu}$  and  $^{90}\text{Y}$ , or  $^{61}\text{Cu}$  and  $^{119}\text{Sb}$ , or  $^{61}\text{Cu}$  and  $^{225}\text{Ac}$ , or  $^{61}\text{Cu}$  and  $^{188}\text{Re}$ , or  $^{61}\text{Cu}$  and  $^{186}\text{Re}$ , or  $^{61}\text{Cu}$  and  $^{211}\text{At}$ , or  $^{61}\text{Cu}$  and  $^{67}\text{Ga}$ , or  $^{67}\text{Cu}$  and  $^{177}\text{Lu}$ , or  $^{67}\text{Cu}$  and  $^{90}\text{Y}$ , or  $^{67}\text{Cu}$  and  $^{119}\text{Sb}$ , or  $^{67}\text{Cu}$  and  $^{225}\text{Ac}$ , or  $^{67}\text{Cu}$  and  $^{188}\text{Re}$ , or  $^{67}\text{Cu}$  and  $^{186}\text{Re}$ , or  $^{67}\text{Cu}$  and  $^{211}\text{At}$ , or  $^{68}\text{Ga}$  and  $^{177}\text{Lu}$ , or  $^{68}\text{Ga}$  and  $^{90}\text{Y}$ , or  $^{68}\text{Ga}$  and  $^{119}\text{Sb}$ , or  $^{68}\text{Ga}$  and  $^{225}\text{Ac}$ , or  $^{68}\text{Ga}$  and  $^{188}\text{Re}$ , or  $^{68}\text{Ga}$  and  $^{186}\text{Re}$ , or  $^{68}\text{Ga}$  and  $^{211}\text{At}$ , or  $^{68}\text{Ga}$  and  $^{67}\text{Cu}$ .

15 Nanoparticles or vesicles comprising one or more radionuclides according to the present invention may be used for clinical imaging and/or radiotherapy. Clinical imaging includes imaging for diagnosis, monitoring the effects of treatment, or monitoring the location of vesicles used for radiotherapy.

20 In a preferred embodiment, vesicles or nanoparticles of the present invention comprise a combination of radionuclides useful for combined positron emission tomography (PET) imaging and radiation therapy, such as  $^{64}\text{Cu}$  and  $^{177}\text{Lu}$ , or such as  $^{64}\text{Cu}$  and  $^{67}\text{Cu}$ , or such as  $^{61}\text{Cu}$  and  $^{67}\text{Cu}$ , or such as  $^{64}\text{Cu}$  and  $^{90}\text{Y}$ , or such as  $^{64}\text{Cu}$  and  $^{119}\text{Sb}$ , or such as  $^{64}\text{Cu}$  and  $^{225}\text{Ac}$ , or such as  $^{64}\text{Cu}$  and  $^{188}\text{Re}$ , or such as  $^{64}\text{Cu}$  and  $^{186}\text{Re}$ , or such as  $^{64}\text{Cu}$  and  $^{211}\text{At}$ .

In an even more preferred embodiment, vesicles or nanoparticles of the present invention comprise a combination of radionuclides useful for combined positron emission tomography (PET) imaging and radiation therapy, such as  $^{64}\text{Cu}$  and  $^{177}\text{Lu}$ .

30 According to the present invention, the nanoparticles may comprise one or more isotopes different from copper which may be associated to the inner or outer surface of the nanoparticle composition via a linker molecule such as a chelator. Such isotopes may be selected from the group of Indium ( $^{111}\text{In}$ ), Technetium ( $^{99\text{m}}\text{Tc}$ ), Rhenium ( $^{186}\text{Re}$ ,  $^{188}\text{Re}$ ), Gallium ( $^{67}\text{Ga}$ ,  $^{68}\text{Ga}$ ), Strontium ( $^{89}\text{Sr}$ ), Samarium ( $^{153}\text{Sm}$ ), Ytterbium ( $^{169}\text{Yb}$ ),

35



Thallium ( $^{201}\text{Tl}$ ), Astatine ( $^{211}\text{At}$ ), Lutetium ( $^{177}\text{Lu}$ ), Actinium ( $^{225}\text{Ac}$ ), Yttrium ( $^{90}\text{Y}$ ), Antimony ( $^{119}\text{Sb}$ ), Tin ( $^{117}\text{Sn}$ ,  $^{113}\text{Sn}$ ), Dysprosium ( $^{159}\text{Dy}$ ), Cobalt ( $^{56}\text{Co}$ ), Iron ( $^{59}\text{Fe}$ ), Ruthenium ( $^{97}\text{Ru}$ ,  $^{103}\text{Ru}$ ), Palladium ( $^{103}\text{Pd}$ ), Cadmium ( $^{115}\text{Cd}$ ), Tellurium ( $^{118}\text{Te}$ ,  $^{123}\text{Te}$ ), Barium ( $^{131}\text{Ba}$ ,  $^{140}\text{Ba}$ ), Gadolinium ( $^{149}\text{Gd}$ ,  $^{151}\text{Gd}$ ), Terbium ( $^{160}\text{Tb}$ ), Gold ( $^{198}\text{Au}$ ,  $^{199}\text{Au}$ ),  
 5 Lanthanum ( $^{140}\text{La}$ ), Radium ( $^{223}\text{Ra}$ ,  $^{224}\text{Ra}$ ), Rhenium ( $^{186}\text{Re}$ ), Strontium ( $^{89}\text{Sr}$ ), Samarium ( $^{153}\text{Sm}$ ), Ytterbium ( $^{169}\text{Yb}$ ), Thallium ( $^{201}\text{Tl}$ ) and Astatine ( $^{211}\text{At}$ ), wherein said isotope of a metal radionuclide may appear in any of the existing oxidation states for the metal. These oxidation states include monovalent cations, divalent cations, trivalent cations, tetravalent cations, pentavalent cations, hexavalent cations and heptavalent  
 10 cations.

According to one embodiment of the present invention, the metal entities can be radionuclides selected from the group consisting of  $^{61}\text{Cu}$ ,  $^{64}\text{Cu}$ ,  $^{67}\text{Cu}$ ,  $^{177}\text{Lu}$ ,  $^{67}\text{Ga}$ ,  $^{68}\text{Ga}$ ,  $^{225}\text{Ac}$ ,  $^{90}\text{Y}$ ,  $^{186}\text{Re}$ ,  $^{188}\text{Re}$ ,  $^{119}\text{Sb}$  and  $^{111}\text{In}$  wherein said isotope of a metal radionuclide may  
 15 appear in any of the existing oxidation states for the metal. These oxidation states include monovalent cations, divalent cations, trivalent cations, tetravalent cations, pentavalent cations, hexavalent cations and heptavalent cations.

In a preferred embodiment of the present invention, the metal entities are radionuclides selected from the group consisting of  $^{61}\text{Cu}$ ,  $^{64}\text{Cu}$ ,  $^{67}\text{Cu}$ ,  $^{111}\text{In}$  and  $^{177}\text{Lu}$  wherein said isotope of a metal radionuclide may appear in any of the existing oxidation states for the metal. These oxidation states include monovalent cations, divalent cations, trivalent cations, tetravalent cations, pentavalent cations, hexavalent cations and heptavalent  
 20 cations.

In one embodiment of the present invention, the metal entities are two or more radionuclides selected from the group consisting of  $^{64}\text{Cu}$  and  $^{67}\text{Cu}$ ,  $^{61}\text{Cu}$  and  $^{67}\text{Cu}$ ,  $^{64}\text{Cu}$  and  $^{90}\text{Y}$ ,  $^{64}\text{Cu}$  and  $^{119}\text{Sb}$ ,  $^{64}\text{Cu}$  and  $^{225}\text{Ac}$ ,  $^{64}\text{Cu}$  and  $^{188}\text{Re}$ ,  $^{64}\text{Cu}$  and  $^{186}\text{Re}$ ,  $^{64}\text{Cu}$  and  $^{211}\text{At}$ ,  $^{64}\text{Cu}$  and  $^{67}\text{Ga}$ ,  $^{61}\text{Cu}$  and  $^{177}\text{Lu}$ ,  $^{61}\text{Cu}$  and  $^{90}\text{Y}$ ,  $^{61}\text{Cu}$  and  $^{119}\text{Sb}$ ,  $^{61}\text{Cu}$  and  $^{225}\text{Ac}$ ,  $^{61}\text{Cu}$  and  $^{188}\text{Re}$ ,  $^{61}\text{Cu}$  and  $^{186}\text{Re}$ ,  $^{61}\text{Cu}$  and  $^{211}\text{At}$ ,  $^{61}\text{Cu}$  and  $^{67}\text{Ga}$ ,  $^{67}\text{Cu}$  and  $^{177}\text{Lu}$ ,  $^{67}\text{Cu}$  and  $^{90}\text{Y}$ ,  
 30  $^{67}\text{Cu}$  and  $^{119}\text{Sb}$ ,  $^{67}\text{Cu}$  and  $^{225}\text{Ac}$ ,  $^{67}\text{Cu}$  and  $^{188}\text{Re}$ ,  $^{67}\text{Cu}$  and  $^{186}\text{Re}$ ,  $^{67}\text{Cu}$  and  $^{211}\text{At}$ ,  $^{68}\text{Ga}$  and  $^{177}\text{Lu}$ ,  $^{68}\text{Ga}$  and  $^{90}\text{Y}$ ,  $^{68}\text{Ga}$  and  $^{119}\text{Sb}$ ,  $^{68}\text{Ga}$  and  $^{225}\text{Ac}$ ,  $^{68}\text{Ga}$  and  $^{188}\text{Re}$ ,  $^{68}\text{Ga}$  and  $^{186}\text{Re}$ ,  $^{68}\text{Ga}$  and  $^{211}\text{At}$ , and  $^{68}\text{Ga}$  and  $^{67}\text{Cu}$ .

In another embodiment of the present invention, the metal entities are two or more radionuclides selected from the group consisting of Copper ( $^{61}\text{Cu}$ ,  $^{64}\text{Cu}$ , and  $^{67}\text{Cu}$ ), such as  $^{61}\text{Cu}$  and  $^{64}\text{Cu}$ , or  $^{61}\text{Cu}$  and  $^{67}\text{Cu}$ , or  $^{64}\text{Cu}$  and  $^{67}\text{Cu}$ , or  $^{61}\text{Cu}$ ,  $^{64}\text{Cu}$  and  $^{67}\text{Cu}$ .

5 In one embodiment of the present invention, the metal entities are selected from the groups of metal entities as mentioned herein, wherein the cations  $\text{Hg}^{2+}$  and  $\text{Cu}^+$ , are excluded.

10 In a further embodiment of the invention, the radionuclide may also be entrapped within another carrier such as a nanoparticle that is useful in diagnosing and/or treating a cancerous disease and, in general a pathological condition associated with leaky blood vessels or another disease in a subject.

15 A detailed description of exemplary vesicle forming components and agent-entrapping components for preparing the liposome compositions of the present invention are set forth below.

#### **Vesicle forming component**

20 A vesicle forming component is a synthetic or naturally-occurring amphiphatic compound which comprises a hydrophilic part and a hydrophobic part. Vesicle forming components include, for example, fatty acids, neutral fats, phosphatides, glycolipids, aliphatic alcohols, and steroids,. Additionally, vesicle forming components may further include lipids, diblock and triblock copolymers bolalipids, ceramides, sphingolipids, phospholipids, pegylated phospholipids and cholesterol.

25 In one embodiment of the present invention, the vesicle forming components allow for a prolonged circulation time of the nanoparticles.

30 The vesicle forming component of the present invention or the method of the present invention may contain a hydrophilic polymer such as for example a polyethylene glycol (PEG) component or a derivate thereof, or a polysaccharide. In such a case the vesicle forming component is said to be derivatized with the hydrophilic polymer (e.g. PEG) or the polysaccharide. In one embodiment, the polymer enables conjugation of proteins or other receptor affinity molecules to the vesicle forming component derivatized with the  
35 polymer. In another embodiment, the attachment of the polymer (e.g. PEG) to the

liposome composition, allows for prolonged circulation time within the blood stream. Vesicles comprising PEG chains on their surface are capable of extravasating leaky blood vessels.

5 Examples of suitable vesicle forming lipids used in the present invention or the method of the present invention include, but are not limited to: phosphatidylcholines such as 1,2-dioleoyl-phosphatidylcholine, 1,2-dipalmitoyl-phosphatidylcholine, 1,2-dimyristoyl-phosphatidylcholine, 1,2-distearoyl-phosphatidylcholine, 1-oleoyl-2-palmitoyl-phosphatidylcholine, 1-oleoyl-2-stearoyl-phosphatidylcholine, 1-palmitoyl-2-oleoyl-phosphatidylcholine and 1-stearoyl-2-oleoyl-phosphatidylcholine; phosphatidylethanolamines such as 1,2-dioleoyl-phosphatidylethanolamine, 1,2-dipalmitoyl-phosphatidylethanolamine, 1,2-dimyristoyl-phosphatidylethanolamine, 1,2-distearoyl-phosphatidylethanolamine, 1-oleoyl-2-palmitoyl-phosphatidylethanolamine, 1-oleoyl-2-stearoyl-phosphatidylethanolamine, 1-palmitoyl-2-oleoyl-phosphatidylethanolamine, 1-stearoyl-2-oleoyl-phosphatidylethanolamine and N-succinyl-dioleoyl-phosphatidylethanolamine; phosphatidylserines such as 1,2-dioleoyl-phosphatidylserine, 1,2-dipalmitoyl-phosphatidylserine, 1,2-dimyristoyl-phosphatidylserine, 1,2-distearoyl-phosphatidylserine, 1-oleoyl-2-palmitoyl-phosphatidylserine, 1-oleoyl-2-stearoyl-phosphatidylserine, 1-palmitoyl-2-oleoyl-phosphatidylserine and 1-stearoyl-2-oleoyl-phosphatidylserine; phosphatidylglycerols such as 1,2-dioleoyl-phosphatidylglycerol, 1,2-dipalmitoyl-phosphatidylglycerol, 1,2-dimyristoyl-phosphatidylglycerol, 1,2-distearoyl-phosphatidylglycerol, 1-oleoyl-2-palmitoyl-phosphatidylglycerol, 1-oleoyl-2-stearoyl-phosphatidylglycerol, 1-palmitoyl-2-oleoyl-phosphatidylglycerol and 1-stearoyl-2-oleoyl-phosphatidylglycerol; pegylated lipids; pegylated phospholipids such as phosphatidylethanolamine-N-[methoxy(polyethyleneglycol)-1000], phosphatidylethanolamine-N-[methoxy(polyethyleneglycol)-2000], phosphatidylethanolamine-N-[methoxy(polyethylene glycol)-3000], phosphatidylethanolamine-N-[methoxy(polyethyleneglycol)-5000]; pegylated ceramides such as N-octanoyl-sphingosine-1-{succinyl[methoxy(polyethyleneglycol)1000]}, N-octanoyl-sphingosine-1-{succinyl[methoxy(polyethylene glycol)2000]}, N-octanoyl-sphingosine-1-{succinyl[methoxy(polyethyleneglycol)3000]}, N-octanoyl-sphingosine-1-{succinyl[methoxy(polyethyleneglycol)5000]}; lyso-phosphatidylcholines, lyso-phosphatidylethanolamines, lyso-phosphatidylglycerols, lyso-phosphatidylserines, ceramides; sphingolipids; glycolipids such as ganglioside GMI; glucolipids; sulphatides;

10  
15  
20  
25  
30  
35

phosphatidic acid, such as di-palmitoyl-glycerophosphatidic acid; palmitic fatty acids; stearic fatty acids; arachidonic fatty acids; lauric fatty acids; myristic fatty acids; lauroleic fatty acids; physeteric fatty acids; myristoleic fatty acids; palmitoleic fatty acids; petroselinic fatty acids; oleic fatty acids; isolauric fatty acids; isomyristic fatty acids; isostearic fatty acids; sterol and sterol derivatives such as cholesterol, cholesterol hemisuccinate, cholesterol sulphate, and cholesteryl-(4-trimethylammonio)-butanoate, ergosterol, lanosterol; polyoxyethylene fatty acids esters and polyoxyethylene fatty acids alcohols; polyoxyethylene fatty acids alcohol ethers; polyoxyethylated sorbitan fatty acid esters, glycerol polyethylene glycol oxy-stearate; glycerol polyethylene glycol ricinoleate; ethoxylated soybean sterols; ethoxylated castor oil; polyoxyethylene polyoxypropylene fatty acid polymers; polyoxyethylene fatty acid stearates; di-oleoyl-*sn*-glycerol; dipalmitoyl-succinylglycerol; 1,3-dipalmitoyl-2-succinylglycerol; 1-alkyl-2-acyl-phosphatidylcholines such as 1-hexadecyl-2-palmitoyl-phosphatidylcholine; 1-alkyl-2-acyl-phosphatidylethanolamines such as 1-hexadecyl-2-palmitoyl-phosphatidylethanolamine; 1-alkyl-2-acyl-phosphatidylserines such as 1-hexadecyl-2-palmitoyl-phosphatidylserine; 1-alkyl-2-acyl-phosphatidylglycerols such as 1-hexadecyl-2-palmitoyl-phosphatidylglycerol; 1-alkyl-2-alkyl-phosphatidylcholines such as 1-hexadecyl-2-hexadecyl-phosphatidylcholine; 1-alkyl-2-alkyl-phosphatidylethanolamines such as 1-hexadecyl-2-hexadecyl-phosphatidylethanolamine; 1-alkyl-2-alkyl-phosphatidylserines such as 1-hexadecyl-2-hexadecyl-phosphatidylserine; 1-alkyl-2-alkyl-phosphatidylglycerols such as 1-hexadecyl-2-hexadecyl-phosphatidylglycerol; N-Succinyl-dioctadecylamine; palmitoylhomocysteine; lauryltrimethylammonium bromide; cetyltrimethyl-ammonium bromide; myristyltrimethylammonium bromide; N-[1,2,3-dioleoyloxy)-propyl]-N,N,N-trimethylammoniumchloride(DOTMA); 1,2-dioleoyloxy-3-(trimethylammonium)propane(DOTAP); and 1,2-dioleoyl-c-(4'-trimethylammonium)-butanoyl-*sn*-glycerol (DOTB).

Such examples of suitable vesicle forming lipids used in the present invention or the methods of the present invention further include hydrogenated soy phosphatidylcholine (HSPC).

In one embodiment the vesicle forming component include compounds selected from the group of DSPC (1,2-distearoyl-*sn*-glycero-3-phosphocholine), CHOL (Cholesterol), DSPE-PEG-2000 (1,2-distearoyl-*sn*-glycero-3-phosphoethanolamine-*N*-[methoxy

(polyethylene glycol)-2000]), POPC (1-palmitoyl-2-oleoyl-*sn*-glycero-3-phosphocholine), DPPC (1,2-dipalmitoyl-*sn*-glycero-3-phosphocholine), DSPE-PEG<sub>2000</sub>-TATE, (1,2-distearoyl-*sn*-glycero-3-phosphoethanolamine-*N*-[methoxy (polyethylene glycol)-2000]-TATE).

5

In one preferred embodiment the vesicle forming component include compounds selected from the group of DSPC (1,2-distearoyl-*sn*-glycero-3-phosphocholine), CHOL (Cholesterol), DSPE-PEG-2000 (1,2-distearoyl-*sn*-glycero-3-phosphoethanolamine-*N*-[methoxy (polyethylene glycol)-2000]), POPC (1-palmitoyl-2-oleoyl-*sn*-glycero-3-phosphocholine), DPPC (1,2-dipalmitoyl-*sn*-glycero-3-phosphocholine), DSPE-PEG<sub>2000</sub>-TATE, (1,2-distearoyl-*sn*-glycero-3-phosphoethanolamine-*N*-[methoxy (polyethylene glycol)-2000]-TATE) and hydrogenated soy phosphatidylcholine (HSPC).

10

15

In one embodiment of the nanoparticle composition, the vesicle forming component consists of amphiphatic compounds selected from the group consisting of 1,2-distearoyl-*sn*-glycero-3-phosphocholine (DSPC) "A", cholesterol "B", and 1,2-distearoyl-*sn*-glycero-3-phosphoethanolamine-*N*-[methoxy (polyethylene glycol)-2000] (DSPE-PEG-2000) "C" in the molar ratio of A:B:C, wherein A is selected from the interval 45 to 65, B is selected from the interval 35 to 45, and C is selected from the interval 2 to 20 and wherein A+B+C = 100.

20

30

In one preferred embodiment of the nanoparticle composition, the vesicle forming component consists of amphiphatic compounds selected from the group consisting of 1,2-distearoyl-*sn*-glycero-3-phosphocholine (DSPC) "A", cholesterol "B", and 1,2-distearoyl-*sn*-glycero-3-phosphoethanolamine-*N*-[methoxy (polyethylene glycol)-2000] (DSPE-PEG-2000) "C" in the molar ratio of A:B:C, wherein A is selected from the interval 45 to 65, B is selected from the interval 35 to 45, and C is selected from the interval 1 to 20 and wherein A+B+C = 100.

25

35

In another preferred embodiment the vesicle forming component include DSPC (1,2-distearoyl-*sn*-glycero-3-phosphocholine), CHOL (Cholesterol), DSPE-PEG-2000 (1,2-distearoyl-*sn*-glycero-3-phosphoethanolamine-*N*-[methoxy (polyethylene glycol)-2000]) in a molar ratio of 50:40:10.

In another embodiment of the disclosed method, the vesicle forming component consists of amphiphatic compounds selected from the group consisting of 1,2-distearoyl-*sn*-glycero-3-phosphocholine (DSPC) "A", cholesterol "B", and 1,2-distearoyl-*sn*-glycero-3-phosphoethanolamine-*N*-[methoxy (polyethylene glycol)-2000] (DSPE-PEG-2000) "C", and 1,2-distearoyl-*sn*-glycero-3-phosphoethanolamine-*N*-[methoxy (polyethylene glycol)-2000]-TATE (DSPE-PEG-2000-TATE) "D" with the molar ratio A:B:C:D, wherein A is selected from the interval 45 to 65, B is selected from the interval 35 to 45, C is selected from the interval 5 to 13, D is selected from the interval 0 to 3, and wherein  $A+B+C+D = 100$ .

10

The radiolabeled nanoparticle composition mentioned above may further comprise a targeting moiety enabling the nanoparticle to specifically bind to target cells bearing the target molecule, or a moiety specifically binding to diseased target. The targeting moiety may be attached to the surface of the nanoparticle composition via a lipid-anchoring molecule or a PEG-conjugated lipid component.

15

The vesicle forming component may further comprise a lipid-conjugate of an antibody or an affibody or a peptide that acts as a targeting moiety to enable the nanoparticle to specifically bind to target cell bearing a target molecule.

20

The vesicle forming component may also consist of a lipid-conjugate of an antibody or an affibody or a peptide that acts as a targeting moiety to enable the nanoparticle to specifically bind to diseased target.

25

The antibodies useful in the present invention may be monospecific, bispecific, trispecific, or of greater multi-specificity. For example, multi-specific antibodies may be specific for different epitopes of a cytokine, cell, or enzyme which may be present in an increased amount at the target site compared to the normal tissues.

30

An "antibody" in accordance with the present specification is defined as a protein that binds specifically to an epitope. The antibody may be polyclonal or monoclonal. Examples of monoclonal antibodies useful in the present invention is selected from the group consisting of, but not limited to, Rituximab, Trastuzumab, Cetuximab, LymphoCide, Vitaxin, Lym-1 and Bevacizumab. In a preferred embodiment, the

monoclonal antibodies are selected from the group consisting of Rituximab, Trastuzumab, Cetuximab, LymphoCide, Vitaxin, Lym-1, and Bevacizumab.

5 An "affibody" is defined as a small and stable antigen-binding molecule that can be engineered to bind specifically to a large number of target proteins. The affibody molecules mimic monoclonal antibodies in many ways, and in addition offer several unique properties making them a superior choice for a number of applications. These applications include incorporating the affibodies as lipid-conjugates in liposome compositions targeted for a tissue or a cell in a neovascular or inflammatory site, 10 wherein the radionuclide, such as a copper isotope, but not limited to,  $^{61}\text{Cu}$ ,  $^{64}\text{Cu}$  and  $^{67}\text{Cu}$ , is included for diagnostic and/or therapeutic applications. Examples of affibody molecules useful in the present invention is collected for the group consisting of, but not limited to, anti-ErbB2 affibody molecule and anti-Fibrinogen affibody molecule.

15 The peptides useful in the present invention act as a targeting moiety to enable the nanoparticle to specifically bind to a diseased target, wherein the peptides are selected from the group consisting of, but not limited to, RGD, somatostatin and analogs thereof, and cell-penetrating peptides. In one embodiment, the peptides are selected from the group consisting of RGD, somatostatin and analogs thereof, and cell-penetrating 20 peptides. In one embodiment, the somatostatin analog is octreotate (TATE).

The vesicle forming components are selected to achieve a specified degree of fluidity or rigidity, to control the stability of the liposome compositions *in vivo* and to control the rate of release of the entrapped agent inside the liposome composition. The rigidity of 25 the liposome composition, as determined by the vesicle forming components, may also play a role in the fusion or endocytosis of the liposome to a targeted cell.

The surface charge of the vesicles may also be an important factor in the loading of the vesicle, for controlling the stability of the liposome compositions *in vivo* and to control 30 the rate of release of the entrapped agent inside the liposome composition. Thus according to the present invention, the vesicle forming components may further be selected in order to control the surface charge of the formed vesicles.

35

**Agent-entrapping component**

The agent-entrapping component of the present invention or the method of the present invention may be a chelating agent that forms a chelating complex with the transition metal or the radiolabeled agent, such as the radionuclide.

5

When a chelator (such as for example DOTA) is present in the aqueous phase of the liposome interior, the equilibrium between the exterior and the interior of the liposome is shifted since metal ions that pass the membrane barrier are effectively removed from the inner membrane leaflet due to tight binding to the chelator. The very effective complex formation of the metal ion with the chelator renders the free metal ion concentration in the liposome interior negligible and loading proceeds until all metal ions have been loaded into the liposome or equilibrium has been reached. If excess of chelator is used, the metal ion concentration in the liposomes will be low at all stages during loading and the trans-membrane gradient will be defined by the free metal ion concentration on the exterior of the liposomes.

15

According to the present invention, chelators may be selected from the group comprising 1,4,7,10-tetraazacyclododecane-1,4,7,10-tetraacetic acid (DOTA) and derivatives thereof; 1,4,8,11-tetraazacyclotetradecane (cyclam) and derivatives thereof; 20 1,4,7,10-tetraazacyclododecane (cyclen) and derivatives thereof; 1,4-ethano-1,4,8,11-tetraazacyclotetradecane (et-cyclam) and derivatives thereof; 1,4,7,11-tetraazacyclotetradecane (isocyclam) and derivatives thereof; 1,4,7,10-tetraazacyclotridecane ([13]aneN<sub>4</sub>) and derivatives thereof; 1,4,7,10-tetraazacyclododecane-1,7-diacetic acid (DO2A) and derivatives thereof; 1,4,7,10-tetraazacyclododecane-1,4,7-triacetic acid (DO3A) and derivatives thereof; 1,4,7,10-tetraazacyclododecane-1,7-di(methanephosphonic acid) (DO2P) and derivatives thereof; 1,4,7,10-tetraazacyclododecane-1,4,7-tri(methanephosphonic acid) (DO3P) and derivatives thereof; 1,4,7,10-tetraazacyclododecane-1,4,7,10-tetra(methanephosphonic acid) (DOTP) and derivatives thereof; 30 ethylenediaminetetraacetic acid (EDTA) and derivatives thereof; diethylenetriaminepentaacetic acid (DTPA) and derivatives thereof; 1,4,8,11-tetraazacyclotetradecane-1,4,8,11-tetraacetic acid (TETA) and derivatives thereof, or other adamanzanes and derivates thereof.



In another embodiment, the agent-entrapping component according to the present invention may be a substance that has the ability to reduce other substances, thus referred to as a reducing agent. Examples of reducing agents comprise ascorbic acid, glucose, fructose, glyceraldehyde, lactose, arabinose, maltose and acetol.

5

In one embodiment of the present invention the loaded copper isotope, which may be Cu(II) or Cu(I) cations, is reduced to a lower oxidation state upon diffusion through the vesicle membrane, thus trapping the copper isotope within the vesicle. In another embodiment, the radionuclide different from copper, is reduced to a lower oxidation state upon diffusion through the vesicle membrane, thus trapping the radionuclide different from copper within the vesicle.

10

In a further embodiment, an agent-entrapping component within the scope of the present invention or the method of present invention may be a substance with which the radionuclide or metal entity, such as copper isotope, forms a low solubility salt. Examples of such are copper phosphates, copper oxalate and copper chlorides. In one embodiment, the low solubility salt formed with copper (Cu(II) or Cu(I)) is selected from the group consisting of copper phosphates, copper oxalate and copper chlorides.

15

In one embodiment of the present invention or the method of the present invention the agent-entrapping component is a chelator selected from the group consisting of macrocyclic compounds comprising adamanzanes; 1,4,7,10-tetraazacyclododecane ([12]aneN<sub>4</sub>) or a derivative thereof; 1,4,7,10-tetraazacyclotridecane ([13]aneN<sub>4</sub>) or a derivative thereof; 1,4,8,11-tetraazacyclotetradecane ([14]aneN<sub>4</sub>) or a derivative thereof; 1,4,8,12-tetraazacyclopentadecane ([15]aneN<sub>4</sub>) or a derivative thereof; 1,5,9,13-tetraazacyclohexadecane ([16]aneN<sub>4</sub>) or a derivative thereof; and other chelators capable of binding metal ions such as ethylene-diamine-tetraacetic-acid (EDTA) or a derivative thereof, diethylene-triamine-penta-acetic acid (DTPA) or a derivative thereof.

20

25

30

In one embodiment of the present invention or the method of the present invention the agent-entrapping component is a chelator selected from the group consisting of 1,4-ethano-1,4,8,11-tetraazacyclotetradecane (et-cyclam) or a derivative thereof; 1,4,7,11-tetraazacyclotetradecane (iso-cyclam) or a derivatives thereof; 1,4,7,10-tetraazacyclododecane-1,4,7,10-tetraacetic acid (DOTA) or a derivative thereof; 2-

35

(1,4,7,10-tetraazacyclododecan-1-yl)acetate (DO1A) or a derivative thereof; 2,2'-(1,4,7,10-tetraazacyclododecane-1,7-diyl) diacetic acid (DO2A) or a derivative thereof; 2,2',2''-(1,4,7,10-tetraazacyclododecane-1,4,7-triyl) triacetic acid (DO3A) or a derivative thereof; 1,4,7,10-tetraazacyclododecane-1,4,7,10-tetra(methanephosphonic acid) (DOTP) or a derivative thereof; 1,4,7,10-tetraazacyclododecane-1,7-di(methanephosphonic acid) (DO2P) or a derivative thereof; 1,4,7,10-tetraazacyclododecane-1,4,7-tri(methanephosphonic acid) (DO3P) or a derivative thereof; 1,4,8,11-15 tetraazacyclotetradecane-1,4,8,11-tetraacetic acid (TETA) or a derivative thereof; 2-(1,4,8,11-tetraazacyclotetradecane-1-yl) acetic acid (TE1A) or a derivative thereof; 2,2'-(1,4,8,11-tetraazacyclotetradecane-1,8-diyl) diacetic acid (TE2A) or a derivative thereof; and other adamanzanes or derivates thereof.

In one embodiment of the present invention or the method of the present invention the agent-entrapping component is selected from the group consisting of 1,4,7,10-tetraazacyclododecane-1,4,7,10-tetraacetic acid (DOTA) or a derivative thereof, 1,4,8,11-15 tetraazacyclotetradecane-1,4,8,11-tetraacetic acid (TETA) or a derivative thereof, 1,4,7,10-tetraazacyclododecane-1,4,7,10-tetra(methanephosphonic acid) (DOTP), cyclam and cyclen.

In a particularly important embodiment of the present invention or method of the present invention, the agent-entrapping component is 1,4,7,10-tetraazacyclododecane-1,4,7,10-tetraacetic acid (DOTA).

### **Ionophores**

Ionophores can be characterized as ion-transporters, lipophilic chelators, channel formers, lipophilic complexes etc. In general an ionophore can be defined as a lipid-soluble molecule that transports ions across the lipid bilayer of cell membranes or liposomes. Ionophores are used to increase permeability of lipid membranes to ions and facilitate transfer of molecules through, into and out of the membrane. There are general two broad classifications of ionophores, where one is; *chemical compounds, mobile carriers or lipophilic chelators* that bind or chelate to a particular ion or molecule, shielding its charge from the surrounding environment, and thus facilitating its crossing of the hydrophobic interior of the lipid membrane. The second classification is; *channel formers* that introduce a hydrophilic pore into the membrane, allowing molecules or

metal ions to pass through while avoiding contact with the hydrophobic interior of the membrane.

5 In conventional methods using ionophores, or other components capable of transporting ions or loading of nanoparticles, the resulting nanoparticles comprise small amounts of the ion-transporter or ionophore used in the loading procedure. The nanoparticles provided by the present invention are prepared without the use of an ion-transporter such as an ionophore. Thus, the present invention relates to nanoparticle compositions, which do not comprise ion-transporters or ionophores.

10 In another embodiment of the present invention, the nanoparticle compositions as defined herein do not comprise any added ionophores.

Ion-transporters or ionophoric compounds which are not comprised in the nanoparticles of the present invention may be selected from the group of 8-hydroxyquinoline (oxine); 8-hydroxyquinoline  $\beta$ -D-galactopyranoside; 8-hydroxyquinoline  $\beta$ -D-glucopyranoside; 15 8-hydroxyquinoline glucuronide; 8-hydroxyquinoline-5-sulfonic acid; 8-hydroxyquinoline- $\beta$ -D-glucuronide sodium salt; 8-quinolinol hemisulfate salt; 8-quinolinol *N*-oxide; 2-amino-8-quinolinol; 5,7-dibromo-8-hydroxyquinoline; 5,7-dichloro-8-hydroxyquinoline; 5,7-diiodo-8-hydroxyquinoline; 5,7-dimethyl-8-quinolinol; 5-amino-8-hydroxyquinoline dihydrochloride; 5-chloro-8-quinolinol; 5-nitro-8-hydroxyquinoline; 7-bromo-5-chloro-8-quinolinol; N-butyl-2,2'-imino-di(8-quinolinol); 8-hydroxyquinoline 20 benzoate; 2-benzyl-8-hydroxyquinoline; 5-chloro-8-hydroxyquinoline hydrochloride; 2-methyl-8-quinolinol; 5-chloro-7-iodo-8-quinolinol; 8-hydroxy-5-nitroquinoline; 8-hydroxy-7-iodo-5-quinolinesulfonic acid; 5,7-dichloro-8-hydroxy-2-methylquinoline, and other quinolines (1-azanaphthalene, 1-benzazine) consisting chemical compounds and derivatives thereof. In one embodiment the ionophoric compound is selected from the group consisting of: 8-hydroxyquinoline (oxine); 8-hydroxyquinoline  $\beta$ -D-galactopyranoside; 8-hydroxyquinoline  $\beta$ -D-glucopyranoside; 8-hydroxyquinoline glucuronide; 8-hydroxyquinoline-5-sulfonic acid; 8-hydroxyquinoline- $\beta$ -D-glucuronide sodium salt; 8-quinolinol hemisulfate salt; 8-quinolinol *N*-oxide; 2-amino-8-quinolinol; 30 5,7-dibromo-8-hydroxyquinoline; 5,7-dichloro-8-hydroxyquinoline; 5,7-diiodo-8-hydroxyquinoline; 5,7-dimethyl-8-quinolinol; 5-amino-8-hydroxyquinoline dihydrochloride; 5-chloro-8-quinolinol; 5-nitro-8-hydroxyquinoline; 7-bromo-5-chloro-8-quinolinol; N-butyl-2,2'-imino-di(8-quinolinol); 8-hydroxyquinoline benzoate; 2-benzyl-8-hydroxyquinoline; 5-chloro-8-hydroxyquinoline hydrochloride; 2-methyl-8-quinolinol; 5-chloro-7-iodo-8-quinolinol; 8-hydroxy-5-nitroquinoline; 8-hydroxy-7-iodo-5-

quinolinesulfonic acid; 5,7-dichloro-8-hydroxy-2-methylquinoline, and other quinolines (1-azanaphthalene, 1-benzazine) consisting chemical compounds and derivatives thereof.

5 Ion-transporters or ionophoric compounds which are not comprised in the nanoparticles or used in the methods of the present invention may additionally be selected from the group consisting of 2-hydroxyquinoline-4-carboxylic acid; 6-chloro-2-hydroxyquinoline; 8-chloro-2-hydroxyquinoline; carbostyryl 124; carbostyryl 165; 4,6-dimethyl-2-hydroxyquinoline; 4,8-dimethyl-2-hydroxyquinoline; or other 2-quinolinol compounds 8-  
10 hydroxyquinoline (oxine); 8-hydroxyquinoline  $\beta$ -D-galactopyranoside; 8-hydroxyquinoline  $\beta$ -D-glucopyranoside; 8-hydroxyquinoline glucuronide; 8-hydroxyquinoline-5-sulfonic acid; 8-hydroxyquinoline- $\beta$ -D-glucuronide sodium salt; 8-quinolinol hemisulfate salt; 8-quinolinol *N*-oxide; 2-amino-8-quinolinol; 5,7-dibromo-8-hydroxyquinoline; 5,7-dichloro-8-hydroxyquinoline; 5,7-diiodo-8-hydroxyquinoline; 5,7-  
15 dimethyl-8-quinolinol; 5-amino-8-hydroxyquinoline dihydrochloride; 5-chloro-8-quinolinol; 5-nitro-8-hydroxyquinoline; 7-bromo-5-chloro-8-quinolinol; *N*-butyl-2,2'-imino-di(8-quinolinol); 8-hydroxyquinoline benzoate; 2-benzyl-8-hydroxyquinoline; 5-chloro-8-hydroxyquinoline hydrochloride; 2-methyl-8-quinolinol; 5-chloro-7-iodo-8-quinolinol; 8-hydroxy-5-nitroquinoline; 8-hydroxy-7-iodo-5-quinolinesulfonic acid; 5,7-  
20 dichloro-8-hydroxy-2-methylquinoline, and other quinolines (1-azanaphthalene, 1-benzazine) consisting chemical compounds and derivatives thereof, [6*S*-[6.alpha.(2*S*\*,3*S*\*), 8.beta.(*R*\*),9.beta.,11.alpha.]]-5-(methylamino)-2-[[3,9,11-trimethyl-8-[1-methyl-2-oxo-2-(1*H*-pyrrol-2-yl)ethyl]-1,7-dioxaspiro[5.5]undec-2-yl]methyl]-4-benzoxazolecarboxylic acid (also called A23187), HMPAO (hexamethyl propylene amine oxime, HYNIC (6-Hydrazinopyridine-3-carboxylic acid), BMEDA (*N,N*-bis (2-mercaptoethyl)-*N,N'*-diethylethylenediamine), DISIDA (diisopropyl iminodiacetic acid, phthaldialdehyde and derivatives thereof, 2,4-dinitrophenol and derivatives thereof, di-benzo-18-crown-6 and derivatives thereof, *o*-xylylenebis(*N,N*-diisobutyldithiocarbamate) and derivatives thereof, *N,N,N',N'*-Tetracyclohexyl-2,2'-  
30 thiodiacetamide and derivatives thereof, 2-(1,4,8,11-Tetrathiacyclotetradec-6-yloxy)hexanoic acid, 2-(3,6,10,13-Tetrathiacyclotetradec-1-oxy)hexanoic acid and derivatives thereof, *N,N*-bis (2-mercaptoethyl)-*N,N'*-diethylethylenediamine and derivatives thereof, beauvericin, enniatin, gramicidin, ionomycin, lasalocid, monesin, nigericin, nonactin, nystatin, salinomycin, valinomycin, pyridoxal isonicotinoyl  
35 hydrazone (PIH), salicylaldehyde isonicotinoyl hydrazone (SIH), 1,4,7-

5 tris(mercaptoethyl)-1,4,7-triazacyclononane, N,N',N''-tris(2-mercaptoethyl)-1,4,7-triazacyclononane, monensis, DP-b99, DP-109, BAPTA, pyridoxal isonicotinoyl hydrazone (PIH), alamethicin, di-2-pyridylketone thiosemicarbazone (HDpT), carbonyl cyanide *m*-chlorophenyl hydrazone (CCCP), lasalocid A (X-537A), 5-bromo derivative of lasalocid; cyclic depsipeptides; cyclic peptides:DECYL-2; N,N,N',N'-tetrabutyl-3,6-dioxaoctanedi[thioamide]; N,N,N',N'-tetracyclohexyl-3-oxa-pentanediamide; N,N-dicyclohexyl-N',N'-dioctadecyl-diglycolic-diamide; N,N'-diheptyl-N,N'-dimethyl-1,-butanediamide; N,N''-octamethylene-bis[N'-heptyl-N'-methyl-malonamide; N,N-dioctadecyl-N',N'-dipropyl-3,6-dioxaoctanediamide; N-[2-(1H-pyrrolyl-methyl)]-N'-(4-penten-3-on-2)-ethane-1,2-diamine (MRP20); and antifungal toxins; avenaciolide or derivatives of the above mentioned ionophores, as well as the ionophores described in WO2011/006510 and other ionophores described in the art.

15 pH gradient loadable agents i.e. agents with one or more ionisable moieties such that the neutral form of the ionisable moiety allows the metal entities to cross the liposome membrane and conversion of the moiety to a charged form causes the metal entity to remain encapsulated within the liposome are also regarded as ionophores according to the present invention. Ionisable moieties may comprise, but are not limited to comprising, amine, carboxylic acid and hydroxyl groups. pH gradient loadable agents that load in response to an acidic interior may comprise ionisable moieties that are charged in response to an acidic environment whereas drugs that load in response to a basic interior comprise moieties that are charged in response to a basic environment. In the case of a basic interior, ionisable moieties including but not limited to carboxylic acid or hydroxyl groups may be utilized.

25

#### Interior PH

The interior pH of the nanoparticles according to the present invention can be controlled to lie in a specific range wherein the features of the nanoparticle are optimized.

30

In one embodiment of the present invention or the method of the present invention, the interior pH of the liposome composition is controlled, thus achieving a desired protonation state of the agent-entrapping component and / or the ionophore, thereby securing efficient loading and entrapment of the radionuclide.

35

In a preferred embodiment of the present invention or the method of the present invention, the interior pH of the liposome composition is controlled, thus achieving a desired protonation state of the agent-entrapping component, thereby securing efficient loading and entrapment of the radionuclide.

5

In another embodiment of the disclosed method for producing a nanoparticle composition loaded with a copper isotope, the interior pH is controlled during synthesis of the nanoparticles in such a way that the interior pH of the nanoparticles is within the range of 1 to 10, such as 1-2, for example 2-3, such as 3-4, for example 4-5, such as 5-6, for example 6-7, such as 7-8, for example 8-9, such as 9-10.

10

In a preferred embodiment of the present invention, the interior pH of the nanoparticles is in the range of 4 to 8.5, such as 4.0 to 4.5, for example 4.5 to 5.0, such as 5.0 to 5.5 for example 5.5 to 6.0, such as 6.0 to 6.5, for example 6.5 to 7.0, such as 7.0 to 7.5, for example 7.5 to 8.0, such as 8.0 to 8.5.

15

In another embodiment of the present invention, the interior pH of the nanoparticles according to the present invention is optimized in order to prolong the stability of the nanoparticles. Such improved stability can for example lead to a longer shelf-life or a wider range of possible storage temperatures and thereby facilitate the use of the nanoparticles. The improved stability can be obtained, for example because the interior pH leads to an increased stability of the vesicle forming components forming a vesicle, due to increased stability of the agent-entrapping component with or without the entrapped radionuclides or due to improved stability of other features of the nanoparticles. An interior pH which is optimized for improved stability may be within the range of 1 to 10, such as 1-2, for example 2-3, such as 3-4, for example 4-5, such as 5-6, for example 6-7, such as 7-8, for example 8-9, such as 9-10.

20

25

In a preferred embodiment of the present invention, the interior pH which leads to an improved stability of the nanoparticles is in the range of 4 to 8.5, such as 4.0 to 4.5, for example 4.5 to 5.0, such as 5.0 to 5.5 for example 5.5 to 6.0, such as 6.0 to 6.5, for example 6.5 to 7.0, such as 7.0 to 7.5, for example 7.5 to 8.0, such as 8.0 to 8.5.

30

35

**Osmotic pressure**

The creation of a small osmotic stress on the vesicle or nanoparticle membrane is favourable in the loading of metal entity and/or radionuclide into the nanoparticles. Osmotic stress is a difference in osmotic pressure, i.e. an imbalance or difference  
5 between interior and exterior osmolarity. Presence of an osmotic stress facilitates the transfer of smaller ions over the membrane, such as metal ions or radionuclide ions, while larger charged molecules such as chelating agents remain trapped within the nanoparticles.

10 According to the present invention, the loading into liposomes can be modulated by controlling the osmolarity of the aqueous solution that is encapsulated in the liposomes as well as the exterior solution during manufacture of the liposomes. The osmolarity (Osm) is a measure of the activity of water (as a function of the chemical potential), which is governed by the presence of solutes in the aqueous solution, including  
15 chelators or other osmotically active agents. Trans-membrane gradients of osmolytes influences the state of the liposome and can either cause the liposome to be flaccid ( $Osm_{interior} < Osm_{exterior}$ ) due to loss of water or to be tense due to uptake of water building up osmotic trans-membrane pressure ( $Osm_{interior} > Osm_{exterior}$ ) and membrane tension. In general, membrane tension will lead to membrane stretching and thus  
20 thinning of the bilayer causing an increased permeability. Furthermore, membrane tension can cause formation of defects (transient pores), which also attributes to increased membrane permeability. It is thus expected that the membrane permeability increases with augmented hyper-osmotic pressure ( $Osm_{interior} > Osm_{exterior}$ ) leading to higher loading rate and loading efficiency. A too high osmotic pressure (tension) can  
25 also induce lysis of the liposomes and cause a gradual release of contents or mechanical failure of the liposome. For example, when 100 nm vesicles are placed in a hypo-osmotic solution with respect to the trapped intra-vesicular medium, it can result in an influx of water causing the vesicles to assume a spherical shape, and osmotic differentials of sufficient magnitude will produce membrane rupture that results in  
30 partial release of the intra-vesicular solutes. However, it is recognized that the presence of cholesterol in the membrane provide mechanical stability thereby increasing the membrane lysis tension resulting overall in a larger tolerance towards osmotic imbalance.

The intra-liposomal osmolarity can be determined by measuring the osmolarity of the solution used to hydrate lipid films during liposome preparation, by using conventional methods in the art such as, but not limited to the freeze-point method, which is commonly used in apparatus for measuring osmolarity. The same method can be  
5 utilized for measuring the osmolarity of the external liposomal buffer. Importantly, the buffer osmolarity is easily influenced by pH adjustment (using e.g. NaOH or HCl) during buffer preparation.

In a preferred embodiment of the present invention, the osmolarity is measured by use  
10 of the freeze point method.

Controlling the osmolarity can be used to create osmotic stress. Such osmotic stress can be controlled by entrapping osmotic agents such as sugars, salts, chelating agents, ions, peptides, proteins, pharmaceutical compounds, buffer molecules and/or  
15 solutes in the nanoparticles.

In one embodiment of the present invention, the osmolarity of the interior of the nanoparticles is 40-800 mOsm/L, such as 40-100 mOsm/L, or such as 100-150 mOsm/L, or such as 150-200 mOsm/L, or such as 200-250 mOsm/L, or such as 250-  
20 300 mOsm/L, or such as 300-350 mOsm/L, or such as 350-400 mOsm/L, or such as 400-450 mOsm/L, or such as 450-500 mOsm/L, or such as 500-550 mOsm/L, or such as 550-600 mOsm/L, or such as 600-650 mOsm/L, or such as 650-700 mOsm/L or such as 700-750 mOsm/L, or such as 750-800 mOsm/L.

In another embodiment of the present invention, the osmolarity of the exterior of the nanoparticles is 40-800 mOsm/L, such as 40-100 mOsm/L, or such as 100-150 mOsm/L, or such as 150-200 mOsm/L, or such as 200-250 mOsm/L, or such as 250-  
25 300 mOsm/L, or such as 300-350 mOsm/L, or such as 350-400 mOsm/L, or such as 400-450 mOsm/L, or such as 450-500 mOsm/L, or such as 500-550 mOsm/L, or such as 550-600 mOsm/L, or such as 600-650 mOsm/L, or such as 650-700 mOsm/L or  
30 such as 700-750 mOsm/L, or such as 750-800 mOsm/L.

In one embodiment of the present invention, the difference in osmolarity between the interior of the nanoparticle and the exterior of the nanoparticle is 5-800 mOsm/L, such  
35 as 5-10 mOsm/L such as 10-20 mOsm/L, or such as 10-20 mOsm/L, or such as 20-



20-30 mOsm/L, or such as 30-40 mOsm/L, or such as 40-50 mOsm/L, or such as 50-60 mOsm/L, or such as 60-70 mOsm/L, or such as 60-70 mOsm/L, or such as 70-80 mOsm/L, or such as 80-90 mOsm/L, or such as 90-100 mOsm/L, or such as 100-150 mOsm/L, or such as 150-200 mOsm/L, or such as 200-250 mOsm/L, or such as 250-300 mOsm/L, or such as 300-350 mOsm/L, or such as 350-400 mOsm/L, or such as 400-450 mOsm/L, or such as 450-500 mOsm/L, or such as 500-550 mOsm/L, or such as 550-600 mOsm/L, or such as 600-650 mOsm/L, or such as 650-700 mOsm/L, or such as 700-750 mOsm/L, or such as 750-800 mOsm/L.

10 In one particular embodiment of the present invention, the difference in osmolarity between the interior of the nanoparticle and the exterior of the nanoparticle is 10-100 mOsm/L.

### Stability

15 The nanoparticles of the present invention have improved stability, which may be measured using different tests.

In one embodiment of the present invention, the stability of the radiolabeled nanoparticles is such that less than 20% leakage of radioactivity is observed following a given time of incubation in buffer or human serum. Such leakage can be less than 20%, for example less than 15% leakage, such as less than 12% leakage, for example less than 10% leakage, such as less than 8% leakage, for example less than 6% leakage, such as less than 4% leakage, for example less than 3% leakage, such as less than 2% leakage, for example less than 1% leakage as measured by conventional methods in the art, including a purification procedure such as size exclusion chromatography (SEC), ion-exchange chromatography or dialysis. The amount of metal entity such as the radionuclide can be measured as radioactivity using a radioactivity detector or by measuring the concentration of the metal entity using inductively coupled plasma mass spectrometry (ICP-MS), inductively coupled plasma atomic emission spectroscopy (ICP-AES) or inductively coupled plasma optical emission spectrometry (ICP-OES).

In one embodiment of the present invention, the stability of the radiolabeled nanoparticles is such that less than 20% leakage of radioactivity is observed following 24 hours incubation in buffer or human serum at 37°C followed by a purification

procedure to separate the radiolabeled nanoparticles from leaked radionuclide, for example less than 15% leakage, such as less than 12% leakage, for example less than 10% leakage, such as less than 8% leakage, for example less than 6% leakage, such as less than 4% leakage, for example less than 3% leakage, such as less than 2% leakage, for example less than 1% leakage. Said purification procedure comprises size exclusion chromatography (SEC), ion-exchange chromatography or dialysis. The amount of metal entity such as the radionuclide is measured as radioactivity using a radioactivity detector or by measuring the concentration of the metal entity using inductively coupled plasma mass spectrometry (ICP-MS), inductively coupled plasma atomic emission spectroscopy (ICP-AES) or inductively coupled plasma optical emission spectrometry (ICP-OES).

#### **Sizes of the nanoparticles**

Nanoparticles according to the present invention may vary in size. The size of the nanoparticles may be optimized for the use of the nanoparticle wherein the nanoparticle is administered to a subject, for example for improving targeting of the particles to sites in the human body, or for improved monitoring of the nanoparticles inside the human body. The size may also be optimized for improved stability of the nanoparticle or for improved or facilitated preparation of the nanoparticles.

In one embodiment, the nanoparticle composition of the present invention has a diameter in the range of 30 nm to 1000 nm; such as 30 nm to 300 nm, such as 30 nm to 60 nm, for example 60 nm to 80 nm, such as 80 nm to 100 nm, for example 100 nm to 120 nm, such as 120 nm to 150 nm, for example 150 nm to 180 nm, such as 180 nm to 210 nm, for example, 210 nm to 240 nm, such as 240 nm to 270 nm for example 270 nm to 300 nm, or such as 300 nm to 600 nm, such as 300 nm to 400 nm, or such as 400 nm to 500 nm, or such as 500 nm to 600 nm, or such as 600 nm to 1000 nm, such as 600 nm to 700 nm, or such as 700 nm to 800 nm, or such as 800 nm to 900 nm, or such as 900 nm to 1000 nm.

In one embodiment, the disclosed method for producing a nanoparticle loaded with radionuclides results in nanoparticles which has a diameter in the range of 30 nm to 1000 nm; such as 30 nm to 300 nm, such as 30 nm to 60 nm, for example 60 nm to 80 nm, such as 80 nm to 100 nm, for example 100 nm to 120 nm, such as 120 nm to 150 nm, for example 150 nm to 180 nm, such as 180 nm to 210 nm, for example, 210 nm to

240 nm, such as 240 nm to 270 nm for example 270 nm to 300 nm, or such as 300 nm to 600 nm, such as 300 nm to 400 nm, or such as 400 nm to 500 nm, or such as 500 nm to 600 nm, or such as 600 nm to 1000 nm, such as 600 nm to 700 nm, or such as 700 nm to 800 nm, or such as 800 nm to 900 nm, or such as 900 nm to 1000 nm.

5

In one embodiment, the disclosed method for producing a nanoparticle loaded with copper results in nanoparticles which has a diameter in the range of 30 nm to 1000 nm; such as 30 nm to 300 nm, such as 30 nm to 60 nm, for example 60 nm to 80 nm, such as 80 nm to 100 nm, for example 100 nm to 120 nm, such as 120 nm to 150 nm, for example 150 nm to 180 nm, such as 180 nm to 210 nm, for example, 210 nm to 240 nm, such as 240 nm to 270 nm for example 270 nm to 300 nm, or such as 300 nm to 600 nm, such as 300 nm to 400 nm, or such as 400 nm to 500 nm, or such as 500 nm to 600 nm, or such as 600 nm to 1000 nm, such as 600 nm to 700 nm, or such as 700 nm to 800 nm, or such as 800 nm to 900 nm, or such as 900 nm to 1000 nm.

10

15

In a preferred embodiment, the nanoparticle composition of the present invention has a diameter in the range of 30 nm to 300 nm; such as 30 nm to 60 nm, for example 60 nm to 80 nm, such as 80 nm to 100 nm, for example 100 nm to 120 nm, such as 120 nm to 150 nm, for example 150 nm to 180 nm, such as 180 nm to 210 nm, for example, 210 nm to 240 nm, such as 240 nm to 270 nm for example 270 nm to 300 nm.

20

In a preferred embodiment, the disclosed method for producing a nanoparticle loaded with radionuclides results in nanoparticles which has a diameter in the range of 30 nm to 300 nm; such as 30 nm to 60 nm, for example 60 nm to 80 nm, such as 80 nm to 100 nm, for example 100 nm to 120 nm, such as 120 nm to 150 nm, for example 150 nm to 180 nm, such as 180 nm to 210 nm, for example, 210 nm to 240 nm, such as 240 nm to 270 nm for example 270 nm to 300 nm.

25

In a preferred embodiment, the disclosed method for producing a nanoparticle loaded with copper results in nanoparticles which has a diameter in the range of 30 nm to 300 nm; such as 30 nm to 60 nm, for example 60 nm to 80 nm, such as 80 nm to 100 nm, for example 100 nm to 120 nm, such as 120 nm to 150 nm, for example 150 nm to 180 nm, such as 180 nm to 210 nm, for example, 210 nm to 240 nm, such as 240 nm to 270 nm for example 270 nm to 300 nm.

30

35

**Methods for preparation**

The present invention provides methods for preparation of nanoparticle compositions as described herein comprising a vesicle forming component, an agent-entrapping component enclosed by the vesicle forming component, and an entrapped metal entity within the nanoparticle composition.

Such methods for preparation of nanoparticles according to the present invention comprise the following steps:

- a. Providing a nanoparticle composition comprising a vesicle forming component and an agent-entrapping component enclosed by said vesicle forming component;
- b. Entrapping the metal entities within the interior of the nanoparticle composition by incubation of the nanoparticle composition in a solution comprising the metal entity at a temperature higher than 22°C.

Preferred methods for preparation of nanoparticles according to the present invention which do not involve the use of ionophore for loading, comprise the following steps:

- a. Providing a nanoparticle composition comprising a vesicle forming component and an agent-entrapping component enclosed by said vesicle forming component;
- b. Entrapping the metal entities within the interior of the nanoparticle composition by enabling transfer of cation metal entities across the membrane of the vesicle forming component by incubation of the nanoparticle composition in a solution comprising the metal entity.

In one embodiment, the methods according to the present invention, the incubation temperature for loading of the nanoparticles is higher than 22°C, such as higher than 30°C, such as higher than 35°C, such as higher than 40°C, such as higher than 45°C, such as higher than 50°C, such as higher than 55°C, such as higher than 60°C, such as higher than 65°C, such as higher than 70°C, such as higher than 75°C.

In another embodiment, the methods according to the present invention, the incubation temperature for loading of the nanoparticles is higher than 10°C, such as

higher than 15 °C, such as higher than 22°C, such as higher than 30°C, such as higher than 35°C, such as higher than 40°C, such as higher than 45°C, such as higher than 50°C, such as higher than 55°C, such as higher than 60°C, such as higher than 65°C, such as higher than 70°C, such as higher than 75°C.

5

In the methods according to the present invention, the incubation temperature for loading of the nanoparticles is lower than a critical temperature where upon the nanoparticles will degrade. Thus according to the present invention, the incubation temperature for loading of the nanoparticles is lower than 100°C, such as lower than 90°C, such as lower than 85°C, such as lower than 80°C.

10

In yet another embodiment of the present invention, incubation temperature for loading of the nanoparticles is between 22°C to 80°C, such as 22°C to 30°C, or in the range of 30°C to 80°C, such as in the range of 30°C to 40°C, such as 30°C to 35°C, or such as 35°C to 40 °C, or in the range of 40°C to 80°C, such as 40°C to 45 °C, or such as 45°C to 50°C, including the range of 50°C to 80°C, such as 50°C to 55°C, or such as 55°C to 60°C, or such as 60°C to 65°C, or such as 65°C to 70°C, or such as 70°C to 75°C, or such as 75°C to 80°C, wherein a range of 30°C to 80°C is preferred and a range of 40°C to 80°C is more preferred.

15

20

In yet another embodiment of the present invention, incubation temperature for loading of the nanoparticles is between 10°C to 80°C, such as 15°C to 80°C, or such as 15°C to 22°C, or in the range of 22°C to 80°C, such as 22°C to 30°C, such as in the range of 30°C to 80°C, such as in the range of 30°C to 40°C, such as 30°C to 35°C, or such as 35°C to 40 °C, or in the range of 40°C to 80°C, such as 40°C to 45 °C, or such as 45°C to 50°C, including the range of 50°C to 80°C, such as 50°C to 55°C, or such as 55°C to 60°C, or such as 60°C to 65°C, or such as 65°C to 70°C, or such as 70°C to 75°C, or such as 75°C to 80°C, wherein a range of 30°C to 80°C is preferred and a range of 40°C to 80°C is more preferred.

25

30

The methods of the present invention allows for a faster loading of the nanoparticles than what is expected from mere diffusion of the metal entities/radionuclides into the nanoparticles.

Thus, in one embodiment of the present invention, the incubation for loading of the nanoparticles can be performed in a time period which is less than 48 hours, such as 36-48 hours, or such as 24-36 hours, or such as 18-24 hours, or such as 16-18 hours, or such as 14-16 hours, or such as 12-14 hours, or such as 10-12 hours, or such as 8-10 hours, or such as 6-8 hours, or such as 4-6 hours, or such as 2-4 hours, or such as 1-2 hours, or such as 30 min to 60 min, or 5 min to 30 min, or 1 min to 5 min.

The incubation time according to the present invention is a time period shorter than 48 hours, such as between 0 minutes to 360 minutes, such as between 1 minutes to 240 minutes preferably between 1 minutes to 120 minutes (including 3 minutes to 120 minutes and 5 minutes to 120 minutes) and more preferably between 1 minutes to 60 minutes, such as 5 minutes to 60 minutes.

The methods of the present invention may comprise one or more steps wherein an osmotic stress as defined herein is created in the nanoparticles. The inventors have found that a difference in the osmolarity of the interior of the nanoparticle compared to the exterior of the nanoparticle improves the loading of the nanoparticles. Said osmotic stress can be created by ensuring that there is an imbalance between the interior ion concentration of the nanoparticles compared to the exterior ion concentration, thus a difference in the osmotic pressure over the membrane of the vesicle.

Such osmotic stress or osmotic pressure can be controlled by an entrapped osmotic agent such as salts, sugars, ions, chelates, peptides, proteins, pharmaceutical compounds, buffer molecules, and/or other solutes.

In one embodiment of the present invention, the osmotic pressure of the membrane is obtained by controlling the osmolarity of the interior of the nanoparticle by preparing the nanoparticle composition in step a) using a solution which has an osmolarity for enhancing the loading, wherein said solution comprises one or more osmotic agents as defined herein.

In another embodiment of the present invention, the osmotic pressure of the membrane is obtained by controlling the osmolarity of the exterior of the nanoparticle by incubating the nanoparticle composition in step b) using a solution which has an osmolarity for

enhancing the loading, wherein said solution comprises one or more osmotic agents as defined herein.

5 Thus in one embodiment of the present invention, the difference in osmolarity of the interior of the nanoparticle compared to the incubation solution (exterior of the nanoparticle) is 5-800 mOsm/L at the starting point of the incubation.

10 The methods of the present invention ensure that a high amount of the radionuclides used in preparation will be entrapped within the nanoparticle. In one embodiment of the present invention or the method of the present invention, the efficiency of loading is higher than 90% when assayed using size exclusion chromatography (SEC, described in examples), ion-exchange chromatography or dialysis. In another embodiment of the present method the efficiency of loading is higher than 35%, for example higher than 40%, such as higher than 50%, for example higher than 60%, such as higher than 15 65%, for example higher than 70%, such as higher than 75%, for example higher than 80%, such as higher than 85%, for example higher than 90%, such as higher than 95%, or such as higher than 96%, or such as higher than 97%, or such as higher than 98%, or such as higher than 99%.

20 In one embodiment of the present invention, the loading efficiency when using incubation times of 1 minutes to 240 minutes is in the range of 10% to 100%, preferably in the range of 80% to 100% and more preferably in the range of 90% to 100%, such as for example in the range of 95%-100% (including 95% to 99.9%, such as 95%-99%).

25 Thus in one embodiment of the present invention, the incubation temperature for loading of nanoparticles is in the range of 30°C to 80°C and the loading efficiency when using incubation times of 1 to 240 minutes is in the range of 10% to 100% preferably in the range of 80% to 100% and more preferably in the range of 90% to 30 100%, such as for example in the range of 95%-100% (including 95% to 99.9%, such as 95%-99%).

In a preferred embodiment of the present invention, the incubation temperature for loading of nanoparticles is in the range of 30°C to 80°C and the loading efficiency when 35 using incubation times of 1 minutes to 60 minutes is in the range of 10% to 100%,

preferably in the range of 80% to 100%, such as 90%-100%, and more preferably in the range of 95% to 100%, such as 95% to 99.9%, or such as 95%-99%).

5 The methods of the present invention may comprise a step wherein the loaded nanoparticles are purified from the incubation solution as mentioned in step b). Thus, in one embodiment of the invention or the disclosed method of the invention, the generated nanoparticles loaded with radionuclides are purified using SEC, ion-exchange chromatography or dialysis.

10 In a preferred embodiment of the invention or the disclosed method of the invention, the generated nanoparticles loaded with copper are purified using SEC, ion-exchange chromatography or dialysis.

15 In one embodiment of the disclosed method, the size of the nanoparticle compositions remains essentially unaltered following loading of said nanoparticles with copper. In another embodiment of the disclosed method, the size of the nanoparticle compositions is altered less than 20% following loading of the nanoparticles with copper isotopes, for example less than 17%, such as less than 14%, for example less than 11%, such as less than 8%, for example less than 5%, such as less than 2%, for example less than  
20 1%.

In one embodiment of the disclosed method, the size of the nanoparticle compositions remains essentially unaltered following loading of said nanoparticles with a radionuclide. In another embodiment of the disclosed method, the size of the  
25 nanoparticle compositions is altered less than 20% following loading of the nanoparticles with a radionuclide, for example less than 17%, such as less than 14%, for example less than 11%, such as less than 8%, for example less than 5%, such as less than 2%, for example less than 1%.

30 In one embodiment of the disclosed method, the zeta potential is altered less than 20% following loading of the nanoparticles with copper isotopes. In another embodiment of the disclosed method, the zeta potential is altered less than 18% following loading of the nanoparticles with copper isotopes, for example less than 16%, such as less than 14%, for example less than 12%, such as less than 10%.

35



In one embodiment of the disclosed method, the zeta potential is altered less than 20% following loading of the nanoparticles with a radionuclide. In another embodiment of the disclosed method, the zeta potential is altered less than 18% following loading of the nanoparticles with a radionuclide, for example less than 16%, such as less than 14%,  
5 for example less than 12%, such as less than 10%.

In a further embodiment the method for preparing nanoparticle compositions encompass controlling the liposome interior pH in the form of protonating or deprotonating the agent-entrapping component, thereby inducing effective loading of  
10 the radionuclide.

The described method for preparing nanoparticle compositions may further comprise a step wherein a moiety is attached or associated to the external layer of the nanoparticle which is targeted for a cancerous disease, and in general, pathological conditions associated with leaky blood vessels. In another embodiment of the present invention,  
15 method for preparing nanoparticle compositions further comprises step wherein a compound with intracellular targeting properties, such as nuclear localization sequence peptide (NLS peptide), is conjugated to the agent-entrapping component, and/or entrapped within the nanoparticle composition..

20

A method for preparation of the disclosed nanoparticle composition may further comprise a step of measuring and/or detecting the amount of radiation emitted from the radionuclide entrapped within the nanoparticle composition.

25 The methods provided by the present invention do not include the use of an ion-transporter such as an ionophore. Thus nanoparticles prepared by the methods of the present invention do not comprise ion-transporters, lipophilic chelators or ionophores.

### **Kit of parts**

30 The present invention provides kit of parts for preparation of the nanoparticles.

According to the present invention, such a kit of parts may comprise:

- a. A nanoparticle composition comprising i) a vesicle forming component, and ii) an agent-entrapping component enclosed by the  
35 vesicle forming component; and

b. A composition containing a metal entity for loading into the nanoparticle,  
wherein all the components are as described herein.

5 In one embodiment, the composition containing a metal entity comprises a radionuclide.

The metal entity or radionuclide is either in storage or delivered from the manufacturer depending on the characteristics of the particular radionuclide. The radionuclide may  
10 be delivered in the form of a (lyophilized) salt or an aqueous solution or may be synthesized on the premises using existing production facilities and starting materials. Before administration of the radionuclide-containing nanoparticles, parts a, and b of the kit are mixed, and incubated at a temperature higher than 22°C for a given time period, wherein the incubation temperature and time period are as defined herein.

15 The efficiency of encapsulation is then tested, preferably using the simple test procedure supplied with the kit. Following test of encapsulation, the drug is administered to the patient.

20 According to the present invention, a kit of parts may also comprise:  
A mixture of a nanoparticle composition comprising a) a vesicle forming component, and b) an agent-entrapping component enclosed by the vesicle forming component; and c) composition containing a metal entity for loading into the nanoparticle, wherein  
25 all the components are as described in the present application. Before administration of the radionuclide-containing nanoparticles the mixture of parts a, b and c is incubated at a temperature higher than 22°C for a given time period, wherein the incubation temperature and time period are as defined herein.

30 If the metal entity comprises a radionuclide e.g. the positron emitter <sup>64</sup>Cu, said radionuclide is delivered directly from a cyclotron facility to the venue of treatment or diagnosis immediately prior to use, in the form of a (lyophilized) salt or an aqueous solution. Before administration of the radionuclide-containing nanoparticles, parts a and b of the kit are mixed and the efficiency of encapsulation is tested, preferably using the simple test procedure supplied with the kit. Following administration the patient may

receive a PET- or a SPECT scan. Optimal visualization may be achieved 4-48 hours after administration.

5 In another embodiment of the present invention, the patient may be subject to magnetic resonance imaging (MRI) following administration of the nanoparticle compositions as mentioned herein. Such MRI may or may not be combined with PET or SPECT scanning according to the present invention.

Thus, according to the present invention, a kit of parts may comprise:

- 10 a. A nanoparticle composition comprising i) a vesicle forming component ii) an agent-entrapping component enclosed by the vesicle forming component and iii) a metal entity useful for MRI; and
- b. A composition containing one or more metal entities for loading into the nanoparticle,

wherein all the components are as described herein,

15

or, a kit of parts may comprise:

- a. A nanoparticle composition comprising i) a vesicle forming component and ii) an agent-entrapping component enclosed by the vesicle forming component; and
- 20 b. A composition comprising one or more metal entities for loading into the nanoparticle,

wherein all the components are as described herein.

25 In one embodiment of the present invention, the kit of parts comprise a combination of radionuclides useful for combined positron emission tomography (PET) imaging and radiation therapy, for example two radionuclides such as  $^{64}\text{Cu}$  and  $^{177}\text{Lu}$ , or such as  $^{64}\text{Cu}$  and  $^{67}\text{Cu}$ , or such as  $^{61}\text{Cu}$  and  $^{67}\text{Cu}$ , or such as  $^{64}\text{Cu}$  and  $^{90}\text{Y}$ , or such as  $^{64}\text{Cu}$  and  $^{119}\text{Sb}$ , or such as  $^{64}\text{Cu}$  and  $^{225}\text{Ac}$ , or such as  $^{64}\text{Cu}$  and  $^{188}\text{Re}$ , or such as  $^{64}\text{Cu}$  and  $^{186}\text{Re}$ , or such as  $^{64}\text{Cu}$  and  $^{211}\text{At}$ .

30

In a preferred embodiment of the present invention, the kit of parts comprise a combination of radionuclides useful for combined positron emission tomography (PET) imaging and radiation therapy, such as  $^{64}\text{Cu}$  and  $^{177}\text{Lu}$ .

In another embodiment of the present invention, said kit of parts is for preparation of nanoparticles comprising radionuclides such as for example isotopes of Copper (<sup>61</sup>Cu, <sup>64</sup>Cu, and <sup>67</sup>Cu), wherein said isotopes may or may not be part of the kit of parts. In such an embodiment of the present invention, such a kit of parts may comprise: A  
5 nanoparticle composition comprising i) a vesicle forming component, and ii) an agent-entrapping component enclosed by the vesicle forming component. In a further embodiment of the present invention, the kit of parts further comprises an incubation buffer for loading of the metal entities into the nanoparticles.

10 In a preferred embodiment, any of the kit of parts further comprises a test procedure to assess the efficiency of encapsulation.

The kits of parts for preparation of nanoparticles according to the present invention, do not include an ion-transporter such as an ionophore.

15

#### **Methods for treatment or diagnosis**

The nanoparticles of the present invention can be used for diagnosis, monitoring or treatment of diseases or conditions associated with leaky blood vessels in an animal  
20 subject in need, for example a mammal in need, such as a human being in need.

Leaky blood vessels are often associated with angiogenesis or neoplastic growth of tissue. Cancer is an example of a disease characterized by leaky blood vessels. Inflammation is another example of a conditions associated with leaky blood vessels.

25

As mentioned herein, cancer is a disease characterized by leaky blood vessels, and the present invention relates to treatment, monitoring or diagnosis of cancerous diseases associated with malignant neoplasia such as malignant neoplasm of lip, mouth or throat, such as malignant neoplasm of the tongue, the base of tongue, gum,  
30 floor of mouth, palate, parotid gland, major salivary glands, tonsil, oropharynx, nasopharynx, piriform sinus, hypopharynx or other parts of lip, mouth or throat or malignant neoplasms of digestive organs such as malignant neoplasms of oesophagus, stomach, small intestine, colon, rectosigmoid junction, rectum, anus and anal canal, liver and intrahepatic bile ducts, gallbladder, other parts of biliary tract,  
35 pancreas and spleen, malignant neoplasms of respiratory and intrathoracic organs

such as malignant neoplasms of the nasal cavity and middle ear, accessory sinuses, larynx, trachea, bronchus and lung, thymus, heart, mediastinum and pleura, malignant neoplasms of bone and articular cartilage such as malignant neoplasm of bone and articular cartilage of limbs, bone and articular cartilage, malignant melanoma of skin, sebaceous glands and sweat glands, malignant neoplasms of mesothelial and soft tissue such as malignant neoplasm of mesothelioma, Kaposi's sarcoma, malignant neoplasm of peripheral nerves and autonomic nervous system, malignant neoplasm of retroperitoneum and peritoneum, malignant neoplasm of connective and soft tissue such as blood vessels, bursa, cartilage, fascia, fat, ligament, lymphatic vessel, muscle, synovia, tendon, head, face and neck, abdomen, pelvis or overlapping lesions of connective and soft tissue, malignant neoplasm of breast or female genital organs such as malignant neoplasms of vulva, vagina, cervix uteri, corpus uteri, uterus, ovary, Fallopian tube, placenta or malignant neoplasms of male genital organs such as malignant neoplasms of penis, prostate, testis, malignant neoplasms of the urinary tract, such as malignant neoplasms of kidney, renal pelvis, ureter, bladder, urethra or other urinary organs, malignant neoplasms of eye, brain and other parts of central nervous system such as malignant neoplasm of eye and adnexa, meninges, brain, spinal cord, cranial nerves and other parts of central nervous system, malignant neoplasms of thyroid and other endocrine glands such as malignant neoplasm of the thyroid gland, adrenal gland, parathyroid gland, pituitary gland, craniopharyngeal duct, pineal gland, carotid body, aortic body and other paraganglia, malignant neoplasms of head, face and neck, thorax, abdomen and pelvis, secondary malignant neoplasm of lymph nodes, respiratory and digestive organs, kidney and renal pelvis, bladder and other and urinary organs, secondary malignant neoplasms of skin, brain, cerebral meninges, or other parts of nervous system, bone and bone marrow, ovary, adrenal gland, malignant neoplasms of lymphoid, haematopoietic and related tissue such as Hodgkin's disease, follicular non-Hodgkin's lymphoma, diffuse non-Hodgkin's lymphoma, peripheral and cutaneous T-cell lymphomas, non-Hodgkin's lymphoma, lymphosarcoma, malignant immunoproliferative diseases such as Waldenström's macroglobulinaemia, alpha heavy chain disease, gamma heavy chain disease, immunoproliferative small intestinal disease, multiple myeloma and malignant plasma cell neoplasms such as plasma cell leukaemia, plasmacytoma, solitary myeloma, lymphoid leukaemia such as acute lymphoblastic leukaemia, myeloid leukaemia, monocytic leukaemia, blast cell leukaemia, stem cell leukaemia, and other and unspecified malignant neoplasms of lymphoid, haematopoietic and related tissue such

as Letterer-Siwe disease, malignant histiocytosis, malignant mast cell tumour, true histiocytic lymphoma or other types of malignant neoplasia.

5 According to the present invention, a disease associated with leaky blood vessels also may be carcinoma in situ of oral cavity, oesophagus, stomach, digestive organs, middle ear and respiratory system, melanoma in situ, carcinoma in situ of skin, carcinoma in situ of breast, carcinoma in situ of female or male genitals, carcinoma in situ of bladder, urinary organs or eye, thyroid and other endocrine glands, or other types of carcinoma in situ.

10

The nanoparticles or vesicles of the present invention are preferably for administration to a subject such as a human being.

15

According to the present invention, the nanoparticles may be administered to a subject in need in a manner which ensures the delivery of the nanoparticles to tissues comprising leaky blood vessels. Such administration may ensure that the nanoparticles are brought into circulation in the blood or the lymph.

20

In one embodiment of the present invention, the nanoparticles are used for intravenous administration.

In another embodiment of the present invention, the nanoparticles are used for oral administration.

25

The vesicles or nanoparticles according to the present invention may be used for one or more types of imaging. Such imaging may or be part of a method for treating, monitoring or diagnosis of a disease, monitoring efficiency of treatment by chemotherapy or radiotherapy or condition associated with leaky blood vessels. Imaging according to the present invention comprises x-ray imaging, computed tomography (CT) imaging, magnetic resonance imaging (MRI), positron emission tomography (PET) imaging, single photon emission computed tomography (SPECT) imaging or nuclear scintigraphy imaging.

30

In one embodiment of the present invention, a method is provided for monitoring, monitoring treatment efficiency, diagnosis or treatment in a subject in need which comprises:

- 5           a. Providing a nanoparticle composition comprising a vesicle forming component, an agent-entrapping component, and one or more entrapped metal entities.
- b. Administering the nanoparticle composition to a subject in need.

10           In another embodiment of the present invention, a method is provided for monitoring, monitoring treatment efficiency, diagnosis or treatment in a subject in need which comprises:

- a. Providing a nanoparticle composition comprising a vesicle forming  
15           component, an agent-entrapping component, and one or more radionuclides entrapped within the nanoparticle.
- b. Administering the nanoparticle composition to a subject by intravenous administration
- c. Measuring the amount of radiation emitted from the radionuclides within the  
20           liposome composition after a given incubation time.

or

- a. Providing a nanoparticle composition comprising a vesicle forming  
25           component, an agent-entrapping component, and one or more metal entities entrapped within the nanoparticle.
- b. Administering the nanoparticle composition to a subject by intravenous administration
- c. Using conventional imaging methods for measuring the presence and/or  
30           location of the metal entities in said subject.

In one embodiment of the present invention, a method for monitoring, monitoring treatment efficiency, diagnosis or treatment of cancer is provided which comprises:

- a. Providing a nanoparticle composition comprising a vesicle forming component, an agent-entrapping component, and a radiolabeled agent comprising one or more radionuclides of the copper isotopes  $^{61}\text{Cu}$ ,  $^{64}\text{Cu}$  and  $^{67}\text{Cu}$  which may be Cu(II) cations or Cu(I) cations.
- 5 b. Administering the nanoparticle composition to a subject by intravenous administration
- c. Measuring the amount of radiation emitted from the radionuclide within the liposome composition after a given incubation time.

10

## Examples

### Example I

15 **Improved loading of  $^{64}\text{Cu}$  and/ or  $^{177}\text{Lu}$  into liposomes comprising a chelating agent**

#### Preparation of liposome composition containing chelating-agent:

Chelating-agent (DOTA) was trapped within the liposomes consisting of 1,2-distearoyl-*sn*-glycero-3-phosphocholine (DSPC), cholesterol (CHOL) and 1,2-distearoyl-*sn*-glycero-3-phosphoethanolamine-*N*-[methoxy(polyethyleneglycol)-2000 (DSPE-PEG-2000) in the molar ratio 50:40:10 using standard thin-film hydration and repeated extrusions. Briefly, the lipids were mixed in chloroform and dried to a lipid-film under a gentle stream of nitrogen. Organic solvent residues were removed under reduced pressure overnight. The lipid-film was dispersed by adding an aqueous solution - a HEPES buffer (10 mM, 150 mM NaCl, pH 7.4) containing the chelating-agent, DOTA, adjusted to either pH 4.0 or pH 7.4 with a concentration of 10 mM and the osmolarity was measured to be 325 mOsm/L. The solution was then hydrated at 65°C for 60 min. Multi-lamellar vesicles (MLVs) were sized to large unilamellar vesicles (LUVs) by multiple extrusions through 100 nm polycarbonate filters using a mini-extruder. Unentrapped chelating-agent was removed by size exclusion chromatography (SEC) on a Sephadex G-25 packed 1 x 25 cm column eluted with a HEPES buffer (10 mM, 150 mM NaCl, pH 7.4, 310 mOsm/L).

#### Loading liposomes with radionuclide:

35 The suspension of liposomes prepared as described in the section above, was added to a dried vial containing a radionuclide such as  $^{64}\text{Cu}$  and/ or  $^{177}\text{Lu}$ . The suspension was



incubated for 60 min at 50-55°C. Radionuclide loading efficiency was greater than 90% for  $^{64}\text{Cu}$  and greater than 80% for  $^{177}\text{Lu}$ . The separation of  $^{64}\text{Cu}$ -Liposomes and free un-entrapped  $^{64}\text{Cu}$  with size exclusion chromatography (SEC) using Sephadex G-25 column is shown in Fig. 1. The separation of  $^{177}\text{Lu}$ -Liposomes and free un-entrapped  $^{177}\text{Lu}$  with size exclusion chromatography (SEC) using Sephadex G-25 column is shown in Fig. 2.

The loading efficiency of  $^{64}\text{Cu}$  as function of temperature is shown in Fig. 3, and compared to ionophoric loading using 2-hydroxyquinoline (2HQ). The loading efficiency of  $^{64}\text{Cu}$  into liposome compositions when using the ionophore 2HQ was slightly increasing as function of temperature with a maximum loading efficiency ( $92.4\% \pm 1.4\%$ ) at 50-55°C. In contrast the loading efficiency of  $^{64}\text{Cu}$  into liposome compositions without using an ionophore was increasing with increasing temperature reaching a higher loading efficiency ( $96.7\% \pm 1.0\%$ ) at 50-55°C compared to the method with ionophore (2HQ).

Storage stability at 37°C for 24 h of  $^{64}\text{Cu}$ -Liposome with a liposomal interior pH 4.0:

A purified 500  $\mu\text{L}$   $^{64}\text{Cu}$ -Liposome solution was incubated at 37°C for 24 h, and the stability of the  $^{64}\text{Cu}$ -Liposome were assayed by separating free  $^{64}\text{Cu}$  from  $^{64}\text{Cu}$ -Liposome by size exclusion chromatography (SEC) on a Sephadex G-25 column. The elution profile was monitored on an in line radioactivity detector. The  $^{64}\text{Cu}$ -Liposomes containing 10 mM DOTA (pH 4.0) retained more than 95% of the total radioactivity. The radionuclide binds preferably to DOTA encapsulated in the interior of the liposome, due to its strong affinity thereto, allowing the entrapment of the radionuclide.

Storage stability at 37°C for 24 h of  $^{64}\text{Cu}$ -Liposome with a liposomal interior pH 7.4:

A purified 500  $\mu\text{L}$   $^{64}\text{Cu}$ -Liposome solution was incubated at 37°C for 24 h, and the stability of the  $^{64}\text{Cu}$ -liposome were assayed by separating free  $^{64}\text{Cu}$  from  $^{64}\text{Cu}$ -Liposome by size exclusion chromatography (SEC) on a Sephadex G-25 column. The elution profile was monitored on an in line radioactivity detector. The  $^{64}\text{Cu}$ -Liposomes containing 10 mM DOTA (pH 7.4) retained more than 95% of the total radioactivity. The radionuclide binds preferably to DOTA encapsulated in the interior of the liposome, due to its strong affinity thereto, allowing the entrapment of the radionuclide.

The disclosed method of producing nanoparticle compositions loaded with radionuclides is a fast and easy preparation of a novel PET imaging agents. The fast preparation is important due to the short half-life of the positron-emitter,  $^{64}\text{Cu}$ , and ideal in manufacturing the product. The method is very robust and consistently gives high loading efficiencies (>95 %) using liposome composition containing a chelating-agent, a controlled osmotic pressure on the inside of the liposomes, and with a pH ranging from 4 to 8. It is an advantage of the disclosed method that there are no carriers such as lipophilic ionophores used to load the radionuclides into the liposomes. The disclosed method of preparing nanoparticles containing radionuclides produces nanoparticles retaining >95% of the entrapped radionuclides, which is a necessity for the utilization of these nanoparticle compositions as imaging and therapeutic agents.

### Example II

#### Preparation of liposome composition containing chelating-agent for Cu(II)-loading:

The loading of non-radioactive  $\text{Cu}^{2+}$  into chelator-containing liposomes was tested, and evaluated by using an ion Cu(II)-selective electrode. The electrode converts the activity of  $\text{Cu}^{2+}$  dissolved in a solution into an electrical potential, which is measured by a voltmeter or pH meter. Thus the Cu(II)-selective electrode responds to un-complexed  $\text{Cu}^{2+}$  ion activity. The sensing part of the electrode is made as an ion-specific membrane, along with a reference electrode.

Chelating-agent (DOTA) was trapped within the liposomes consisting of DSPC, cholesterol and DSPE-PEG-2000 in the molar ratio 50:40:10 using standard thin-film hydration and repeated extrusions. Briefly, the lipids were mixed in chloroform and dried to a lipid-film under a gentle stream of nitrogen. Organic solvent residues were removed under reduced pressure overnight. The lipid-film was dispersed by adding an aqueous solution - a HEPES buffer (10 mM, 150 mM  $\text{NaNO}_3$ , pH 6.85) containing the chelating-agent, DOTA, adjusted to pH 4.0. The solution was then hydrated at  $65^\circ\text{C}$  for 60 min. Multi-lamellar vesicles (MLVs) were sized to large unilamellar vesicles (LUVs) by multiple extrusions through 100 nm polycarbonate filters using a mini-extruder. Untrapped chelating-agent was removed by size exclusion chromatography (SEC) on a Sephadex G-25 packed 1 x 25 cm column eluted with a HEPES buffer (10 mM, 150 mM  $\text{NaNO}_3$ , pH 6.85, 310 mOsm/L).

#### Loading liposomes with Cu(II):

A sequence of  $\text{Cu}(\text{NO}_3)_2$  standard solutions were prepared and measured using a Cu(II)-selective electrode (Fig. 4). The Cu(II)-selective electrode responds to uncomplexed copper ion activity.  $\text{Cu}(\text{NO}_3)_2$  was added to the liposomes (final concentration of 25 ppm) and the Cu(II)-electrode response was measured to 141 mV (Fig. 4) corresponding to 18.1 ppm uncomplexed Cu(II). The liposome suspension was incubated for 60 min at 50-55°C for loading Cu(II) into the liposome compositions, giving a Cu(II)-electrode response of 94 mV corresponding to 1.2 ppm Cu(II). The blank (background) measurement (10 mM HEPES buffer, 150 mM  $\text{NaNO}_3$ , pH 6.85) without Cu(II) added gave a Cu(II)-electrode response of 104 mV corresponding to 2.2 ppm Cu(II).

To calculate the loading efficiency the following equation (4) was used:

$$\left(1 - \frac{1.2 \text{ ppm}}{25 \text{ ppm}}\right) \cdot 100\% > 95\% \quad (\text{equation 4})$$

These results strongly indicates a very high loading efficiency (>95%) of Cu(II) into the liposomes compositions (Fig. 4), when using the disclosed method.

#### **Example III**

To test whether the ionophore free loading method was limited to divalent cations, the two radioactive trivalent cations,  $^{177}\text{Lu}^{3+}$  and  $^{111}\text{In}^{3+}$ , were tested. Loading of the radioactive pertechnetate ( $^{99\text{m}}\text{Tc}$ ), was also tested.  $^{99\text{m}}\text{Tc}$  is an oxoanion with the chemical formula  $\text{TcO}_4^-$ . Successful loading of both  $^{177}\text{Lu}^{3+}$  and  $^{111}\text{In}^{3+}$  into chelator-containing liposomes without using ionophores was obtained. In contrast no loading was observed of  $^{99\text{m}}\text{TcO}_4^-$  (see Table 1).

The chelator-containing liposomes consisted of DSPC/CHOL/DSPE-PEG<sub>2000</sub> in the molar ratio 50:40:10. An isotonic HEPES buffer (10 mM HEPES, 150 mM NaCl, pH 7.4, 300 mOsm/L) was used as exterior buffer, and a HEPES buffer containing chelator (10 mM DTPA or DOTA, 10 mM HEPES, 150 mM NaCl, pH 7.4) was used as interior buffer. Approximately 10  $\mu\text{L}$  of radioactive  $^{177}\text{LuCl}_3$ ,  $^{111}\text{InCl}_3$  or  $^{99\text{m}}\text{Tc}$  pertechnetat was added to purified chelator-containing liposomes (500  $\mu\text{L}$ ) followed by incubation for 60 min at 50-55°C. The radioactive  $^{177}\text{LuCl}_3$  and  $^{111}\text{InCl}_3$  was purchased from Pelkin Elmer, Denmark, and the  $^{99\text{m}}\text{Tc}$  pertechnetat was kindly provided from Køge Hospital, radiology department, Denmark.

- 5 Table 1: Loading efficiencies of  $^{64}\text{Cu}^{2+}$ ,  $^{111}\text{In}^{3+}$ ,  $^{177}\text{Lu}^{3+}$  and  $^{99\text{m}}\text{TcO}_4^-$  into liposomes consisting of DSPC/CHOL/DSPE-PEG<sub>2000</sub> (50:40:10) with 10 mM chelator entrapped. The loading was carried out for 60 min at 50-55°C without using ionophore and evaluated by SEC.

Radionuclide	Entrapped chelator	Loading efficiency [%]
$^{64}\text{Cu}^{2+}$	DOTA	98
$^{64}\text{Cu}^{2+}$	DTPA	95
$^{111}\text{In}^{3+}$	DOTA	96
$^{177}\text{Lu}^{3+}$	DOTA	81/88*
$^{99\text{m}}\text{TcO}_4^-$	DTPA	0

\*: loading for 4 hours at 65°C

10

The results in Table 1 indicate that the loading method leads to cation permeability ( $^{64}\text{Cu}^{2+}$ ,  $^{177}\text{Lu}^{3+}$  and  $^{111}\text{In}^{3+}$ ) of liposome compositions with highly favourable loading kinetics.

15

To characterize and optimize the loading methods of the present invention different experiments were performed and the following parameters were tested; (1) Effect of lipid composition, (2) Effect of lipid concentration and entrapped volume, (3) Effect of free fatty acids, (4) Effect of monovalent ions ( $\text{Na}^+$ ,  $\text{Cl}^-$ ) and competing divalent ion ( $\text{Ca}^{2+}$ ), (5) Effect of chelating components on the exterior, (6) Effect of interior liposomal pH, (7) Phase behavior and effect of loading temperature, (8) Loading kinetics and influence of temperature, (9) Hyper- and hypo-osmotic pressure and (10)  $\text{Cu}^{2+}$  loading kinetics with and without ionophore.

20

### (1) Effects of lipid composition

25

Liposome compositions within this study are formed from phosphatidylcholines (PC) as 1,2-distearoyl-*sn*-glycero-3-phosphocholine (DSPC) and polyethyleneglycol (PEG) derivatized phosphatidyl ethanolamine as 1,2-distearoyl-*sn*-glycero-3-

phosphoethanolamine-*N*-[methoxy(polyethyleneglycol)-2000] (DSPE-PEG<sub>2000</sub>). Besides DSPC and DSPE-PEG<sub>2000</sub>, cholesterol is incorporated in the membrane. Generally, cholesterol increases bilayer thickness and fluidity while decreasing membrane permeability, and does not add any charge to the membrane. DSPE-PEG<sub>2000</sub> is negatively charged. The liposomes evaluated here were composed of DSPC, cholesterol and DSPE-PEG<sub>2000</sub>. The overall membrane potential of the liposome composition (evaluated via the zeta-potential) is slightly negative for a liposome with the lipid composition DSPC/CHOL/DSPE-PEG<sub>2000</sub> 50:40:10; approximately -15 mV when measured in 10 mM HEPES buffer supplemented with 300 mM glucose, pH 7.4, 336 mOsm/L (Table 2). The different liposome compositions in Table 2 were loaded with <sup>64</sup>Cu<sup>2+</sup> by incubating liposome compositions with <sup>64</sup>Cu<sup>2+</sup> for 60 min at 50-55°C without using ionophore and evaluated by SEC.

Table 2: Loading efficiencies of <sup>64</sup>Cu<sup>2+</sup> into different liposome compositions containing 10 mM DOTA encapsulated. Loading was performed without using ionophore and by incubating for 60 min at 50-55°C and evaluated by SEC.

Liposome composition (% molar ratio)	Loading efficiency [%]	Zeta potential [mV]
DSPC/CHOL/DSPE-PEG <sub>2000</sub> (50:40:10)	98	-16.2*/-2.8**
DSPC/CHOL/DSPE-PEG <sub>2000</sub> (55:40:5)	98	-15.2*/-6.3**
DSPC/CHOL (60:40)	92	-11.5*/+2.9**
DSPC	92	-8.6*/+12.9**

\*Zeta potential was measured in a 10 mM HEPES buffer supplemented with 300 mM glucose, pH 7.4, 336 mOsm/L.

\*\*Zeta potential was measured in a 10 mM HEPES buffer supplemented with 300 mM glucose and 1 mM CaCl<sub>2</sub>, pH 7.4, 339 mOsm/L.

The negative membrane potential could influence the high loading efficiencies of the cationic metal ions into the liposomes (Table 1). In order to evaluate this, loading experiments were conducted on neutral liposome compositions excluding DSPE-PEG<sub>2000</sub> only consisting of pure DSPC or a mixture of DSPC and cholesterol in the molar ratio 60:40. All liposome compositions contained high chelator concentrations

(DOTA, 10 mM) in the interior. The chelator-containing liposomes were added to a dried vial with radioactive  $^{64}\text{CuCl}_2$  and incubated for 60 min at 50-55°C. High  $^{64}\text{Cu}^{2+}$  loading efficiencies were observed with all liposomes compositions (see Table 2).

## 5 (2) Effect of lipid concentration and entrapped volume

Classical means of entrapping drugs (known as loading) into liposomes involves encapsulating the desired drug during the preparation of the liposomes (passive entrapment). Passive entrapment techniques are less efficient in encapsulating drugs or other entities compared to active loading methods (wherein the metal is loaded after  
10 preparation of the liposomes). In passive entrapment, the drug or the radionuclide is simply included in the buffer solution from which the liposomes are formed. The liposome size is highly important for passive loading, as passive entrapment strongly depends on the entrapped aqueous volume of the liposomes.

15 Here, a passive entrapment of  $^{64}\text{Cu}^{2+}$  was tested. The passive entrapment was carried out as described in the following: A lipid-film was made by mixing the lipids (DSPC, cholesterol and DSPE-PEG<sub>2000</sub> in the molar ratio of 55:40:5 with a lipid concentration of 50 mM) in chloroform and dried under a gentle stream of nitrogen. Organic solvent residues were removed under reduced pressure overnight. The lipid-film was the  
20 dispersed by adding an aqueous solution - a HEPES buffer (10 mM, 150 mM NaCl, pH 7.4) containing the chelating-agent, DOTA, adjusted to either pH 4.0 or pH 7.4 with a concentration of 10 mM together with radioactive  $^{64}\text{CuCl}_2$ . The solution was passively loaded with  $^{64}\text{Cu}^{2+}$  by hydrating the solution at 65°C for 60 min. Passively  $^{64}\text{Cu}$ -loaded multi-lamellar vesicles (MLVs) were sized to large unilamellar vesicles (LUVs)  $^{64}\text{Cu}$ -  
25 loaded by multiple extrusions through 100 nm polycarbonate filters using a automated dispenser system applicable for radioactive samples and the loading efficiency was evaluated by SEC. An encapsulation efficiency of 6.25% was obtained in a 100 nm sized liposome solution composed of DSPC, cholesterol and DSPE-PEG<sub>2000</sub> in the molar ratio of 55:40:5 with a lipid concentration of 50 mM. From this the following  
30 conclusion was made; ~0.14%  $^{64}\text{Cu}^{2+}$  is passively encapsulated or associated with the membrane per mM lipid in 100 nm liposomes. This assumption is consistent with estimates of the entrapped volume and encapsulation degree of 100 nm sized unilamellar liposomes:

35

$$\left( (V_{\text{entrap}}/V_{\text{tot}}) / C_{\text{lip}} \right) = Na \cdot a_{\text{lip}} \cdot \frac{R}{6} \sim 0.20\%/mM \quad \text{Equation 5}$$

$V_{\text{entrap}}$  and  $V_{\text{tot}}$  being the entrapped and total volume,  $C_{\text{lip}}$  is the lipid concentration,  $Na$  is the Avogadro's number,  $a_{\text{lip}} = 40\text{\AA}^2$  is the approximate average cross-sectional area of the lipid composition used and  $R$  is the liposome radius.

5 To test if the method of loading metal cations into preformed liposomes is proportional to the lipid concentration and the entrapped volume, the uptake of radioactive  $^{64}\text{Cu}^{2+}$  into neutral membrane compositions consisting of a mixture of DSPC and CHOL in the molar ratio 60:40 without any chelating agent encapsulated was observed. Chelator-free liposomes were prepared as follows: The lipids (DSPC and  
10 CHOL) were mixed in chloroform and dried to a lipid-film under a gentle stream of nitrogen. Organic solvent residues were removed under reduced pressure overnight. The lipid-film was dispersed by adding an aqueous solution - a HEPES buffer (10 mM, 150 mM NaCl, pH 7.4) and the osmolarity was measured to be 300 mOsm/L. The solution was then hydrated at 65°C for 60 min. Multi-lamellar vesicles (MLVs) were  
15 sized to large unilamellar vesicles (LUVs) by multiple extrusions through 100 nm polycarbonate filters using a mini-extruder. The buffer used in this experiment was the same used in all other experiments; an isotonic HEPES buffer (10 mM HEPES, 150 mM NaCl, pH 7.4, 300 mOsm/L). The liposomes were incubated with  $^{64}\text{Cu}^{2+}$  for 60 min at 50-55°C and evaluated by SEC. The liposomal loaded radioactivity was 0.75% when  
20 the lipid concentration was low (5 mM) and 5.3% when the lipid concentration was 10-fold higher (50 mM) (see Table 3).

Table 3: Percent radioactivity associated to the liposome compositions without chelator encapsulated. The incubations were carried out for 60 min at 50-55°C without using  
25 ionophore and evaluated by SEC.

Radionuclide	Liposome composition (% molar ratio)	Lipid concentration [mM]	Loading efficiency [%]
$^{64}\text{Cu}^{2+}$	DSPC/CHOL (60:40)	50	5.3 ± 1.0
$^{64}\text{Cu}^{2+}$	DSPC/CHOL (60:40)	5	0.75
$^{111}\text{In}^{3+}$	DSPC/CHOL/DSPE- PEG <sub>2000</sub> (50:40:10)	50	4

It is clear that the loading efficiency of passive loading using temperatures of 50-55°C is significantly lower (6.25%) than the loading efficiency obtained by using the loading methods of the present invention (e.g. Table 1 and 2). The results in Table 3 also indicate that loading of  $^{64}\text{Cu}^{2+}$  into the liposomes without chelator encapsulated using the method of the present invention is proportional to the entrapped volume and/or the lipid concentration of the liposomes, indicating that loading/association of  $\text{Cu}^{2+}$  into preformed liposomes can occur unassisted by an entrapped chelator. The hypothesis was also tested with the trivalent metal ion,  $^{111}\text{In}^{3+}$ , showing similar trends as for  $^{64}\text{Cu}^{2+}$  (see Table 3). Either the metal ions are trapped or transported passively in the aqueous phase of preformed liposomes due to simple transmembrane ion equilibrium or the metal ions are associated to the lipids in the membrane of the liposome. The metal ions could bind to or associate to the phosphate moiety in the polar head group of PC. The results in Table 3 clearly demonstrate a correlation between the lipid concentration and/or the entrapped liposomal volume and the  $\text{Cu}^{2+}$  and  $\text{In}^{3+}$  ions association to or transport into the liposomes.

### (3) Effect of free fatty acids

Free fatty acids (FFA) are known to diffuse (or flip-flop) rapidly across phospholipid bilayers in their protonated form. However, whether flip-flop through the hydrophobic core of the bilayer or desorption from the membrane into the aqueous phase is the rate-limiting step in FFA transport through membranes is still debated. Nevertheless, FFAs are well known to have a destabilizing effect on some liposomal membranes enhancing the permeability of membranes and facilitating the passage of entities over the membrane; however, exceptions are known where FFAs stabilize the gel state of fully saturated lipid membranes. The addition of FFA to lipid bilayer solutions such as liposomes have been shown to dramatically enhance membrane permeability in the presence of e.g. palmitic acid and  $\text{Ca}^{2+}$  ions [Agafonov et al., BBA, 1609:153-160, 2003]. To evaluate if the high radionuclide loading into the aqueous phase of liposomes without the use of ionophores found for the present invention, could be dependent on the presence of FFA that enhance the trans-bilayer diffusion rate of free metal ions (acyl phospholipids contain small impurities of FFA), the  $^{64}\text{Cu}^{2+}$  loading efficiency was measured for non-FFA containing liposomal membranes. 1,2-Di-O-Hexadecyl-sn-Glycero-3-phosphocholine (1,2-Di-O-DPPC) was used as FFA free lipid component replacing DSPC in the liposome composition (see Fig. 5).

35



The chelator-containing non-FFA containing liposomes were prepared as described in Example I: Preparation of liposome composition containing chelating-agent, using 1,2-Di-O-Hexadecyl-sn-Glycero-3-phosphocholine (1,2-Di-O-DPPC) and CHOL as vesicle-forming components in the molar ratio 60:40. The chelator-free non-FFA containing liposomes were prepared as described in the above section **(2)** using 1,2-Di-O-Hexadecyl-sn-Glycero-3-phosphocholine (1,2-Di-O-DPPC) and CHOL as vesicle-forming components in the molar ratio 60:40.

The chelator-containing (10 mM DOTA) non-FFA containing liposomes or chelator-free non-FFA containing liposomes were added to a dried vial with radioactive  $^{64}\text{CuCl}_2$  and incubated for 60 min at 50-55°C and evaluated by SEC. A high loading of  $^{64}\text{Cu}^{2+}$  into the interior of the chelator-containing non-FFA containing liposomes was observed (Table 4) with chelator-free non-FFA containing liposomes serve as a control.

Table 4: Loading efficiencies of  $^{64}\text{Cu}^{2+}$  into liposome compositions containing 1,2-Di-O-Hexadecyl-sn-Glycero-3-phosphocholine (1,2-Di-O-DPPC) and CHOL in the molar ratio 60:40 with and without 10 mM DOTA encapsulated. The loading were carried out for 60 min at 50-55°C without using ionophore and evaluated by SEC.

Chelator	Liposome composition (% molar ratio)	Lipid concentration [mM]	Loading efficiency [%]
With	1,2-Di-O-DPPC/CHOL (60:40)	10	93
Without	1,2-Di-O-DPPC/CHOL (60:40)	50	6

1,2-Di-O-DPPC: 1,2-Di-O-Hexadecyl-sn-Glycero-3-phosphocholine

This excludes the possibility that FFAs are inducing the permeability of the free metal ions into the liposomes. Non-FFA containing liposomes without chelator encapsulated served as a control, and gave similar results as for DSPC/CHOL (60:40) without encapsulated chelators (Table 3). The conclusion is that liposomes both with and without FFA in the membrane can be used in the present invention.

25

#### **(4) Effect of monovalent ions ( $\text{Na}^+$ , $\text{Cl}^-$ ) and competing divalent ions ( $\text{Ca}^{2+}$ )**

In a study by Hauser and Dawson it was observed that monovalent ions like  $\text{Na}^+$  and  $\text{K}^+$  were only effective at displacing  $\text{Ca}^{2+}$  when they were present at a concentration about  $10^4$  times that of  $\text{Ca}^{2+}$  [Hauser and Dawson, J. Biochem., 1:61-69, 1967], which agrees with the predictions of the double layer theory [Lyklema, ISBN:0-12-460530-3,

30

5:3.208, 1995]. The double layer is a structure that appears on the surface of an object when it is placed into liquid containing ions. The object might be a solid particle such as a nanoparticle or liposome. In the first layer, the surface charge (either positive or negative) comprises ions adsorbed directly onto the object. The second layer is composed of ions attracted to the surface charge via Coulomb force, thereby electrically screening the first layer. This second layer is loosely associated with the nanoparticle, because it is made of free ions which move in the liquid under the influence of electric attraction and thermal motion rather than being firmly anchored.

As reported above, 5.3% radioactivity was associated/loaded to the liposomes when an isotonic HEPES buffer (10 mM HEPES, 150 mM NaCl, pH 7.4, 300 mOsm/L) was used (Table 3), but if no monovalent ions (Na<sup>+</sup> and Cl<sup>-</sup>) were added (10 mM HEPES, pH 7.4, 5 mOsm/L), 11% radioactivity was associated with the DSPC/CHOL membrane (50 mM) (see Table 5).

Table 5: Loading efficiencies of <sup>64</sup>Cu<sup>2+</sup> into liposome compositions without chelator encapsulated. The liposome composition consisted of lipid components DSPC and CHOL in the molar ratio 60:40 with a total lipid concentration of 50 mM. The incubations were carried out for 60 min at 50-55°C without using ionophore and loading was subsequently evaluated by SEC.

External and internal buffer solution	Loading efficiency [%]
10 mM HEPES (pH 7.4, 5 mOsm/L)	11
10 mM HEPES, 150 mM NaCl (pH 7.4, 300 mOsm/L)	5.3 ± 1.0
10 mM HEPES, 150 mM NaCl, 10 mM CaCl <sub>2</sub> (pH 7.4, 315 mOsm/L)	3 ± 1

This is in agreement with double layer theory predicting a stronger interaction between the negatively charged lipid membrane and Cu<sup>2+</sup> as the screening is reduced by the removal of NaCl. In order to substantiate this point, we repeated the loading experiment with the DSPC/CHOL membrane (50 mM) at higher ionic strength adding 10 mM of Ca<sup>2+</sup> (using 10 mM HEPES, 150 mM NaCl, 10 mM CaCl<sub>2</sub>, pH 7.4, 315 mOsm/L). A significant reduction (3%) of radioactivity was associated to the membrane (see Table 5), indicating that monovalent ions such as Na<sup>+</sup> and divalent ions as Ca<sup>2+</sup> effectively displace <sup>64</sup>Cu<sup>2+</sup> at the membrane surface thereby reducing the <sup>64</sup>Cu<sup>2+</sup>

loading rate. This observation is furthermore in agreement with previous investigations on interactions of divalent cations such as  $\text{Ca}^{2+}$  and  $\text{Zn}^{2+}$  with phospholipid membranes [Altenbach and Seelig, *Biochemistry*, 23:3913-3920, 1984; Binder et al., *Bio-phys. Chem.*, 90:57-74, 2001; Huster et al., *Biophys. J.*, 78:3011-3018, 2000]. In addition the study by Binder and Zschörnig [Binder and Zschörnig, *Chem. Phys. Lipids*, 115:39-61, 2002] showed that  $\text{Ca}^{2+}$  clearly binds to the lipid headgroup of pure POPC lipid bilayers. From the results reported here it is suggested that the primary binding of the metal cation,  $\text{Cu}^{2+}$  to the membrane, is reduced by charge screening effects by mono- and divalent ions such as  $\text{Ca}^{2+}$  and  $\text{Na}^+$ .

Importantly, it can be seen from the results in Table 5 that the loading methods of the present invention of  $\text{Cu}^{2+}$  (divalent ions, radioactive and non-radioactive, as well as radioactive trivalent cations,  $^{177}\text{Lu}^{3+}$  and  $^{111}\text{In}^{3+}$ ) into chelator-containing liposomes can be conducted both in presence or absence of  $\text{Ca}^{2+}$ ,  $\text{Na}^+$  and  $\text{Cl}^-$ .

#### (5) Effect of chelating components

The distribution between, and binding of free metal ions (radionuclides) to, various components on the outside of the liposomes (such as un-removed chelator, buffer molecules etc.) are important in determining the chemical activity of the free metal ions with respect to trans-membrane diffusion and overall remote loading kinetics. When residual chelators or other metal binding components are present on the outside of the liposomes, the loading kinetics and efficiency is lowered dramatically. This was observed when a chelator-containing liposome solution was spiked with  $10^{-6}$  M DOTA prior to incubation. The loading efficiency was lowered to 2% compared to when no chelator components were present on the outside (>95%). To achieve high loading efficiency (for all cations tested ( $^{64}\text{Cu}^{2+}$ ,  $^{177}\text{Lu}^{3+}$  and  $^{111}\text{In}^{3+}$ )) it is important to remove residual chelators (e.g. DOTA) from the outside of the chelator-containing liposomes during preparation. The presence of chelating components on the liposome exterior lowers the cation concentration (e.g.  $^{64}\text{Cu}^{2+}$ ,  $^{177}\text{Lu}^{3+}$  and  $^{111}\text{In}^{3+}$ ) in the aqueous phase and thereby the concentration of the membrane associated fraction, which leads to a very low loading efficiency within an appropriate time scale (hours).

Besides chelators, buffer components are able to complex metal ions. It is known that the buffer HEPES (4-(2-hydroxyethyl)-1-piperazineethanesulfonic acid) interacts with  $\text{Cu}^{2+}$  and forms complexes that undergoes alkaline hydrolysis above pH 6, resulting in  $\text{Cu}(\text{OH})_2$  precipitation [Sokolowska and Bal, *J. Inorg. Biochem.*, 99:1653-

1660, 2005]. It has been proposed that HEPES contain small impurities that have relatively high affinity for  $\text{Cu}^{2+}$  [Mash and Chin, Anal. Chem., 75:671-677, 2003]. Hypothetically, HEPES could act as carrier molecule of metal ions within the loading methods of the present invention, shedding and transporting the ions over the membrane where they preferentially bind to the pre-encapsulated chelator.

Since similar high loading efficiencies (>95%) of  $^{64}\text{Cu}^{2+}$  into chelator-containing liposomes (DSPC/CHOL/DSPE-PEG<sub>2000</sub> in the molar ratio 50:40:10), were obtained when using other buffers such as phosphate buffered saline (PBS) and the “non-coordinating” buffer 2-(N-morpholino)ethanesulfonic acid (MES), HEPES may not act as carrier molecule of Cu(II) (see Table 6). The preparation of the liposomes was carried out as described in Example I: Preparation of chelator-containing liposomes, where HEPES buffer was replaced by PBS or MES buffer. The loading was performed for 60 min at 50-55°C and the loading efficiency was evaluated by SEC.

Table 6: Loading efficiencies of  $^{64}\text{Cu}^{2+}$  into liposome compositions (DSPC/CHOL/DSPE-PEG<sub>2000</sub> in the molar ratio 50:40:10) containing 10 mM DOTA encapsulated with different external buffer solutions. Loading was performed for 60 min at 50-55°C without using ionophores and evaluated by SEC.

External buffer solution	Loading efficiency [%]
10 mM HEPES, 150 mM NaCl (pH 7.4, 300 mOsm/L)	98 ± 2
10 mM MES, 150 mM NaCl (pH 5.9, 300 mOsm/L)	95
9.5 mM PBS, 150 mM NaCl (pH 7.4, 300 mOsm/L)	95 ± 3

The present results show that a high loading efficiency is obtained using the methods of the present invention with an incubation solution comprising different loading buffers,

However, the solubility of dried  $^{64}\text{CuCl}_2$  was found to be higher and more rapid in HEPES buffer compared to PBS and sterile water at pH 7.4 at 22°C temperature, which is convenient for the preparation procedure. At higher temperatures the solubility of dried  $^{64}\text{CuCl}_2$  in HEPES, PBS and sterile water was equal.

### (6) Effect of Interior liposomal pH

An important discovery in liposome loading techniques was that trans-membrane ion gradients can be generated and utilized to actively load and encapsulate ionizable drugs in the aqueous liposome lumen [U.S. patent Nos. 5,736,155; 5,077,056; and 5,762,957]. The method involves establishing a pH gradient across a liposome bilayer such that an ionizable drug, to be encapsulated within a liposome, is uncharged in the external buffer and charged within the aqueous interior. This allows the drug to cross the bilayer membrane of the liposome in a neutral form and to be trapped within the aqueous interior of the liposome due to conversion to the charged form. Leakage of drug from actively loaded liposomes has also been found to follow the loss of the proton gradient.

In a previous study on  $^{64}\text{Cu}^{2+}$  loading into liposomes using the ionophore 2-hydroxyquinoline (2HQ) [Petersen et al., *Biomaterials*, 32:2334-2341, 2011], >95% and 70% loading efficiency was observed for chelator-containing liposomes with interior pH of 4.0 and 5.9 respectively. The lower degree of loading obtained at pH 5.9 was explained by the less favorable exchange of  $^{64}\text{Cu}^{2+}$  from 2HQ to DOTA. Another ionophore, oxine, was also evaluated, but provided unstable liposomes with respect to  $^{64}\text{Cu}^{2+}$  retention. This instability (release of  $^{64}\text{Cu}^{2+}$ ) was explained by the ionophore's ability to dissipate the transmembrane pH gradient, causing the liposomal interior pH to increase, which in the case of oxine, resulted in a reduction of the ligand exchange by several orders of magnitude. Thus ionophores can facilitate the release of entrapped metal ions from liposome compositions.

The influence of interior liposomal pH on the loading efficiency and retention of metal ions was tested with the loading methods of the present invention. Chelating-agent ( $C_{\text{DOTA}} = 10 \text{ mM}$ ) was trapped within the liposomes (DSPC/CHOL/DSPE-PEG<sub>2000</sub> in the molar ratio 50:40:10) adjusted to either pH 4.0 or pH 7.4 as previously described in Example I: Preparation of chelator-containing liposomes. The external buffer was an isotonic HEPES buffer (10 mM HEPES, 150 mM NaCl, pH 7.4, 300 mOsm/L). The incubations of liposomes with  $^{64}\text{Cu}^{2+}$  were carried out for 60 min at 50-55°C and followingly evaluated by SEC. High loading efficiencies (>95%) of  $^{64}\text{Cu}^{2+}$  were obtained for both interior liposomal pH (4.0 and 7.4) (see Table 7).

Table 7: Loading efficiencies of  $^{64}\text{Cu}^{2+}$  into liposome compositions (DSPC/CHOL/DSPE-PEG<sub>2000</sub> in the molar ratio 50:40:10) containing 10 mM DOTA encapsulated with different interior pH (pH 4.0 or 7.4). Loading was performed for 60 min at 50-55°C without using ionophores and followingly evaluated by SEC. External buffer was an isotonic HEPES buffer (10 mM HEPES, 150 mM NaCl, pH 7.4, 300 mOsm/L).

Internal buffer pH	Loading efficiency [%]	Leakage [%]
4.0	98 ± 2	<1%
7.4	98 ± 2	<1%

In addition,  $^{64}\text{Cu}^{2+}$  loaded liposomes were tested for radionuclide retention by incubating the liposome solutions for 24 h at 37°C and 20°C. Additionally, stability in human serum of the liposome solutions was tested by mixing human serum and liposome solution (1:1) at 37°C for 24 h. No release of entrapped radionuclide,  $^{64}\text{Cu}^{2+}$ , was observed from any of the liposome solutions (see Table 7).

From the results obtained provided in Table 7 it is clear that the interior pH can easily be raised to pH 7.4 without any influence on loading efficiency or radionuclide retention. Thus the loading method of the present invention is not dependent on any pH gradient across the membrane. An interior pH 7.4 of the liposome is preferable due to possible lipid hydrolysis at lower pH such as pH 4.0. The shelf-life of the chelator-containing liposomes is therefore also significantly prolonged when using interior pH 7.4 compared to pH 4.0.

20

#### (7) Phase behavior and effect of loading temperature

Conventional approaches to liposome formulation dictate inclusion of substantial amounts (e.g. 30-45 mol%) of cholesterol or equivalent membrane rigidifying agents (such as other sterols). Generally, cholesterol increases the bilayer thickness and fluidity while decreasing membrane permeability of the liposome. For example, it has been reported that including increasing amounts of cholesterol in phosphatidylcholine (PC) containing liposomes decreased the leakage of calcein (a fluorescent marker compound) from liposomes in the presence and absence of an osmotic gradient [Allen, et al. Biochim, Biophys. Acta, 597:418-426, 1980]. Another feature of adding cholesterol to lipid bilayers is the formation of a liquid-ordered phase inheriting the

30

stability properties of the liquid-crystalline phase and mobility of the fluid phase. When the DSPC bilayer is supplemented with more than ~35 mol% of cholesterol, the main phase transition is completely abolished, and the membrane can be considered to exist in a liquid-ordered phase over a wide temperature range. From differential scanning calorimetry (DSC) experiments it is observed that the liposomal membrane composed of DSPC, CHOL and DSPE-PEG<sub>2000</sub> in the molar ratio of 50:40:10 does not exhibit any thermal transitions in the range 45-60°C and thus exists in a single (liquid-ordered like) phase within this temperature range (Fig. 6). Still as shown in Figure 3, the loading efficiency of <sup>64</sup>Cu<sup>2+</sup> into liposome compositions without the use of an ionophore was increasing with increasing temperature reaching a high loading efficiency (96.7% ± 1.0%) at 50-55°C for 60 min. The efficiencies presented here for loading without use of ionophores are proportional with the increasing temperatures, however, since no phase transition temperature occurs in the liposome composition (Fig. 6), the augmented loading efficiencies are not caused by a phase transition behavior.

#### (8) Loading kinetics and loading temperature

The kinetics of <sup>64</sup>Cu<sup>2+</sup> loading into chelator-containing liposomes (DSPC/CHOL/DSPE-PEG<sub>2000</sub> in the molar ratio 50:40:10), were examined by radio thin layer chromatography (radio-TLC) as the ratio between complexed <sup>64</sup>Cu (e.g. <sup>64</sup>Cu-DOTA) and the total <sup>64</sup>Cu amount (sum of complexed (<sup>64</sup>Cu-DOTA) and free <sup>64</sup>Cu<sup>2+</sup>) as function of time. The loading experiments were carried out in a reaction vial at 30°C, 40°C and 50°C and 2 µL samples were spotted on TLC plates at different time points. Thus when <sup>64</sup>Cu<sup>2+</sup> is loaded into the liposomes, the metal ion binds preferentially to DOTA and <sup>64</sup>Cu-DOTA complex is formed. The TLC plates were run in an organic eluent (10% ammonium acetate:methanol (50:50)) where <sup>64</sup>Cu-DOTA complexes were separated from free <sup>64</sup>CuCl<sub>2</sub>. The retention factor (R<sub>f</sub>) of <sup>64</sup>Cu-DOTA was approximately 0.3 while ionic <sup>64</sup>Cu<sup>2+</sup> remained on the origin (R<sub>f</sub> = 0). When the liposome samples were spotted on TLC plates, the liposomes immediately dry out and the interior (<sup>64</sup>Cu-DOTA) runs on the TLC plate. The ratio between the interior <sup>64</sup>Cu-DOTA complex and the total <sup>64</sup>Cu amount (sum of complexed (<sup>64</sup>Cu-DOTA) and free <sup>64</sup>Cu<sup>2+</sup>) was calculated as the loading efficiency (defined in equation 1). As a control, free <sup>64</sup>Cu<sup>2+</sup> was spotted on a TLC plate followed by non-radioactive chelator-containing liposomes on top of <sup>64</sup>Cu<sup>2+</sup>. This control was done to eliminate an erroneous estimation of <sup>64</sup>Cu<sup>2+</sup> and DOTA complexation occurring on the TLC plate. Since no <sup>64</sup>Cu-DOTA peak was present on the TLC plate, no complexation is occurring on the TLC plate.

The loading of metal ions into liposomes can be divided into several steps including: (i) binding/coordination/adsorption of the ion to the lipid membrane, (ii) trans-bilayer ion diffusion and (iii) binding of ions to the chelator. In the current loading procedure the lipid and chelator are in large excess compared to the  $^{64}\text{Cu}^{2+}$  and the kinetics thus only depends on the  $^{64}\text{Cu}^{2+}$  concentration. The rate of coordination/binding of  $\text{Cu}^{2+}$  to the membrane is rapid (likely to be diffusion limited) and binding of  $\text{Cu}^{2+}$  to DOTA occurs on timescale of seconds (verified by radio-TLC) rendering trans-membrane ion diffusion as the most probable rate limiting step. In general, the rate of trans-membrane diffusion will depend on the concentration gradient of the transported entity (according to Ficks 1<sup>st</sup> law), the membrane phase state (gel, fluid or liquid-ordered) and physicochemical (hydrophilicity vs. hydrophobicity) properties of the transported entity. These arguments substantiate the first order equation (Equation 6) presented below. The loading kinetics (example shown in Fig. 7-8) can be characterized by the equation

$$\%load = \frac{A_{\text{Cu-chelator}}}{A_{\text{Cu}} + A_{\text{Cu-chelator}} + A_{\text{Cu(ionophore)}}} = a(1 - be^{-ct}) \quad \text{Equation 6}$$

where  $A_{\text{Cu}}$ ,  $A_{\text{Cu-chelator}}$  and  $A_{\text{Cu(ionophore)}}$  denote the TLC activity of the  $^{64}\text{Cu}^{2+}$ ,  $^{64}\text{Cu}$ -DOTA and  $^{64}\text{Cu}(\text{2HQ})_2$  specie. The fitting parameter  $a$ , describes the plateau level ( $a \sim 100\%$  if loading proceeds according to 1<sup>st</sup> order kinetics),  $b$  describes offset and uncertainty in  $t$  ( $b = 1$  when offset and uncertainties in  $t$  are small) and  $c$  describes the loading rate. By fitting of equation 7, each loading profile can be characterized by: (i) the initial velocity:

$$v_{ini} = a \cdot b \cdot c \quad (\text{equation 7}),$$

(ii) the time required to reach 95% loading:

$$t_{(95\%)} = -\ln((1 - (95\%)/a)/b)/c \quad (\text{equation 8}),$$

, and (iii) the degree of loading reached at 60 min ( $\%load_{1h}$ ). The latter is directly comparable to the loading degree achieved using the method based on SEC (presented in Fig. 3 and Tables 1, 2, 6 and 7).

The first order rate constant ( $c$ ) depends on different parameters such as temperature (see Fig. 7-8) and osmolarity (see next section) at which the loading is conducted. The initial velocity ( $v_{ini}$ ),  $t_{(95\%)}$  and  $\%load_{1h}$  is given in Table 8 for a set of loading conditions.



Table 8: Kinetic parameters for loading conducted at 30°C, 40°C and 50°C, without ionophore for iso-osmotic and hyper-osmotic conditions, and with ionophore (2HQ). The kinetics are characterized by the initial velocity,  $v_{ini}$ , the time required to achieve 95% loading,  $t_{(95\%)}$  and the loading efficiency obtained after 60 min,  $\%load_{1h}$ . All parameters were derived from radio-TLC measurements shown in Fig. 7-8.

5

	$v_{ini}$ [%/min]	$t_{(95\%)}$ [min]	$\%load_{1h}$ [%]
Iso-osmotic			
30 °C	0.6	220	33
40 °C	3	*	62
50 °C	23	18	99
Hyper-osmotic			
30 °C	0.9	240	42
40 °C	7	*	86
50 °C	51	9	99
With ionophore (2HQ)			
30 °C	3	80	82
40 °C	7	60	94
50 °C	100	6	100

\* Extrapolation not possible

The loading efficiency of  $^{64}\text{Cu}^{2+}$  into liposomes at 50°C at iso-osmotic conditions (Fig. 8) displays a rapid initial rate which gradually declines and saturates as function of time. Upon lowering of the temperature the initial velocity is decreased significantly (Table 8) and the time required for loading 95% is increased from 30 min to several hours (at iso-osmotic loading). Similar temperature effects are observed for loading at hyper-osmotic conditions (discussed in section 9) and for ionophore assisted loading (discussed in section 10).

15

**(9) Hyper- and hypo-osmotic pressure**

In order to investigate whether hyper-osmotic conditions increase the loading rate and loading efficiency of metal ions, loading experiments of  $^{64}\text{Cu}^{2+}$  into chelator-containing liposomes having a hyper-osmotic ( $\Delta(\text{mOsm/L}) = +75$ ), a hypo-osmotic ( $\Delta(\text{mOsm/L}) = -40$ ) as well as an iso-osmotic gradient ( $\Delta(\text{mOsm/L}) = 0$ ) (see Table 9) were conducted. The preparation of liposomes and loading experiments were performed as described in Example I, except for changes in the osmolarity of the buffers (see Table 9 below).

Table 9: Loading efficiencies of  $^{64}\text{Cu}^{2+}$  into liposomes consisting of DSPC/CHOL/DSPE-PEG<sub>2000</sub> (50:40:10) using different intra- and extra-liposomal osmolarties. Loading was performed for 60 min at 50-55°C without using ionophore and evaluated by SEC followingly.

* $\Delta(\text{mOsm/L})$ (Interior buffer #/Exterior buffer#)	Loading efficiency [%]
0 (#1/#3)	96
+ 80 (#2/#3)	98
- 40 (#2/#4)	96
0 (#2/#5)	95

\* $\Delta(\text{mOsm/L})$ : difference between the internal and external osmolarity liposomal buffer solution. + is higher internal osmolarity and – is lower internal osmolarity.

#1: 10 mM DOTA, 10 mM HEPES, 140 mM NaCl, pH 7.4, 295 mOsm/L

#2: 10 mM DOTA, 10 mM HEPES, 150 mM NaCl, pH 7.4, 375 mOsm/L

#3: 10 mM HEPES, 150 mM NaCl, pH 7.4, 295 mOsm/L

#4: 10 mM HEPES, 200 mM NaCl, pH 7.4, 415 mOsm/L

#5: 10 mM HEPES, 150 mM NaCl, pH 7.4, 75 mM Sucrose, 375 mOsm/L

20

The liposome compositions consisted of DSPC/CHOL/DSPE-PEG<sub>2000</sub> in the molar ratio 50:40:10 contained high chelator concentrations (DOTA, 10 mM) in the interior. The osmolarity was controlled by adjusting the NaCl concentration or by adding sucrose (see Table 9). The loading efficiency (evaluated after 60 min) conducted at 50-55°C (results are compiled in Table 9) showed that high loading efficiency of  $\text{Cu}^{2+}$  (>94%) is obtained in all cases within the timeframe of the experiment. However, results shown in Table 8 indicate a difference in loading rate between the different osmolarities.

25

$^{64}\text{Cu}^{2+}$  loading kinetics were in addition evaluated as function of time at three different temperatures (30°C, 40°C and 50°C) and at two osmotic conditions (iso- and hyper-osmotic) using radio-TLC (Fig. 7-8) with chelator-containing liposomes (DSPC/CHOL/DSPE-PEG<sub>2000</sub> in the molar ratio 50:40:10). These data (Fig. 7-8) confirm an increased loading rate (initial velocity ( $v_{ini}$ ) in Table 8) and loading efficiency ( $\%load_{1h}$  in Table 8) with increased temperature for both iso- and hyper-osmotic conditions. The rate and efficiency was further augmented when loading was conducted at hyper-osmotic conditions when compared to iso-osmotic conditions. The largest change in loading rate and loading efficiency upon increased osmolarity were observed at 30°C and 40°C, whereas little change was found at 50°C.

These results evidence that the loading rate and efficiency can be modulated significantly by tuning parameters as the temperature and the osmolarity. These parameters are important for the effectiveness of the loading method.

15

#### **(10) $\text{Cu}^{2+}$ loading kinetics with and without ionophore**

As shown in Figure 3, the loading efficiency ( $\%load_{1h}$  evaluated by SEC) of  $^{64}\text{Cu}^{2+}$  into liposome compositions when using the ionophore 2HQ was weakly increasing as function of temperature with a maximum loading efficiency ( $92.4\% \pm 1.4\%$ ) at 50-55°C for 60 min. In contrast, the loading efficiency of  $^{64}\text{Cu}^{2+}$  into liposome compositions without the use of an ionophore showed a larger increase with augmented temperature reaching a higher loading efficiency ( $96.7\% \pm 1.0\%$ ) at 50-55°C for 60 min compared to the method with ionophore. These results indicate an increase in loading efficiencies at temperatures below 50°C, when incubating  $^{64}\text{Cu}^{2+}$ , liposomes and ionophore compared to loading without ionophore. The concentration of ionophore used in the loading experiments in Figure 3 was 100  $\mu\text{M}$ . Ionophores may be toxic to mammals, and therefore the loaded liposomes need to be purified before intravenous injection, which would be a disadvantage in liposome production.

The  $^{64}\text{Cu}^{2+}$  loading kinetics into the aqueous phase of liposomes consisting of DSPC/CHOL/DSPE-PEG<sub>2000</sub> in the molar ratio 50:40:10 with and without the use of ionophore ( $C_{2HQ} = 100 \mu\text{M}$ ) was compared. To investigate the influence of osmotic pressure on the results of the kinetics, the liposomes were prepared having iso-osmotic conditions. The solutions were incubated at different temperatures (30°C, 40°C and 50°C) and evaluated by radio-TLC as function of time (as described above). The radio-TLC results (Table 8) substantiated by results from Figure 3 show, that the use of an

35

ionophore: (i) increases the loading rate (initial velocity ( $v_{ini}$ )) and loading efficiency ( $\%load_{1h}$ ) (below 50°C) and (ii) lowers the time required to load 95% ( $t_{(95\%)}$ ). The ionophore assisted loading method furthermore reduces the activation energy for loading, resulting in smaller changes in loading rate and efficiency as a function of temperature variations when compared to non-assisted loading.

Previous studies have shown low ion permeability of phospholipid bilayers such as liposome compositions, which has lead to highly unfavorable loading kinetics for charged ion species [Paula et al., Biophys. J., 74:319-327, 1998; Hauser et al., Nature, 239:342-344, 1972; Ceh et al., J. Phys. Chem. B, 102:3036-3043, 1998; Mills et al., Biochim. Biophys. Acta, 1716:77-96, 2005; Papahadjopoulos et al., Biochim. Biophys. Acta, 266:561-583, 1971; Puskin, J. Membrane Biol, 35:39-55, 1977]. The results from the experiments utilizing the loading methods of the present invention show the opposite, where charged ions as  $^{64}\text{Cu}^{2+}/^{63}\text{Cu}^{2+}$ ,  $^{111}\text{In}^{3+}$  and  $^{177}\text{Lu}^{3+}$  are loaded fast and efficiently into chelator-containing liposomes. The results show that the use of ionophores or other lipophilic complexes to increase trans-bilayer diffusion rates only moderately improves or increases the loading of divalent and trivalent cations, as previously thought.

### Summary

The present examples show that divalent and trivalent ions (such as for example  $^{64}\text{Cu}^{2+}$ ,  $^{111}\text{In}^{3+}$  and  $^{177}\text{Lu}^{3+}$ ) are passively transported through liposomal membranes encapsulated in high concentrations in the interior of liposome compositions due to complexation to pre-encapsulated chelators.

**References**

- Agafonov et al., BBA, 1609:153-160, 2003
- 5 Allen, et al. Biochim, Biophys. Acta, 597:418-426, 1980
- Allen, Science, 303: 1818-1822, 2004
- 10 Altenbach and Seelig, Biochemistry, 23:3913-3920, 1984
- Anderson et al., J Nucl Med., 36: 2315-2325, 1998
- Binder et al., Bio-phys. Chem., 90:57-74, 2001
- 15 Binder and Zschörnig, Chem. Phys. Lipids, 115:39-61, 2002
- Ceh et al., J. Phys. Chem. B, 102:3036-3043, 1998
- 20 Dehdashti et al., J Nucl Med. 38: 103P, 1997
- Gabizon et al., J Liposome Res., 1: 123-125, 1988
- Gabizon et al., Cancer Res., 50: 6371-6378, 1990
- 25 Goto et al., Chem harm Bull.(Tokyo), 37: 1351-1354, 1989
- Hauser and Dawson, J. Biochem., 1:61-69, 1967
- 30 Hauser et al., Nature, 239:342-344, 1972
- Henriksen et al., Nucl Med Bio., 31: 441-449, 2004
- Huster et al., Biophys. J., 78:3011-3018, 2000
- 35 Hwang et al., Biochim Biophys Acta., 716: 101-109, 1982
- Kostarelos et al., J Liposome Res, 9:407-424, 1999
- 40 Lyklema, ISBN:0-12-460530-3, 5:3.208, 1995
- Mash and Chin, Anal. Chem., 75:671-677, 2003
- Mills et al., Biochim. Biophys. Acta, 1716:77-96, 2005
- 45 Morgan et al., J Med Microbiol., 14: 213-217, 1981
- Papahadjopoulos et al., Biochim. Biophys. Acta, 266:561-583, 1971
- 50 Paula et al.,Biophys. J., 74:319-327, 1998
- Petersen et al., 2011, Biomaterials, 32:2334-2341, 2011

Phillips, Adv Drug Deliv Rev., 37: 13-32, 1999

Phillips et al., Int J Rad Appl Instrum B, 19: 539-547, 1992

5 Puskin, J. Membrane Biol, 35:39-55, 1977

Seo et al., Bioconjugate Chem., 19: 2577-2584, 2008

10 Seo, Curr. Radiopharm., 1: 17-21, 2008

Sokolowska and Bal, J. Inorg. Biochem., 99:1653-1660, 2005

15

**Claims**

- 5 1. A method for preparation of a nanoparticle composition loaded with metal entities such as radionuclides, wherein said method does not involve the use of ionophore, said method comprising:
- a) Providing a nanoparticle composition comprising a vesicle forming component and an agent-entrapping component enclosed by said vesicle forming component;
- 10 b) Entrapping the metal entities within the interior of the nanoparticle composition by enabling transfer of cation metal entities across a membrane formed by the vesicle forming component by incubation of the nanoparticle composition in a solution comprising the metal entities.
- 15 2. The method method of claim 1 wherein loading efficiency or entrapment of radionuclide is greater than 10% such as greater than 40%, for example greater than 50%, such as greater than 60%, for example greater than 70%, such as greater than 80% for example greater than 85%, such as greater than 90%, or such as greater than 95%, or such as greater than 97%, or such as greater than 99%.
- 20 3. The method of any of the preceding claims wherein the nanoparticle composition is incubated at a temperature lower than 100°C.
- 25 4. The method of any of the preceding claims wherein the nanoparticle composition is incubated at a temperature between 10°C and 80°C, such as between 22°C to 80°C, or such as between 30°C to 80°C.
- 30 5. The method of any of the preceding claims wherein the nanoparticle composition is incubated for a time period shorter than 48 hours.
- 35 6. The method of any of the preceding claims wherein the nanoparticle composition is incubated for a time period of 1 to 240 minutes.

7. The method of any of the preceding claims wherein the nanoparticle composition is incubated for a time period which is between 1 min to 120 min.
- 5 8. The method of any of the preceding claims wherein the nanoparticle composition is incubated for a time period which is between 1 min to 60 min.
9. The method of any of the preceding claims, wherein the loading efficiency when using incubation times of 1 to 240 minutes is in the range of 10% to 100%.
- 10 10. The method of any of the preceding claims, wherein the loading efficiency when using incubation times of 1 to 240 minutes is in the range of 80% to 100%
11. The method of any of the preceding claims, wherein the loading efficiency when using incubation times of 1 to 240 minutes is in the range of 95% to 100%.
- 15 12. The method of any of the preceding claims, wherein the incubation temperature for loading of nanoparticles is in the range of 30°C to 80°C and wherein the loading efficiency when using incubation times of 1 to 240 minutes is in the range of 10% to 100%.
- 20 13. The method of any of the preceding claims, wherein the incubation temperature for loading of nanoparticles is in the range of 30°C to 80°C and the loading efficiency when using incubation times of 1 to 60 minutes is in the range of 10% to 100%.
- 25 14. The method of any of the preceding claims, wherein the incubation temperature for loading of nanoparticles is in the range of 30°C to 80°C and the loading efficiency when using incubation times of 1 to 60 minutes is in range of 80% to 100%.
- 30 15. The method of any of the preceding claims, wherein the incubation temperature for loading of nanoparticles is in the range of 40°C to 80°C and the loading efficiency when using incubation times of 1 to 60 minutes is in the range of 95% to 100%.
- 35



16. The method of any of the preceding claims wherein the metal entities are cations.
17. The method of any of the preceding claims wherein said cation metal entities  
5 are divalent or trivalent cations and/or wherein said metal entities are divalent or trivalent cations.
18. The method of any of the preceding claims wherein the metal entities comprise  
10 one or more radionuclides selected from the group consisting of Copper ( $^{61}\text{Cu}$ ,  $^{64}\text{Cu}$ , and  $^{67}\text{Cu}$ ), Indium ( $^{111}\text{In}$ ), Technetium ( $^{99\text{m}}\text{Tc}$ ), Rhenium ( $^{186}\text{Re}$ ,  $^{188}\text{Re}$ ), Gallium ( $^{67}\text{Ga}$ ,  $^{68}\text{Ga}$ ), Strontium ( $^{89}\text{Sr}$ ), Samarium ( $^{153}\text{Sm}$ ), Ytterbium ( $^{169}\text{Yb}$ ), Thallium ( $^{201}\text{Tl}$ ), Astatine ( $^{211}\text{At}$ ), Lutetium ( $^{177}\text{Lu}$ ), Actinium ( $^{225}\text{Ac}$ ), Yttrium ( $^{90}\text{Y}$ ), Antimony ( $^{119}\text{Sb}$ ), Tin ( $^{117}\text{Sn}$ ,  $^{113}\text{Sn}$ ), Dysprosium ( $^{159}\text{Dy}$ ), Cobalt ( $^{56}\text{Co}$ ), Iron ( $^{59}\text{Fe}$ ), Ruthenium ( $^{97}\text{Ru}$ ,  $^{103}\text{Ru}$ ), Palladium ( $^{103}\text{Pd}$ ), Cadmium ( $^{115}\text{Cd}$ ), Tellurium  
15 ( $^{118}\text{Te}$ ,  $^{123}\text{Te}$ ), Barium ( $^{131}\text{Ba}$ ,  $^{140}\text{Ba}$ ), Gadolinium ( $^{149}\text{Gd}$ ,  $^{151}\text{Gd}$ ), Terbium ( $^{160}\text{Tb}$ ), Gold ( $^{198}\text{Au}$ ,  $^{199}\text{Au}$ ), Lanthanum ( $^{140}\text{La}$ ), and Radium ( $^{223}\text{Ra}$ ,  $^{224}\text{Ra}$ ).
19. The method of any of the preceding claims, wherein the metal entities are  
20 radionuclides selected from the group consisting of  $^{61}\text{Cu}$ ,  $^{64}\text{Cu}$ ,  $^{67}\text{Cu}$ ,  $^{177}\text{Lu}$ ,  $^{67}\text{Ga}$ ,  $^{68}\text{Ga}$ ,  $^{225}\text{Ac}$ ,  $^{90}\text{Y}$ ,  $^{186}\text{Re}$ ,  $^{188}\text{Re}$ ,  $^{119}\text{Sb}$  and  $^{111}\text{In}$ .
20. The method of any of the preceding claims wherein the metal entities are  
25 radionuclides selected from the group consisting of  $^{61}\text{Cu}$ ,  $^{64}\text{Cu}$ ,  $^{67}\text{Cu}$ ,  $^{111}\text{In}$  and  $^{177}\text{Lu}$ .
21. The method of any of the preceding claims wherein the metal entities are  
radionuclides selected from the group consisting of  $^{61}\text{Cu}$ ,  $^{64}\text{Cu}$  and  $^{67}\text{Cu}$ .
22. The method of any of the preceding claims wherein one or more metal entities  
30 are selected from the group of Gd, Dy, Ti, Cr, Mn, Fe, Co, Ni including divalent or trivalent ions thereof.
23. The method of any of the preceding claims wherein the metal entities are  
combinations selected from the group of  $^{64}\text{Cu}$  and Gd(III),  $^{64}\text{Cu}$  and Dy(III),

<sup>64</sup>Cu and Ti(II), <sup>64</sup>Cu and Cr(III), <sup>64</sup>Cu and Mn(II), <sup>64</sup>Cu and Fe(II), <sup>64</sup>Cu and Fe(III), <sup>64</sup>Cu and Co(II), <sup>64</sup>Cu and Ni(II), <sup>68</sup>Ga and Gd(III), <sup>68</sup>Ga and Dy(III), <sup>68</sup>Ga and Ti(II), <sup>68</sup>Ga and Cr(III), <sup>68</sup>Ga and Mn(II), <sup>68</sup>Ga and Fe(II), <sup>68</sup>Ga and Fe(III), <sup>68</sup>Ga and Co(II), <sup>68</sup>Ga and Ni(II), <sup>111</sup>In and Gd(III), <sup>111</sup>In and Dy(III), <sup>111</sup>In and Ti(II), <sup>111</sup>In and Cr(III), <sup>111</sup>In and Mn(II), <sup>111</sup>In and Fe(II), <sup>111</sup>In and Fe(III), <sup>111</sup>In and Co(II), <sup>111</sup>In and Ni(II), <sup>99m</sup>Tc and Gd(III), <sup>99m</sup>Tc and Dy(III), <sup>99m</sup>Tc and Ti(II), <sup>99m</sup>Tc and Cr(III), <sup>99m</sup>Tc and Mn(II), <sup>99m</sup>Tc and Fe(II), <sup>99m</sup>Tc and Fe(III), <sup>99m</sup>Tc and Co(II), <sup>99m</sup>Tc and Ni(II), <sup>177</sup>Lu and Gd(III), <sup>177</sup>Lu and Dy(III), <sup>177</sup>Lu and Ti(II), <sup>177</sup>Lu and Cr(III), <sup>177</sup>Lu and Mn(II), <sup>177</sup>Lu and Fe(II), <sup>177</sup>Lu and Fe(III), <sup>177</sup>Lu and Co(II), <sup>177</sup>Lu and Ni(II), <sup>67</sup>Ga and Gd(III), <sup>67</sup>Ga and Dy(III), <sup>67</sup>Ga and Ti(II), <sup>67</sup>Ga and Cr(III), <sup>67</sup>Ga and Mn(II), <sup>67</sup>Ga and Fe(II), <sup>67</sup>Ga and Fe(III), <sup>67</sup>Ga and Co(II), <sup>67</sup>Ga and Ni(II), <sup>201</sup>Tl and Gd(III), <sup>201</sup>Tl and Dy(III), <sup>201</sup>Tl and Ti(II), <sup>201</sup>Tl and Cr(III), <sup>201</sup>Tl and Mn(II), <sup>201</sup>Tl and Fe(II), <sup>201</sup>Tl and Fe(III), <sup>201</sup>Tl and Co(II), <sup>201</sup>Tl and Ni(II), <sup>90</sup>Y and Gd(III), <sup>90</sup>Y and Dy(III), <sup>90</sup>Y and Ti(II), <sup>90</sup>Y and Cr(III), <sup>90</sup>Y and Mn(II), <sup>90</sup>Y and Fe(II), <sup>90</sup>Y and Fe(III), <sup>90</sup>Y and Co(II) and <sup>90</sup>Y and Ni(II), wherein said isotope of metal radionuclide may appear in any of the existing oxidation states for the metal including monovalent cations, divalent cations, trivalent cations, tetravalent cations, pentavalent cations, hexavalent cations and heptavalent cations.

20

24. The method of any of the preceding claims wherein the metal entities are two or more radionuclides selected from the group defined in claim 18.

25. The method of any of the preceding claims, wherein the metal entities are two or more radionuclides selected from the group consisting of <sup>64</sup>Cu and <sup>67</sup>Cu, <sup>61</sup>Cu and <sup>67</sup>Cu, <sup>64</sup>Cu and <sup>90</sup>Y, <sup>64</sup>Cu and <sup>119</sup>Sb, <sup>64</sup>Cu and <sup>225</sup>Ac, <sup>64</sup>Cu and <sup>188</sup>Re, <sup>64</sup>Cu and <sup>186</sup>Re, <sup>64</sup>Cu and <sup>211</sup>At, <sup>64</sup>Cu and <sup>67</sup>Ga, <sup>61</sup>Cu and <sup>177</sup>Lu, <sup>61</sup>Cu and <sup>90</sup>Y, <sup>61</sup>Cu and <sup>119</sup>Sb, <sup>61</sup>Cu and <sup>225</sup>Ac, <sup>61</sup>Cu and <sup>188</sup>Re, <sup>61</sup>Cu and <sup>186</sup>Re, <sup>61</sup>Cu and <sup>211</sup>At, <sup>61</sup>Cu and <sup>67</sup>Ga, <sup>67</sup>Cu and <sup>177</sup>Lu, <sup>67</sup>Cu and <sup>90</sup>Y, <sup>67</sup>Cu and <sup>119</sup>Sb, <sup>67</sup>Cu and <sup>225</sup>Ac, <sup>67</sup>Cu and <sup>188</sup>Re, <sup>67</sup>Cu and <sup>186</sup>Re, <sup>67</sup>Cu and <sup>211</sup>At, <sup>68</sup>Ga and <sup>177</sup>Lu, <sup>68</sup>Ga and <sup>90</sup>Y, <sup>68</sup>Ga and <sup>119</sup>Sb, <sup>68</sup>Ga and <sup>225</sup>Ac, <sup>68</sup>Ga and <sup>188</sup>Re, <sup>68</sup>Ga and <sup>186</sup>Re, <sup>68</sup>Ga and <sup>211</sup>At, and <sup>68</sup>Ga and <sup>67</sup>Cu.

26. The method of any of the preceding claims, wherein the metal entities are two or more radionuclides selected from the group consisting of Copper (<sup>61</sup>Cu, <sup>64</sup>Cu,

35

and  $^{67}\text{Cu}$ ), such as  $^{61}\text{Cu}$  and  $^{64}\text{Cu}$ , or  $^{61}\text{Cu}$  and  $^{67}\text{Cu}$ , or  $^{64}\text{Cu}$  and  $^{67}\text{Cu}$ , or  $^{61}\text{Cu}$ ,  $^{64}\text{Cu}$  and  $^{67}\text{Cu}$ .

- 5 27. The method of any of the preceding claims, wherein there is a difference in osmotic pressure between the exterior of the nanoparticles and the interior of the nanoparticles during incubation.
- 10 28. The method of claim 27 wherein the difference in osmotic pressure between the exterior of the nanoparticles and the interior of the nanoparticles is 5-800 mOsm/L.
- 15 29. The method of claims 27-28 wherein the difference in osmotic pressure between the exterior of the nanoparticles and the interior of the nanoparticles is 5-100 mOsm/L.
- 20 30. The method of any of the preceding claims, wherein said vesicle-forming component comprises one or more of the compounds selected from the group consisting of lipids, ceramides, sphingolipids, phospholipids, pegylated phospholipids.
- 25 31. The method of any of the preceding claims, wherein the vesicle forming component comprises one or more amphiphatic compounds selected from the group of HSPC, DSPC, DPPC, POPC, CHOL, DSPE-PEG-2000 and DSPE-PEG-2000-TATE.
- 30 32. The method of any of the preceding claims, wherein said agent-entrapping component is selected from the group consisting of chelators, reducing agents and agents that form low solubility salts with said radionuclides.
33. The method of any of the preceding claims, wherein said agent-entrapping component is a chelator selected from the group consisting of 1,4,7,10-tetraazacyclododecane ( $^{12}\text{aneN}_4$ ); 1,4,7,10-tetraazacyclotridecane ( $^{13}\text{aneN}_4$ ); 1,4,8,11-tetraazacyclotetradecane ( $^{14}\text{aneN}_4$ ); 1,4,8,12-tetraazacyclopentadecane ( $^{15}\text{aneN}_4$ ); 1,5,9,13-tetraazacyclohexadecane

([16]aneN4); ethylene-diamine-tetraacetic-acid (EDTA); and diethylene-triamine-penta-acetic acid (DTPA).

- 5 34. The method of any of the preceding claims, wherein said agent-entrapping component is a chelator selected from the group consisting of 1,4-ethano-1,4,8,11-tetraazacyclotetradecane (et-cyclam); 1,4,7,11-tetraazacyclotetradecane (iso-cyclam); 1,4,7,10-tetraazacyclododecane-1,4,7,10-tetraacetic acid (DOTA); 2-(1,4,7,10-tetraazacyclododecan-1-yl)acetate (DO1A); 2,2'-(1,4,7,10-tetraazacyclododecane-1,7-diyl) diacetic acid (DO2A); 2,2',2''-(1,4,7,10-tetraazacyclododecane-1,4,7-triyl) triacetic acid (DO3A); 1,4,7,10-tetraazacyclododecane-1,4,7,10-tetra(methanephosphonic acid) (DOTP); 1,4,7,10-tetraazacyclododecane-1,7-di(methanephosphonic acid) (DO2P); 1,4,7,10-tetraazacyclododecane-1,4,7-tri(methanephosphonic acid) (DO3P); 1,4,8,11-15 tetraazacyclotetradecane-1,4,8,11-tetraacetic acid (TETA); 15 2-(1,4,8,11-tetraazacyclotetradecane-1-yl) acetic acid (TE1A); 2,2'-(1,4,8,11-tetraazacyclotetradecane-1,8-diyl) diacetic acid (TE2A); ethylene-diamine-tetraacetic-acid (EDTA), and diethylene-triamine-penta-acetic acid (DTPA).
- 20 35. The method of any of the preceding claims, wherein said agent-entrapping component is a chelator selected from the group consisting of 1,4,7,10-tetraazacyclododecane-1,4,7,10-tetraacetic acid (DOTA), 1,4,8,11-15 tetraazacyclotetradecane-1,4,8,11-tetraacetic acid (TETA), 1,4,7,10-tetraazacyclododecane-1,4,7,10-tetra(methanephosphonic acid) (DOTP), cyclam and cyclen.
- 25 36. The method of any of the preceding claims, wherein said agent-entrapping component is a reducing agent selected from the group consisting of ascorbic acid, glucose, fructose, glyceraldehyde, lactose, arabinose, maltose and acetol.
- 30 37. The method of any of the preceding claims, wherein the interior pH of the nanoparticle is within the range of 4 to 8.5, such as 4.0 to 4.5, or such as 4.5 to 5.0, or such as 5.0 to 5.5, or such as 5.5 to 6.0, or such as 6.0 to 6.5, or such as 6.5 to 7.0, or such as 7.0 to 7.5, or such as 7.5 to 8.0, or such as 8 to 8.5.

38. The method of any of the preceding claims, wherein the stability of the radiolabeled nanoparticles is such that less than 20% leakage of radioactivity is observed, for example less than 15% leakage, such as less than 12% leakage, for example less than 10% leakage, such as less than 8% leakage, for example less than 6% leakage, such as less than 4% leakage, for example less than 3% leakage, such as less than 2% leakage, for example less than 1% leakage.

39. A kit of parts for loading of nanoparticles without the use of ionophores comprising:

10 a. A nanoparticle composition comprising i) a vesicle forming component, and ii) an agent-entrapping component enclosed by the vesicle forming component; and

b. A composition containing a metal entity for loading into the nanoparticle,

15

40. The kit of parts according to claim 39 wherein the metal entity comprises one or more radionuclides as defined in claim 16 to 26.

41. The kit of parts according to claims 39 to 40, wherein the metal entity is one or more radionuclide isotopes selected from of copper ( $^{61}\text{Cu}$ ,  $^{64}\text{Cu}$ , and  $^{67}\text{Cu}$ ).

20

42. A nanoparticle composition prepared by use of the method as defined in claims 1 to 38.

25 43. The nanoparticle composition of claim 42 loaded with metal entities comprising:

i. a vesicle forming component,

ii. an agent-entrapping component enclosed by said vesicle-forming component;

iii. a metal entity entrapped on the interior side of the nanoparticle composition,

30

said nanoparticle composition being devoid of any trace of ionophore.

44. The nanoparticle composition of claims 42 to 43 wherein the metal entity comprises one or more metal entities as defined in claims 16 to 26.

35

45. The nanoparticle composition of claims 42 to 44, further comprising an amphiphatic compound derivatized with PEG.
- 5 46. The nanoparticle composition of claims 42 to 45, wherein the vesicle-forming component comprises one or more amphiphatic compounds.
- 10 47. The nanoparticle composition of claims 42 to 46, wherein the vesicle forming component comprises one or more amphiphatic compounds selected from the group of HSPC, DSPC, POPC, DPPC, CHOL, DSPE-PEG-2000 and DSPE-PEG-2000-TATE.
- 15 48. The nanoparticle composition of claims 42 to 47, wherein said agent-entrapping component is a chelator.
- 20 49. The nanoparticle composition of claims 42 to 48, wherein said agent-entrapping component is a chelator selected from the group of 1,4,7,10-tetraazacyclododecane-1,4,7,10-tetraacetic acid (DOTA), 1,4,8,11-15 tetraazacyclotetradecane-1,4,8,11-tetraacetic acid (TETA), 1,4,7,10-tetraazacyclododecane-1,4,7,10-tetra(methanephosphonic acid) (DOTP), cyclam and cyclen.
- 25 50. The nanoparticle composition of claims 42 to 49, wherein the metal entity comprises one or more radionuclides selected from the group consisting of  $^{61}\text{Cu}$ ,  $^{64}\text{Cu}$ ,  $^{67}\text{Cu}$ ,  $^{177}\text{Lu}$ ,  $^{67}\text{Ga}$ ,  $^{68}\text{Ga}$ ,  $^{225}\text{Ac}$ ,  $^{90}\text{Y}$ ,  $^{186}\text{Re}$ ,  $^{188}\text{Re}$ ,  $^{119}\text{Sb}$ .
- 30 51. The nanoparticle composition of claims 42 to 50 wherein the metal entity comprises two radionuclides selected from the group consisting of  $^{64}\text{Cu}$  and  $^{67}\text{Cu}$ ,  $^{61}\text{Cu}$  and  $^{67}\text{Cu}$ ,  $^{64}\text{Cu}$  and  $^{90}\text{Y}$ ,  $^{64}\text{Cu}$  and  $^{119}\text{Sb}$ ,  $^{64}\text{Cu}$  and  $^{225}\text{Ac}$ ,  $^{64}\text{Cu}$  and  $^{188}\text{Re}$ ,  $^{64}\text{Cu}$  and  $^{186}\text{Re}$ ,  $^{64}\text{Cu}$  and  $^{211}\text{At}$ ,  $^{64}\text{Cu}$  and  $^{67}\text{Ga}$ ,  $^{61}\text{Cu}$  and  $^{177}\text{Lu}$ ,  $^{61}\text{Cu}$  and  $^{90}\text{Y}$ ,  $^{61}\text{Cu}$  and  $^{119}\text{Sb}$ ,  $^{61}\text{Cu}$  and  $^{225}\text{Ac}$ ,  $^{61}\text{Cu}$  and  $^{188}\text{Re}$ ,  $^{61}\text{Cu}$  and  $^{186}\text{Re}$ ,  $^{61}\text{Cu}$  and  $^{211}\text{At}$ ,  $^{61}\text{Cu}$  and  $^{67}\text{Ga}$ ,  $^{67}\text{Cu}$  and  $^{177}\text{Lu}$ ,  $^{67}\text{Cu}$  and  $^{90}\text{Y}$ ,  $^{67}\text{Cu}$  and  $^{119}\text{Sb}$ ,  $^{67}\text{Cu}$  and  $^{225}\text{Ac}$ ,  $^{67}\text{Cu}$  and  $^{188}\text{Re}$ ,  $^{67}\text{Cu}$  and  $^{186}\text{Re}$ ,  $^{67}\text{Cu}$  and  $^{211}\text{At}$ ,  $^{68}\text{Ga}$  and  $^{177}\text{Lu}$ ,  $^{68}\text{Ga}$  and  $^{90}\text{Y}$ ,  $^{68}\text{Ga}$  and  $^{119}\text{Sb}$ ,  $^{68}\text{Ga}$  and  $^{225}\text{Ac}$ ,  $^{68}\text{Ga}$  and  $^{188}\text{Re}$ ,  $^{68}\text{Ga}$  and  $^{186}\text{Re}$ ,  $^{68}\text{Ga}$  and  $^{211}\text{At}$ , and  $^{68}\text{Ga}$  and  $^{67}\text{Cu}$ .
- 35

52. The nanoparticle composition of claims 42 to 51, further comprising a targeting moiety selected from the group consisting of antibodies, affibodies, and peptide components.
- 5 53. The nanoparticle composition of claims 42 to 52, comprising a compound with intracellular targeting properties such as nuclear localization sequence peptide (NLS peptide) which is conjugated to the agent-entrapping component.
- 10 54. The nanoparticle composition of claims 42 to 53, wherein the interior pH of the nanoparticle is within the range of 4 to 8.5, such as 4.0 to 4.5, or such as 4.5 to 5.0, such as 5.0 to 5.5, or such as 5.5 to 6.0, or such as 6.0 to 6.5, or such as 6.5 to 7.0, or such as 7.0 to 7.5, or such as 7.5 to 8.0, or such as 8.0 to 8.5.
- 15 55. The nanoparticle composition of claims 42 to 54, wherein the interior pH of the nanoparticle is within the range of 6 to 8, such as 6.0 to 6.5, such as 6.5 to 7.0, such as 7.0 to 7.5, such as 7.5 to 8.
- 20 56. The nanoparticle composition of claims 42 to 55, wherein the diameter of the nanoparticle is in the range of 30 nm to 1000 nm.
- 25 57. The nanoparticle composition of claims 42 to 56, wherein the stability of the radiolabeled nanoparticles is such that less than 20% leakage is observed, such as less than 15% leakage, such as less than 12% leakage, for example less than 10% leakage, such as less than 8% leakage, for example less than 6% leakage, such as less than 4% leakage, for example less than 3% leakage, such as less than 2% leakage, for example less than 1% leakage.
- 30 58. The nanoparticle composition of claims 42 to 57 for use in a method for treating, monitoring, monitoring treatment efficiency or diagnosis in a subject in need.
- 35 59. The nanoparticle composition of claims 42 to 58 for use in imaging.
60. The nanoparticle composition of claims 42 to 59 for use in positron emission tomography (PET) scanning and/or single photon emission computed tomography (SPECT) scanning and/or magnetic resonance imaging (MRI).

61. The nanoparticle composition of claims 42 to 60 for use as a medicament.

5



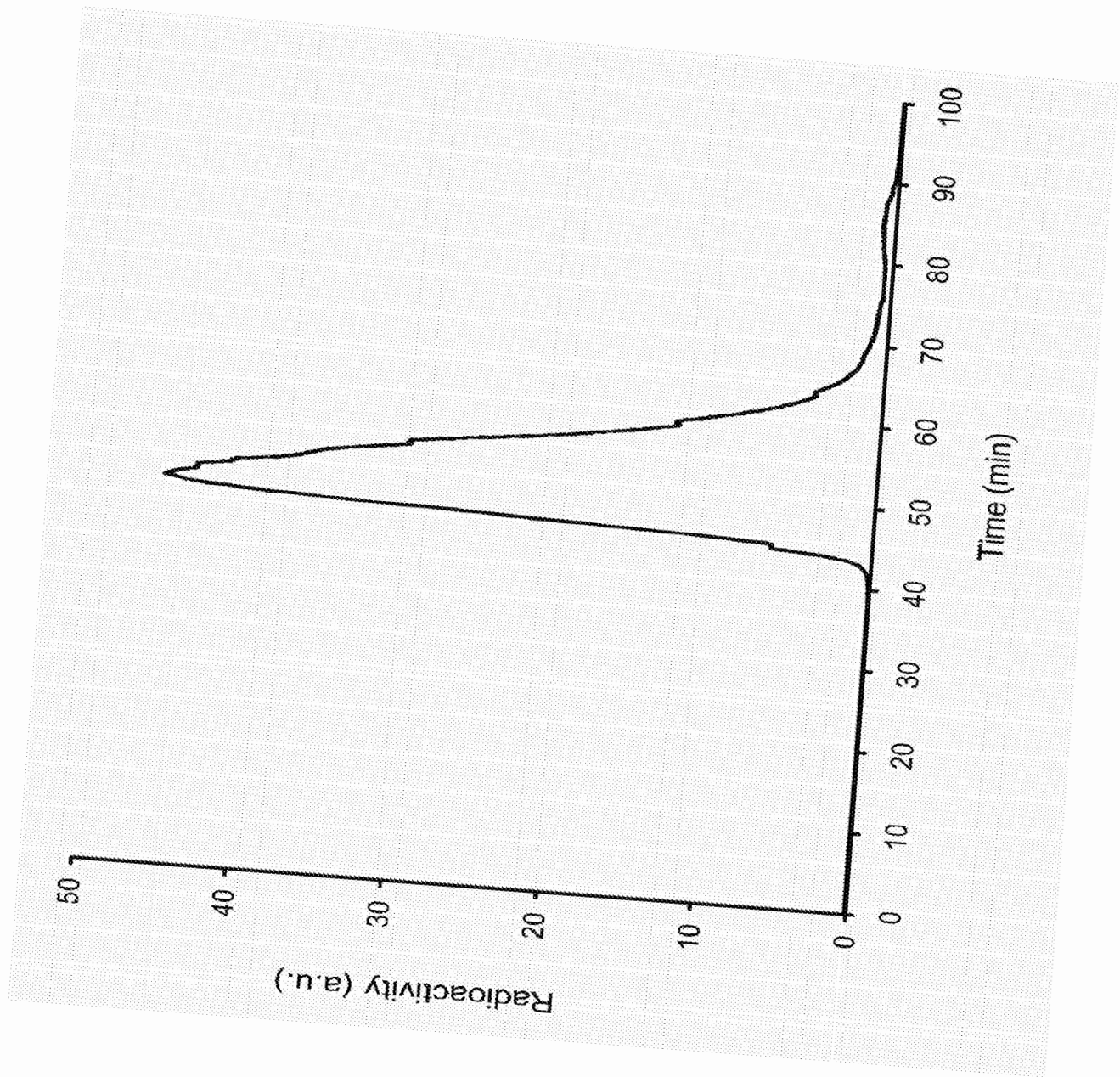


Fig. 1

2 / 7

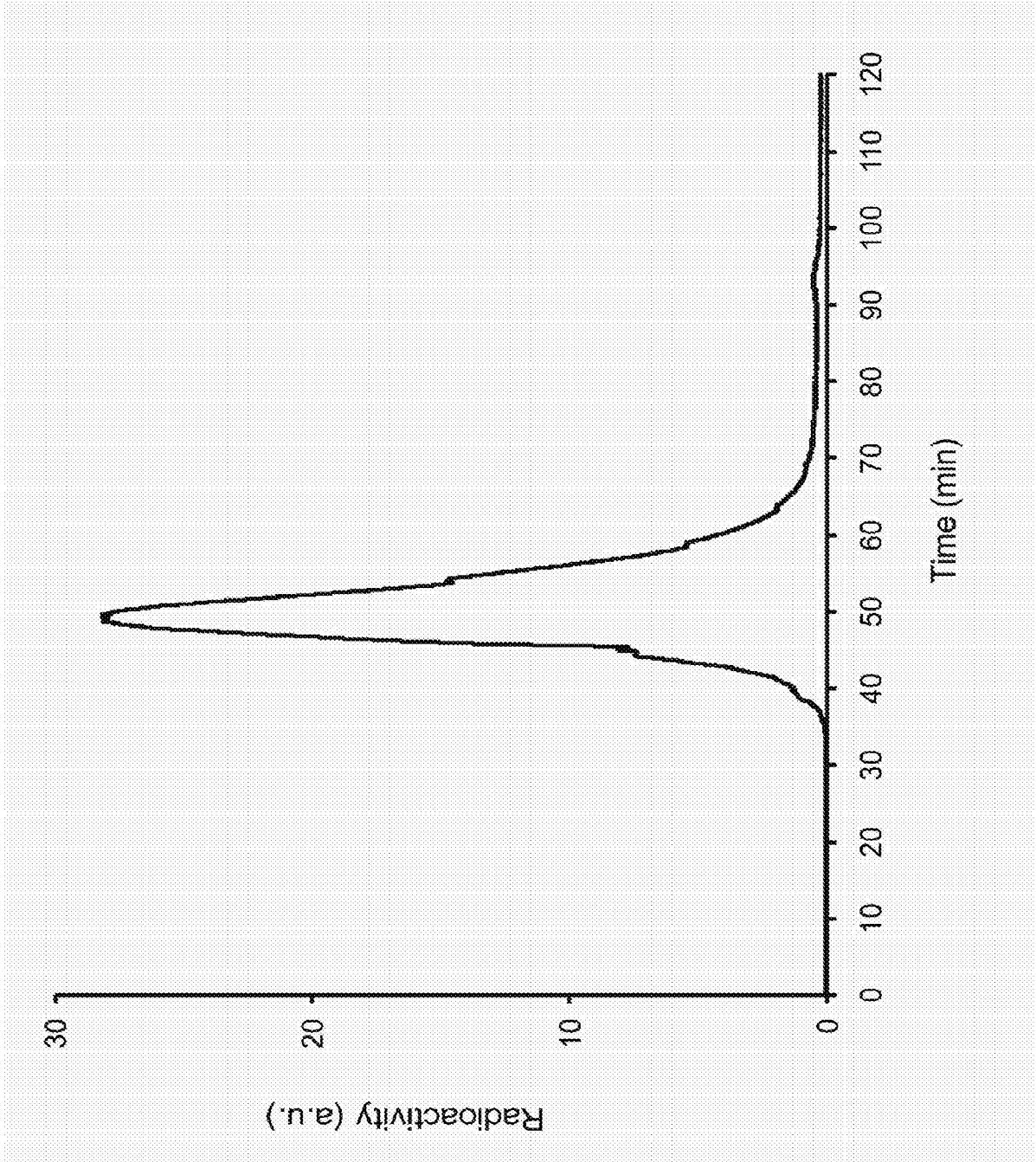


Fig. 2

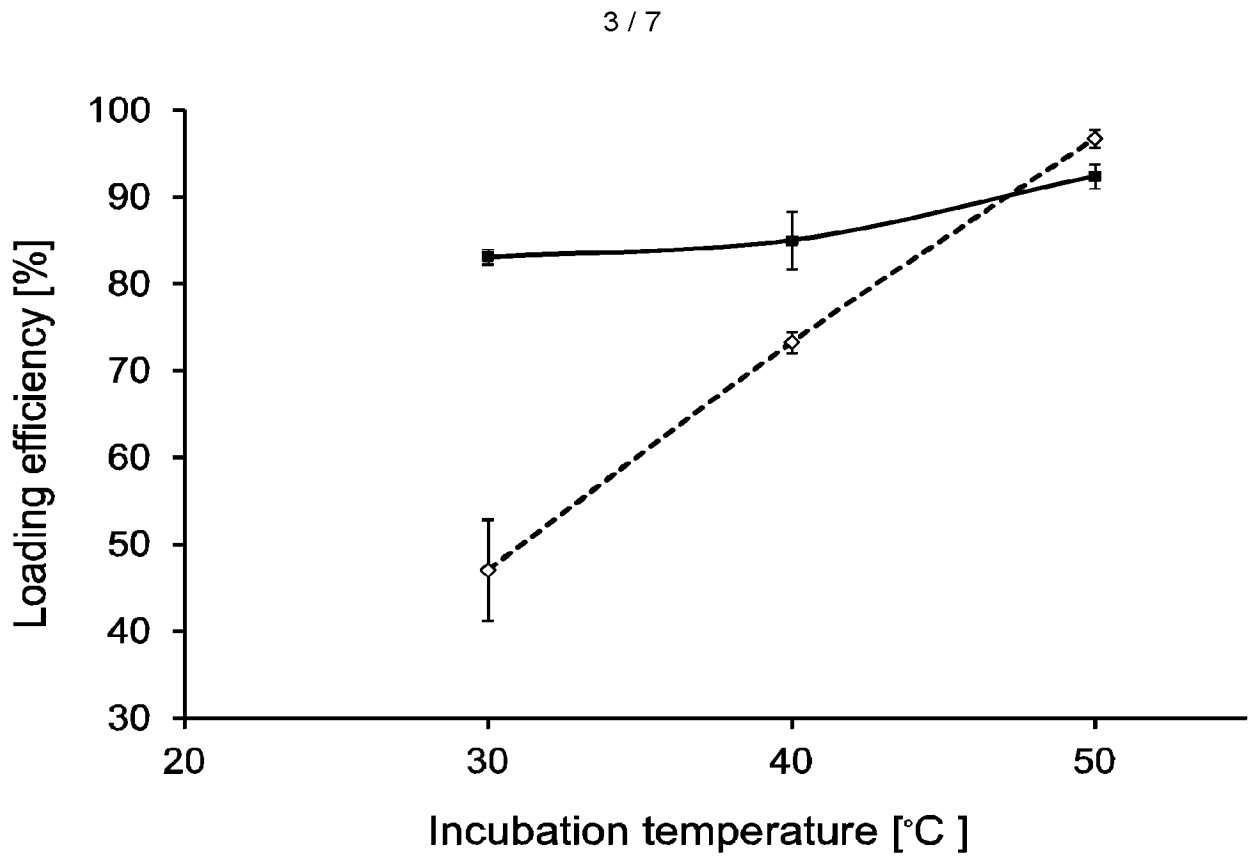


Fig. 3

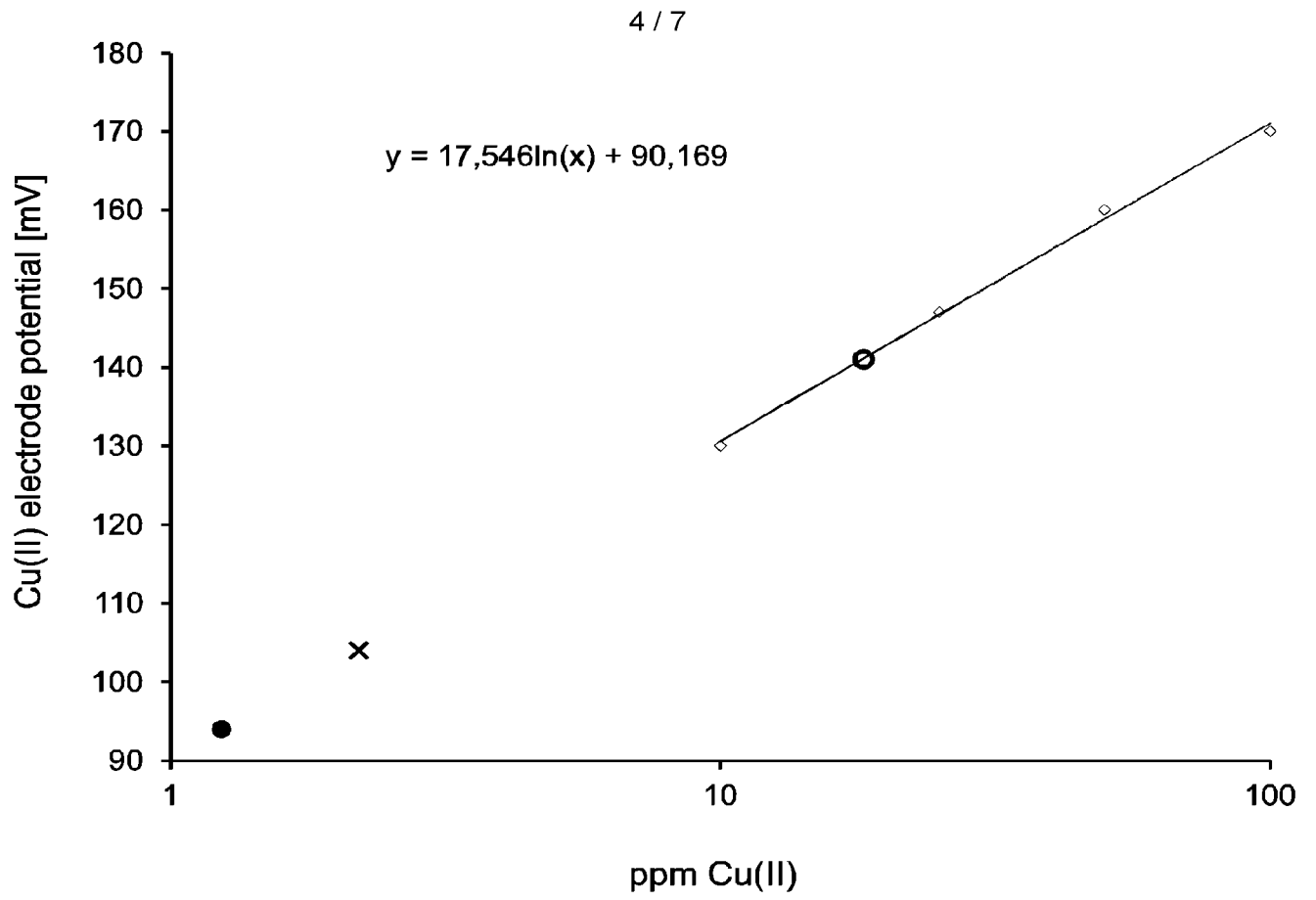


Fig. 4

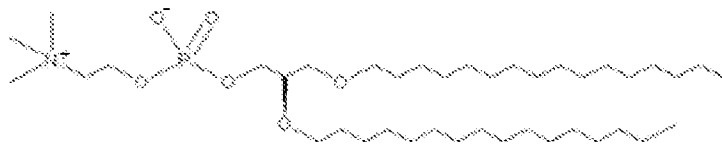


Fig. 5

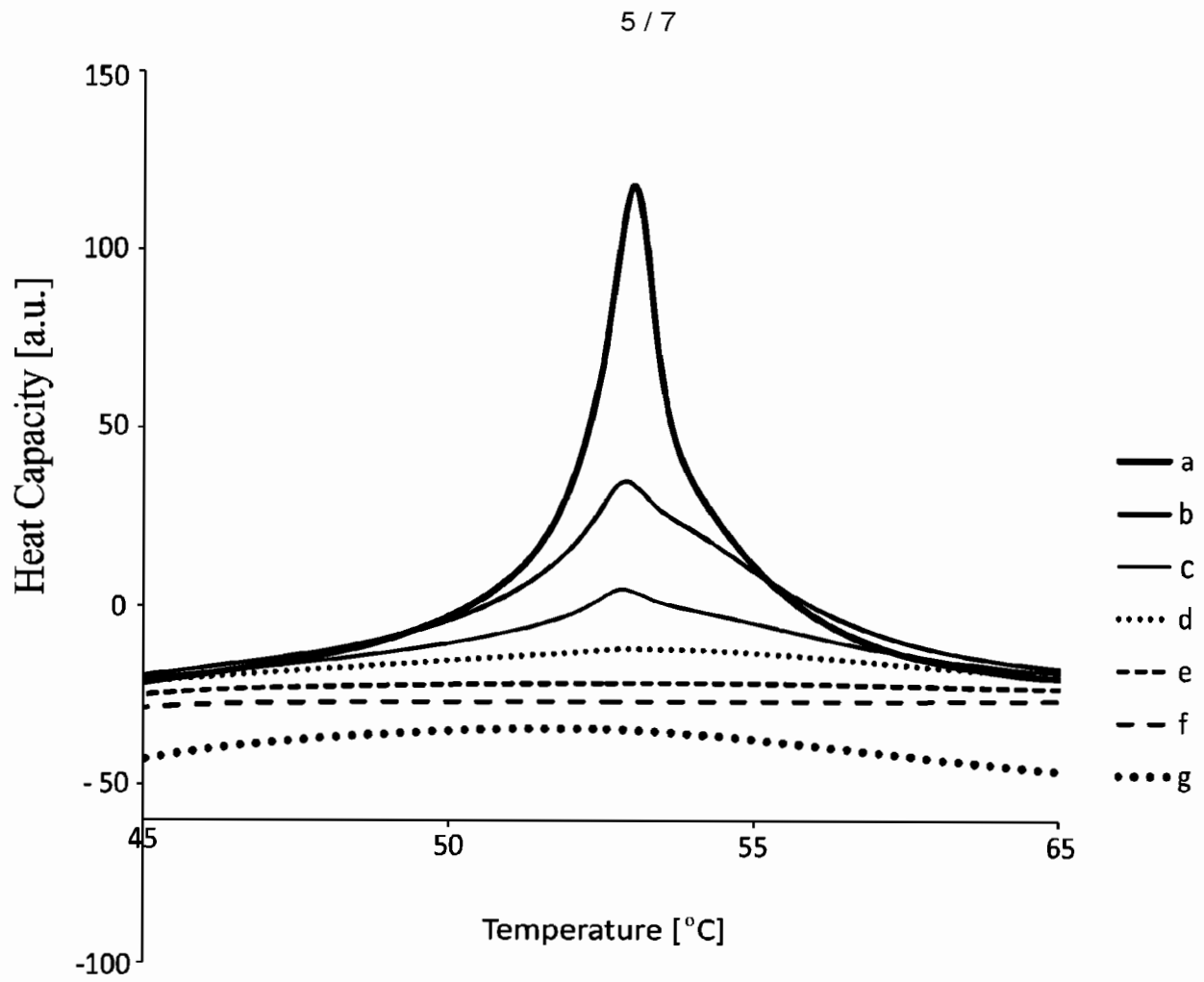


Fig. 6

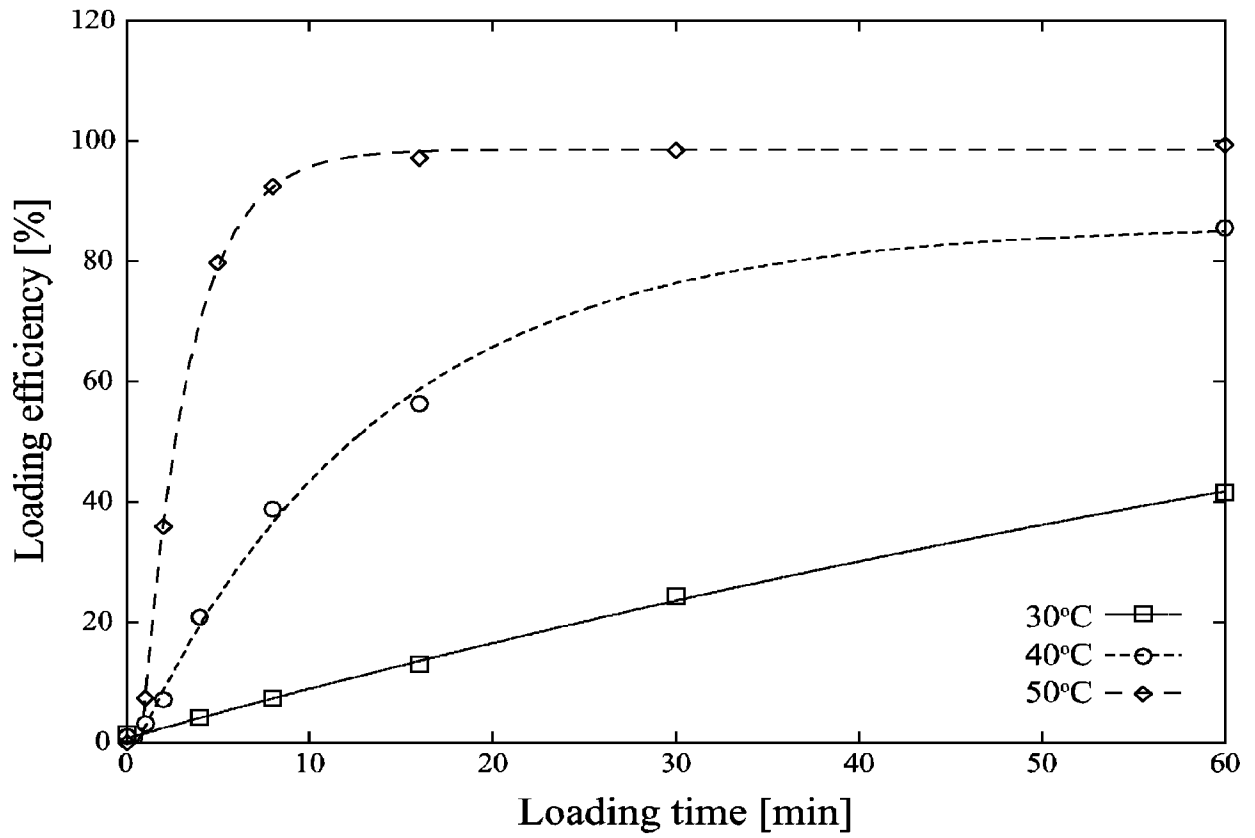


Fig. 7

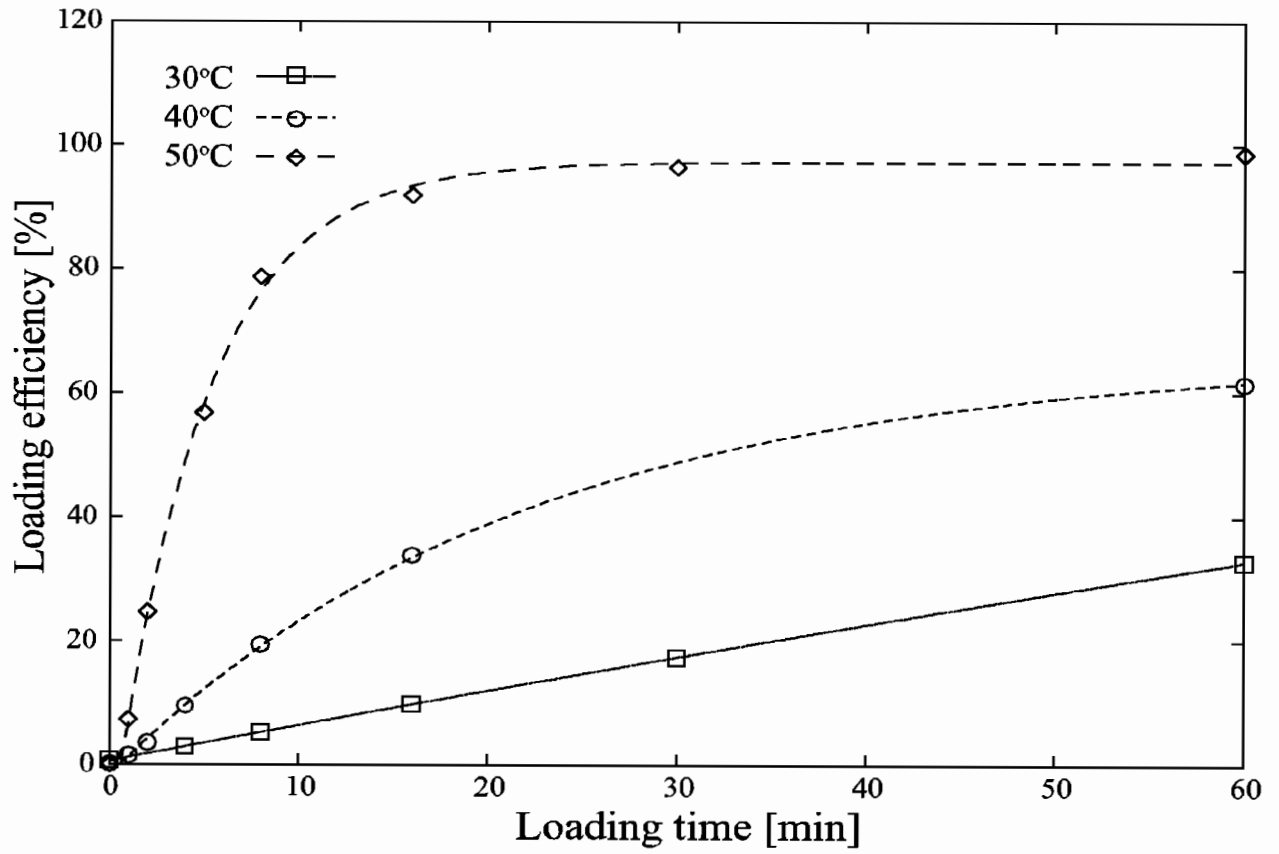


Fig. 8

INTERNATIONAL SEARCH REPORT

International application No

PCT/DK2011/050479

A. CLASSIFICATION OF SUBJECT MATTER  
 INV. A61K47/28 A61K47/44 A61K51/12  
 ADD.  
 According to International Patent Classification (IPC) or to both national classification and IPC

B. FIELDS SEARCHED

Minimum documentation searched (classification system followed by classification symbols)  
 A61K

Documentation searched other than minimum documentation to the extent that such documents are included in the fields searched

Electronic data base consulted during the international search (name of data base and, where practical, search terms used)  
 EPO-Internal

C. DOCUMENTS CONSIDERED TO BE RELEVANT

Category*	Citation of document, with indication, where appropriate, of the relevant passages	Relevant to claim No.
X	WO 2006/043083 A2 (ALGETA ASA) 27 April 2006 (2006-04-27) page 18, lines 29-34 page 6, lines 18-30 pages 17-19; claims 1-5 page 23, line 27 - page 24, line 25; claims 10, 12, 21 -----	1-5, 10-15
X Y	US 4 310 506 A (BALDESCHWIELER JOHN D ET AL) 12 January 1982 (1982-01-12) column 7, lines 3-8, 41-45 column 2, lines 8-13; claim 1 column 3, lines 36-37 column 5, line 68 - column 6, line 2; example II column 6, lines 64-66; example II column 6, lines 66-68 - column 7, lines 45-48; example II ----- -/--	1-5,7,8, 10-15 2-14

Further documents are listed in the continuation of Box C.

See patent family annex.

\* Special categories of cited documents :

"A" document defining the general state of the art which is not considered to be of particular relevance  
 "E" earlier document but published on or after the international filing date  
 "L" document which may throw doubts on priority claim(s) or which is cited to establish the publication date of another citation or other special reason (as specified)  
 "O" document referring to an oral disclosure, use, exhibition or other means  
 "P" document published prior to the international filing date but later than the priority date claimed

"T" later document published after the international filing date or priority date and not in conflict with the application but cited to understand the principle or theory underlying the invention  
 "X" document of particular relevance; the claimed invention cannot be considered novel or cannot be considered to involve an inventive step when the document is taken alone  
 "Y" document of particular relevance; the claimed invention cannot be considered to involve an inventive step when the document is combined with one or more other such documents, such combination being obvious to a person skilled in the art.  
 "&" document member of the same patent family

Date of the actual completion of the international search  8 March 2012	Date of mailing of the international search report  15/03/2012
---	--

Name and mailing address of the ISA/ European Patent Office, P.B. 5818 Patentlaan 2 NL - 2280 HV Rijswijk Tel. (+31-70) 340-2040, Fax: (+31-70) 340-3016	Authorized officer  Kanbier, Titia
--	--



## INTERNATIONAL SEARCH REPORT

International application No

PCT/DK2011/050479

C(Continuation). DOCUMENTS CONSIDERED TO BE RELEVANT

Category*	Citation of document, with indication, where appropriate, of the relevant passages	Relevant to claim No.
X	US 2009/081121 A1 (TING GANN [TW] ET AL) 26 March 2009 (2009-03-26) paragraphs [0063] - [0064], [0067] - [0069]; claims 1, 3, 7, 9, 10, 12, 15, 18 paragraphs [0012] - [0013], [0046] - [0055] -----	1,3-5,7, 8,10-15
X	WO 2004/082626 A2 (ETHICON INC) 30 September 2004 (2004-09-30) cited in the application pages 27-28; example 1 -----	1,3-5,7, 8,10-15
X	EP 1 486 216 A1 (AMATO PHARM PROD LTD) 15 December 2004 (2004-12-15)  paragraphs [0053], [0055], [0067] sentences 18-19, paragraph 73 - sentences 30-32, paragraph 74 -----	1,3,4,7, 8,10-12, 14,15
X	WO 01/60417 A2 (ANTICANCER THERAPEUTIC INV S A) 23 August 2001 (2001-08-23) cited in the application claims 1-3, 12, 14-15, 24, 26-32; examples 7-9 -----	1,3-5, 10-15
Y	FISCHER P W F ET AL: "Copper transport by intestinal brush border membrane vesicles from rats fed high zinc or copper deficient diets", NUTRITION RESEARCH 1985 US, vol. 5, no. 7, 1985, pages 759-767, XP002650386, ISSN: 0271-5317 page 766, paragraph 1-2 page 761, line 1, paragraph 3; figure 4 -----	2-14
Y	WO 03/041682 A2 (CELATOR TECHNOLOGIES INC) 22 May 2003 (2003-05-22) page 6, paragraph 20-21; claims 1-3, 5, 9, 14-15 paragraphs [0039] - [0043] page 12, paragraph 47-51 claim 9; figure 7; examples 3, 5, 7, 8 -----	2-11
A	HENRIKSEN G ET AL: "Sterically stabilized liposomes as a carrier for alpha-emitting radium and actinium radionuclides", NUCLEAR MEDICINE AND BIOLOGY, ELSEVIER, NY, US, vol. 31, no. 4, 1 May 2004 (2004-05-01), pages 441-449, XP004503655, ISSN: 0969-8051, DOI: DOI:10.1016/J.NUCMEDBIO.2003.11.004 pages 443-4 -----	1-15
	----- -/--	

INTERNATIONAL SEARCH REPORT

International application No  
PCT/DK2011/050479

C(Continuation). DOCUMENTS CONSIDERED TO BE RELEVANT		
Category*	Citation of document, with indication, where appropriate, of the relevant passages	Relevant to claim No.
A	<p>FERRARA KATHERINE W ET AL: "Lipid-shelled vehicles: engineering for ultrasound molecular imaging and drug delivery.", ACCOUNTS OF CHEMICAL RESEARCH 21 JUL 2009 LNKD- PUBMED:19552457, vol. 42, no. 7, 21 July 2009 (2009-07-21), pages 881-892, XP002650387, ISSN: 1520-4898 page 882, right-hand column; figure 1a page 886, left-hand column, paragraph 2 page 884</p> <p style="text-align: center;">-----</p>	7-14

## INTERNATIONAL SEARCH REPORT

Information on patent family members

International application No

PCT/DK2011/050479

Patent document cited in search report	Publication date	Patent family member(s)	Publication date	
WO 2006043083	A2	27-04-2006	AU 2005297082 A1	27-04-2006
			BR PI0517006 A	30-09-2008
			CA 2583367 A1	27-04-2006
			CN 101060886 A	24-10-2007
			EA 200700686 A1	26-10-2007
			EP 1812115 A2	01-08-2007
			JP 2008517049 A	22-05-2008
			KR 20070108851 A	13-11-2007
			US 2008193374 A1	14-08-2008
			WO 2006043083 A2	27-04-2006
			ZA 200704035 A	27-08-2008
US 4310506	A	12-01-1982	NONE	
US 2009081121	A1	26-03-2009	TW 200922630 A	01-06-2009
			US 2009081121 A1	26-03-2009
WO 2004082626	A2	30-09-2004	EP 1603535 A2	14-12-2005
			WO 2004082626 A2	30-09-2004
EP 1486216	A1	15-12-2004	AU 2003211666 A1	09-09-2003
			CA 2480408 A1	04-09-2003
			CN 1649628 A	03-08-2005
			EP 1486216 A1	15-12-2004
			JP 4360917 B2	11-11-2009
			US 2005129613 A1	16-06-2005
			WO 03072142 A1	04-09-2003
WO 0160417	A2	23-08-2001	AT 300316 T	15-08-2005
			AU 3782701 A	27-08-2001
			BR 0108572 A	19-11-2002
			CA 2400994 A1	23-08-2001
			CN 1404402 A	19-03-2003
			CZ 20023164 A3	16-04-2003
			DE 60112251 D1	01-09-2005
			DE 60112251 T2	30-03-2006
			DK 1257299 T3	21-11-2005
			EP 1257299 A2	20-11-2002
			ES 2247069 T3	01-03-2006
			JP 2003522808 A	29-07-2003
			MX PA02008110 A	11-12-2003
			NO 20000855 A	22-08-2001
			NZ 520848 A	25-02-2005
			PL 358541 A1	09-08-2004
			UA 73160 C2	15-10-2002
			US 2001048914 A1	06-12-2001
			WO 0160417 A2	23-08-2001
			ZA 200206500 A	14-08-2003
WO 03041682	A2	22-05-2003	AT 373466 T	15-10-2007
			AU 2002340670 A1	26-05-2003
			DE 60222580 T2	12-06-2008
			EP 1448165 A2	25-08-2004
			ES 2290333 T3	16-02-2008
			WO 03041682 A2	22-05-2003



- (51) **International Patent Classification:**  
*C07K 14/435* (2006.01)
- (21) **International Application Number:**  
PCT/US2012/045235
- (22) **International Filing Date:**  
2 July 2012 (02.07.2012)
- (25) **Filing Language:** English
- (26) **Publication Language:** English
- (30) **Priority Data:**  
61/504,633 5 July 2011 (05.07.2011) US  
61/558,945 11 November 2011 (11.11.2011) US
- (71) **Applicants (for all designated States except US):** **MERRIMACK PHARMACEUTICALS, INC.** [US/US]; One Kendall Square, Suite B7201, Cambridge, MA 02139 (US). **ADIMAB, LLC** [US/US]; 7 Lucent Drive, Lebanon, NH 03766 (US).
- (72) **Inventors; and**
- (75) **Inventors/Applicants (for US only):** **BUKHALID, Raghida** [US/US]; 80 Ferdinand Street, Melrose, MA 02176 (US). **FELDHAUS, Michael** [US/US]; P.o. Box 1888, Grantham, NH 03753 (US). **KING, Anne** [US/US]; 17 Otis St., #402, Cambridge, MA 02141 (US). **KOHLI, Neeraj** [IN/US]; 39 Shepard Street, Apt. 17, Brighton, MA 02135 (US). **KRAULAND, Eric** [US/US]; 10 High St., Apt. 3, Lebanon, NH 03766 (US). **KEARNS, Jeffrey, David** [US/US]; 42 Everett St., #2, Arlington, MA 02474-6902 (US). **LUGOVSKOY, Alexey, A.** [US/US]; 24 Cen-

ter Street, Woburn, MA 01801 (US). **NIELSEN, Ulrik** [DK/US]; 18 Thomas Street, Quincy, MA 02169 (US).

(74) **Agents:** **REMILLARD, Jane, E.** et al.; Nelson Mullins Riley & Scarborough LLP, One Post Office Square, Boston, MA 02109-2127 (US).

(81) **Designated States (unless otherwise indicated, for every kind of national protection available):** AE, AG, AL, AM, AO, AT, AU, AZ, BA, BB, BG, BH, BR, BW, BY, BZ, CA, CH, CL, CN, CO, CR, CU, CZ, DE, DK, DM, DO, DZ, EC, EE, EG, ES, FI, GB, GD, GE, GH, GM, GT, HN, HR, HU, ID, IL, IN, IS, JP, KE, KG, KM, KN, KP, KR, KZ, LA, LC, LK, LR, LS, LT, LU, LY, MA, MD, ME, MG, MK, MN, MW, MX, MY, MZ, NA, NG, NI, NO, NZ, OM, PE, PG, PH, PL, PT, QA, RO, RS, RU, RW, SC, SD, SE, SG, SK, SL, SM, ST, SV, SY, TH, TJ, TM, TN, TR, TT, TZ, UA, UG, US, UZ, VC, VN, ZA, ZM, ZW.

(84) **Designated States (unless otherwise indicated, for every kind of regional protection available):** ARIPO (BW, GH, GM, KE, LR, LS, MW, MZ, NA, RW, SD, SL, SZ, TZ, UG, ZM, ZW), Eurasian (AM, AZ, BY, KG, KZ, RU, TJ, TM), European (AL, AT, BE, BG, CH, CY, CZ, DE, DK, EE, ES, FI, FR, GB, GR, HR, HU, IE, IS, IT, LT, LU, LV, MC, MK, MT, NL, NO, PL, PT, RO, RS, SE, SI, SK, SM, TR), OAPI (BF, BJ, CF, CG, CI, CM, GA, GN, GQ, GW, ML, MR, NE, SN, TD, TG).

**Published:**  
— without international search report and to be republished upon receipt of that report (Rule 48.2(g))



**WO 2013/006547 A2**

(54) **Title:** ANTIBODIES AGAINST EPIDERMAL GROWTH FACTOR RECEPTOR (EGFR) AND USES THEREOF

(57) **Abstract:** Anti- EGFR antibodies, therapeutic compositions comprising combinations of anti-EGFR antibodies, as well as methods for using such antibodies and compositions to treat EGFR-related disorders (e.g., cancers), are disclosed.

**ANTIBODIES AGAINST EPIDERMAL GROWTH FACTOR RECEPTOR  
(EGFR) AND USES THEREOF**

**Cross-Reference to Related Applications**

5           This application claims the benefit of priority of U.S. Provisional Application No. 61/504633 (filed July 5, 2011) and U.S. Provisional Application No. 61/558945 (filed November 11, 2011), both of which are incorporated herein by reference.

**Background**

10           The natural immune system has evolved to make antibodies for efficient neutralization of pathogens. Natural antibody preparations isolated from immunized animals are polyclonal in origin, and exhibit immunodominance as compared to individual antibodies, which are restricted to one or a few epitopes of a particular antigen. Anti-tumor antibodies are able to block growth or kill tumor cells to which they  
15 bind have been developed as highly effective cancer therapeutic agents. Mixtures of anti-tumor antibodies may achieve tumor suppressive effects that are greater than achieved by any individual antibody in the mixture

          Such results have been achieved by combining two or more neutralizing antibodies against the epidermal growth factor receptor, EGFR (ErbB1). Antibodies that  
20 bind to and inhibit EGFR have proven to provide useful anti-cancer benefits and are of great medical and commercial value. Particular combinations of pairs of antagonistic, yet non-competitive, anti-EGFR antibodies resulted in downregulation of EGFR which was faster and more effective than application of either antibody alone (Friedman *et al.* (2005) PNAS 102:1915-1920). The combination of two cross-competitive (*i.e.*,  
25 competitive with each other for binding to antigen) anti-EGFR antibodies has shown to be non-synergistic. It is possible that binding of a plurality of antibodies to distinct epitopes of EGFR forms lattices of complexed receptors on cell surfaces, leading to more efficient internalization and degradation than obtained with antibodies targeting a single epitope. The combination of a particular pair of anti-EGFR receptor antibodies  
30 have also been reported to result in additive and in some cases synergistic, antitumor activity *in vivo* (Perera *et al.* (2005) Clin Cancer Res 11:6390-6399). Monoclonal antibody 806, raised against the mutant de2-7 EGFR, combined with antagonistic antibody 528 displayed significantly higher anti-tumor activity in a glioma xenograft model than treatment with either antibody alone. The mechanism of the synergistic anti-

tumor activity was shown to be associated with rapid downregulation of EGFR, which was not induced by treatment with the individual antibodies. Similarly EGFR phosphorylation was greatly reduced in the presence of another pair of anti-EGFR antibodies, cetuximab and EMD55900 (Kamat *et al.* (2008) *Cancer Biol Ther* 7:726-33).

5           Certain combinations of antibodies targeting the related receptor, ErbB2, have also been shown to function in synergy (Friedman *et al.* (2005). Trastuzumab combined with pertuzumab inhibited the survival of BT474 breast cancer cells at doses in which individual antibodies are ineffective (Nahta *et al.* (2004) *Cancer Res* 64:2343-2346). In another study three non-competitive anti-ErbB2 antibodies demonstrated far more  
10 effective *in vitro* killing of BT474 cells in combination than individually and similar results were obtained in a BT474 *in vivo* xenograft model (Spiridon *et al.* (2002) *Clin Cancer Res* 8:1699-701).

          Other evidence that combining more than one antibody may enhance the growth suppressive (*e.g.*, cytotoxic) effect of antibodies on tumor cells has been reported. For  
15 example, monoclonal antibodies to the tumor antigen 17-1A were combined, tumor cell lysis was studied, and it was found that monoclonal antibodies, as well as combinations of competing antibodies, were ineffective, whereas combinations of two or more non-competing antibodies resulted in complete tumor cell lysis.

          In addition to combining antibodies, higher antibody potency has also been  
20 achieved by increasing the antigen affinity of recombinantly expressed anti-tumor antibodies through recombinant DNA techniques known as affinity maturation.

          Accordingly, additional approaches and methods for producing anti-tumor antibody action so as to enhance the responsiveness of tumors to anti-EGFR antibodies and antibody combinations are still needed, including anti-EGFR antibodies with higher  
25 tumor affinity and combinations of such high-affinity anti-EGFR antibodies that enhance signaling inhibition and provide more effective cytostatic or cytotoxic anti-tumor outcomes.

### **Summary**

          Novel monoclonal antibodies that bind to EGFR and inhibit various EGFR  
30 functions are provided herein. These antibodies provide useful therapeutic effects, and when combined with each other or with other anti-ErbB receptor antibodies (*e.g.*, other anti-EGFR antibodies), are capable of exhibiting a synergistic or additive therapeutic effect compared to the administration of each antibody alone. These antibodies, when

administered individually or in combinations as herein provided, are useful for treating a variety of disorders (*e.g.*, cancers) associated with EGFR-mediated cellular signaling. Accordingly, isolated novel monoclonal antibodies that exhibit the properties of binding to EGFR and inhibiting various EGFR functions, and combinations of such antibodies  
5 that exhibit such properties are also provided herein. Uses of these antibodies for diagnostic and therapeutic purposes are also provided, as are uses of the antibodies and antibody combinations herein disclosed.

In one embodiment, a monoclonal antibody is provided which binds EGFR extracellular domain and comprises heavy and light chain CDR1, CDR2, and CDR3,  
10 sequences, wherein the heavy and light chain CDR1, CDR2, and CDR3, sequences are selected from the group consisting of:

- (a) heavy chain CDR1, CDR2, and CDR3 sequences of SEQ ID NOs: 1, 2, and 3 respectively, and light chain CDR1, CDR2, and CDR3 sequences of SEQ ID NOs: 4, 5, and 6, respectively;
- 15 (b) heavy chain CDR1, CDR2, and CDR3 sequences of SEQ ID NOs: 7, 8, and 9, respectively, and light chain CDR1, CDR2, and CDR3 sequences of SEQ ID NOs: 10, 11 and 12, respectively; and
- (c) heavy chain CDR1, CDR2, and CDR3 sequences of SEQ ID NOs: 13, 14, and 15, respectively, and light chain CDR1, CDR2, and CDR3 sequences of SEQ ID  
20 NOs: 16, 17, and 18, respectively.

In another embodiment, a monoclonal antibody is provided that binds to EGFR extracellular domain and comprises a heavy chain variable region and a light chain variable region, wherein the heavy and light chain variable region sequences are selected from the group consisting of:

- 25 (a) a heavy chain variable region comprising SEQ ID NO: 19 and a light chain variable region comprising SEQ ID NO: 20;
- (b) a heavy chain variable region comprising SEQ ID NO: 21 and a light chain variable region comprising SEQ ID NO: 22; and
- (c) a heavy chain variable region comprising SEQ ID NO: 23 and a light chain  
30 variable region comprising SEQ ID NO: 24.

The aforementioned monoclonal antibodies can bind to EGFR with a  $K_D$  of, for example, better than 100 nM, or better than 10 nM, or better than 1 nM, or better than 100 pM, or better than 10 pM, or better than 1 pM. The monoclonal antibodies can

exhibit one or more of the functional properties disclosed herein. The monoclonal antibody can be, for example, a human antibody. In other embodiments, the antibody can be a bispecific antibody, immunoconjugate, Fab, Fab'2, ScFv, affibody®, avimer, nanobody or a domain antibody. In other embodiments, the monoclonal antibody can  
5 be, e.g., an IgG1, IgG2, IgG3, IgG4, IgM, IgA1, IgA2, IgAsec, IgD, or IgE isotype antibody.

Also provided are pharmaceutical compositions comprising any one or more of the aforementioned anti-EGFR monoclonal antibodies and a pharmaceutically acceptable carrier. Kits are also provided. The kit can comprise, for example, a  
10 pharmaceutical composition in a container. Methods of treating cancer in a subject, comprising administering to the subject an effective amount of the pharmaceutical composition comprising any one or more of the aforementioned anti-EGFR monoclonal antibodies are also provided. The aforementioned anti-EGFR monoclonal antibodies or combinations thereof for the the treatment of a cancer (or for manufacture of a  
15 medicament for the treatment of a cancer) are also provided.

In another embodiment, a composition comprising two or three monoclonal antibodies which bind to EGFR extracellular domain is provided, wherein the two or three monoclonal antibodies are selected from the group consisting of:

(a) a monoclonal antibody comprising heavy chain CDR1, CDR2, and CDR3  
20 sequences of SEQ ID NOs: 1, 2, and 3 respectively, and light chain CDR1, CDR2, and CDR3 sequences of SEQ ID NOs: 4, 5, and 6, respectively;

(b) a monoclonal antibody comprising heavy chain CDR1, CDR2, and CDR3 sequences of SEQ ID NOs: 7, 8, and 9, respectively, and light chain CDR1, CDR2, and CDR3 sequences of SEQ ID NOs: 10, 11 and 12, respectively and

25 (c) a monoclonal antibody comprising heavy chain CDR1, CDR2, and CDR3 sequences of SEQ ID NOs: 13, 14, and 15, respectively, and light chain CDR1, CDR2, and CDR3 sequences of SEQ ID NOs: 16, 17 and 18, respectively;

and wherein the composition comprises (a) and (b), (a) and (c), (b) and (c) or (a), (b) and (c).

30 In yet another embodiment, a composition comprising two or three monoclonal antibodies which bind to EGFR extracellular domain is provided, wherein the two or three monoclonal antibodies are selected from the group consisting of:



(a) a monoclonal antibody comprising a heavy chain variable region comprising SEQ ID NO: 19 and a light chain variable region comprising SEQ ID NO: 20;

(b) a monoclonal antibody comprising a heavy chain variable region comprising SEQ ID NO: 21 and a light chain variable region comprising SEQ ID NO: 22; and

5 (c) a monoclonal antibody comprising a heavy chain variable region comprising SEQ ID NO: 23 and a light chain variable region comprising SEQ ID NO: 24; and wherein the composition comprises (a) and (b), (a) and (c), (b) and (c) or (a) (b) and (c).

Each of monoclonal antibodies (a), (b) and (c) in the aforementioned  
10 compositions comprising two or three antibodies can bind to EGFR with a  $K_D$  of, for example, better than 100 nM, or better than 10 nM or better than 1 nM. Each of monoclonal antibodies (a), (b) and (c) can exhibit one or more of the functional properties disclosed herein. Each of monoclonal antibodies (a), (b) and (c) can be, for example, a human antibody. In other embodiments, one or more of monoclonal  
15 antibodies (a), (b), and (c) is independently selected from the group consisting of a bispecific antibody, immunoconjugate, Fab, Fab'2, ScFv, affibody®, avimer, nanobody, and a domain antibody. In other embodiments, each of monoclonal antibodies (a), (b), and (c) is independently selected from the group consisting of IgG1, IgG2, IgG3, IgG4, IgM, IgA1, IgA2, IgAsec, IgD and IgE isotype antibodies. Monoclonal antibodies (a),  
20 (b) and (c) may also be in the form of IgY and camelid antibodies .

Also provided is a pharmaceutical composition comprising any one of the aforementioned compositions comprising two or three anti-EGFR monoclonal antibodies and a pharmaceutically acceptable carrier. Kits are also provided. The kit can comprise, for example, a pharmaceutical composition in a container. Methods of  
25 treating cancer in a subject, comprising administering to the subject an effective amount of the pharmaceutical composition comprising any one of the aforementioned compositions comprising two or three anti-EGFR monoclonal antibodies are also provided. The aforementioned compositions comprising two or three anti-anti-EGFR monoclonal antibodies (and their use for the manufacture of a medicament) for the  
30 treatment of a cancer are also provided.

In another embodiment, a composition is provided comprising three monoclonal anti-EGFR antibodies, said composition comprising a first antibody, a second antibody and a third antibody, wherein (i) the first antibody comprises heavy chain CDR1, CDR2,

and CDR3 sequences of SEQ ID NOs: 1, 2, and 3 respectively, and light chain CDR1, CDR2, and CDR3 sequences of SEQ ID NOs: 4, 5, and 6, respectively; (ii) the second antibody comprises heavy chain CDR1, CDR2, and CDR3 sequences of SEQ ID NOs: 7, 8, and 9, respectively, and light chain CDR1, CDR2, and CDR3 sequences of SEQ ID NOs: 10, 11 and 12, respectively; and (iii) the third antibody comprises heavy chain CDR1, CDR2, and CDR3 sequences of SEQ ID NOs: 13, 14, and 15 respectively, and light chain CDR1, CDR2, and CDR3 sequences of SEQ ID NOs: 16, 17, and 18, respectively, and wherein the first second and third antibodies are present at a molar ratio of 2:2:1 to each other.

10 In yet another embodiment, a composition is provided comprising three monoclonal anti-EGFR antibodies, said composition comprising a first antibody, a second antibody and a third antibody, wherein (i) the first antibody comprises a heavy chain variable region comprising SEQ ID NO: 19 and a light chain variable region comprising SEQ ID NO: 20; (ii) the second antibody comprises a heavy chain variable region comprising SEQ ID NO: 21 and a light chain variable region comprising SEQ ID NO: 22; and (iii) the third antibody comprises a heavy chain variable region comprising SEQ ID NO: 23 and a light chain variable region comprising SEQ ID NO: 24, and wherein the first second and third antibodies are present at a molar ratio of 2:2:1 to each other.

20 Each of the first, second and third antibodies in the aforementioned compositions can bind to EGFR with a  $K_D$  of, for example, better than 100 nM, or better than 10 nM or better than 1 nM. In another embodiment, the first antibody binds to EGFR with a  $K_D$  in a range of  $1 \times 10^{-9}$  M to  $1.1 \times 10^{-11}$  M, the second antibody binds to EGFR with a  $K_D$  in a range of  $1 \times 10^{-9}$  M to  $7.0 \times 10^{-11}$  M and the third antibody binds to EGFR with a  $K_D$  in a range of  $1 \times 10^{-9}$  M to  $3.6 \times 10^{-10}$  M. Each of the first, second and third antibodies in the aforementioned compositions can exhibit one or more of the functional properties disclosed herein. Each of the first, second and third antibodies in the aforementioned compositions can be, for example, a human antibody. In other embodiments, one or more of the first antibody, the second antibody and the third antibody is independently  
25  
30 selected from the group consisting of a bispecific antibody, immunoconjugate, Fab, Fab'2, ScFv, affibody, avimer, nanobody, and a domain antibody. In other embodiments, each of the first antibody, the second antibody and the third antibody is

independently selected from the group consisting of IgG1, IgG2, IgG3, IgG4, IgM, IgA1, IgA2, IgAsec, IgD and IgE isotype antibodies.

Also provided are pharmaceutical compositions comprising any one of the aforementioned anti-EGFR compositions comprising a first antibody, a second antibody  
5 and a third antibody at a 2:2:1 ratio, and a pharmaceutically acceptable carrier. In one embodiment, the pharmaceutical composition is a sterile composition. In another embodiment, the pharmaceutical composition is suitable for injection. In yet another embodiment, the pharmaceutical composition is a sterile composition suitable for intravenous injection. Kits are also provided. The kit can comprise, for example, a  
10 pharmaceutical composition in a container. Methods of treating cancer in a subject, comprising administering to the subject an effective amount of the pharmaceutical composition comprising any one of the aforementioned anti-EGFR compositions comprising first, second and third antibodies at a 2:2:1 ratio are also provided. Use of any of the aforementioned anti-EGFR compositions comprising first, second and third  
15 antibodies at a 2:2:1 ratio for the manufacture of a medicament for the treatment of a cancer are also provided.

In another embodiment, a method of preparing an anti-EGFR antibody composition is provided, the method comprising combining in a single composition:

(a) a monoclonal antibody comprising heavy chain CDR1, CDR2, and CDR3  
20 sequences of SEQ ID NOs: 1, 2, and 3 respectively, and light chain CDR1, CDR2, and CDR3 sequences of SEQ ID NOs: 4, 5, and 6, respectively;

(b) a monoclonal antibody comprising heavy chain CDR1, CDR2, and CDR3 sequences of SEQ ID NOs: 7, 8, and 9, respectively, and light chain CDR1, CDR2, and CDR3 sequences of SEQ ID NOs: 10, 11 and 12, respectively; and

25 (c) a monoclonal antibody comprising heavy chain CDR1, CDR2, and CDR3 sequences of SEQ ID NOs: 13, 14, and 15 respectively, and light chain CDR1, CDR2, and CDR3 sequences of SEQ ID NOs: 16, 17, and 18, respectively;

wherein (a), (b) and (c) are combined at a molar ratio of 2:2:1 to each other.

In another embodiment, a method of preparing an anti-EGFR antibody  
30 composition is provided, the method comprising combining in a single composition:

(a) a monoclonal antibody comprising a heavy chain variable region comprising SEQ ID NO: 19 and a light chain variable region comprising SEQ ID NO:20;

(b) a monoclonal antibody comprising a heavy chain variable region comprising SEQ ID NO: 21 and a light chain variable region comprising SEQ ID NO: 22; and

(c) a monoclonal antibody comprising a heavy chain variable region comprising SEQ ID NO: 23 and a light chain variable region comprising SEQ ID NO: 24;

5 wherein (a), (b) and (c) are combined at a molar ratio of 2:2:1 to each other.

In another embodiment, a method of treating a subject with anti-EGFR antibodies is provided, the method comprising administering to the subject:

(a) a monoclonal antibody comprising heavy chain CDR1, CDR2, and CDR3 sequences of SEQ ID NOs: 1, 2, and 3 respectively, and light chain CDR1, CDR2, and  
10 CDR3 sequences of SEQ ID NOs: 4, 5, and 6, respectively;

(b) a monoclonal antibody comprising heavy chain CDR1, CDR2, and CDR3 sequences of SEQ ID NOs: 7, 8, and 9, respectively, and light chain CDR1, CDR2, and CDR3 sequences of SEQ ID NOs: 10, 11 and 12, respectively; and

(c) a monoclonal antibody comprising heavy chain CDR1, CDR2, and CDR3  
15 sequences of SEQ ID NOs: 13, 14, and 15 respectively, and light chain CDR1, CDR2, and CDR3 sequences of SEQ ID NOs: 16, 17, and 18, respectively;

wherein (a), (b) and (c) are administered to the subject at a molar ratio of 2:2:1 to each other.

In another embodiment, a method of treating a subject with anti-EGFR  
20 antibodies is provided, the method comprising administering to the subject:

(a) a monoclonal antibody comprising a heavy chain variable region comprising SEQ ID NO: 19 and a light chain variable region comprising SEQ ID NO:20;

(b) a monoclonal antibody comprising a heavy chain variable region comprising SEQ ID NO: 21 and a light chain variable region comprising SEQ ID NO: 22; and

25 (c) a monoclonal antibody comprising a heavy chain variable region comprising SEQ ID NO: 23 and a light chain variable region comprising SEQ ID NO: 24;

wherein (a), (b) and (c) are administered to the subject at a molar ratio of 2:2:1 to each other.

Other features and advantages of the invention will be apparent from the  
30 following detailed description, and from the claims.

### **Brief Description of the Figures**

Figure 1A is a bar graph showing the results of a direct ELISA epitope binning experiment with the P1X, P2X and P3X antibodies using wild-type EGFR-ECD antigen (WT), a Bin 1 epitope mutant (Bin 1 MT) and a Bin 3 epitope mutant (Bin 3 MT).

Figure 1B is a graph showing the results of a surface plasmon resonance epitope binning experiment using the ICR10 epitope (Bin 2) conjugated on a Biacore chip, with injection of wild-type EGFR-ECD antigen, followed by sequential injection of the P1X, P2X and P3X antibodies.

Figure 2A is a graph showing the results of a surface plasmon resonance epitope binning experiment using the P1X antibody conjugated on a Biacore chip, with injection of wild-type EGFR-ECD antigen, followed by sequential injection of the P3X, P2X and P1X antibodies.

Figure 2B is a graph showing the results of a surface plasmon resonance epitope binning experiment using the P2X antibody conjugated on a Biacore chip, with injection of wild-type EGFR-ECD antigen, followed by sequential injection of the P3X, P2X and P1X antibodies.

Figure 2C is a graph showing the results of a surface plasmon resonance epitope binning experiment using the P3X antibody conjugated on a Biacore chip, with injection of wild-type EGFR-ECD antigen, followed by sequential injection of the P3X, P2X and P1X antibodies.

Figure 3 is a graph showing the results of P1X, P2X and P3X antibody binding kinetics to EGFR on A431 cells as measured via flow cytometry (FACS plot).

Figure 4 is a graph showing the results of a phospho-EGFR (pEGFR) ELISA, demonstrating pEGFR inhibition by single antibodies: single-agent treatment with P1X, P2X or P3X antibody.

Figure 5A is a graph showing the results of a phospho-ERK (pERK) ELISA, demonstrating the effect of affinity maturation on pERK inhibition by comparison of pERK inhibition by parental (ca antibody) and affinity matured P1X antibody.

Figure 5B is a graph showing the results of a phospho-ERK (pERK) ELISA, comparing pERK inhibition by parental (ca and ch antibodies) and affinity matured P1X+P3X antibodies.

Figure 5C is a graph showing the results of a phospho-ERK (pERK) ELISA, comparing pERK inhibition by parental (ca and cd antibodies) and affinity matured P1X+P2X antibodies.

Figure 6A is a graph showing the results of a phospho-ERK (pERK) ELISA, demonstrating pERK inhibition by P1X antibody, with an  $IC_{50}$  value of approximately 25 nM.

Figure 6B is a graph showing the results of a phospho-ERK (pERK) ELISA for  
5 A431 cells treated with a dilution series of 5 combination ratios of P3X + P2X in combination with a constant P1X concentration of 25nM.

Figure 6C is a graph showing the results of a phospho-ERK (pERK) ELISA for A431 cells treated with a dilution series of 6 combination ratios of P1X:P2X:P3X.

Figure 6D is a graph showing the results of a phospho-ERK (pERK) ELISA for  
10 A431 cells treated with a dilution series of 5 combination ratios of P1X:P2X.

Figure 7A is a graph showing the results of a phospho-EGFR (pEGFR) ELISA (circles) and a phospho-ERK (pERK) ELISA (triangles), demonstrating inhibition by a 2:2:1 combination of P1X:P2X:P3X.

Figure 7B is a graph showing the results of a phospho-ERK (pERK) ELISA,  
15 demonstrating inhibition by a 2:2:1 formulation of P1X:P2X:P3X (P1X+P2X+P3X) versus P1X single antibody alone.

Figure 7C is a graph showing the results of a phospho-ERK (pERK) ELISA, demonstrating inhibition by P1X+P2X+P3X versus P2X single antibody alone.

Figure 8A is a bar graph showing western blot analysis results for total EGFR  
20 (tEGFR) internalization kinetics of H1975 cells pre-treated with P1X+P2X+P3X antibodies for various periods of time before stimulation with EGF.

Figure 8B is a bar graph showing western blot analysis results for H1975 cells pre-treated with P1X+P2X+P3X antibodies before stimulation with EGF, showing levels of tEGFR, pERK, phospho-AKT (pAKT) and phospho-c-Jun (p-c-Jun) in the cells,  
25 normalized to the loading control (PCNA) and to lysates of control untreated cells.

Figure 9A is a graph showing the results of a cell viability assay for HCC827 cells, demonstrating inhibition of tumor cell proliferation by treatment with P1X+P2X+P3X antibodies, as compared to cetuximab, in the presence of EGF ligand.

Figure 9B is a graph showing the results of a cell viability assay for H1975 cells,  
30 demonstrating inhibition of tumor cell proliferation by treatment with P1X+P2X+P3X antibodies, as compared to cetuximab, in the presence of EGF ligand.

Figure 9C is a graph showing the results of a cell viability assay for HCC827 cells, demonstrating inhibition of tumor cell proliferation by treatment with

P1X+P2X+P3X antibodies, as compared to cetuximab, in the presence of amphiregulin (AREG) ligand.

Figure 9D is a graph showing the results of a cell viability assay for H1975 cells, demonstrating inhibition of tumor cell proliferation by treatment with P1X+P2X+P3X antibodies, as compared to cetuximab, in the presence of AREG ligand.

Figure 10A is a graph showing the results of a DU145 tumor xenograft mouse model experiment, demonstrating decreased tumor volume *in vivo* in mice treated with P1X+P2X+P3X antibodies, as compared to PBS and cetuximab controls.

Figure 10B is a graph showing the results of an H1975 tumor xenograft mouse model experiment, demonstrating decreased tumor volume *in vivo* in mice treated with P1X+P2X+P3X antibodies, as compared to PBS control.

Figure 11 is a graph showing the results of a ligand antagonism cell binding assay, demonstrating the EGF ligand blocking ability of P1X, P2X or P3X alone at low doses.

Figure 12A is a graph showing the results of a ligand antagonism cell binding assay, demonstrating the EGF ligand blocking ability of P1X, P2X or P3X alone, or in triple combination, at high doses.

Figure 12B is a graph showing the results of a ligand antagonism cell binding assay, demonstrating the EGF ligand blocking ability of P1X Fab, P2X Fab or P3X Fab alone, or in triple combination, at high doses.

Figure 13A is a graph showing the results of a phospho-EGFR inhibition assay, demonstrating the inhibitory ability of triple combinations of P1X+P2X+P3X or P1X Fab+P2X Fab+P3X Fab at low doses (50 ng/ml; 8 nM).

Figure 13B is a graph showing the results of a phospho-EGFR inhibition assay, demonstrating the inhibitory ability of triple combinations of P1X+P2X+P3X or P1X Fab+P2X Fab+P3X Fab at high doses (500 ng/ml; 80 nM).

Figure 13C is a graph showing the results of a phospho-ERK inhibition assay, demonstrating the inhibitory ability of triple combinations of P1X+P2X+P3X or P1X Fab+P2X Fab+P3X Fab at low doses (50 ng/ml; 8 nM).

Figure 13D is a graph showing the results of a phospho-ERK inhibition assay, demonstrating the inhibitory ability of triple combinations of P1X+P2X+P3X or P1X Fab+P2X Fab+P3X Fab at high doses (500 ng/ml; 80 nM).

Figure 14 is an immunoblot of an EGF-receptor downregulation assay in cells pre-treated with triple combinations of P1X+P2X+P3X or P1X Fab+P2X Fab+P3X Fab or with cetuximab. The housekeeping protein pcna was used as a control.

## 5 **Detailed Description**

### **I. Definitions**

The terms “EGFR,” “ErbB1,” and “EGF receptor” are used interchangeably herein to refer to human EGFR protein; see UniProtKB/Swiss-Prot entry P00533. The amino acid sequence of the extracellular domain of human EGFR (EGFR-ECD) is  
10 shown in Example 1 and in SEQ ID NO:33.

The term “inhibition” as used herein, refers to any statistically significant decrease in biological activity, including full blocking of the activity. For example, “inhibition” can refer to a statistically significant decrease of about 10%, 20%, 30%, 40%, 50%, 60%, 70%, 80%, 90%, or about 100% in biological activity.

15 Inhibition of phosphorylation, as used herein, refers to the ability of an antibody to statistically significantly decrease the phosphorylation of a substrate protein relative to the signaling in the absence of the antibody (control). As is known in the art, intracellular signaling pathways include, for example, phosphoinositide 3'-kinase/Akt (PI3K/Akt/*PTEN* or “AKT”) and/or mitogen-activated protein kinase (MAPK/ERK or  
20 “ERK”) pathways. As is also known in the art, EGFR mediated signaling can be measured by assaying for the level phosphorylation of the substrate (*e.g.*, phosphorylation or no phosphorylation of AKT and/or ERK). Accordingly, in one embodiment, anti-EGFR antibody combinations and compositions provide statistically significant inhibition of the level of phosphorylation of either or both of AKT and ERK  
25 by at least 10%, or at least 20%, or at least 30%, or at least 40%, or at least 50%, or at least 60%, or at least 70%, or at least 80%, or at least 90%, or about 100% relative to the level of phosphorylation of AKT and/or ERK in the absence of such antibody (control). Such EGFR mediated signaling can be measured using art recognized techniques which measure a protein in a cellular cascade involving EGFR, *e.g.*, ELISA, western, or  
30 multiplex methods, such as Luminex®.

The phrase “inhibition of the growth of cells expressing EGFR,” as used herein, refers to the ability of an antibody to statistically significantly decrease the growth of a cell expressing EGFR relative to the growth of the cell in the absence of the antibody



(control) either *in vivo* or *in vitro*. In one embodiment, the growth of a cell expressing EGFR (*e.g.*, a cancer cell) may be decreased by at least 10%, or at least 20%, or at least 30%, or at least 40%, or at least 50%, or at least 60%, or at least 70%, or at least 80%, or at least 90%, or about 100% when the cells are contacted with an antibody composition  
5 of combination disclosed herein, relative to the growth measured in the absence of the antibody composition of combination (control). Cellular growth can be assayed using art recognized techniques which measure the rate of cell division, the fraction of cells within a cell population undergoing cell division, and/or the rate of cell loss from a cell population due to terminal differentiation or cell death (*e.g.*, using a cell titer glow assay  
10 or thymidine incorporation).

The phrase “inhibition of an EGFR ligand binding to EGFR,” as used herein, refers to the ability of an antibody to statistically significantly decrease the binding of an EGFR ligand to its receptor, EGFR, relative to the EGFR ligand binding in the absence of the antibody (control). This means that, in the presence of the antibody, the amount  
15 of the EGFR ligand that binds to EGFR relative to a control (no antibody), is statistically significantly decreased. The amount of an EGFR ligand which binds EGFR may be decreased in the presence of an antibody composition or combination disclosed herein by at least 10%, or at least 20%, or at least 30%, or at least 40%, or at least 50%, or at least 60%, or at least 70%, or at least 80%, or at least 90%, or about 100% relative to the  
20 amount in the absence of the antibody (control). A decrease in EGFR ligand binding can be measured using art-recognized techniques that measure the level of binding of labeled EGFR ligand (*e.g.*, radiolabelled EGF or radiolabeled betacellulin) to cells expressing EGFR in the presence or absence (control) of the antibody.

The phrase “inhibition of EGFR dimerization,” as used herein, refers to the  
25 ability of an antibody to statistically significantly decrease EGFR dimerization (pairing with another ErbB receptor to form homodimers, *e.g.*, ErbB1 / ErbB1 pairings, or heterodimers, *e.g.*, ErbB1 / ErbB3 pairings) relative to EGFR dimerization in the absence of the antibody (control). In one embodiment, dimerization of EGFR may be decreased by at least 10%, or at least 20%, or at least 30%, or at least 40%, or at least  
30 50%, or at least 60%, or at least 70%, or at least 80%, or at least 90%, or about 100% when cells expressing EGFR are contacted with an antibody composition or combination disclosed herein, relative to dimerization of EGFR measured in the absence of the antibody (control). A decrease in EGFR dimerization can be measured using art-

recognized techniques that measure the level of EGFR dimerization in the presence or absence (control) of the antibody.

The phrase “downregulation of EGFR expression,” as used herein, refers to the ability of an antibody to statistically significantly decrease the expression of EGFR on a cell surface, for example, by increasing internalization of EGFR and/or by decreasing recycling of EGFR from intracellular vesicles relative to EGFR expression in the absence of the antibody (control). In one embodiment, expression of EGFR may be decreased by at least 10%, or at least 20%, or at least 30%, or at least 40%, or at least 50%, or at least 60%, or at least 70%, or at least 80%, or at least 90%, or about 100% when cells expressing EGFR are contacted with an antibody composition of combination provided herein, relative to expression of EGFR on the cell surface measured in the absence of the antibody (control). Downregulation of EGFR expression on a cell surface includes, for example, an increase in internalization / recycling of the receptor, and/or an increase in internalization / degradation of the receptor. An increase in EGFR internalization can be measured using art-recognized techniques that measure the level of EGFR internalization in the presence or absence (control) of the antibody.

With respect to combinations of EGFR antibodies (described herein), the words “additive” or “additivity,” as used herein, refer to the activity of two or more antibodies wherein their combined activity (relative to a particular function, *e.g.*, inhibition of cell growth) is equal to the sum of their individual activities. That is, the sum of the activities of two or more antibodies provided herein, when acting individually on a cell expressing EGFR, is approximately equivalent to the combined effect of the same antibodies acting together on the same cell. In one embodiment, the additive effect is measured with respect to any of the properties discussed above (*e.g.*, inhibition of AKT or ERK phosphorylation, inhibition of the growth of cells expressing EGFR, *etc.*).

The words “synergy” or “synergistic,” as used herein, refer to the activity of two or more antibodies wherein their combined activity (relative to a particular function, *e.g.*, inhibition of cell growth) is greater than the expected additive effect of their individual activities. For example, the expected additive effect can be defined according to Bliss independence criteria. In accordance with the Bliss criteria, the effect of two or more drugs (*e.g.*, antibodies) is equal to the sum of the effects of the individual drugs minus the multiplication of the effects of the individual drugs:

$$E12 = E1 + E2 - E1 * E2$$

where E1 is the % inhibition by drug 1, E2 is the % inhibition by drug 2, and E12 is the expected % inhibition by the combination.

5           The synergistic effect can apply to any of the properties discussed herein (*e.g.*, inhibition of EGFR-dependant AKT or ERK phosphorylation, inhibition of the growth of cells expressing EGFR, *etc.*). In a particular embodiment, at least 10%, or at least 20%, or at least 30%, or at least 40%, or at least 50%, or at least 60%, or at least 70%, or at least 80%, or at least 90%, or greater increase in activity of the combined antibodies  
10 relative to the additive effect of their individual activities is achieved.

          The term “antibody” or “immunoglobulin,” as used interchangeably herein, includes whole antibodies and any antigen binding fragment (antigen-binding portion) or single chain cognates thereof. An “antibody” comprises at least one heavy (H) chain and one light (L) chain. In naturally occurring IgGs, for example, these heavy and light  
15 chains are inter-connected by disulfide bonds and there are two paired heavy and light chains, these two also inter-connected by disulfide bonds. Each heavy chain is comprised of a heavy chain variable region (abbreviated herein as V<sub>H</sub>) and a heavy chain constant region. The heavy chain constant region is comprised of three domains, CH1, CH2 and CH3. Each light chain is comprised of a light chain variable region  
20 (abbreviated herein as V<sub>L</sub>) and a light chain constant region. The light chain constant region is comprised of one domain, CL. The V<sub>H</sub> and V<sub>L</sub> regions can be further subdivided into regions of hypervariability, termed complementarity determining regions (CDR), interspersed with regions that are more conserved, termed framework regions (FR) or Joining (J) regions (J<sub>H</sub> or J<sub>L</sub> in heavy and light chains respectively).  
25 Each V<sub>H</sub> and V<sub>L</sub> is composed of three CDRs three FRs and a J domain, arranged from amino-terminus to carboxy-terminus in the following order: FR1, CDR1, FR2, CDR2, FR3, CDR3, J. The variable regions of the heavy and light chains bind with an antigen. The constant regions of the antibodies may mediate the binding of the immunoglobulin to host tissues or factors, including various cells of the immune system (*e.g.*, effector  
30 cells) or humoral factors such as the first component (C1q) of the classical complement system. Thus one or more fragments of an antibody that retain the ability to specifically bind to an antigen (*e.g.*, EGFR) may be used in the combinations disclosed herein. It has been shown that fragments of a full-length antibody can perform the antigen-binding function of an antibody. Examples of binding fragments denoted as an antigen-binding

portion or fragment of an antibody include (i) a Fab fragment, a monovalent fragment consisting of the  $V_L$ ,  $V_H$ , CL and CH1 domains; (ii) a  $F(ab')_2$  fragment, a bivalent fragment comprising two Fab fragments linked by a disulfide bridge at the hinge region; (iii) a Fd fragment consisting of the  $V_H$  and CH1 domains; (iv) a Fv fragment consisting of the  $V_L$  and  $V_H$  domains of a single arm of an antibody, (v) a dAb including  $V_H$  and  $V_L$  domains; (vi) a dAb fragment (Ward *et al.* (1989) *Nature* 341, 544-546), which consists of a  $V_H$  domain; (vii) a dAb which consists of a  $V_H$  or a  $V_L$  domain; and (viii) an isolated complementarity determining region (CDR) or (ix) a combination of two or more isolated CDRs which may optionally be joined by a synthetic linker. Furthermore, although the two domains of the Fv fragment,  $V_L$  and  $V_H$ , are coded for by separate genes, they can be joined, using recombinant methods, by a synthetic linker that enables them to be made as a single protein chain in which the  $V_L$  and  $V_H$  regions are paired to form monovalent molecules (such a single chain cognate of an immunoglobulin fragment is known as a single chain Fv (scFv). Such single chain antibodies are also intended to be encompassed within the term "antibody". Antibody fragments are obtained using conventional techniques known to those with skill in the art, and the fragments are screened for utility in the same general manner as are intact antibodies. Antigen-binding portions can be produced by recombinant DNA techniques, or by enzymatic or chemical cleavage of intact immunoglobulins.

The term "monoclonal antibody" as used herein refers to an antibody obtained from a population of substantially homogeneous antibodies, *i.e.*, the individual antibodies comprising the population are identical except for possible naturally occurring mutations that may be present in minor amounts. Antigen binding fragments (including scFvs) of such immunoglobulins are also encompassed by the term "monoclonal antibody" as used herein. Monoclonal antibodies are highly specific, being directed against a single antigenic site. Furthermore, in contrast to conventional (polyclonal) antibody preparations, which typically include different antibodies, directed against different determinants (epitopes), each monoclonal antibody is directed against a single determinant on the antigen. Monoclonal antibodies can be prepared using any art recognized technique and those described herein such as, for example, a hybridoma method, a transgenic animal, recombinant DNA methods (see, *e.g.*, U.S. Pat. No. 4,816,567), or using phage antibody libraries using the techniques described in, for example, US Patent No. 7,388,088 and US patent application Ser. No. 09/856,907 (PCT

Int. Pub. No. WO 00/31246). Monoclonal antibodies include chimeric antibodies, human antibodies and humanized antibodies and may occur naturally or be produced recombinantly.

The term “recombinant antibody,” refers to antibodies that are prepared,  
5 expressed, created or isolated by recombinant means, such as (a) antibodies isolated from an animal (*e.g.*, a mouse) that is transgenic or transchromosomal for immunoglobulin genes (*e.g.*, human immunoglobulin genes) or a hybridoma prepared therefrom, (b) antibodies isolated from a host cell transformed to express the antibody, *e.g.*, from a transfectoma, (c) antibodies isolated from a recombinant, combinatorial  
10 antibody library (*e.g.*, containing human antibody sequences) using phage display, and (d) antibodies prepared, expressed, created or isolated by any other means that involve splicing of immunoglobulin gene sequences (*e.g.*, human immunoglobulin genes) to other DNA sequences. Such recombinant antibodies may have variable and constant regions derived from human germline immunoglobulin sequences. In certain  
15 embodiments, however, such recombinant human antibodies can be subjected to *in vitro* mutagenesis and thus the amino acid sequences of the V<sub>H</sub> and V<sub>L</sub> regions of the recombinant antibodies are sequences that, while derived from and related to human germline V<sub>H</sub> and V<sub>L</sub> sequences, may not naturally exist within the human antibody germline repertoire *in vivo*.

20 The term “chimeric immunoglobulin” or antibody refers to an immunoglobulin or antibody whose variable regions derive from a first species and whose constant regions derive from a second species. Chimeric immunoglobulins or antibodies can be constructed, for example by genetic engineering, from immunoglobulin gene segments belonging to different species.

25 The term “human antibody,” as used herein, is intended to include antibodies having variable regions in which both the framework and CDR regions are derived from human germline immunoglobulin sequences as described, for example, by Kabat et al. (See Kabat, *et al.* (1991) *Sequences of proteins of Immunological Interest, Fifth Edition*, U.S. Department of Health and Human Services, NIH Publication No. 91-3242).  
30 Furthermore, if the antibody contains a constant region, the constant region also is derived from human germline immunoglobulin sequences. The human antibodies may include amino acid residues not encoded by human germline immunoglobulin sequences (*e.g.*, mutations introduced by random or site-specific mutagenesis *in vitro* or by somatic

mutation *in vivo*). However, the term "human antibody", as used herein, is not intended to include antibodies in which CDR sequences derived from the germline of another mammalian species, such as a mouse, have been grafted onto human framework sequences.

5           The human antibody can have at least one or more amino acids replaced with an amino acid residue, *e.g.*, an activity enhancing amino acid residue that is not encoded by the human germline immunoglobulin sequence. Typically, the human antibody can have up to twenty positions replaced with amino acid residues that are not part of the human germline immunoglobulin sequence. In a particular embodiment, these  
10       replacements are within the CDR regions as described in detail below.

          The term "humanized antibody" refers to an antibody that includes at least one humanized antibody chain (*i.e.*, at least one humanized light or heavy chain). The term "humanized antibody chain" (*i.e.*, a "humanized immunoglobulin light chain") refers to an antibody chain (*i.e.*, a light or heavy chain, respectively) having a variable region that  
15       includes a variable framework region substantially from a human antibody and complementarity determining regions (CDRs) (*e.g.*, at least one CDR, two CDRs, or three CDRs) substantially from a non-human antibody, and further includes constant regions (*e.g.*, one constant region or portion thereof, in the case of a light chain, and preferably three constant regions in the case of a heavy chain).

20           "Isolated," as used herein, is intended to refer to an antibody or combination of two, three or four antibodies that is substantially free of other antibodies having different antigenic specificities (*e.g.*, an isolated composition of antibodies ca, cf, and ch, each of which specifically bind to EGFR, is substantially free of antibodies that specifically bind antigens other than EGFR). In addition, an isolated antibody is typically substantially  
25       free of other cellular material and/or chemicals. In one embodiment, a combination of "isolated" monoclonal antibodies having different EGFR binding specificities are combined in a well-defined composition.

          As used herein, "isotype" refers to the antibody class (*e.g.*, IgM or IgG1) that is encoded by heavy chain constant region genes. In some embodiments, a monoclonal  
30       antibody composition provided herein comprises only antibodies of the IgG1 isotype. In other embodiments, a monoclonal antibody composition provided herein comprises only antibodies of the IgG2 isotype. In other embodiments, a monoclonal antibody composition provided herein comprises antibodies of two or three different isotypes.

An “antigen” is an entity (*e.g.*, a proteinaceous entity or peptide) to which an antibody binds. In various embodiments, an antigen is EGF. In a particular embodiment, an antigen is human EGFR.

Accordingly, also encompassed by the present disclosure are combinations of  
5 antibodies that bind to epitopes on EGFR which comprise all or a portion of the epitopes recognized by the particular antibodies of the combinations described herein. In another embodiment, the antibodies are provided that compete for binding to EGFR with the antibodies described herein. Competing antibodies and antibodies that recognize the same or an overlapping epitope can be identified using routine techniques such as an  
10 immunoassay, for example, by showing the ability of one antibody to block the binding of another antibody to a target antigen, *i.e.*, a competitive binding assay. Competitive binding may be determined using an assay such as described in the Examples below.

The terms “specific binding,” “specifically binds,” “selective binding,” and “selectively binds,” mean that an antibody exhibits appreciable affinity for a particular  
15 antigen or epitope and, generally, does not exhibit significant cross-reactivity with other antigens and epitopes. “Appreciable” or preferred binding includes binding with a  $K_D$  of  $10^6$ ,  $10^7$ ,  $10^8$ ,  $10^9$ , or  $10^{10} M^{-1}$  or better. The  $K_D$  of an antibody antigen interaction (the affinity constant) indicates the concentration of antibody at which 50% of antibody and antigen molecules are bound together. Thus, at a suitable fixed antigen concentration,  
20 50% of a higher (*i.e.*, stronger) affinity antibody will bind antigen molecules at a lower antibody concentration than would be required to achieve the same percent binding with a lower affinity antibody. Thus a lower  $K_D$  value indicates a higher (stronger) affinity. As used herein, “better” affinities are stronger affinities, and are of lower numeric value than their comparators, with a  $K_D$  of  $10^7 M^{-1}$  being of lower numeric value and therefore  
25 representing a better affinity than a  $K_D$  of  $10^6 M^{-1}$ . Affinities better (*i.e.*, with a lower  $K_D$  value and therefore stronger) than  $10^7 M^{-1}$ , preferably better than  $10^8 M^{-1}$ , are generally preferred. Values intermediate to those set forth herein are also contemplated, and a preferred binding affinity can be indicated as a range of affinities, for example preferred binding affinities for anti-EGFR antibodies disclosed herein are,  $10^6$  to  $10^{12} M^{-1}$ ,  
30 preferably  $10^7$  to  $10^{12} M^{-1}$ , more preferably  $10^8$  to  $10^{12} M^{-1}$ . An antibody that “does not exhibit significant cross-reactivity” is one that will not appreciably bind to an off target antigen (*e.g.*, a non-EGFR protein). For example, in one embodiment, an antibody that specifically binds to EGFR will exhibit at least a two, and preferably three, or four or

more orders of magnitude better binding affinity (i.e., binding exhibiting a two, three, or four or more orders of magnitude lower  $K_D$  value) for EGFR than for ErbB molecules other than ErbB1 (EGFR) or for non-ErbB proteins or peptides. Specific or selective binding can be determined according to any art-recognized means for determining such binding, including, for example, according to Scatchard analysis and/or competitive (competition) binding assays as described herein.

The term “ $K_D$ ,” as used herein, is intended to refer to the dissociation equilibrium constant of a particular antibody-antigen interaction or the affinity of an antibody for an antigen. In one embodiment, the antibody provided herein binds an antigen (e.g., EGFR) with an affinity ( $K_D$ ) of 100 nM or better (i.e., or less) (e.g., 90 nM, 80 nM, 70 nM, 60nM, 50nM, 40nM, 30nM, 20nM, 10 nM, 5 nM, 1 nM or less), as measured using a surface plasmon resonance assay, a cell binding assay, or an equilibrium dialysis assay. In a particular embodiment, an antibody binds EGFR with an affinity (as represented by dissociation constant  $K_D$ ) of 8 nM or better (e.g., 7 nM, 6 nM, 5 nM, 4 nM, 2 nM, 1.5 nM, 1.4 nM, 1.3 nM, 1.2nM, 1.1nM, 1nM or lower), as measured by a surface plasmon resonance assay or a cell binding assay. In other embodiments, an antibody binds an antigen (e.g., EGFR) with an affinity ( $K_D$ ) of approximately less than  $10^{-7}$  M, such as approximately less than  $10^{-8}$  M,  $10^{-9}$  M or  $10^{-10}$  M or even lower when determined by surface plasmon resonance (SPR) technology in a BIACORE 3000 instrument using recombinant EGFR as the analyte and the antibody as the ligand, and binds to the predetermined antigen with an affinity that is at least two-fold greater than its affinity for binding to a non-specific antigen (e.g., BSA, casein) other than the predetermined antigen or a closely-related antigen. Other methods for determining  $K_D$  include equilibrium binding to live cells expressing EGFR via flow cytometry (FACS) or in solution using KinExA® technology.

The term “ $K_{off}$ ,” as used herein, is intended to refer to the off rate constant for the dissociation of an antibody from the antibody/antigen complex.

The terms “IC50” and “IC90,” as used herein, refer to the measure of the effectiveness of a compound (e.g., an anti-EGFR antibody) in inhibiting a biological or biochemical function (e.g., the function or activity of EGFR) by 50% and 90%, respectively. For example, IC50 indicates how much of an anti-EGFR antibody is needed to inhibit the activity of EGFR (e.g., the growth of a cell expressing EGFR) by half. That is, it is the half maximal (50%) inhibitory concentration (IC) of an anti-EGFR



antibody (50% IC, or IC<sub>50</sub>). According to the FDA, IC<sub>50</sub> represents the concentration of a drug that is required for 50% inhibition *in vitro*. The IC<sub>50</sub> and IC<sub>90</sub> can be determined by techniques known in the art, for example, by constructing a dose-response curve and examining the effect of different concentrations of the antagonist  
5 (*i.e.*, the anti-EGFR antibody) on reversing EGFR activity.

As used herein, “glycosylation pattern” is defined as the pattern of carbohydrate units that are covalently attached to a protein, more specifically to an immunoglobulin protein.

The term “nucleic acid molecule,” as used herein, is intended to include DNA  
10 molecules and RNA molecules. A nucleic acid molecule may be single-stranded or double-stranded, but preferably is double-stranded DNA.

The term “isolated nucleic acid molecule,” as used herein in reference to nucleic acids encoding antibodies or antibody fragments (*e.g.*, V<sub>H</sub>, V<sub>L</sub>, CDR3), is intended to refer to a nucleic acid molecule in which the nucleotide sequences are essentially free of  
15 other genomic nucleotide sequences, *e.g.*, those encoding antibodies that bind antigens other than EGFR, which other sequences may naturally flank the nucleic acid in human genomic DNA.

The term “modifying,” or “modification,” as used herein, is intended to refer to changing one or more amino acids in the antibodies or antigen-binding portions thereof.  
20 The change can be produced by adding, substituting or deleting an amino acid at one or more positions. The change can be produced using known techniques, such as PCR mutagenesis. For example, in some embodiments, an antibody or an antigen-binding portion thereof identified using the methods provided herein can be modified, to thereby modify the binding affinity of the antibody or antigen-binding portion thereof to EGFR.  
25 “Conservative amino acid substitutions” in the sequences of the antibodies are provided, *i.e.*, nucleotide and amino acid sequence modifications which do not abrogate the binding of the antibody encoded by the nucleotide sequence or containing the amino acid sequence, to the antigen, *i.e.*, EGFR. Conservative amino acid substitutions include the substitution of an amino acid in one class by an amino acid of the same class, where  
30 a class is defined by common physicochemical amino acid side chain properties and high substitution frequencies in homologous proteins found in nature, as determined, for example, by a standard Dayhoff frequency exchange matrix or BLOSUM matrix. Six general classes of amino acid side chains have been categorized and include: Class I

(Cys); Class II (Ser, Thr, Pro, Ala, Gly); Class III (Asn, Asp, Gln, Glu); Class IV (His, Arg, Lys); Class V (Ile, Leu, Val, Met); and Class VI (Phe, Tyr, Trp). For example, substitution of an Asp for another class III residue such as Asn, Gln, or Glu, is a conservative substitution. Thus, a predicted nonessential amino acid residue in an anti-EGFR antibody is preferably replaced with another amino acid residue from the same class. Methods of identifying nucleotide and amino acid conservative substitutions which do not eliminate antigen binding are well-known in the art.

The term “non-conservative amino acid substitution” refers to the substitution of an amino acid in one class with an amino acid from another class; for example, substitution of an Ala, a class II residue, with a class III residue such as Asp, Asn, Glu, or Gln.

Alternatively, in another embodiment, mutations (conservative or non-conservative) can be introduced randomly along all or part of an anti-EGFR antibody coding sequence, such as by saturation mutagenesis, and the resulting modified anti-EGFR antibodies can be screened for binding activity.

A “consensus sequence” is a sequence formed from the most frequently occurring amino acids (or nucleotides) in a family of related sequences. In a family of proteins, each position in the consensus sequence is occupied by the amino acid occurring most frequently at that position in the family. If two amino acids occur equally frequently, either can be included in the consensus sequence. A “consensus framework” of an immunoglobulin refers to a framework region in the consensus immunoglobulin sequence. Similarly, the consensus sequence for the CDRs of can be derived by optimal alignment of the CDR amino acid sequences of EGFR antibodies provided herein.

For nucleic acids, the term “substantial homology” indicates that two nucleic acids, or designated sequences thereof, when optimally aligned and compared, are identical, with appropriate nucleotide insertions or deletions, in at least about 80% of the nucleotides, usually at least about 90% to 95%, and more preferably at least about 98% to 99.5% of the nucleotides. Alternatively, substantial homology exists when the segments will hybridize under selective hybridization conditions, to the complement of the strand.

The nucleic acids may be present in whole cells, in a cell lysate, or in a partially purified or substantially pure form. A nucleic acid is “isolated” or “rendered

substantially pure” when purified away from other cellular components or other contaminants, *e.g.*, other cellular nucleic acids or proteins, by standard techniques, including alkaline/SDS treatment, CsCl banding, column chromatography, agarose gel electrophoresis and others well known in the art.

5           The nucleic acid compositions, while often comprising a native sequence (except for modified restriction sites and the like), from either cDNA, genomic or mixtures thereof may alternately be mutated, in accordance with standard techniques to provide altered gene sequences. For coding sequences, these mutations, may modify the encoded amino acid sequence as desired. In particular, DNA sequences substantially  
10 homologous to native V, D, J, constant, switches and other such sequences described herein are contemplated.

          The term “operably linked” refers to a nucleic acid sequence placed into a functional relationship with another nucleic acid sequence. For example, DNA for a presequence or secretory leader is operably linked to DNA for a polypeptide if it is  
15 expressed as a pre-protein that participates in the secretion of the polypeptide; a promoter or enhancer is operably linked to a coding sequence if it affects the transcription of the sequence; or a ribosome binding site is operably linked to a coding sequence if it is positioned so as to facilitate translation. Generally, “operably linked” means that the DNA sequences being linked are contiguous, and, in the case of a  
20 secretory leader, contiguous and in reading phase. However, enhancers do not have to be contiguous. Linking is accomplished by ligation at convenient restriction sites. If such sites do not exist, the synthetic oligonucleotide adaptors or linkers are used in accordance with conventional practice. A nucleic acid is “operably linked” when it is placed into a functional relationship with another nucleic acid sequence. For instance, a  
25 promoter or enhancer is operably linked to a coding sequence if it affects the transcription of the sequence. With respect to transcription regulatory sequences, operably linked means that the DNA sequences being linked are contiguous and, where necessary to join two protein coding regions, contiguous and in reading frame. For switch sequences, operably linked indicates that the sequences are capable of effecting  
30 switch recombination.

          The term “vector,” as used herein, is intended to refer to a nucleic acid molecule capable of transporting another nucleic acid to which it has been linked. One type of vector is a “plasmid,” which refers to a circular double stranded DNA loop into which

additional DNA segments may be ligated. Another type of vector is a viral vector, wherein additional DNA segments may be ligated into the viral genome. Certain vectors are capable of autonomous replication in a host cell into which they are introduced (*e.g.*, bacterial vectors having a bacterial origin of replication and episomal mammalian  
5 vectors). Other vectors (*e.g.*, non-episomal mammalian vectors) can be integrated into the genome of a host cell upon introduction into the host cell, and thereby are replicated along with the host genome. Moreover, certain vectors are capable of directing the expression of genes to which they are operatively linked. Such vectors are referred to herein as “recombinant expression vectors” (or simply, “expression vectors”). In  
10 general, expression vectors of utility in recombinant DNA techniques are often in the form of plasmids. The terms, “plasmid” and “vector” may be used interchangeably. However, other forms of expression vectors, such as viral vectors (*e.g.*, replication defective retroviruses, adenoviruses and adeno-associated viruses), which serve equivalent functions are also contemplated.

15 The term “recombinant host cell” (or simply “host cell”), as used herein, is intended to refer to a cell into which a recombinant expression vector has been introduced. It should be understood that such terms are intended to refer not only to the particular subject cell but to the progeny of such a cell. Because certain modifications may occur in succeeding generations due to either mutation or environmental influences,  
20 such progeny may not, in fact, be identical to the parent cell, but are still included within the scope of the term “host cell” as used herein.

The terms “treat,” “treating,” and “treatment,” as used herein, refer to therapeutic or preventative measures described herein. The methods of “treatment” employ administration to a subject, an antibody or antibody pair or trio disclosed herein, for  
25 example, a subject having a disease or disorder associated with EGFR dependent signaling or predisposed to having such a disease or disorder, in order to prevent, cure, delay, reduce the severity of, or ameliorate one or more symptoms of the disease or disorder or recurring disease or disorder, or in order to prolong the survival of a subject beyond that expected in the absence of such treatment.

30 The term “disease associated with EGFR dependent signaling,” or “disorder associated with EGFR dependent signaling,” as used herein, includes disease states and/or symptoms associated with a disease state, where increased levels of EGFR and/or activation of cellular cascades involving EGFR are found. The term “disease associated

with EGFR dependent signaling,” also includes disease states and/or symptoms associated with the activation of alternative EGFR signaling pathways. In general, the term “disease associated with EGFR dependent signaling,” refers to any disorder, the onset, progression or the persistence of the symptoms of which requires the participation  
5 of EGFR. Exemplary EGFR-mediated disorders include, but are not limited to, for example, cancer.

The terms “cancer” and “cancerous” refer to or describe the physiological condition in mammals that is typically characterized by unregulated cell growth. Examples of cancer include but are not limited to, carcinoma, lymphoma, blastoma,  
10 sarcoma, and leukemia. More particular examples of such cancers include squamous cell cancer, small-cell lung cancer, non-small cell lung cancer, gastric cancer, pancreatic cancer, glial cell tumors such as glioblastoma and neurofibromatosis, cervical cancer, ovarian cancer, liver cancer, bladder cancer, hepatoma, breast cancer, colon cancer, melanoma, colorectal cancer, endometrial carcinoma, salivary gland carcinoma, kidney  
15 cancer, renal cancer, prostate cancer, vulval cancer, thyroid cancer, hepatic carcinoma and various types of head and neck cancer. In a particular embodiment, a cancer treated or diagnosed using the methods disclosed herein is selected from melanoma, breast cancer, ovarian cancer, renal carcinoma, gastrointestinal/colon cancer, lung cancer, and prostate cancer.

20 The term “effective amount,” as used herein, refers to that amount of an antibody or an antigen binding portion thereof that binds EGFR, which is sufficient to effect treatment, prognosis or diagnosis of a disease associated with EGFR dependent signaling, as described herein, when administered to a subject. Therapeutically effective amounts of antibodies provided herein, when used alone or in combination, will vary  
25 depending upon the relative activity of the antibodies and combinations (*e.g.*, in inhibiting cell growth) and depending upon the subject and disease condition being treated, the weight and age of the subject, the severity of the disease condition, the manner of administration and the like, which can readily be determined by one of ordinary skill in the art. The dosages for administration can range from, for example,  
30 about 1 ng to about 10,000 mg, about 5 ng to about 9,500 mg, about 10 ng to about 9,000 mg, about 20 ng to about 8,500 mg, about 30 ng to about 7,500 mg, about 40 ng to about 7,000 mg, about 50 ng to about 6,500 mg, about 100 ng to about 6,000 mg, about 200 ng to about 5,500 mg, about 300 ng to about 5,000 mg, about 400 ng to about 4,500

mg, about 500 ng to about 4,000 mg, about 1  $\mu$ g to about 3,500 mg, about 5  $\mu$ g to about 3,000 mg, about 10  $\mu$ g to about 2,600 mg, about 20  $\mu$ g to about 2,575 mg, about 30  $\mu$ g to about 2,550 mg, about 40  $\mu$ g to about 2,500 mg, about 50  $\mu$ g to about 2,475 mg, about 100  $\mu$ g to about 2,450 mg, about 200  $\mu$ g to about 2,425 mg, about 300  $\mu$ g to about 2,000, about 400  $\mu$ g to about 1,175 mg, about 500  $\mu$ g to about 1,150 mg, about 0.5 mg to about 1,125 mg, about 1 mg to about 1,100 mg, about 1.25 mg to about 1,075 mg, about 1.5 mg to about 1,050 mg, about 2.0 mg to about 1,025 mg, about 2.5 mg to about 1,000 mg, about 3.0 mg to about 975 mg, about 3.5 mg to about 950 mg, about 4.0 mg to about 925 mg, about 4.5 mg to about 900 mg, about 5 mg to about 875 mg, about 10 mg to about 850 mg, about 20 mg to about 825 mg, about 30 mg to about 800 mg, about 40 mg to about 775 mg, about 50 mg to about 750 mg, about 100 mg to about 725 mg, about 200 mg to about 700 mg, about 300 mg to about 675 mg, about 400 mg to about 650 mg, about 500 mg, or about 525 mg to about 625 mg, of an antibody. Dosage regimens may be adjusted to provide the optimum therapeutic response. An effective amount is also one in which any toxic or detrimental effects (*i.e.*, side effects) of an antibody are minimized and/or outweighed by the beneficial effects.

The term “therapeutic agent” is intended to encompass any and all compounds that have an ability to decrease or inhibit the severity of the symptoms of a disease or disorder, or increase the frequency and/or duration of symptom-free or symptom-reduced periods in a disease or disorder, or inhibit or prevent impairment or disability due to a disease or disorder affliction, or inhibit or delay progression of a disease or disorder, or inhibit or delay onset of a disease or disorder, or inhibit or prevent infection in an infectious disease or disorder. Non-limiting examples of therapeutic agents include small organic molecules, monoclonal antibodies, bispecific antibodies, recombinantly engineered biologics, RNAi compounds, tyrosine kinase inhibitors, and commercial antibodies. In certain embodiments, tyrosine kinase inhibitors include, *e.g.*, one or more of erlotinib, gefitinib, and lapatinib, which are currently marketed pharmaceuticals. Commercially available pharmaceutical anti-EGFR antibodies include cetuximab and panitumumab. Other pharmaceutical anti-EGFR antibodies include zalutumumab, nimotuzumab, and matuzumab, which are in development.

The term “patient” includes human and other mammalian subjects that receive either prophylactic or therapeutic treatment.

The term “subject” includes any mammal, *e.g.*, a primate. For example, the methods and compositions herein disclosed can be used to treat a subject having cancer. In a particular embodiment, the subject is a human.

The term “sample” refers to tissue, body fluid, or a cell (or a fraction of any of the foregoing) taken from a patient or a subject. Normally, the tissue or cell will be removed from the patient, but *in vivo* diagnosis is also contemplated. In the case of a solid tumor, a tissue sample can be taken from a surgically removed tumor and prepared for testing by conventional techniques. In the case of lymphomas and leukemias, lymphocytes, leukemic cells, or lymph tissues can be obtained (*e.g.*, leukemic cells from blood) and appropriately prepared. Other samples, including urine, tears, serum, plasma, cerebrospinal fluid, feces, sputum, cell extracts *etc.* can also be useful for particular cancers.

Various aspects of the disclosure are described in further detail in the following subsections.

15 **II. Anti-EGFR Antibodies and Combinations Thereof**

Novel anti-EGFR monoclonal antibodies are disclosed herein, including three referred to in the Examples as P1X, P2X and P3X. The P1X, P2X and P3X monoclonal antibodies are affinity matured antibodies of parental antibodies referred to as ca, cd and ch, respectively, disclosed in PCT Application No. PCT/US2011/35238. The CDR amino acid sequences of the parental and affinity matured antibodies are shown below, with the changed amino acids in the affinity matured antibodies bolded and underlined:

25	ca V <sub>H</sub>	<u>CDR1</u> SYAIS (SEQ ID NO: 1)	<u>CDR2</u> IIPFGTANY (SEQ ID NO: 27)	<u>CDR3</u> DPSVDL (SEQ ID NO: 28)
30	P1X V <sub>H</sub>	<u>CDR1</u> SYAIS (SEQ ID NO: 1)	<u>CDR2</u> IIPFGT <u>V</u> NY (SEQ ID NO: 2)	<u>CDR3</u> DPSV <u>N</u> L (SEQ ID NO: 3)
	ca V <sub>L</sub>	<u>CDR1</u> QSISSWLA (SEQ ID NO: 29)	<u>CDR2</u> DASSL (SEQ ID NO: 5)	<u>CDR3</u> QQFAAHA (SEQ ID NO: 30)
35	P1X V <sub>L</sub>	<u>CDR1</u> QSISSW <u>W</u> A (SEQ ID NO: 4)	<u>CDR2</u> DASSL (SEQ ID NO: 5)	<u>CDR3</u> QQY <u>H</u> A <u>H</u> P (SEQ ID NO: 6)

5	cd V <sub>H</sub>	<u>CDR1</u> SYAIS (SEQ ID NO: 7)	<u>CDR2</u> IPIFGTANY (SEQ ID NO: 27)	<u>CDR3</u> MGRGKV (SEQ ID NO: 9)
10	P2X V <sub>H</sub>	<u>CDR1</u> SYAIS (SEQ ID NO: 7)	<u>CDR2</u> IPIFGAANP (SEQ ID NO: 8)	<u>CDR3</u> MGRGKV (SEQ ID NO: 9)
15	cd V <sub>L</sub>	<u>CDR1</u> QSVLYSSNNKNYLA (SEQ ID NO: 31)	<u>CDR2</u> WASTR (SEQ ID NO: 11)	<u>CDR3</u> QQYYGSP (SEQ ID NO: 12)
15	P2X V <sub>L</sub>	<u>CDR1</u> QSVLYSPNNKNYLA (SEQ ID NO: 10)	<u>CDR2</u> WASTR (SEQ ID NO: 11)	<u>CDR3</u> QQYYGSP (SEQ ID NO: 12)
20	ch V <sub>H</sub>	<u>CDR1</u> SYGIN (SEQ ID NO: 13)	<u>CDR2</u> ISAYNGNTNY (SEQ ID NO: 32)	<u>CDR3</u> DLGGYGSGS (SEQ ID NO: 15)
25	P3X V <sub>H</sub>	<u>CDR1</u> SYGIN (SEQ ID NO: 13)	<u>CDR2</u> ISAYNGNTYY (SEQ ID NO: 14)	<u>CDR3</u> DLGGYGSGS (SEQ ID NO: 15)
30	ch V <sub>L</sub>	<u>CDR1</u> QSVSSNLA (SEQ ID NO: 16)	<u>CDR2</u> GASTR (SEQ ID NO: 17)	<u>CDR3</u> QDYRTWPR (SEQ ID NO: 18)
35	P3X V <sub>L</sub>	<u>CDR1</u> QSVSSNLA (SEQ ID NO: 16)	<u>CDR2</u> GASTR (SEQ ID NO: 17)	<u>CDR3</u> QDYRTWPR (SEQ ID NO: 18)

The full-length V<sub>H</sub> and V<sub>L</sub> amino sequences for P1X are shown in SEQ ID NO: 19 and 20, respectively. The full-length V<sub>H</sub> and V<sub>L</sub> amino sequences for P2X are shown in SEQ ID NO: 21 and 22, respectively. The full-length V<sub>H</sub> and V<sub>L</sub> amino sequences for P3X are shown in SEQ ID NO: 23 and 24, respectively. Additionally, the V<sub>H</sub> and V<sub>L</sub> CDR segments as presented herein are arranged, *e.g.*, in the amino to carboxy terminal order of CDR1, CDR2 and CDR3.



In one embodiment, a monoclonal antibody is provided which binds EGFR extracellular domain and comprises heavy and light chain CDR1, CDR2, and CDR3, sequences, wherein the heavy and light chain CDR1, CDR2, and CDR3, sequences are selected from the group consisting of:

5 (a) heavy chain CDR1, CDR2, and CDR3 sequences of SEQ ID NOs: 1, 2, and 3 respectively, and light chain CDR1, CDR2, and CDR3 sequences of SEQ ID NOs: 4, 5, and 6, respectively;

(b) heavy chain CDR1, CDR2, and CDR3 sequences of SEQ ID NOs: 7, 8, and 9, respectively, and light chain CDR1, CDR2, and CDR3 sequences of SEQ ID NOs: 10,  
10 11 and 12, respectively; and

(c) heavy chain CDR1, CDR2, and CDR3 sequences of SEQ ID NOs: 13, 14, and 15, respectively, and light chain CDR1, CDR2, and CDR3 sequences of SEQ ID NOs: 16, 17, and 18, respectively.

In another embodiment, a monoclonal antibody is provided that binds to EGFR  
15 extracellular domain and comprises a heavy chain variable region and a light chain variable region, wherein the heavy and light chain variable region sequences are selected from the group consisting of:

(a) a heavy chain variable region comprising SEQ ID NO: 19 and a light chain variable region comprising SEQ ID NO: 20;

20 (b) a heavy chain variable region comprising SEQ ID NO: 21 and a light chain variable region comprising SEQ ID NO: 22; and

(c) a heavy chain variable region comprising SEQ ID NO: 23 and a light chain variable region comprising SEQ ID NO: 24.

Combinations of the aforementioned anti-EGFR antibodies are also provided.  
25 Such combinations can contain, for example, any combination of two of the aforementioned anti-EGFR antibodies. Another combination can comprise all three of the aforementioned anti-EGFR antibodies. Accordingly, in another aspect, a composition comprising two or three monoclonal antibodies which bind to EGFR extracellular domain is provided, wherein the two or three monoclonal antibodies are  
30 selected from the group consisting of:

(a) a monoclonal antibody comprising heavy chain CDR1, CDR2, and CDR3 sequences of SEQ ID NOs: 1, 2, and 3 respectively, and light chain CDR1, CDR2, and CDR3 sequences of SEQ ID NOs: 4, 5, and 6, respectively;

(b) a monoclonal antibody comprising heavy chain CDR1, CDR2, and CDR3 sequences of SEQ ID NOs: 7, 8, and 9, respectively, and light chain CDR1, CDR2, and CDR3 sequences of SEQ ID NOs: 10, 11 and 12, respectively and

(c) a monoclonal antibody comprising heavy chain CDR1, CDR2, and CDR3  
5 sequences of SEQ ID NOs: 13, 14, and 15, respectively, and light chain CDR1, CDR2, and CDR3 sequences of SEQ ID NOs: 16, 17 and 18, respectively;  
and wherein the composition comprises (a) and (b), (a) and (c), (b) and (c) or (a), (b) and (c).

In yet another embodiment, a composition comprising two or three monoclonal  
10 antibodies which bind to EGFR extracellular domain is provided, wherein the two or three monoclonal antibodies are selected from the group consisting of:

(a) a monoclonal antibody comprising a heavy chain variable region comprising SEQ ID NO: 19 and a light chain variable region comprising SEQ ID NO: 20;

(b) a monoclonal antibody comprising a heavy chain variable region comprising  
15 SEQ ID NO: 21 and a light chain variable region comprising SEQ ID NO: 22; and

(c) a monoclonal antibody comprising a heavy chain variable region comprising SEQ ID NO: 23 and a light chain variable region comprising SEQ ID NO: 24;  
and wherein the composition comprises (a) and (b), (a) and (c), (b) and (c) or (a) (b) and (c).

20 The anti-EGFR antibodies disclosed herein, whether as a single antibody or in a combination of antibodies, can bind to EGFR with a  $K_D$  of, for example, better than 100 nM, or better than 10 nM or better than 1 nM. As used herein with respect to  $K_D$ , the term “better than \_\_\_ nM” means that an antibody has a  $K_D$ , expressed as a nanomolar concentration, that is lower than the indicated number. For example, a  $K_D$  that is “better  
25 than” 100 nM indicates a  $K_D$ , expressed as a nanomolar concentration, that is lower in value than 100 nM (e.g., is 50 nM).

In other embodiments, a PIX-related antibody, such as an antibody comprising heavy chain CDR1, CDR2, and CDR3 sequences of SEQ ID NOs: 1, 2, and 3 respectively, and light chain CDR1, CDR2, and CDR3 sequences of SEQ ID NOs: 4, 5,  
30 and 6, respectively, or an antibody comprising  $V_H$  and  $V_L$  sequences of SEQ ID NOs: 19 and 20, respectively, can bind to EGFR with a  $K_D$  in a range of about  $1 \times 10^{-9}$  M to  $1.1 \times 10^{-11}$  M or better.

In other embodiments, a P2X-related antibody, such as an antibody comprising heavy chain CDR1, CDR2, and CDR3 sequences of SEQ ID NOs: 7, 8 and 9 respectively, and light chain CDR1, CDR2, and CDR3 sequences of SEQ ID NOs: 10, 11, and 12, respectively, or an antibody comprising V<sub>H</sub> and V<sub>L</sub> sequences of SEQ ID  
5 NOs: 21 and 22, respectively, can bind to EGFR with a K<sub>D</sub> in a range of about 1 x 10<sup>-9</sup> M to 7.0 x 10<sup>-11</sup> M or better.

In other embodiments, a P3X-related antibody, such as an antibody comprising heavy chain CDR1, CDR2, and CDR3 sequences of SEQ ID NOs: 13, 14 and 15 respectively, and light chain CDR1, CDR2, and CDR3 sequences of SEQ ID NOs: 16,  
10 17, and 18, respectively, or an antibody comprising V<sub>H</sub> and V<sub>L</sub> sequences of SEQ ID NOs: 23 and 24, respectively, can bind to EGFR with a K<sub>D</sub> in a range of about 1 x 10<sup>-9</sup> M to 3.6 x 10<sup>-10</sup> M or better.

The anti-EGFR antibodies disclosed herein, whether as a single antibody or in a combination of antibodies, can exhibit one or more other functional properties as  
15 disclosed herein, including but not limited to

- (a) inhibition of AKT or ERK phosphorylation, *e.g.*, EGFR-dependant AKT or ERK phosphorylation, as measured in a cell-based assay;
- (b) inhibition of the growth of cells expressing EGFR;
- (c) inhibition of EGF ligand binding to EGFR (*e.g.*, inhibition of binding of one  
20 or more ligands that bind EGFR, including EGF, heparin binding EGF-like growth factor (HB-EGF), transforming growth factor (TGF), epigen, epiregulin, betacellulin, or amphiregulin);
- (d) inhibition of EGFR dimerization;
- (e) downregulation of EGFR on cell surfaces (*e.g.*, by internalization and  
25 recycling of the receptor, and/or internalization and degradation of the receptor);
- (f) inhibition of *in vitro* tumor cell proliferation; and/or
- (g) inhibition of *in vivo* tumor growth.

Antibodies disclosed herein include all known forms of antibodies and other protein scaffolds with antibody-like properties. For example, the antibody can be a  
30 human antibody, a humanized antibody, a bispecific antibody, an immunoconjugate, a chimeric antibody or a protein scaffold with antibody-like properties, such as fibronectin or ankyrin repeats. The antibody also can be a Fab, Fab'2, ScFv, affibody®, avimer, nanobody, or a domain antibody. The antibody also can have any isotype, including any

of the following isotypes: IgG1, IgG2, IgG3, IgG4, IgM, IgA1, IgA2, IgAsec, IgD, and IgE. IgG antibodies are preferred. Full-length antibodies can be prepared from V<sub>H</sub> and V<sub>L</sub> sequences using standard recombinant DNA techniques and nucleic acid encoding the desired constant region sequences to be operatively linked to the variable region  
5 sequences. Non-limiting examples of suitable constant region sequences include the kappa light chain constant region disclosed in SEQ ID NO: 25 and the IgG1 heavy chain constant region disclosed in SEQ ID NO: 26.

As disclosed in the examples, it has been discovered that triple combinations of the P1X + P2X + P3X antibodies are particularly efficacious when used at a  
10 P1X:P2X:P3X molar ratio of 2:2:1. Thus, for such a triple antibody combination, 40% of the total concentration is selected to be P1X, 40% of the total concentration is selected to be P2X and 20% of the total concentration is selected to be P3X.

Accordingly, in another embodiment, a composition is provided comprising three monoclonal anti-EGFR antibodies, said composition comprising a first antibody, a  
15 second antibody and a third antibody, wherein (i) the first antibody comprises heavy chain CDR1, CDR2, and CDR3 sequences of SEQ ID NOs: 1, 2, and 3 respectively, and light chain CDR1, CDR2, and CDR3 sequences of SEQ ID NOs: 4, 5, and 6, respectively; (ii) the second antibody comprises heavy chain CDR1, CDR2, and CDR3 sequences of SEQ ID NOs: 7, 8, and 9, respectively, and light chain CDR1, CDR2, and  
20 CDR3 sequences of SEQ ID NOs: 10, 11 and 12, respectively; and (iii) the third antibody comprises heavy chain CDR1, CDR2, and CDR3 sequences of SEQ ID NOs: 13, 14, and 15 respectively, and light chain CDR1, CDR2, and CDR3 sequences of SEQ ID NOs: 16, 17, and 18, respectively, and wherein the first second and third antibodies are present at a molar ratio of 2:2:1 to each other.

25 In yet another embodiment, a composition is provided comprising three monoclonal anti-EGFR antibodies, said composition comprising a first antibody, a second antibody and a third antibody, wherein (i) the first antibody comprises a heavy chain variable region comprising SEQ ID NO: 19 and a light chain variable region comprising SEQ ID NO: 20; (ii) the second antibody comprises a heavy chain variable  
30 region comprising SEQ ID NO: 21 and a light chain variable region comprising SEQ ID NO: 22; and (iii) the third antibody comprises a heavy chain variable region comprising SEQ ID NO: 23 and a light chain variable region comprising SEQ ID NO: 24, and

wherein the first second and third antibodies are present at a molar ratio of 2:2:1 to each other.

Methods of preparing anti-EGFR antibody compositions comprising three antibodies are provided, wherein the antibodies are prepared at a 2:2:1 ratio. More specifically, in another embodiment, a method of preparing an anti-EGFR antibody composition is provided, the method comprising combining in a single composition:

(a) a monoclonal antibody comprising heavy chain CDR1, CDR2, and CDR3 sequences of SEQ ID NOs: 1, 2, and 3 respectively, and light chain CDR1, CDR2, and CDR3 sequences of SEQ ID NOs: 4, 5, and 6, respectively;

10 (b) a monoclonal antibody comprising heavy chain CDR1, CDR2, and CDR3 sequences of SEQ ID NOs: 7, 8, and 9, respectively, and light chain CDR1, CDR2, and CDR3 sequences of SEQ ID NOs: 10, 11 and 12, respectively; and

(c) a monoclonal antibody comprising heavy chain CDR1, CDR2, and CDR3 sequences of SEQ ID NOs: 13, 14, and 15 respectively, and light chain CDR1, CDR2, 15 and CDR3 sequences of SEQ ID NOs: 16, 17, and 18, respectively;

wherein (a), (b) and (c) are combined at a molar ratio of 2:2:1 to each other.

In another embodiment, a method of preparing an anti-EGFR antibody composition is provided, the method comprising combining in a single composition:

(a) a monoclonal antibody comprising a heavy chain variable region comprising 20 SEQ ID NO: 19 and a light chain variable region comprising SEQ ID NO:20;

(b) a monoclonal antibody comprising a heavy chain variable region comprising SEQ ID NO: 21 and a light chain variable region comprising SEQ ID NO: 22; and

(c) a monoclonal antibody comprising a heavy chain variable region comprising SEQ ID NO: 23 and a light chain variable region comprising SEQ ID NO: 24;

25 wherein (a), (b) and (c) are combined at a molar ratio of 2:2:1 to each other.

Methods of treating a subject with three anti-EGFR antibodies wherein the antibodies are administered to the subject at a 2:2:1 ratio are also provided. More specifically, a method of treating a subject with anti-EGFR antibodies is provided, the method comprising administering to the subject:

30 (a) a monoclonal antibody comprising heavy chain CDR1, CDR2, and CDR3 sequences of SEQ ID NOs: 1, 2, and 3 respectively, and light chain CDR1, CDR2, and CDR3 sequences of SEQ ID NOs: 4, 5, and 6, respectively;

(b) a monoclonal antibody comprising heavy chain CDR1, CDR2, and CDR3 sequences of SEQ ID NOs: 7, 8, and 9, respectively, and light chain CDR1, CDR2, and CDR3 sequences of SEQ ID NOs: 10, 11 and 12, respectively; and

(c) a monoclonal antibody comprising heavy chain CDR1, CDR2, and CDR3 sequences of SEQ ID NOs: 13, 14, and 15 respectively, and light chain CDR1, CDR2, and CDR3 sequences of SEQ ID NOs: 16, 17, and 18, respectively;

wherein (a), (b) and (c) are administered to the subject at a molar ratio of 2:2:1 to each other.

In another embodiment, a method of treating a subject with anti-EGFR antibodies is provided, the method comprising administering to the subject:

(a) a monoclonal antibody comprising a heavy chain variable region comprising SEQ ID NO: 19 and a light chain variable region comprising SEQ ID NO:20;

(b) a monoclonal antibody comprising a heavy chain variable region comprising SEQ ID NO: 21 and a light chain variable region comprising SEQ ID NO: 22; and

(c) a monoclonal antibody comprising a heavy chain variable region comprising SEQ ID NO: 23 and a light chain variable region comprising SEQ ID NO: 24;

wherein (a), (b) and (c) are administered to the subject at a molar ratio of 2:2:1 to each other.

Further details on formulating anti-EGFR antibodies into pharmaceutical compositions and methods of using such compositions in EGFR-related diseases are described in subsections below.

### **III. Methods for Producing Antibodies**

#### **(i) Monoclonal Antibodies**

The monoclonal antibodies of provided herein most typically are prepared by standard recombinant DNA techniques based on the amino acid sequences of the V<sub>H</sub> and V<sub>L</sub> regions disclosed herein.

Additionally or alternatively, monoclonal antibodies can be produced using a variety of known techniques, such as the standard somatic cell hybridization technique, viral or oncogenic transformation of B lymphocytes, or yeast or phage display techniques using libraries of human antibody genes. In particular embodiments, the antibodies are fully human monoclonal antibodies.

Accordingly, in one embodiment, a hybridoma method is used for producing an antibody that binds EGFR. In this method, a mouse or other appropriate host animal can be immunized with a suitable antigen in order to elicit lymphocytes that produce or are capable of producing antibodies that will specifically bind to the antigen used for  
5 immunization. Alternatively, lymphocytes may be immunized *in vitro*. Lymphocytes can then be fused with myeloma cells using a suitable fusing agent, such as polyethylene glycol, to form a hybridoma cell. Culture medium in which hybridoma cells are growing is assayed for production of monoclonal antibodies directed against the antigen. After hybridoma cells are identified that produce antibodies of the desired specificity,  
10 affinity, and/or activity, the clones may be subcloned by limiting dilution procedures and grown by standard methods. Suitable culture media for this purpose include, for example, D-MEM or RPMI-1640 medium. In addition, the hybridoma cells may be grown *in vivo* as ascites tumors in an animal. The monoclonal antibodies secreted by the subclones can be separated from the culture medium, ascites fluid, or serum by  
15 conventional immunoglobulin purification procedures such as, for example, protein A-Sepharose, hydroxylapatite chromatography, gel electrophoresis, dialysis, or affinity chromatography.

In another embodiment, antibodies that bind EGFR can be isolated from antibody libraries generated using well know techniques such as those described in, for  
20 example, U.S. Patent Nos. 5,223,409; 5,403,484; and 5,571,698 to Ladner *et al.*; U.S. Patent Nos. 5,427,908 and 5,580,717 to Dower *et al.*; U.S. Patent Nos. 5,969,108 and 6,172,197 to McCafferty *et al.*; and U.S. Patent Nos. 5,885,793; 6,521,404; 6,544,731; 6,555,313; 6,582,915 and 6,593,081 to Griffiths *et al.*. Additionally, production of high affinity (nM range) human antibodies by chain shuffling, as well as combinatorial  
25 infection and *in vivo* recombination as a strategy for constructing very large phage libraries may also be used. See, e.g., US patent application Ser. No. 09/856,907 (PCT Int. Pub. No. WO 00/31246)

In a particular embodiment, the monoclonal antibody that binds EGFR is produced using phage display. This technique involves the generation of a human Fab  
30 library having a unique combination of immunoglobulin sequences isolated from human donors and having synthetic diversity in the heavy-chain CDRs is generated. The library is then screened for Fabs that bind to EGFR.

In yet another embodiment, human monoclonal antibodies directed against EGFR can be generated using transgenic or transchromosomal mice carrying parts of the human immune system rather than the mouse system (see *e.g.*, U.S. Patent Nos. 5,545,806; 5,569,825; 5,625,126; 5,633,425; 5,789,650; 5,877,397; 5,661,016; 5 5,814,318; 5,874,299; and 5,770,429; all to Lonberg and Kay; U.S. Patent No. 5,545,807 to Surani *et al.*; PCT Publication Nos. WO 92/03918, WO 93/12227, WO 94/25585, WO 97/13852, WO 98/24884 and WO 99/45962, all to Lonberg and Kay; and PCT Publication No. WO 01/14424 to Korman *et al.*).

In another embodiment, human antibodies can be raised using a mouse that 10 carries human immunoglobulin sequences on transgenes and transchromosomes, such as a mouse that carries a human heavy chain transgene and a human light chain transchromosome (see *e.g.*, PCT Publication WO 02/43478 to Ishida *et al.*).

Still further, alternative transgenic animal systems expressing human immunoglobulin genes are available in the art and can be used to raise anti-EGFR 15 antibodies. For example, an alternative transgenic system referred to as the Xenomouse (Abgenix, Inc.) can be used; such mice are described in, for example, U.S. Patent Nos. 5,939,598; 6,075,181; 6,114,598; 6,150,584 and 6,162,963 to Kucherlapati *et al.*

Moreover, alternative transchromosomal animal systems expressing human immunoglobulin genes are available in the art and can be used to raise anti-EGFR 20 antibodies. For example, mice carrying both a human heavy chain transchromosome and a human light chain transchromosome can be used. Furthermore, cows carrying human heavy and light chain transchromosomes have been described in the art and can be used to raise anti-EGFR antibodies.

In yet another embodiment, antibodies can be prepared using a transgenic plant 25 and/or cultured plant cells (such as, for example, tobacco, maize and duckweed) that produce such antibodies. For example, transgenic tobacco leaves expressing antibodies can be used to produce such antibodies by, for example, using an inducible promoter. Also, transgenic maize can be used to express such antibodies and antigen binding portions thereof. Antibodies can also be produced in large amounts from transgenic 30 plant seeds including antibody portions, such as single chain antibodies (scFv's), for example, using tobacco seeds and potato tubers.

The binding specificity of monoclonal antibodies (or portions thereof) that bind EGFR prepared using any technique including those disclosed here, can be determined



by immunoprecipitation or by an *in vitro* binding assay, such as radioimmunoassay (RIA) or enzyme-linked immunoabsorbent assay (ELISA). The binding affinity of a monoclonal antibody or portion thereof also can be determined by Scatchard analysis.

In certain embodiments, an EGFR antibody produced using any of the methods  
5 discussed above may be further altered or optimized to achieve a desired binding specificity and/or affinity using art recognized techniques, such as those described herein.

In one embodiment, partial antibody sequences derived from an EGFR antibody may be used to produce structurally and functionally related antibodies. For example,  
10 antibodies interact with target antigens predominantly through amino acid residues that are located in the six heavy and light chain complementarity determining regions (CDRs). For this reason, the amino acid sequences within CDRs are more diverse between individual antibodies than sequences outside of CDRs. Because CDR sequences are responsible for most antibody-antigen interactions, it is possible to  
15 express recombinant antibodies that mimic the properties of specific naturally occurring antibodies by constructing expression vectors that include CDR sequences from the specific naturally occurring antibody grafted onto framework sequences from a different antibody with different properties. Such framework sequences can be obtained from public DNA databases that include germline antibody gene sequences.

20 Thus, one or more structural features of an anti-EGFR antibody, such as the CDRs, can be used to create structurally related anti-EGFR antibodies that retain at least one desired functional property, *e.g.*, inhibiting growth of cells expressing EGFR.

In a particular embodiment, one or more CDR regions disclosed herein is combined recombinantly with known human framework regions and CDRs to create  
25 additional, recombinantly-engineered, anti-EGFR antibodies. The heavy and light chain variable framework regions can be derived from the same or different antibody sequences.

It is well known in the art that antibody heavy and light chain CDR3 domains play a particularly important role in the binding specificity/affinity of an antibody for an  
30 antigen. Accordingly, in certain embodiments, antibodies are generated that include the heavy and/or light chain CDR3s of the particular antibodies described herein. The antibodies can further include the heavy and/or light chain CDR1 and/or CDR2s of the antibodies disclosed herein.

The CDR 1, 2, and/or 3 regions of the engineered antibodies described above can comprise the exact amino acid sequence(s) as those disclosed herein. However, the ordinarily skilled artisan will appreciate that some deviation from the exact CDR sequences may be possible, particularly for CDR1 and CDR2 sequences, which can tolerate more variation than CDR3 sequences without altering epitope specificity (such deviations are, e.g., conservative amino acid substitutions). Accordingly, in another embodiment, the engineered antibody may be composed of one or more CDR1s and CDR2s that are, for example, 90%, 95%, 98%, 99% or 99.5% identical to the corresponding CDRs of an antibody named herein.

10 In another embodiment, one or more residues of a CDR may be altered to modify binding to achieve a more favored on-rate of binding. Using this strategy, an antibody having ultra high binding affinity of, for example,  $10^{10} \text{ M}^{-1}$  or more, can be achieved. Affinity maturation techniques, well known in the art and those described herein, can be used to alter the CDR region(s) followed by screening of the resultant binding molecules for the desired change in binding. Accordingly, as CDR(s) are altered, changes in binding affinity as well as immunogenicity can be monitored and scored such that an antibody optimized for the best combined binding and low immunogenicity are achieved.

20 Modifications can also be made within one or more of the framework or joining regions of the heavy and/or the light chain variable regions of an antibody, so long as antigen binding affinity subsequent to these modifications is better than  $10^6 \text{ M}^{-1}$ .

In another embodiment, the antibody is further modified with respect to effector function, so as to enhance the effectiveness of the antibody in treating cancer, for example. For example cysteine residue(s) may be introduced in the Fc region, thereby allowing interchain disulfide bond formation in this region. The homodimeric antibody thus generated may have improved internalization capability and/or increased complement-mediated cell killing and antibody-dependent cellular cytotoxicity (ADCC). Homodimeric antibodies with enhanced anti-tumor activity may also be prepared using heterobifunctional cross-linkers. Alternatively, an antibody can be engineered which has dual Fc regions and may thereby have enhanced complement lysis and ADCC capabilities.

30 Also provided are bispecific antibodies and immunoconjugates, as discussed below.

(ii) Bispecific Antibodies

Bispecific antibodies herein include at least two binding specificities for EGFR which preferably bind non-overlapping or non-competing epitopes. Such bispecific antibodies can include additional binding specificities, *e.g.*, a third EGFR binding  
5 specificity and/or a binding specificity for another ErbB receptor (*e.g.*, ErbB3) or another antigen, such as the product of an oncogene. Bispecific antibodies can be prepared as full length antibodies or antibody fragments (*e.g.* F(ab')<sub>2</sub> bispecific antibodies).

Methods for making bispecific antibodies are well known in the art (see, *e.g.*,  
10 WO 05117973 and WO 06091209). For example, production of full length bispecific antibodies can be based on the coexpression of two paired immunoglobulin heavy chain-light chains, where the two chains have different specificities. Various techniques for making and isolating bispecific antibody fragments directly from recombinant cell culture have also been described. For example, bispecific antibodies have been  
15 produced using leucine zippers. Another strategy for making bispecific antibody fragments by the use of single-chain Fv (sFv) dimers has also been reported.

In a particular embodiment, the bispecific antibody comprises a first antibody (or binding portion thereof) which binds to EGFR derivatized or linked to another functional molecule, *e.g.*, another peptide or protein (*e.g.*, another antibody or ligand for  
20 a receptor) to generate a bispecific molecule that binds to at least two different binding sites or target molecules. An antibody may be derivatized or linked to more than one other functional molecule to generate multispecific molecules that bind to more than two different binding sites and/or target molecules; such multispecific molecules are also intended to be encompassed by the term "bispecific molecule" as used herein. To  
25 create a bispecific molecule, an antibody disclosed herein can be functionally linked (*e.g.*, by chemical coupling, genetic fusion, noncovalent association or otherwise) to one or more other binding molecules, such as another antibody, antibody fragment, peptide or binding mimetic, such that a bispecific molecule results.

Accordingly, bispecific molecules comprising at least one first binding  
30 specificity for EGFR and a second binding specificity for a second target epitope are contemplated. In a particular embodiment, the second target epitope is an Fc receptor, *e.g.*, human FcγRI (CD64) or a human Fcα receptor (CD89). Therefore, bispecific molecules capable of binding both to FcγR, FcαR or FcεR expressing effector cells (*e.g.*,

monocytes, macrophages or polymorphonuclear cells (PMNs)), and to target cells expressing EGFR are also provided. These bispecific molecules target EGFR expressing cells to effector cell and trigger Fc receptor-mediated effector cell activities, such as phagocytosis of an EGFR expressing cells, antibody dependent cell-mediated cytotoxicity (ADCC), cytokine release, or generation of superoxide anion.

In one embodiment, the bispecific molecules comprise as a binding specificity at least one antibody, or an antibody fragment thereof, including, *e.g.*, an Fab, Fab', F(ab')<sub>2</sub>, Fv, or a single chain Fv. The antibody may also be a light chain or heavy chain dimer, or any minimal fragment thereof such as a Fv or a single chain construct as described in Ladner *et al.* U.S. Patent No. 4,946,778.

The bispecific molecules can be prepared by conjugating the constituent binding specificities, *e.g.*, the anti-FcR and anti-EGFR binding specificities, using methods known in the art. For example, each binding specificity of the bispecific molecule can be generated separately and then conjugated to one another. When the binding specificities are proteins or peptides, a variety of coupling or cross-linking agents can be used for covalent conjugation. Examples of cross-linking agents include protein A, carbodiimide, N-succinimidyl-S-acetyl-thioacetate (SATA), 5,5'-dithiobis(2-nitrobenzoic acid) (DTNB), o-phenylenedimaleimide (oPDM), N-succinimidyl-3-(2-pyridyldithio)propionate (SPDP), and sulfosuccinimidyl 4-(N-maleimidomethyl) cyclohexane-1-carboxylate (sulfo-SMCC). Preferred conjugating agents are SATA and sulfo-SMCC, both available from Pierce Chemical Co. (Rockford, IL).

When the binding specificities are antibodies, they can be conjugated via sulfhydryl bonding of the C-terminus hinge regions of the two heavy chains. In a particularly preferred embodiment, the hinge region is modified to contain an odd number of sulfhydryl residues, preferably one, prior to conjugation.

Alternatively, both binding specificities can be encoded in the same vector and expressed and assembled in the same host cell. This method is particularly useful where the bispecific molecule is a mAb x mAb, mAb x Fab, Fab x F(ab')<sub>2</sub> or ligand x Fab fusion protein. A bispecific molecule can be a single chain molecule comprising one single chain antibody and a binding determinant, or a single chain bispecific molecule comprising two binding determinants. Bispecific molecules may comprise at least two single chain molecules. Methods for preparing bispecific molecules are described for example in U.S. Patent Number 5,260,203; U.S. Patent Number 5,455,030; U.S. Patent

Number 4,881,175; U.S. Patent Number 5,132,405; U.S. Patent Number 5,091,513; U.S. Patent Number 5,476,786; U.S. Patent Number 5,013,653; U.S. Patent Number 5,258,498; and U.S. Patent Number 5,482,858.

Binding of the bispecific molecules to their specific targets can be confirmed by, for example, enzyme-linked immunosorbent assay (ELISA), radioimmunoassay (RIA), FACS analysis, bioassay (*e.g.*, growth inhibition), or western blot assay. Each of these assays generally detects the presence of protein-antibody complexes of particular interest by employing a labeled reagent (*e.g.*, an antibody) specific for the complex of interest. For example, the FcR-antibody complexes can be detected using *e.g.*, an enzyme-linked antibody or antibody fragment which recognizes and specifically binds to the antibody-FcR complexes. Alternatively, the complexes can be detected using any of a variety of other immunoassays. For example, the antibody can be radioactively labeled and used in a radioimmunoassay (RIA). The radioactive isotope can be detected by such means as the use of a  $\alpha$   $\gamma$ - $\beta$ counter or a scintillation counter or by autoradiography.

(iii) Immunoconjugates

Immunoconjugates provided herein can be formed by conjugating the antibodies described herein to another therapeutic agent. Suitable agents include, for example, a cytotoxic agent (*e.g.*, a chemotherapeutic agent), a toxin (*e.g.* an enzymatically active toxin of bacterial, fungal, plant or animal origin, or fragments thereof), and/or a radioactive isotope (*i.e.*, a radioconjugate).

Chemotherapeutic agents useful in the generation of such immunoconjugates have been described above. Enzymatically active toxins and fragments thereof which can be used include diphtheria A chain, nonbinding active fragments of diphtheria toxin, exotoxin A chain (from *Pseudomonas aeruginosa*), ricin A chain, abrin A chain, modeccin A chain, alpha-sarcin, Aleurites fordii proteins, dianthin proteins, *Phytolaca americana* proteins (PAPI, PAPII, and PAP-S), momordica charantia inhibitor, curcin, crotin, sapaonaria officinalis inhibitor, gelonin, mitogellin, restrictocin, phenomycin, enomycin and the tricothecenes. A variety of radionuclides are available for the production of radioconjugated anti-EGFR antibodies. Examples include  $^{212}\text{Bi}$ ,  $^{131}\text{I}$ ,  $^{131}\text{In}$ ,  $^{90}\text{Y}$  and  $^{186}\text{Re}$ .

Immunoconjugates can be made using a variety of bifunctional protein coupling agents such as N-succinimidyl-3-(2-pyridyldithiol) propionate (SPDP), iminothiolane

(IT), bifunctional derivatives of imidoesters (such as dimethyl adipimidate HCL), active esters (such as disuccinimidyl suberate), aldehydes (such as glutaredehyde), bis-azido compounds (such as bis (p-azidobenzoyl) hexanediamine), bis-diazonium derivatives (such as bis-(p-diazoniumbenzoyl)-ethylenediamine), diisocyanates (such as tolyene 2,6-  
5 diisocyanate), and bis-active fluorine compounds (such as 1,5-difluoro-2,4-dinitrobenzene). Carbon-14-labeled 1-isothiocyanatobenzyl-3-methyldiethylene triaminepentaacetic acid (MX-DTPA) is an exemplary chelating agent for conjugation of radionucleotide to the antibody (see, *e.g.*, WO94/11026).

#### 10 IV. Methods for Screening Antibodies

Subsequent to producing antibodies they can be screened for various properties, such as those described herein, using a variety of assays that are well known in the art.

In one embodiment, the antibodies are screened (*e.g.*, by flow cytometry or ELISA) for binding to EGFR using, for example, purified EGFR and/or EGFR-  
15 expressing cells, such as A431 cells. The epitopes bound by the anti-EGFR antibodies can further be identified and compared, for example, to identify non-competing antibodies (*e.g.*, antibodies that bind different epitopes), as well as antibodies which compete for binding and/or bind the same or overlapping epitopes.

Competitive antibodies and non-competitive antibodies can be identified using  
20 routine techniques. Such techniques include, for example, an immunoassay, which shows the ability of one antibody to block (or not block) the binding of another antibody to a target antigen, *i.e.*, a competitive binding assay. Competitive binding is determined in an assay in which the immunoglobulin under test inhibits specific binding of a reference antibody to a common antigen, such as EGFR. Numerous types of  
25 competitive binding assays are known, for example: solid phase direct or indirect radioimmunoassay (RIA), solid phase direct or indirect enzyme immunoassay (EIA), sandwich competition assay; solid phase direct biotin-avidin EIA; solid phase direct labeled assay, solid phase direct labeled sandwich assay; solid phase direct <sup>125</sup>I labeled RIA; solid phase direct biotin-avidin EIA; and direct labeled RIA.. The surface plasmon  
30 resonance technique set forth in the Materials and Methods of the Examples and in Example 2, below, can also be used advantageously for this purpose. Typically, such an assay involves the use of purified antigen bound to a solid surface or cells bearing either of these, an unlabeled test immunoglobulin and a labeled reference immunoglobulin.

Competitive inhibition is measured by determining the amount of label bound to the solid surface or cells in the presence of the test immunoglobulin. Usually the test immunoglobulin is present in excess. Usually, when a competing antibody is present in excess, it will inhibit specific binding of a reference antibody to a common antigen by at least 50-55%, 55-60%, 60-65%, 65-70% 70-75% or more.

Other screening techniques for determining the epitope bound by antibodies disclosed herein include, for example, x-ray analysis of crystals of antigen:antibody complexes, which provides atomic resolution of the epitope. Other methods monitor the binding of the antibody to antigen fragments or mutated variations of the antigen where loss of binding due to a modification of an amino acid residue within the antigen sequence is often considered an indication of an epitope component. In addition, computational combinatorial methods for epitope mapping can also be used. These methods rely on the ability of the antibody of interest to affinity isolate specific short peptides from combinatorial phage display peptide libraries. The peptides are then regarded as leads for the definition of the epitope corresponding to the antibody used to screen the peptide library. For epitope mapping, computational algorithms have also been developed which have been shown to map conformational discontinuous epitopes.

In another embodiment, the antibodies (*e.g.*, non-competing antibodies anti-EGFR antibodies) are screened for the ability to bind to epitopes exposed upon binding to ligand, *e.g.*, EGF (*i.e.*, do not inhibit the binding of EGFR-binding ligands to EGFR). Such antibodies can be identified by, for example, contacting cells which express EGFR (*e.g.* A431 cells) with a labeled EGFR ligand (*e.g.*, radiolabeled or biotinylated EGF) in the absence (control) or presence of the anti-EGFR antibody. If the antibody does not inhibit EGF binding to EGFR, then no statistically significantly decrease in the amount of label recovered, relative to the amount in the absence of the antibody, will be observed. Alternatively, if the antibody inhibits EGF binding to EGFR, then a statistically significantly decrease in the amount of label recovered, relative to the amount in the absence of the antibody, will be observed.

Antibodies also can be screened (tested) for their binding affinity. This can be done, for example, using a plasmon resonance assay, *e.g.*, as described below.

Antibodies also can be screened for their ability to inhibit signaling through EGFR using signaling assays, such as, those described herein. For example, the ability of an antibody to inhibit EGFR ligand mediated phosphorylation of EGFRs can be

assessed by treating cells expressing EGFR with an EGFR ligand (*e.g.*, EGF) in the presence and absence of the antibody. The cells can then be lysed, crude lysates centrifuged to remove insoluble material, and EGFR phosphorylation measured, for example, by western blotting followed by probing with an anti-phosphotyrosine  
5 antibody.

Alternatively, the ability of an antibody to inhibit downstream signaling through EGFR can be measured by kinase assays for known substrates of EGFR such as, for example, AKT and/or ERK, following EGFR stimulation by EGF ligand. For example, cells expressing EGFR can be incubated with a candidate antibody and stimulated with  
10 EGF ligand. Cell lysates subsequently prepared from such cells can be immunoprecipitated with an antibody for a substrate of EGFR (or a protein in a cellular pathway involving EGFR) such as, an anti-AKT antibody, and assayed for kinase activity (*e.g.*, AKT kinase activity) using art-recognized techniques. A decrease in or complete disappearance in level or activity (*e.g.*, kinase activity) of a EGFR substrate or  
15 protein in a pathway involving EGFR in the presence of the antibody, relative to the level or activity in the absence of the antibody is indicative of an antibody which inhibits EGFR signaling.

Antibodies that decrease levels of EGFR on cell surfaces can be identified by their ability to downregulate or inhibit EGFR expression on tumor cells. In certain  
20 embodiments, the antibodies decrease EGFR on cell surfaces by inducing internalization (or increasing endocytosis) of EGFR (*e.g.*, by internalization and recycling of the receptor and/or internalization and degradation of the receptor) or by inhibiting recycling of internalized EGFR. To test this, EGFR can be biotinylated and the number of EGFR molecules on the cell surface can be readily determined, for example, by measuring the  
25 amount of biotin on a monolayer of cells in culture in the presence or absence of an antibody, followed by immunoprecipitation of EGFR and probing with streptavidin. A decrease in detection of biotinylated EGFR over time in the presence of an antibody is indicative of an antibody that decreases EGFR levels on cell surfaces.

Antibodies and antibody combinations can also be tested for their ability to  
30 inhibit growth of cells expressing EGFR (either *in vivo* or *in vitro*), such as tumor cells, using art recognized techniques, including the Cell Titer-Glo Assay described in the Examples below and Tritium-labeled thymidine incorporation assay. Antibodies also can be screened for the ability to inhibit spheroid growth of cells expressing EGFR.



This can be done by using an assay that approximates conditions of a developing tumor growth as described herein.

In another embodiment, combinations of anti-EGFR antibodies are screened for IC50 and/or IC90 values relative to inhibiting a particular EGFR activity or function, such as EGFR-mediated signaling (*e.g.*, as measured by ELISA, Western, or multiplex methods, such as Luminex®). Combinations of antibodies, each of which possesses a particularly desired IC50 and/or IC90 value (*e.g.*, an IC90 of about 80nM for inhibiting EGFR signaling) can then be selected. In one embodiment, the combination has a greater IC50 or IC90 value than a known reference antibody (*e.g.*, cetuximab). In another embodiment, the combination has an additive IC50 or IC90 (*i.e.*, the sum of the activities of the antibodies, when acting individually on a cell expressing EGFR, is approximately equivalent to the combined effect of the same antibodies acting together on the same cell) In another embodiment, the combination has a synergistic IC50 or IC90 (*i.e.*, the sum of the effects of the antibodies, when acting individually on a cell expressing EGFR, is less than the combined effect of the same antibodies acting together on the same cell).

#### **V. Pharmaceutical Compositions**

In another aspect, herein provided is a composition, *e.g.*, a pharmaceutical composition, containing one or a combination of the anti-EGFR monoclonal antibodies disclosed herein, formulated together with a pharmaceutically acceptable carrier. In one embodiment, the compositions include a combination of multiple (*e.g.*, two or three) isolated antibodies that bind different epitopes on EGFR. Such antibodies preferably have an additive or synergistic effect relative to inhibiting a particular EGFR activity or function, such as EGFR-mediated signaling. Preferred pharmaceutical compositions are sterile compositions, compositions suitable for injection, and sterile compositions suitable for injection by a desired route of administration, such as by intravenous injection.

As used herein, “pharmaceutically acceptable carrier” includes any and all solvents, dispersion media, coatings, antibacterial and antifungal agents, isotonic and absorption delaying agents, and the like that are physiologically compatible. Preferably, the carrier is suitable for intravenous, intramuscular, subcutaneous, parenteral, spinal or epidermal administration (*e.g.*, by injection or infusion). Depending on the route of

administration, the active compound, *i.e.*, antibody, bispecific and multispecific molecule, may be coated in a material to protect the compound from the action of acids and other natural conditions that may inactivate the compound.

Compositions can be administered alone or in combination therapy, *i.e.*,  
5 combined with other agents. For example, the combination therapy can include a composition provided herein with at least one or more additional therapeutic agents, such as the anti-cancer agents described herein. In one embodiment, combination therapy can use a composition provided herein of two or three of the anti-EGFR antibodies disclosed herein. In another embodiment, combination therapy can use a  
10 composition comprising at least one of the anti-EGFR antibodies disclosed herein combined with one or more other antibodies, such as one or more other anti-EGFR antibodies known in the art (*e.g.*, anti-EGFR antibodies as disclosed in PCT Application No. PCT/US2011/3528). The compositions can also be administered in conjunction with radiation therapy and/or surgery. Particular combinations of anti-EGFR antibodies  
15 may also be administered separately or sequentially, with or without additional therapeutic agents.

Compositions can be administered by a variety of methods known in the art. As will be appreciated by the skilled artisan, the route and/or mode of administration will vary depending upon the desired results. The antibodies can be prepared with carriers  
20 that will protect the antibodies against rapid release, such as a controlled release formulation, including implants, transdermal patches, and microencapsulated delivery systems. Biodegradable, biocompatible polymers can be used, such as ethylene vinyl acetate, polyanhydrides, polyglycolic acid, collagen, polyorthoesters, and polylactic acid. Many methods for the preparation of such formulations are patented or generally  
25 known to those skilled in the art.

To administer compositions by certain routes of administration, it may be necessary to coat the constituents, *e.g.*, antibodies, with, or co-administer the compositions with, a material to prevent its inactivation. For example, the compositions may be administered to a subject in an appropriate carrier, for example, liposomes, or a  
30 diluent. Acceptable diluents include saline and aqueous buffer solutions. Liposomes include water-in-oil-in-water CGF emulsions as well as conventional liposomes.

Acceptable carriers include sterile aqueous solutions or dispersions and sterile powders for the extemporaneous preparation of sterile injectable solutions or dispersion.

The use of such media and agents for pharmaceutically active substances is known in the art. Except insofar as any conventional medium or agent is incompatible with the antibodies, use thereof in compositions provided herein is contemplated. Supplementary active constituents can also be incorporated into the compositions.

- 5           Therapeutic compositions typically must be sterile and stable under the conditions of manufacture and storage. The composition can be formulated as a solution, microemulsion, liposome, or other ordered structure suitable to high drug concentration. The carrier can be a solvent or dispersion medium containing, for example, water, ethanol, polyol (for example, glycerol, propylene glycol, and liquid  
10 polyethylene glycol, and the like), and suitable mixtures thereof. The proper fluidity can be maintained, for example, by the use of a coating such as lecithin, by the maintenance of the required particle size in the case of dispersion and by the use of surfactants. In many cases, it will be preferable to include isotonic agents, for example, sugars, polyalcohols such as mannitol, sorbitol, or sodium chloride in the composition.
- 15 Including in the composition an agent that delays absorption, for example, monostearate salts and gelatin can bring about prolonged absorption of the injectable compositions.

- Sterile injectable solutions can be prepared by incorporating the monoclonal antibodies in the required amount in an appropriate solvent with one or a combination of ingredients enumerated above, as required, followed by sterilization microfiltration.
- 20 Generally, dispersions are prepared by incorporating the antibodies into a sterile vehicle that contains a basic dispersion medium and the required other ingredients from those enumerated above. In the case of sterile powders for the preparation of sterile injectable solutions, the preferred methods of preparation are vacuum drying and freeze-drying (lyophilization) that yield a powder of the active ingredient plus any additional desired  
25 ingredient from a previously sterile-filtered solution thereof.

- Dosage regimens are adjusted to provide the optimum desired response (*e.g.*, a therapeutic response). For example, a single bolus may be administered, several divided doses may be administered over time or the dose may be proportionally reduced or increased as indicated by the exigencies of the therapeutic situation. For example,  
30 human antibodies may be administered once or twice weekly by subcutaneous injection or once or twice monthly by subcutaneous injection.

          It is especially advantageous to formulate parenteral compositions in dosage unit form for ease of administration and uniformity of dosage. Dosage unit form as used

herein refers to physically discrete units suited as unitary dosages for the subjects to be treated; each unit contains a predetermined quantity of antibodies calculated to produce the desired therapeutic effect in association with the required pharmaceutical carrier.

The specification for the dosage unit forms provided herein are dictated by and directly  
5 dependent on (a) the unique characteristics of the antibodies and the particular therapeutic effect to be achieved, and (b) the limitations inherent in the art of compounding such antibodies for the treatment of sensitivity in individuals.

Examples of pharmaceutically-acceptable antioxidants include: (1) water soluble antioxidants, such as ascorbic acid, cysteine hydrochloride, sodium bisulfate, sodium  
10 metabisulfite, sodium sulfite and the like; (2) oil-soluble antioxidants, such as ascorbyl palmitate, butylated hydroxyanisole (BHA), butylated hydroxytoluene (BHT), lecithin, propyl gallate, alpha-tocopherol, and the like; and (3) metal chelating agents, such as citric acid, ethylenediamine tetraacetic acid (EDTA), sorbitol, tartaric acid, phosphoric acid, and the like.

15 For the therapeutic compositions, formulations include those suitable for oral, nasal, topical (including buccal and sublingual), rectal, and parenteral administration. Parenteral administration is the most common route of administration for therapeutic compositions comprising antibodies. The formulations may conveniently be presented in unit dosage form and may be prepared by any methods known in the art of pharmacy.  
20 The amount of antibodies that can be combined with a carrier material to produce a single dosage form will vary depending upon the subject being treated, and the particular mode of administration. This amount of antibodies will generally be an amount sufficient to produce a therapeutic effect. Generally, out of one hundred per cent, this amount will range from about 0.001 per cent to about ninety percent of antibody by  
25 mass, preferably from about 0.005 per cent to about 70 per cent, most preferably from about 0.01 per cent to about 30 per cent.

The phrases "parenteral administration" and "administered parenterally" as used herein means modes of administration other than enteral and topical administration, usually by injection, and includes, without limitation, intravenous, intramuscular,  
30 intraarterial, intrathecal, intraventricular, intracapsular, intraorbital, intracardiac, intradermal, intraperitoneal, transtracheal, subcutaneous, subcuticular, intraarticular, subcapsular, subarachnoid, intraspinal, epidural and intrasternal injection and infusion.

Examples of suitable aqueous and nonaqueous carriers which may be employed in the pharmaceutical compositions provided herein include water, ethanol, polyols (such as glycerol, propylene glycol, polyethylene glycol, and the like), and suitable mixtures thereof, vegetable oils, such as olive oil, and injectable organic esters, such as ethyl  
5 oleate. Proper fluidity can be maintained, for example, by the use of coating materials, such as lecithin, by the maintenance of the required particle size in the case of dispersions, and by the use of surfactants.

These compositions may also contain adjuvants such as preservatives, wetting agents, emulsifying agents and dispersing agents. Particular examples of adjuvants  
10 which are well-known in the art include, for example, inorganic adjuvants (such as aluminum salts, *e.g.*, aluminum phosphate and aluminum hydroxide), organic adjuvants (*e.g.*, squalene), oil-based adjuvants, virosomes (*e.g.*, virosomes which contain a membrane-bound heagglutinin and neuraminidase derived from the influenza virus).

Prevention of presence of microorganisms may be ensured both by sterilization  
15 procedures and by the inclusion of various antibacterial and antifungal agents, for example, paraben, chlorobutanol, phenol sorbic acid, and the like. It may also be desirable to include isotonic agents, such as sugars, sodium chloride, and the like into the compositions. In addition, prolonged absorption of the injectable pharmaceutical form may be brought about by the inclusion of one or more agents that delay absorption  
20 such as aluminum monostearate or gelatin.

When compositions are administered as pharmaceuticals, to humans and animals, they can be given alone or as a pharmaceutical composition containing, for example, 0.001 to 90% (more preferably, 0.005 to 70%, such as 0.01 to 30%) of active ingredient in combination with a pharmaceutically acceptable carrier.

25 Regardless of the route of administration selected, compositions provided herein, may be used in a suitable hydrated form, and they may be formulated into pharmaceutically acceptable dosage forms by conventional methods known to those of skill in the art.

Actual dosage levels of the antibodies in the pharmaceutical compositions  
30 provided herein may be varied so as to obtain an amount of the active ingredient which is effective to achieve the desired therapeutic response for a particular patient, composition, and mode of administration, without being toxic to the patient. The selected dosage level will depend upon a variety of pharmacokinetic factors including

the activity of the particular compositions employed, or the ester, salt or amide thereof, the route of administration, the time of administration, the rate of excretion of the particular compound being employed, the duration of the treatment, other drugs, compounds and/or materials used in combination with the particular compositions employed, the age, sex, weight, condition, general health and prior medical history of the patient being treated, and like factors well known in the medical arts. A physician or veterinarian having ordinary skill in the art can readily determine and prescribe the effective amount of the composition required. For example, the physician or veterinarian could start doses of the antibodies at levels lower than that required to achieve the desired therapeutic effect and gradually increasing the dosage until the desired effect is achieved. In general, a suitable daily dose of compositions provided herein will be that amount of the antibodies which is the lowest dose effective to produce a therapeutic effect. Such an effective dose will generally depend upon the factors described above. It is preferred that administration be intravenous, intramuscular, intraperitoneal, or subcutaneous, preferably administered proximal to the site of the target. If desired, the effective daily dose of a therapeutic composition may be administered as two, three, four, five, six or more sub-doses administered separately at appropriate intervals throughout the day, optionally, in unit dosage forms. While it is possible for antibodies to be administered alone, it is preferable to administer antibodies as a formulation (composition).

Therapeutic compositions can be administered with medical devices known in the art, such as, for example, those disclosed in U.S. Patent Nos. 5,399,163, 5,383,851, 5,312,335, 5,064,413, 4,941,880, 4,790,824, 4,596,556, 4,487,603, 4,486,194, 4,447,233, 4,447,224, 4,439,196, and 4,475,196.

In certain embodiments, the monoclonal antibodies can be formulated to ensure proper distribution *in vivo*. For example, the blood-brain barrier (BBB) excludes many highly hydrophilic compounds. To ensure that therapeutic antibodies cross the BBB (if desired), they can be formulated, for example, in liposomes. For methods of manufacturing liposomes, see, *e.g.*, U.S. Patents 4,522,811; 5,374,548; 5,399,331; 5,891,468; 6,056,973; 6,210,707, 6,224,903; 6,316,024; 7,122,202; 7,135,177; and 7,507,407 and US Patent Publication 20070116753. The liposomes may comprise one or more moieties that attach to and/or are selectively transported into specific cells or organs, thus enhance targeted drug delivery.

Pharmaceutical compositions are provided that comprise trios of anti-EGFR antibodies at a 2:2:1 ratio, that is the composition comprises three different anti-EGFR antibodies, in particular a P1X-related antibody, a P2X-related antibody and a P3X-related antibody, which bind to different EGFR epitopes, formulated at a specific 2:2:1 ratio. In addition to the three antibodies, these pharmaceutical compositions can comprise a pharmaceutically acceptable carrier and/or other excipient(s) such as those described in detail above. The pharmaceutical composition can be supplied in a single container containing all three antibodies or, alternatively, the pharmaceutical composition can comprise a package comprising three distinct containers each containing one of the three different anti-EGFR antibodies (as well as a pharmaceutically acceptable carrier and/or other excipient(s) as described above).

Uses of the above-described anti-EGFR antibodies are provided, either alone (as single agents), in pair combinations (two antibodies), or in triple combinations (three antibodies) in the manufacture of a medicament for the treatment of a disease associated with EGFR dependent signaling. The above-described anti-EGFR antibodies are also provided, either alone (as single agents), in pair combinations (two antibodies), or in triple combinations (three antibodies) for the treatment of cancer (or to be used in the manufacture of a medicament for the treatment of cancer), such as an EGFR-expressing cancer, such as a cancer including, but not limited to melanoma, breast cancer, ovarian cancer, renal carcinoma, gastrointestinal cancer, colon cancer, lung cancer, pancreatic cancer, skin cancer, head and neck cancer glioblastoma, prostate cancer and other solid and/or metastatic tumors.

Additionally, contemplated compositions may further include, or be prepared for use as a medicament in combination therapy with, an additional therapeutic agent, *e.g.*, an additional anti-cancer agent. An “anti-cancer agent” is a drug used to treat tumors, cancers, malignancies, and the like. Drug therapy (*e.g.*, with antibody compositions disclosed herein) may be administered without other treatment, or in combination with other treatments such as surgery, heat, or radiation therapy (*e.g.*, with ionizing radiation). Several classes of anti-cancer agents may be used in cancer treatment, depending on the nature of the organ or tissue involved. For example, breast cancers are commonly stimulated by estrogens, and may be treated with drugs which inactive sex hormones. Similarly, prostate cancer may be treated with drugs that inactivate androgens. Anti-cancer agents for use in combination with antibody compositions

disclosed herein include, among others, those listed in Appendix A, which should not be construed as limiting. One or more anti-cancer agents may be administered either simultaneously or before or after administration of an antibody composition disclosed herein. Antibody compositions disclosed herein can be administered sequentially or  
5 together with the additional anti-cancer agent, *e.g.*, an anti cancer agent disclosed in Appendix A, below.

Also provided are kits comprising one or more anti-EGFR antibodies disclosed herein, optionally contained in a single vial or container, and include, *e.g.*, instructions for use in treating or diagnosing a disease associated with EGFR upregulation and/or  
10 EGFR dependent signaling (*e.g.*, a cancer such as those described in subsection VI below). The kits may include a label indicating the intended use of the contents of the kit. The term label includes any writing, marketing materials or recorded material supplied on or with the kit, or which otherwise accompanies the kit. Such kits may comprise the antibody composition in unit dosage form, such as in a single dose vial or a  
15 single dose pre-loaded syringe. Kits comprising a combination of the anti-EGFR antibodies disclosed herein (*e.g.*, a combination of a P1X-related antibody, a P2X-related antibody, and a P3X-related antibody) can comprise a single vial containing all components of the combination or, alternatively, the kit can comprise each component in separate vials with instructions for administration of the antibodies in combination  
20 therapy. In a preferred embodiment, a P1X-related antibody, a P2X-related antibody, and a P3X-related antibody are supplied in a 2:2:1 ratio in a single vial or, alternatively, are supplied each in separate vials with instructions for administering the three antibodies at a 2:2:1 ratio.

## 25 VI. Methods of Using Antibodies

Antibodies and compositions disclosed herein can be used in a broad variety of therapeutic and diagnostic applications, particularly oncological applications. Accordingly, in another aspect, provided herein are methods for inhibiting EGFR activity in a subject by administering one or more antibodies or compositions described  
30 herein in an amount sufficient to inhibit EGFR-mediated activity. Particular therapeutic indications which can be treated include, for example, cancers of organs or tissues such as skin, brain and central nervous system, head and neck, esophagus, stomach, colon, rectum, anus, liver, pancreas, bile duct, gallbladder, lung or bronchus, breast, ovary,



uterus, cervix, vagina, testis, germ cells, prostate, kidney, ureter, urinary bladder, adrenal, pituitary, thyroid, bone, muscle or other connective tissues, leukemia, multiple myeloma, Hodgkin's lymphoma and non-Hodgkin's lymphoma.

Antibodies of disclosed herein also can be used to diagnose or prognose diseases  
5 (*e.g.*, cancers) associated with EGFR, for example, by contacting one or more antibodies, antibody pairs or antibody trios disclosed herein (*e.g.*, *ex vivo* or *in vivo*) with cells from the subject, and measuring the level of binding to EGFR on the cells, wherein abnormally high levels of binding to EGFR indicate that the subject has a cancer associated with EGFR.

10 Also provided are methods of using the anti-EGFR antibodies disclosed herein in a variety of *ex vivo* and *in vivo* diagnostic and therapeutic applications involving EGFR dependent signaling, including a variety of cancers.

Accordingly, in one embodiment, a method is provided for treating a disease associated with EGFR dependent signaling by administering to a subject an antibody or  
15 preferably a combination of antibodies provided herein in an amount effective to treat the disease. Suitable diseases include, for example, a variety of cancers including, but not limited to, melanoma, breast cancer, ovarian cancer, renal carcinoma, gastrointestinal cancer, colon cancer, lung cancer, pancreatic cancer, skin cancer, head and neck cancer glioblastoma, prostate cancer and other solid and/or metastatic tumors.

20 The antibody can be administered alone or with another therapeutic agent that acts in conjunction with or synergistically with the antibody to treat the disease associated with EGFR mediated signaling. Such therapeutic agents include those described herein, for example, small organic molecules, monoclonal antibodies, bispecific antibodies, recombinantly engineered biologics, RNAi compounds, tyrosine  
25 kinase inhibitors, and commercial antibodies, as well as anticancer agents (*e.g.*, cytotoxins, chemotherapeutic agents, small molecules and radiation). Non-limiting examples of anti-cancer agents that can be used in combination therapy with one or more of the anti-EGFR antibodies disclosed herein include those listed in Appendix A.

Other embodiments are described in the following non-limiting Examples.  
30

## Examples

### Materials and Methods for The Examples

In general, in the following examples, unless otherwise indicated, conventional  
5 techniques of chemistry, molecular biology, recombinant DNA technology, immunology  
(especially, *e.g.*, antibody technology), and standard techniques in recombinant  
immunoglobulin preparation were used.

### Cell Lines

10 All the cell lines to be used in the experiments described below are obtained  
from the National Cancer Institute or ATCC.

#### Cell Lines:

A431 – epidermoid carcinoma

DU145 – prostate carcinoma

15 H1975 – lung adenocarcinoma; non-small cell lung cancer

HCC827 – lung adenocarcinoma; non-small cell lung cancer

### Protein Purification of EGFR Extracellular Domain (EGFR-ECD) Mutants

20 Mutants of the EGFR extracellular domain (EGFR-ECD) are generated for mAb  
epitope binning. Mutations were designed based upon both the cetuximab (Li S. *et al.*,  
Cancer Cell. **7**: 301-311, 2005) and H11 (Spangler J. *et al.* PNAS. **107**: 13252-13257,  
2010) epitopes and upon structural analysis of the EGFR-ECD structure (Protein Data  
Bank ID: 1NQL; Ferguson K.M. *et al.* Mol Cell. **11**: 507-517, 2003). Residues are  
25 mutated to alanines as noted in the protein sequences included in this application. DNA  
synthesis of expression constructs may be commercially obtained from DNA2.0  
(www.dna20.com). Subsequent DNA subcloning, protein expression in 293F cells and  
protein purification are completed using conventional methods.

### Inhibition of EGF-Mediated Signaling of EGFR or ERK in Tumor Cells

Inhibition of ligand-mediated tumor cell signaling is investigated as follows:  
A431 or Du145 cells are seeded at a density of 35,000 cells/well or 17,500 cells per half  
well in 96 well tissue culture plates and grown in DMEM or RPMI-1640 medium  
supplemented with antibiotics, 2 mM L-glutamine and 10% fetal bovine serum (FBS)

for 24 hours at 37°C and 5% carbon dioxide. Cells are serum starved in 1% FBS medium with antibiotics and 2mM L-glutamine for about 20 hours at 37°C and 5% carbon dioxide. Cells are then preincubated with varying concentrations of anti-EGFR antibodies for 2 hrs, and then stimulated with human EGF ligand (50 ng/ml) (PeproTech, cat # AF-100-15) for 10 minutes at 37°C and 5% carbon dioxide. Cells are washed with ice-cold PBS and lysed in 50µl ice-cold Lysis buffer (Mammalian Protein Extract Lysis buffer (MPER-Pierce, #78505) amended with 150mM NaCl and protease inhibitor cocktail (Sigma, P714)) by incubating on ice for 30 minutes. Lysates are either analyzed immediately by ELISA for ERK (a downstream effector of EGFR) and EGFR phosphorylation, or frozen at -80°C until use.

### ELISA Assays

For the phospho-EGFR sandwich ELISA, 96-half well GREINER high binding plates (Cat. #675077; GREINER BIO-ONE, Monroe, NC) are coated with 50 µL of an EGFR antibody (EGFR Ab-11, Clone: 199.12, without BSA and azide, Fisher Scientific, cat# MS396PIABX), and incubated overnight at room temperature. The next morning, the plates are washed 3 times with 100 µl/well PBST (0.05% Tween-20) on a BIOTEK plate washer. Plates are subsequently blocked for about 1 hour at room temperature with 2 % BSA in PBS. The plates are washed 3 times with 100 µl/well PBST (0.05% Tween-20) on the BIOTEK plate washer. Cell lysates (50µl) or standards (pEGFR pY1068 ELISA kit, R&D Systems, cat# DYC3570) are diluted in 50% Lysis buffer and 1% BSA-PBS (per the manufacturer's recommendations) and are added to the plates in duplicates and incubated for 2 hrs at room temperature or overnight at 4°C with shaking. Plates are then washed 3 times with 100 µl/well in the BIOTEK plate washer with PBST (PBS with 0.05% Tween-20). About 50 µl of a detection antibody conjugated to horse radish peroxidase (HRP) (pEGFR pY1068 ELISA kit, R&D Systems, cat# DYC3570) diluted in 2% BSA, PBS is added and incubated for about 2 hour at room temperature. The plate is washed 3 times with 100 µl/well in the BIOTEK plate washer with PBST (0.05% Tween-20). About 50 µL of SUPERSIGNAL PICO ELISA substrate is added and the plate is read using an Envision (Perkin Elmer) plate reader. For data analysis, duplicate samples are averaged and error bars are used to represent the standard deviation between the two replicates. Inhibition curves and corresponding IC50 values are calculated using GraphPad Prism software (GraphPad

Software, Inc.) via regression of the data to a 4 parameter logistic equation.

The phospho-ERK ELISA is performed similarly to the phospho-EGFR ELISA with the following changes: Human pERK ELISA DuoSet kit is purchased from R&D Systems (cat# DYC1018-5) and used as recommended by the manufacturer.

5 A direct ELISA is performed using EGFR-ECD wild-type (WT), a Bin1 epitope mutant, or a Bin3 epitope mutant as capture reagents (4 $\mu$ g/ml). 96-half well GREINER high binding plates (Cat. #675077; GREINER BIO-ONE, Monroe, NC) are coated with 50  $\mu$ L of capture reagent and incubated overnight at room temperature. Next morning, plates are washed 3 times with 100  $\mu$ L/well in a BIOTEK plate washer with PBST  
10 (0.05% Tween-20) and blocked for about 1 hour at room temperature with 1% BSA in PBS, pH7.2. Varying concentrations (1, 0.25, 0.06, and 0.02  $\mu$ g/ml) of monoclonal antibodies (mAbs) diluted in 1 % BSA in PBS, pH7.2 are incubated with the capture reagents at room temperature for 2 hours, followed by detection with 1:50,000 dilution in 1 % BSA in PBS, pH7.2 of Peroxidase-Conjugated AffiniPure Goat Anti-Human IgG  
15 Fc Fragment (Jackson ImmunoResearch Catalog #109-035-008) for 2 hours. About 50  $\mu$ L of Supersignal PICO ELISA substrate is added and the plate is read using an Envision (Perkin Elmer) plate reader. For data analysis, duplicate samples are averaged and error bars are used to represent the standard deviation between the two replicates.

#### 20 Binding Affinity: Kinetic Exclusion Assay (KinExA)

Affinities and cross reactivity of antibodies are measured in solution with recombinant EGF receptor using KinExA instrumentation (SAPIDYNE Instruments, Boise, ID). Materials used for this assay are a KinExA 3000 instrument and software (Sapidyne Instruments, Boise, ID), polymethylmethacrylate (PMMA) beads (Sapidyne  
25 Instruments), human anti-EGFR IgG, recombinant human EGFR, Cy5-conjugated goat anti-human IgG (Jackson ImmunoResearch, West Grove, PA), phosphate buffered saline (PBS), and bovine serum albumin in PBS (100 mg/ml).

To couple the recombinant EGF receptor to PMMA beads, 100  $\mu$ g of recombinant EGFR is added to a pre-measured aliquot of 200 mg PMMA beads, and  
30 PBS is added to make the total volume 1 ml. The beads are incubated for 1 hr at room temperature on a rotating wheel. Then the beads are briefly centrifuged and the supernatant is removed. 100  $\mu$ L of 100 mg/ml BSA in PBS is added to the beads, with further addition of PBS to make a total volume of 1 ml. The beads are incubated again

for 1 hr at room temperature on a rotating wheel. The beads are then transferred to a glass bottle containing 27 mL of PBS.

To determine the monovalent antibody binding affinity, a twelve-step dilution series of recombinant EGFR (75 nM, 25 nM, 8.3 nM, 2.8 nM, 0.9 nM, 0.3 nM, 100 pM, 5 33 pM, 11 pM, 4 pM, 1.3 pM, 0 pM) is prepared in 5 ml PBS having a constant concentration of anti-EGFR antibody. For accurate affinity measurement, the total antibody binding site concentration (“ABC”; twice the molar concentration of antibody, due to valence) should be less than the monovalent affinity of the antibody for EGFR. The antibody-receptor mixtures are incubated for 2 hr at room temperature in order to 10 achieve equilibrium. Depending upon the expected affinity of the antibody-receptor complex, this equilibration time may be adjusted accordingly. In a separate tube, 15 mL of 2 µg/mL Cy5-conjugated anti-human IgG secondary antibody is prepared, using a 1:1000 dilution of stock (2 mg/mL) antibody into PBS. Then, the KinExA instrument lines are attached to each of the 12 antibody-receptor solution tubes. Each solution is 15 injected through a packed EGFR-bead column. (The KinExA instrument automatically packs a fresh bead column for each injection.) After a wash step, the labeled secondary antibody is passed through the column. Finally, using the measured amount of uncomplexed receptor at different receptor concentrations, the equilibrium titration data is fit to a 1:1 binding model in the KinExA software to yield an affinity value  $K_D$ . The 20 lower the value of  $K_D$  the better (stronger, sometimes stated as higher) the binding affinity. Therefore a recitation that an antibody binds with a  $K_D$  of x nM or better means it binds with a  $K_D$  value of, e.g.,  $1 \times 10^{-8}$  M (10 nM) or with a lower  $K_D$  value, e.g.,  $1 \times 10^{-10}$  M (0.1 nM), with the lower  $K_D$  value indicating better (higher) affinity.

To determine the binding on-rate using the KinExA “direct method”, the 25 equilibrium monovalent binding affinity ( $K_D$ ) is determined using the above approach and total antibody binding site concentration (ABC). Then, using the “Theoretical Binding Curve Demonstration” software (Sapidyne Instruments), the starting antigen concentration ( $L_0$ ) is determined for the kinetics experiment. To do this, the affinity and ABC values determined in the monovalent binding affinity experiment are entered, and 30 a starting antigen concentration is selected as that concentration where roughly 20% of antibody will be unbound to antigen at equilibrium. This assures good signal-to-noise ratio in the experiment. 15 mL of 2 µg/mL Cy5-conjugated anti-human IgG secondary antibody is prepared, using a 1:1000 dilution of stock (2 mg/mL) antibody into PBS. In

a separate tube, 8 mL of anti-EGFR antibody solution is prepared at a concentration of 2 x ABC. This concentration is double the running concentration, since it is mixed with 8 mL of antigen solution prior to the experiment. In a separate tube, 8 mL of recombinant EGFR solution is prepared at a concentration of 2 x L0. This concentration is also  
 5 double the running concentration, since it is mixed with 8 mL of antibody solution prior to the experiment. Then, the EGFR coated beads and secondary antibody solution are placed in the appropriate container and line, respectively. The antibody and antigen solution are mixed thoroughly and immediately connected to the appropriate line, and the KinExA software is used to measure the amount of free antibody as a function of  
 10 time in the resulting solution. To determine the association constant  $k_{on}$  ( $K_{on}$ ), the KinExA software is used to fit the depletion of the amount of free antibody as a function of time to a reversible bimolecular rate equation. The dissociation constant  $K_{off}$  ( $K_{off}$ ) is equal to the  $K_{on} * K_D$  ( $K_D$ ).

#### 15 Binding Affinity: Surface Plasmon Resonance Assay

The Surface Plasmon Resonance Assay is performed as follows:

either antibody or antigen (300 RU) is immobilized on a CM5 chip using amine coupling. Different concentrations of antibodies or antigens are then injected to study their association and dissociation with the immobilized protein. Between different  
 20 injections, the chip is regenerated using suitable regeneration buffer (such as glycine, pH 2.5). The dissociation phase is fitted using Equation 1 to determine  $K_{off}$  (dissociate rate):

$$R = R_0 * \exp(-K_{off} * t) \quad (1)$$

The association phase is fitted using this value of  $K_{off}$  and Equation 2 to determine  $K_{on}$  (association rate) and  $K_D$  (equilibrium constant).

$$25 \quad R = \frac{R_{max} * C}{K_D + C} (1 - \exp(-(K_{on} * C + K_{off})t)) \quad (2)$$

where  $C$  represents either the antigen or antibody concentration in solution,  $R_{max}$  represents the saturation signal and  $t$  represents the time.

#### Epitope Binning: Surface Plasmon Resonance Assay

30 Epitope binning is performed using surface plasmon resonance assay, as described above. One of the antibodies is immobilized on the surface of the chip. Recombinantly expressed human EGFR extracellular domain (EGFR-ECD) is then injected. As EGFR-ECD associates with the antibody conjugated to the surface of the

chip, the resonance signal increases. Sequential injections of antibodies that belong to the three bins 1, 2 and 3 are performed. If the antibody binds overlapping epitopes with the injected antibody, then the signal will not change compared to the previous injection. If the antibody binds to a non-overlapping epitope, the signal on the chip will be higher than the previous injection. The antibody conjugated to the chip is finally injected as free ligand to confirm lack of binding with overlapping epitopes.

#### Cell Binding Assay

Cell binding assays for determining the  $K_D$  values are performed as follows:

10 A431 cells are detached with 3 mLs trypsin-EDTA at 37 °C for 5 minutes. Complete DMEM (10 mLs) is added immediately to the trypsinized cells, resuspended gently and spun down in a Beckman tabletop centrifuge at 1100 rpm for 5 minutes. Cells are resuspended in stain buffer (PBS + 0.2% BSA+ 0.1% sodium azide) at a concentration of  $2 \times 10^6$  cells per ml and 50  $\mu$ l ( $1 \times 10^5$  cells) aliquots are plated in a 96-well titer plate.

15 A 300  $\mu$ l stock solution of 2000 nM anti-EGFR antibody is prepared in stain buffer and 100  $\mu$ l of it is serially diluted into 200  $\mu$ l of stain buffer. The concentrations of the diluted antibody range from 2000 nM to 0.1 nM. 150  $\mu$ l aliquots of the different protein dilutions are then added directly to the 50  $\mu$ l cell suspension giving final concentrations of 1500 nM, 500 nM, 166.7 nM, 55.6 nM, 18.5 nM, 6.17 nM, 2.05 nM, 20 0.68 nM, 0.23 nM and 0.076 nM antibody.

Aliquoted cells in the 96-well plate are incubated with the antibody dilutions for 2 hr at room temperature with shaking and washed 3 times with 300  $\mu$ l stain buffer. Cells are then incubated with 100  $\mu$ l of a 1:750 dilution of Alexa 647-labeled goat anti-human IgG in BD stain buffer for 45 minutes with shaking at 4°C. Finally, cells are washed twice, pelleted and resuspended in 250  $\mu$ l stain buffer + 0.5  $\mu$ g/ml propidium iodide. Analysis of 10,000 cells is done in a FACSCALIBUR flow cytometer using the FL4 channel. MFI values and the corresponding concentrations of the anti-EGFR-antibodies are plotted on the y-axis and x-axis, respectively. The  $K_D$  of the molecule is determined using GRAPHPAD PRISM software using the one-site binding model for a non-linear regression curve.

30 The  $K_D$  value is calculated based on the formula  $Y = B_{max} * X / K_D + X$  ( $B_{max}$  = fluorescence at saturation.  $X$  = antibody concentration.  $Y$  = degree of binding).

### Measurement of EGFR levels via immunoblotting

To prepare cell lysates, H1975 cells are trypsinized, harvested, counted, and plated in 6 well dishes at  $1 \times 10^6$  cells per well and incubated overnight to allow attachment to the culture plate. Cells are pre-treated with  $1 \mu\text{M}$  concentration of P1X+P2X+P3X (P1X+P2X+P3X or P1X, P2X, & P3X indicates a combination at a 2:2:1 molar ratio of P1X, P2X, and P3X) for 1, 2, 5, and 24 hours before stimulation with rhEGF (Peprotech, cat# 100-15) for 10 minutes. Cells are lysed with  $100 \mu\text{l}$  of Mammalian Protein Extraction Reagent (Pierce, cat# 78505). Protein extraction reagent is supplemented with PhosSTOP (Roche, cat# 04906837001) and Protease Inhibitor Cocktail tablets (Roche, cat# 04693124001). Extracts of H1975 cells are denatured by boiling for 5 minutes in sample buffer, subjected to reducing conditions, and electrophoresed using SDS-PAGE 4-12% polyacrylamide gels for 50 minutes at 200V. Following transfer of proteins to a nitrocellulose membrane, nonspecific sites are blocked by incubation with Odyssey blocking buffer (LI-COR, cat# 927-400-00) for one hour at room temperature. Membranes are incubated as required with mouse monoclonal anti-EGFR (1F4 – labeling tEGFR; Cell Signaling, cat# 2239); rabbit monoclonal anti-phospho44/42 MAPK (Erk1/2, Thr202/Tyr204, D13.14.4E – labeling pERK; Cell Signaling, cat# 4370); rabbit monoclonal anti-phosphoAKT (Ser473, 193H12; Cell Signaling, cat# 4058); rabbit monoclonal phospho-c-Jun (Ser73, D47G9 – labeling p-c-Jun; Cell Signaling, cat# 3270) and rabbit anti-PCNA (FL-261) (Santa Cruz Biotechnology, cat# sc-7907). Following overnight incubation with the primary antibodies, immunoblots are incubated with the appropriate IRDye-labeled secondary antibody (IR800CW goat anti-mouse (Odyssey, cat# 926-3210) or IR800CW goat anti-rabbit (Odyssey, cat#926-3211)) for 10 minutes and vacuumed through the membrane using SNAP i.d., Protein Detection System (Millipore). Bands are detected using LI-COR Odyssey Infrared Imaging System and analyzed using Odyssey software.

### Inhibition of Tumor Cell Proliferation *In Vitro*

Inhibition of cellular proliferation of cells expressing EGFR is examined *in vitro* as follows: HCC827 and H1975 cancer cells are seeded in 96 well tissue culture plates at 5,000 cells per well and grown in RPMI-1640 medium supplemented with antibiotics, 2mM L-glutamine and 10% fetal calf serum (FCS) for 24 hours at  $37^\circ\text{C}$  and 5% carbon dioxide. Medium is then switched to RPMI-1640 (with antibiotics, 2mM L-glutamine,



1% FBS) supplemented with 50ng/mL EGF or 200ng/ml AREG (amphiregulin; R&D Systems) in the presence of varying concentrations of P1X+P2X+P3X or cetuximab (Bristol-Myers Squibb). Cell viability is measured using the CellTiter-Glo® (CTG) Luminescent Cell Viability Assay (Promega Corporation, cat# G7572) according to  
5 manufacturer's instructions. The CTG assay measures the number of viable cells in culture based upon quantitation of ATP present, which is an indicator of metabolically active cells. Control treatments include cells treated with RPMI-1640 with antibiotics, 2mM L-glutamine, 1% FCS in the presence (referred to as "+EGF" or "+AREG") or absence (referred to as "-EGF" or "-AREG") of 50ng/mL EGF or 200ng/ml AREG.

10

#### DU145 & H1975 Mouse Xenograft Studies

A combination of P1X, P2X, and P3X Nu/nu mice (Charles River Labs) are injected subcutaneously with cells. The resultant tumors are allowed to grow until they reach an average size of 300mm<sup>3</sup>. Dosing is then initiated with the indicated  
15 concentrations of combinations of P1X with P2X, and P3X, cetuximab or matched volume of PBS as vehicle control. Measurements are taken at 4 day intervals and tumor volumes calculated using the formula  $Volume = \pi/6 \times (W \times L^2)$ . Cetuximab and P1X+P2X+P3X doses are normalized to provide uniform serum exposures.

Efficacy of a combination of P1X with P2X, and P3X *in vivo* is assessed in a  
20 DU145 prostate cancer cell xenograft murine mouse model.  $8 \times 10^6$  DU145 cells are injected subcutaneously into the flank of nu/nu mice. Once tumors reach an average size of 300mm<sup>3</sup>, treatment is initiated. Groups of 10 mice are treated with either vehicle control (PBS); 2.075mg/kg of cetuximab, P1X with P2X, and P3X at component concentrations that were at a "murine ratio" designed to provide a 2:2:1 C<sub>max</sub> for P1X,  
25 for P2X and for P3X, respectively, in the mouse, as follows : P1X=2.53mg/kg, P2X=7.26mg/kg and P3X=0.66mg/kg. Mice in the cetuximab group are dosed every four days. Mice in the P1X+P2X+P3X group are dosed every two days. These doses and dosing intervals are chosen to give an equivalent serum exposure of cetuximab and the murine ratio antibody trio.

30

### Ligand Antagonism Cell Binding Assay

Cell binding assays for determining the binding of EGF ligand in the presence of single or multiple antibodies are performed as follows: A431 cells are detached with 5 mL trypsin-EDTA at 37 °C for 5 minutes. Complete DMEM (10 mL) is added  
5 immediately to the trypsinized cells, resuspended gently and spun down in a Beckman tabletop centrifuge at 1200 rpm for 7 minutes. Cells are resuspended in stain buffer (PBS + 2% FBS + 0.1% sodium azide) at a concentration of  $3 \times 10^5$  cells per ml and 100  $\mu$ l ( $3 \times 10^4$  cells) aliquots are plated in a 96-well titer plate.

A 5 mL 2x stock solution of anti-EGFR antibody is prepared in stain buffer at  
10 the concentrations indicated in each example. A 10 mL 3x stock solution of recombinant human EGF ligand conjugated to a biotin tag (biotin-EGF) is prepared in stain buffer and 100  $\mu$ l of it is serially diluted into 200  $\mu$ l of stain buffer. The concentrations of the diluted biotin-EGF range from 600 nM to 9 pM. 100  $\mu$ l aliquots of the anti-EGFR antibody are then added directly to the 100  $\mu$ l cell suspension giving a final  
15 concentration as indicated in each example. Aliquoted cells in the 96-well plate are incubated with the antibody dilutions for 1 hr at room temperature. 100  $\mu$ l aliquots of the biotin-EGF are then added directly to the 100  $\mu$ l cell suspension giving a final concentration of 200 nM, 66.67 nM, 22.22 nM, 7.41 nM, 2.47 nM, 0.82 nM, 0.27 nM, 0.09 nM, 0.03 nM, 0.01 nM, and 0.003 nM biotin-EGF. Aliquoted cells in the 96-well  
20 plate are incubated with the antibody and biotin-EGF dilutions for 10 min at room temperature, washed 1 time with 100  $\mu$ l stain buffer, and then spun down in a Beckman tabletop centrifuge at 1200 rpm for 7 minutes. Cells are resuspended in 100  $\mu$ l of a 1:500 dilution of Alexa Fluor® 647 Streptavidin conjugate (Invitrogen Life Technologies) in stain buffer for 30 minutes at room temperature in the dark. Finally, cells are washed  
25 twice with 100  $\mu$ l stain buffer, pelleted and resuspended in 80  $\mu$ l fixing buffer (PBS + 2% FBS + 2% paraformaldehyde) and transferred to 96-well U-bottom Assay Plates (Becton Dickinson) and sealed with foil and stored at 4°C.

Analysis of 10,000 cells is done in a FACSCALIBUR flow cytometer using the FL4 channel. Data are analyzed using WinList 6.0 software. Mean Fluorescence  
30 Intensity (MFI) values and the corresponding concentrations of the biotin-EGF ligand are plotted on the y-axis and x-axis, respectively.

**Example 1: Epitope mapping/binning**

Antibodies P1X, P2X, and P3X were generated via affinity maturation of parental antibodies. Respective parental antibodies ca, cd, and ch are disclosed in copending patent application Serial No. PCT/US2011/3528. Epitope mapping and binning experiments were performed to demonstrate that P1X, P2X, and P3X share the same non-overlapping epitopes as their respective parental molecules.

The Bins were designed so that selected antibodies would span three distinct, non-overlapping epitopes on the extracellular domain (ECD) of EGFR. These are grouped into three bins: Bin1 is mapped to Domain III of EGFR and represents the c225 epitope (the site of cetuximab binding); Bin2 is mapped to Domain I and represents the ICR10 epitope (Abcam Ab231) (Cochran *et al.* (2004) *Journal of Immunological Methods*, 287:147-158); and Bin3 is mapped to Domain III and represents the clone H11 epitope (Spangler J. *et al.* *PNAS*. **107**: 13252-13257, 2010). Bin1 (B1-7MT-Ala) and Bin3 (B3-4MT) mutants were generated for epitope mapping at the amino acid positions shown below in bold in the EGFR extracellular domain.

EGFR ECD (SEQ ID NO: 33)

```

1   MRPSGTAGAA LLALLAALCP ASRALEEKKV CQGTSNKLTQ LGTFEDHFLS LQRMFNNCEV
61  VLG NLEITYV Q RNYDLSFLK TIQEVAGYVL IALNTVERIP LENLQIIRGN MYYENSYALA
121 VLSNYDANKT GLKELPMRNL QEILHGAVRF SNNPALCNVE SIQWRDIVSS DFLSNMSMDF
20 181 QNHLGSCQKC DPSCPNGSCW GAGEENCQKL TKIICAQQCS GRCRGKSPSD CCHNQCAAGC
241 TGPRES DCLV CRKFRDEATC KDTCPPLMLY NPTTYQMDVN PEGKYSEFAT CVKCKPRNYV
301 VTDHGSCVRA CGADSYEMEE DGVRKCKKCE GPCRKVCNGI GIGEFKDSLS INATNIKHKFK
361 NCTSI SGDLH ILPVAFRGDS FTHTPPLDPQ ELDILKTVKE ITGFLLIQAW PENRTDLHAF
421 ENLEIIRGRT KQHGQFSLAV VSLNITSLGL RSLKEISDGD VIISGNKNLC YANTINWKKL
25 481 FGTSGQKTKI ISNRGENSCK ATGQVCHALC SPEGCWGPEP RDCVSCRNVS RGRECVDKCN
541 LLEGEPPREFV ENSECIQCHP ECLPQAMNIT CTGRGPDNCI QCAHYIDGPH CVKTCPAGVM
601 GENNTLVWKY ADAGHVCHLC HPNCTYGCTG PGLEGCP TNG PKIPSHHHHH H
    
```

The following substitution mutants were made at the bolded amino acid positions using standard recombinant DNA technology to create the Bin1 (B1) and Bin3 (B3) epitope mutants with the following mutant residues:

Mutants

Bin1 (B1) Mutant Residues

B1-7MT-Ala: Q408A, Q432M, H433E, K467A, K489A, I491A, N497A

Bin3 (B3) Mutant Residues

B3-4MT: S380A, F381G, T382A, H383G

A direct ELISA was performed using EGFR-ECD wild-type (WT), a Bin1 epitope mutant (c225 epitope), or a Bin3 epitope mutant (H11 epitope) as capture reagents. Varying concentrations (1, 0.25, 0.06, and 0.02 µg/ml) of monoclonal

antibodies (mAbs) P1X (Bin1), P2X (Bin2), and P3X (Bin3) were incubated with the capture reagents at room temperature for 2 hours, followed by detection with HRP-conjugated anti-human Fc polyclonal antibody for 1 hour. As shown in Figure 1A, all three antibodies bound to the WT extracellular domain of EGFR, whereas the Bin1  
5 antibody P1X did not bind to the Bin1 mutant epitope, and the P3X antibody did not bind to the Bin3 mutant epitope.

A surface plasmon resonance experiment was performed to demonstrate that P2X associates to the ICR10 epitope on Domain I of EGFR extraceullular domain (Figure 1B). ICR10 was conjugated to the surface of a BIACORE chip. 0.5  $\mu$ M EGFR-  
10 ECD was injected followed by sequential injections of 0.5  $\mu$ M of antibodies P1X (Bin1), P2X (Bin2), and P3X (Bin3). While P1X and P3X are observed to simultaneously associate with ICR10-bound EGFR-ECD, P2X is shown to not associate.

In order to demonstrate that the epitopes for P1X, P2X, and P3X are distinct and non-overlapping, a series of three surface plasmon resonance binning experiments were  
15 performed. P1X (Figure 2A), P2X (Figure 2B), or P3X (Figure 2C) were conjugated to the surface of a BIACORE chip. 0.5  $\mu$ M EGFR-ECD was injected followed by sequential injections of 0.5  $\mu$ M of antibodies P3X, P2X, and P1X. Injection of the same antibody as conjugated on the BIACORE chip serves as a negative control. In all three experiments, the two antibodies from the remaining bins are observed to associate with  
20 EGFR-ECD. Thus, the results of the three experiments demonstrate that P1X, P2X, and P3X have non-overlapping, distinct epitopes and can simultaneously associate with EGFR-ECD.

### **Example 2: Binding affinities**

25 The monovalent affinities of P1X, P2X, and P3X to EGFR were measured by KinExA. Data are shown below in Table 1. Affinities of P1X, P2X, and P3X are all better than 0.4 nM and are all improved relative to the parent molecules. The affinity of P1X (11pM) is 13.18 times better than the Bin 1 parent molecule ca (145pM). The affinity of P2X (70pM) is 7.71 times better than the Bin 2 parent molecule cd (540pM).  
30 The affinity of P3X (360pM) is 2.10 times better than the Bin 3 parent molecule ch (757pM).

**Table 1**

Antibody	Association Rate (1/M*sec)	Dissociation Rate (1/sec)	K <sub>D</sub> (M)
P1X	3.73E+06	4.10E-05	1.10E-11
ca (P1X parent)	<i>N.D.</i>	<i>N.D.</i>	1.45E-10
P2X	7.06E+05	4.94E-05	7.00E-11
cd (P2X parent)	9.62E+05	5.20E-04	5.40E-10
P3X	1.16E+06	4.16E-04	3.60E-10
ch (P3X parent)	5.87E+05	4.44E-04	7.57E-10

**Example 3: Cell binding assays with single antibodies**

A cell binding assay was performed to demonstrate that monoclonal antibodies

5 P1X, P2X, and P3X can associate with EGFR on A431 cells (Figure 3). A431 cells were incubated with a dilution series of single antibody for 2 hr and the amount of bound antibody measured by quantitative flow cytometry, as described in the methodology section above. The concentrations used in the dilution series for the antibodies are shown below in Table 2. The ordinarily skilled artisan will understand that each specific

10 concentration value in Table 2 is subject to some minor experimental variability, so that each specific concentration given indicates a value of about the indicated concentration (*e.g.*, a concentration indicated in a table as 0.1 nM represents a value of about 0.1 nM).

**Table 2**

Conc, Log(Molar)	Conc, nM
-7.00	100.00
-7.48	33.33
-7.95	11.11
-8.43	3.70
-8.91	1.23
-9.39	0.41
-9.86	0.14
-10.34	0.05
-10.82	0.02
-11.29	0.01
-11.77	0.00

The on-cell binding affinities under these experimental conditions were calculated, via

15 regression to a 4 parameter logistic equation using GraphPad Prism® software, to be 168pM (P1X), 340pM (P2X) and 748pM (P3X).

**Example 4: Phospho-EGF receptor signaling inhibition by single antibodies**

A431 cells were treated with single antibodies and their ability to inhibit EGF-dependent phospho-EGFR activity was measured by phospho-EGFR ELISA. P1X and P2X potently inhibit phospho-EGFR activity in a dose-dependent manner, with respective IC<sub>50</sub> values of 3.09nM and 4.19nM, while treatment with P3X elicits partial phospho-EGFR inhibition (Figure 4). The concentrations used in the dilution series for the antibodies are shown below in Table 3. The ordinarily skilled artisan will understand that each specific concentration value in Table 3 is subject to some minor experimental variability, so that each specific concentration given indicates a value of about the indicated concentration (*e.g.*, a concentration indicated in a table as 0.1 nM represents a value of about 0.1 nM).

**Table 3**

Conc, Log(Molar)	Conc, nM
-6.60	250.00
-7.20	62.50
-7.81	15.62
-8.41	3.91
-9.01	0.98
-9.61	0.24
-10.21	0.06
-10.82	0.02
-11.42	0.00

15 **Example 5: Phospho-ERK signaling inhibition by single and pairwise combinations of antibodies and comparison to parental antibodies**

A431 cells were treated with a dilution series of single P1X or ca antibody and phospho-ERK inhibition measured by phospho-ERK ELISA (Figure 5A). P1X elicited dose-dependent inhibition of phospho-ERK activity while the ca parental antibody elicited only partial inhibition.

A431 cells were treated with a dilution series of pairwise combinations of P1X+P3X or their respective parent antibodies ca+ch and phospho-ERK inhibition measured by phospho-ERK ELISA (Figure 5B). Both combinations inhibit phospho-ERK generation in a dose-dependent manner, but the combination of P1X+P3X provides superior inhibition. The combination of P1X+P3X elicited 82% inhibition of phospho-

ERK activity while the parental combination elicited only 71%, as calculated by a fit to a 4 parameter logistic equation using GraphPad Prism software.

A431 cells were treated with a dilution series of pairwise combinations of P1X+P2X or their respective parent antibodies ca+cd and phospho-ERK inhibition measured by phospho-ERK ELISA (Figure 5C). Both combinations inhibit phospho-ERK generation in a dose-dependent manner, but the combination of P1X+P2X demonstrates an observable improvement in the IC90 value versus the parental combination.

The concentrations used in the dilution series for the antibodies are shown below in Table 4 (for the data in Figure 5A) and in Table 5 (for the data in Figures 5B and 5C). The ordinarily skilled artisan will understand that each specific concentration value in Tables 4 and 5 is subject to some minor experimental variability, so that each specific concentration given indicates a value of about the indicated concentration (*e.g.*, a concentration indicated in a table as 0.1 nM represents a value of about 0.1 nM).

15 **Table 4**

Conc, Log(Molar)	Conc, nM
-5.70	2000.00
-6.18	666.67
-6.65	222.22
-7.13	74.07
-7.61	24.69
-8.21	6.17
-8.81	1.54
-9.41	0.39
-10.02	0.10

**Table 5**

Conc, Log(Molar)	Conc, nM
-5.69897	2000.00
-6.176091	666.67
-6.653213	222.22
-7.130334	74.07
-7.607455	24.69
-8.209515	6.17
-8.811575	1.54
-9.413635	0.39
-10.01569	0.10
-10.61775	0.02

It is noted that the concentrations shown in Table 5 are total concentrations for the pairs of antibodies used. The ratio used is 1:1 so each individual antibody in the pair comprises half of the total concentration.

**Example 6: Phospho-ERK signaling inhibition by different combination ratios of P1X, P2X, and P3X**

A431 cells were treated with a dilution series of P1X and phospho-ERK inhibition measured by ELISA (Figure 6A). The concentrations used in the dilution series for the antibodies are shown below in Table 6. The ordinarily skilled artisan will understand that each specific concentration value in Table 6 is subject to some minor experimental variability, so that each specific concentration given indicates a value of about the indicated concentration (*e.g.*, a concentration indicated in a table as 0.1 nM represents a value of about 0.1 nM).

**Table 6**

Conc, Log(Molar)	Conc, nM
-5.69897	2000.00
-6.176091	666.67
-6.653213	222.22
-7.130334	74.07
-7.607455	24.69
-8.084577	8.23
-8.561698	2.74
-9.038818	0.91
-9.51594	0.30
-9.993061	0.10

The experiment was carried out as described in the methodology section. Under these experimental conditions, P1X inhibits 81% of phospho-ERK activity at saturating doses with an IC50 value of about 25 nM (27nM). Therefore the approximate location on the plot of the IC50 is indicated in Figure 6A by “25nM” and 25 nM was set as the constant concentration of P1X in the following experiments.

A431 cells were treated with dilution series of 5 combination ratios of P3X + P2X in combination with a constant P1X concentration of 25nM and phospho-ERK inhibition measured by ELISA (Figure 6B). The concentrations used in the dilution series for the antibodies are shown below in Table 7. The ordinarily skilled artisan will understand that each specific concentration value in Table 7 is subject to some minor experimental variability, so that each specific concentration given indicates a value of



about the indicated concentration (*e.g.*, a concentration indicated in a table as 0.1 nM represents a value of about 0.1 nM).

**Table 7**

Conc, Log(Molar)	Conc, nM
-5.69897	2000.00
-6.176091	666.67
-6.653213	222.22
-7.130334	74.07
-7.607455	24.69
-8.084577	8.23
-8.561698	2.74
-9.038818	0.91
-9.51594	0.30
-9.993061	0.10

It is noted that the concentrations shown in Table 7 are total concentrations for  
 5 P2X+P3X. The individual concentration of P2X and P3X is dependent on the indicated ratio. The experiment was carried out as described in the methodology section. The ratios of P3X:P2X used were 1:0, 0:1, 1:2, 2:1, and 1:1. All ratios inhibited greater than 70% of phospho-ERK activity, with those combinations containing all three antibodies providing the highest degree of inhibition.

10 A431 cells were treated with dilution series of 6 combination ratios of P1X:P2X:P3X and phospho-ERK inhibition measured by ELISA (Figure 6C). The concentrations used in the dilution series for the antibodies are shown below in Table 8. The ordinarily skilled artisan will understand that each specific concentration value in  
 15 Table 8 is subject to some minor experimental variability, so that each specific concentration given indicates a value of about the indicated concentration (*e.g.*, a concentration indicated in a table as 0.1 nM represents a value of about 0.1 nM).

**Table 8**

LogM	nM	Ratio (P1X:P2X:P3X)					
		1:0.01:1	1:0.1:1	1:1:1	2:0.1:1	2:0.1:1	2:2:1
-10.8148	0.0153	X					
-10.8141	0.0153				X		
-10.7958	0.0160		X				
-10.7889	0.0163					X	
-10.6409	0.0229			X			

-	10.5951	0.0254					X
-	10.3377	0.0460	X				
-	10.3370	0.0460			X		
-	10.3187	0.0480		X			
-	10.3118	0.0488				X	
-	10.1638	0.0686			X		
-	10.1180	0.0762					X
-	-9.8606	0.1379	X				
-	-9.8598	0.1381			X		
-	-9.8415	0.1440		X			
-	-9.8347	0.1463				X	
-	-9.6866	0.2058			X		
-	-9.6409	0.2286					X
-	-9.3834	0.4136	X				
-	-9.3827	0.4143			X		
-	-9.3644	0.4321		X			
-	-9.3576	0.4390				X	
-	-9.2095	0.6173			X		
-	-9.1638	0.6859					X
-	-8.9063	1.2407	X				
-	-8.9056	1.2428			X		
-	-8.8873	1.2963		X			
-	-8.8805	1.3169				X	
-	-8.7324	1.8519			X		
-	-8.6866	2.0576					X
-	-8.4292	3.7222	X				
-	-8.4285	3.7284			X		
-	-8.4102	3.8889		X			
-	-8.4033	3.9506				X	
-	-8.2553	5.5555			X		
-	-8.2095	6.1728					X
-	-7.9521	11.1667	X				
-	-7.9514	11.1852			X		
-	-7.9331	11.6667		X			
-	-7.9262	11.8518				X	
-	-7.7782	16.6667			X		
-	-7.7324	18.5185					X
-	-7.4750	33.5000	X				
-	-7.4742	33.5555			X		
-	-7.4559	35.0000		X			
-	-7.4491	35.5556				X	
-	-7.3010	50.0000			X		

-7.2553	55.5556						X
-6.9978	100.5000	X					
-6.9971	100.6667				X		
-6.9788	104.9999		X				
-6.9720	106.6665					X	
-6.8239	149.9999			X			
-6.7782	166.6668						X
-6.5207	301.4998	X					
-6.5200	302.0000				X		
-6.5017	315.0003		X				
-6.4949	320.0000					X	
-6.3468	450.0005			X			
-6.3010	500.0000						X

The experiment was carried out as described in the methodology section. The ratios of P1X:P2X:P3X used were 1:0.01:1, 1:0.1:1, 1:1:1, 2:0.01:1, 2:0.1:1, and 2:2:1. All ratios inhibited greater than 70% of phospho-ERK activity.

A431 cells were treated with dilution series of 5 combination ratios of P1X:P2X and phospho-ERK inhibition measured by ELISA (Figure 6D). The concentrations used in the dilution series for the antibodies are shown below in Table 9. The ordinarily skilled artisan will understand that each specific concentration value in Table 9 is subject to some minor experimental variability, so that each specific concentration given indicates a value of about the indicated concentration (*e.g.*, a concentration indicated in a table as 0.1 nM represents a value of about 0.1 nM).

**Table 9**

Conc, Log(Molar)	Conc, nM
-6.522879	300.00
-7	100.00
-7.477121	33.33
-7.954243	11.11
-8.431364	3.70
-8.908485	1.23
-9.385606	0.41
-9.862727	0.14
-10.33985	0.05
-10.81697	0.02

It is noted that the concentrations shown in Table 9 are total concentrations for P1X+P2X. The individual concentration of P1X and P2X is dependent on the indicated ratio. The experiment was carried out as described in the methodology section. The ratios of P1X:P2X used were 1:2, 5:1, 9:1, 50:1, and 1:5. All ratios except 1:5

(P1X:P2X) inhibited greater than 70% of phospho-ERK activity within the concentration range used in the experiment. However, fitting a 4 parameter logistic inhibition curve to the 1:5 ratio (P1X:P2X) data predicts that this combination will achieve 70% phospho-ERK inhibition at a concentration of 35.7nM, marginally higher than the dose used in the experiment and well within the range achievable under physiological conditions.

**Example 7: Phospho-EGFR and Phospho-ERK signaling inhibition by a 2:2:1 ratio combination of P1X, P2X, and P3X**

A431 cells were treated with a dilution series of a 2:2:1 molar ratio combination of antibodies P1X, P2X, and P3X (this combination at this molar ratio is referred to herein as “P1X+P2X+ P3X”) and phospho-EGFR and phospho-ERK inhibition measured by ELISA (Figure 7A). The concentrations used in the dilution series for the antibodies are shown below in Table 10. The ordinarily skilled artisan will understand that each specific concentration value in Table 10 is subject to some minor experimental variability, so that each specific concentration given indicates a value of about the indicated concentration (*e.g.*, a concentration indicated in a table as 0.1 nM represents a value of about 0.1 nM).

**Table 10**

Conc, Log(Molar)	Conc, nM
-6.30	500.00
-6.78	166.67
-7.26	55.56
-7.73	18.52
-8.21	6.17
-8.69	2.06
-9.16	0.69
-9.64	0.23
-10.12	0.08
-10.60	0.03

It is noted that the concentrations shown in Table 10 are total concentrations for P1X+P2X+P3X. The ratio used is 2:2:1, so the individual concentrations of P1X, P2X and P3X are 40%, 40% and 20%, respectively. Experiments were carried out as described in the methodology section. The combination of three antibodies is a potent

inhibitor of both phospho-EGFR and phospho-ERK activities, with respective IC50 values of 2.30nM and 9.87nM.

P1X+P2X+ P3X was compared to P1X single (Figure 7B) and P2X single (Figure 7C). A431 cells were treated with a dilution series of antibody and phospho-ERK inhibition measured by ELISA. The concentrations used in the dilution series for the antibodies for the experiments shown in Figures 7B and 7C are shown below in Table 11. The ordinarily skilled artisan will understand that each specific concentration value in Table 11 is subject to some minor experimental variability, so that each specific concentration given indicates a value of about the indicated concentration (*e.g.*, a concentration indicated in a table as 0.1 nM represents a value of about 0.1 nM).

**Table 11**

Conc, Log(Molar)	Conc, nM
-5.69897	2000.00
-6.176091	666.67
-6.653213	222.22
-7.130334	74.07
-7.607455	24.69
-8.084577	8.23
-8.561698	2.74
-9.038818	0.91
-9.51594	0.30
-9.993061	0.10

It is noted that the concentrations shown in Table 11 are total concentrations for P1X+P2X+P3X. The ratio used is 2:2:1, so the individual concentrations of P1X, P2X and P3X are 40%, 40% and 20%, respectively. Experiments were carried out as described in the methodology section with the exception that 80nM of EGF ligand was used to stimulate cells. The 2:2:1 ratio combination of antibodies is a potent inhibitor of phospho-ERK activity compared to P1X and P2X, which respectively provide partial and no inhibition.

**Example 8: EGF receptor down-regulation and inhibition of pERK, pAKT and p-c-Jun signaling in H1975 cells following treatment with P1X+P2X+P3X**

Cells were pre-incubated for 2 hours with of P1X+P2X+P3X equaling 1 $\mu$ M total antibody prior to stimulation with 50 ng/ml rhEGF (PeproTech) for 10 minutes, as described in the methodology section above. Immunoblots of cell lysates were

separately probed with antibodies against tEGFR, pERK, pAKT or p-c-Jun and densitometry of the bands was normalized to the loading control PCNA and to lysates of control untreated cells. EGF receptor down-regulation in response to P1X+P2X+P3X treatment is shown in Figure 8A and inhibition of pERK, pAKT and p-c-Jun signaling in response to P1X+P2X+P3X treatment is shown in Figure 8B.

**Example 9: Inhibition of tumor cell proliferation in vitro**

Inhibition of tumor cell proliferation *in vitro* was analyzed by the methods described above or minor variations thereof. The non-small cell lung cancer (NSCLC) lines HCC827 and H1975 were plated at 5000 cells/well and treated with antibody combinations ranging from 0.1-1 μM (final concentration). Figures 9A-9D show inhibition of cell proliferation using CellTiter-Glo® (CTG) Luminescent Cell Viability Assay (Promega Corporation) that measures the number of viable cells in culture based upon quantitation of ATP present, which is an indicator of metabolically active cells. Figures 9A and 9B show potent inhibition of growth of HCC827 and H1975 cells over a range of P1X+P2X+P3X concentrations, but not by cetuximab treatment or assay medium alone (1% FCS) in the presence of EGF ligand. Figures 9C and 9D show potent inhibition of growth of HCC827 and H1975 cells over a range of concentrations for both P1X+P2X+P3X and cetuximab, but not by assay medium alone (1% FCS) in the presence of AREG ligand. These results demonstrate the ability of P1X+P2X+P3X to inhibit tumor cell proliferation *in vitro* in response to both high-affinity (EGF) and low-affinity (AREG) ligands, whereas cetuximab is only effective in cells treated with low-affinity (AREG) ligand. The concentrations used in the dilution series for the antibodies for the experiments shown in Figures 9A-D are shown below in Table 12. The ordinarily skilled artisan will understand that each specific concentration value in Table 12 is subject to some minor experimental variability, so that each specific concentration given indicates a value of about the indicated concentration (*e.g.*, a concentration indicated in a table as 0.1 nM represents a value of about 0.1 nM).

**Table 12**

Conc, Log(Molar)	Conc, nM
-6.000000	1000.00
-6.301030	500.00
-6.602060	250.00
-6.903090	125.00
-7.204120	62.50

-7.806180	15.63
-8.408240	3.91
-9.010300	0.98
-9.913390	0.12

It is noted that the concentrations shown in Table 12 are total concentrations for P1X+P2X+P3X. The ratio used is 2:2:1, so the individual concentrations of P1X, P2X and P3X are 40%, 40% and 20%, respectively.

5

**Example 10: Inhibition of tumor cell proliferation *in vivo***

Efficacy of P1X+P2X+P3X *in vivo* was assessed in a H1975 lung cancer cell xenograft murine mouse model.  $2 \times 10^6$  NCI-H1975 cells were injected subcutaneously into the flank of nu/nu mice. Once tumors had reached an average size of  $300\text{mm}^3$  treatment was initiated. Groups of 10 mice were treated with either vehicle control (PBS); or the murine ratio antibody trio at the following component concentrations: murine ratio antibody trio-Low P1X=2.53mg/kg, P2X=7.26mg/kg and P3X=0.66mg/kg or murine ratio antibody trio-Medium P1X=5.06mg/kg, P2X=14.52mg/kg and P3X=1.33mg/kg. Mice were treated every two days.

The results shown in Figure 10A (DU145 xenograft model) and Figure 10B (H1975 xenograft model) demonstrate the ability of P1X+P2X+P3X to inhibit tumor cell proliferation *in vivo*.

15

**Example 11: Ligand antagonism cell binding assays with single antibodies**

A cell binding assay was performed to demonstrate that monoclonal antibodies P1X, P2X, and P3X can antagonize the interaction of EGF ligand and EGF receptor on A431 cells. A431 cells were incubated with one dose of single antibody for 1 hr followed by a dilution series of biotin-EGF ligand and the amount of bound biotin-EGF ligand measured by quantitative flow cytometry, as described in the methods section above. The concentrations for the antibodies are shown below in Table 13 and represent a sub-saturating concentration (approx. EC90 concentration) of cell binding as determined from the analysis demonstrated in Example 3. The concentrations used in the dilution series for the biotin-EGF are shown below in Table 14. The values in Table 13 and Table 14 are subject to some minor experimental variability, so that each specific

25

concentration given indicates a value of about the indicated concentration (*e.g.*, a concentration indicated in a table as 0.1 nM represents a value of about 0.1 nM).

**Table 13**

Antibody	Conc, Log(Molar)	Conc, nM
P1X	-9.01	0.97
P2X	-8.70	2.00
P3X	-8.33	4.68

5 **Table 14**

Conc, Log(Molar)	Conc, nM
-6.70	200
-7.18	66.67
-7.65	22.22
-8.13	7.41
-8.61	2.47
-9.08	0.82
-9.56	0.27
-10.04	0.09
-10.52	0.03
-11.00	0.01
-11.52	0.003

The results are shown in Figure 11, which demonstrates that each of the single antibodies (P1X, P2X and P3X) alone are capable of antagonizing the interaction of EGF ligand and EGF receptor on A431 cells, with P1X and P2X exhibiting more potent  
10 inhibitory activity than P3X.

**Example 12: Ligand antagonism cell binding assays with single and combinations of antibodies or Fabs**

A cell binding assay was performed to determine the extent to which single  
15 antibodies and multiple antibody combinations of monoclonal antibodies P1X, P2X, and P3X and single and multiple combinations of monovalent Fab fragments P1X Fab, P2X Fab, and P3X Fab can antagonize the interaction of EGF ligand and EGF receptor on A431 cells. A431 cells were incubated with one dose of antibody or Fab for 1 hr followed by a dilution series of biotin-EGF ligand and the amount of bound biotin-EGF  
20 ligand measured by quantitative flow cytometry, as described in the methodology section above. The concentration of antibodies and Fab was 10nM. The combinations of three antibodies (P1X+P2X+P3X) and three antibodies (P1X Fab + P2X Fab + P3X



Fab) were formulated in a ratio of 2:2:1 and were dosed at a total concentration of 10 nM. The concentrations used in the dilution series for the biotin-EGF are shown above in Table 14. The ordinarily skilled artisan will understand that each specific concentration value in Table 14 is subject to some minor experimental variability, so that each specific concentration given indicates a value of about the indicated concentration (*e.g.*, a concentration indicated in a table as 0.1 nM represents a value of about 0.1 nM).

The results are shown in Figure 12A (single and combinations of monoclonal antibodies P1X, P2X, and P3X) and Figure 12B (single and combinations of monovalent Fab fragments P1X Fab, P2X Fab, and P3X Fab). The results in Figure 12A demonstrate that again all three antibodies alone were capable of antagonizing the interaction of EGF ligand and EGF receptor on A431 cells, with P1X and P2X exhibiting more potent inhibitory activity than P3X, and the triple combination of P1X+P2X+P3X also showed potent inhibitory activity. The results in Figure 12B demonstrate that P1X Fab showed the strongest inhibitory activity alone, with P3X Fab alone showing intermediate inhibitory activity alone and P2X Fab showing only minimal inhibitory activity alone. The triple combination of P1X Fab + P2X Fab + P3X Fab also showed strong inhibitory activity, although less potent than P1X Fab alone.

**Example 13: Phospho-EGFR and Phospho-ERK signaling inhibition by a 2:2:1 molar ratio combination of P1X, P2X, and P3X antibodies or Fabs**

A431 cells were treated with a dilution series of a 2:2:1 molar ratio combination of antibodies P1X, P2X, and P3X (“P1X+P2X+P3X”) or Fabs P1X Fab, P2X Fab, P3X Fab (this combination at this molar ratio is referred to herein as “P1X Fab+P2X Fab+P3X Fab”) and phospho-EGFR and phospho-ERK inhibition measured by ELISA. Experiments were performed with rhEGF (PeproTech) dosed at a concentration of 50ng/mL or 500 ng/mL. The concentrations used in the dilution series for the antibodies and Fabs are shown below in Table 15. The ordinarily skilled artisan will understand that each specific concentration value in Table 15 is subject to some minor experimental variability, so that each specific concentration given indicates a value of about the indicated concentration (*e.g.*, a concentration indicated in a table as 0.1 nM represents a value of about 0.1 nM).

**Table 15**

Conc, Log(Molar)	Conc, nM
-5.70	2000.00
-6.18	666.67
-6.65	222.22
-7.13	74.07
-7.61	24.70
-8.08	8.23
-8.56	2.74
-9.04	0.91
-9.52	0.30
-9.99	0.10

The results are shown in Figures 13A-D, wherein Figures 13A and 13B show the results of the phospho-EGFR inhibition assay and Figures 13C and 13D show the results of the phospho-ERK inhibition assay, with Figures 13A and 13C showing the results at low doses (50 ng/ml or 8 nM) and with Figures 13B and 13D showing the results at high doses (500 ng/ml or 80 nM).

With respect to inhibition of phospho-EGFR, the results in Figures 13A and 13B demonstrate that both triple combinations, P1X+P2X+P3X mAbs and P1X Fab+P2X Fab+P3X Fab fragments, exhibited strong inhibition at both the low dose and the high dose tested.

With respect to inhibition of phospho-ERK, the results in Figures 13C and 13D demonstrate that both triple combinations, P1X+P2X+P3X mAbs and P1X Fab+P2X Fab+P3X Fab fragments, exhibited inhibition at both the low dose and the high dose tested, with the P1X+P2X+P3X mAb combination exhibiting more potent inhibition than the P1X Fab+P2X Fab+P3X Fab fragment combination.

**Example 14: EGF receptor down-regulation in DU-145 cells following treatment with P1X+P2X+P3X, P1X Fab +P2X Fab +P3X Fab, or cetuximab**

Cells were pre-incubated for 2, 6, or 24 hours with of P1X+P2X+P3X, P1X Fab +P2X Fab +P3X Fab, or cetuximab equaling 50 nM, 100 nM, and 50 nM, respectively. The Fab combination is dosed at twice the concentration as P1X+P2X+P3X and cetuximab to account for a single binding moiety on a Fab molecule versus two binding moieties on and IgG molecule. Immunoblots of cell lysates were probed with antibodies against transmembrane EGFR (tEGFR) and the pcna housekeeping protein as a control,

as described in the methodology section above. EGF receptor down-regulation in response to treatment is shown in Figure 14. The results demonstrate that treatment with P1X+P2X+P3X led to observable down-regulation of EGFR, in a time dependent manner, whereas treatment with P1X Fab+P2X Fab+P3X Fab or cetuximab did not lead to observable down-regulation of EGFR on visual inspection of the immunoblots.

### **Equivalents**

Those skilled in the art will recognize, or be able to ascertain using no more than routine experimentation, many equivalents of the specific embodiments described herein. Such equivalents are intended to be encompassed by the following claims. Any combination of the embodiments disclosed in the any plurality of the dependent claims is contemplated to be within the scope of the disclosure.

### **Incorporation by Reference**

All, patents, pending patent applications and patent publications referred to hereinabove are hereby incorporated by reference in their entireties.

**APPENDIX A**  
**ANTI-CANCER AGENTS**

<b>Anti-Cancer Agent</b>	<b>Comments</b>	<b>Examples</b>
Antibodies	Antibodies which bind IGF-1R (insulin-like growth factor type 1 receptor), which is expressed on the cell surface of most human cancers	A12 (fully humanized mAb) 19D12 (fully humanized mAb) CP751-871 (fully humanized mAb) H7C10 (humanized mAb) alphaIR3 (mouse) scFV/FC (mouse/human chimera) EM/164 (mouse) AMG 479 (fully humanized mAb; Amgen) IMCA 12 (fully humanized mAb; Imclone) NSC-742460 (Dyax) MR-0646, F50035 (Pierre Fabre Medicament, Merck)
	Antibodies which bind EGFR; Mutations affecting EGFR expression or activity can result in cancer	matuzumab (EMD72000) Erbix® / cetuximab (Imclone) Vectibix® / panitumumab (Amgen) mAb 806 nimotuzumab (TheraCIM®) INCB7839 (Incyte) panitumumab (Vectibix®; Amgen)
	Antibodies which bind cMET (mesenchymal epithelial transition factor); a member of the MET family of receptor tyrosine kinases)	AV299 (AVEO) AMG102 (Amgen) 5D5 (OA-5D5) (Genentech)
	Anti-ErbB3 antibodies	MM-121 (Merrimack Pharmaceuticals) Ab #14 described in WO 2008/100624 1B4C3; 2D1D12 (U3 Pharma AG) U3-1287/AMG888 (U3 Pharma/Amgen)

	Anti-ErbB2 (HER2) antibodies	Herceptin® (trastuzumab; Genentech/Roche); Omnitarg® (pertuzumab; 2C4,R1273; Genentech/Roche)
Small Molecules Targeting IGF1R	IGF-1R (insulin-like growth factor type 1 receptor), which is expressed on the cell surface of most human cancers	NVP-AEW541-A BMS-536,924 (1H-benzoimidazol-2-yl)-1H-pyridin-2-one) BMS-554,417 Cycloligan TAE226 PQ401
Small Molecules Targeting EGFR	EGFR; Mutations affecting EGFR expression or activity can result in cancer	Iressa® / gefitinib (AstraZeneca) CI-1033 (PD 183805) (Pfizer) TYVERB / lapatinib (GlaxoSmithKline) Tykerb® / lapatinib ditosylate (SmithKline Beecham) Tarceva®/ Erlotinib HCL (OSI Pharma) PKI-166 (Novartis) PD-158780 EKB-569 Tyrphostin AG 1478(4-(3-Chloroanillino)-6,7-dimethoxyquinazoline)
Small Molecules Targeting ErbB2	ErbB2, also known as HER2, a member of the ErbB family of receptors, which is expressed on certain cancer cells	HKI-272 (neratinib; Wyeth) KOS-953 (tanespimycin; Kosan Biosciences)
Small Molecules Targeting cMET	cMET (Mesenchymal epithelial transition factor); a member of the MET family of receptor tyrosine kinases)	PHA665752 ARQ 197 (ArQule) ARQ-650RP (ArQule)

Antimetabolites	<p>An antimetabolite is a chemical with a similar structure to a substance (a metabolite) required for normal biochemical reactions, yet different enough to interfere with the normal functions of cells, including cell division.</p>	<p>flourouracil (5-FU)                      capecitabine / XELODA® (HLR Roche)                      5-trifluoromethyl-2'-deoxyuridine                      methotrexate sodium (Trexall) (Barr)                      raltitrexed / Tomudex® (AstraZaneca)                      pemetrexed / Alimta® (Lilly)                      tegafur                      cytosine arabinoside (Cytarabine, Ara-C)                      / tioguanine / Lanvis® (GlaxoSmithKline)                      5-azacytidine                      6-mercaptopurine (Mercaptopurine, 6-MP)                      azathioprine / Azasan® (AAIPHARMA LLC)                      6-thioguanine (6-TG) / Purinethol® (TEVA)                      pentostatin / Nipent® (Hospira Inc.)                      fludarabine phosphate / Fludara® (Bayer Health Care)                      cladribine / Leustatin® (2-CdA, 2-chlorodeoxyadenosine) (Ortho Biotech)                      floxuridine (5-fluoro-2'-deoxyuridine) / FUDR® (Hospira, Inc.)</p>
Alkylating agents	<p>An alkylating antineoplastic agent is an alkylating agent that attaches an alkyl group to DNA. Since cancer cells generally proliferate unrestrictedly more than do healthy cells they are more sensitive to DNA damage, and alkylating agents are used clinically to treat a variety of tumors.</p>	<p>Ribonucleotide Reductase Inhibitor (RNR)                      cyclophosphamide / Cytoxan® (BMS) / Neosar® (TEVA)                      ifosfamide /Mitoxana® (ASTA Medica)                      ThioTEPA (Bedford, Abraxis, Teva)                      BCNU→ 1,3-bis(2-chloroethyl)-1-nitrosourea                      CCNU→ 1, -(2-chloroethyl)-3-cyclohexyl-1-nitrosourea (methyl CCNU)                      hexamethylmelamine (altretamine, HMM) / Hexalen® (MGI Pharma Inc.)                      busulfan / Myleran® (GlaxoSmithKline)</p>

procarbazine HCL / Matulane® (Sigma Tau)  
 Dacarbazine (DTIC®)  
 chlorambucil / Leukaran® (SmithKline Beecham)  
 Melphalan / Alkeran® (GlaxoSmithKline)  
 cisplatin (Cisplatinum, CDDP) / Platinol (Bristol Myers)  
 carboplatin / Paraplatin (BMS)  
 oxaliplatin / Eloxitan® (Sanofi-Aventis US)  
 Bendamustine  
 carboquone  
 carmustine  
 chloromethine  
 dacarbazine (DTIC)  
 fotemustine  
 lomustine  
 mannosulfan  
 nedaplatin  
 nimustine  
 prednimustine  
 ranimustine  
 satraplatin  
 semustine  
 streptozocin  
 temozolomide  
 treosulfan  
 triaziquone  
 triethylene melamine  
 triplatin tetranitrate  
 trofosfamide  
 uramustine

Topoisomerase inhibitors

Topoisomerase inhibitors are chemotherapy agents designed to interfere with the action of

doxorubicin HCL / Doxil® (Alza)  
 daunorubicin citrate / Daunoxome® (Gilead)  
 mitoxantrone HCL/Novantrone (EMD)

	<p>topoisomerase enzymes (topoisomerase I and II), which are enzymes that control the changes in DNA structure by catalyzing the breaking and rejoining of the phosphodiester backbone of DNA strands during the normal cell cycle.</p>	<p>Serono)                  actinomycin D                  etoposide / Vepesid® (BMS)/                  Etopophos® (Hospira, Bedford, Teva Parenteral, Etc.)                  topotecan HCL / Hycamtin® (GlaxoSmithKline)                  teniposide (VM-26) / Vumon® (BMS)                  irinotecan HCL(CPT-11) /                  camptosar® (Pharmacia &amp; Upjohn)                  camptothecin (CPT)                  belotecan                  rubitecan</p>
<p>Microtubule targeting agents</p>	<p>Microtubules are one of the components of the cytoskeleton. They have diameter of apporximately 24 nm and length varying from several micrometers to possibly millimeters in axons of nerve cells. Microtubules serve as structural components within cells and are involved in many cellular processes including mitosis, cytokinesis, and vesicular transport.</p>	<p>vincristine / Oncovin® (Lilly)                  vinblastine sulfate/Velban®(discontinued) (Lilly)                  vinorelbine tartrate / Navelbine® (PierreFabre)                  vindesine sulphate / Eldisine® (Lilly)                  paclitaxel / Taxol® (BMS)                  docetaxel / Taxotere® (Sanofi Aventis US)                  Nanoparticle paclitaxel (ABI-007) / Abraxane® (Abraxis BioScience, Inc.)                  ixabepilone / IXEMPRA™ (BMS)                  larotaxel                  ortataxel                  tesetaxel                  vinflunine</p>
<p>Kinase inhibitors</p>	<p>Tyrosine kinases are enzymes within the cell that function to attach phosphate groups to the amino acid tyrosine. By blocking the ability of protein tyrosine kinases</p>	<p>imatinib mesylate / Gleevec (Novartis)                  sunitinib malate / Sutent® (Pfizer)                  sorafenib tosylate / Nexavar® (Bayer)                  nilotinib hydrochloride monohydrate / Tasigna® (Novartis)                  AMG 386 (Amgen)                  axitinib (AG-013736; Pfizer, Inc.)</p>



	to function, these compounds provide a tool for controlling cancerous cell growth.	<p>bosutinib (SKI-606; Wyeth)</p> <p>brivanib alalinate (BMS-582664; BMS)</p> <p>cediranib (AZD2171; Recentin, AstraZeneca)</p> <p>dasatinib (BMS-354825; Sprycel®; BMS)</p> <p>lestaurtinib (CEP-701; Cephalon)</p> <p>motesanib diphosphate (AMG-706; Amgen/Takeda)</p> <p>pazopanib HCL (GW786034; Armala, GSK)</p> <p>semaxanib (SU5416; Pharmacia)</p> <p>vandetanib (AZD647; Zactima; AstraZeneca)</p> <p>vatalanib (PTK-787; Novartis, Bayer Schering Pharma)</p> <p>XL184 (NSC718781; Exelixis, GSK)</p>
Protein synthesis inhibitors	Induces cell apoptosis	L-asparaginase / Elspar® (Merck & Co.)
Immunotherapeutic agents	Induces cancer patients to exhibit immune responsiveness	<p>Alpha interferon</p> <p>Angiogenesis Inhibitor / Avastin® (Genentech)</p> <p>IL-2→ Interleukin 2 (Aldesleukin) / Proleukin® (Chiron)</p> <p>IL-12→ Interleukin 12</p>
Hormonal therapies	<p>Hormonal therapies associated with menopause and aging seek to increase the amount of certain hormones in the body to compensate for age- or disease-related hormonal declines.</p> <p>Hormonal therapy as a cancer treatment</p>	<p>Ttoremifene citrate / Fareston® (GTX, Inc.)</p> <p>fulvestrant / Faslodex® (AstraZeneca)</p> <p>raloxifene HCL / Evista® (Lilly)</p> <p>anastrozole / Arimidex® (AstraZeneca)</p> <p>letrozole / Femara® (Novartis)</p> <p>fadrozole (CGS 16949A )</p> <p>exemestane / Aromasin® (Pharmacia &amp; Upjohn)</p> <p>leuprolide acetate / Eligard® (QTL USA)</p> <p>Lupron® (TAP Pharm.)</p>

generally either reduces the level of one or more specific hormones, blocks a hormone from interacting with its cellular receptor or otherwise alters the cancer's ability to be stimulated by hormones to grow and spread. Such hormonal therapies thus include hormone antagonists and hormone synthesis inhibitors. In some instances hormone agonists may also be used as anticancer hormonal therapies.

goserelin acetate / Zoladex® (AstraZeneca)  
 triptorelin pamoate / Trelstar® (Watson Labs)  
 buserelin / Suprefact® (Sanofi Aventis)  
 nafarelin  
 cetrotirelix / Cetrotide® (EMD Serono)  
 bicalutamide / Casodex® (AstraZeneca)  
 nilutamide / Nilandron® (Aventis Pharm.)  
 megestrol acetate / Megace® (BMS)  
 somatostatin Analogs (e.g., Octreotide acetate / Sandostatin® (Novartis))  
 abarelix (Plenaxis™ ; Amgen)  
 abiraterone acetate (CB7630; BTG plc)  
 afimoxifene (TamoGel; Ascend Therapeutics, Inc.)  
 aromatase inhibitor (Atamestane plus toremifene; Intarcia Therapeutics, Inc.)  
 arzoxifene (Eli Lilly & Co)  
 Asentar™; DN-101 (Novacea; Oregon Health Sciences U)  
 flutamide (Eulexin®, Schering; Prostacur, Laboratorios Almirall, S.A)  
 letrozole (CGS20267) (Femara®, Chugai; Estrochek®, (Jagsonpal Pharmaceuticals Ltd;)  
 Delestrogen®, estradiol valerate (Jagsonpal)  
 magestrol acetate / Megace®  
 medroxyprogesterone acetate (Veraplex®; Combiphar)  
 MT206 (Medisyn Technologies, Inc.)  
 nandrolone decanoate (Zestabolin®; Mankind Pharma Ltd)  
 tamoxifen (Taxifen®, Yung Shin Pharmaceutical; Tomifen®, Alkem Laboratories Ltd.)  
 tamoxifen citrate (Nolvadex,

		AstraZeneca; soltamox, EUSA Pharma Inc; tamoxifen citrate SOPHARMA, Sopharma JSCo.)
Glucocorticoids	Anti-inflammatory drugs used to reduce swelling that causes cancer pain.	prednisolone dexamethasone / Decadron® (Wyeth) prednisone (Deltasone, Orasone, Liquid Pred, Sterapred®)
Aromatase inhibitors	Includes imidazoles	ketoconazole
mTOR inhibitors	The mTOR signaling pathway was originally discovered during studies of the immunosuppressive agent rapamycin. This highly conserved pathway regulates cell proliferation and metabolism in response to environmental factors, linking cell growth factor receptor signaling via phosphoinositide-3-kinase (PI-3K) to cell growth, proliferation, and angiogenesis.	sirolimus (Rapamycin) /Rapamune® (Wyeth) Temsirolimus (CCI-779) / Torisel® (Wyeth) Deforolimus (AP23573) (Ariad Pharm.) Everolimus (RAD001) /Certican® (Novartis)
Chemotherapeutic agents		adriamycin, 5-fluorouracil, cytoxin, bleomycin, mitomycin C, daunomycin, carminomycin, aminopterin, dactinomycin, mitomycins, esperamicins, clofarabine, mercaptopurine, pentostatin, thioguanine, cytarabine, decitabine, floxuridine, gemcitabine (Gemzar), enocitabine,

	sapacitabine
Protein Kinase B (PKB) Inhibitors	<p>AKT Inhibitor Astex® (Astex Therapeutics)</p> <p>AKT Inhibitors NERVIANO (Nerviano Medical Sciences)</p> <p>AKT Kinase Inhibitor TELIK (Telik Inc)</p> <p>AKT DECIPHERA (Deciphera Pharmaceuticals, LLC)</p> <p>perifosine (KRX0401, D-21266; Keryx Biopharmaceuticals Inc, AEterna Zentaris Inc)</p> <p>perifosine with Docetaxel (Keryx Biopharmaceuticals Inc, AEterna Zentaris Inc)</p> <p>perifosine with Gemcitabine (AEterna Zentaris Inc)</p> <p>perifosine with paclitaxel (AEterna Zentaris Inc)</p> <p>protein kinase-B inhibitor DEVELOGEN (DeveloGen AG)</p> <p>PX316 (Oncothyreon, Inc.)</p> <p>RX0183 (Rexahn Pharmaceuticals Inc)</p> <p>RX0201 (Rexahn Pharmaceuticals Inc)</p> <p>VQD002 (VioQuest Pharmaceuticals Inc)</p> <p>XL418 (Exelixis Inc)</p> <p>ZEN027 (AEterna Zentaris Inc)</p>
Phosphatidylinositol 3-Kinase (PI3K) Inhibitors	<p>BEZ235 (Novartis AG)</p> <p>BGT226 (Novartis AG)</p> <p>CAL101 (Calistoga Pharmaceuticals, Inc.)</p> <p>CHR4432 (Chroma Therapeutics Ltd)</p> <p>Erk/PI3K Inhibitors ETERNA (AEterna Zentaris Inc)</p> <p>GDC0941 (Genentech Inc/Piramed Limited/Roche Holdings Ltd)</p> <p>enzastaurin HCL (LY317615; Enzastaurin; Eli Lilly)</p>

		LY294002/Wortmannin PI3K Inhibitors SEMAFORE (Semafore Pharmaceuticals) PX866 (Oncothyreon, Inc.) SF1126 (Semafore Pharmaceuticals) VMD-8000 (VM Discovery, Inc.) XL147 (Exelixis Inc) XL147 with XL647 (Exelixis Inc) XL765 (Exelixis Inc) PI-103 (Roche/Piramed)
Cyclin Dependent Kinase Inhibitors		CYC200, R-roscovitine (Seliciclib; Cyclacel Pharma) NSC-649890, L86-8275, HMR-1275 (alvocidib; NCI)
TLr9, CD289		IMOXine (Merck KGaA) HYB2055 (Idera) IMO-2055 (Isis Pharma) 1018 ISS (Dynavax Technologies/UCSF) PF-3512676 (Pfizer)
Enzyme Inhibitor		lonafarnib(SCH66336; Sarasar; SuperGen, U Arizona)
Anti-TRAIL		AMG-655 (Aeterna Zentaris, Keryx Biopharma) Apo2L/TRAIL, AMG951 (Genentech, Amgen) APOMAB (fully humanized mAb; Genentech)
MEK Inhibitors	[Mitogen-Activated Protein Kinase Kinase 1 (MAP2K1); Mitogen-Activated Protein Kinase Kinase 2 (MAP2K2)]	ARRY162 (Array BioPharma Inc) ARRY704 (Array BioPharma Inc) ARRY886 (Array BioPharma Inc) AS703026 (Merck Serono S.A) AZD6244 (AstraZeneca Plc) AZD8330 (AstraZeneca Plc)

Miscellaneous  
Inhibitors

RDEA119 (Ardea Biosciences, Inc.)  
RDEA436 (Ardea Biosciences, Inc.)  
XL518 (Exelixis Inc; Genentech Inc)

Imprime PGG (Biothera)  
CHR-2797 (AminopeptidaseM1 inhibitor;  
Chroma Therapeutics)  
E7820, NSC 719239 (Integrin-alpha2  
inhibitor, Eisai)  
INCB007839 (ADAM 17, TACE  
Inhibitor; Incyte)  
CNF2024,BIIB021 (Hsp90 Inhibitor;  
Biogen Idec)  
MP470, HPK-56 (Kit/Mel/Ret Inhibitor;  
Schering-Plough)  
SNDX-275/MS-275 (HDAC Inhibitor;  
Syndax)  
Zarnestra™ ,Tipifarnib, R115777 (Ras  
Inhibitor; Janssen Pharma)  
volociximab; Eos 200-4,M200 (alpha581  
integrin inhibitor; Biogen Idec; Eli  
Lilly/UCSF/PDL BioPharma)  
apricoxib (TP2001; COX-2 Inhibitor,  
Daiichi Sankyo; Tragara Pharma)

SEQUENCE LISTING SUMMARY

P1X V <sub>H</sub> CDR1	SYAIS	SEQ ID NO: 1
P1X V <sub>H</sub> CDR2	IPIFGTVNY	SEQ ID NO: 2
P1X V <sub>H</sub> CDR3	DPSVNL	SEQ ID NO: 3
P1X V <sub>L</sub> CDR1	QSISSWWA	SEQ ID NO: 4
P1X V <sub>L</sub> CDR2	DASSL	SEQ ID NO: 5
P1X V <sub>L</sub> CDR3	QQYHAHP	SEQ ID NO: 6
P2X V <sub>H</sub> CDR1	SYAIS	SEQ ID NO: 7
P2X V <sub>H</sub> CDR2	IPIFGAANP	SEQ ID NO: 8
P2X V <sub>H</sub> CDR3	MGRGKV	SEQ ID NO: 9
P2X V <sub>L</sub> CDR1	QSVLYSPNNKNYLA	SEQ ID NO: 10
P2X V <sub>L</sub> CDR2	WASTR	SEQ ID NO: 11
P2X V <sub>L</sub> CDR3	QQYYGSP	SEQ ID NO: 12
P3X V <sub>H</sub> CDR1	SYGIN	SEQ ID NO: 13
P3X V <sub>H</sub> CDR2	ISAYNGNTYY	SEQ ID NO: 14
P3X V <sub>H</sub> CDR3	DLGGYGS	SEQ ID NO: 15
P3X V <sub>L</sub> CDR1	QSVSSNLA	SEQ ID NO: 16
P3X V <sub>L</sub> CDR2	GASTR	SEQ ID NO: 17
P3X V <sub>L</sub> CDR3	QDYRTWPR	SEQ ID NO: 18
P1X V <sub>H</sub>	MGFGLSWLFLVAILKGVQC QVQLVQSGAEVKKPGSSVKV SCKASGGTFSSYAISWVRQA PGQGLEWMGSIPIFGTVNY AQKFQGRVTITADESTSTAY MELSSLRSEDVAVYYCARDP SVNLYWYFDLWGRGTLVTVSS	SEQ ID NO: 19
P1X V <sub>L</sub>	MGTPAQLLFLLLLWLPDTTG DIQMTQSPSTLSASVGRVT ITCRASQSISSWWAWYQQK GKAPKLLIYDASSLESGVPS RFSGSGSGTEFTLTISSLP DDFATYYCQQYHAHPTTFGG GTKVEIK	SEQ ID NO: 20
P2X V <sub>H</sub>	MGFGLSWLFLVAILKGVQC QVQLVQSGAEVKKPGSSVKV SCKASGGTFSSYAISWVRQA PGQGLEWMGSIPIFGAANP AQKSQGRVTITADESTSTAY MELSSLRSEDVAVYYCAKMG	SEQ ID NO: 21

	RGKVAFDIWGQGTMVTVSS	
P2X V <sub>L</sub>	MGTPAQLLFLLLLWLPDTTG DIVMTQSPDSLAVSLGERAT INCKSSQSVLYSPNNKNYLA WYQQKPGQPPKLLIYWASTR ESGVPDRFSGSGSGTDFLT ISSLQAEDVAVYYCQQYYGS PITFGGGTKVEIK	SEQ ID NO: 22
P3X V <sub>H</sub>	MGFGLSWLFLVAILKGVQC QVQLVQSGAEVKKPGASVKV SCKASGYAFTSYGINWVRQA PGQGLEWMGWISAYNGNTYY AQKLRGRVTMTTDTSTSTAY MELRSLRSDDTAVYYCARDL GGYGSGSVFPDPWGQGLVTVSS	SEQ ID NO: 23
P3X V <sub>L</sub>	MGTPAQLLFLLLLWLPDTTG EIVMTQSPATLSVSPGERAT LSCRASQSVSSNLAWYQQKP GQAPRLLIYGASTRATGIPA RFSGSGSGTEFTLTISLQS EDFAVYYCQDYRTWPRRVFG GGTKVEIK	SEQ ID NO: 24
pMP10K_IgG1 Light Chain Kappa-Constant	RTVAAPSVFIFPPSDEQLKS GTASVCLLNFPYFREAKVQ WKVDNALQSGNSQESVTEQD SKDSTYLSSTLTLSKADYE KHKVYACEVTHQGLSSPVTK SFNRGEC	SEQ ID NO: 25
pMP10K_IgG1 Heavy Chain (EEM)_Constant	ASTKGPSVFPLAPSSKSTSG GTAALGCLVKDYFPEPVTVS WNSGALTSGVHTFPAVLQSS GLYSLSSVVTVPSSSLGTQT YICNVNHKPSNTKVDKKVEP KSCDKTHTCPPCPAPELLGG PSVFLFPPKPKDTLMIS RTP EVTCCVVVDVSHEDPEVKFNW YVDGVEVHNAKTKPREEQYN STYRVVSVLTVLHQDWLNGK EYKCKVSNKALPAPIEKTIS KAKGQPREPQVYTLPPSREE MTKNQVSLTCLVKGFYPSDI	SEQ ID NO: 26



	AVEWESNGQPENNYKTTTPPV LDS DG SFFLYSKLTVDKSRW QQGNVFSCSVMHEALHNHYT QKSLSLSPGK	
ca/cd V <sub>H</sub> CDR2	IIPIFGTANY	SEQ ID NO: 27
ca V <sub>H</sub> CDR3	DPSVDL	SEQ ID NO: 28
ca V <sub>L</sub> CDR1	QSISSWLA	SEQ ID NO: 29
ca V <sub>L</sub> CDR3	QQFAAHA	SEQ ID NO: 30
cd V <sub>L</sub> CDR1	QSVLYSSNNKNYLA	SEQ ID NO: 31
ch V <sub>H</sub> CDR2	ISAYNGNTNY	SEQ ID NO: 32

EGFR ECD (SEQ ID NO: 33)

1 MRPSGTAGAA LLALLAALCP ASRALEEKV CQGTSNKLTQ LGTFEDHFLS LQRMFNNCEV  
 61 VLG NLEITYV QRNYDLSFLK TIQEVAGYVL IALNTVERIP LENLQIIRGN MYYENSYALA  
 5 121 VLSNYDANKT GLKELPMRNL QEILHGAVRF SNNPALCNVE SIQWRDIVSS DFLSNMSMDF  
 181 QNHLGSCQKC DPSCPNGSCW GAGEENCQKL TKIICAQQCS GRCRGKSPSD CCHNQCAAGC  
 241 TGPRESDECLV CRKFRDEATC KDTCPLMLY NPTTYQMDVN PEGKYSEFGAT CVKKCPRNYV  
 301 VTDHGSCVRA CGADSYEMEE DGVRKCKKCE GPCRKVCNGI GIGEFKDSLS INATNIKHFK  
 361 NCTSI SGDLH ILPVAFRGDS FTHTPPLDPQ ELDILKTVKE ITGFLLIQAW PENRTDLHAF  
 10 421 ENLEIIRGRT KQHGFSLAV VSLNITSLGL RSLKEISDGD VIISGNKNLC YANTINWKKL  
 481 FGTSGQKTKI ISNRGENSCK ATGQVCHALC SPEGCWGPEP RDCVSCRNVS RGRECVDKCN  
 541 LLEGEPPREFV ENSECIQCHP ECLPQAMNIT CTGRGPDNCI QCAHYIDGPH CVKTCPAGVM  
 601 GENNTLVWKY ADAGHVCHLC HPNCTYGCTG PGLEGCP TNG PKIPSHHHHH H

15

What is claimed is:

1. A monoclonal antibody which binds EGFR extracellular domain and  
5 comprises heavy and light chain CDR1, CDR2, and CDR3 sequences, wherein the  
heavy and light chain CDR1, CDR2, and CDR3 sequences are selected from the group  
consisting of:
  - (a) heavy chain CDR1, CDR2, and CDR3 sequences of SEQ ID NOs: 1, 2, and 3  
respectively, and light chain CDR1, CDR2, and CDR3 sequences of SEQ ID NOs: 4, 5,  
10 and 6, respectively;
  - (b) heavy chain CDR1, CDR2, and CDR3 sequences of SEQ ID NOs: 7, 8, and  
9, respectively, and light chain CDR1, CDR2, and CDR3 sequences of SEQ ID NOs: 10,  
11 and 12, respectively; and
  - (c) heavy chain CDR1, CDR2, and CDR3 sequences of SEQ ID NOs: 13, 14,  
15 and 15, respectively, and light chain CDR1, CDR2, and CDR3 sequences of SEQ ID  
NOs: 16, 17, and 18, respectively.
  
2. A monoclonal antibody that binds to EGFR extracellular domain and  
comprises a heavy chain variable region and a light chain variable region, wherein the  
20 heavy and light chain variable region sequences are selected from the group consisting  
of:
  - (a) a heavy chain variable region comprising SEQ ID NO: 19 and a light chain  
variable region comprising SEQ ID NO: 20;
  - (b) a heavy chain variable region comprising SEQ ID NO: 21 and a light chain  
25 variable region comprising SEQ ID NO: 22; and
  - (c) a heavy chain variable region comprising SEQ ID NO: 23 and a light chain  
variable region comprising SEQ ID NO: 24.
  
3. The monoclonal antibody of claim 1 or 2, which binds to EGFR with a  $K_D$  of  
30 better than 100 nM.
  
4. The monoclonal antibody of claim 3, which binds to EGFR with a  $K_D$  of better  
than 10 nM.

5. The monoclonal antibody of claim 3, which binds to EGFR with a  $K_D$  of better than 1 nM.
- 5 6. The monoclonal antibody of claim 1 or 2, which is a human antibody.
7. The monoclonal antibody of claim 1 or 2, wherein the antibody is selected from the group consisting of a bispecific antibody, immunoconjugate, Fab, Fab'2, ScFv, avimer, nanobody and a domain antibody.
- 10 8. The monoclonal antibody of claim 1 or 2, wherein the monoclonal antibody is selected from the group consisting of IgG1, IgG2, IgG3, IgG4, IgM, IgA1, IgA2, IgAsec, IgD and IgE isotype antibodies.
- 15 9. A pharmaceutical composition comprising the monoclonal antibody of claim 1 or 2 and a pharmaceutically acceptable carrier.
10. A kit comprising the pharmaceutical composition of claim 9 in a container.
- 20 11. A method of treating cancer in a subject, comprising administering to the subject an effective amount of the pharmaceutical composition of claim 9.
12. The monoclonal antibody of claim 1 or 2 for the treatment of a cancer.
- 25 13. A composition comprising two or three monoclonal antibodies which bind to EGFR extracellular domain, wherein the two or three monoclonal antibodies are selected from the group consisting of:
- (a) a monoclonal antibody comprising heavy chain CDR1, CDR2, and CDR3 sequences of SEQ ID NOs: 1, 2, and 3 respectively, and light chain CDR1, CDR2, and
- 30 CDR3 sequences of SEQ ID NOs: 4, 5, and 6, respectively;
- (b) a monoclonal antibody comprising heavy chain CDR1, CDR2, and CDR3 sequences of SEQ ID NOs: 7, 8, and 9, respectively, and light chain CDR1, CDR2, and CDR3 sequences of SEQ ID NOs: 10, 11 and 12, respectively and

(c) a monoclonal antibody comprising heavy chain CDR1, CDR2, and CDR3 sequences of SEQ ID NOs: 13, 14, and 15, respectively, and light chain CDR1, CDR2, and CDR3 sequences of SEQ ID NOs: 16, 17 and 18, respectively; and wherein the composition comprises (a) and (b), (a) and (c), (b) and (c) or (a), (b) and  
5 (c).

14. A composition comprising two or three monoclonal antibodies which bind to EGFR extracellular domain, wherein the two or three monoclonal antibodies are selected from the group consisting of:

10 (a) a monoclonal antibody comprising a heavy chain variable region comprising SEQ ID NO: 19 and a light chain variable region comprising SEQ ID NO: 20;

(b) a monoclonal antibody comprising a heavy chain variable region comprising SEQ ID NO: 21 and a light chain variable region comprising SEQ ID NO: 22; and

(c) a monoclonal antibody comprising a heavy chain variable region comprising  
15 SEQ ID NO: 23 and a light chain variable region comprising SEQ ID NO: 24;

and wherein the composition comprises (a) and (b), (a) and (c), (b) and (c) or (a) (b) and (c).

15. The composition of claim 13 or 14, wherein each of monoclonal antibodies (a),  
20 (b) and (c) binds to EGFR with a  $K_D$  of better than 100 nM.

16. The composition of claim 15, wherein each of monoclonal antibodies (a), (b) and (c) binds to EGFR with a  $K_D$  of better than 10 nM.

25 17. The composition of claim 15, wherein each of monoclonal antibodies (a), (b) and (c) binds to EGFR with a  $K_D$  of better than 1nM.

18. The composition of claim 13 or 14, wherein each of monoclonal antibodies (a), (b) and (c) is a human antibody.  
30

19. The composition of claim 13 or 14, wherein one or more of monoclonal antibodies (a), (b), and (c) is independently selected from the group consisting of a

bispecific antibody, immunoconjugate, Fab, Fab'2, ScFv, avimer, nanobody and a domain antibody.

20. The composition of claim 13 or 14, wherein each of monoclonal antibodies (a),  
5 (b), and (c) is independently selected from the group consisting of IgG1, IgG2, IgG3, IgG4, IgM, IgA1, IgA2, IgAsec, IgD and IgE isotype antibodies.

21. The composition of claim 13 or 14, which further comprises a pharmaceutically acceptable carrier.

10

22. A kit comprising the composition of claim 21 in a container.

23. A method of treating cancer in a subject, comprising administering to the subject an effective amount of the composition of claim 21.

15

24. The composition of claim 13 or 14 for the treatment of a cancer.

25. A composition comprising three monoclonal anti-EGFR antibodies, said composition comprising a first antibody, a second antibody and a third antibody,  
20 wherein (i) the first antibody comprises heavy chain CDR1, CDR2, and CDR3 sequences of SEQ ID NOs: 1, 2, and 3 respectively, and light chain CDR1, CDR2, and CDR3 sequences of SEQ ID NOs: 4, 5, and 6, respectively; (ii) the second antibody comprises heavy chain CDR1, CDR2, and CDR3 sequences of SEQ ID NOs: 7, 8, and 9, respectively, and light chain CDR1, CDR2, and CDR3 sequences of SEQ ID NOs: 10,  
25 11 and 12, respectively; and (iii) the third antibody comprises heavy chain CDR1, CDR2, and CDR3 sequences of SEQ ID NOs: 13, 14, and 15 respectively, and light chain CDR1, CDR2, and CDR3 sequences of SEQ ID NOs: 16, 17, and 18, respectively, and wherein the first second and third antibodies are present at a molar ratio of 2:2:1 to each other.

30

26. A composition comprising three monoclonal anti-EGFR antibodies, said composition comprising a first antibody, a second antibody and a third antibody, wherein (i) the first antibody comprises a heavy chain variable region comprising SEQ

ID NO: 19 and a light chain variable region comprising SEQ ID NO: 20; (ii) the second antibody comprises a heavy chain variable region comprising SEQ ID NO: 21 and a light chain variable region comprising SEQ ID NO: 22; and (iii) the third antibody comprises a heavy chain variable region comprising SEQ ID NO: 23 and a light chain variable region comprising SEQ ID NO: 24, and wherein the first second and third antibodies are present at a molar ratio of 2:2:1 to each other.

27. The composition of claim 25 or 26, wherein each of the first antibody, the second antibody and the third antibody binds to EGFR with a  $K_D$  of better than 100 nM.

10

28. The composition of claim 27, wherein each of the first antibody, the second antibody and the third antibody binds to EGFR with a  $K_D$  of better than 10 nM.

29. The composition of claim 27, wherein each of the first antibody, the second antibody and the third antibody binds to EGFR with a  $K_D$  of better than 1nM.

15

30. The composition of claim 25 or 26, wherein the first antibody binds to EGFR with a  $K_D$  in a range of  $1 \times 10^{-9}$  M to  $1.1 \times 10^{-11}$  M, the second antibody binds to EGFR with a  $K_D$  in a range of  $1 \times 10^{-9}$  M to  $7.0 \times 10^{-11}$  M and the third antibody binds to EGFR with a  $K_D$  in a range of  $1 \times 10^{-9}$  M to  $3.6 \times 10^{-10}$  M.

20

31. The composition of claim 25 or 26, wherein each of the first antibody, the second antibody and the third antibody are human antibodies.

25 32. The composition of claim 25 or 26, wherein one or more of the first antibody, the second antibody and the third antibody are independently selected from the group consisting of a bispecific antibody, immunoconjugate, Fab, Fab'2, ScFv, avimer, nanobody and a domain antibody.

30 33. The composition of claim 25 or 26, wherein each of the first antibody, the second antibody and the third antibody is independently selected from the group consisting of IgG1, IgG2, IgG3, IgG4, IgM, IgA1, IgA2, IgAsec, IgD and IgE isotype antibodies

34. The composition of claim 25 or 26, which further comprises a pharmaceutically acceptable carrier.
35. The composition of claim 34, which is a sterile composition.
- 5 36. The composition of claim 34, which is suitable for injection.
37. The composition of claim 34, which is a sterile composition suitable for intravenous injection.
- 10 38. A kit comprising the composition of claim 34 in a container.
39. A method of treating cancer in a subject, comprising administering to the subject an effective amount of the composition of claim 34.
- 15 40. the composition of claim 25 or 26 for the treatment of a cancer.
41. A method of preparing an anti-EGFR antibody composition, the method comprising combining in a single composition:
- 20 (a) a monoclonal antibody comprising heavy chain CDR1, CDR2, and CDR3 sequences of SEQ ID NOs: 1, 2, and 3 respectively, and light chain CDR1, CDR2, and CDR3 sequences of SEQ ID NOs: 4, 5, and 6, respectively;
- (b) a monoclonal antibody comprising heavy chain CDR1, CDR2, and CDR3 sequences of SEQ ID NOs: 7, 8, and 9, respectively, and light chain CDR1, CDR2, and
- 25 CDR3 sequences of SEQ ID NOs: 10, 11 and 12, respectively; and
- (c) a monoclonal antibody comprising heavy chain CDR1, CDR2, and CDR3 sequences of SEQ ID NOs: 13, 14, and 15 respectively, and light chain CDR1, CDR2, and CDR3 sequences of SEQ ID NOs: 16, 17, and 18, respectively;
- wherein (a), (b) and (c) are combined at a molar ratio of 2:2:1 to each other.
- 30 42. A method of preparing an anti-EGFR antibody composition, the method comprising combining in a single composition:

(a) a monoclonal antibody comprising a heavy chain variable region comprising SEQ ID NO: 19 and a light chain variable region comprising SEQ ID NO:20;

(b) a monoclonal antibody comprising a heavy chain variable region comprising SEQ ID NO: 21 and a light chain variable region comprising SEQ ID NO: 22; and

5 (c) a monoclonal antibody comprising a heavy chain variable region comprising SEQ ID NO: 23 and a light chain variable region comprising SEQ ID NO: 24;

wherein (a), (b) and (c) are combined at a molar ratio of 2:2:1 to each other.

43. A method of treating a subject with anti-EGFR antibodies, the method  
10 comprising administering to the subject:

(a) a monoclonal antibody comprising heavy chain CDR1, CDR2, and CDR3 sequences of SEQ ID NOs: 1, 2, and 3 respectively, and light chain CDR1, CDR2, and CDR3 sequences of SEQ ID NOs: 4, 5, and 6, respectively;

(b) a monoclonal antibody comprising heavy chain CDR1, CDR2, and CDR3  
15 sequences of SEQ ID NOs: 7, 8, and 9, respectively, and light chain CDR1, CDR2, and CDR3 sequences of SEQ ID NOs: 10, 11 and 12, respectively; and

(c) a monoclonal antibody comprising heavy chain CDR1, CDR2, and CDR3 sequences of SEQ ID NOs: 13, 14, and 15 respectively, and light chain CDR1, CDR2, and CDR3 sequences of SEQ ID NOs: 16, 17, and 18, respectively;

20 wherein (a), (b) and (c) are administered to the subject at a molar ratio of 2:2:1 to each other.

44. A method of treating a subject with anti-EGFR antibodies, the method  
comprising administering to the subject:

25 (a) a monoclonal antibody comprising a heavy chain variable region comprising SEQ ID NO: 19 and a light chain variable region comprising SEQ ID NO:20;

(b) a monoclonal antibody comprising a heavy chain variable region comprising SEQ ID NO: 21 and a light chain variable region comprising SEQ ID NO: 22; and

(c) a monoclonal antibody comprising a heavy chain variable region comprising  
30 SEQ ID NO: 23 and a light chain variable region comprising SEQ ID NO: 24;

wherein (a), (b) and (c) are administered to the subject at a molar ratio of 2:2:1 to each other.



1/33

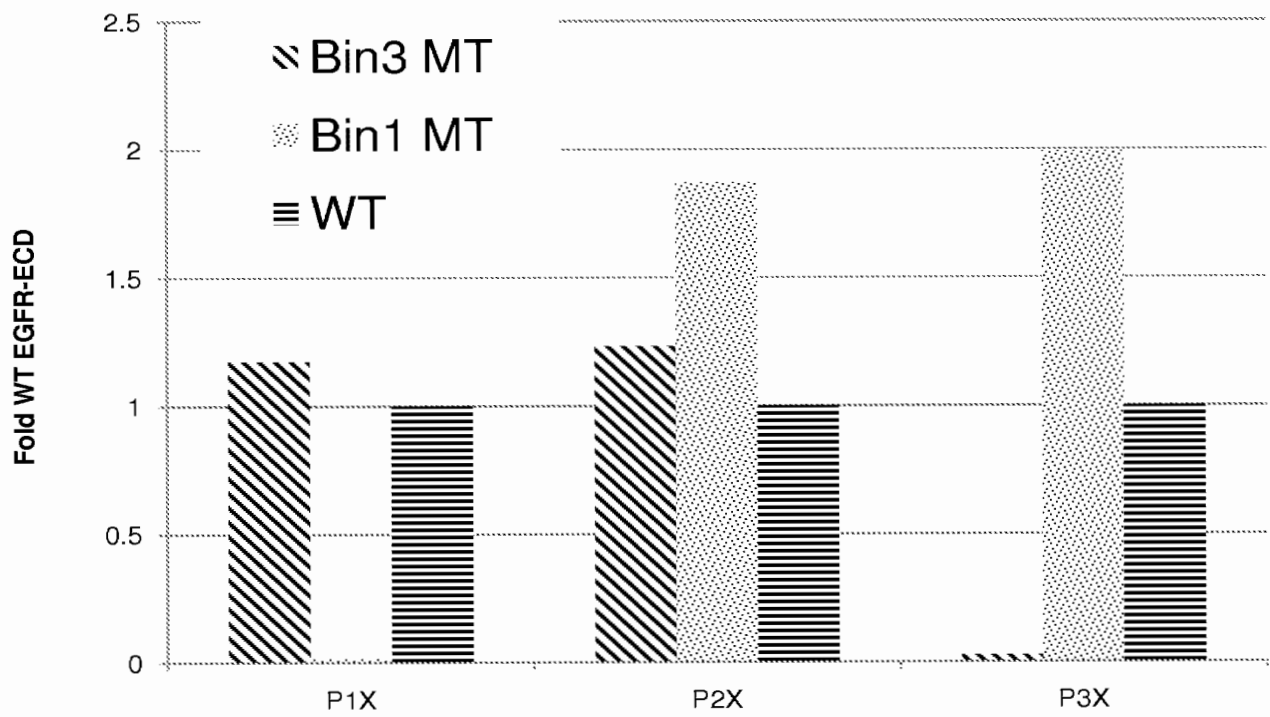


**Fig. 1A**

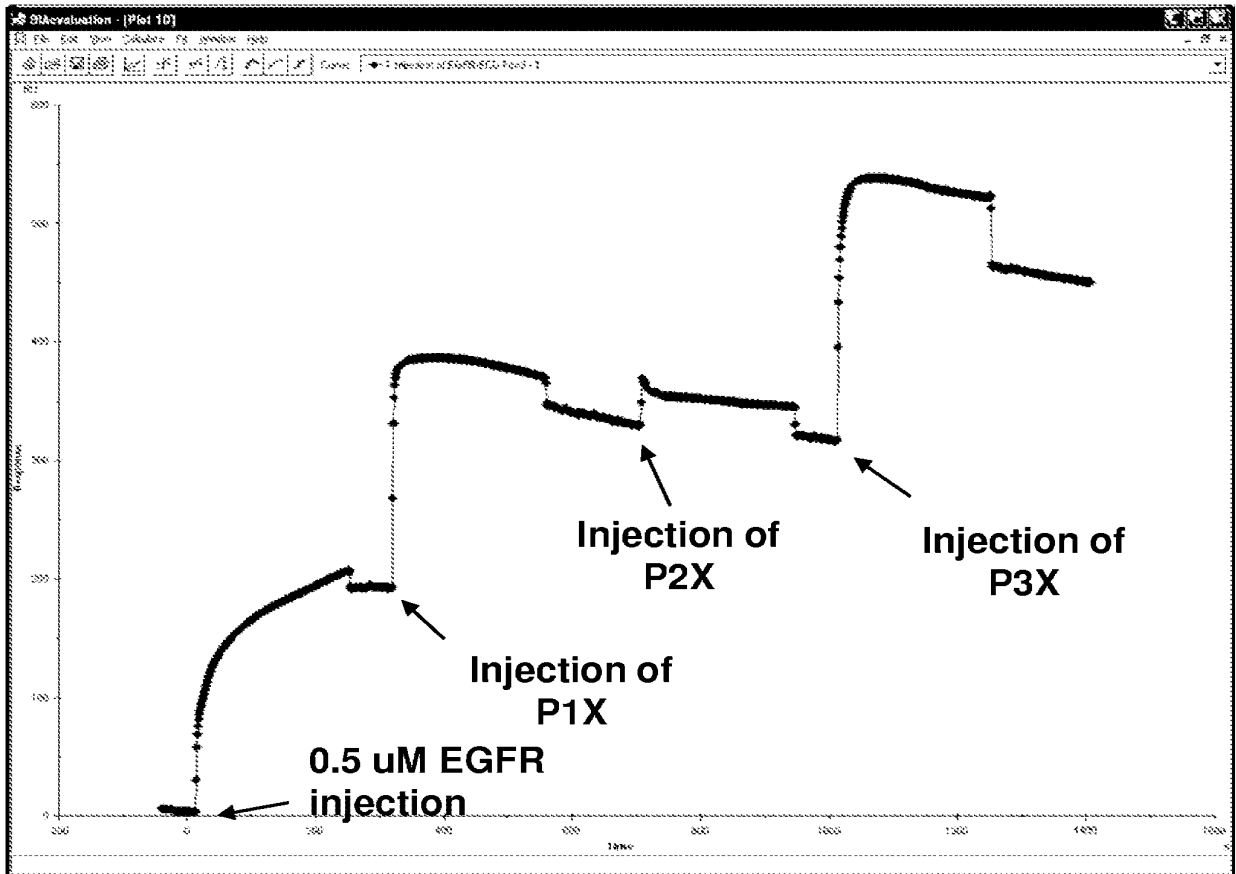


**Fig. 1B**

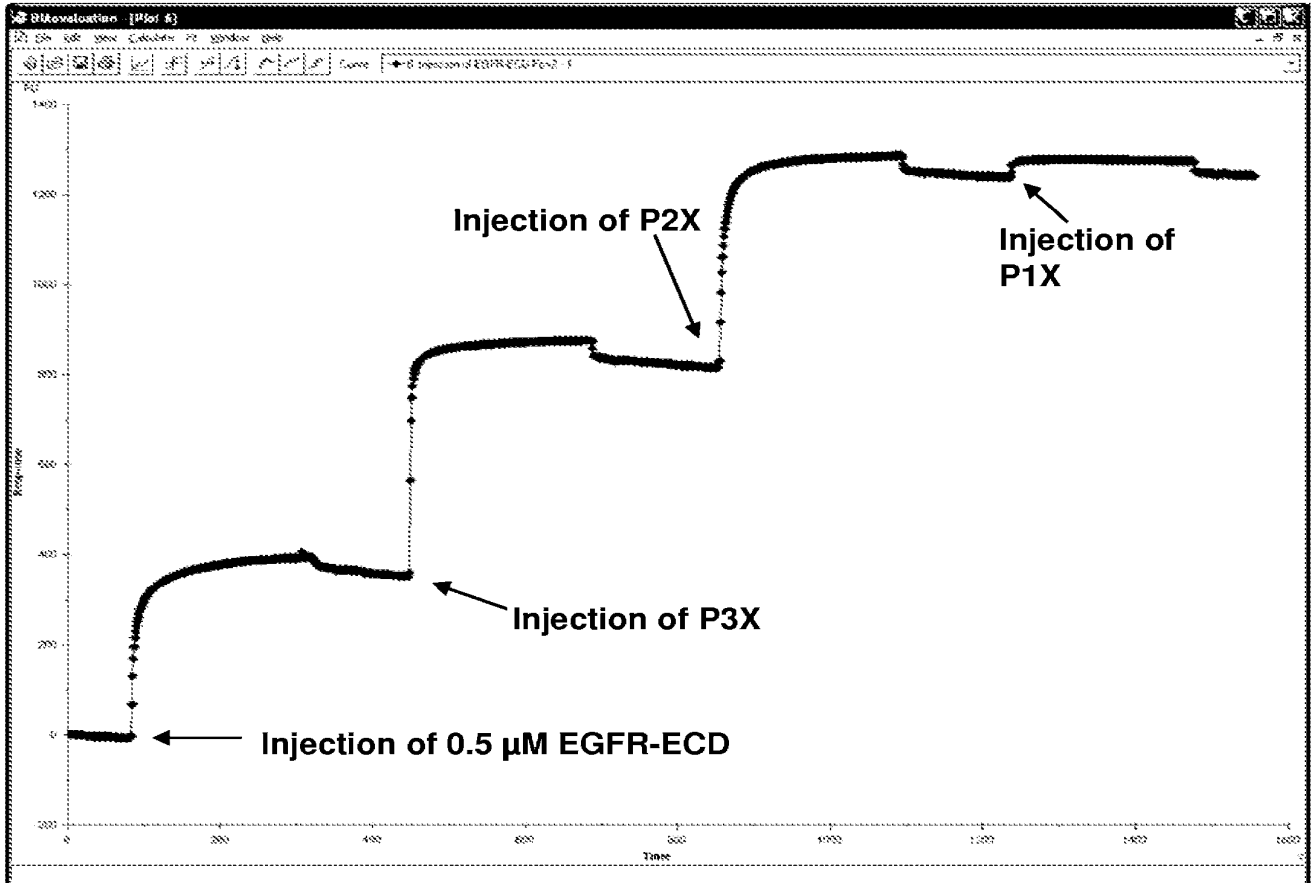


**Fig. 2A**

4/33

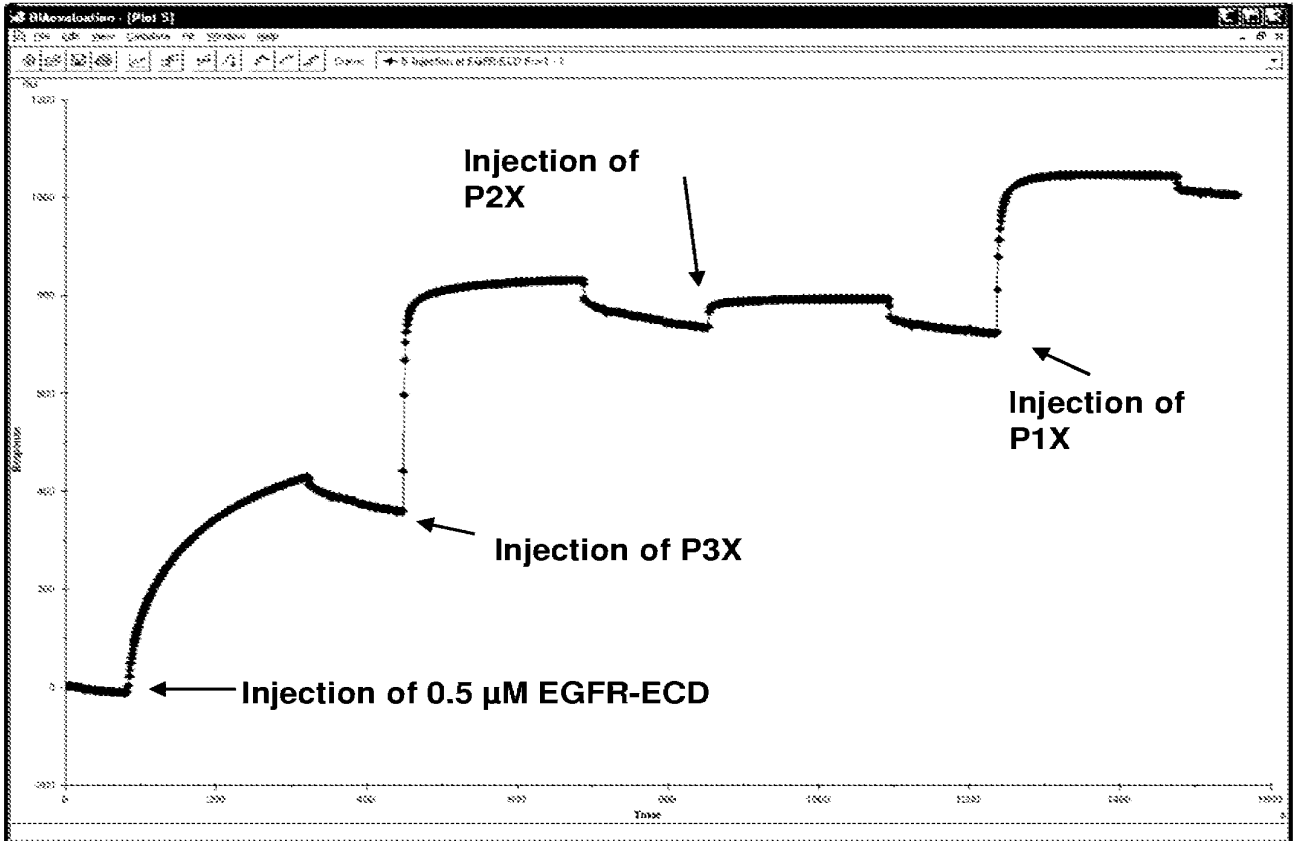


**Fig. 2B**

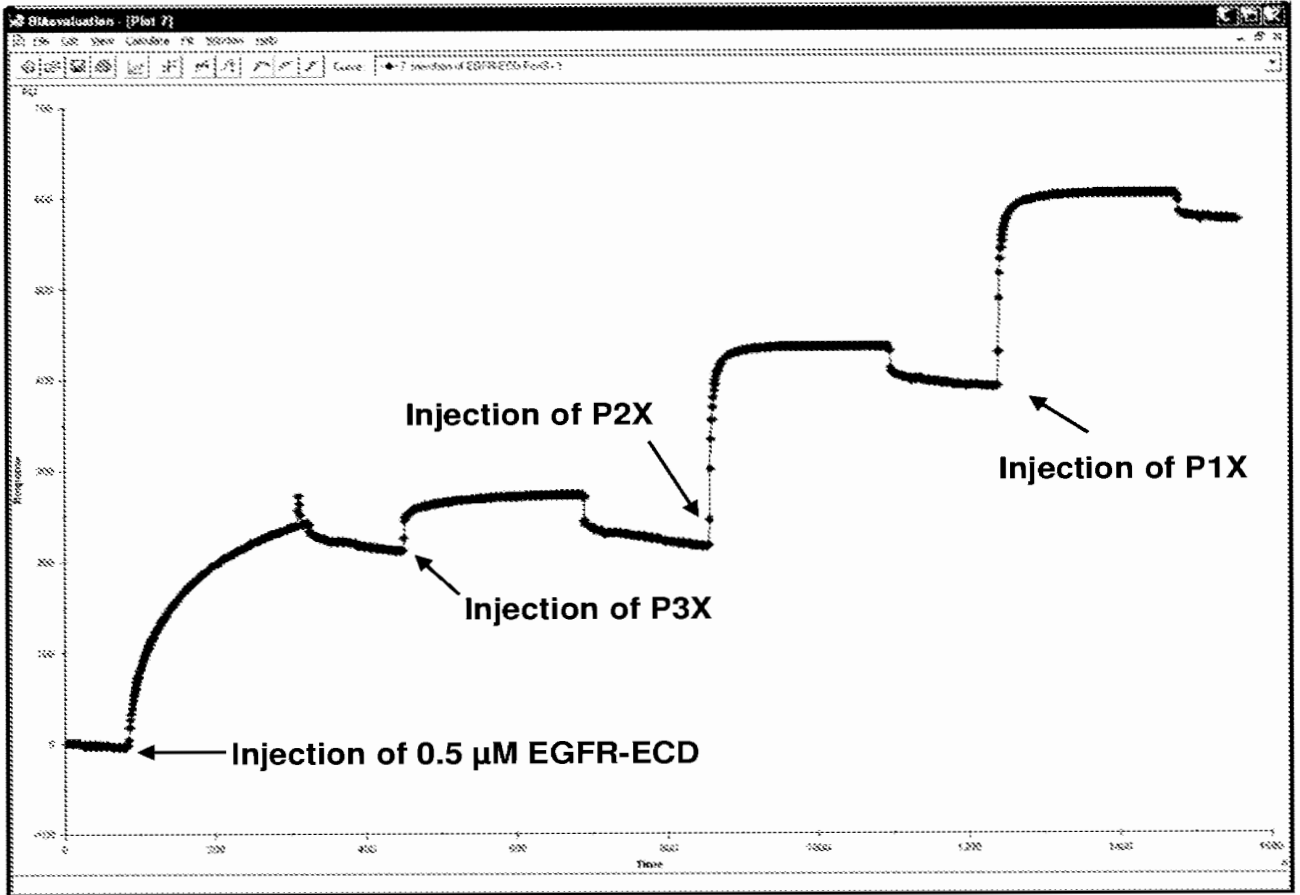


**Fig. 2C**

6/33

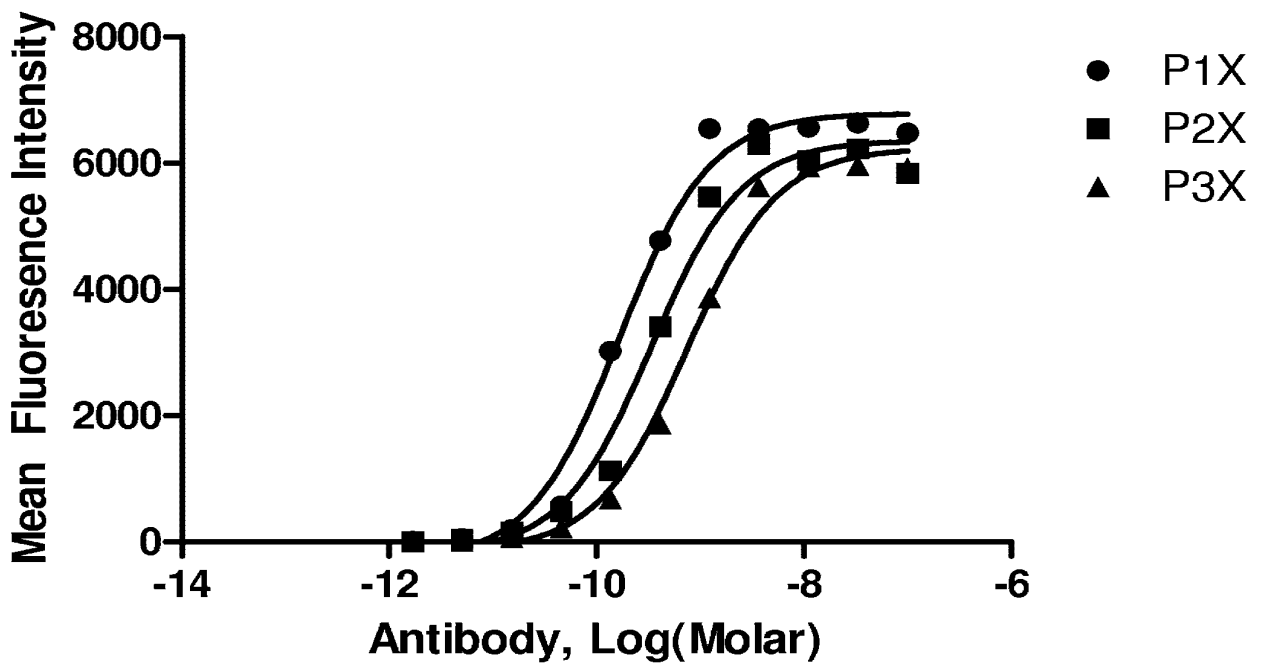


*Fig. 3*

7/33

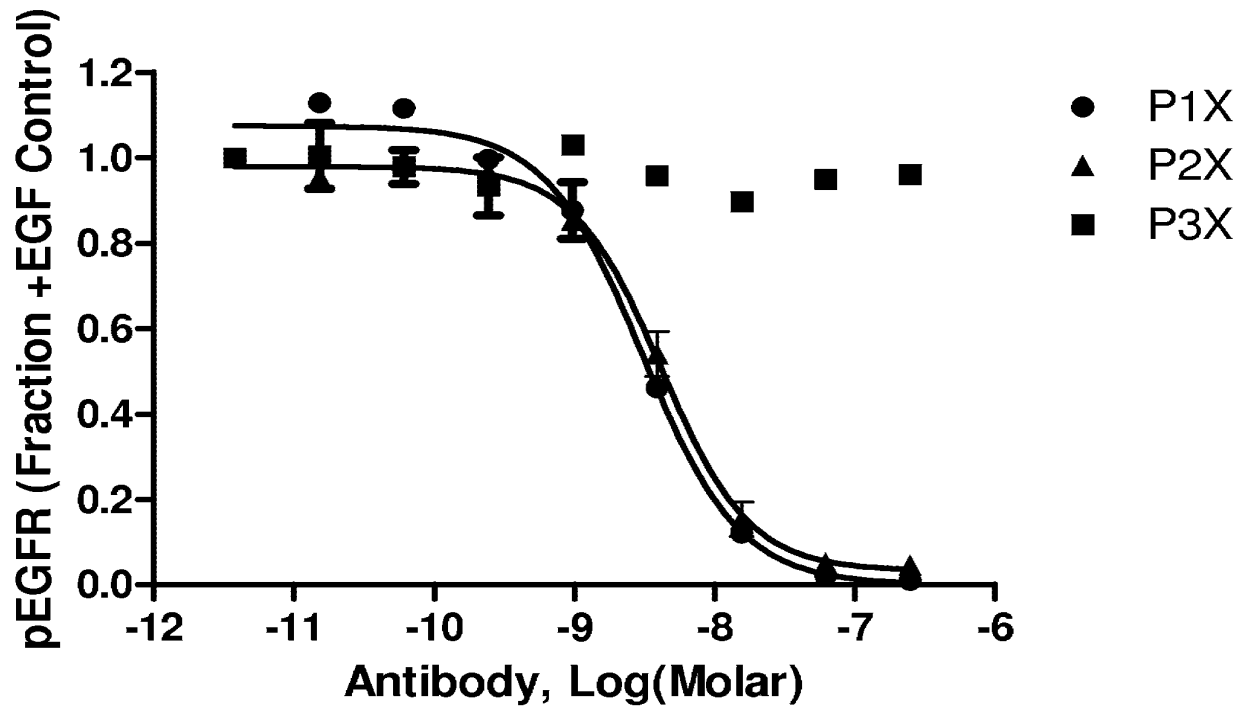
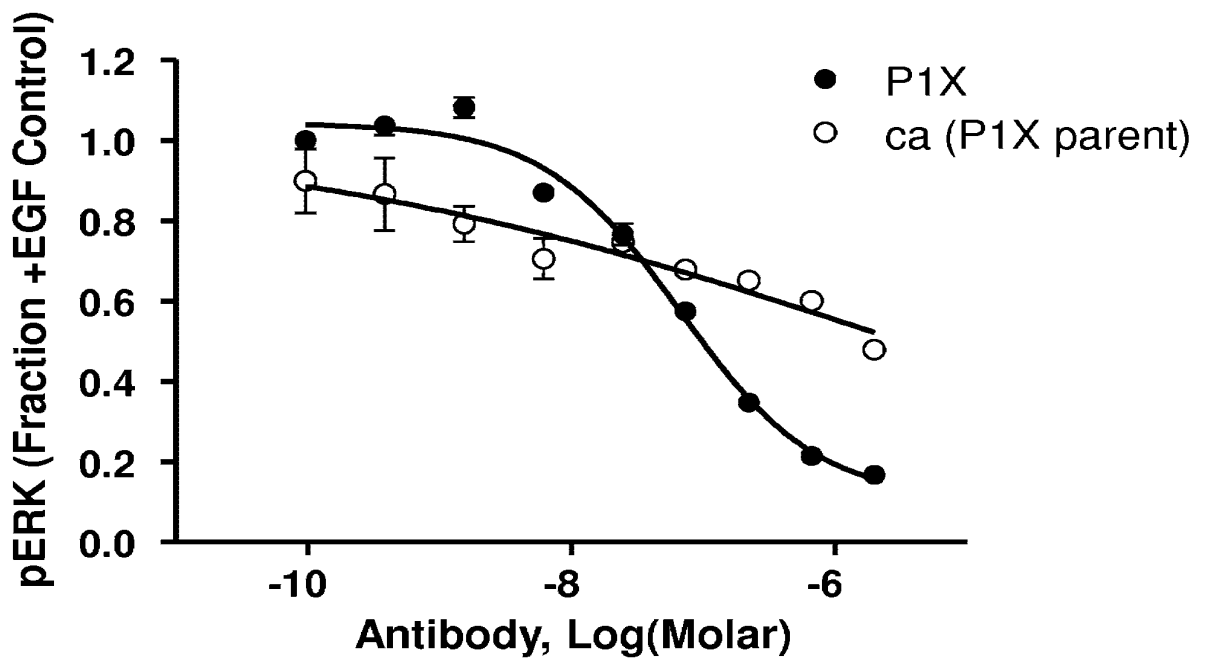


Fig. 4

8/33



**Fig. 5A**



9/33

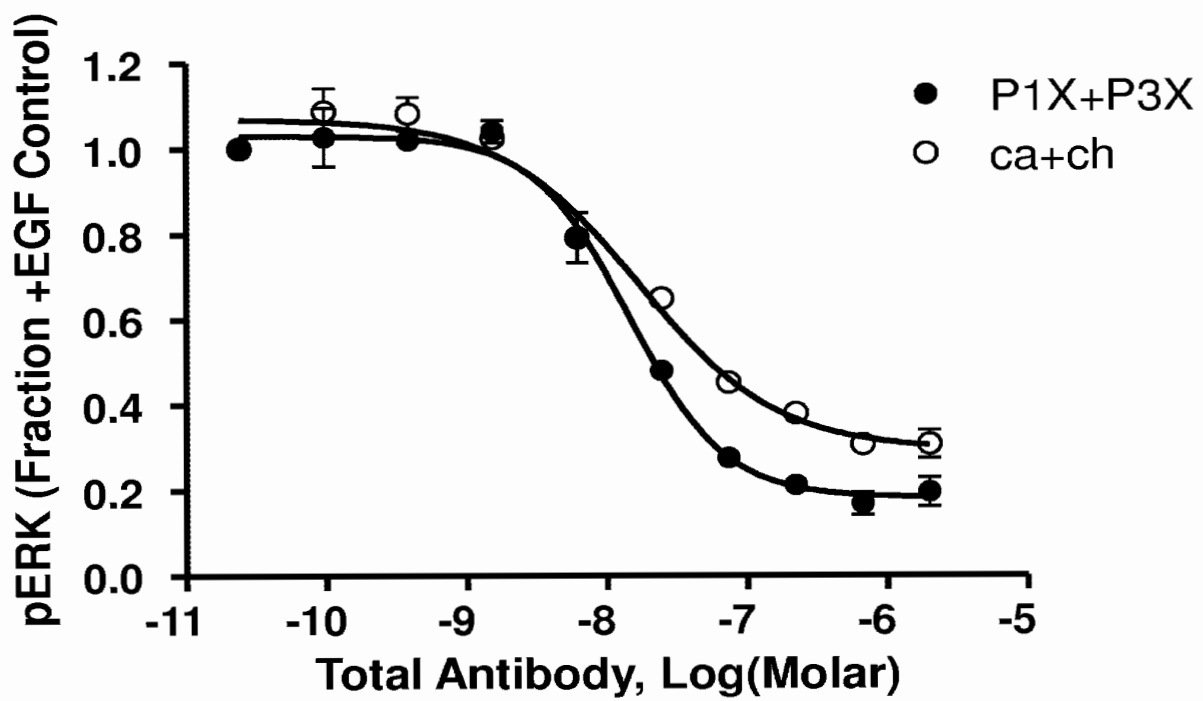


**Fig. 5B**

10/33

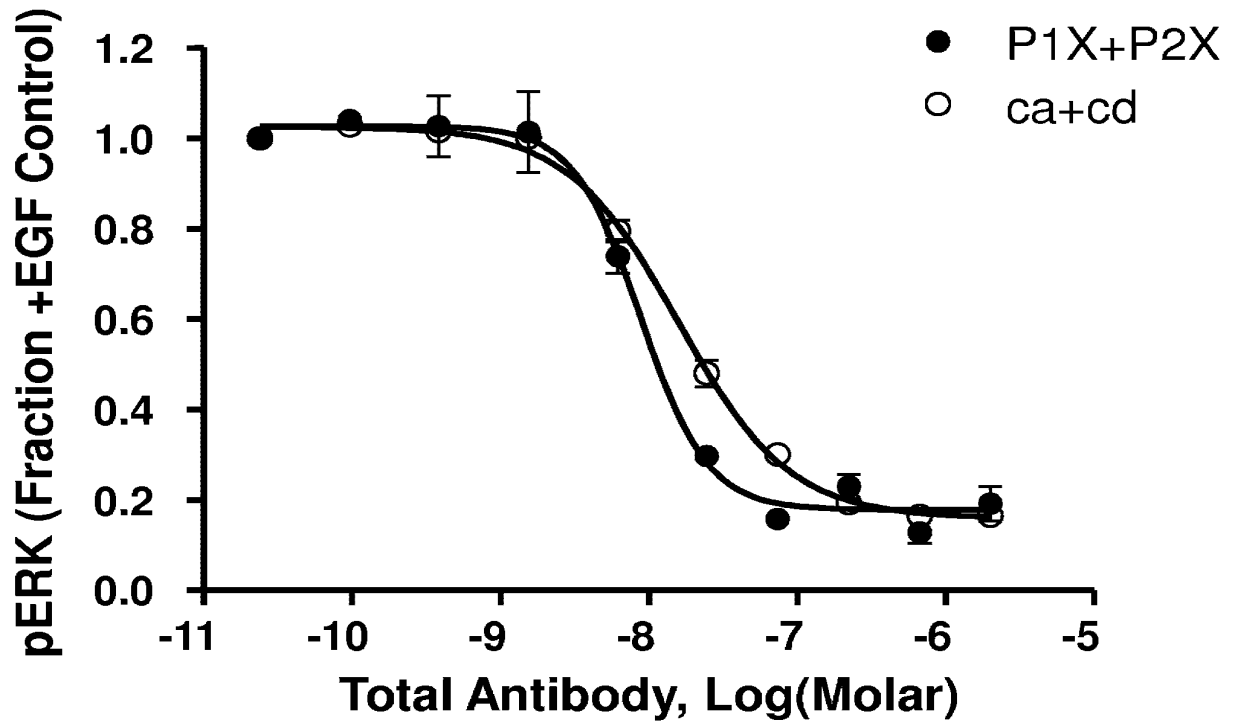


*Fig. 5C*

11/33

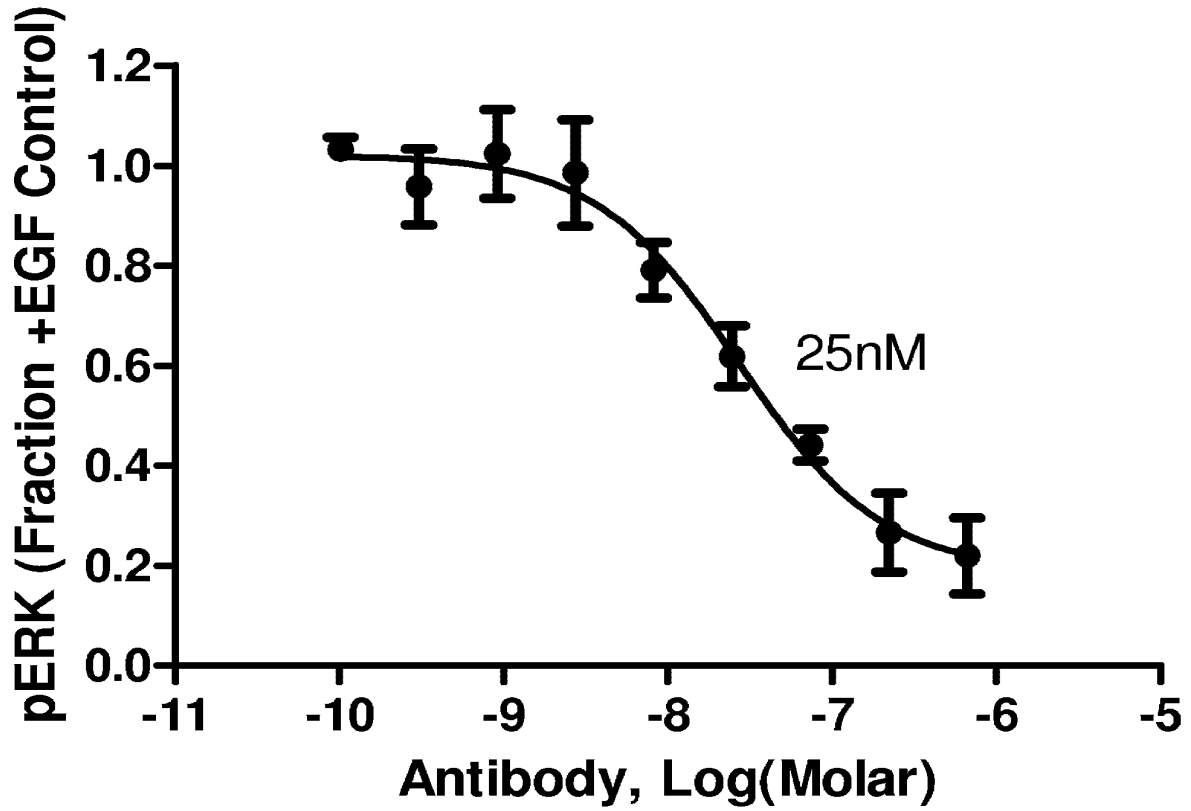


*Fig. 6A*

12/33

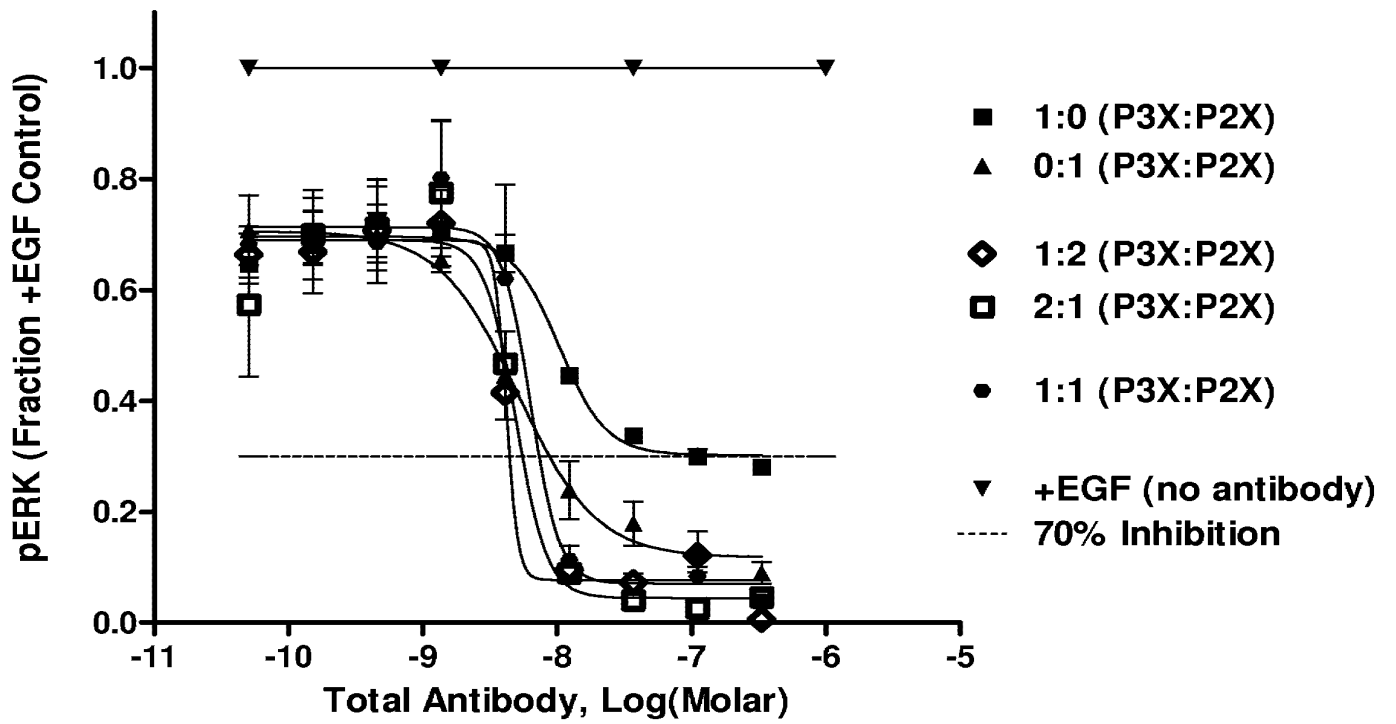


**Fig. 6B**

13/33

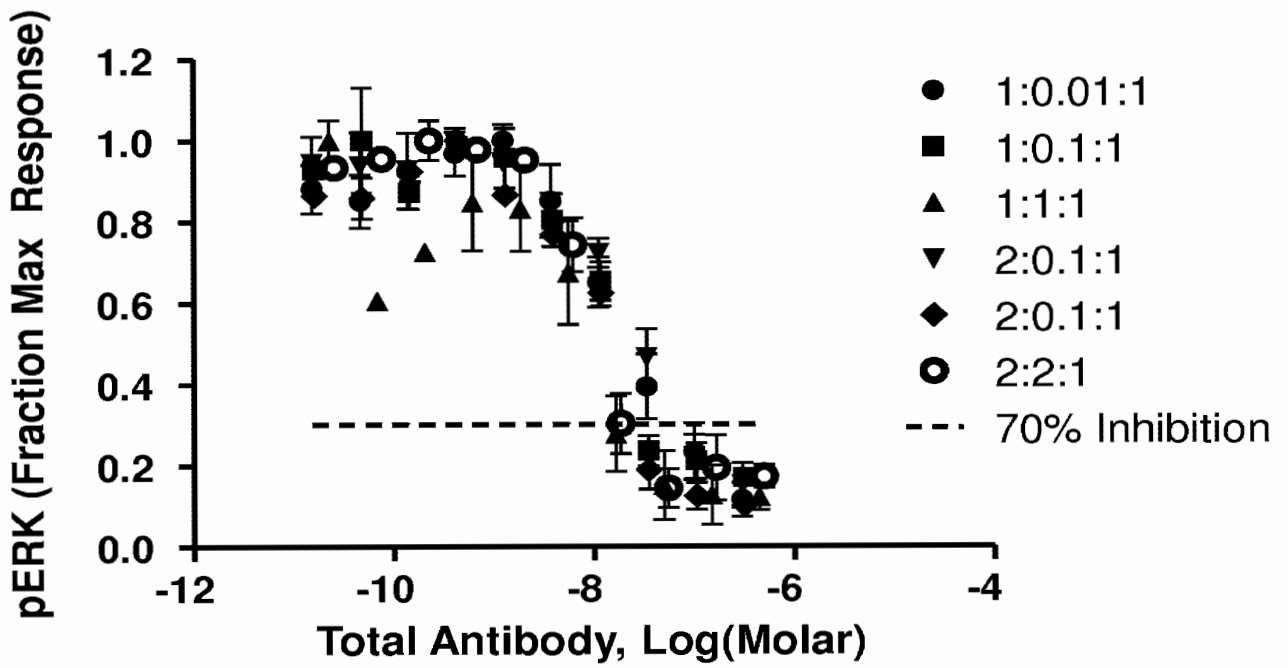


Fig. 6C

14/33

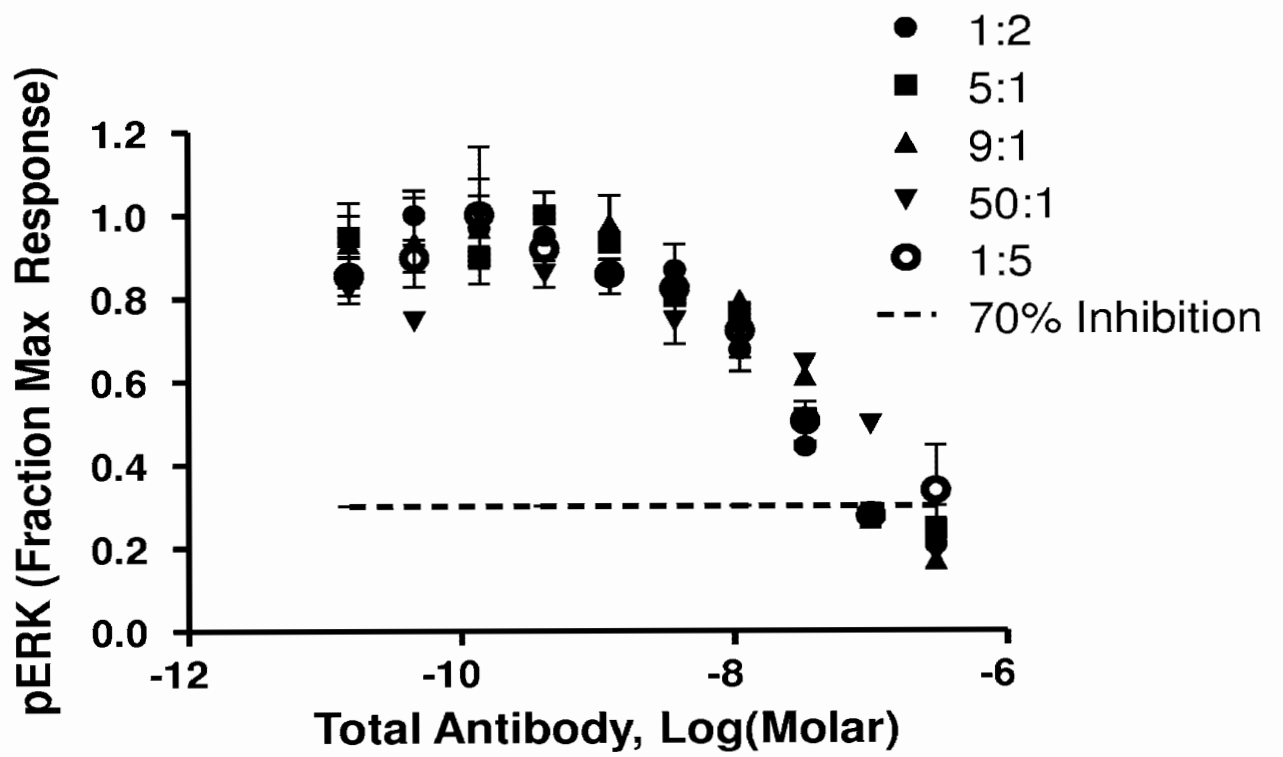
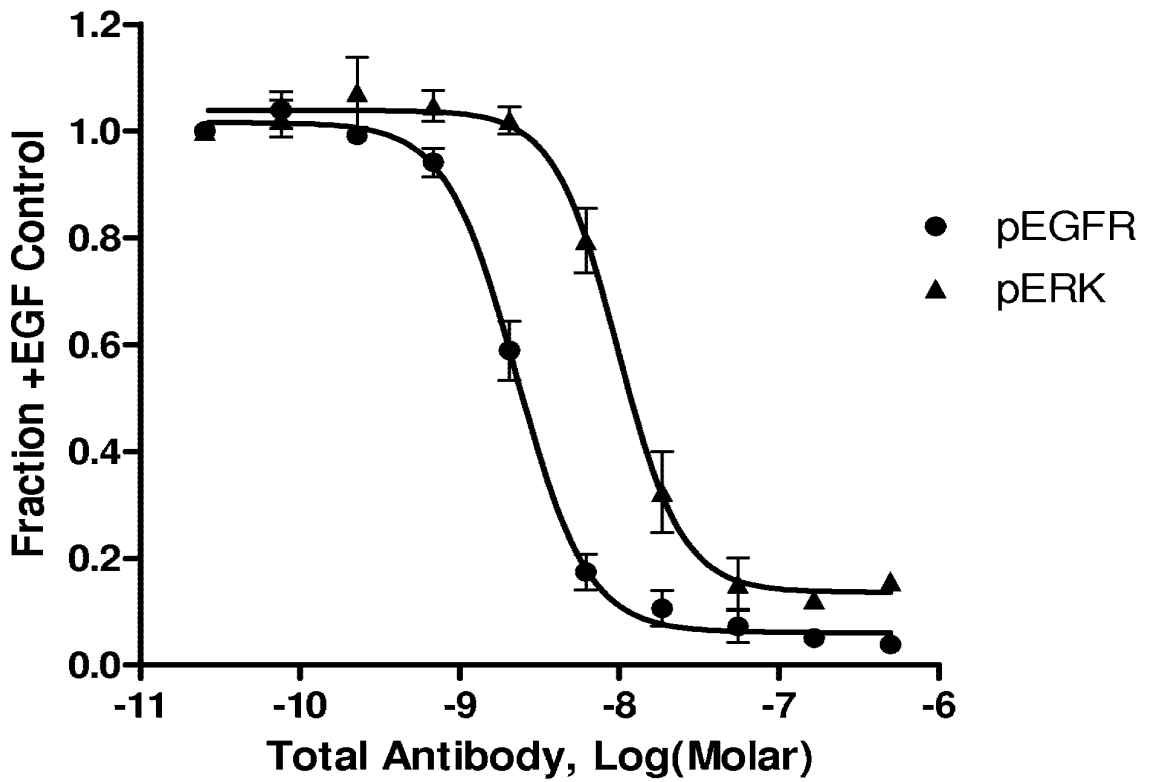


Fig. 6D

15/33



**Fig. 7A**

16/33

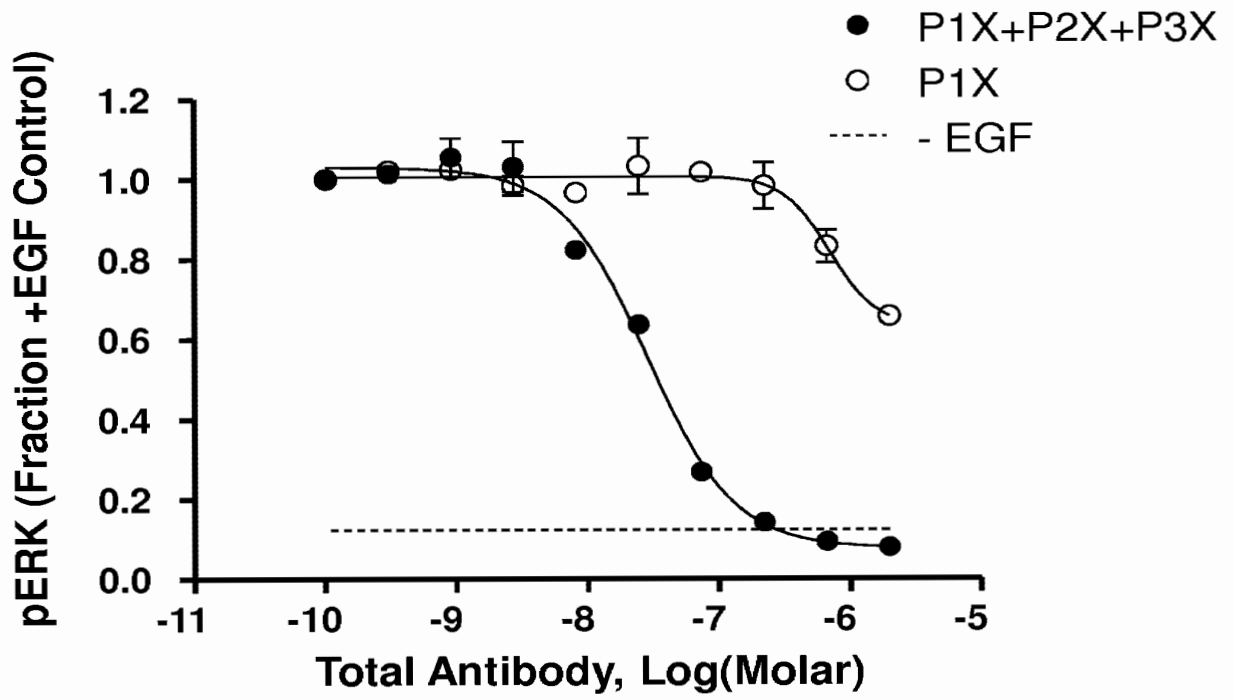


**Fig. 7B**



17/33

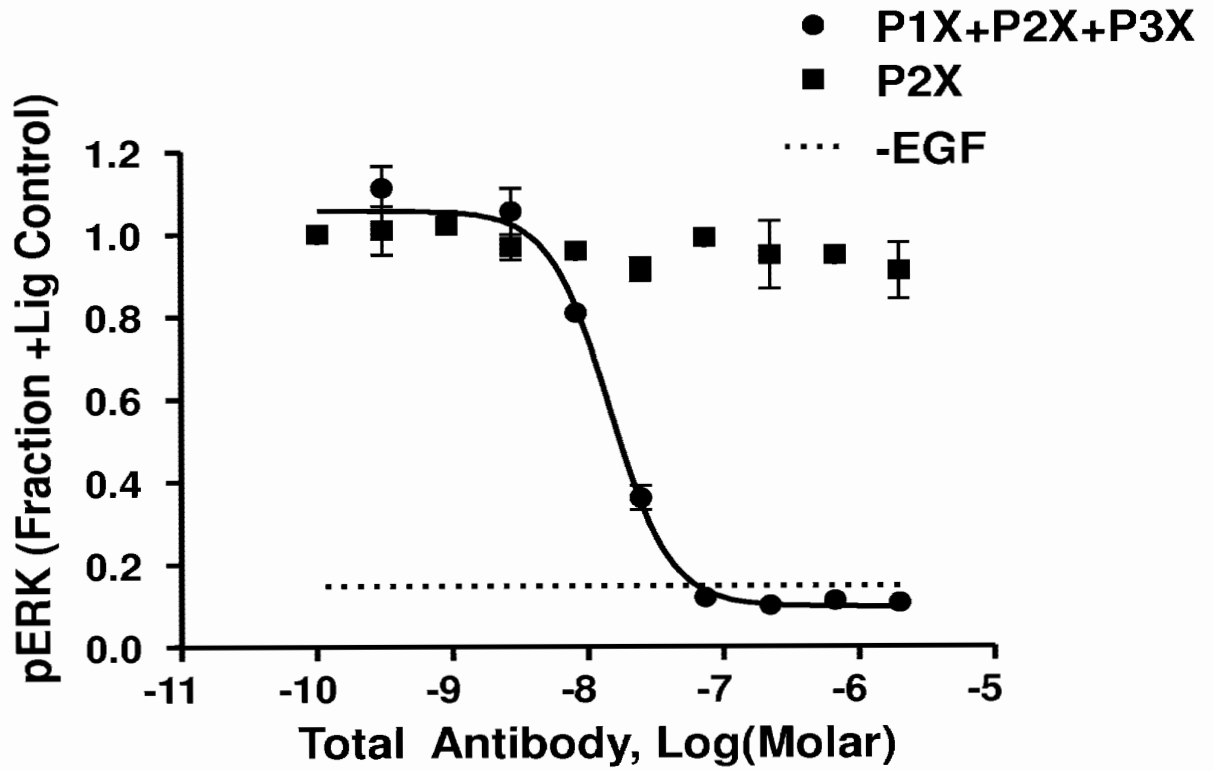
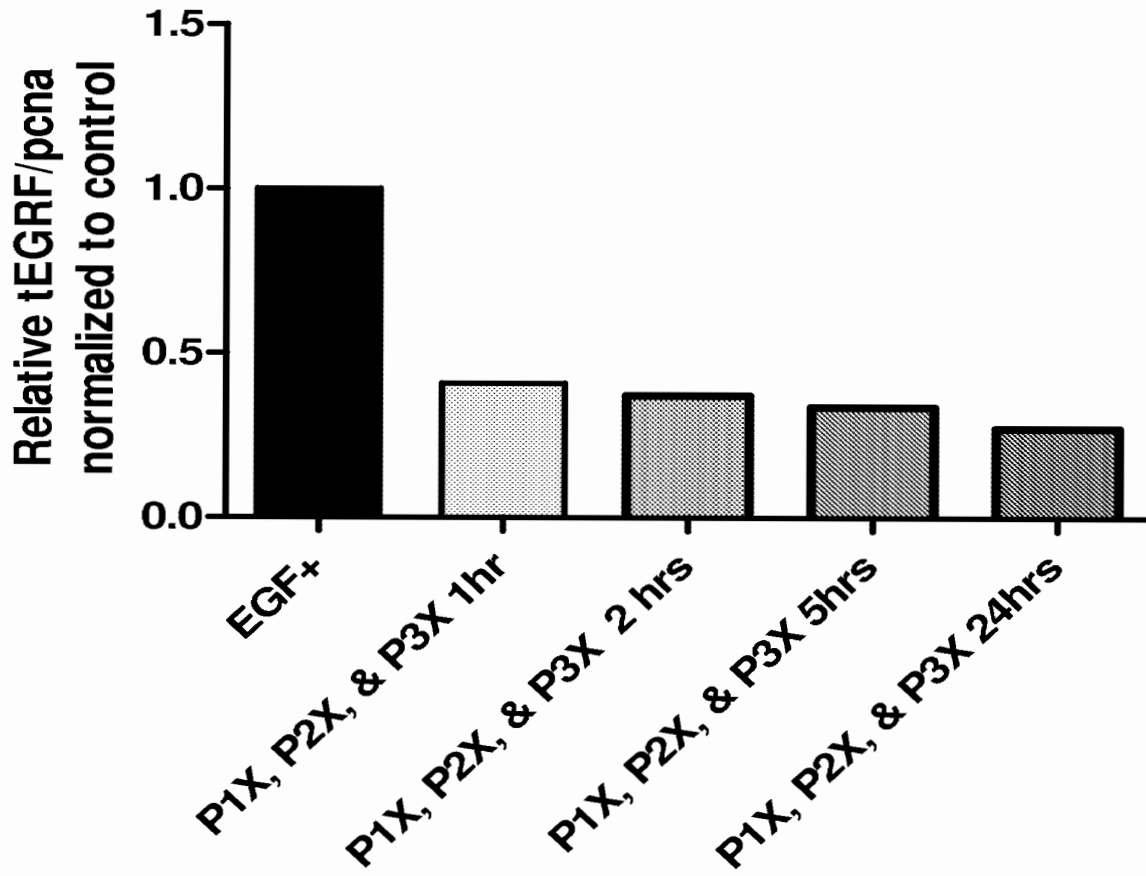


Fig. 7C

18/33



**Fig. 8A**

19/33

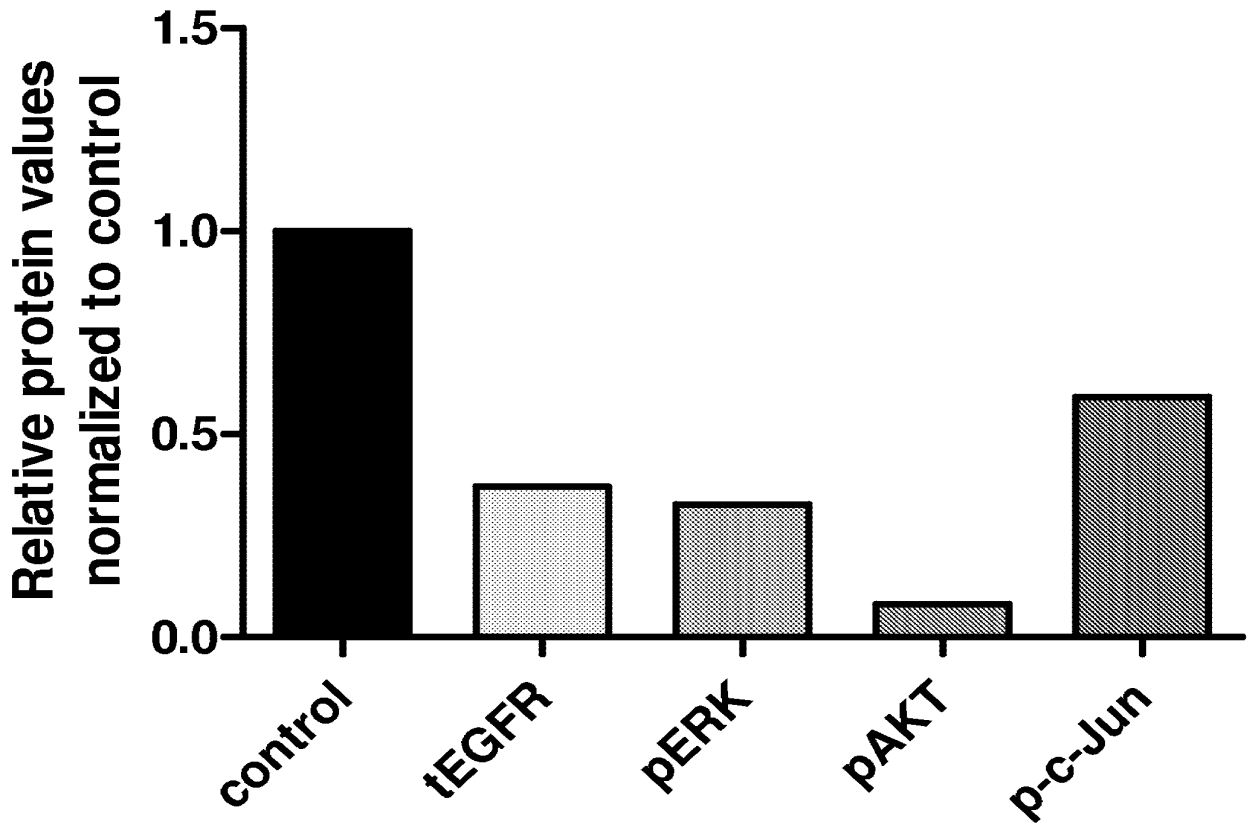


**Fig. 8B**

20/33

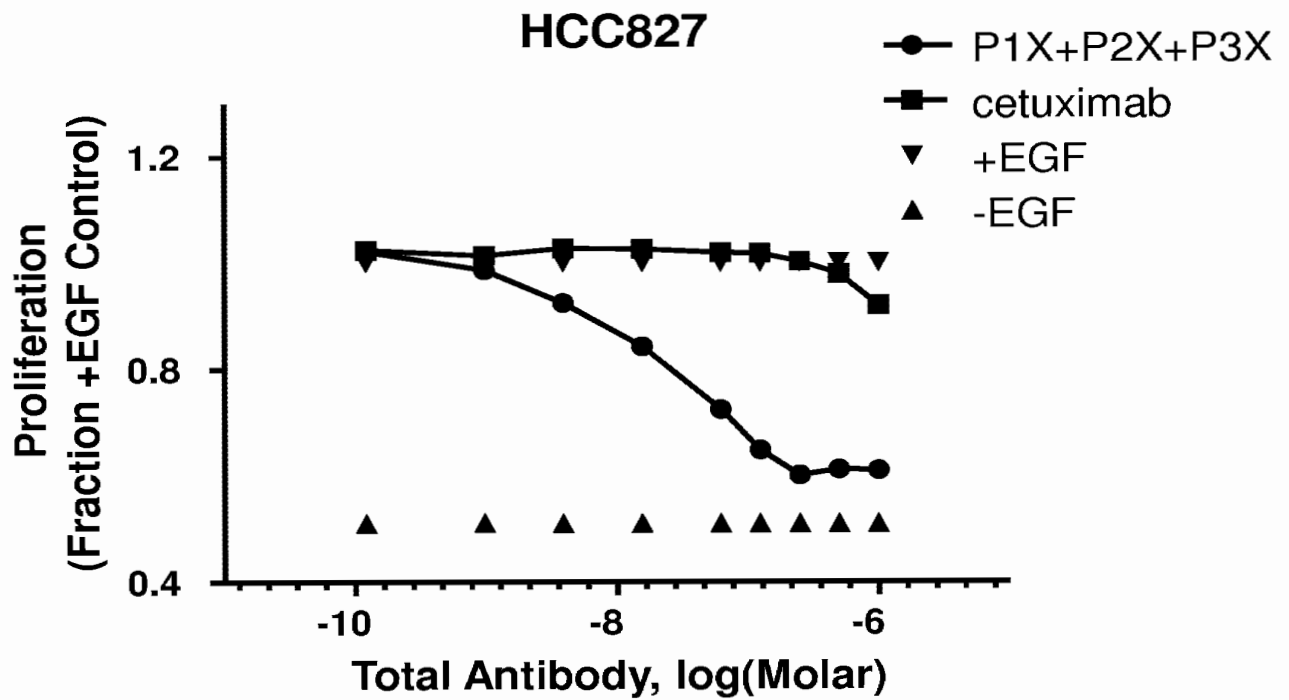


**Fig. 9A**

21/33

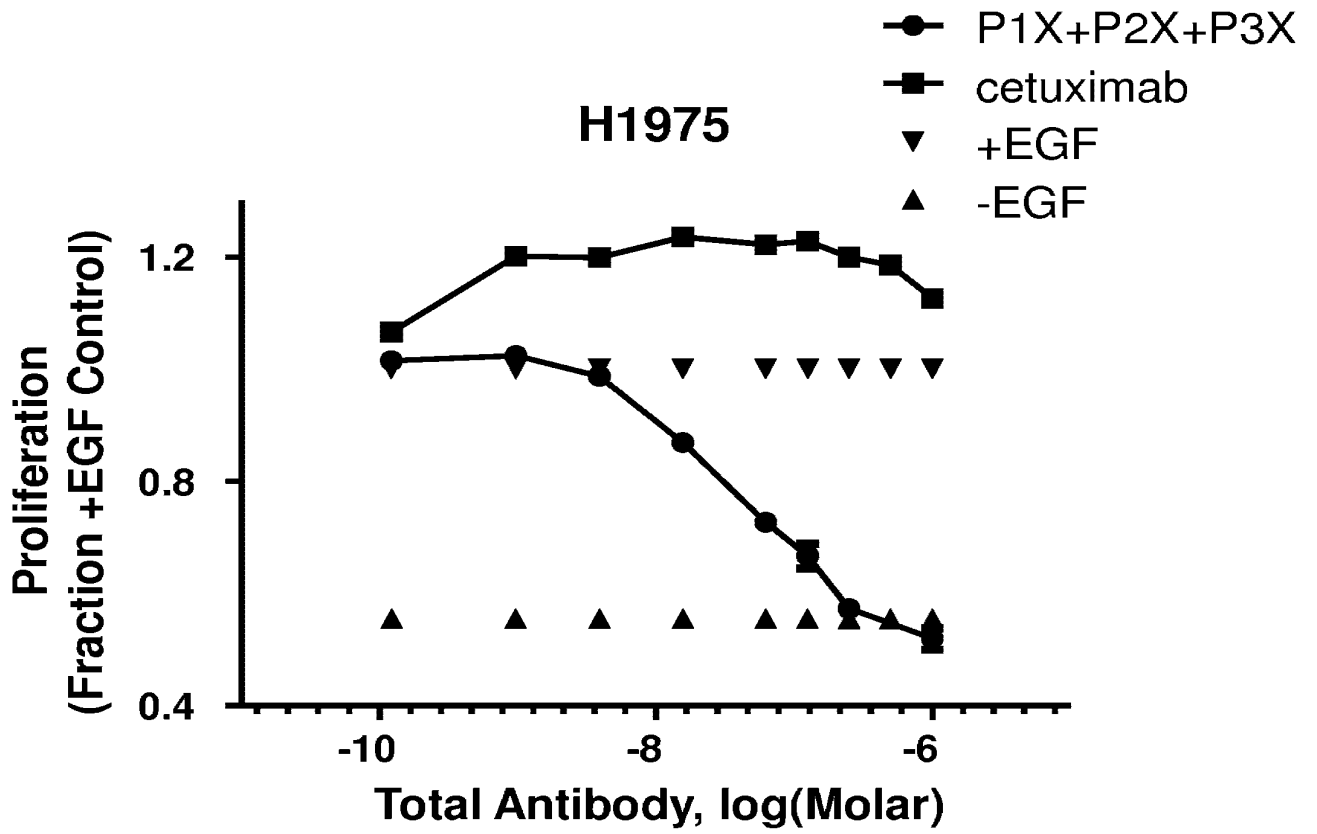


*Fig. 9B*

22/33

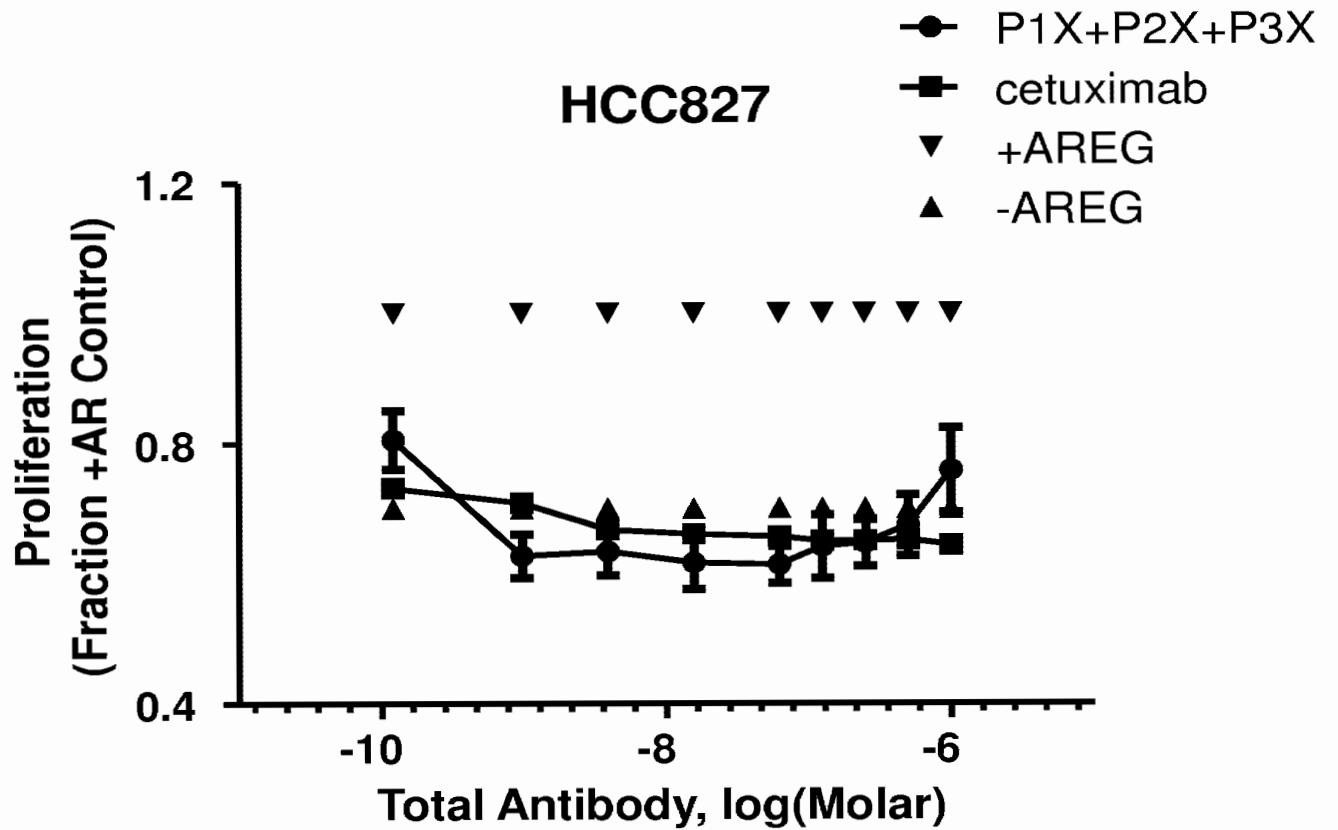


*Fig. 9C*

23/33

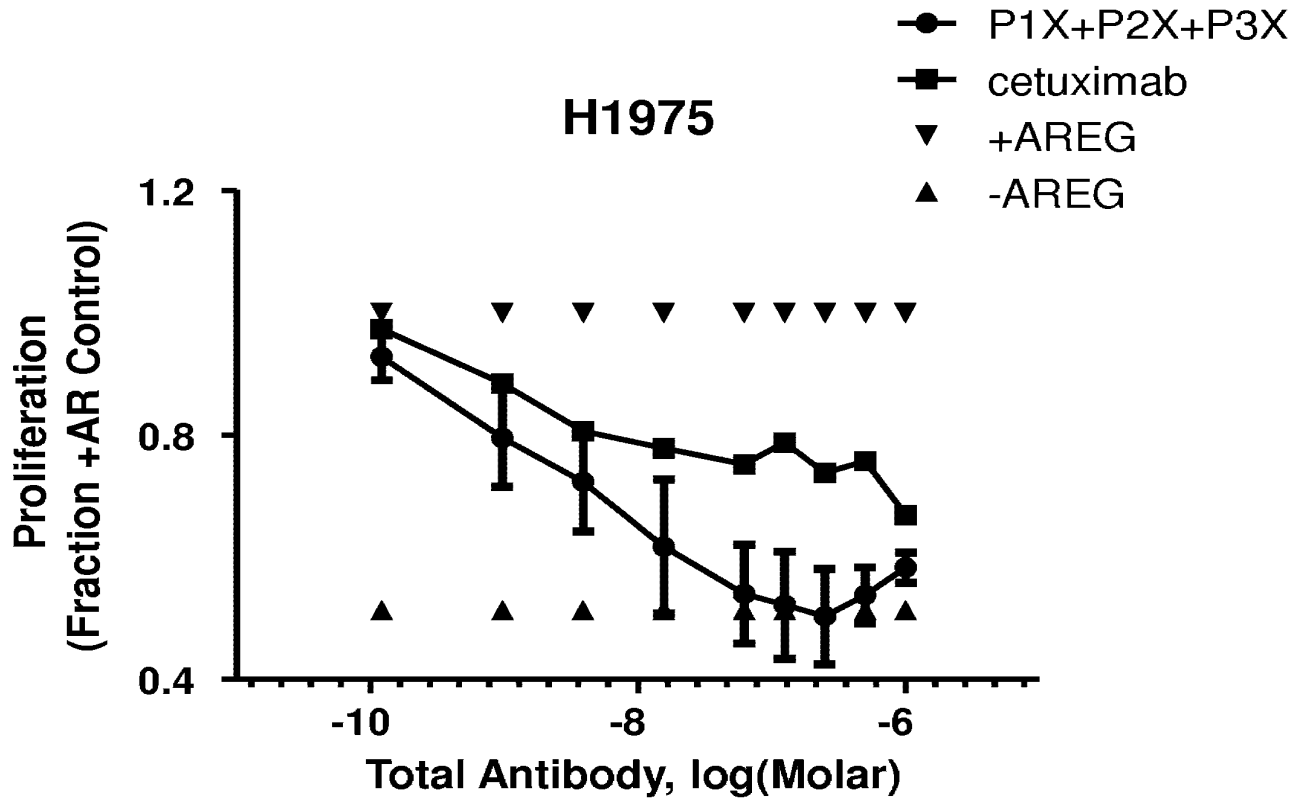


**Fig. 9D**

24/33

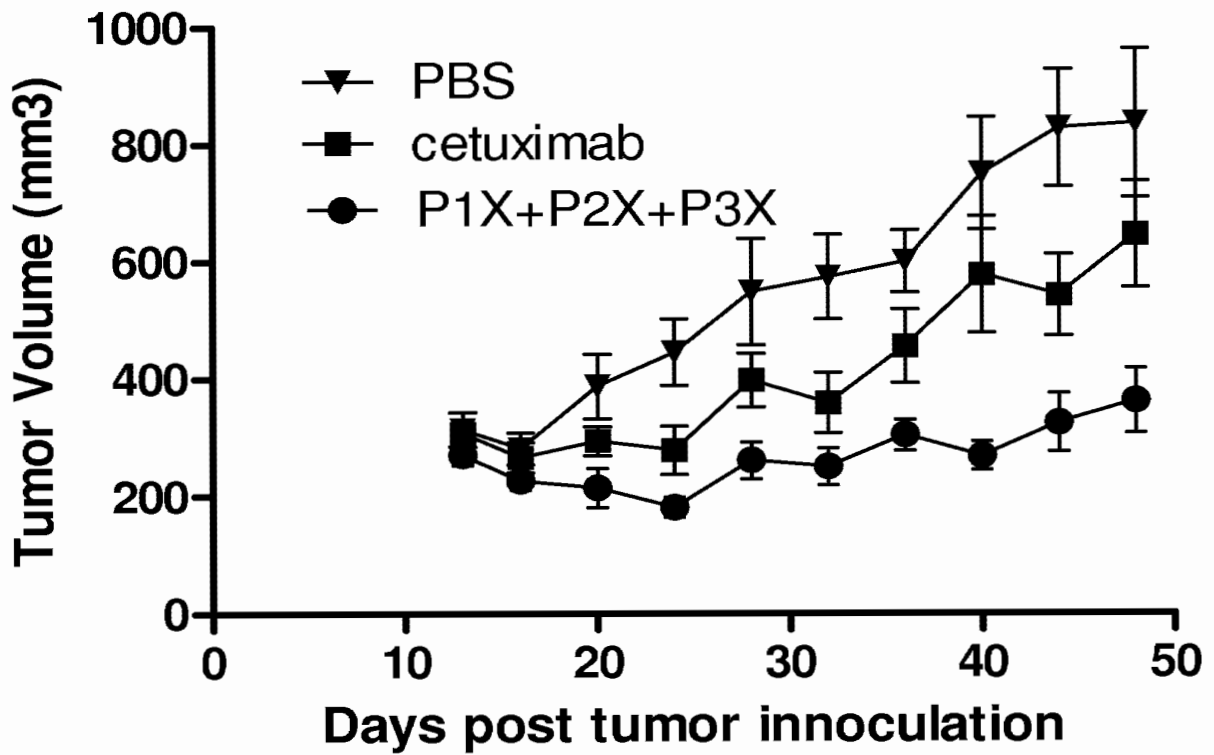


*Fig. 10A*



25/33

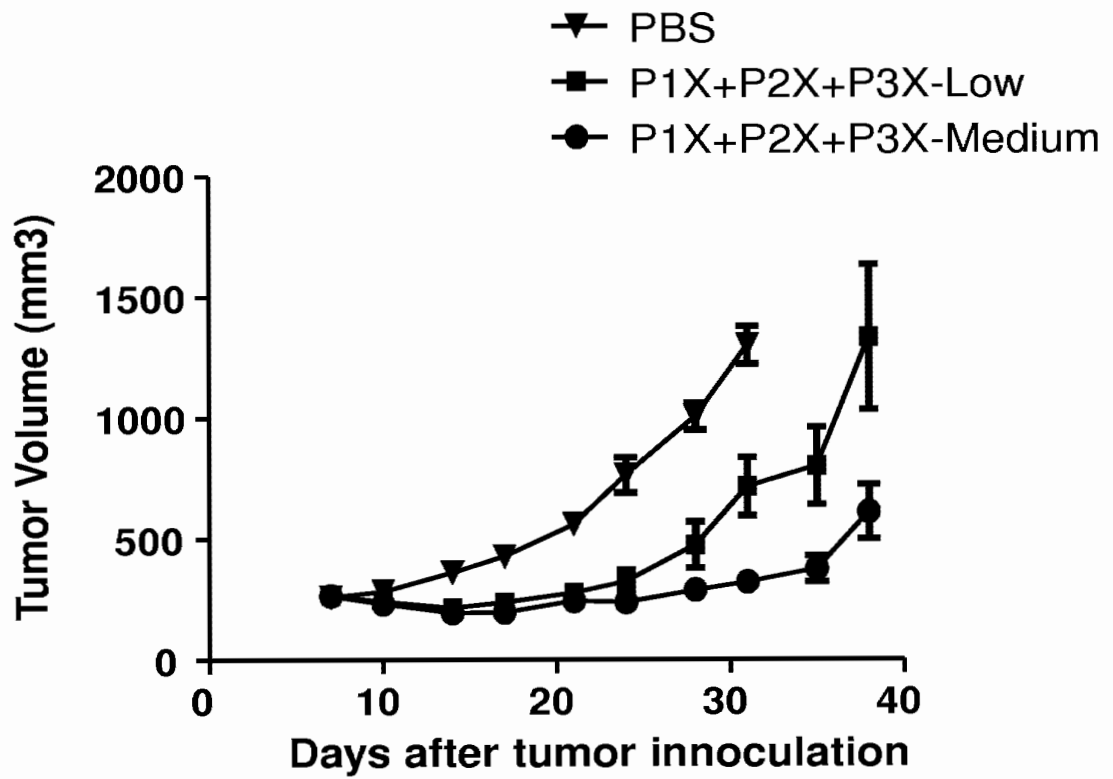


**Fig. 10B**

26/33

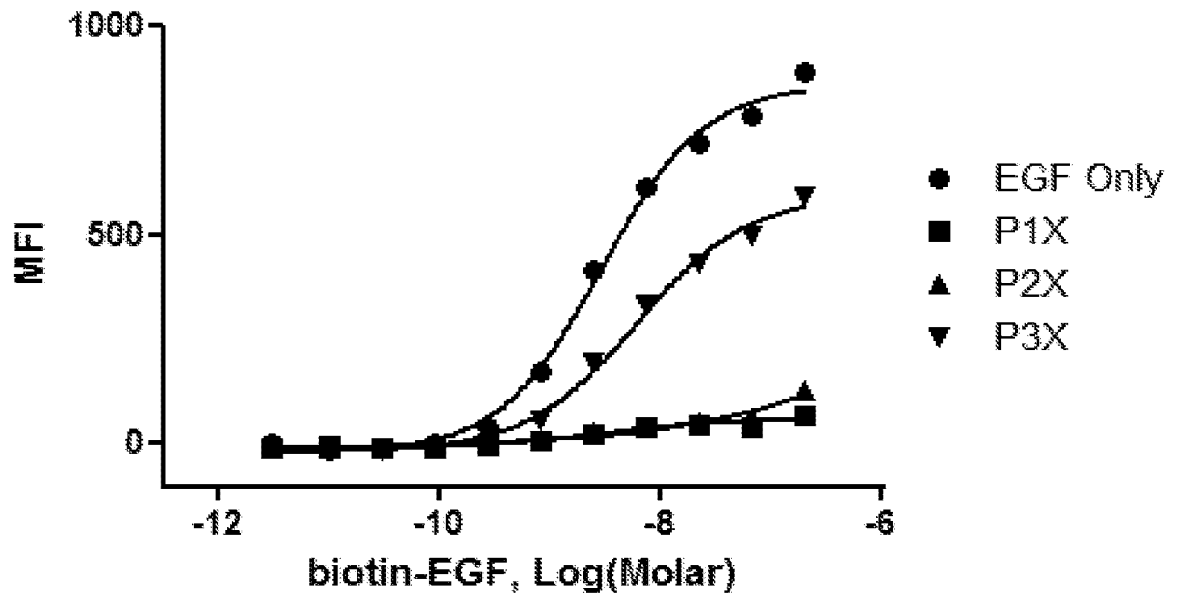


**Fig. 11**

27/33

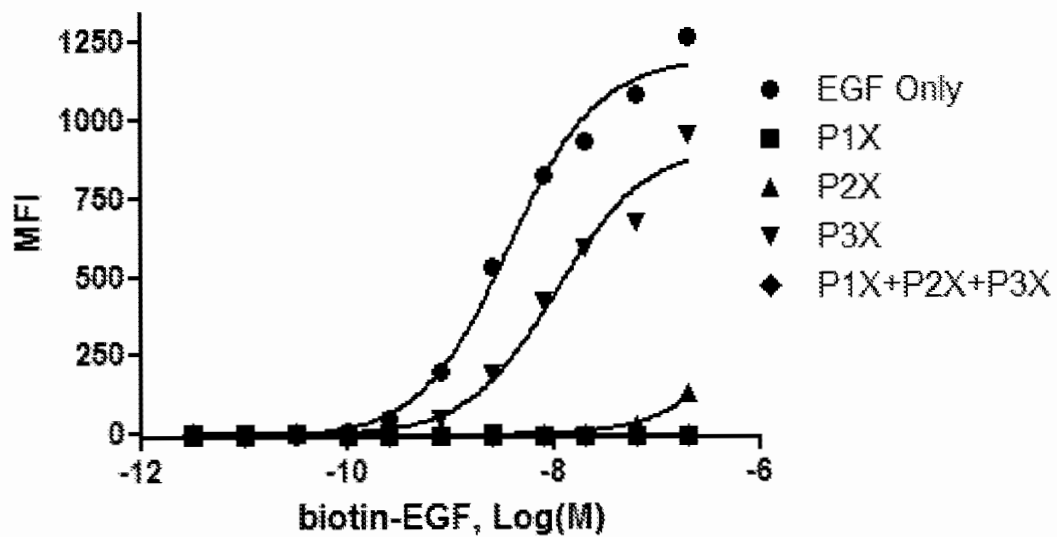


**Fig. 12A**

28/33

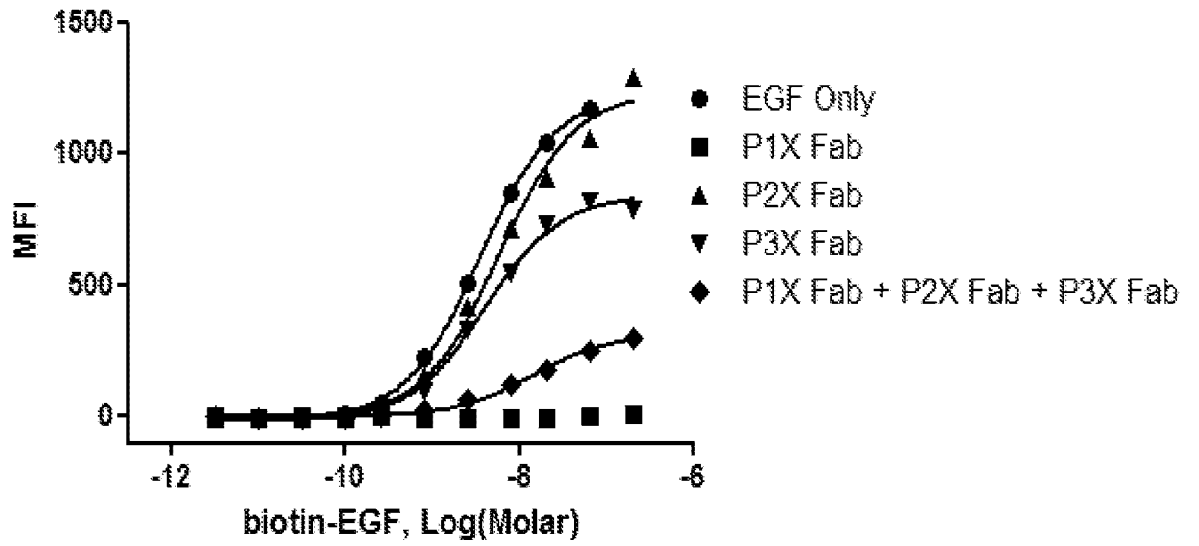


**Fig. 12B**

29/33

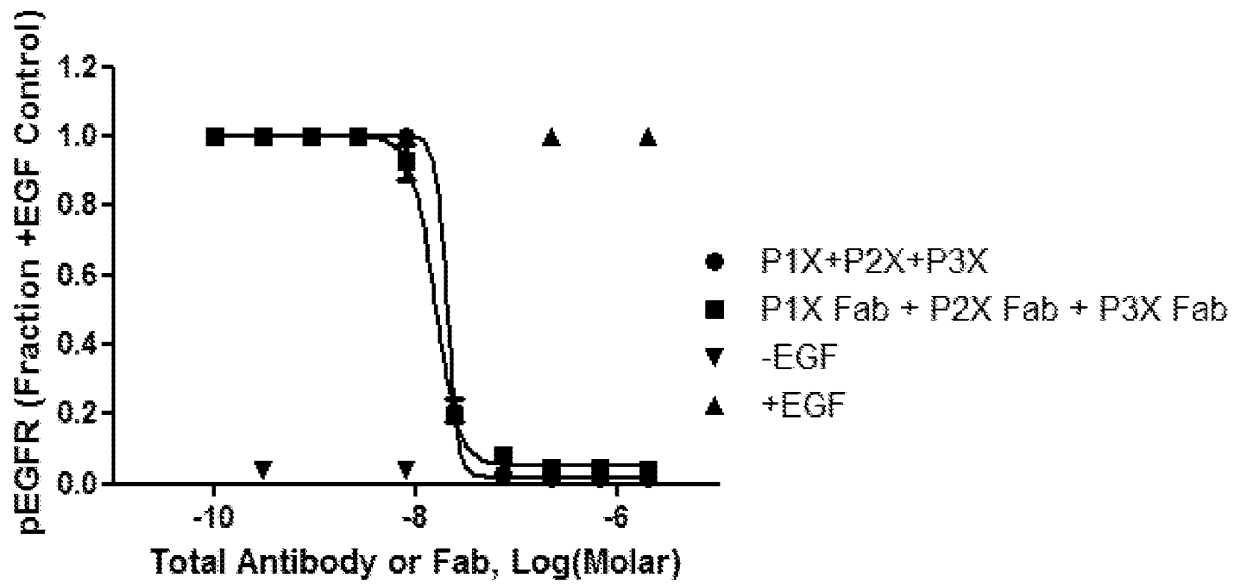


**Fig. 13A**

30/33

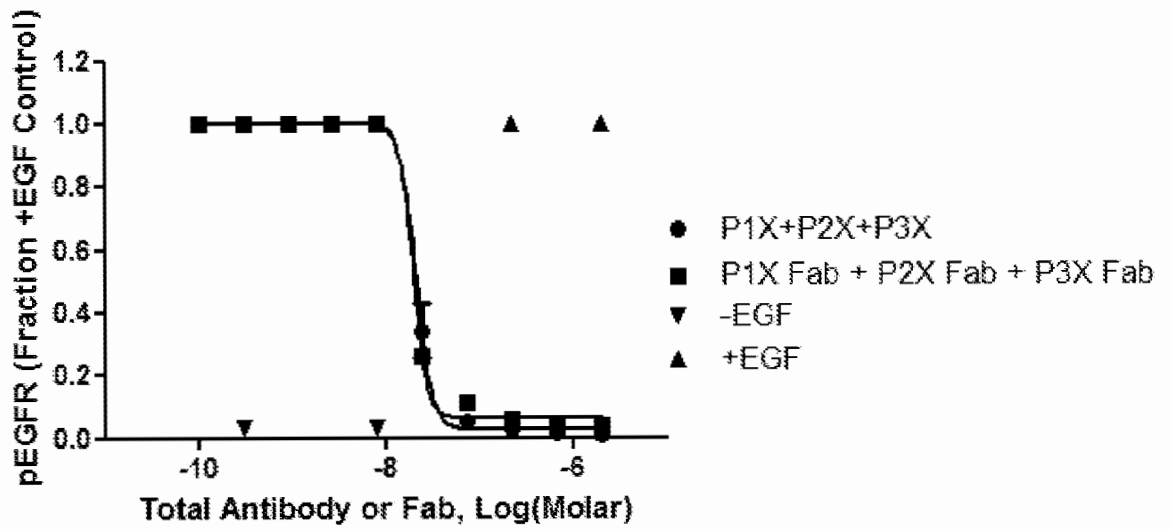


**Fig. 13B**

31/33

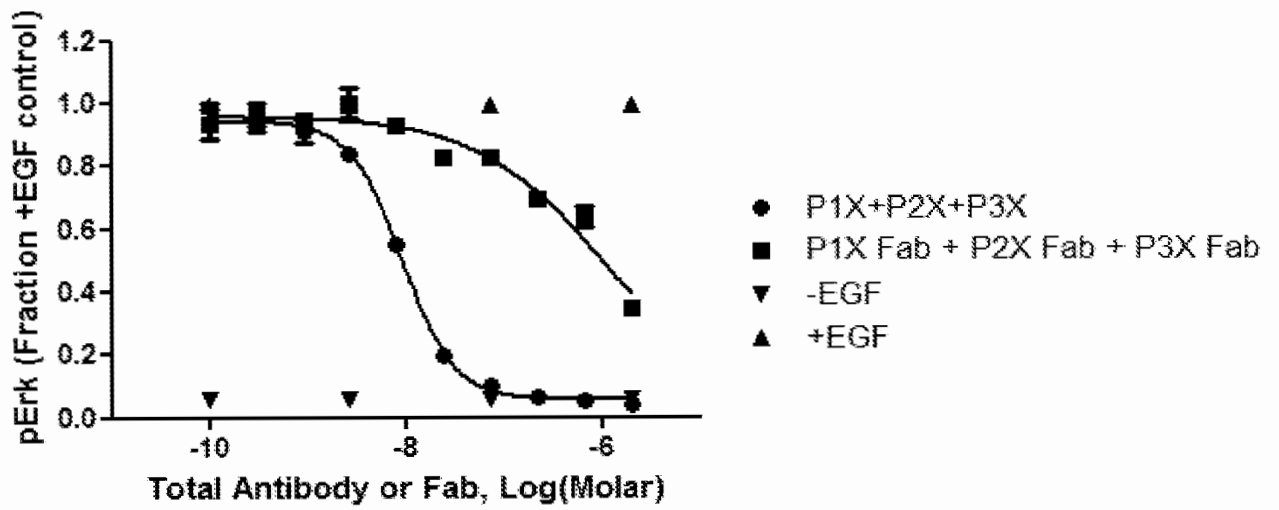


**Fig. 13C**

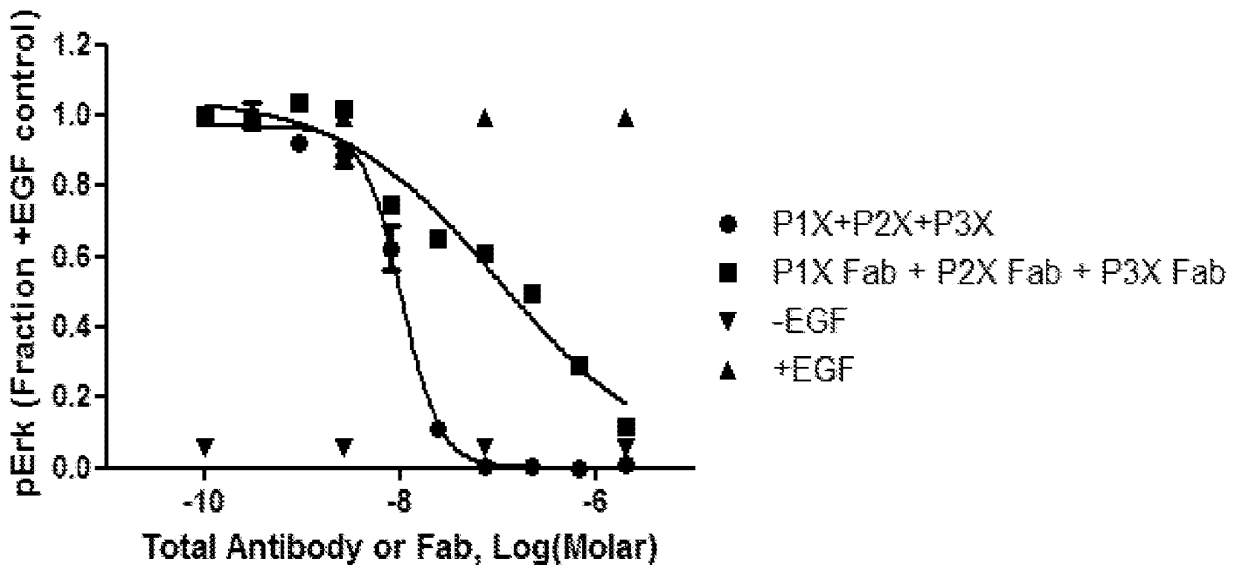


**Fig. 13D**



33/33

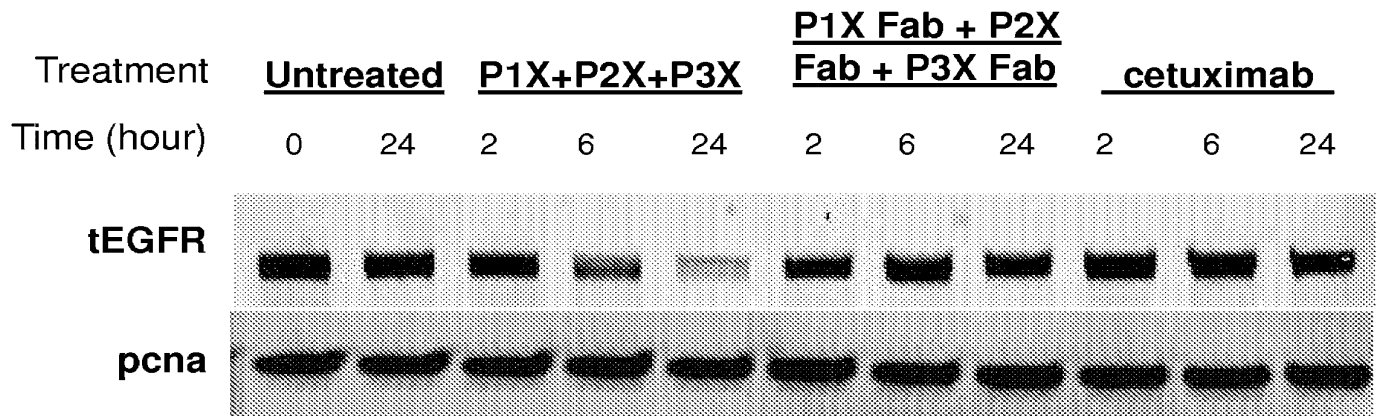


**Fig. 14**



- (51) **International Patent Classification:**  
*C07C 337/08* (2006.01)
- (21) **International Application Number:**  
PCT/US2013/037033
- (22) **International Filing Date:**  
17 April 2013 (17.04.2013)
- (25) **Filing Language:** English
- (26) **Publication Language:** English
- (30) **Priority Data:**  
61/625,670 17 April 2012 (17.04.2012) US  
61/696,560 4 September 2012 (04.09.2012) US  
61/798,855 15 March 2013 (15.03.2013) US
- (71) **Applicant:** **MERRIMACK PHARMACEUTICALS, INC.** [US/US]; One Kendall Square, Suite B7201, Cambridge, MA 02139-1670 (US).
- (72) **Inventors:** **DRUMMOND, Daryl, C.**; Merrimack Pharmaceuticals, Inc., One Kendall Square, Suite B7201, Cambridge, MA 02139-1670 (US). **KIRPOTIN, Dmitiri, B.**; Merrimack Pharmaceuticals, Inc., One Kendall Square, Suite B7201, Cambridge, MA 02139-1670 (US). **WICKHAM, Thomas**; Merrimack Pharmaceuticals, Inc., One Kendall Square, Suite B7201, Cambridge, MA 02139-1670 (US). **HENDRIKS, Bart, S.**; Merrimack Pharmaceuticals, Inc., One Kendall Square, Suite B7201, Cambridge, MA 02139-1670 (US). **AGRESTA, Samuel**; Merrimack Pharmaceuticals, Inc., One Kendall Square, Suite B7201, Cambridge, MA 02139-1670 (US). **LEE, Helen**; Merrimack Pharmaceuticals, Inc., One Kendall Square, Suite B7201, Cambridge, MA 02139-1670 (US).
- (74) **Agents:** **RUSSETT, Mark, D.** et al.; Edwards Wildman Palmer LLP, P.O. Box 55874, Boston, MA 02205 (US).
- (81) **Designated States** (*unless otherwise indicated, for every kind of national protection available*): AE, AG, AL, AM, AO, AT, AU, AZ, BA, BB, BG, BH, BN, BR, BW, BY, BZ, CA, CH, CL, CN, CO, CR, CU, CZ, DE, DK, DM, DO, DZ, EC, EE, EG, ES, FI, GB, GD, GE, GH, GM, GT, HN, HR, HU, ID, IL, IN, IS, JP, KE, KG, KM, KN, KP, KR, KZ, LA, LC, LK, LR, LS, LT, LU, LY, MA, MD, ME, MG, MK, MN, MW, MX, MY, MZ, NA, NG, NI, NO, NZ, OM, PA, PE, PG, PH, PL, PT, QA, RO, RS, RU, RW, SC, SD, SE, SG, SK, SL, SM, ST, SV, SY, TH, TJ, TM, TN, TR, TT, TZ, UA, UG, US, UZ, VC, VN, ZA, ZM, ZW.
- (84) **Designated States** (*unless otherwise indicated, for every kind of regional protection available*): ARIPO (BW, GH, GM, KE, LR, LS, MW, MZ, NA, RW, SD, SL, SZ, TZ, UG, ZM, ZW), Eurasian (AM, AZ, BY, KG, KZ, RU, TJ, TM), European (AL, AT, BE, BG, CH, CY, CZ, DE, DK, EE, ES, FI, FR, GB, GR, HR, HU, IE, IS, IT, LT, LU, LV, MC, MK, MT, NL, NO, PL, PT, RO, RS, SE, SI, SK, SM, TR), OAPI (BF, BJ, CF, CG, CI, CM, GA, GN, GQ, GW, ML, MR, NE, SN, TD, TG).
- Published:**
- *with international search report (Art. 21(3))*
  - *before the expiration of the time limit for amending the claims and to be republished in the event of receipt of amendments (Rule 48.2(h))*

(54) **Title:** COMPOSITIONS AND METHODS FOR NON-INVASIVE IMAGING

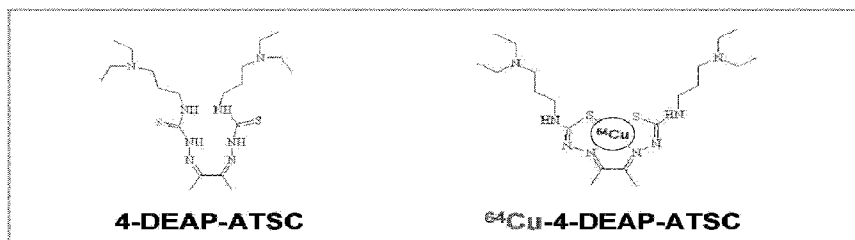


**FIGURE 1**

(57) **Abstract:** The present invention relates to a novel composition useful in targeted diagnostic and/or therapy of a target site, such as cancerous tissue. The composition and methods disclosed herein find particular use in diagnosing and imaging cancerous tissue. The present invention provides a new diagnostic tool for the utilization of positron emission tomography (PET) imaging technique.



## COMPOSITIONS AND METHODS FOR NON-INVASIVE IMAGING

### RELATED APPLICATIONS

This application claims the benefit of and priority to U.S. Provisional Patent Application Nos.  
5 61/625,670, filed April 17, 2012, 61/696,560, filed September 4, 2012, and 61/798,855, filed March  
15, 2013. The contents of each of the foregoing applications are incorporated herein by reference in  
their entireties.

### BACKGROUND

10 Liposomes have proved a valuable tool for delivering various pharmacologically active  
molecules, such as anti-neoplastic agents, to cells, organs, or tumors. However, it has been found that  
deposition of liposomes into tumors can be highly variable between not only tumors of different  
subtypes between patients, but also between tumors of similar subtype within the same patient. The  
outcome of treatment with liposomally-delivered therapeutic agents can therefore be somewhat  
15 unpredictable for a given patient.

Liposome delivery has been shown to improve the pharmacokinetic profile and widen the  
therapeutic index of certain anticancer drugs, especially the anthracycline class. Improved efficacy is  
in part a result of passive targeting to tumor sites based on the enhanced permeability and retention  
(EPR) effect. To fully exploit this process, drug carriers should be engineered to retain drug while  
20 circulating, thereby preventing premature drug release before accumulating in the tumor but still  
allowing for release of drug once in the vicinity of the tumor. Antibody-targeted nanoparticles, such  
as immunoliposomes against HER2 or epidermal growth factor receptor, represent another strategy  
for more efficient drug delivery to tumor cells.

It has been found, however, that deposition of liposomal drugs into tumors varies. Tumors  
25 that have higher drug deposition will have improved clinical outcomes. Liposomal drugs have been  
shown to enter tumors via a mechanism termed the enhanced permeability and retention (EPR) effect  
whereby liposomes can preferentially escape from the bloodstream into the tumor interstitium *via*  
leaky tumor vasculature and then become trapped in the tumor by virtue of their large size and the  
lack of functional lymphatics. However, the degree to which liposomal particles can deposit into  
30 tumors has been shown to be highly variable in both preclinical tumor models and in clinical studies  
whereby liposomes have been used as imaging agents to quantify the level and variability of tumor  
deposition. The invention provides liposomal imaging agents that can be used to predict which  
patients' tumors will have low or high deposition of liposomal drugs and ultimately which will benefit  
from a particular liposomal drug.

35 Non-invasive methods for determining whether a liposomally-delivered therapeutic agent is  
suitable for use in a patient before treatment (*e.g.*, to predict clinical outcomes of targeted and  
untargeted liposomal therapeutics) are therefore needed.

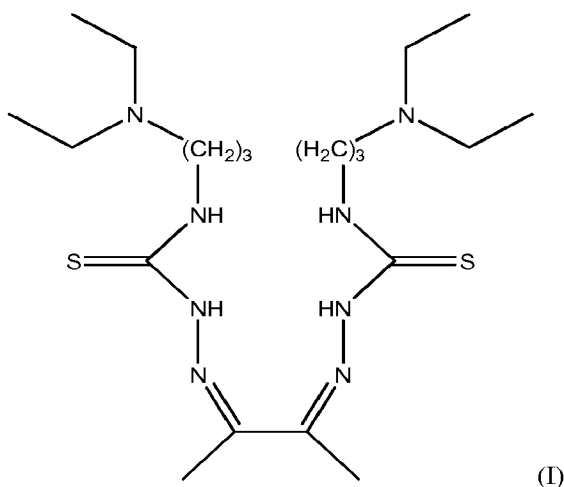
## SUMMARY

The present invention provides compositions and methods for non-invasive imaging, and more particularly, non-invasive imaging for liposomal therapeutics. Such compositions and methods are useful in imaging cancer or another disease, and/or for drug delivery to a target site, *e.g.*,

5 cancerous tissue.

Other features and advantages will be apparent from the detailed description, and from the claims.

Provided in one aspect is the DEAP-ASTC compound of formula I:

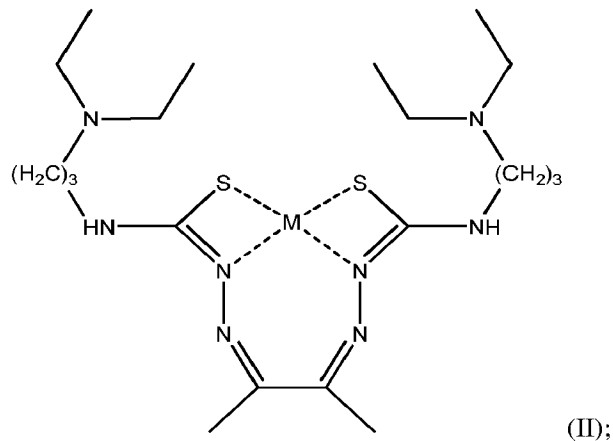


10

or a pharmaceutically acceptable salt thereof. In one embodiment the compound is stored at a temperature of -20 °C, -4 °C, room temperature (22-25 °C), 30 °C, 37 °C or 40 °C. In one embodiment the compound is stored for 3 months, 4 months, 5 months, or 6 months. In another embodiment, following storage for 3 months, 4 months, 5 months, or 6 months days at a temperature of from 4°C to

15 40 °C, less than 15% of the compound has degraded. In one embodiment the % of the compound that has degraded is measured by high performance liquid chromatography.

Provided in another aspect is a DEAP-ASTC compound of formula II:



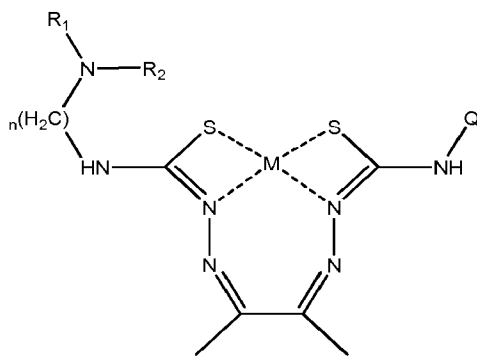
in which M is a metal ion with a valency of 2 or 3 or 4, or a metal oxide ion. In one embodiment, M is a divalent cation, e.g., a copper cation. In another embodiment, M is  $\text{Cu}^{2+}$ . In one embodiment, M is a radioisotope, e.g.,  $^{64}\text{Cu}$  or  $^{67}\text{Cu}$ , or another suitable isotope of a divalent cation.

5 Provided in another aspect is a composition comprising liposomes in an aqueous medium (e.g., a pharmaceutically acceptable medium) said liposomes each having an interior space and a membrane separating said interior from said medium, said membrane comprising one or more lipids; and a compound of formula I or formula II (or formula III, *infra*), either with or without a chelated divalent cation, entrapped in at least one liposome of the liposomes in the composition. In one embodiment, where a divalent metal cation is chelated, the composition comprises at least about 10 0.1  $\mu\text{Ci}$  of radioactivity. In another embodiment, M is a radioisotope of  $\text{Cu}^{2+}$  selected from  $^{64}\text{Cu}$  and  $^{67}\text{Cu}$ . In yet another embodiment, the composition comprises about 0.01, 1, 2, 3, 4, 5, 10, 15 or 20  $\mu\text{Ci}$  of radioactivity. In various embodiments the membranes comprises cholesterol and a phosphatidylcholine. In other embodiments, the liposomes are stable after a storage period of 3 months, 4 months, 5 months, or 6 months, wherein stability is measured by a functional readout, e.g., 15 *in vivo* stability or loadability. A liposome is considered loadable (stable) if, after loading of  $^{64}\text{Cu}$ :4-DEAP-ATSC into the liposomes, about 90% of  $^{64}\text{Cu}$ :4-DEAP-ATSC is in the liposome fraction after size exclusion chromatography. In one embodiment, the membranes of the liposomes comprise cholesterol and a phosphatidylcholine. In another embodiment, the membranes of the liposomes comprise a non-hydrolysable lipid. An exemplary non-hydrolysable lipid is a sphingolipid. In yet 20 another embodiment, the membranes of the liposomes comprise one or more of sphingomyelin, HSPC, DSPC and a non-hydrolysable lipid.

In various aspects, the liposomes in an aqueous medium are prepared as unloaded liposomes prior to the compound of Formula III being entrapped in the at least one liposome, and the unloaded liposomes are stable after a storage period of 3 months, 4 months, 5 months, or 6 months, wherein 25 stability is measured by a functional readout obtained following loading of the liposomes with the compound of Formula III after the storage period. The functional readout may be loading efficiency, e.g., of  $^{64}\text{Cu}$ :4-DEAP-ATSC into the liposomes, wherein a liposome is stable if, after loading, at least 90% of  $^{64}\text{Cu}$ :4-DEAP-ATSC is in the liposome fraction after size exclusion chromatography. In other aspects the liposomes in the aqueous medium are prepared as unloaded liposomes prior to the 30 compound of Formula III being entrapped in the at least one liposome, and a plurality of the unloaded liposomes comprise either or both of TEA-SOS and ammonium sulfate in their interior spaces.

In any of the liposomal compositions or methods herein provided, the liposomes may comprise either or both of TEA-SOS and ammonium sulfate in their interior spaces in an amount sufficient to form an electro-chemical gradient across the membrane.

35 In another embodiment, the compound is a compound of formula III:



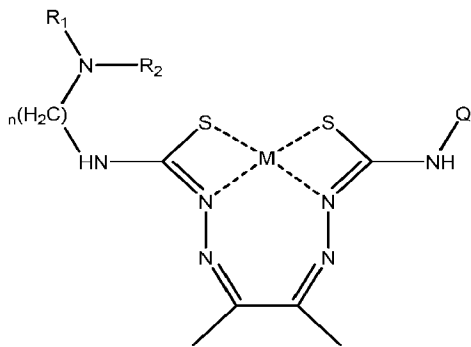
in which: Q is H, substituted or unsubstituted C<sub>1</sub>-C<sub>6</sub>alkyl, or -(CH<sub>2</sub>)<sub>n</sub>-NR<sub>3</sub>R<sub>4</sub>; R<sub>1</sub>, R<sub>2</sub>, R<sub>3</sub> and R<sub>4</sub> are each independently selected from H, substituted or unsubstituted C<sub>1</sub>-C<sub>6</sub>alkyl, or substituted or unsubstituted aryl or wherein either or both of (1) R<sub>1</sub> and R<sub>2</sub> and (2) R<sub>3</sub> and R<sub>4</sub> are joined to form a heterocyclic ring; M is a metal cation with a valency of 2 or 3 or 4, and n is independently, for each occurrence, an integer from 1 to 5. In various embodiments, Q is -(CH<sub>2</sub>)<sub>n</sub>-NR<sub>3</sub>R<sub>4</sub>. In other embodiments, M is Cu<sup>2+</sup>. In other embodiments the composition comprises at least about 0.1 μCi of radioactivity.

In other embodiments, following storage for at least 90 days at a temperature from 4°C to 40°C, less than 15% of the compound is degraded. For example, the compound in some embodiments may be stored at a room temperature of about 25°C or incubated at about 37 °C In one embodiment, the % of the compound that has degraded is measured by high performance liquid chromatography. In some embodiments, following storage for 4 months, 5 months, or 6 months, less than 15% of the compound is degraded.

15

In another aspect, a method is provided for preparing a liposomal imaging agent, the method comprising:

(a) providing a first solution comprising a quantity of a compound of Formula III,



20 in which

Q is H, substituted or unsubstituted C<sub>1</sub>-C<sub>6</sub>alkyl, or -(CH<sub>2</sub>)<sub>n</sub>-NR<sub>3</sub>R<sub>4</sub>;

R<sub>1</sub>, R<sub>2</sub>, R<sub>3</sub> and R<sub>4</sub> are each independently selected from H, substituted or unsubstituted C<sub>1</sub>-C<sub>6</sub>alkyl, or substituted or unsubstituted aryl or wherein either or both of (1) R<sub>1</sub> and R<sub>2</sub> and (2) R<sub>3</sub> and R<sub>4</sub> are joined to form a heterocyclic ring;

M absent or is a metal ion,

5 and

n is independently, for each occurrence, an integer from 1 to 5; and

(b) providing a preparation of liposomes in a aqueous medium, a plurality of the liposomes each having an interior space and a membrane separating the interior space from the medium, the interior space comprising a second solution creating an electro-chemical gradient across the membrane, and  
10 either (c) where M is present, preparing a mixture by combining the first solution with the preparation of liposomes, and incubating the mixture under conditions such that a fraction of the quantity of the compound of Formula III becomes encapsulated by at least one liposome of the plurality of liposomes, to form a liposomal imaging agent, or (d) where M is absent, preparing a mixture by combining the first solution with the preparation of liposomes, and incubating the mixture under  
15 conditions such that a fraction of the quantity of the compound of Formula III becomes encapsulated by at least one liposome of the plurality of liposomes, and subsequently adding a solution comprising radioactive metal ion to the at least one liposome so that radioactive metal ion becomes encapsulated by the at least one liposome to that to form a liposomal imaging agent. In certain aspects of this method, prior to the mixture being prepared, the second solution is essentially free of any metal  
20 chelating moiety. In other aspects, prior to the mixture being prepared, the first solution is essentially free of lipid. In still other aspects, the conditions include a temperature of 40 °C or above, or 60 °C or above. In these aspects, the imaging agent so prepared may be suitable for use by injection into a patient without fractionation, other than sterile filtration, subsequent to the preparation of the mixture. In additional aspects, prior to becoming encapsulated by at least one liposome, the compound of  
25 Formula III is uncharged, and subsequent to becoming encapsulated by at least one liposome, the compound of Formula III is charged. In various embodiments, subsequent to the incubating, the mixture is subjected to filtration that is optionally paper filtration, membrane filtration, or gel filtration. In yet another aspect, the fraction of the compound of Formula III in the first solution that does not become encapsulated is less than 15 % or less than 10%. In various aspects of this method,  
30 the preparation of liposomes of (b) comprises within a plurality of the liposomes therein, an antineoplastic therapeutic agent, which is optionally a chemotherapeutic agent such as doxorubicin or irinotecan.

Another method of preparing a liposomal imaging agent is provided, the method comprising:

(a) providing a first solution comprising a quantity of an uncharged composition that is radioactive  
35 metal chelated by a chelator; and (b) providing a preparation of liposomes in a aqueous medium, a plurality of said liposomes each having an interior space and a membrane separating said interior space from said medium, said interior space comprising a second solution creating an electro-

chemical gradient across the membrane, and (c) preparing a mixture by combining the first solution with the preparation of liposomes, and incubating the mixture under conditions such that a fraction of the quantity of the composition becomes encapsulated by at least one liposome of the plurality of liposomes and becomes charged, to form a liposomal imaging agent.

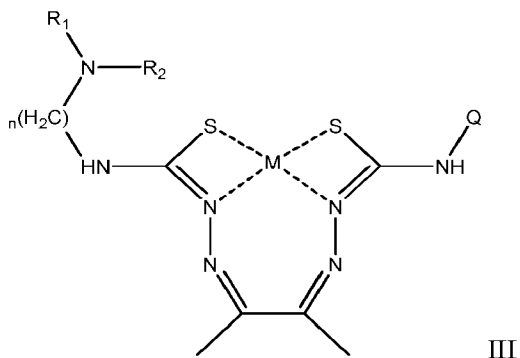
- 5 Also provided is a method of imaging a tissue in a patient, the method comprising:
- (a) injecting the patient with a liposomal imaging agent comprising the composition of claim 9 in an amount sufficient to provide a dose of at least 0.1  $\mu\text{Ci}$  of radioactivity to the patient; and
  - (b) within 48 hours following the injection, scanning the location of the tissue using a scanning method that detects radiation emitted by the radioisotope to obtain an image of the tissue. In certain
- 10 aspects of this method the tissue is a tumor.

Further provided is a method of determining whether a patient having a tumor should be treated with an antineoplastic liposomal therapeutic agent, the method comprises

- (a) injecting the patient with a liposomal imaging agent comprising the composition of claim 9 in an amount sufficient to provide a dose of at least 0.1  $\mu\text{Ci}$  of radioactivity to the patient;
  - 15 (b) within 48 hours following the injection, scanning the location of the tumor using a scanning method that detects radiation emitted by the radioisotope to obtain an image; and
  - (c) examining the image. If the image shows that the liposomal imaging agent is deposited in the tumor at levels higher than background, then the patient is determined to be a patient that should be treated with the liposomal therapeutic agent. Background may be determined by scanning tumor-free
- 20 muscle tissue within 48 hours following the injection. In various aspects, if the image shows that the liposomal imaging agent is deposited in the tumor at levels higher than background, then the patient is treated with the liposomal therapeutic agent and if the image shows that the liposomal imaging agent is not deposited in the tumor at levels higher than background, then the patient is not treated with the liposomal therapeutic agent.

- 25 Also provided is a kit for preparing a liposomal imaging agent, the kit comprising a package containing:

(a) a first container comprising a compound of Formula III



in which



M is absent;

Q is H, substituted or unsubstituted C<sub>1</sub>-C<sub>6</sub>alkyl, or -(CH<sub>2</sub>)<sub>n</sub>-NR<sub>3</sub>R<sub>4</sub>; R<sub>1</sub>, R<sub>2</sub>, R<sub>3</sub> and R<sub>4</sub> are each independently selected from H, substituted or unsubstituted C<sub>1</sub>-C<sub>6</sub>alkyl, or substituted or unsubstituted aryl or wherein either or both of (1) R<sub>1</sub> and R<sub>2</sub> and (2) R<sub>3</sub> and R<sub>4</sub> are joined to form a heterocyclic ring; and n is independently, for each occurrence, an integer from 1 to 5; and

5 (b) a second container comprising a preparation of liposomes in a pharmaceutically acceptable medium, said liposomes having an interior space and a membrane separating said interior from said medium, said interior space comprising a solution creating an electro-chemical gradient across the membrane. The kit may further comprise instructions for, in sequence: (i) combining the compound of  
10 formula III with a metal ion to yield a compound of formula III in which M is not absent and is the metal ion; (ii) preparing a mixture by combining the compound of formula III in which M is the metal ion with the preparation of liposomes, and incubating the mixture under conditions such that the compound of formula III in which M is the metal ion becomes encapsulated in liposomes of the preparation of liposomes; and (iii) administering the encapsulated compound of formula III in which  
15 M is the metal ion to the patient.

In additional embodiments, a method of preparing a liposomal imaging agent is provided, the method comprising: (a) providing a first solution comprising a quantity of an uncharged composition that is radioactive metal chelated by a chelator; and (b) providing a preparation of liposomes in a  
20 aqueous medium, a plurality of said liposomes each having an interior space and a membrane separating said interior space from said medium, said interior space comprising a second solution creating an electro-chemical gradient across the membrane, and (c) preparing a mixture by combining the first solution with the preparation of liposomes, and incubating the mixture under conditions such that a fraction of the quantity of the composition becomes encapsulated by at least one liposome of the plurality of liposomes and becomes charged, to form a liposomal imaging agent.

25

### BRIEF DESCRIPTION OF THE DRAWINGS

Figure 1 shows the molecular structure of a representative chelator alone, and when complexed with <sup>64</sup>Cu.

Figure 2 shows the molecular structure of the ATSM chelator complexed with Cu.

30 Figure 3 is a schematic depicting a protocol for preparing labeled liposomes.

Figure 4 is a schematic depicting chelation of 4-DEAP-ATSC with a molar excess of <sup>64</sup>Cu.

Figure 5 is a schematic showing the process of liposome loading.

Figure 6 shows a schematic representation of the structure of Liposome A. <sup>64</sup>Cu:4-DEAP-ATSC chelation complex is in red color. Non-complexed, protonated 4-DEAP-ATSC is depicted as  
35 V2<sup>+</sup>. The internal aqueous space contains <sup>64</sup>Cu:4-DEAP-ATSC, 4-DEAP-ATSC, ammonium sulfate, and sodium sulfate.

Figure 7 is a graph showing the  $^{64}\text{Cu}$  chelating efficiency of 4-DEAP-ATSC as assessed by instant thin layer chromatography.

Figure 8 depicts the chemical structures of exemplary lipid components of a liposome.

Figure 9 depicts two graphs and a bar chart. The graphs depict a fitting of model results to published pharmacokinetic data for Doxil®, and the bar graph depicts the fitting of model results to the published pharmacokinetic data for Doxil® and a corresponding sensitivity analysis.

Figure 10 shows three graphs depicting Liposome A kinetics of deposition and anticipated variability of deposition based on simulations derived from reported literature data.

Figure 11 is a graph depicting the stability of Liposome A in human plasma after 48 hours.

Figure 12 shows an example of PET-CT image registration to produce a PET-CT fusion image.

Figure 13 depicts PET-CT imaging of  $^{64}\text{Cu}$ -loaded Liposome B in tumor bearing mice.

Figure 14A and 14B show a graph and a bar chart, respectively. Figure 14A depicts the pharmacokinetics of two batches of Liposome A in CD-1 mice. Figure 14B shows the bio-distribution of Liposome A in heart, liver, lung, kidney, and spleen of CD-1 mice.

Figure 15A and 15B show a graph and a bar chart, respectively. Figure 15A depicts the pharmacokinetics of two batches of Liposome A, uncomplexed  $^{64}\text{Cu}$  or  $^{64}\text{Cu}$ :4-DEAP-ATSC in CD-1 mice. Figure 15B shows the biodistribution of two batches of Liposome A, uncomplexed  $^{64}\text{Cu}$  or  $^{64}\text{Cu}$ :4-DEAP-ATSC in heart, liver, lung, kidney, and spleen of CD-1 mice.

Figure 16A-C shows a graph and two bar charts, respectively. Figure 16A depicts the pharmacokinetics of Liposome A in comparison to  $^{64}\text{Cu}$ -labeled Liposome B containing doxorubicin in CD-1 mice, as well as Liposome B in both an NCI-N87 and BT474-M3 mouse xenograft models. Figures 16B and 16C show the biodistribution of Liposome A in comparison to  $^{64}\text{Cu}$ -labeled Liposome B in CD-1 mice and BT474-M3 mouse xenograft models, respectively.

Figure 17 is a graph showing quantification of Liposome A in liver (square), heart (solid circle), kidneys (open circle) and BT474-MFP Tumor. The y-axis is intensity in mega-Becquerels (MBq) per mL, and the x-axis is organ counts in MBq per gram.

Figure 18 is a composite of images showing PET-CT images of H520 (NSCLC) and BT474-M3 (breast) tumor-bearing mice injected with Liposome A. Images were taken at 10 minutes, 6 hours, and 20 hours post-injection.

Figure 19 is a series of graphs showing stability of various 4-DEAP-ATSC formulations stored under a number of conditions, including those of varying pH (A), varying temperature (B), lyophilization (C), lyophilization with mannitol (D), inert gas/air atmosphere (E) and inert gas/air-filled lyophilized formulations (F).

Figure 20 is a series of graphs showing storage stability of various excipient liposome formulations. Multiple lipid compositions and two distinct internal buffers (ammonium sulfate and triethylammonium sucrose octasulfate (TEA-SOS) were tested. (A) shows functional stability of

HSPC, DSPC, and sphingomyelin formulations at 1 to 6 months storage at varying temperatures, and illustrates that the HSPC – ammonium sulfate formulation is functionally stable for at least 15 months when stored at 4°C; (B) shows degradation of lipid in HSPC and DSPC formulations (as measured by HPLC/ELSD) after 1 to 5 months at varying storage temperatures; (C) shows stability of a <sup>64</sup>Cu-DEAP-ATSC-loaded HSPC liposome *in vivo* after up to 6 months storage of the liposome preparation (without radiolabel) at room temperature; (D-F) show stability of sphingomyelin formulations up to 3 months of storage at 4°C, 30°C, and 37°C, respectively; (G) shows storage stability of PEG-DSGE, PEG-DSG, or a liposomal formulation made by post-insertion of (reduced amount) PEG-DSPE into preformed liposomes.

10 Figure 21 is a series of graphs showing storage stability of excipient liposome formulations with various strengths of electro-chemical loading gradient. (A) shows the effect of loading gradient strengths on the <sup>64</sup>Cu:4-DEAP-ATSC loading efficiency of HSPC liposomes (A), DSPC liposomes (B), and liposomes comprising sphingomyelin (C).

15 Figure 22 is a graph showing the effect of storage pH on the storage stability of sphingomyelin liposomes over a four-month period, with loadability of the liposomes as a functional measurement.

Figure 23 is a graph showing that Liposome A is an imaging marker for predicting patient treatment response to liposomal therapeutic. The graph shows correlation between tumor uptake of Liposome A to treatment response to Liposome B.

20 Figure 24 is a series of graphs showing changes in tumor deposition of Liposome A in mammary fat pad tumors (A), and subcutaneous tumors (B) in a BT474-M3 mouse xenograft tumor model and comparison of dose 3 to dose 1 (C).

25 Figure 25 is a graph showing that liposome targeting has no effect on the total tumor deposition of Liposome B and its untargeted counterpart, but rather, increases the liposome uptake by tumor cells within the tumors (insert).

Figure 26 is a graph showing tumor deposition of Liposome B in mouse xenograft models expressing various levels of HER2. Tumor depositions of Liposome B were found to vary with no correlation with HER2 expression in the tumors.

30 Figure 27 is three graphs showing the *in vivo* stability of Liposome A (25A), Liposome B (25B), and Liposome C (25C) after injection into CD-1 mice.

#### DETAILED DESCRIPTION

The present invention provides compositions and methods for non-invasive imaging, and more particularly, non-invasive imaging for liposomal therapeutics.

35 The invention is based, at least in part, on the discovery that diacetyl 4,4'-bis (3-(N,N-diethylamino)propyl)thiosemicarbazone (4-DEAP-ATSC) is useful as a non-invasive imaging reagent

for determining whether a subject is a candidate for treatment with a liposomal therapeutic, as well as for monitoring treatment of a subject with a liposomal therapeutic.

### Definitions

5 Unless specifically stated or obvious from context, as used herein, the term “about” is understood as within a range of normal tolerance in the art, for example within 2 standard deviations of the mean. “About” can be understood as within 10%, 9%, 8%, 7%, 6%, 5%, 4%, 3%, 2%, 1%, 0.5%, 0.1%, 0.05%, or 0.01% of the stated value. Unless otherwise clear from the context, all numerical values provided herein are modified by the term “about.”

10 By “loading” is meant the process of incorporating a chelating agent, chemical agent, therapeutic agent, nucleic acid, and/or polypeptide into an exosome, liposome, or vesicle.

By “nanoparticle” is meant a liposome, exosome, polymersome, microvesicle, apoptotic body, or other lipid or polymer shell structure that constitutes a membrane surrounding an aqueous core. Such nanoparticles may be either synthetically made, or endogenously derived from a cell or a population of cells.

15 Ranges provided herein are understood to be shorthand for all of the values within the range. For example, a range of 1 to 50 is understood to include any number, combination of numbers, or sub-range from the group consisting of 1, 2, 3, 4, 5, 6, 7, 8, 9, 10, 11, 12, 13, 14, 15, 16, 17, 18, 19, 20, 21, 22, 23, 24, 25, 26, 27, 28, 29, 30, 31, 32, 33, 34, 35, 36, 37, 38, 39, 40, 41, 42, 43, 44, 45, 46, 47, 48, 20 49, or 50.

### Liposomal Imaging Agents

In a general aspect, the invention provides liposomal imaging agents having at least two components: (1) A liposome, which will be suspended or solubilized in a liquid medium (such as a buffer or other pharmaceutically acceptable carrier); (2) a chelator moiety capable of chelating a metal ion; and optionally (3) a metal ion suitable for imaging or otherwise assessing the in vitro or in vivo uptake of the liposomal imaging agent into cells, organs, or tumors. In some embodiments, the metal ion has a valency of 2 or 3 or 4. In exemplary embodiments, the metal ion has a valency of 2.

### Liposomes

The liposomes of the liposomal imaging agents disclosed herein can be any liposome known or later discovered in the art. In general, the liposomes can have any liposome structure, *e.g.*, structures having an inner space sequestered from the outer medium by one or more lipid bilayers, or any microcapsule that has a semi-permeable membrane with a lipophilic central part where the membrane sequesters an interior. A lipid bilayer can be any arrangement of amphiphilic molecules characterized by a hydrophilic part (hydrophilic moiety) and a hydrophobic part (hydrophobic moiety). Usually amphiphilic molecules in a bilayer are arranged into two dimensional sheets in which hydrophobic moieties are oriented inward relative to the sheet, while hydrophilic moieties are oriented outward. Amphiphilic molecules forming the liposomes disclosed herein can be any known or later discovered amphiphilic molecules, *e.g.*, lipids of synthetic or natural origin or biocompatible lipids. Liposomes disclosed herein can also be formed by amphiphilic polymers and surfactants, *e.g.*, polymerosomes and niosomes. For the purpose of this disclosure, without limitation, these liposome-forming materials also are referred to as "lipids".

In certain embodiments, the liposome comprises hydrogenated soy phosphatidylcholine (HSPC), cholesterol, and poly(ethylene glycol) (PEG) (Mol. weight 2000)-derivatized distearoylphosphatidylethanolamine (PEG-DSPE) (3:1:0.05 molar ratio).

In certain embodiments, the liposome comprises poly(ethylene glycol)-derivatized phosphatidylethanolamines such as 1,2-distearoyl-sn-glycero-3-phosphatidyl ethanolamine-N-[methoxy(poly(ethylene glycol)-2000)] (ammonium salt); 1,2-dipalmitoyl- sn-glycero-3-phosphatidyl ethanolamine-N-[methoxy(poly(ethylene glycol)-2000)] (ammonium salt); 1,2-dimyristoyl-sn-glycero-3-phosphatidyl ethanolamine-N-[methoxy(poly(ethylene glycol)-2000)] (ammonium salt); or 1,2-dioleoyl-sn-glycero-3-phosphatidyl ethanolamine-N-[methoxy(poly(ethylene glycol)-2000)] (ammonium salt). In certain embodiments, the molecular weight of PEG is 750, 1000, 1500, 2000, 3000, 3500, or 5000.

In certain embodiments the liposome comprises poly(ethylene glycol)-derivatized diacyl glycerols such as such as 1,2-distearoyl-glycerol-[methoxy(poly(ethylene glycol)-2000)] 1,2-dimyristoyl -glycerol-[methoxy(poly(ethylene glycol)-2000)], 1,2-dipalmitoyl-glycerol-[methoxy(poly(ethylene glycol)-2000)]; or 1,2-dioleoyl-glycerol-[methoxy(poly(ethylene glycol)-

2000)]. In certain embodiments, the molecular weight of PEG is 750, 1000, 1500, 2000, 3000, 3500, or 5000.

In certain embodiments the liposome comprises 1,2-dioctadecyl glycerol-N-[methoxy(poly(ethylene glycol)-2000)], dihexadecyl glycerol-N-[methoxy(poly(ethylene glycol)-2000)] ditetradecyl glycerol-N-[methoxy(poly(ethylene glycol)-2000)]. In certain embodiments, the  
5 molecular weight of PEG is 750, 1000, 1500, 2000, 3000, 3500, or 5000.

In certain embodiments the liposome comprises PEG-ceramides, such as N-octadecanoyl-sphingosine-1-[succinoyl[methoxy(poly(ethylene glycol)-2000)]]; N-tetradecanoyl-sphingosine-1-[succinoyl[methoxy(poly(ethylene glycol)-2000)]]; N-hexadecanoyl-sphingosine-1-  
10 {succinoyl[methoxy(poly(ethylene glycol)-2000)]]; N-octadecanoyl-sphingosine-1-[methoxy(poly(ethylene glycol)-2000)]; N-tetradecanoyl-sphingosine-1-[methoxy(poly(ethylene glycol)-2000)]; or N-hexadecanoyl-sphingosine-1-[methoxy(poly(ethylene glycol)-2000)]. In certain embodiments the molecular weight of PEG is 750, 1000, 1500, 2000, 3000, 3500, or 5000.

15 Additional examples of suitable nanoparticle or liposome forming lipids that may be used in the compositions or methods include, but are not limited to, the following: phosphatidylcholines such as diacyl-phosphatidylcholine, dialkylphosphatidylcholine, 1,2-dioleoyl-phosphatidylcholine, 1,2-dipalmitoyl-phosphatidylcholine, 1,2-dimyristoyl-phosphatidylcholine, 1,2-distearoyl-phosphatidylcholine, 1-oleoyl-2-palmitoyl-phosphatidylcholine, 1-oleoyl-2-stearoyl-phosphatidylcholine, 1-palmitoyl-2-oleoyl-phosphatidylcholine and 1-stearoyl-2-oleoyl-phosphatidylcholine; phosphatidylethanolamines such as 1,2-dioleoyl-phosphatidylethanolamine, 1,2-dipalmitoyl-phosphatidylethanolamine, 1,2-dimyristoyl-phosphatidylethanolamine, 1,2-distearoyl-phosphatidylethanolamine, 1-oleoyl-2-palmitoyl-phosphatidylethanolamine, 1-oleoyl-2-stearoyl-phosphatidylethanolamine, 1-palmitoyl-2-oleoyl-phosphatidylethanolamine, 1-stearoyl-2-oleoyl-phosphatidylethanolamine and N-succinyl-dioleoyl-phosphatidylethanolamine;  
25 phosphatidylserines such as 1,2-dioleoyl-phosphatidylserine, 1,2-dipalmitoyl-phosphatidylserine, 1,2-dimyristoyl-phosphatidylserine, 1,2-distearoyl-phosphatidylserine, 1-oleoyl-2-palmitoyl-phosphatidylserine, 1-oleoyl-2-stearoyl-phosphatidylserine, 1-palmitoyl-2-oleoyl-phosphatidylserine and 1-stearoyl-2-oleoyl-phosphatidylserine; phosphatidylglycerols such as 1,2-dioleoyl-phosphatidylglycerol, 1,2-dipalmitoyl-phosphatidylglycerol, 1,2-dimyristoyl-phosphatidylglycerol, 1,2-distearoyl-phosphatidylglycerol, 1-oleoyl-2-palmitoyl-phosphatidylglycerol, 1-oleoyl-2-stearoyl-phosphatidylglycerol, 1-palmitoyl-2-oleoyl-phosphatidylglycerol and 1-stearoyl-2-oleoyl-phosphatidylglycerol; pegylated lipids; pegylated phospholipids such as phosphatidylethanolamine-N-[methoxy(polyethyleneglycol)-1000], phosphatidylethanolamine-N-[methoxy(polyethyleneglycol)-2000], phosphatidylethanolamine-N-[methoxy(polyethylene glycol)-3000], phosphatidylethanolamine-N-  
35 N-

[methoxy(polyethyleneglycol)-5000]; lyso-phosphatidylcholines, lyso-phosphatidylethanolamines, lyso-phosphatidylglycerols, lyso-phosphatidylserines, ceramides,; sphingolipids, *e.g.*, sphingomyelin; phospholipids; glycolipids such as ganglioside GMI; glucolipids; sulphatides; phosphatidic acid, such as di-palmitoyl- glycerophosphatidic acid; palmitic fatty acids; stearic fatty acids; arachidonic fatty acids; lauric fatty acids; myristic fatty acids; lauroleic fatty acids; physcetric fatty acids; myristoleic fatty acids; palmitoleic fatty acids; petroselinic fatty acids; oleic fatty acids; isolauric fatty acids; isomyristic fatty acids; isostearic fatty acids; sterol and sterol derivatives such as cholesterol, cholesterol hemisuccinate, cholesterol sulphate, and cholesteryl-(4-trimethylammonio)-butanoate, ergosterol, lanosterol; poly- oxyethylene fatty acids esters and polyoxyethylene fatty acids alcohols; poly- oxyethylene fatty acids alcohol ethers; polyoxyethylated sorbitan fatty acid esters, glycerol polyethylene glycol oxy-stearate; glyccrol polyethylcnc glycol ricinoleate; ethoxylated soybean sterols; ethoxylated castor oil; polyoxyethylene polyoxypropyl- ene fatty acid polymers; polyoxyethylene fatty acid stearates; di-oleoyl-sn-glycerol; dipalmitoyl-succiny I glycerol; 1,3-dipalmitoyl-2-succinylglycerol; 1-alkyl-2-acyl- phosphatidylcholines such as i-hexadecyl-2-palmitoyl-phosphatidylcholine; 1-alkyl- 2-acyl-p hospatidylethanolamines such as 1-hexadecyl-2-palmitoyl- phosphatidylethanolamine; 1-alkyl-2-acyl-phosphatidylserines such as 1-hexadecyl- 2-palmitoyl-phosphatidylserine; 1-alkyl-2-acyl-phosphatidylglycerols such as 1-hexadecyl-2-palmitoyl-phosphatidylglycerol; 1-alkyl-2-alkyl-phosphatidylcholines such as 1-hexadecyl-2-hexadecyl-phosphatidylcholine; 1 -alkyl-2-alkyl- phosphatidylethanolamines such as 1-hexadecyl-2-hexadecyl- phosphatidylethanolamine; 1-alkyl-2-alkyl-phosphatidylserines such as 1-hexadecyl- 2-hexadecyl-phosphatidylserine; 1-alkyl-2-alkyl-phosphatidylglycerols such as 1-hexadecyl^hexadecyl-phosphatidylglycerol; N-Succinyl-dioctadecylamine; palmitoylhomocysteine; lauryltrimethylammonium bromide; cetyltrimethyl-ammonium bromide; myristyltrimethylammonium bromide; N-[1,2,3-dioleoyloxy)-propyl]- N,N,Ntrimethylammoniumchloride (DOTMA); 1,2-dioleoyloxy-3 (trimethyl- ammonium)propane(DOTAP); and 1,2-dioleoyl-c-(4'-trimethylammonium)-butanoyl- sn-glycerol (DOTB).

The liposomes contained in the liposomal imaging agents disclosed herein can be untargeted liposomes or targeted liposomes, *e.g.*, liposomes containing one or more targeting moieties or biodistribution modifiers on the surface of the liposomes. A targeting moiety can be any agent that is capable of specifically binding or interacting with a desired target. In one embodiment, a targeting moiety is a ligand. The ligand, according to the present invention, preferentially binds to and/or internalizes into, a cell in which the liposome-entrapped entity exerts its desired effect (a target cell). A ligand is usually a member of a binding pair where the second member is present on, or in, a target cell(s) or in a tissue comprising the target cell. Examples of ligands suitable for the present invention are: folic acid, protein, *e.g.*, transferrin, a growth factor, an enzyme, a peptide, a receptor, an antibody or antibody fragment (such as, *e.g.*, Fab', Fv, single chain Fv, single-domain antibody), or any other polypeptide comprising antigen-binding sequences (CDRs) of an antibody molecule. A ligand-

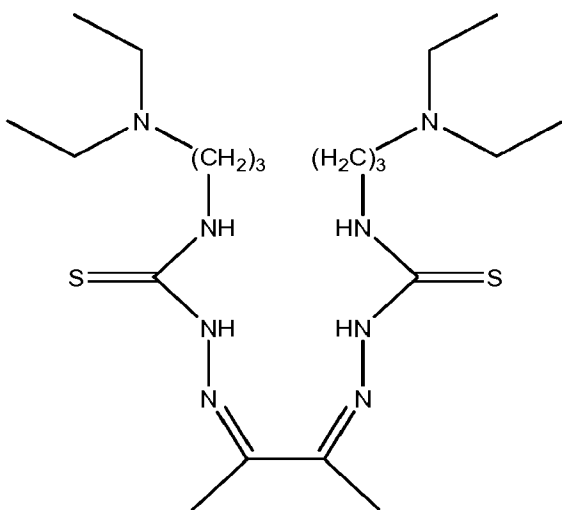
targeted liposome wherein a targeting moiety is an antibody or a target antigen-binding fragment thereof is called an immunoliposome. In a preferred embodiment, the liposome carrying a targeting moiety, *e.g.*, a ligand, is internalized by a target cell. In yet another embodiment, a targeting moiety is a ligand that specifically interacts with a tyrosine kinase receptor such as, for example, EGFR, HER2, HER3, HER4, PDGFR, VEGFR, FGFR or IGFR receptors. In still another embodiment, the targeting moiety specifically interacts with a growth factor receptor, an angiogenic factor receptor, a transferrin receptor, a cell adhesion molecule, or a vitamin receptor.

In certain embodiments, the liposomes of the liposomal imaging agents exhibit a transmembrane gradient formed by a gradient-forming agent such as a substituted ammonium compound. Alternate loading modalities are described, *e.g.*, in U.S. patent No. 8,147,867. Preferably, the higher concentration of the gradient forming agent is in the interior (inner) space of the liposomes. In addition, a liposome composition disclosed herein can include one or more trans-membrane gradients in addition to the gradient created by the substituted ammonium and/or polyanion disclosed herein. For example, liposomes contained in liposome compositions disclosed herein can additionally include a transmembrane pH gradient, ion gradient, electro-chemical potential gradient, and/or solubility gradient.

It will be appreciated that when a trapping agent is used, excess gradient forming agent can be removed from the liposomes (*e.g.*, by diafiltration) after the metal chelator moiety has been entrapped within the liposome.

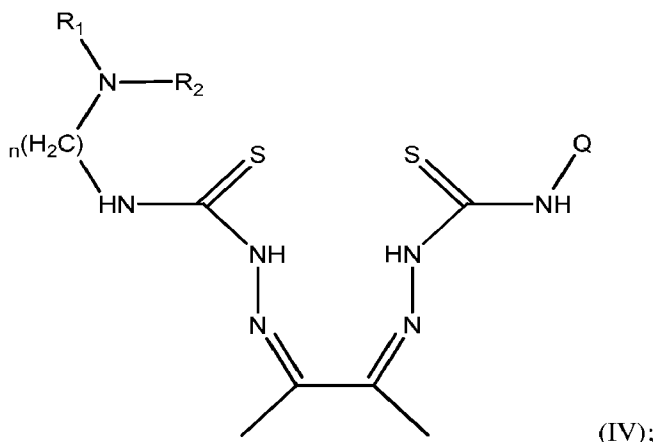
#### Metal chelator

The metal chelating moiety of the liposomal imaging agent can be any agent capable of stably chelating a divalent metal cation and being retained in the interior of the liposome. Examples of such metal chelating moieties include the compound:



Additional examples of suitable chelators include compounds represented by Formula (IV):





in which

Q is H, substituted or unsubstituted C<sub>1</sub>-C<sub>6</sub>alkyl or -(CH<sub>2</sub>)<sub>n</sub>-NR<sub>3</sub>R<sub>4</sub>;

R<sub>1</sub>, R<sub>2</sub>, R<sub>3</sub> and R<sub>4</sub> are each independently selected from H, substituted or unsubstituted C<sub>1</sub>-  
 5 C<sub>6</sub>alkyl, or substituted or unsubstituted aryl or wherein either or both of (1) R<sub>1</sub> and R<sub>2</sub> and (2) R<sub>3</sub> and R<sub>4</sub> are joined to form a heterocyclic ring;

M is a metal ion,

and

n is independently, for each occurrence, an integer from 1 to 5.

#### 10 Divalent metal cation

In some embodiments the metal ion is a divalent metal cation. The metal cation for use in the liposomal imaging agents disclosed herein can be any suitable divalent metal cation, *e.g.*, of the alkaline earth, transition metal, lanthanide, or actinide series. A divalent metal cation can be selected according to the intended use of the liposomal imaging agent.

15 For example, for use in positron emission tomography (PET scanning), a positron-emitting radioisotope (such as a divalent ion of <sup>44</sup>Sc<sup>2+</sup>, <sup>64</sup>Cu<sup>2+</sup>, <sup>110</sup>In<sup>2+</sup> or <sup>128</sup>Cs<sup>2+</sup>) can be employed. In certain embodiments, the divalent metal cation is <sup>64</sup>Cu<sup>2+</sup>.

Alternatively, the divalent metal cation can be a metal cation capable of providing contrast when deposited within a cell or organ (*e.g.*, Au<sup>2+</sup> or Ag<sup>2+</sup>).

20

#### Preparation of liposomal imaging agents

Gradient-based drug loading technologies, in which electrochemical gradients drive the accumulation of drugs in the liposome interior, can be used to prepare liposomes according to the present invention. Thus, a liposome having an electrochemical gradient between the interior and the exterior of the lipid bilayer can be loaded with cationic chelation complexes of divalent metals by  
 25 addition of the cationic chelator complex to the liposome preparation.

Thus, a transmembrane gradient system can comprise a polymeric anionic trapping agent (such as polyphosphate) or a nonpolymeric anionic trapping agent (sucrose octasulfate). The use of

polymeric polyanions such as heparin or dextran sulfate to improve liposomal drug retention has also been reported. However, polyanionic polymers such as heparin and dextran sulfate have notable anticoagulant activity and, thus, heparin and dextran sulfate are less preferred. In many instances, sucrose octasulfate provides better retention of a cationic moiety than polyanionic polymers, resulting in good encapsulation stability. Sucrose octasulfate is a known pharmaceutical ingredient, *e.g.*, of the basic aluminum salt (sucralfate). Advantageously, sucrose octasulfate is chemically well defined, does not have known anticoagulant or anti-macrophage activity, and its salts can be produced in pure crystalline form.

In general, liposomes can be prepared according to any method known in the art. Methods of making and loading liposomes are known in the art. For example, U.S. Patent No. 4,192,869, describes a method for creating synthetic lipid vesicles loaded with inositol hexaphosphate (IHP). Other methods for producing nanoparticles/liposomes are known to one of skill in the art (see, *e.g.*, U.S. Patent Application Nos. 20030118636; 20080318325; and 20090186074 and U.S. Patent Nos 4,192,869; 4,397,846; 4,394,448; 4,394,149; 4,241,046; 4,598,051; 4,429,008; 4,755,388; 4,911,928; 6,426,086; 6,803,053; and 7,871,620.

Alternatively, a liposome can be loaded with a chelator moiety (*i.e.*, without a metal cation complexed to the chelator moiety), followed by addition of the divalent metal cation to the liposomal formulation. In one embodiment, the intraliposomal pH is adjusted so that <sup>64</sup>Cu enters the lipid bilayer and forms a complex with the chelator inside the liposome.

## Diagnostics

The present invention provides methods of patient stratification or determination of the suitability of a patient for a candidate liposome-based therapy. The invention also provides a method of determining whether a patient is a candidate for therapy with a liposomal therapeutic agent, the method comprising:

- (a) injecting the patient with a liposomal imaging agent;
- (b) imaging the patient to determine the distribution of the liposomal imaging agent within the body of the patient; and
- (c) determining that the patient is a candidate for therapy with the liposomal therapeutic agent if the liposomal imaging agent is distributed to a location within the body of the patient in need of the liposomal therapeutic agent.

In another aspect, the invention provides a method of monitoring treatment of a location within the patient by a liposomal therapeutic agent, the method comprising:

- (a) injecting the patient with a liposomal imaging agent liposomal imaging agent; and
- (b) imaging the patient, wherein a treatment that reduces or eliminates distribution of the liposomal imaging agent to the location within the patient is identified as effective.

In general, the liposomal imaging agents disclosed herein may be used to image a variety of neoplasias including, but not limited to, fibrosarcoma, myxosarcoma, liposarcoma, chondrosarcoma, osteogenic sarcoma, chordoma, angiosarcoma, endotheliosarcoma, lymphangiosarcoma, lymphangioendotheliosarcoma, synovioma, mesothelioma, Ewing's tumor, leiomyosarcoma, rhabdomyosarcoma, colon carcinoma, breast cancer, ovarian cancer, prostate cancer, squamous cell carcinoma, basal cell carcinoma, adenocarcinoma, sweat gland carcinoma, sebaceous gland carcinoma, papillary carcinoma, papillary adenocarcinomas, cystadenocarcinoma, medullary carcinoma, bronchogenic carcinoma, renal cell carcinoma, hepatoma, bile duct carcinoma, choriocarcinoma, seminoma, embryonal carcinoma, Wilm's tumor, cervical cancer, uterine cancer, testicular cancer, lung carcinoma, small cell lung carcinoma, bladder carcinoma, epithelial carcinoma, glioma, glioblastoma multiforme, astrocytoma, medulloblastoma, craniopharyngioma, ependymoma, pinealoma, hemangioblastoma, acoustic neuroma, lymphoma, oligodendroglioma, schwannoma, meningioma, melanoma, neuroblastoma, and retinoblastoma.

In another embodiment, liposomal imaging agents may be used to image vascular damage caused by a variety of infectious agents including, but not limited to, bacteria, fungi, and viruses. Likewise, the liposomal imaging agents may be used to monitor a patient during treatment for vascular disorders such as hand-foot syndrome (also known as palmar-plantar erythrodysesthesia (PPE), plantar palmar toxicity, palmoplantar keratoderma, and cutaneous toxicity), which is a side effect of some chemotherapy drugs. Hand-foot syndrome results when a small amount of an anti-neoplastic agent leaks out of the smallest blood vessels in the palms of the hands and soles of the feet. The amount of drug in the capillaries of the hands and feet increases due to the friction and subsequent heat that is generated in those extremities. As a result, more drug may leak out of capillaries in these areas. Once out of the blood vessels, the chemotherapy drug damages surrounding tissues. Liposomal imaging agents may be used to image such damage and treatment of the patient can be adjusted accordingly, either by adjusting the dose of drug or by increasing adjunctive therapies such as administration of anti-inflammatory therapeutics. Liposomal imaging agents may also be used to predict those patients who are most likely to experience such side effects and prophylactic adjunctive therapies may be employed.

The quantity of liposome composition necessary to image a target cell or tissue can be determined by routine *in vitro* and *in vivo* methods. Safety testing of such compositions will be analogous to those methods common in the art of drug testing. Typically the dosages for a liposome composition disclosed herein ranges between about 0.0007 and about 10 mg of the liposomes per kilogram of body weight. In an exemplary embodiment, the dosage is about 0.0007 mg of the liposomes per kilogram of body weight.

Typically, the liposome pharmaceutical composition disclosed herein is prepared as a topical or an injectable, either as a liquid solution or suspension. However, solid forms suitable for solution in, or suspension in, liquid vehicles prior to injection can also be prepared.

The liposome composition disclosed herein can be administered in any way which is medically acceptable which may depend on the neoplasia being imaged. Possible administration routes include injections, by parenteral routes such as intramuscular, subcutaneous, intravenous, intraarterial, intraperitoneal, intraarticular, intraepidural, intrathecal, or others, as well as oral, nasal, ophthalmic, rectal, vaginal, topical, or pulmonary, *e.g.*, by inhalation. The compositions may also be directly applied to tissue surfaces.

### Kits

The present invention provides kits for use in the diagnostic methods described herein.

In one aspect, the invention provides a kit for determining whether a patient is a candidate for therapy with a liposomal therapeutic agent, the kit comprising:

- (a) a container comprising a divalent metal chelating moiety;
- (b) a preparation of liposomes in a pharmaceutically acceptable medium, said liposomes having an interior space and a membrane separating said interior from said medium, said interior space comprising a solution having an electro-chemical gradient relative to the pharmaceutically acceptable medium; and
- (c) instructions for
  - (i) combining the divalent metal chelating moiety with a divalent metal to form a solution of a divalent metal complexed with a divalent metal chelating moiety;
  - (ii) combining the solution of the divalent metal complexed with a divalent metal chelating moiety with the preparation of liposomes, under conditions such that a liposomal imaging agent is prepared; and
  - (iii) administering the liposomal imaging agent to the patient for determining whether the patient is a candidate for therapy with the liposomal therapeutic agent.

In general, the kits are provided so that a technician can prepare a liposomal imaging agent on site before administration to a patient. Thus, the kits will generally include at least a container comprising divalent metal chelating moiety (which can be solution of the divalent metal chelating moiety); a preparation of liposomes in a pharmaceutically acceptable medium; and instructions for combining the divalent metal chelating moiety with a divalent metal to form a solution of a divalent metal complexed with a divalent metal chelating moiety, and combining the solution of the divalent metal complexed with a divalent metal chelating moiety with the preparation of liposomes, under conditions such that a liposomal imaging agent is prepared. If the divalent metal cation is a radioisotope having a short half-life, the kits allow the technician to prepare the liposomal imaging agent immediately before administration of the liposomal imaging agent to the patient. If the divalent

metal cation is a stable isotope, then the kit may optionally further include a container comprising the divalent metal cation. Alternatively, if the divalent metal cation is a stable isotope, then the kit may comprise a solution of the divalent metal already complexed with the divalent metal chelating moiety.

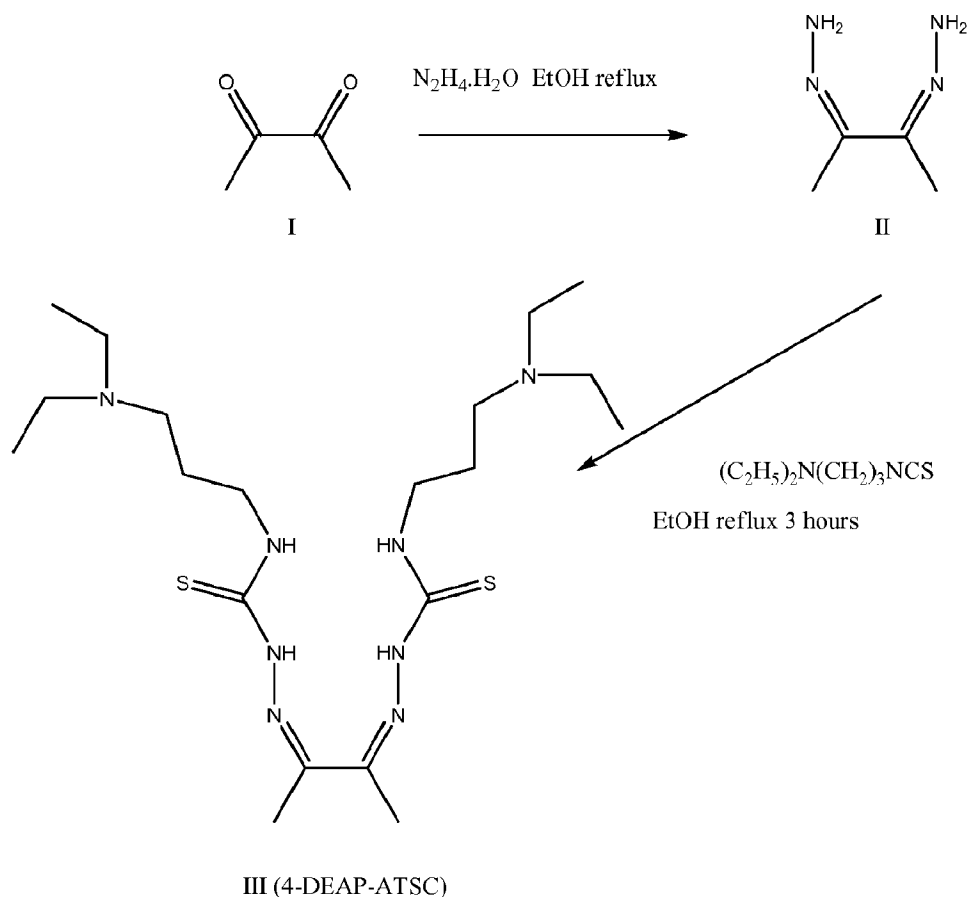
5           The following examples are put forth so as to provide those of ordinary skill in the art with a complete disclosure and description of how to make and use the assay, screening, and therapeutic methods described herein, and are not intended to limit the scope of what the inventors regard as their invention.

10

### EXAMPLES

**Example 1: Preparation of diacetyl 4,4'bis (3-(N,N-diethylamino)propyl)thiosemicarbazone (4-DEAP-ATSC)**

15           Figure 1 shows the chemical structure of diacetyl 4,4'bis (3-(N,N-diethylamino)propyl)thiosemicarbazone (4-DEAP-ATSC), as well as the structure of 4-DEAP-ATSC complexed with  $^{64}\text{Cu}$ . The chelator 4-DEAP-ATSC can be prepared via a two-step synthesis as shown in Scheme 1:



Scheme 1

*Step 1. Synthesis of diacetyldihydrazone*

- 5           The synthesis of diacetyldihydrazone was performed according to the general method described by Busch, D.II. and Bailar, J.C. Jr. (*J.Am. Chem. Soc.*, v. 78, p. 1137-1142, 1956).
- 10           In a 100-ml round flask with a heating mantle, magnetic stir bar, straight reflux condenser, and a drip funnel attached to the top of the condenser, 60 mL of 200 proof reagent ethanol and 7.7 ml (7.9 g) of hydrazine hydrate (Sigma-Aldrich) were added. The solution was brought to boiling with stirring and reflux, and from the funnel, 5 ml of butane-2,3-dione (diacetyl, I) (Sigma-Aldrich) was added at the rate of about 1 drop in 8 seconds over the course of about 30 minutes, at which point the addition was complete. The reaction mixture was then refluxed for 1 hour, and then 50 ml of distilled water were added. The condenser was changed into distilling position (using a Klaisen-type adapter), and with continuing heating, about 70 ml of the solvent (ethanol) were distilled out at ambient
- 15           pressure (boiling range 80-95°C). The residue was briefly placed on a rotary evaporator, and shortly after applying vacuum, the solution crystallized copiously. After 2 hours in the refrigerator (about 4°C), the crystals were filtered off on a polypropylene frit funnel under suction and air-dried. The yellow product was dissolved in 75 ml of the boiling 200 proof ethanol and allowed to cool down and recrystallized. After an overnight incubation in the refrigerator (about 4°C), the recrystallized product

was filtered off under suction, washed 4 times with 4 ml of cold ethanol, air-dried, and then incubated for 1 hour at 110µm Hg. This synthesis yielded of 4.27g (63% based on the diacetyl) of almost colorless crystals of II, with a calculated molecular weight 114.

5 *Step 2. Synthesis of 4,4-bis-(3-diethylamino)propyl)thiocarbazonc of diacetyl.*

The synthesis of the 4,4-bis-(3-diethylamino)propyl)thiocarbazonc of diacetyl was based on the general procedure for preparing thiosemicarbazones by reaction of diketones with substituted isothiocyanates as described in, for example, French Patent No. 1.528.968, filed May 6, 1967, to Farbwerke Hoechst A.G.

10 The same reflux-addition assembly as in Step 1 was used. 1.171 g of bis-hydrazone of diacetyl were suspended in 10 ml of 200 proof reagent ethanol, brought to boiling, and more ethanol was added until all solids were dissolved (total 18 ml of ethanol). 3.8 ml (3.6 g) of diethylaminopropyl isothiocyanate (Sigma, 97%) were dissolved in 2.5 ml of ethanol and passed through a layer of Celite® 545 filter aid under suction. The Celite® was rinsed 2 times with 2 ml of ethanol, and the rinses were combined with the isothiocyanate solution. This solution was added drop wise at a rate of approximately 1 drop/second to the boiling solution of diacetyl bis-hydrazone, and the reflux was continued for a total of 2.5 hours. The reflux was then changed to distillation, and about 13 ml of ethanol was distilled out. The remaining reaction mixture was chilled on ice, and the reaction product crystallized from the chilled mixture. After 1 hour in the refrigerator (about 4°C) the crystalline precipitate was filtered off with suction on the PP porous plate funnel, washed with 2 times with 4 ml of the cold ethanol, and air dried. Yield of the crude product **III** was 2.05 g as a tan powder.

15 20 25 30  
1.03 g of the crude product **III** was then mixed with 1.5 ml of 3 N HCl and 3 ml of water. Upon addition of 1 drop of 3 N HCl, the solution was clear, with a pH of about 3 (as determined by paper indicator). The solution was filtered through Whatman® No.2 paper filter, and concentrated Na<sub>2</sub>CO<sub>3</sub> was added to raise the pH to about 9.5. The precipitated product was filtered out on a PP funnel, washed 2 times with 2 ml of cold water, briefly air-dried, and the resulting paste was transferred into a 20-ml vial and dissolved in 4 ml of boiling ethanol. Upon chilling, the product crystallized. After 30 minutes on an ice bath, the precipitate was filtered off on the funnel under suction, washed 2 times with 2 ml of cold ethanol, 2 times with 2 ml of anhydrous ether, and dried in vacuum for about 1 hour. This stage of the synthesis yielded 0.701 g, with a calculated molecular weight of 458. Upon addition of a CuSO<sub>4</sub> solution to the aqueous solution of III, a yellow-brown color (tea-like) develops, which signifies the formation of the copper complex. Addition of copper sulfate solution to the aqueous solution of **II** produces a complex having a green color.

35 *Synthesis of ATSM*

For comparison, diacetyl 4-methylthiosemicarbazone (ATSM) was synthesized essentially as described in Gingras, et al., *Can. J. Chem.*, v. 40, p. 1053-1059, 1962. First, 0.087 ml (86 mg,

d=0.990, 1 mMol) of diacetyl were dissolved in 5 ml of ethanol. 0.21 g of 4-methylthiosemicarbazone (Sigma-Aldrich) was then dissolved in 5 ml of water and 0.4 ml glacial acetic acid, and added to the diacetyl solution with stirring at about 40°C. In about 1 minute crystalline precipitate began to form. After stirring for 1 hour at room temperature the reaction mix was placed in the refrigerator (about  
5 4°C) overnight. The next day the precipitate was filtered off on the PP frit funnel under suction, washed 2 times with 3 ml water, 2 times with 3 ml ethanol, 1 time with 3 ml acetone (it was observed that the precipitate partially dissolved at this stage), and air-dried. After additional drying in 110 µm Hg vacuum for 30 minutes, the yield was 0.1934 g (74% theory) with a molecular weight of 260 (calculated). The structure of ATSM complexed with <sup>64</sup>Cu is shown in Figure 2.

10

### Example 2: Preparation of a liposomal imaging agent

A liposomal imaging agent was prepared for injection by combining three components (*e.g.*, in the radiopharmacy):

1. <sup>64</sup>Cu, supplied as a radiochemical (*e.g.*, from Washington University);
- 15 2. The chelator 4-DEAP-ATSC (*e.g.*, from Albany Molecular Research, Inc. (Albany, NY, or prepared as described herein); and
3. Excipient liposomes (*i.e.*, liposomes not containing chelated <sup>64</sup>Cu).

These components were sequentially combined to prepare a liposomal imaging agent for clinical use, according to a two-step procedure (see Figure 3). In the first step, uncomplexed <sup>64</sup>Cu  
20 supplied in 0.1 M HCl as a radiochemical was added to a pH-buffered solution containing the chelating agent, 4-DEAP-ATSC, to prepare complexed <sup>64</sup>Cu:4-DEAP-ATSC. Figure 1 shows the chemical structures of the uncomplexed and complexed chelating agent. In one embodiment, chelation of <sup>64</sup>Cu to 4-DEAP-ATSC is facilitated by heating the mixture briefly at 65°C with subsequent cooling in an ice water bath. In another embodiment, chelation of <sup>64</sup>Cu to 4-DEAP-ATSC  
25 is performed at room temperature (22-25°C). Figure 4 shows the schematic of the reaction in which a molar excess of the chelator is reacted with the <sup>64</sup>Cu. In the second step, the chelated <sup>64</sup>Cu solution is then added through a 0.2µm filter to PEGylated liposomes prepared with a chemical gradient that enables >90% loading of the <sup>64</sup>Cu:4-DEAP-ATSC into the liposomes to create liposomal imaging agent. Figure 5 shows a schematic of the liposomal loading depicting complexed and uncomplexed  
30 chelator entering the excipient liposomes, which contain an ammonium sulfate pH gradient. As indicated in Figure 5, the two chelator species become positively charged after they pick up a proton from the ammonium ion and become trapped in the liposome while the free uncharged ammonia is able to exit the liposome.

35 *Preparing 4-DEAP-ATSC solution for testing using radiometals.*

In a 1-dr glass vial with PTFE-lined screw cap, 16.9 mg of 4-DEAP-ATSC (Example 1) was dissolved in 1.85 ml DMSO, and 24 µl of 3 N HCl was added, yielding a solution with a final



concentration of 4-DEAP-ATSC of 20 mM. The solution, at first yellow, turned colorless upon addition of the acid. Alternatively, 4-DEAP-ATSC solution can also be prepared in the absence of DMSO for in vivo study purposes. In one example, 10 mg of 4-DEAP-ATSC was dissolved in 1 mL of 0.05 M citric acid (10 mg/mL final concentration of 4-DEAP-ATSC). The concentrated solution  
5 can then be diluted into other pH-buffered solutions (e.g., 0.02 – 0.1M citrate buffer, pH 5-8) at desired concentrations for use.

*Validation of loadability of Cu-III into gradient-bearing liposomes*

To test the loadability of Cu-III in gradient-bearing liposomes, the following working solutions were prepared:

- 10 1. 20 mM CuSO<sub>4</sub> in water; 5.0 mg/ml of CuSO<sub>4</sub>·5H<sub>2</sub>O in distilled water; 16.7 mg CuSO<sub>4</sub>·5H<sub>2</sub>O dissolved in 3.34 ml distilled H<sub>2</sub>O.
- 15 2. 20 mM DEAPATSC (III): 9.16 mg/ml DEAPATSC in DMSO + equivalent amount of 3N HCl to titrate the free base of III into dihydrochloride. (Free base solution is yellow, dihydrochloride almost colorless.) 28.2 mg of III dissolved in 3.08 ml DMSO (Aldrich 471267 lot 52596AK), and  
15 added 43 µl of 3 N HCl.
3. 20 mM ATSM 5.2 mg/ml in DMSO. 14.8 mg dissolved in 2.84 ml DMSO.
4. 10 mM histidine-100 g/L sucrose buffer, pH 6.5 (HS buffer). In a tared, dry 250-ml volumetric flask, Sucrose (Sigma) 25.03 g (theory, 25 g) and L-Histidine USP (Spectrum Chemicals) 0.3867 g (theory 0.388 g) were added, and then distilled water added, the Sucrose and L-Histidine  
20 were dissolved and brought to the 250-ml mark. The volumetric flask was then weighed, and the solution weight was 259.0 g. The calculated density was 1.036, based on the weight of the water being 233.6 g. The solution was transferred into a beaker, and the pH was adjusted to 6.50 with 1 drop of concentrated HCl and 3 drops of 3 N HCl. The solution was filtered using SteriTop®/SteriCup® 250 ml, 0.22 µm, under vacuum.
- 25 5. Liposomes: HSPC-Chol-PEG(2000)DSPE (3:1:0.05 molar ratio) liposomes were prepared by extrusion of the ethanol-injected MLVs at 100 mM HSPC in a 10 vol% ethanol/90 vol% 250 mM (NH<sub>4</sub>)<sub>2</sub>SO<sub>4</sub> and 65°C via 1x200nm and 6x100 nm stacked PCTE membranes 2 times.

*Cu<sup>2+</sup> complexation and loading into ammonium-gradient liposomes.*

Gradient-bearing liposomes were created as follows. A fresh PD-10 column with Sephadex  
30 G25M was equilibrated with 2 CV of HS buffer. One ml of HSPC-Chol-PEG(2000)DSPE (3:1:0.05 molar ratio) liposomes (see above) was applied and eluted with HS. The liposome fraction was collected between 3 and 5.5 ml, and adjusted to 7.5 ml with HS, resulting in approximately 12.5 mM phospholipid.

Cu:4-DEAP-ATSC and Cu:ATSM complexes were formed as follows. In 1 mL HS were  
35 added 5 µL of 20 mM CuSO<sub>4</sub> and 5 µl of 20 mM 4-DEAP-ATSC (in DMSO) or 5 µL of 20 mM ATSM (in DMSO). The ATSM sample became turbid and developed a brown precipitate. The 4-

DEAP-ATSC sample developed a yellow-brown color, but remained clear, without any signs of precipitation. The chelator and Cu concentration was 0.1 mM.

2 mM working solution of 4-DEAP-ATSC-Cu was prepared as follows. 0.8 ml of HS, 0.1 mL of 20 mM 4-DEAP-ATSC solution, and 0.1 mL 20 mM CuSO<sub>4</sub> solution were mixed, heated for 1 minute at 60°C, and cooled to ambient room temperature. A yellow-brown solution was obtained.

The liposomes were loaded as follows. 0.5 mL of the gradient-bearing liposomes (step 1 above) were mixed with 0.1 ml of 2 mM DEAP-ATSC-Cu chelate and heated in a water bath at 60°C for 5 minutes, and then chilled on ice. The liposomes were applied on a PD-10 column equilibrated with HS buffer. All visibly detectable color of Cu:DEAP-ATSC complex was eluted in the void volume fraction (between 3 and 4.5 ml). This fraction was collected and saved. These results show that the Cu:DEAP-ATSC was effectively loaded into the ammonium-gradient bearing liposomes.

Chromatography of Cu:4-DEAP-ATSC complex on a PD-10 column (Sephadex G25). 0.1 ml of 2 mM DEAP-ATSC-Cu was diluted with 0.5 mL of HS buffer and chromatographed on a PD-10 column as above. The complex moves as a clearly visible yellow-brown band, and begins to appear in the eluate at about 10 ml (full column bed volume) and eluted in approximately 3.5 ml.

When prepared in the radiopharmacy, the liposomal imaging agent is a sterile, injectable parenteral liquid formulation of long-circulating nanoliposomes containing <sup>64</sup>Cu. The unilamellar liposome particles have an average size in the range of 75-100 nm, and consist of a bilayer membrane composed of fully hydrogenated soy phosphatidylcholine (HSPC), cholesterol, and a small amount of poly(ethylene glycol)(Mol. weight 2000)-derivatized distearoylphosphatidylethanolamine (PEG-DSPE). The liposome membrane encloses an interior space where the chelated <sup>64</sup>Cu is contained. A schematic representation of the liposomal imaging agent is shown in Figure 6. The liposomal imaging agent contains no pharmacologically active pharmaceutical ingredient. In addition to the <sup>64</sup>Cu, it contains 10.2 mg/mL of HSPC, 3.39 mg/ml of cholesterol, 0.18 mg/mL of methoxy-terminated polyethylene glycol (MW2000)-distearoylphosphatidylethanolamine (PEG-DSPE), 10 mM Hepes buffer (pH 6.5), 150 mM sodium chloride to maintain isotonicity, ammonium sulfate in a concentration of less than 0.8 mg/mL, sodium sulfate in a concentration of less than 0.8 mg/mL, and sodium citrate in a concentration of less than 1.5 mg/ml.

### Example 3: 4-DEAP-ATSC chelates <sup>64</sup>Cu and is loaded into a liposome

The following data demonstrate the ability of 4-DEAP-ATSC to chelate <sup>64</sup>Cu and to be subsequently loaded into a liposome according to the steps described in Figure 3.

Under conditions outlined in an exemplary radiopharmacy protocol, 109 nmol of 4-DEAP-ATSC was used to chelate 20 millicuries (mCi) of <sup>64</sup>Cu for 1 minute at 65°C, resulting in a targeted specific radioactivity of approximately 0.2 mCi/nmol. An instant thin layer chromatography (ITLC) assay was used for quantifying the fractions of uncomplexed <sup>64</sup>Cu and <sup>64</sup>Cu(II)-4-DEAP-ATSC

complex in the chelation mixture. The uncomplexed <sup>64</sup>Cu can be detected at the solvent front, while the <sup>64</sup>Cu(II)-4-DEAP-ATSC complex remained at the origin where the sample is spotted.

Using the ITLC assay described above (Figure 7), the efficiency of chelation has been observed to be in the range of 94-99% for preparations of <sup>64</sup>Cu with specific radioactivities ranging from 0.07-0.3 mCi/nmol (see Table 1).

**Table 1. Chelation Efficiencies of 4-DEAP-ATSC in Step 2 for <sup>64</sup>Cu Preparations.**

Specific Radioactivity (mCi/nmol)	Chelation Efficiency
0.01	11-46%
0.04	98%
0.07	68-97%
0.08	99%
0.09	99%
0.1	99-100%
0.15	98-99%
0.17	96%
0.18	94%
0.2	96-99%
0.3	98%
0.65	99%
13.1	99%

More generally, the key components to prepare the liposomal imaging agent can be combined according to the steps outlined in Figure 3. Prior to beginning the labeling procedure, the following preparation steps should be followed: Prepare heat bath @ 65°C and an ice water bath. Add contents of the <sup>64</sup>Cu vial to the chelator vial. Place <sup>64</sup>Cu-chelator vial either in a 65°C heat bath for 1 min or incubate at room temperature for 1 min. Cool to room temp using ice bath if heated. Transfer the entire contents to the liposome vial, *e.g.*, with a filtration syringe. Place the liposome vial in 65°C heat bath for 10 min and then cool to room temp with the ice bath. A sample is taken to check loading efficiency.

**Example 4: Efficiency of <sup>64</sup>Cu loading into liposomes**

The efficiency of liposome loading for Step 2 (see Figure 3) was determined. Liposomes were loaded with <sup>64</sup>Cu:4-DEAP-ATSC over a range of 4-DEAP-ATSC:lipid ratios of 0.013 – 4.2 mole%. Encapsulated (liposomal) radioactivity was separated from total radioactivity using size exclusion chromatography. From this it was determined that >90% of the <sup>64</sup>Cu was loaded into the liposome at 4-DEAP-ATSC:lipid ratios < 2 mol% as shown in Table 2. From these data, the 4-DEAP-ATSC to lipid ratio was chosen to be 0.07 mol%.

**Table 2. Efficiency of  $^{64}\text{Cu}$  Loading into Liposomes as a Function of Varying Chelator to Lipid Ratios.**

<b>4-DEAP-ATSC:Lipid Ratio (mol%)</b>	<b><math>^{64}\text{Cu}</math> Loading Efficiency</b>
0.01%	96-98%
0.04%	96-98%
0.10%	95-97%
0.15%	92-97%
0.25%	92-97%
0.40%	94-98%
0.50%	92-96%
0.67%	96%
0.75%	92%
1%	93-98%
2%	91-97%
4.20%	86%
5.00%	92-93%
10%	82-92%
25%	90%
50%	71%

In an exemplary embodiment,  $^{64}\text{Cu}$  meets the specifications shown in Table 3.

5 **Table 3:  $^{64}\text{Cu}$  radioisotope purity**

<i>Identity</i>	<i>Purity</i>
$^{55}\text{Co}$	<0.176%
$^{60}\text{Cu}$	n/a
$^{61}\text{Co}$	<6.600%
$^{61}\text{Cu}$	<0.550%

Radionuclide purity is assessed by the measurement of  $^{40}\text{K}$ ,  $^{55}\text{Co}$ ,  $^{56}\text{Co}$ ,  $^{57}\text{Co}$ ,  $^{58}\text{Co}$ ,  $^{60}\text{Co}$ , and  $^{67}\text{Ga}$ , as indicated on their Certificates of Analysis.  $^{64}\text{Cu}$  in 0.1 M HCl is provided in a plastic vial with volumes 20 to 100  $\mu\text{L}$  and specific activity of 50-400 mCi/ $\mu\text{g}$ .

10

#### **Example 5: Lipid components**

The liposomes described herein can be formed using a variety of lipid components. The structures of representative lipids are shown Figure 8. The selection of lipids is not meant to be limiting.

Table 4 shows the composition of the liposomal excipients and the composition of the excipient liposomes for the 10 mL solution in the final container (Excipient Liposome in Figure 3).

**Table 4. Qualitative and Quantitative Composition of the Liposomal Excipients**

Component	Concentration, mg/mL	Concentration, mg/vial (10 mL)
HSPC	10.2	102
Cholesterol	3.4	34
PEG-DSPE	0.18	1.8
Sodium chloride	8.77	87.7
Hepes	2.38	23.8
Ammonium sulfate	< 0.8	< 8
Sodium sulfate	< 0.8	< 8
Sodium Hydroxide	For pH adjustment	For pH adjustment
Water for Injection	QS to 1.0 mL	QS to 10.0 mL

5 Table 5 shows the functions of the components in the liposomal excipient.

**Table 5. Functions of the Components in the liposomal excipient**

Component	Function
HSPC	Lipid
Cholesterol	Lipid
PEG-DSPE	Lipid
Hepes	Buffer
Sodium Chloride	Isotonicity
Ethanol*	Solvent for lipids
Ammonium sulfate**	drug loading and trapping agent
Sodium sulfate **	osmolarity adjusting agent
NaOH, HCl	pH adjustment

\*removed by diafiltration

\*\*extraliposomal ammonium sulfate and sodium sulfate removed during diafiltration

10 Other excipient liposome formulations comprised of different lipid components and loading gradients have been prepared for loading of  $^{64}\text{Cu}$ :4-DEAP-ATSC. The liposome compositions and loading efficiencies of samples stored at 4°C (Table 6) and at 4°C, 30°C, and 37 °C (Table 7) are listed below:

**Table 6: Liposome compositions and loading efficiencies**

Sample	Lipid Composition	External pH	Loading Gradient	Loading Efficiency (samples stored at 4°C) (%)
D1	DSPC:Cholesterol:PEG-DSPE (3:1:1 wt ratio)	6.5	50 mM Ammonium Sulfate + 50 mM Sodium Sulfate	96%
D2	DSPC:Cholesterol:PEG-DSPE (3:1:1 wt ratio)	6.5	125 mM Ammonium Sulfate	97%
D3	DSPC:Cholesterol:PEG-DSPE (3:1:1 wt ratio)	6.5	250 mM Ammonium Sulfate	97%
D4	DSPC:Cholesterol:PEG-DSPE (3:1:1 wt ratio)	7.2	0.142 N Triethylammonium Sucrose Octasulfate	96%
D5	DSPC:Cholesterol:PEG-DSPE (3:1:1 wt ratio)	7.2	0.215 N Triethylammonium Sucrose Octasulfate	96%
D5	DSPC:Cholesterol:PEG-DSPE (3:1:1 wt ratio)	7.2	0.43 N Triethylammonium Sucrose Octasulfate	96%
SM1	Sphingomyelin:Cholesterol:PEG-DSPE (3:1:1 wt ratio)	6.5	50 mM Ammonium Sulfate + 50 mM Sodium Sulfate	97%
SM2	Sphingomyelin:Cholesterol:PEG-DSPE (3:1:1 wt ratio)	6.5	125 mM Ammonium Sulfate	97%
SM3	Sphingomyelin:Cholesterol:PEG-DSPE (3:1:1 wt ratio)	6.5	250 mM Ammonium Sulfate	97%
SM4	Sphingomyelin:Cholesterol:PEG-DSPE (3:1:1 wt ratio)	7.4	50 mM Ammonium Sulfate + 50 mM Sodium Sulfate	98%
SM5	Sphingomyelin:Cholesterol:PEG-DSPE (3:1:1 wt ratio)	7.4	125 mM Ammonium Sulfate	96%
SM6	Sphingomyelin:Cholesterol:PEG-DSPE (3:1:1 wt ratio)	7.4	250 mM Ammonium Sulfate	97%
SM7	Sphingomyelin:Cholesterol:PEG-DSG (3:1:1 wt ratio)	6.5	50 mM Ammonium Sulfate + 50 mM Sodium Sulfate	97%
SM8	Sphingomyelin:Cholesterol:PEG-DSG (3:1:1 wt ratio)	6.5	125 mM Ammonium Sulfate	95%
SM9	Sphingomyelin:Cholesterol:PEG-DSG (3:1:1 wt ratio)	7.4	50 mM Ammonium Sulfate + 50 mM Sodium Sulfate	96%
SM10	Sphingomyelin:Cholesterol:PEG-DSG (3:1:1 wt ratio)	7.4	125 mM Ammonium Sulfate	96%
SM11	Sphingomyelin:Cholesterol:PEG-DSGE (3:1:1 wt ratio)	6.5	50 mM Ammonium Sulfate + 50 mM Sodium Sulfate	96%

SM12	Sphingomyelin:Cholesterol:PEG-DSGE (3:1:1 wt ratio)	6.5	125 mM Ammonium Sulfate	91%
SM13	Sphingomyelin:Cholesterol:PEG-DSPE (3:1:0.5 wt ratio) [PEG-DSPE Inserted post-extrusion]	7.4	50 mM Ammonium Sulfate + 50 mM Sodium Sulfate	94%
SM14	Sphingomyelin:Cholesterol:PEG-DSPE (3:1:0.5 wt ratio) [PEG-DSPE Inserted post-extrusion]	7.4	125 mM Ammonium Sulfate	92%

**Table 7: Liposome compositions and loading efficiencies**

Sample	Lipid Composition	External pH	Loading Gradient	4°C Storage – Loading Efficiencies	30°C Storage – Loading Efficiencies	37°C Storage – Loading Efficiencies
<b>D5</b>	DSPC:Cholesterol:PEG-DSPE (3:1:1 wt ratio)	7.2	0.215 N Triethylammonium Sucrose Octasulfate	96%	95%	N/A
<b>D6</b>	DSPC:Cholesterol:PEG-DSPE (3:1:1 wt ratio)	7.2	0.43 N Triethylammonium Sucrose Octasulfate	96%	95%	N/A
<b>SM4</b>	Sphingomyelin:Cholesterol:PEG-DSPE (3:1:1 wt ratio)	7.4	50 mM Ammonium Sulfate + 50 mM Sodium Sulfate	99%	98%	98%
<b>SM5</b>	Sphingomyelin:Cholesterol:PEG-DSPE (3:1:1 wt ratio)	7.4	125 mM Ammonium Sulfate	97%	98%	96%
<b>SM6</b>	Sphingomyelin:Cholesterol:PEG-DSPE (3:1:1 wt ratio)	7.4	250 mM Ammonium Sulfate	98%	96%	97%
<b>SM7</b>	Sphingomyelin:Cholesterol:PEG-DSG (3:1:1 wt ratio)	6.5	50 mM Ammonium Sulfate + 50 mM Sodium Sulfate	96%	96%	97%
<b>SM8</b>	Sphingomyelin:Cholesterol:PEG-DSG (3:1:1 wt ratio)	6.5	125 mM Ammonium Sulfate	96%	96%	95%
<b>SM9</b>	Sphingomyelin:Cholesterol:PEG-DSG (3:1:1 wt ratio)	7.4	50 mM Ammonium Sulfate + 50 mM Sodium Sulfate	96%	97%	96%
<b>SM10</b>	Sphingomyelin:Cholesterol:PEG-DSG	7.4	125 mM Ammonium	97%	96%	96%

	(3:1:1 wt ratio)		Sulfate			
SM11	Sphingomyelin:Cholesterol: PEG-DSGE (3:1:1 wt ratio)	6.5	50 mM Ammonium Sulfate + 50 mM Sodium Sulfate	96%	95%	96%
SM12	Sphingomyelin:Cholesterol: PEG-DSGE (3:1:1 wt ratio)	6.5	125 mM Ammonium Sulfate	90%	91%	91%
SM13	Sphingomyelin:Cholesterol: PEG-DSPE (3:1:0.5 wt ratio) [PEG-DSPE Inserted post- extrusion]	7.4	50 mM Ammonium Sulfate + 50 mM Sodium Sulfate	96%	96%	94%
SM14	Sphingomyelin:Cholesterol: PEG-DSPE (3:1:0.5 wt ratio) [PEG-DSPE Inserted post- extrusion]	7.4	125 mM Ammonium Sulfate	96%	95%	92%

#### Example 6: Use of $^{64}\text{Cu}$ :4-DEAP-ATSC in untargeted liposomal imaging agents

As described herein, in one embodiment, the liposomal imaging agent is an untargeted liposome containing entrapped chelator (4-DEAP-ATSC) and a  $^{64}\text{Cu}$  chelation complex ( $^{64}\text{Cu}$ :4-DEAP-ATSC) (herein after, "Liposome A"). 4-DEAP-ATSC is derived from the ATSM structure by adding two diethylamino(propyl) groups (compare structures in Figures 1 and 2).  $^{64}\text{Cu}$ -ATSM (see structure in Figure 2) is currently being clinically tested as a PET imaging agent in cancer patients. 4-DEAP-ATSC is similar to ATSM in that it retains the  $^{64}\text{Cu}$  chelating activity of ATSM; however, it has the unexpected property of being rapidly entrapped within PEGylated liposomes containing a chemical gradient, thereby creating a liposomal imaging agent, as described above.

#### Example 7: Effect of liposome targeting on tumor deposition

Preclinical studies have examined the effect of liposome targeting on total tumor deposition. These studies have shown that the targeting of PEGylated liposomes to the HER2 receptor on tumors did not affect its pharmacokinetics or overall tumor deposition compared to an untargeted liposome. Kirpotin *et al* labeled liposomes with  $^{67}\text{Ga}$  and showed similar tumor deposition % injected dose per gram (%i.d./g) for a HER2-targeted liposome and a corresponding untargeted liposome (*Cancer Research* (66)6732 (2006). Similar results were obtained by comparing tumor deposition by HER2-targeted Liposome B and untargeted liposomes (disclosed in co-pending Patent Application Serial No. PCT/US2011/064496) in an NCI-N87 (ATCC® #CRL-5822™) gastric carcinoma mouse xenograft model, as well as in BT474-M3 breast carcinoma mouse xenograft model in which the two liposome formulations only result in difference in tumor cell uptake (Figure 25 insert) with no significant difference detected in total liposome deposition in the tumors (Figure 25). Figure 26 further



illustrates that liposome targeting does not have any obvious effect on tumor deposition as no correlation can be established between tumor depositions of Liposome B in tumors with varying HER2 expression. Similarly, in the BT474-M3 tumor model (HER2-overexpressing tumors), the HER2-targeted liposome B were shown to have similar tumor deposition as the non-targeted liposome

5 A

The importance of liposome deposition in dictating total delivery of drug to tumors is also supported by results from kinetic computational modeling. The inventors have developed a physiologically-based pharmacokinetic model of liposome delivery to tumors based on literature data. The model includes liposome and free drug pharmacokinetics, as well as a physiologically-based tumor compartment that captures vascular, interstitial, and cellular spaces.

10

The model was trained on literature data. As shown in Figure 9, a sensitivity analysis of the model indicated that factors related to liposome deposition such as, *e.g.*, vascular surface area and permeability of vasculature to liposomes, are the most important determinants of total delivery of drug to tumor cells.

15

This kinetic model was adapted to create a model of Liposome A deposition in tumors. As shown in Figure 10, the model simulated profiles of Liposome A concentration in plasma, tumor vasculature, and tumor interstitium. This model allowed estimation of the fraction of total tumor signal expected to arise from deposited (interstitial) liposomes vs. liposomes in the tumor vascular space. Furthermore, it also allowed simulation of the effect of  $^{64}\text{Cu}$  decay on signal (Figure 10B), as well as the anticipated variability across patients (Figure 10C), based on patient data from Harrington, *et al.*, *Clin. Cancer Res.* (2001) Feb;7(2):243-54. Variability in tumor deposition was also observed across multiple preclinical xenograft models with Liposome B (Figure 26), as well as other  $^{64}\text{Cu}$ -loaded liposomes.

20

#### 25 **Example 8: *In vitro* stability of $^{64}\text{Cu}$ :4-DEAP-ATSC-loaded liposome (Liposome A) in human plasma**

$^{64}\text{Cu}$  was shown to be effectively retained in the liposome after incubation of  $^{64}\text{Cu}$ :4-DEAP-ATSC-loaded liposome (Liposome A) in human plasma for 48 hours (Figure 11). The *in vitro* stability of Liposome A was examined by incubating the  $^{64}\text{Cu}$ :4-DEAP-ATSC-loaded liposome with human plasma at 37°C. At the designated incubation time (up to 48 hours), encapsulated (liposomal) radioactivity was separated from released/unencapsulated radioactivity using size exclusion chromatography (CL4B column which allows for separating liposomal, protein, and  $^{64}\text{Cu}$ :4-DEAP-ATSC/uncomplexed  $^{64}\text{Cu}$  fractions). The data show that Liposome A is highly stable in human plasma at physiological temperature, with < 5% of unencapsulated  $^{64}\text{Cu}$  detected up to 48 hours.

30

#### 35 **Example 9: *In vivo* imaging of $^{64}\text{Cu}$ -loaded Liposome B**

Figure 12 shows the process by which PET-CT fusion images are generated by registration of a CT-image with a PET-image. The ability to image  $^{64}\text{Cu}$ -loaded liposomes was shown using  $^{64}\text{Cu}$ -loaded Liposome B. PET/CT imaging was performed in BT474-M3 tumor bearing mice (inoculated at mammary fat pad) injected intravenously with Liposome B loaded with  $^{64}\text{Cu}$ :4-DEAP-ATSC. As shown in Figure 13,  $^{64}\text{Cu}$ -loaded Liposome B accumulated mainly in the liver and spleen, as well as in the circulatory system as a result of the long-circulating characteristics of liposome. Significant accumulation of  $^{64}\text{Cu}$ -loaded Liposome B was also detected at the tumor site at 10 and 24 hours post-injection.

#### 10 **Example 10: Pharmacokinetics and biodistribution of Liposome A**

The pharmacokinetics and biodistribution of Liposome A was evaluated in non-tumor bearing CD-1® mice (Charles River Laboratories, Wilmington MA). Mice were injected with one of two batches of Liposome A (100-200  $\mu\text{Ci}/\text{mouse}$ , 20  $\mu\text{mol}$  phospholipid/kg). Blood samples were withdrawn from the saphenous vein at the indicated time points. Plasma concentration of  $^{64}\text{Cu}$  was measured using the gamma-counter (Figure 14A). Data are also included for comparison from pharmacokinetic studies with  $^{64}\text{Cu}$ -loaded Liposome B in CD-1 mice (quantified  $^{64}\text{Cu}$  radioactivity and doxorubicin content), as well as Liposome B administered in NCI-N87 and BT474-M3 mouse xenograft models (quantified doxorubicin content). The pharmacokinetics of Liposome A was shown to be highly reproducible between different batches, and was consistent with plasma clearance profiles of Liposome B, which has similar formulation properties. Biodistribution of Liposome A was studied by quantifying the amount of  $^{64}\text{Cu}$  in different organs using a gamma-counter. The liver, spleen, and kidneys were found to show significant accumulation of Liposome A (Figure 14B).

#### 25 **Example 11: *In vivo* PK and biodistribution of Liposome A compared to uncomplexed $^{64}\text{Cu}$ and $^{64}\text{Cu}$ :4-DEAP-ATSC Complex**

CD-1 mice were injected intravenously with uncomplexed  $^{64}\text{Cu}$  or  $^{64}\text{Cu}$ :4-DEAP-ATSC complex A (100-200  $\mu\text{Ci}/\text{mouse}$ ). As shown in Figure 15A, plasma clearances of uncomplexed  $^{64}\text{Cu}$  and  $^{64}\text{Cu}$ :4-DEAP-ATSC complexes were significantly faster than Liposome A, suggesting that the  $^{64}\text{Cu}$ :4-DEAP-ATSC complexes are stably encapsulated within the excipient liposomes. Biodistribution of Liposome A was evaluated using the same method as in the previous Example. The heart liver, spleen, and kidneys were found to show significant accumulation of Liposome A (Figure 15B).

#### 35 **Example 12: *In vivo* PK and biodistribution of Liposome A compared to other liposomal formulations**

The Her2-targeted liposomal doxorubicin, Liposome B, was loaded with  $^{64}\text{Cu}$ :4-DEAP-ATSC complex using the same protocol as described for Liposome A. Unexpectedly, it was found that the

residual pH gradient in the liposome following loading with doxorubicin was sufficient to induce stable entrapment of the  $^{64}\text{Cu}$ :4-DEAP-ATSC complex within the liposome. Pharmacokinetics of  $^{64}\text{Cu}$ -loaded Liposome B was studied by quantifying both the plasma levels of  $^{64}\text{Cu}$  and doxorubicin using gamma-counter and HPLC, respectively. As shown in Figure 16A, there was no significant  
5 difference between the plasma clearance of  $^{64}\text{Cu}$  and doxorubicin, indicating that the  $^{64}\text{Cu}$ :4-DEAP-ATSC complex is stably entrapped within the liposome *in vivo*. In addition, the plasma clearance of  $^{64}\text{Cu}$ -loaded Liposome B was comparable to the plasma clearance of Liposome B in tumor-bearing mice. Importantly, the pharmacokinetics of Liposome A resembles that of  $^{64}\text{Cu}$ -loaded Liposome B. The biodistribution of Liposome A was also similar to that of  $^{64}\text{Cu}$ -loaded Liposome B in CD-1 mice  
10 (Figure 16B). Importantly, these results suggest that the  $^{64}\text{Cu}$ :4-DEAP-ATSC complex is highly stable within the liposome and is representative of the *in vivo* distribution of the liposome.

Liposome A or Liposome B loaded with  $^{64}\text{Cu}$ :4-DEAP-ATSC was administered intravenously in BT474-M3 tumor bearing mice (inoculated at mammary fat pad). After 48 hours post-injection, tumor accumulations of  $^{64}\text{Cu}$ -loaded Liposome B and Liposome A were found to be approximately  
15 4% injected dose per gram of tissue (i.d./g), similar to that previously reported by Kirpotin *et al.*, as well as data obtained with Liposome B in the BT474-M3 breast cancer and NCI-N87 gastric cancer mouse xenograft tumor models. These results show that  $^{64}\text{Cu}$  remains stably-associated with liposomes for at least 48 hours (Figure 16C). This suggests that 4-DEAP-ATSC provides an effective means for radiolabeling liposomes and is suitable as a PET agent for tracking tumor deposition of a  
20 liposomal imaging agent.

### Example 13: $^{64}\text{Cu}$ :4-DEAP-ATSC toxicity estimates and dose levels

The reference range for copper (Cu) in human blood is 70 – 150  $\mu\text{g}/\text{dL}$  (ATSDR Toxicological Profile for Copper, 2004). Toxic dose levels are estimated to be >10 mg/person/day  
25 (~154  $\mu\text{g}/\text{kg}$ ; 65 kg adult) over several weeks. Liposome A will be dosed at 0.2  $\mu\text{g}/\text{patient}$  (~0.003  $\mu\text{g}/\text{kg}$ ), which is ~51,000 times lower than the potentially toxic repeat dose range for copper. Additionally, all Liposome A associated copper will be chelated and encapsulated prior to administration.

### 30 Example 14: Validating Liposome A as a quantifiable PET agent for accurately measuring liposome biodistribution

Organ uptake of Liposome A in tumor-bearing mice was quantified using volume of interest (VOI)-based analysis of PET images, as well as gamma-counting of the excised organs (*i.e.* traditional biodistribution study). The mice were imaged using PET at 48 hours after injected with Liposome A.  
35 Immediately following imaging the mice were sacrificed for organ collection. Each individual organ was then subjected to gamma-counting for quantifying the amount of radioactivity (*i.e.*  $^{64}\text{Cu}$ ). VOI analyses on the PET images were performed by contouring the organs based on the CT-images

registered on the PET images. As shown in Figure 17, the radioactivity measured for each organ on the PET images correlates well with the radioactivity measured via gamma-counting for the corresponding organs. A similar study was performed on a set of PET images acquired at 18 hours post-injection; the results obtained were in agreement with the aforementioned data set collected at 48  
5 hours post-injection. This demonstrates that biodistribution of Liposome A can be studied via PET scan of subject injected with Liposome A.

**Example 15: Liposome A as a tool for measuring tumor deposition of liposomal drugs**

In order to demonstrate that Liposome A can be used as a tool for measuring the variability of  
10 liposomal drugs in tumors; PET-CT imaging was performed on xenografts bearing two different types of tumor. Mice inoculated with H520 (NSCLC model cell line ATCC® #HTB-182™) and BT474-M3 (breast cancer model cell line, see (see Noble, *Cancer Chemother. Pharmacol.* 2009 64:741-51) cells on the right and left flanks, respectively, were injected with Liposome A. PET-CT imaging was performed at 10 minutes, 6 hours, and 20 hours, post-injection. As shown in Figure 18, at 10 minutes  
15 post-injection, Liposome A was seen mainly in circulation, which is known to be characteristics of long-circulating liposome. At 6 hours post-injection, accumulation of Liposome A was clearly visible in the spleen and liver, along with significant deposition in the H520 tumor. At 20 hours post-injection, accumulation of Liposome A in the H520 and BT474-M3 tumors reached 23% i.d./g and 3% i.d./g according to VOI analysis on the PET images; demonstrating that variability of liposomal  
20 deposition in tumors can be measured using Liposome A and PET imaging. The amounts of tumor deposition of Liposome A in the two tumors were also confirmed via organ excision and gamma-scintillation counting.

**Example 16: <sup>64</sup>Cu loading into drug-containing liposomes (Liposome B, Liposome C)**

Using a similar loading procedure as described above for Liposome A, <sup>64</sup>Cu:4-DEAP-ATSC  
25 has also been successfully loaded into other liposomal formulations that contain chemotherapeutic agents via the residual chemical gradient. Examples of such liposomal formulations include the HER2-targeted doxorubicin-loaded Liposome B, the irinotecan-loaded Liposome C, as well as the commercially available doxorubicin-loaded Doxil®. <sup>64</sup>Cu:4-DEAP-ATSC with chelation efficiency >  
30 90% was mixed with varying amounts of Liposome B, Liposome C, or Doxil®. The mixture was then incubated in a water bath at 65°C for 10 minutes and the loading procedure was subsequently quenched in an ice water bath. Using size exclusion chromatography, it was determined that more than 90% of <sup>64</sup>Cu:4-DEAP-ATSC can be loaded into Liposome B (Table 8), Liposome C (Table 9), and Doxil® (Table 10) below.

35

<b>Table 8: <sup>64</sup>Cu-loaded Liposome B</b>	
<b>4-DEAP-ATSC:Doxorubicin Ratio (mol %)</b>	<b><sup>64</sup>Cu Loading Efficiency</b>
0.16 mol%	98%
0.7 mol%	95%
1.0 mol%	92%
1.6 mol%	95%
2.0 mol%	92%
2.7 mol%	96%
4.0 mol%	93%
8.0 mol%	93%
40 mol%	90%

<b>Table 9: <sup>64</sup>Cu-loaded Liposome C</b>	
<b>4-DEAP-ATSC:Irinotecan Ratio (mol %)</b>	<b><sup>64</sup>Cu Loading Efficiency</b>
0.01 mol%	97%
0.2 mol%	95%
0.6 mol%	97%
2.5 mol%	97%
12.5 mol%	90%

<b>Table 10: <sup>64</sup>Cu-loaded Doxil<sup>®</sup></b>	
<b>4-DEAP-ATSC:Doxorubicin Ratio (mol %)</b>	<b><sup>64</sup>Cu Loading Efficiency</b>
0.6 mol%	94%
2.0 mol%	96%
4.0 mol%	96%
8.0 mol%	96%
40 mol%	91%

**5 Example 17: Storage Stability of 4-DEAP-ATSC Formulations**

Various 4-DEAP-ATSC formulations (see Table 10 below) were stored under different conditions. At designated time points, samples were collected where their storage stability were evaluated by functional readouts.

**Table 11. 4-DEAP-ATSC Formulations and Storage Conditions**

<b>Sample</b>	<b>Buffer</b>	<b>Buffer Strength</b>	<b>pH</b>	<b>Formulation</b>	<b>Fill</b>	<b>Temperature</b>
C1	Citrate Buffer	0.1 M	6	Liquid	Air	-20°C, 4°C, 30°C, 37°C
C2	Citrate Buffer	0.1 M	6	Liquid	Argon	-20°C, 4°C, 30°C, 37°C
C3	Citrate Buffer	0.1 M	6	Lyophilized	Air	-20°C, 4°C, 30°C, 37°C

C4	Citrate Buffer	0.1 M	6	Lyophilized	Argon	-20°C, 4°C, 30°C, 37°C
C5	Citrate Buffer	0.1 M	6.5	Liquid	Air	-20°C, 4°C, 30°C, 37°C
C6	Citrate Buffer	0.1 M	7	Liquid	Air	-20°C, 4°C, 30°C, 37°C
C7	Citrate Buffer	0.1 M	7	Liquid	Argon	-20°C, 4°C, 30°C, 37°C
C8	Citrate Buffer	0.005 M	6	Liquid	Air	-20°C, 4°C, 30°C, 37°C
C9	Citrate Buffer	0.005 M	7	Liquid	Air	-20°C, 4°C, 30°C, 37°C
C10	Citrate Buffer	0.005 M	7	Liquid	Argon	-20°C, 4°C, 30°C, 37°C
C11	Water	(Contains 0.0005M Citric acid)		Liquid	Air	-20°C, 4°C, 30°C, 37°C
C12	Water	(Contains 0.0005M Citric acid)		Liquid	Argon	-20°C, 4°C, 30°C, 37°C
C13	Water	(Contains 0.0005M Citric acid)		Lyophilized	Argon	-20°C, 4°C, 30°C, 37°C
C14	Citrate Buffer	0.1 M (with 20 mg/mL mannitol)	6	Lyophilized	Air	-20°C, 4°C, 30°C, 37°C
C15	Citrate Buffer	0.005 M (with 20 mg/mL mannitol)	6	Lyophilized	Air	-20°C, 4°C, 30°C, 37°C
C16	Citrate Buffer	0.1 M	4	Liquid	Air	4°C, 37°C
C16	Citrate Buffer	0.1 M	5	Liquid	Air	4°C, 37°C
C17	Citrate Buffer	0.02 M	4	Liquid	Air	4°C, 37°C
C16	Citrate Buffer	0.02 M	5	Liquid	Air	4°C, 37°C

#### Effect of Storage pH

4-DEAP-ATSC was formulated in citrate buffer in a range of pH (pH 4-7). As seen in Figure 19A, the amount of 4-DEAP-ATSC degradation decreases as the storage pH increases in the formulation. At a pH of between 6 and 7, the rates of degradation were very similar, with less than 15% degradation observed over a 4-month period when stored at -20°C or 4°C.

#### Effect of Storage Temperature

4-DEAP-ATSC formulated in citrate buffer was stored at 4 different temperatures (-20°C, 4°C, 30°C, and 37°C). As seen in Figure 19B, significant degradation was observed when the 4-DEAP-ATSC formulations were stored at 30°C and 37°C (> 60%) over a 1-month period. On the other hand, 4-DEAP-ATSC formulations stored at -20°C and 4°C can be stably preserved with less than 15% of degradation detected over a period of 4 months.

#### Lyophilized Formulations

Various 4-DEAP-ATSC formulations were lyophilized and stored under different conditions to study the effect of lyophilization on their storage stability. Figure 19C illustrates that lyophilization is an effective method to inhibit degradation of 4-DEAP-ATSC, reversing any temperature-related degradation process as described previously. In addition, mannitol was added to the formulation to serve as a bulking agent for lyophilization. As shown in Figure 19D, mannitol has no effect on the storage stability of 4-DEAP-ATSC.

Storage under Inert Gas Atmosphere

A set of 4-DEAP-ATSC formulations was filled with argon as an alternative means to improve storage stability of the liquid formulations. Figure 19E illustrates that storage under inert gas atmosphere did not improve storage stability of 4-DEAP-ATSC liquid formulations. Significant degradation was still detected in formulations stored at elevated temperatures (30°C and 37°C). Additionally, storage stability of inert gas-filled lyophilized formulations was similar to air-filled lyophilized formulations (Figure 19F).

**Example 18: Storage Stability of Excipient Liposome of Various Compositions**

Various excipient liposome formulations (see Table 12 and 13 below) were stored under different conditions. At designated time points, samples were collected and their storage stability was evaluated by functional readouts (loading of <sup>64</sup>Cu:4-DEAP-ATSC and *in vivo* stability of <sup>64</sup>Cu:4-DEAP-ATSC-loaded liposomes), as well as degradation of lipid components, as determined by HPLC/ELSD (high performance liquid chromatography coupled to an evaporative light scattering detector).

**Table 12: Excipient Lipid Formulations with Ammonium Sulfate Gradients and Storage Conditions**

Sample	Lipid Composition	External pH	Ammonium Sulfate	Sodium Sulfate	Temperature
L1	HSPC:Cholesterol:PEG-DSPE (3:1:1 wt ratio)	6.5	20 mM	70 mM	4°C, 37°C
L2	HSPC:Cholesterol:PEG-DSPE (3:1:1 wt ratio)	6.5	50 mM	50 mM	4°C, RT, 37°C
L3	DSPC:Cholesterol:PEG-DSPE (3:1:1 wt ratio)	6.5	50 mM	50 mM	4°C, 30°C, 37°C
L4	DSPC:Cholesterol:PEG-DSPE (3:1:1 wt ratio)	6.5	125 mM	-	4°C, 30°C, 37°C
L5	DSPC:Cholesterol:PEG-DSPE (3:1:1 wt ratio)	6.5	250 mM	-	4°C, 30°C, 37°C
L6	Sphingomyelin:Cholesterol:PEG- DSPE (3:1:1 wt ratio)	6.5	50 mM	50 mM	4°C, 30°C, 37°C
L7	Sphingomyelin:Cholesterol:PEG- DSPE (3:1:1 wt ratio)	6.5	125 mM	-	4°C, 30°C, 37°C
L8	Sphingomyelin:Cholesterol:PEG-	6.5	250 mM	-	4°C, 30°C,

	DSPE (3:1:1 wt ratio)				37°C
L9	Sphingomyelin:Cholesterol:PEG- DSPE (3:1:1 wt ratio)	7.4	50 mM	50 mM	4°C, 30°C, 37°C
L10	Sphingomyelin:Cholesterol:PEG- DSPE (3:1:1 wt ratio)	7.4	125 mM	-	4°C, 30°C, 37°C
L11	Sphingomyelin:Cholesterol:PEG- DSPE (3:1:1 wt ratio)	7.4	250 mM	-	4°C, 30°C, 37°C
L12	Sphingomyelin:Cholesterol:PEG- DSG (3:1:1 wt ratio)	6.5	50 mM	50 mM	4°C, 30°C, 37°C
L13	Sphingomyelin:Cholesterol:PEG- DSG (3:1:1 wt ratio)	6.5	125 mM	-	4°C, 30°C, 37°C
L14	Sphingomyelin:Cholesterol:PEG- DSG (3:1:1 wt ratio)	7.4	50 mM	50 mM	4°C, 30°C, 37°C
L15	Sphingomyelin:Cholesterol:PEG- DSG (3:1:1 wt ratio)	7.4	125 mM	-	4°C, 30°C, 37°C
L16	Sphingomyelin:Cholesterol:PEG- DSGE (3:1:1 wt ratio)	6.5	50 mM	50 mM	4°C, 30°C, 37°C
L17	Sphingomyelin:Cholesterol:PEG- DSGE (3:1:1 wt ratio)	6.5	125 mM	-	4°C, 30°C, 37°C
L18	Sphingomyelin:Cholesterol:PEG- DSPE (3:1:0.5 wt ratio) [PEG-DSPE Inserted post- extrusion]	7.4	50 mM	50 mM	4°C, 30°C, 37°C
L19	Sphingomyelin:Cholesterol:PEG- DSPE (3:1:0.5 wt ratio) [PEG-DSPE Inserted post- extrusion]	7.4	125 mM	-	4°C, 30°C, 37°C

**Table 13: Excipient Lipid Formulations with Triethylammonium Sucrose Octasulfate Gradients and Storage Conditions**

Sample	Lipid Composition	External pH	Triethylammonium Sucrose Octasulfate	Temperature
L20	DSPC:Cholesterol:PEG- DSPE (3:1:1 wt ratio)	7.2	0.142 N	4°C, 30°C



<b>L21</b>	DSPC:Cholesterol:PEG-DSPE (3:1:1 wt ratio)	7.2	0.215 N	4°C, 30°C
<b>L22</b>	DSPC:Cholesterol:PEG-DSPE (3:1:1 wt ratio)	7.2	0.43 N	4°C, 30°C
<b>L23</b>	DSPC:Cholesterol:PEG-DSPE (3:1:1 wt ratio)	6.5	0.43 N	4°C, 30°C
<b>L24</b>	DSPC:Cholesterol:PEG-DSPE (3:1:1 wt ratio)	7.4	0.43 N	4°C, 30°C
<b>L25</b>	HSPC:Cholesterol:PEG-DSPE (3:1:1 wt ratio)	7.2	0.043 N	4°C, 30°C
<b>L26</b>	HSPC:Cholesterol:PEG-DSPE (3:1:1 wt ratio)	7.2	0.086 N	4°C, 30°C
<b>L27</b>	IISPC:Cholesterol:PEG-DSPE (3:1:1 wt ratio)	7.2	0.142 N	4°C, 30°C
<b>L28</b>	HSPC:Cholesterol:PEG-DSPE (3:1:1 wt ratio)	7.2	0.215 N	4°C, 30°C
<b>L29</b>	HSPC:Cholesterol:PEG-DSPE (3:1:1 wt ratio)	7.2	0.43 N	4°C, 30°C
<b>L30</b>	Sphingomyelin:Cholesterol:PEG-DSPE (3:1:1 wt ratio)	7.2	0.215 N	4°C, 30°C
<b>L31</b>	Sphingomyelin:Cholesterol:PEG-DSPE (3:1:1 wt ratio)	7.2	0.43 N	4°C, 30°C

*Excipient Liposome with Various Lipid Compositions*

All liposome formulations listed above were shown to result in acceptable <sup>64</sup>Cu:4-DEAP-ATSC loading (> 95%) at the beginning of the study. HSPC – Ammonium Sulfate formulations were demonstrated to retain the ability to load <sup>64</sup>Cu:4-DEAP-ATSC over a 6-month storage period when stored at room temperature (room temperature (RT) is defined as temperatures varying between 22-25°C), and for at least 15 months when stored at 4°C. At 1-month, DSPC – Ammonium Sulfate formulations did not retain an acceptable level of <sup>64</sup>Cu:4-DEAP-ATSC loading (acceptable level of loading defined as >90%) (Figure 20A). All sphingomyelin formulations retained the ability to load

<sup>64</sup>Cu:4-DEAP-ATSC at all storage temperatures for at least four months. DSPC formulations encapsulating triethylammonium sucrose octasulfate (TEA-SOS) maintained the ability to load <sup>64</sup>Cu:4-DEAP-ATSC for at least 4 months when stored at 4°C.

HPLC/ELSD results support the above observation where significant amounts of lipid degradation were detected in both HSPC and DSPC formulations encapsulating ammonium sulfate (Figure 20B). Lipid breakdown in the sphingomyelin formulations was minimal with a small amount of stearic acid detected at 2-months onwards, which may be attributed to the degradation of PEG-DSPE located on the inner liposomal membrane. Similarly, lipid breakdown in DSPC formulations encapsulating TEA-SOS was minimal over a period of 2 months at 30°C storage, with no lipid degradation detected over 5 months at 4°C storage (Figure 20B).

An *in vivo* stability study was performed as described in Example 10 to investigate the pharmacokinetics profiles of the liposome formulations that were stored under the aforementioned conditions. Even though a significant amount of lipid was degraded in the HSPC formulations, the <sup>64</sup>Cu-DEAP-ATSC-loaded HSPC liposome still performed stably *in vivo* after 6-month storage at room temperature (Figure 20C). Similar results were obtained for the sphingomyelin formulations over a 3-month storage period at elevated temperatures (Figure 20D (4°C), 20E (30°C), and 20F (37°C)).

Additional formulations were also studied by varying the types and amount of PEG-lipid. Since sphingomyelin was not susceptible to hydrolysis, the PEG-DSPE in the sphingomyelin formulation remains the source of lipid degradation induced by the low intraliposomal pH (presence of ammonium sulfate as a loading gradient). In place of the PEG-DSPE lipid, variations of the sphingomyelin formulations were studied, including PEG-DSGE, PEG-DSG, or post-insertion of (reduced amount) PEG-DSPE into preformed liposomes. All these formulations were shown to result in excellent <sup>64</sup>Cu:4-DEAP-ATSC loading (>90%) following 4-months of storage at elevated temperatures (Figure 20G).

#### **Example 19: Storage Stability of Excipient Liposome Containing Various Loading Gradient Strengths**

Liposome formulations with various strengths of loading gradient containing 20, 50, 125, 250mM of ammonium sulfate were prepared. The effects of loading gradient strengths on the <sup>64</sup>Cu:4-DEAP-ATSC loading and storage stability were examined. Figure 21A illustrates the effect of loading gradient strengths on the <sup>64</sup>Cu:4-DEAP-ATSC loading efficiency of HSPC liposome stored under different conditions. The 20mM formulation of liposomes was shown to fail loadability criteria sooner than the 50mM formulation. This may be attributed to lipid bilayer degradation in the HSPC formulation, as suggested by the HPLC/ELSD data, leading to dissipation of the loading gradient. It is likely that over extended storage time at an elevated temperature, the 20mM formulation did not

retain sufficient intraliposomal ammonium sulfate to allow satisfactory loading of  $^{64}\text{Cu}$ -4-DEAP-ATSC.

5 A similar study was performed with the DSPC liposome formulations, where DSPC liposomes containing 50, 125, or 250mM of ammonium sulfate were included in the storage stability study (Figure 21B). Following a 1-month storage period, liposomes that were stored at elevated temperatures also showed <90% of  $^{64}\text{Cu}$ :4-DEAP-ATSC loading. This is also attributed to significant degradation of the DSPC component, leading to gradient dissipation.

10 On the other hand, the sphingomyelin formulations were found to be stable over a 4-month storage at elevated temperatures (Figure 21C). As described above, lipid degradation in the sphingomyelin formulations was insignificant, indicating increased storage stability of the formulations. This also indicates that the minor breakdown of the PEG-DSPE lipid detected in the sphingomyelin formulations did not compromise its storage stability functionally.

#### **Example 20: Storage Stability of Excipient Liposome Formulated in Varying Storage pH**

15 The effect of storage pH on the storage stability of sphingomyelin liposomes is illustrated in Figure 22. Over a 12-month storage, the liposomes retain loadability at a storage pH of 6.5-7.4 when stored refrigerated at 2-8°C. Similar results were obtained in other pH 6.5 and pH 7.4 formulations listed in the table above. When stored at elevated temperature (30°C), at pH 6.5 the liposomes start to show a  $^{64}\text{Cu}$ :4-DEAP-ATSC loading dropping below 90%.

20

#### **Example 21: Liposome A as an imaging marker for predicting patient treatment response to liposomal therapeutics**

25 Mice bearing BT474-M3 tumors (inoculated at mammary fat pad and subcutaneous) were injected intravenously with Liposome A 24h prior to Liposome B treatment. PET/CT imaging was performed at 16h post Liposome A injection, and tumor uptake (% i.d./g) of Liposome A was determined from the PET data set by measuring radioactivity in the volume of interest (VOI) (*i.e.* tumor regions). The mice were then treated with Liposome B (q7d) for 3 weeks at 3 mg/kg. Response to Liposome B treatment was quantified as tumor volume changes measured over a 2-month period by MRI and caliper measurement.

30 Tumor deposition of Liposome A was found to range between 3-6 % i.d./g, which is comparable to tumor uptake levels of Liposome B. As shown in Figure 23, tumor deposition of Liposome A correlates with treatment response to Liposome B (Spearman correlation coefficient of -0.891 and a p-value of 0.0004). Specifically, increased Liposome A accumulation in tumors predicted for improved tumor growth inhibition following Liposome B treatment.

35

#### **Example 22: Liposome A as an imaging marker for monitoring changes in tumor deposition after treatment**

Mice bearing B1474-M3 tumors (inoculated at mammary fat pad and subcutaneous) were injected intravenously with Liposome A 24h prior to Liposome B treatment for 3 weeks (3 doses of Liposome A, and 3 doses of Liposome B). For each dose of Liposome A, PET/CT imaging was performed at 16h post-injection, and tumor uptake (% i.d./g) of Liposome A was determined from the PET data set using VOI analysis.

As shown in Figure 24, changes in tumor deposition of Liposome A can be detected in mammary fat pad (Figure 24A) and subcutaneous (Figure 24B) tumors from the PET data set following consecutive doses of Liposome B compared to baseline uptake (at day 22, "D22"). In the instance where tumor deposition of Liposome A dose 3 (D36) was compared to dose 1 (D22), an increased in the tumor uptake of the liposome was observed according to 2-way ANOVA ( $p = 0.0003$ ) for both subcutaneous and mammary fat pad tumors (Figure 24C).

### **Example 23: In vivo stability of $^{64}\text{Cu}$ :4-DEAP-ATSC-loaded liposomes**

The *in vivo* stability of  $^{64}\text{Cu}$ :4-DEAP-ATSC-loaded Liposome A (Figure 27A), Liposome B (Figure 27B), and Liposome C (Figure 27C) were also examined in CD-1 mouse, up to 24 hours post-injection. CD-1 naïve mice were injected with  $^{64}\text{Cu}$ :4-DEAP-ATSC-loaded Liposome A,  $^{64}\text{Cu}$ :4-DEAP-ATSC-loaded Liposome B, and  $^{64}\text{Cu}$ :4-DEAP-ATSC-loaded Liposome C via tail vein injection (100-200  $\mu\text{Ci}/\text{mouse}$ , 20  $\mu\text{mol}$  phospholipid/kg). At 5 minutes and 24 hours post-injection, blood was collected via cardiac puncture, and was subsequently centrifuged for plasma collection. Encapsulated (liposomal) radioactivity in the plasma was separated from released/unencapsulated radioactivity using size exclusion column (a CL4B column which allows for separating liposomal, protein, and  $^{64}\text{Cu}$ :4-DEAP-ATSC/uncomplexed  $^{64}\text{Cu}$  fractions) similar to the method described in Example 8. The data show that Liposome A and Liposome B are highly stable *in vivo* with < 6% of unencapsulated  $^{64}\text{Cu}$  detected up to 24 hours post-injection. For Liposome C, at 5 minutes and 24 hours post-injection, only 74% and 22% of the  $^{64}\text{Cu}$  in the plasma were detected in the liposomal fractions.

### **Equivalents**

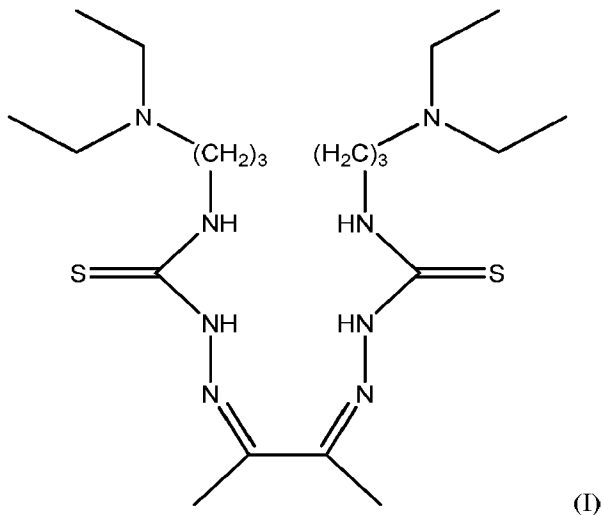
Those skilled in the art will recognize, or be able to ascertain using no more than routine experimentation, many equivalents of the specific embodiments described herein. Such equivalents are intended to be encompassed by the following claims. Any combinations of the embodiments disclosed in the dependent claims are contemplated to be within the scope of the invention.

### **Incorporation by Reference**

Each and every, issued patent, patent application and publication referred to herein is hereby incorporated herein by reference in its entirety.

We claim:

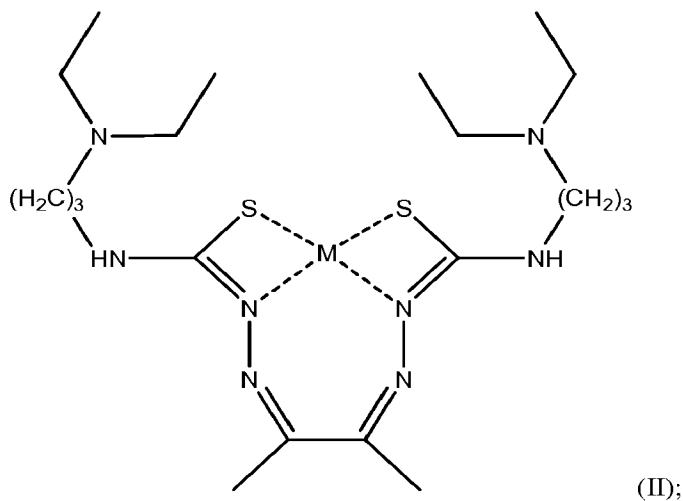
1. The compound DEAP-ATSC:



5

or a pharmaceutically acceptable salt thereof.

2. A DEAP-ATSC compound of formula II:



10 in which M is a metal cation with a valency of 2 or 3 or 4.

3. The compound of claim 2, wherein M is a cation of copper.

4. The compound of claim 3, wherein M is Cu<sup>2+</sup>.

15

5. The compound of claim 2 or claim 3 or claim 4, wherein M is a radioisotope.

6. The compound of claim 5 wherein M is  $^{64}\text{Cu}$ .

7. The compound of claim 5, wherein M is  $^{67}\text{Cu}$ .

8. A composition comprising:

(a) liposomes in a pharmaceutically acceptable medium, said liposomes each having an interior space and a membrane separating said interior from said medium, said membrane comprising one or more lipids; and

(b) a compound of any one of claims 2-7 entrapped in at least one liposome of the liposomes of (a).

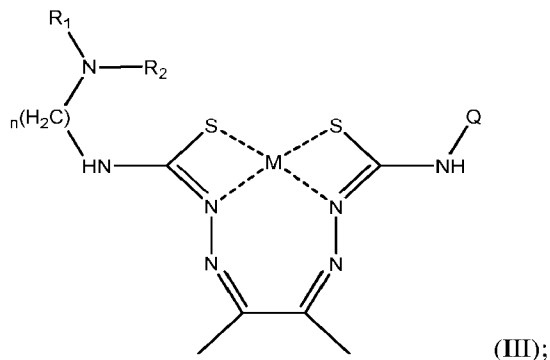
9. The composition of claim 8 wherein the composition comprises at least 0.1  $\mu\text{Ci}$  of radioactivity.

10. The composition of claim 8 M is a radioisotope of  $\text{Cu}^{2+}$  selected from  $^{64}\text{Cu}$  and  $^{67}\text{Cu}$ .

11. A composition comprising:

(a) liposomes in an aqueous medium, said liposomes each having an interior space and a membrane separating said interior from said medium, said membrane comprising one or more lipids; and

(b) entrapped in at least one liposome of the liposomes of (a), a compound of Formula III



in which

Q is H, substituted or unsubstituted  $\text{C}_1\text{-C}_6$ alkyl, or  $-(\text{CH}_2)_n\text{-NR}_3\text{R}_4$ ;

$\text{R}_1$ ,  $\text{R}_2$ ,  $\text{R}_3$  and  $\text{R}_4$  are each independently selected from H, substituted or unsubstituted  $\text{C}_1\text{-C}_6$ alkyl, or substituted or unsubstituted aryl or wherein either or both of (1)  $\text{R}_1$  and  $\text{R}_2$  and (2)  $\text{R}_3$  and  $\text{R}_4$  are joined to form a heterocyclic ring;

M is a metal cation with a valency of 2 or 3 or 4,

and

n is independently, for each occurrence, an integer from 1 to 5.

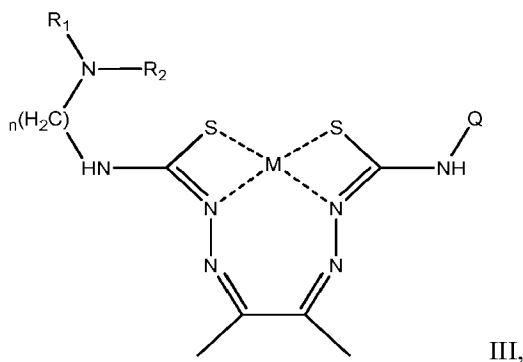
12. The composition of claim 11, in which Q is  $-(\text{CH}_2)_n-\text{NR}_3\text{R}_4$ .
- 5 13. The composition of claim 11, in which M is  $\text{Cu}^{2+}$ .
14. The composition of claim 11 wherein the membrane comprises cholesterol and a phosphatidylcholine.
- 10 15. The composition of claim 13, wherein M is  $\text{Cu}^{2+}$  and the composition comprises at least 0.1  $\mu\text{Ci}$  of a radioisotope of copper.
16. The compound of claim 2, wherein, following storage for 90 days at a temperature of from  $4^\circ\text{C}$  to  $40^\circ\text{C}$ , less than 15% of the compound has degraded.
- 15 17. The compound of claim 16, wherein the % of the compound that has degraded is measured by high performance liquid chromatography.
18. The compound of claim 16, wherein the temperature is a room temperature of about  $25^\circ\text{C}$ .
- 20 19. The compound of claim 16, wherein the temperature is  $37^\circ\text{C}$ .
20. The compound of any one of claims 16 – 19 wherein following storage for 4 months, 5 months, or 6 months, less than 15% of the compound has degraded.
- 25 21. The composition of any of claims 11-15, wherein the liposomes in an aqueous medium are prepared as unloaded liposomes prior to the compound of Formula III being entrapped in the at least one liposome, and the unloaded liposomes are stable after a storage period of 3 months, 4 months, 5 months, or 6 months, wherein stability is measured by a functional readout obtained following loading of the liposomes with the compound of Formula III after the storage period.
- 30 22. The composition of claim 21, wherein the functional readout is loading efficiency of  $^{64}\text{Cu}$ :4-DEAP-ATSC into the liposomes, wherein a liposome is stable if at least 90% of  $^{64}\text{Cu}$ :4-DEAP-ATSC is in the liposome fraction after size exclusion chromatography.
- 35 23. The composition of claim 21 or 22, wherein the membranes of the liposomes comprise cholesterol and a phosphatidylcholine.

24. The composition of any of claims 21-23, wherein the membranes of the liposomes comprise a non-hydrolysable lipid.

5 25. The composition of any of claims 21-24, wherein the membranes of the liposomes comprise one or more of sphingomyelin, HSPC and DSPC.

26. A method of preparing a liposomal imaging agent, the method comprising:

(a) providing a first solution comprising a quantity of a compound of Formula III,



10

in which

Q is H, substituted or unsubstituted C<sub>1</sub>-C<sub>6</sub>alkyl, or -(CH<sub>2</sub>)<sub>n</sub>-NR<sub>3</sub>R<sub>4</sub>;

R<sub>1</sub>, R<sub>2</sub>, R<sub>3</sub> and R<sub>4</sub> are each independently selected from H, substituted or unsubstituted C<sub>1</sub>-C<sub>6</sub>alkyl, or substituted or unsubstituted aryl or wherein either or both of (1) R<sub>1</sub> and R<sub>2</sub> and (2) R<sub>3</sub> and R<sub>4</sub> are joined to form a heterocyclic ring;

15

M absent or is a metal ion,

and

n is independently, for each occurrence, an integer from 1 to 5; and

(b) providing a preparation of liposomes in an aqueous medium, a plurality of the liposomes each having an interior space and a membrane separating the interior space from the medium, the interior space comprising a second solution creating an electro-chemical gradient across the membrane, and either

20

(c) where M is present, preparing a mixture by combining the first solution with the preparation of liposomes, and incubating the mixture under conditions such that a fraction of the quantity of the compound of Formula III becomes encapsulated by at least one liposome of the plurality of liposomes, to form a liposomal imaging agent, or

25

(d) where M is absent, preparing a mixture by combining the first solution with the preparation of liposomes, and incubating the mixture under conditions such that a fraction of the quantity of the compound of Formula III becomes encapsulated by at least one liposome



of the plurality of liposomes, and subsequently adding a solution comprising radioactive metal ion to the at least one liposome so that radioactive metal ion becomes encapsulated by the at least one liposome to that to form a liposomal imaging agent.

5 27. The method of claim 26, wherein, prior to the mixture being prepared, the second solution is essentially free of any metal chelating moiety.

28. The method of claim 26 wherein, prior to the mixture being prepared, the first solution is essentially free of lipid.

10

29. The method of claim 26 wherein the conditions include a temperature of 40 °C or above, or 60 °C or above.

15

30. The method of claim 26, wherein the imaging agent is suitable for use by injection into a patient without fractionation, other than sterile filtration, subsequent to the preparation of the mixture.

31. The method of claim 26, wherein prior to becoming encapsulated by at least one liposome, the compound of Formula III is uncharged, and subsequent to becoming encapsulated by at least one liposome, the compound of Formula III is charged.

20

32. A method of imaging a tissue in a patient, the method comprising:  
(a) injecting the patient with a liposomal imaging agent comprising the composition of claim 9 in an amount sufficient to provide a dose of at least 0.1  $\mu\text{Ci}$  of radioactivity to the patient;  
(b) within 48 hours following the injection, scanning the location of the tissue using a  
25 scanning method that detects radiation emitted by the radioisotope to obtain an image of the tissue.

33. The method of claim 32 wherein the tissue is a tumor.

30

34. A method of determining whether a patient having a tumor should be treated with an antineoplastic liposomal therapeutic agent, the method comprising:

35

(a) injecting the patient with a liposomal imaging agent comprising the composition of claim 9 in an amount sufficient to provide a dose of at least 0.1  $\mu\text{Ci}$  of radioactivity to the patient;  
(b) within 48 hours following the injection, scanning the location of the tumor using a scanning method that detects radiation emitted by the radioisotope to obtain an image; and  
(c) examining the image,

wherein, if the image shows that the liposomal imaging agent is deposited in the tumor at levels higher than background, then the patient is determined to be a patient that should be treated with the liposomal therapeutic agent.

5 35. The method of claim 34 wherein background is determined by scanning tumor-free muscle tissue within 48 hours following the injection.

36. The method of claim 34 or of claim 35, further wherein, if the image shows that the liposomal imaging agent is deposited in the tumor at levels higher than background, then the patient is treated  
10 with the liposomal therapeutic agent and if the image shows that the liposomal imaging agent is not deposited in the tumor at levels higher than background, then the patient is not treated with the liposomal therapeutic agent.

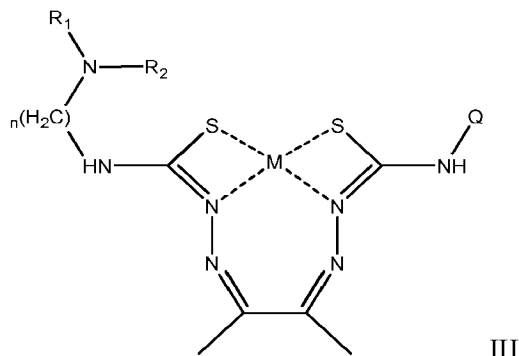
37. The method of claim 26, wherein, subsequent to the incubating, the mixture is subjected to  
15 filtration.

38. The method of claim 37, wherein the filtration is paper filtration, membrane filtration, or gel filtration.

20 39. The method of claim 26, wherein the fraction of the compound of Formula III in the first solution that does not become encapsulated is less than 10%.

40. A kit for determining whether a patient is to be treated with a liposomal therapeutic agent, the kit comprising a package containing:

25 (a) a first container comprising a compound of Formula III



in which

M is absent;

Q is H, substituted or unsubstituted C<sub>1</sub>-C<sub>6</sub>alkyl, or -(CH<sub>2</sub>)<sub>n</sub>-NR<sub>3</sub>R<sub>4</sub>;

R<sub>1</sub>, R<sub>2</sub>, R<sub>3</sub> and R<sub>4</sub> are each independently selected from H, substituted or unsubstituted C<sub>1</sub>-C<sub>6</sub>alkyl, or substituted or unsubstituted aryl or wherein either or both of (1) R<sub>1</sub> and R<sub>2</sub> and (2) R<sub>3</sub> and R<sub>4</sub> are joined to form a heterocyclic ring; and

n is independently, for each occurrence, an integer from 1 to 5; and

5 (b) a second container comprising a preparation of liposomes in a pharmaceutically acceptable medium, said liposomes having an interior space and a membrane separating said interior from said medium, said interior space comprising a solution creating an electro-chemical gradient across the membrane.

10 41. The kit of claim 40 further comprising instructions for, in sequence:

(i) combining the compound of formula III with a metal ion to yield a compound of formula III in which M is not absent and is the metal ion;

(ii) preparing a mixture by combining the compound of formula III in which M is the metal ion with the preparation of liposomes, and incubating the mixture under conditions such that  
15 the compound of formula III in which M is the metal ion becomes encapsulated in liposomes of the preparation of liposomes; and

(iii) administering the encapsulated compound of formula III in which M is the metal ion to the patient.

20 42. The composition of any one of claims 11-15, wherein the liposomes in a pharmaceutically acceptable medium are prepared as unloaded liposomes prior to the compound of Formula III being entrapped in the at least one liposome, and a plurality of the unloaded liposomes comprise either or both of TEA-SOS and ammonium sulfate in their interior spaces.

25 43. The composition of any one of claims 11-15, or the method of any one of claims 26-30 wherein the liposomes comprise either or both of TEA-SOS and ammonium sulfate in their interior spaces in an amount sufficient to form an electro-chemical gradient across the membrane.

30 44. The method of any one of claims 26-30 wherein the preparation of liposomes of (b) comprises within a plurality of the liposomes, an antineoplastic therapeutic agent.

45. The method of claim 44 wherein the antineoplastic therapeutic agent is doxorubicin or irinotecan.

35 46. A method of preparing a liposomal imaging agent, the method comprising:

(a) providing a first solution comprising a quantity of an uncharged composition that is radioactive metal chelated by a chelator; and

(b) providing a preparation of liposomes in a aqueous medium, a plurality of said liposomes each having an interior space and a membrane separating said interior space from said medium, said interior space comprising a second solution creating an electro-chemical gradient across the membrane, and

5 (c) preparing a mixture by combining the first solution with the preparation of liposomes, and incubating the mixture under conditions such that a fraction of the quantity of the composition becomes encapsulated by at least one liposome of the plurality of liposomes and becomes charged, to form a liposomal imaging agent.

10

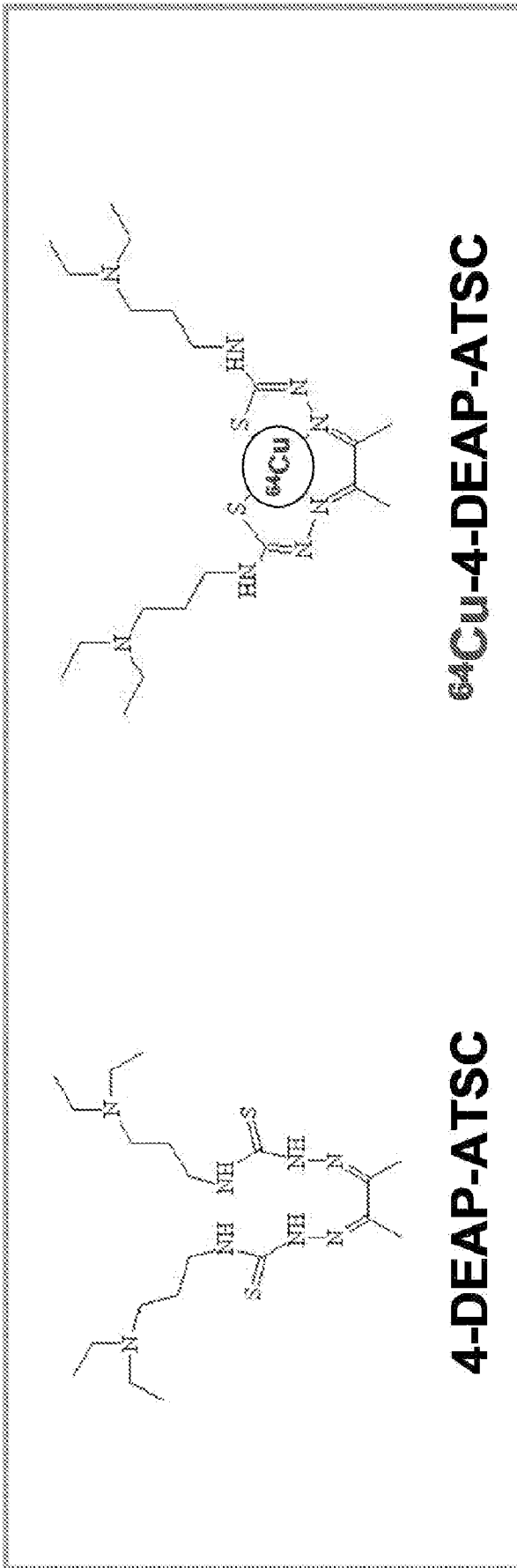


**FIGURE 1**

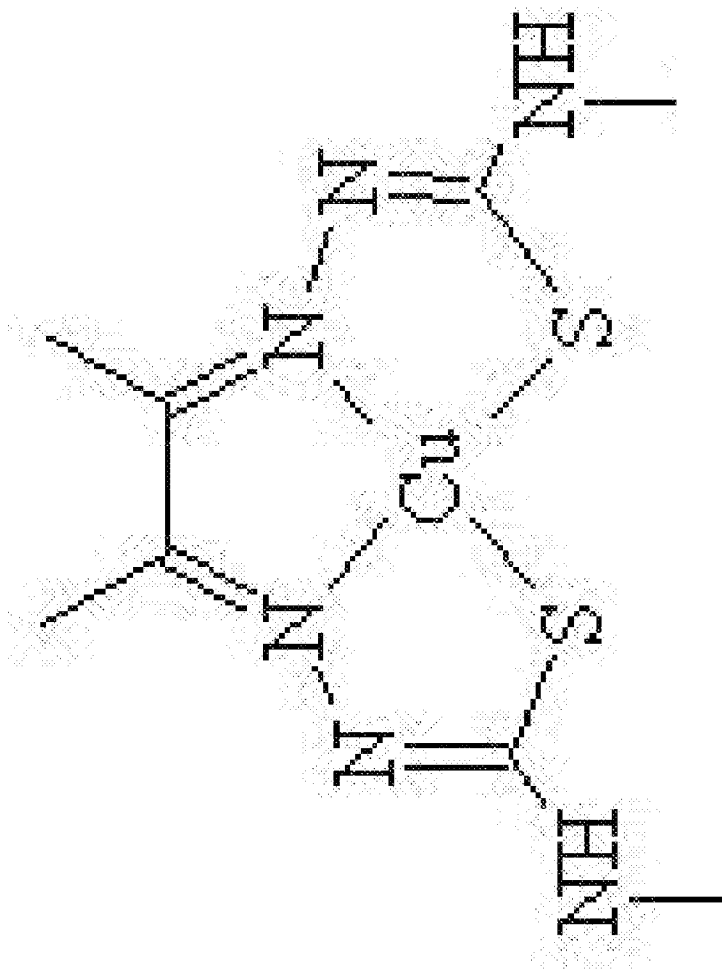


**FIGURE 2**

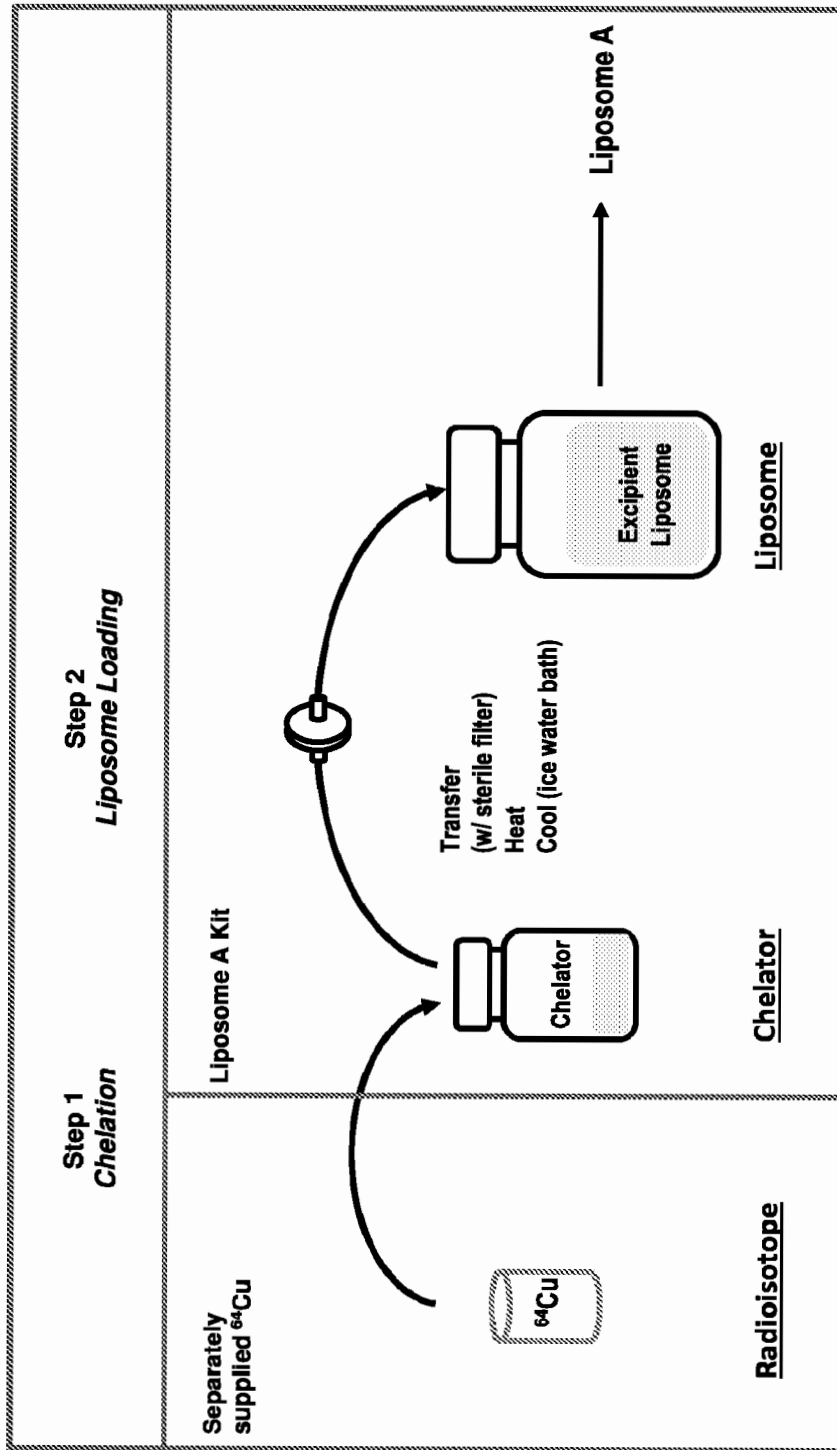


**FIGURE 3**

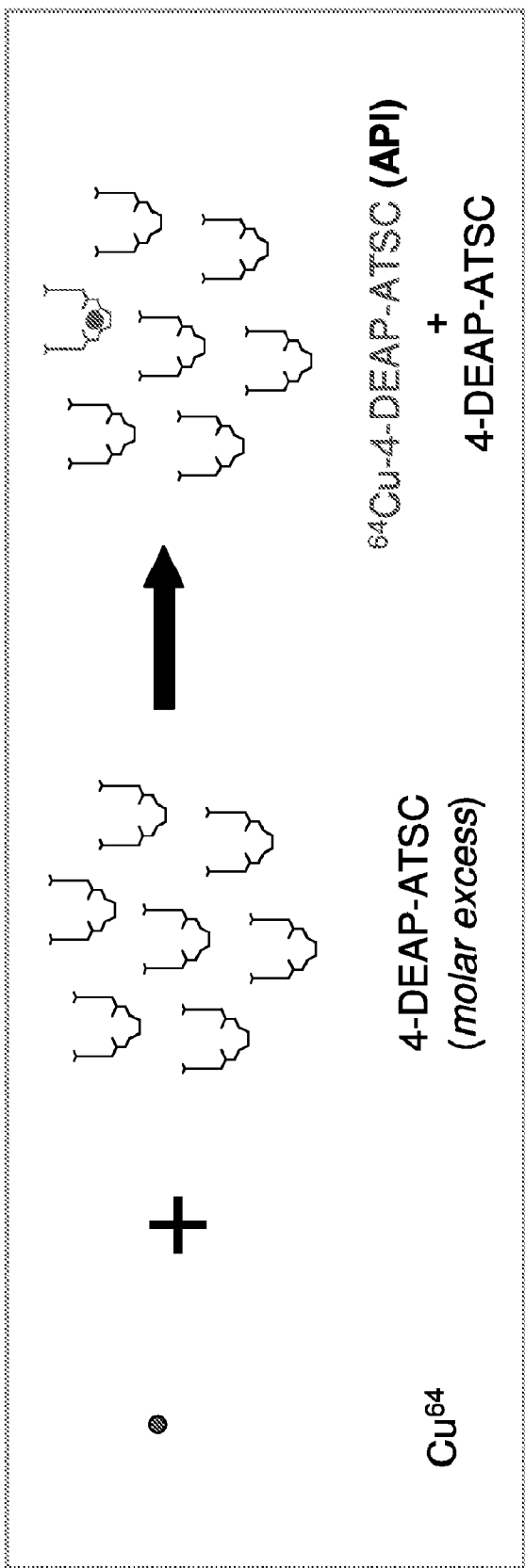


**FIGURE 4**



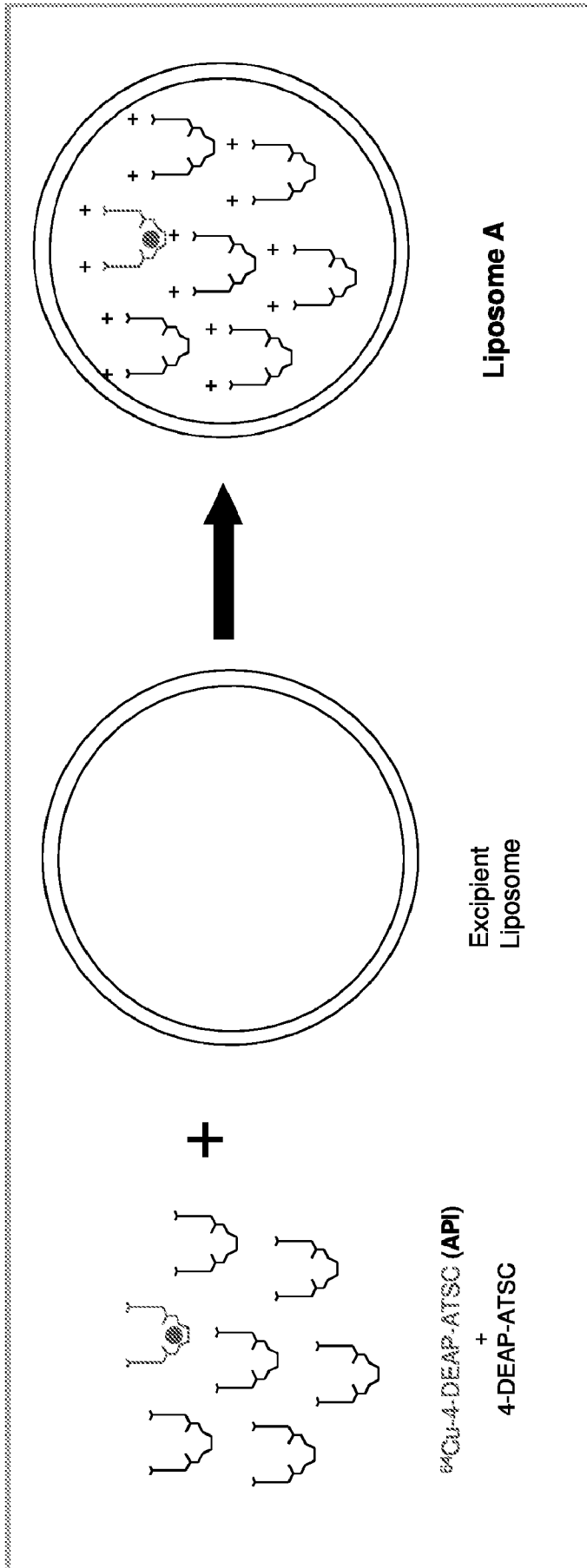
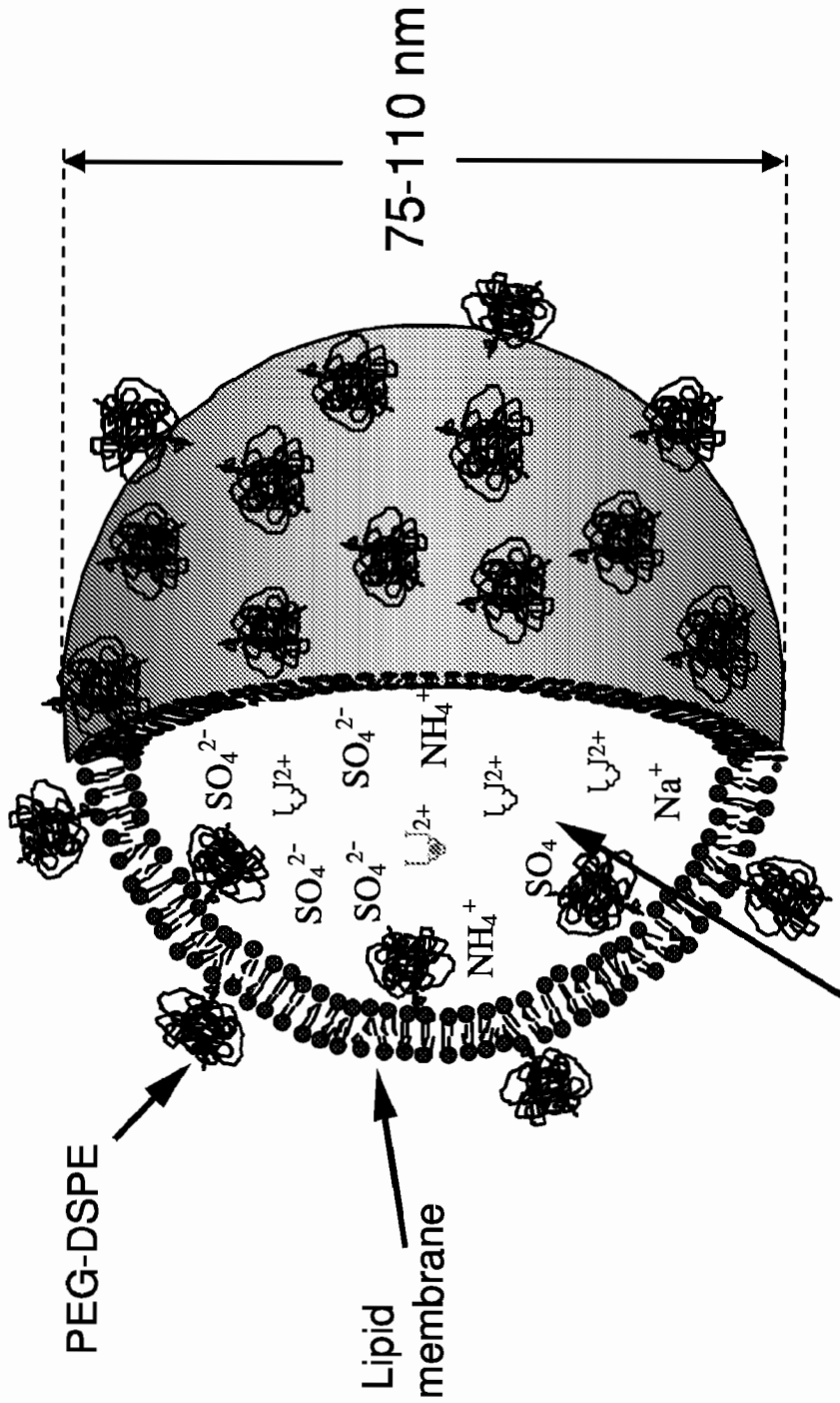


**FIGURE 5**



Internal aqueous space containing  $^{64}\text{Cu}$ -DEAP-ATSC, DEAP-ATSC, ammonium sulfate, and sodium sulfate.

# FIGURE 6

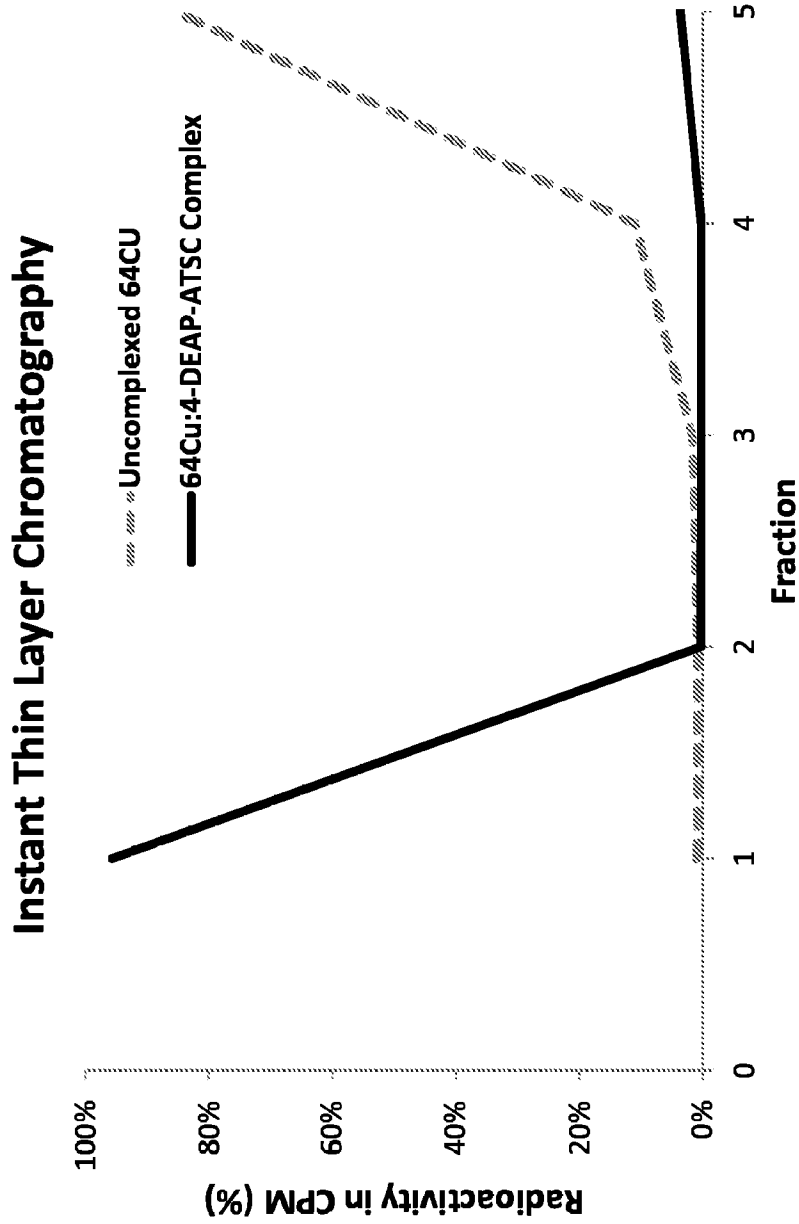
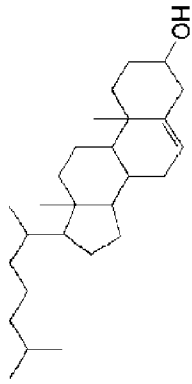
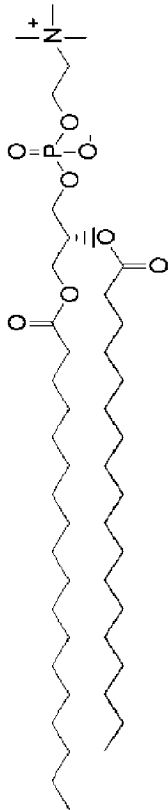


**FIGURE 7**



Cholesterol

PEG<sub>2000</sub>-DSPE



HSPC

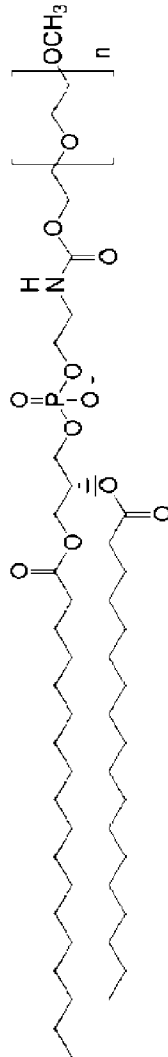


**FIGURE 8**

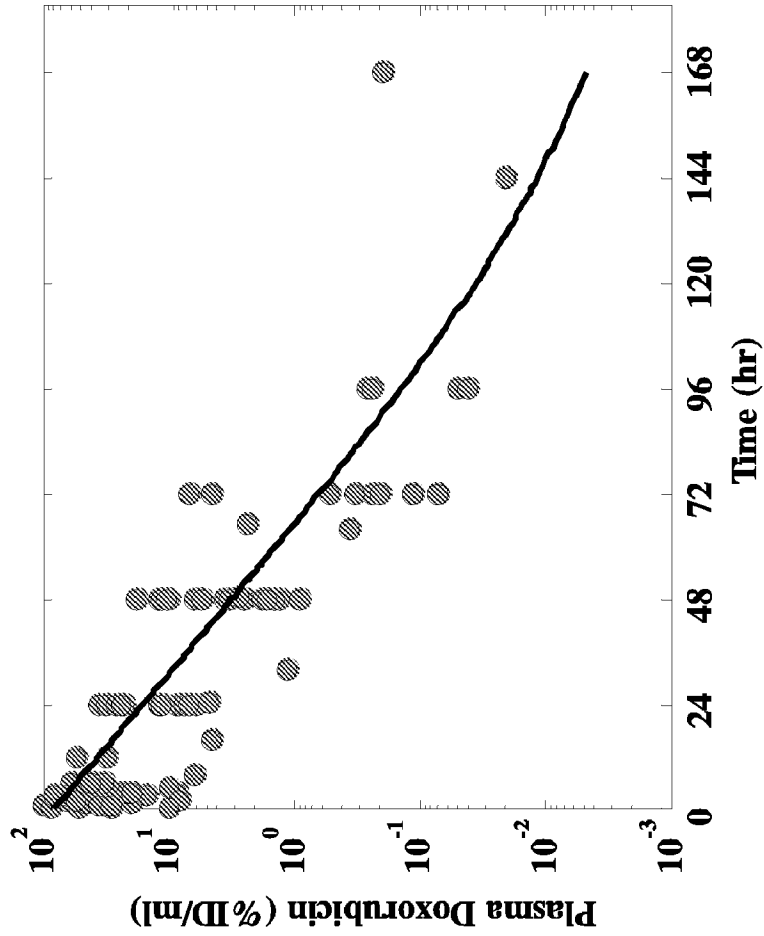


**FIGURE 9A**

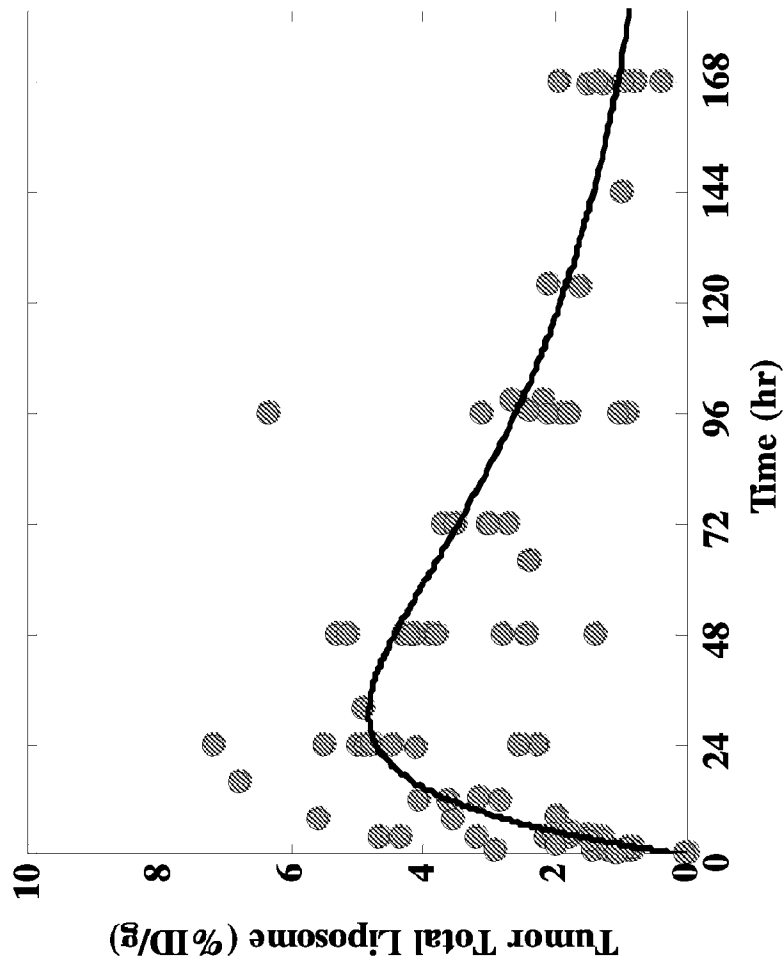


**FIGURE 9B**

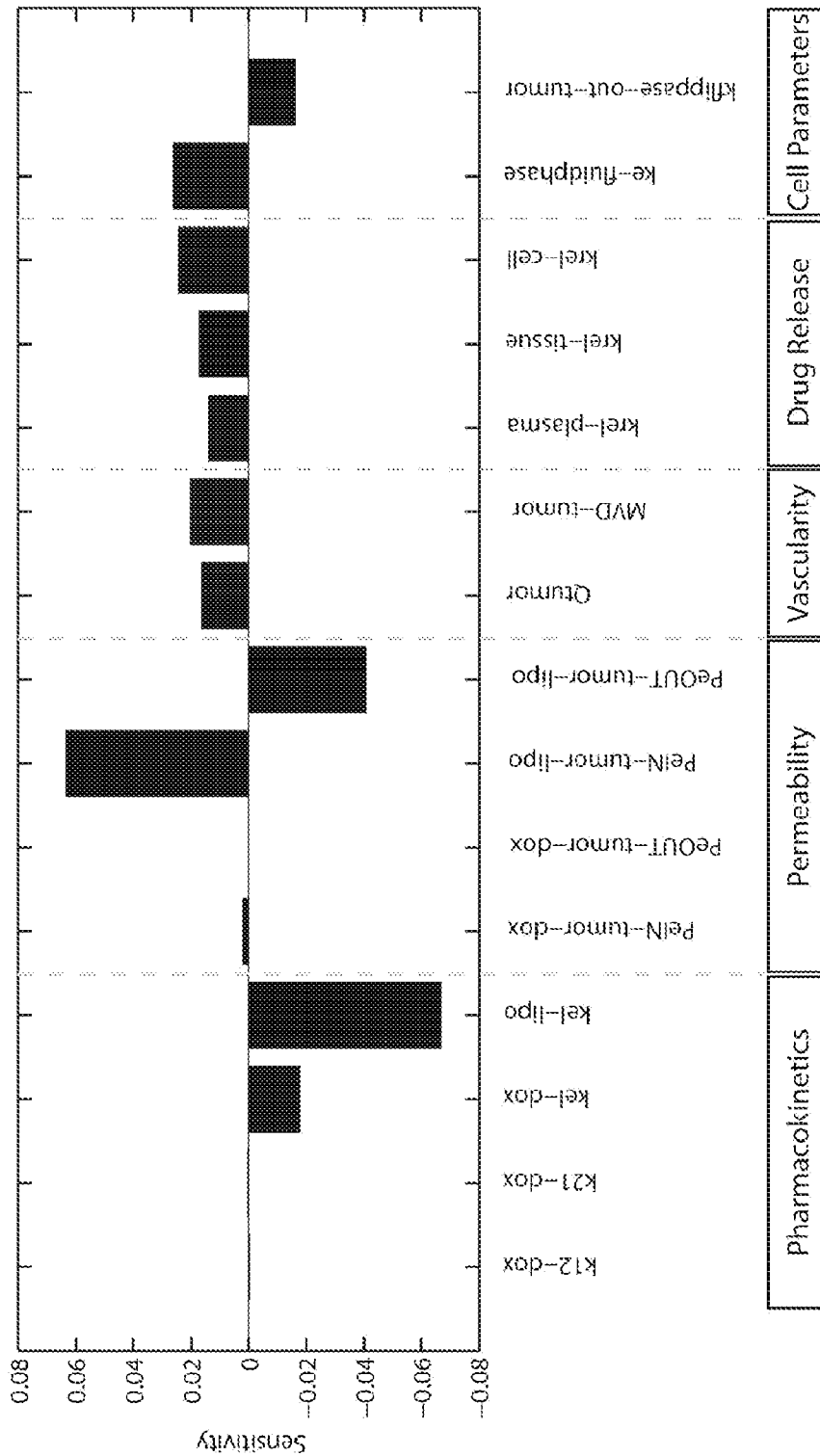


**FIGURE 9C**

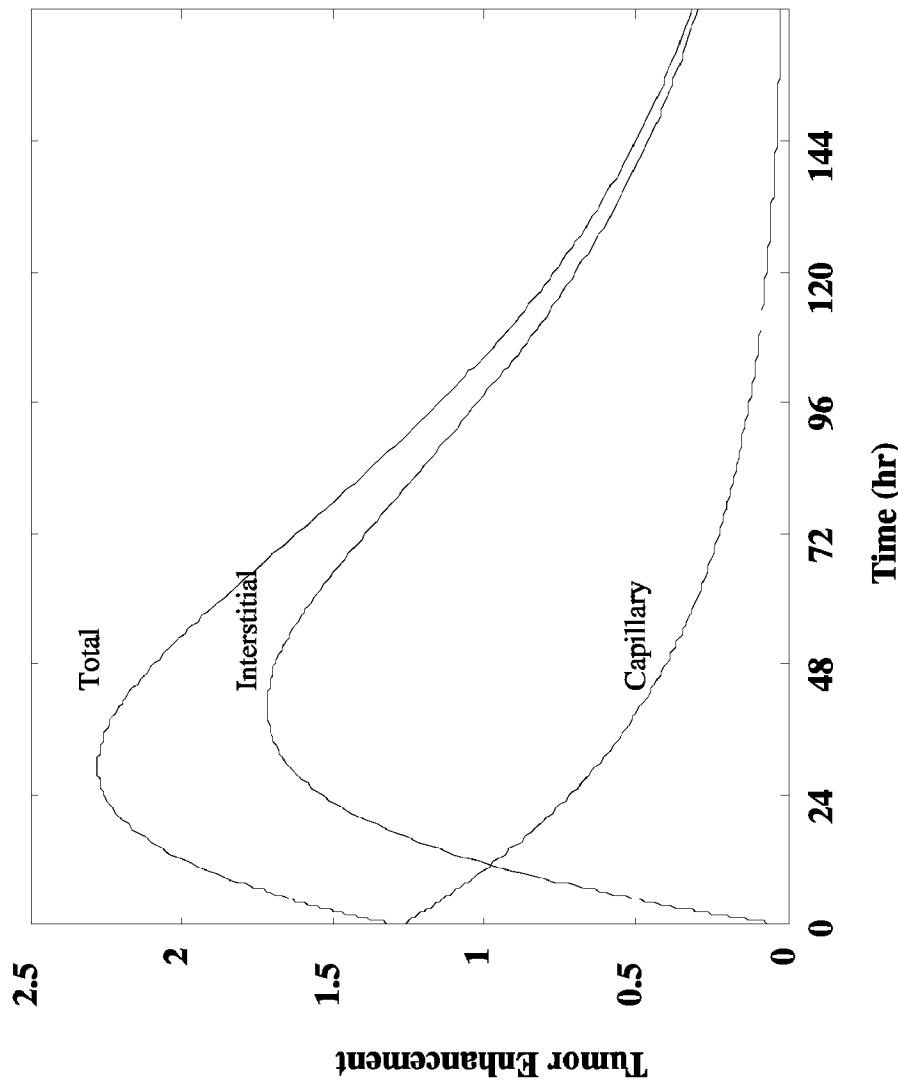


**FIGURE 10A**



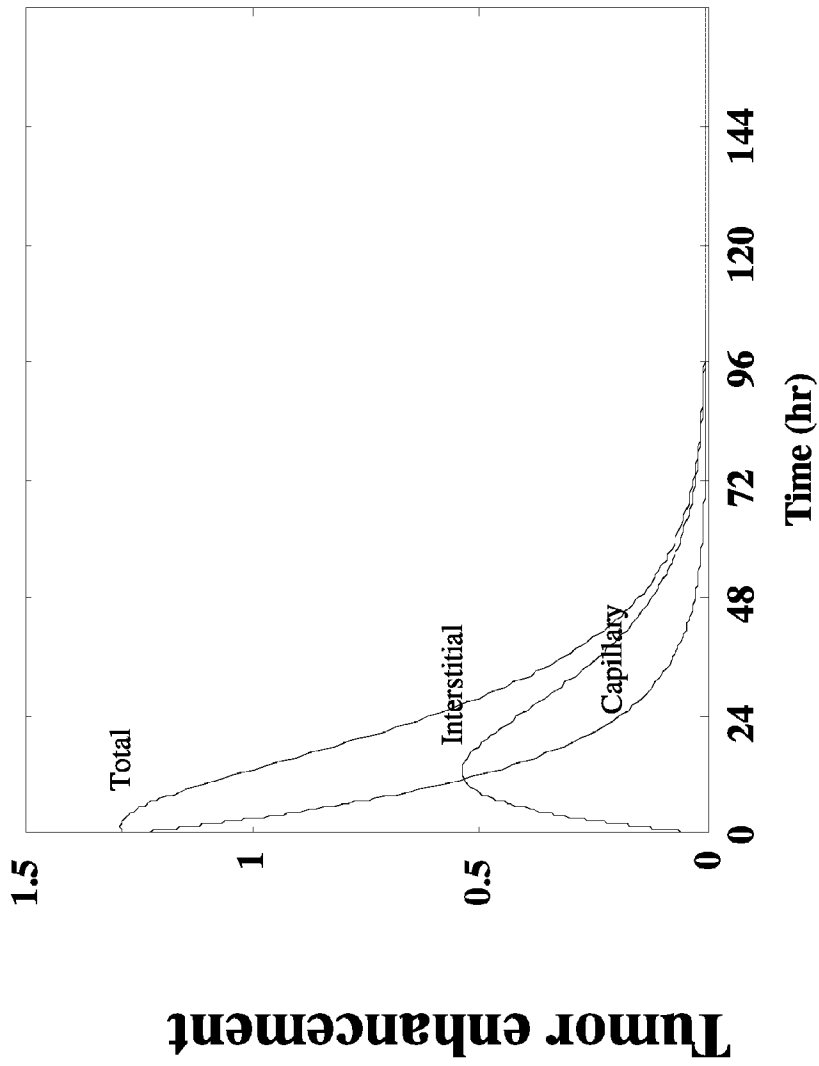


**FIGURE 10B**

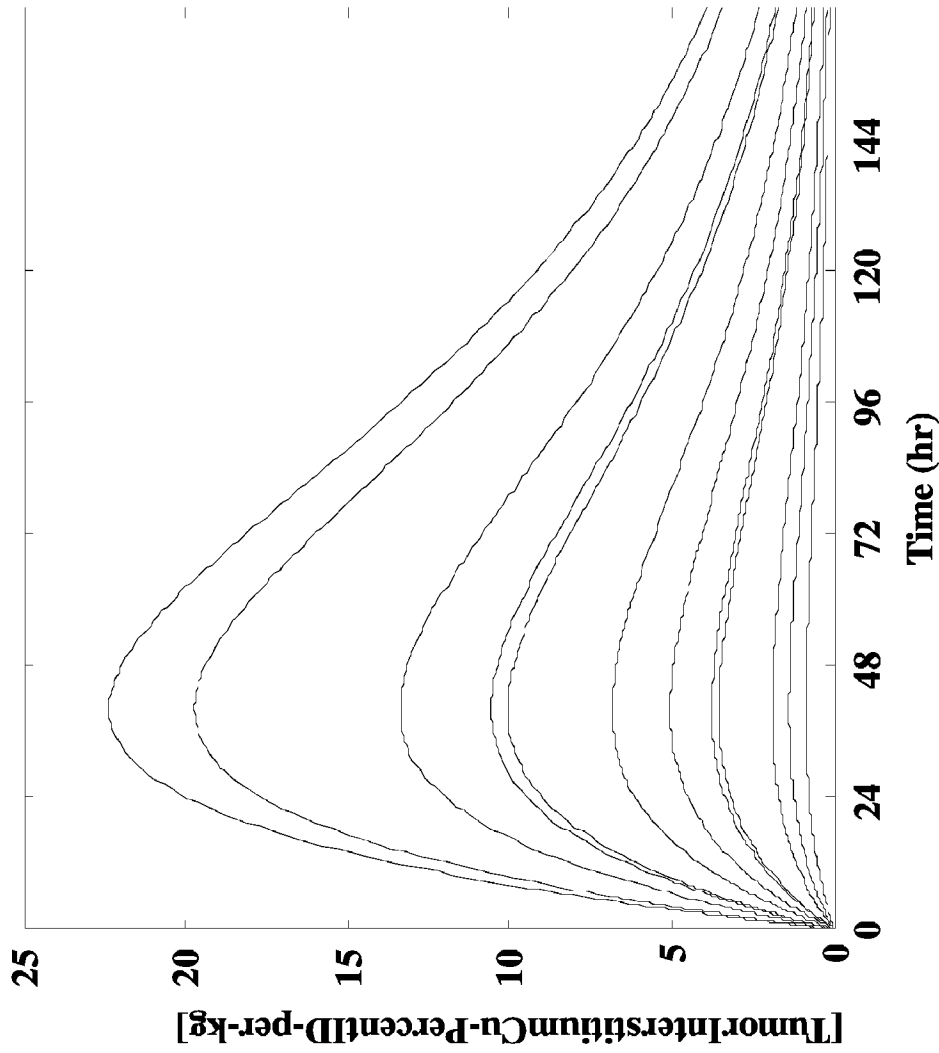


**FIGURE 10C**

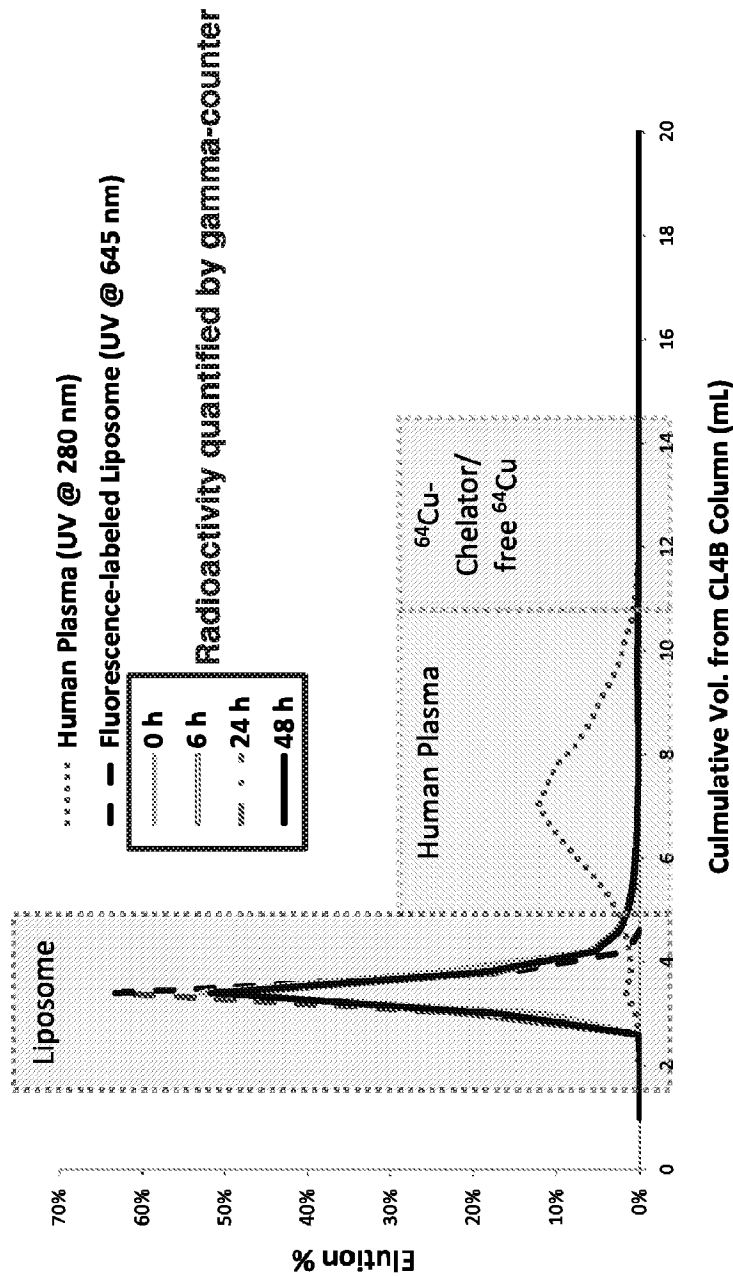


**FIGURE 11**

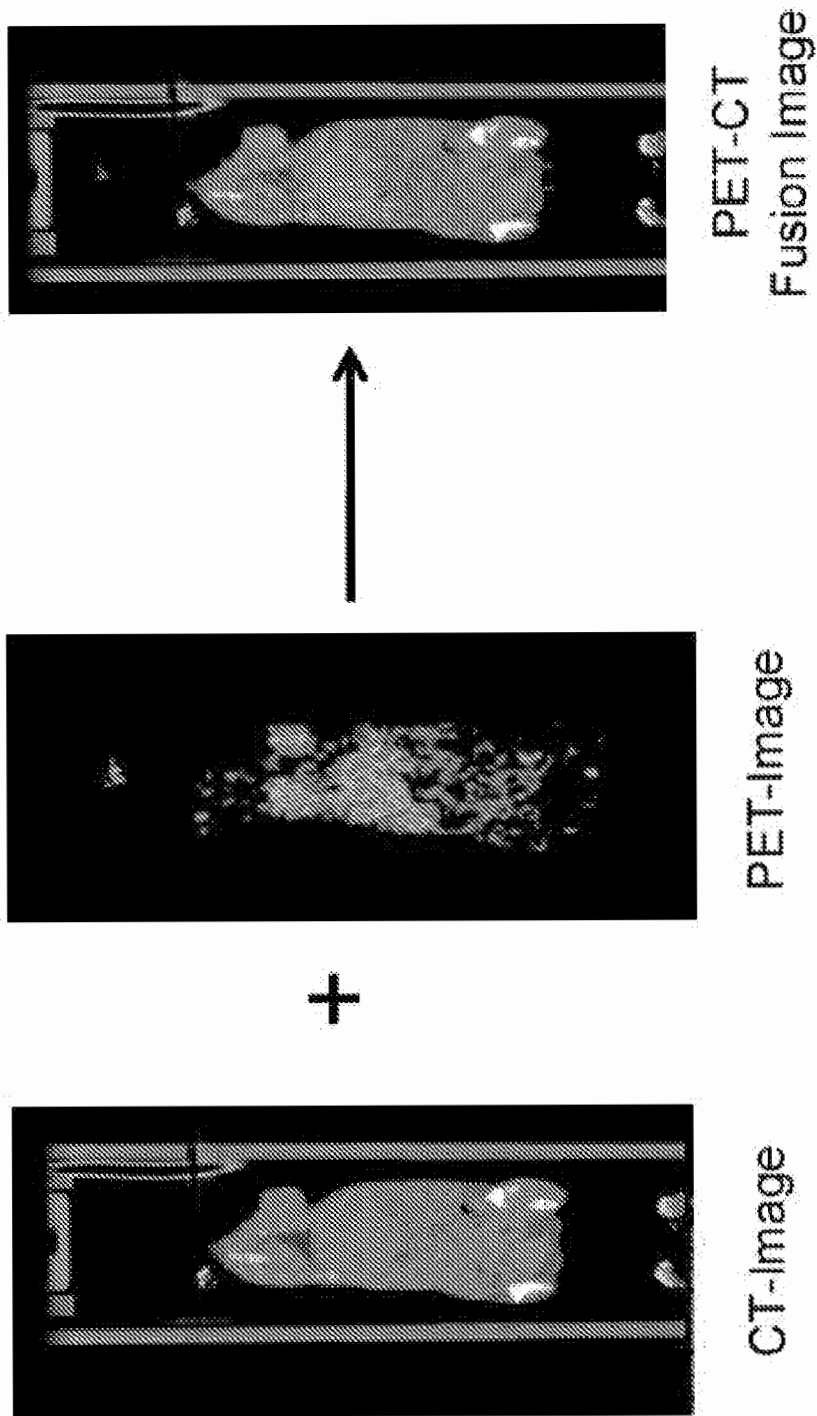


**FIGURE 12**

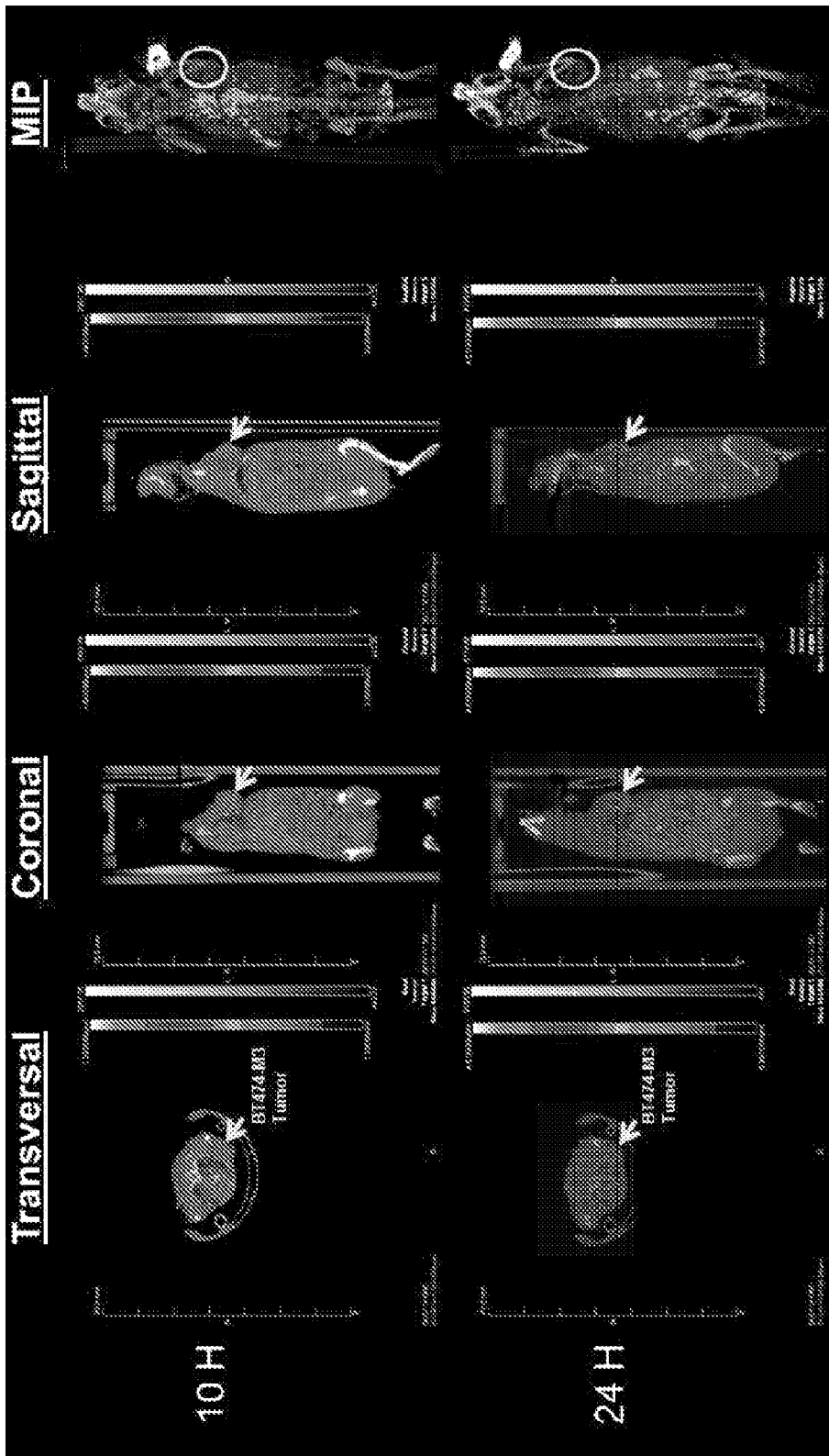


**FIGURE 13**

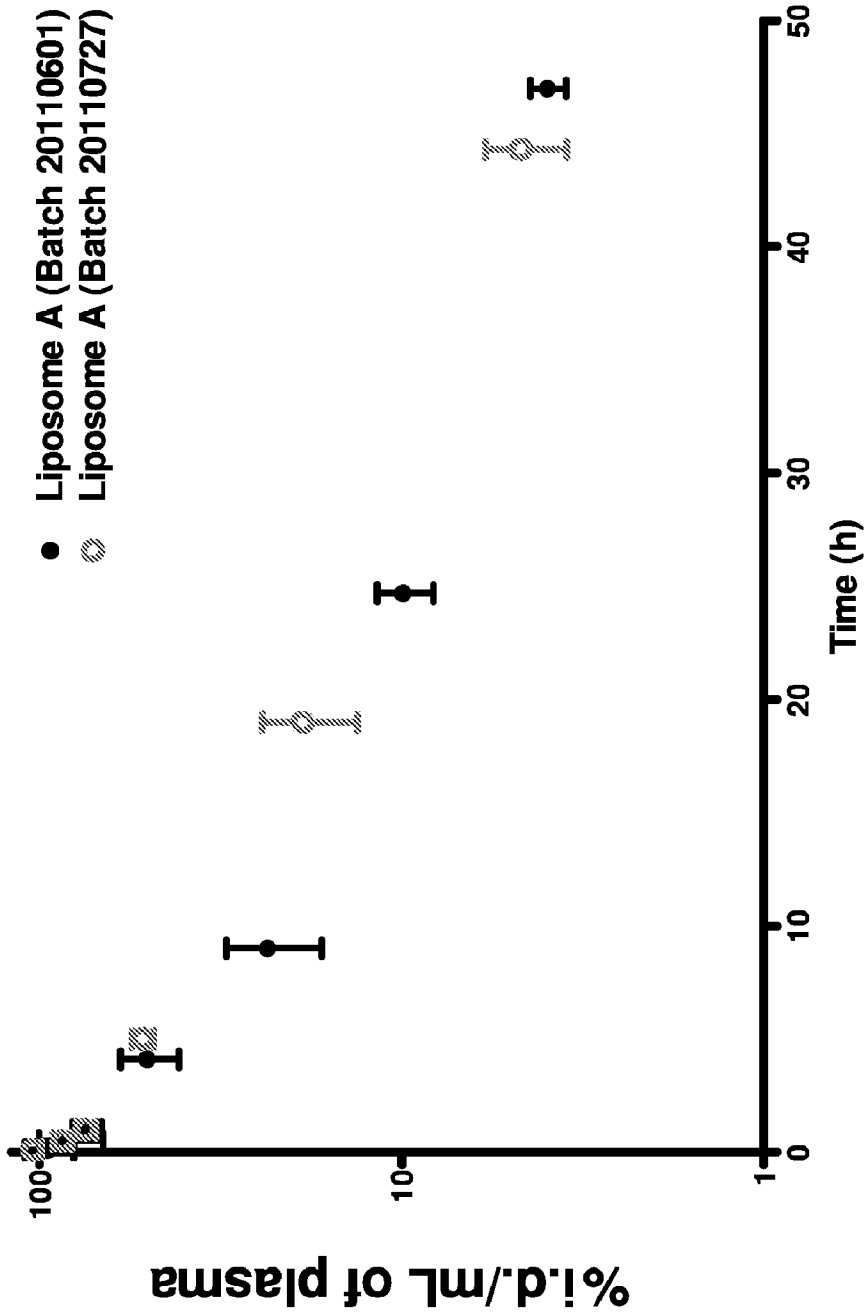


**FIGURE 14A**

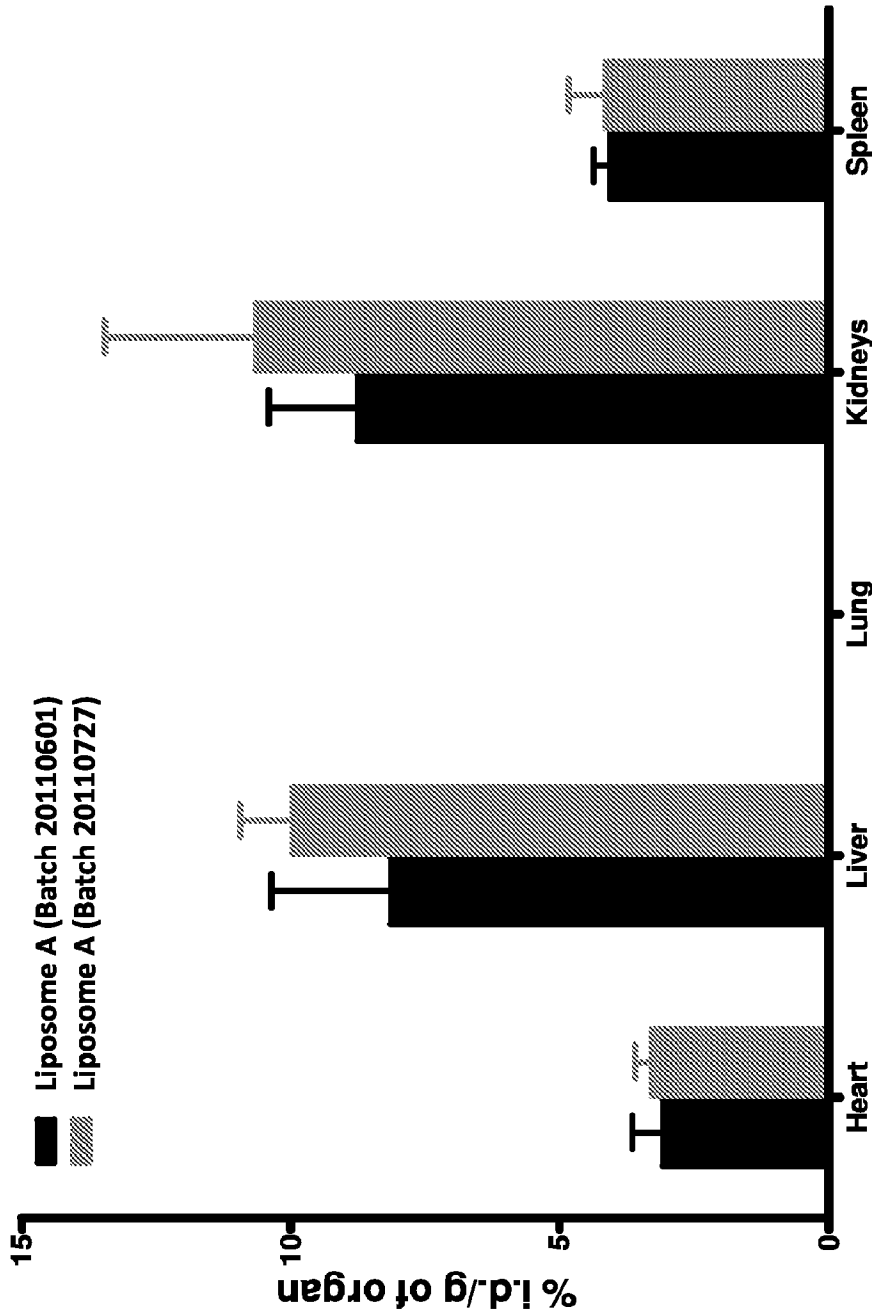


**FIGURE 14B**

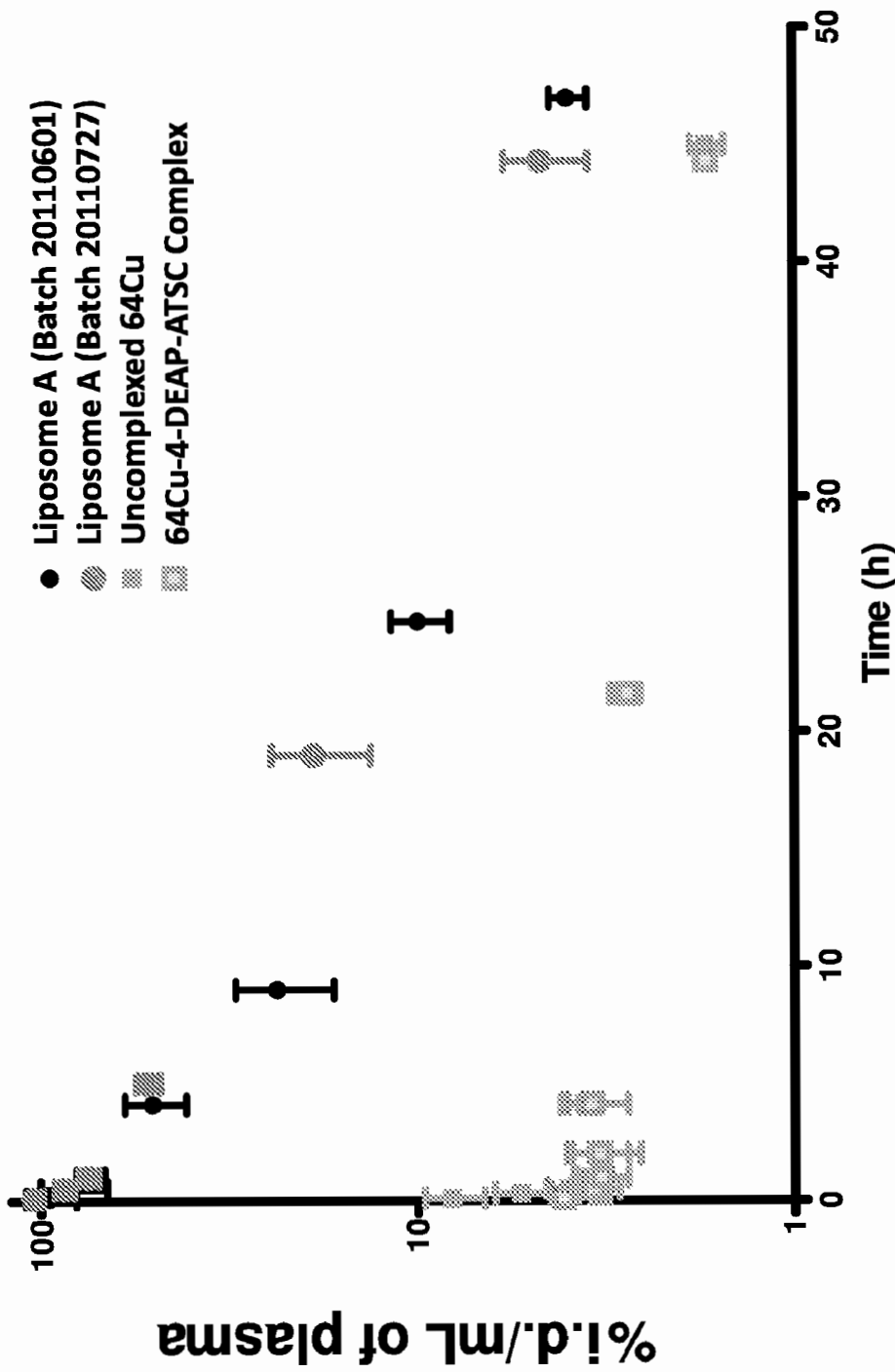


**FIGURE 15A**



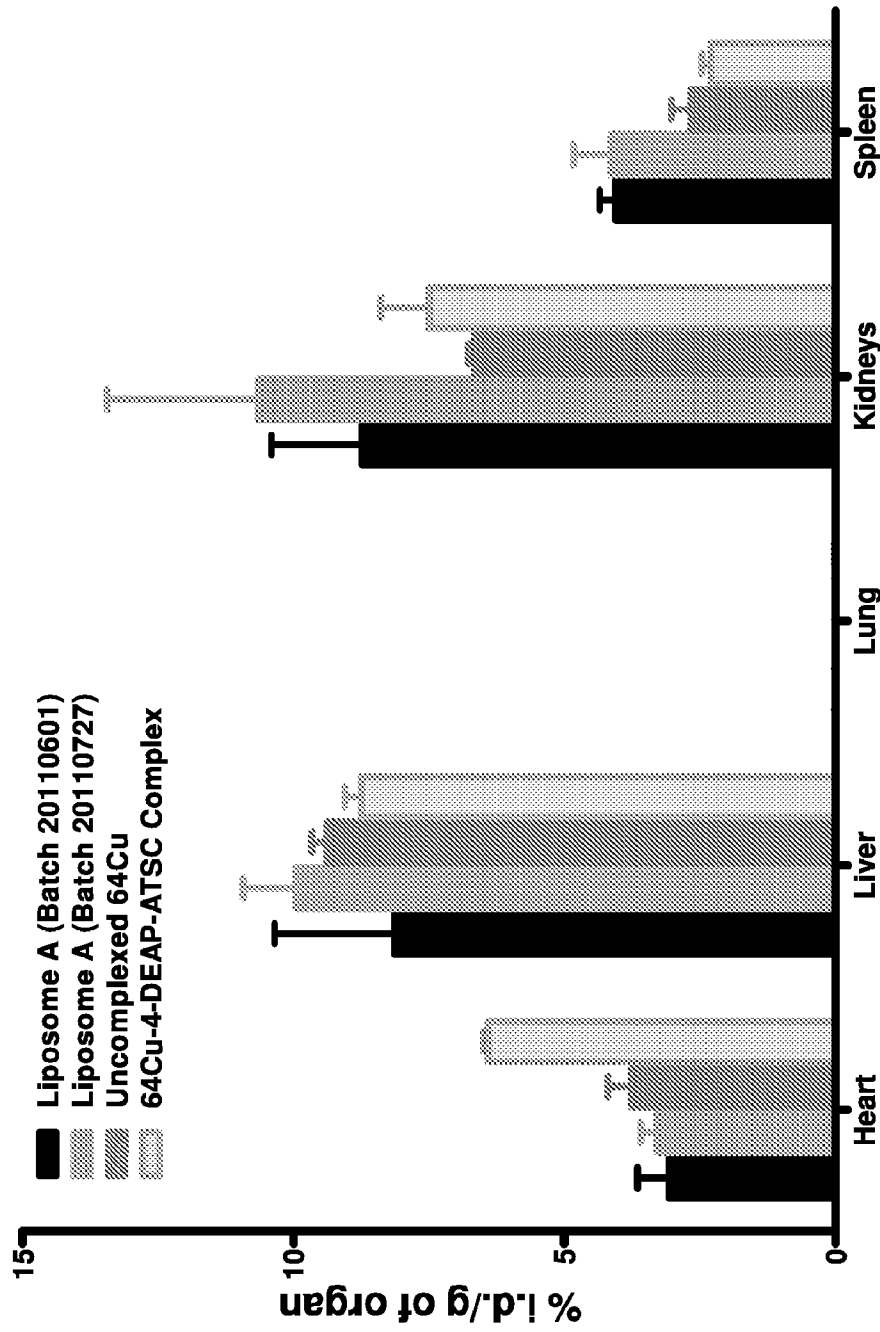


**FIGURE 15B**

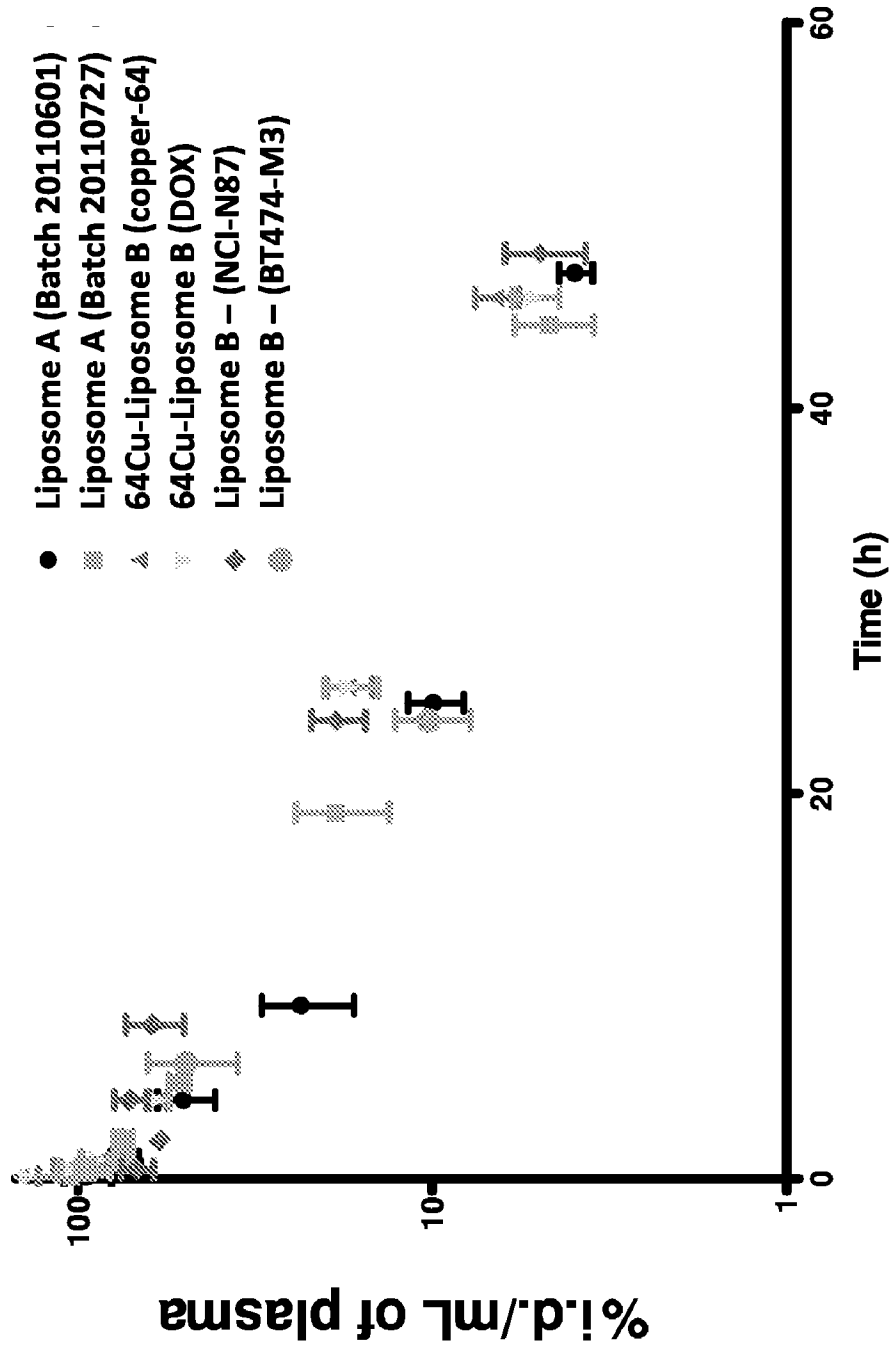
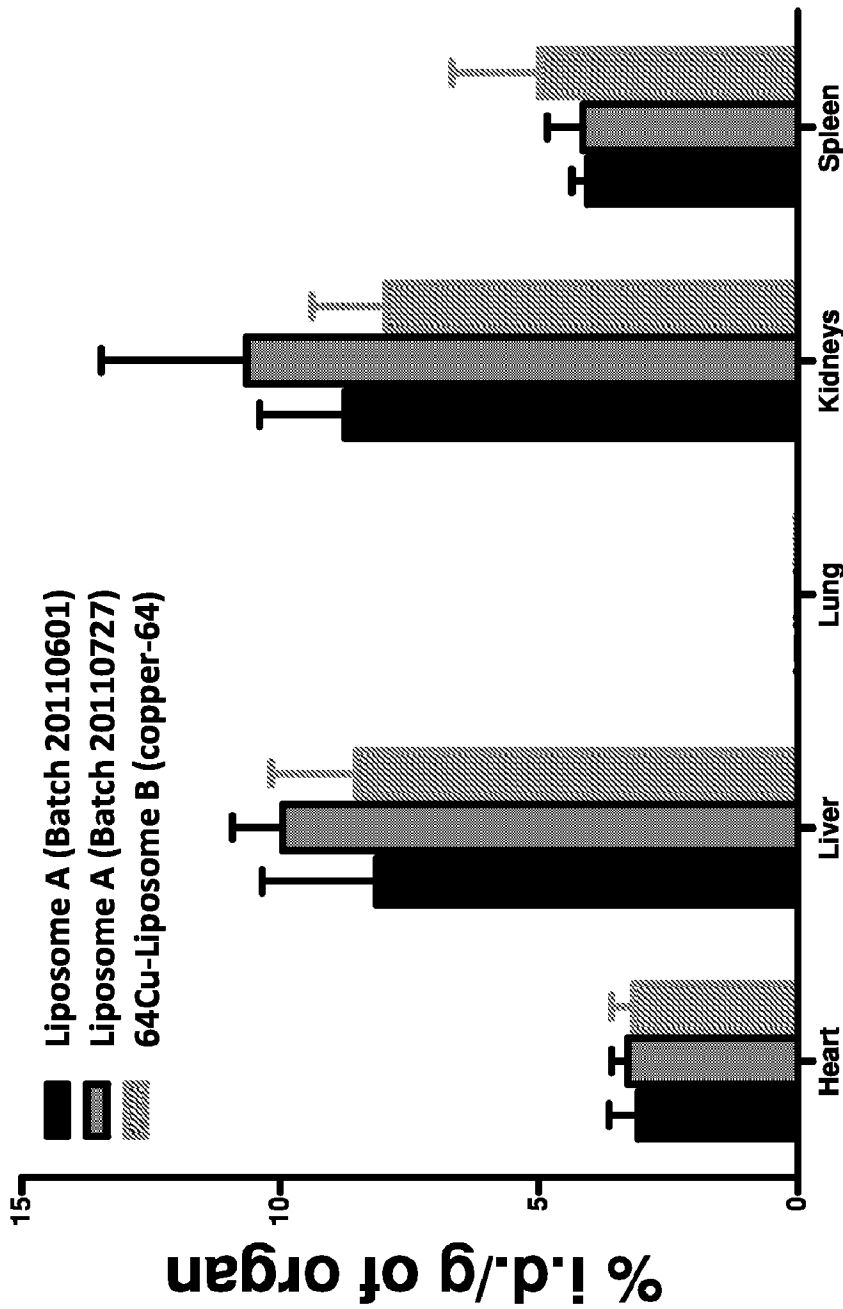
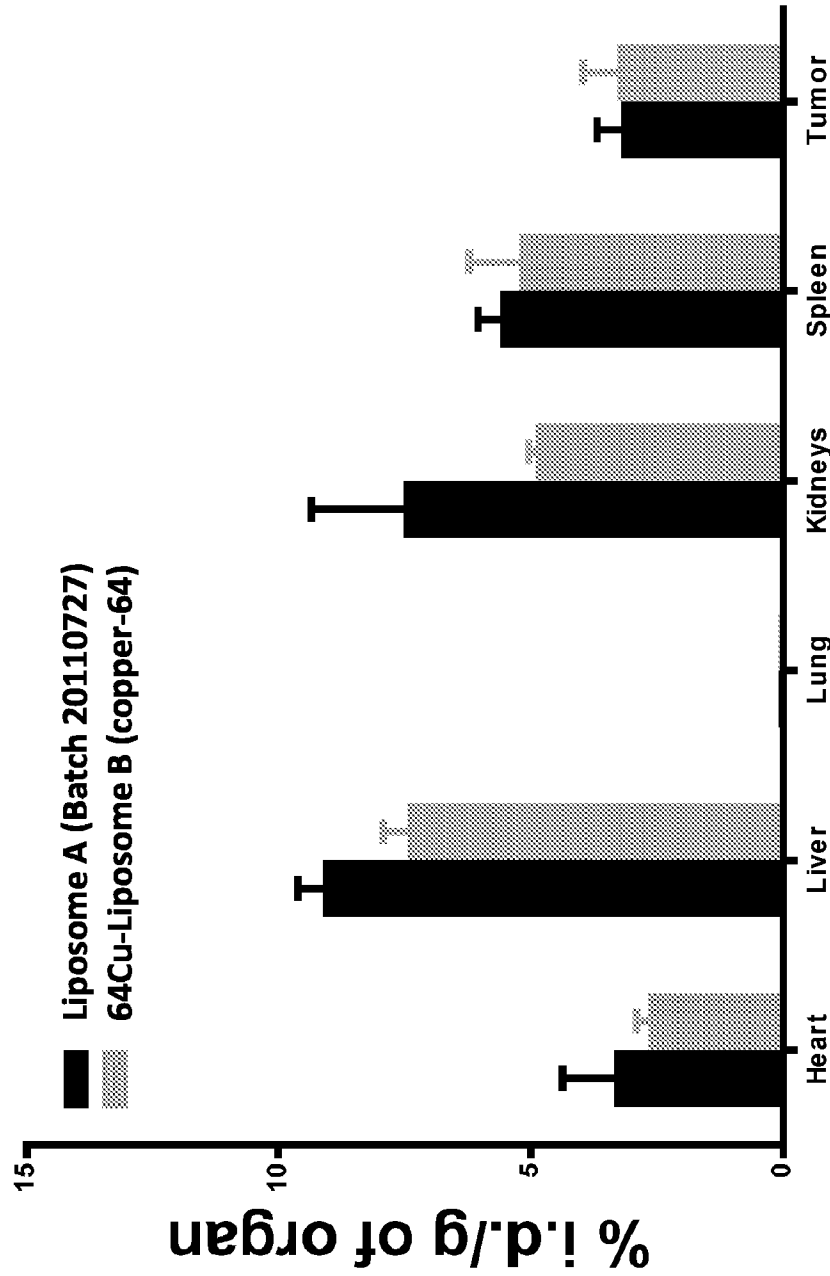


FIGURE 16A



**FIGURE 16B**



**FIGURE 16C**

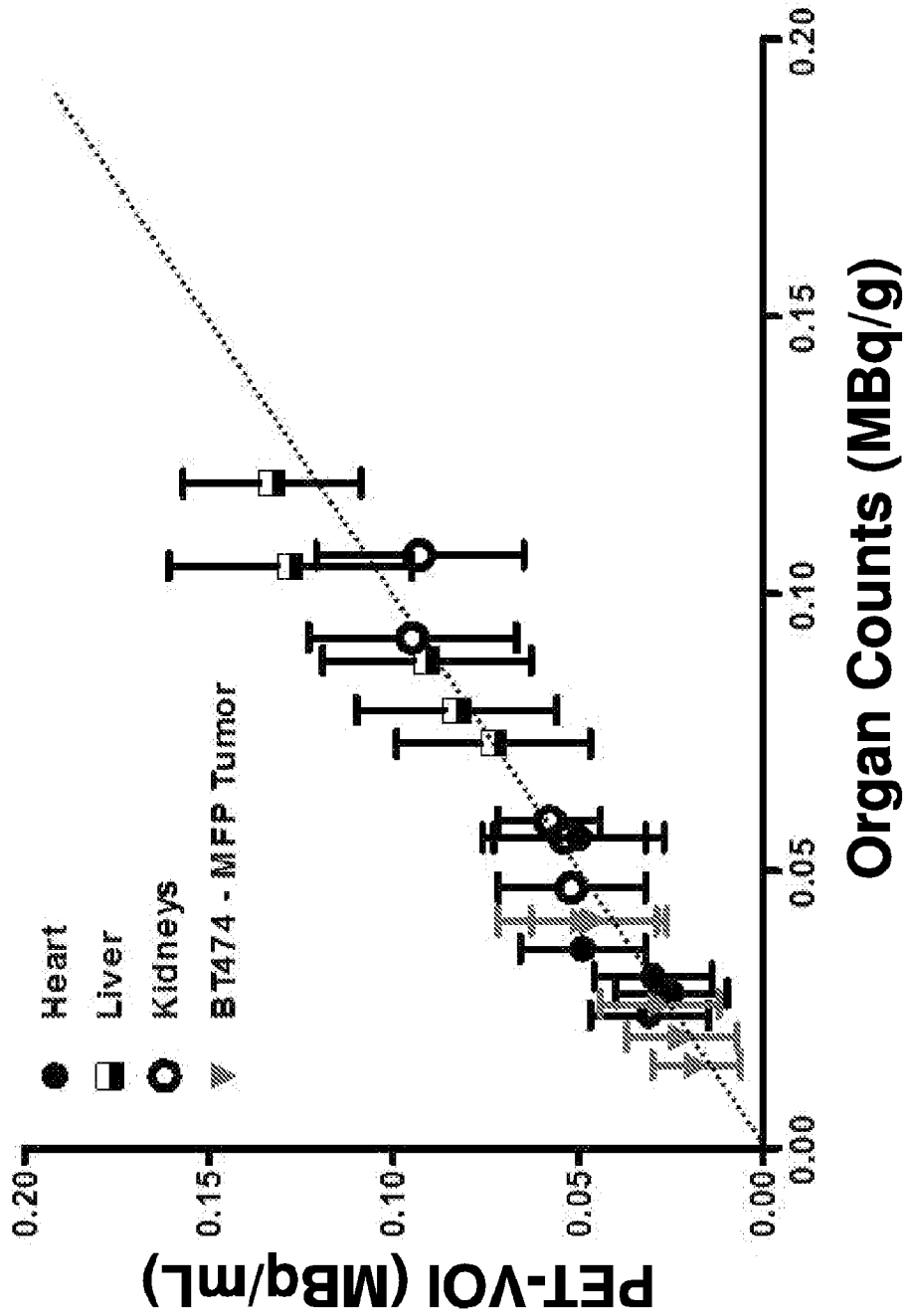
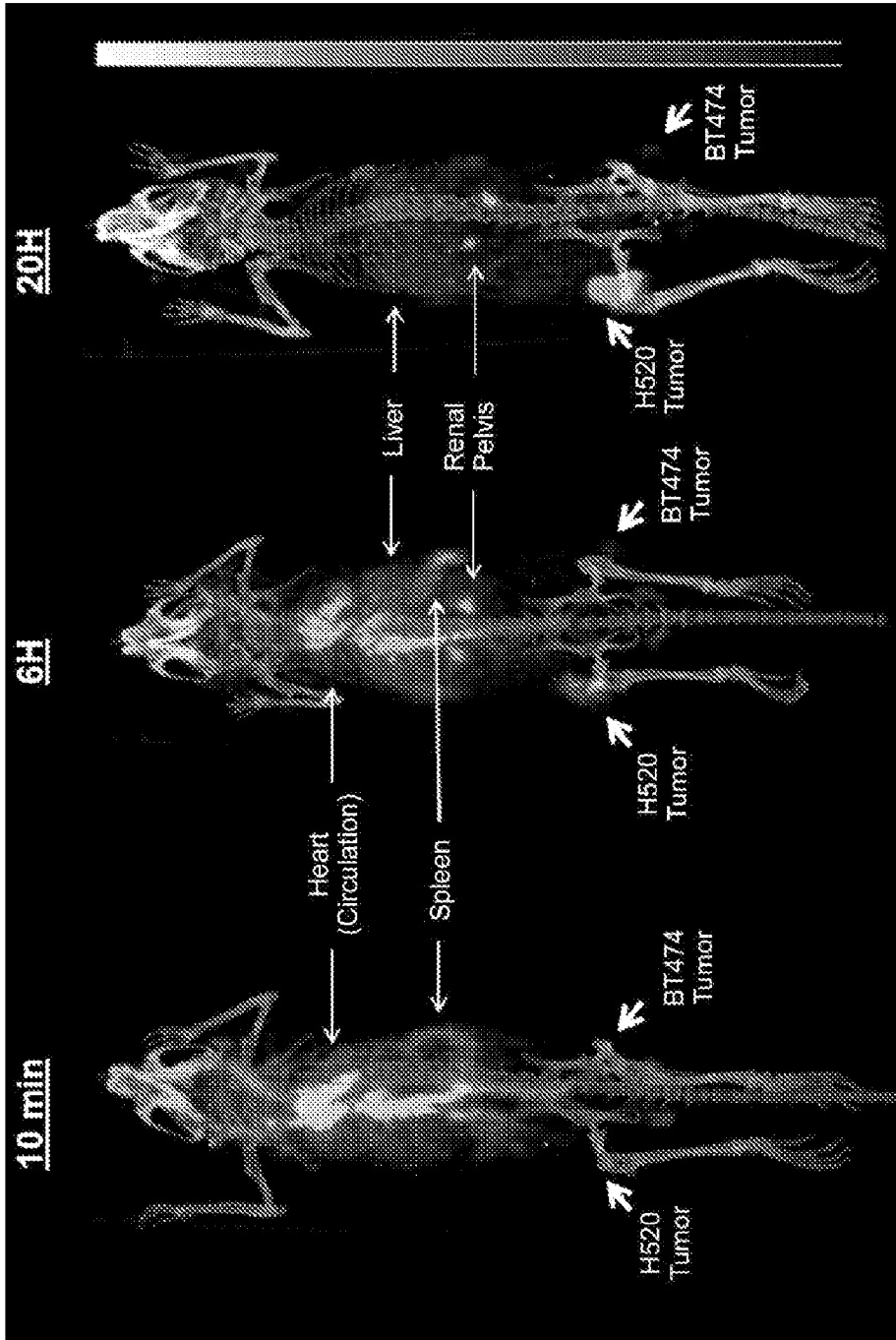
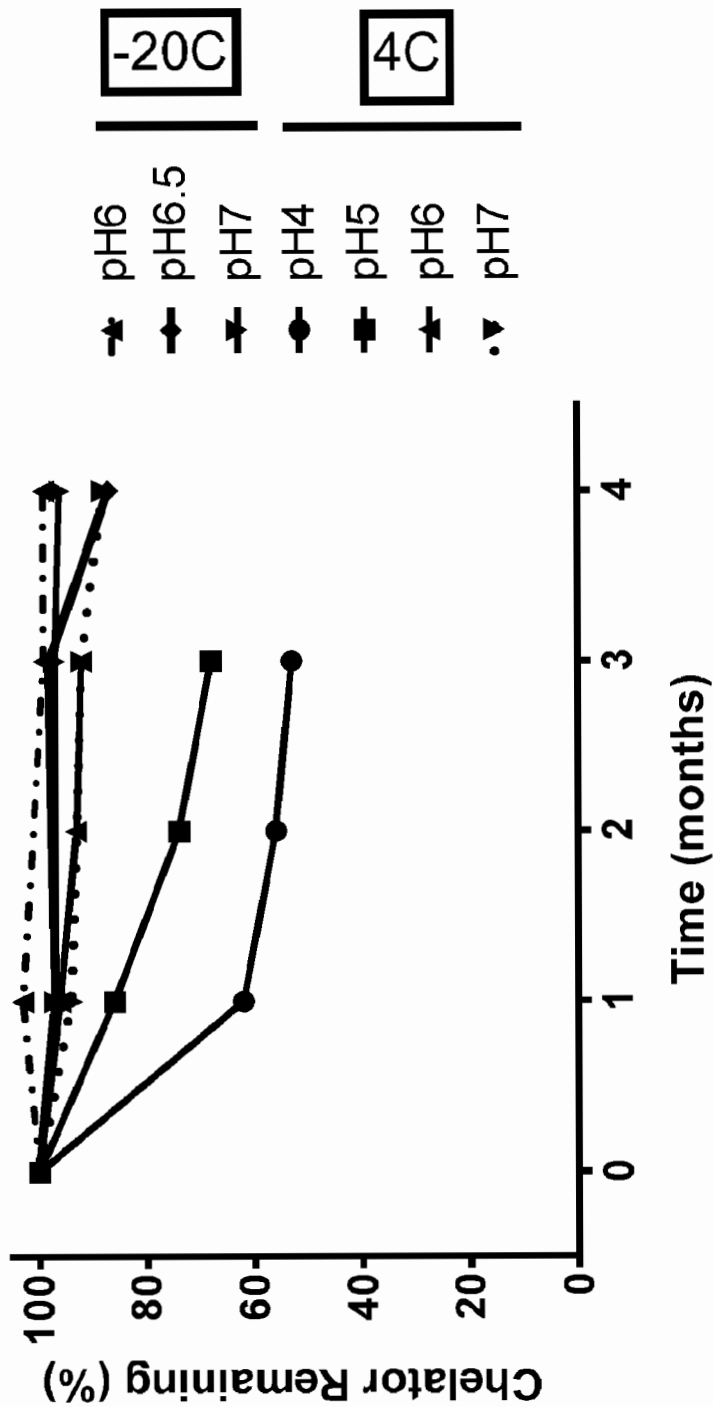


FIGURE 17



**FIGURE 18**



**FIGURE 19A**

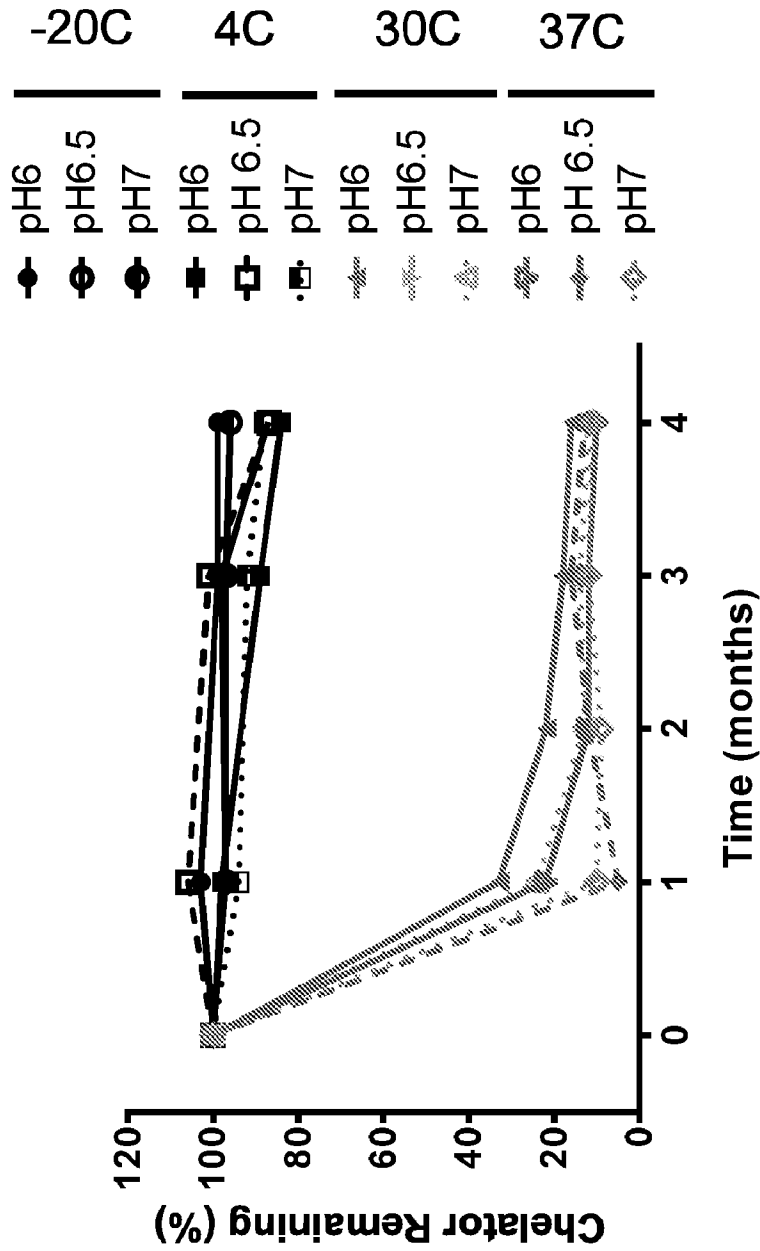


FIGURE 19B



Updated to 4 months

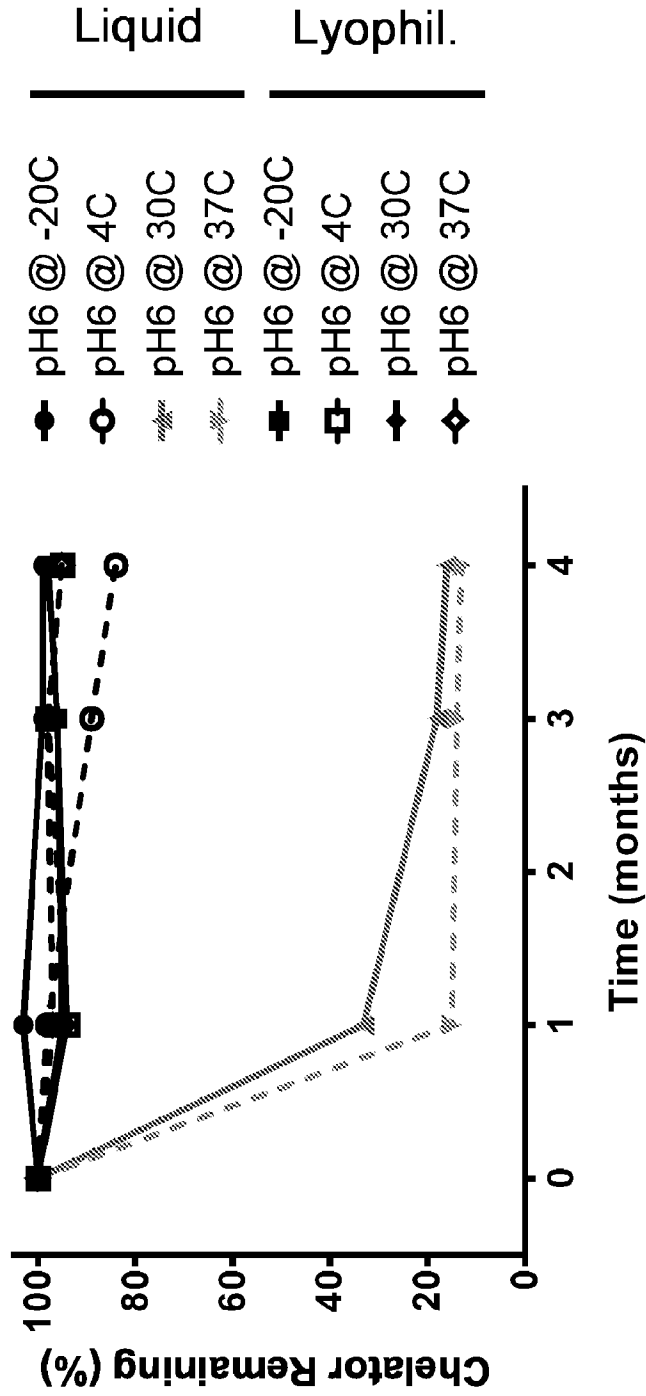
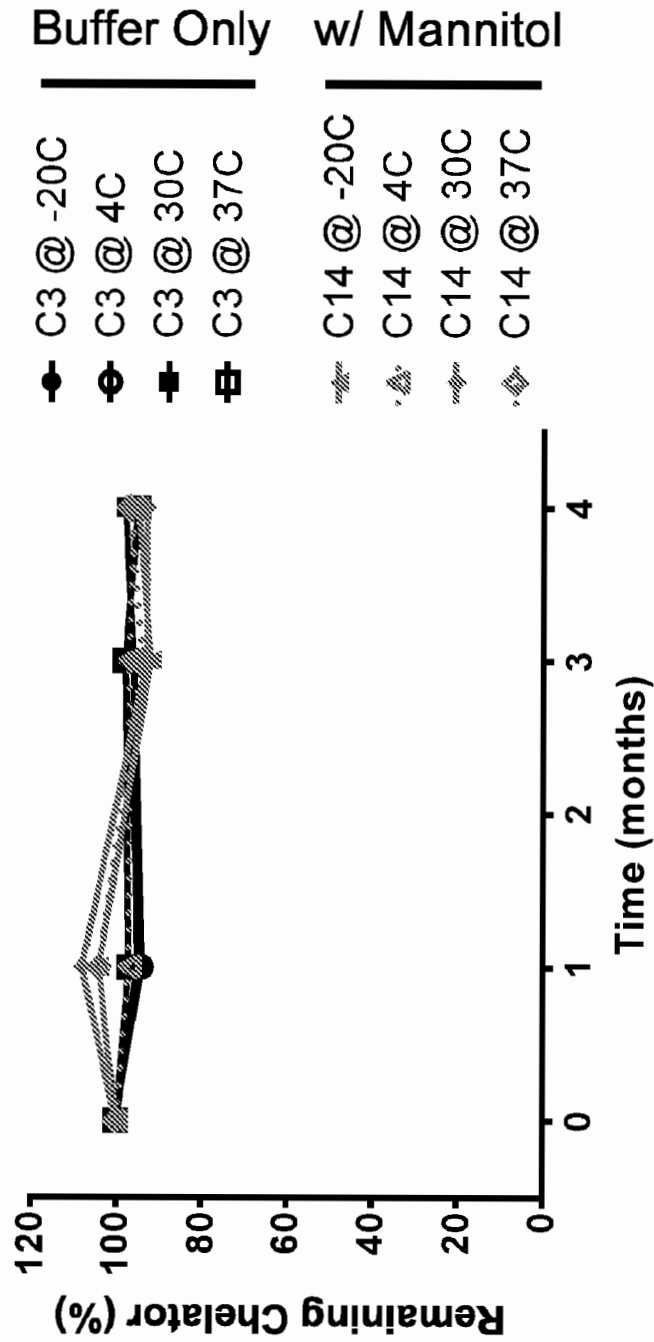


FIGURE 19C



**FIGURE 19D**

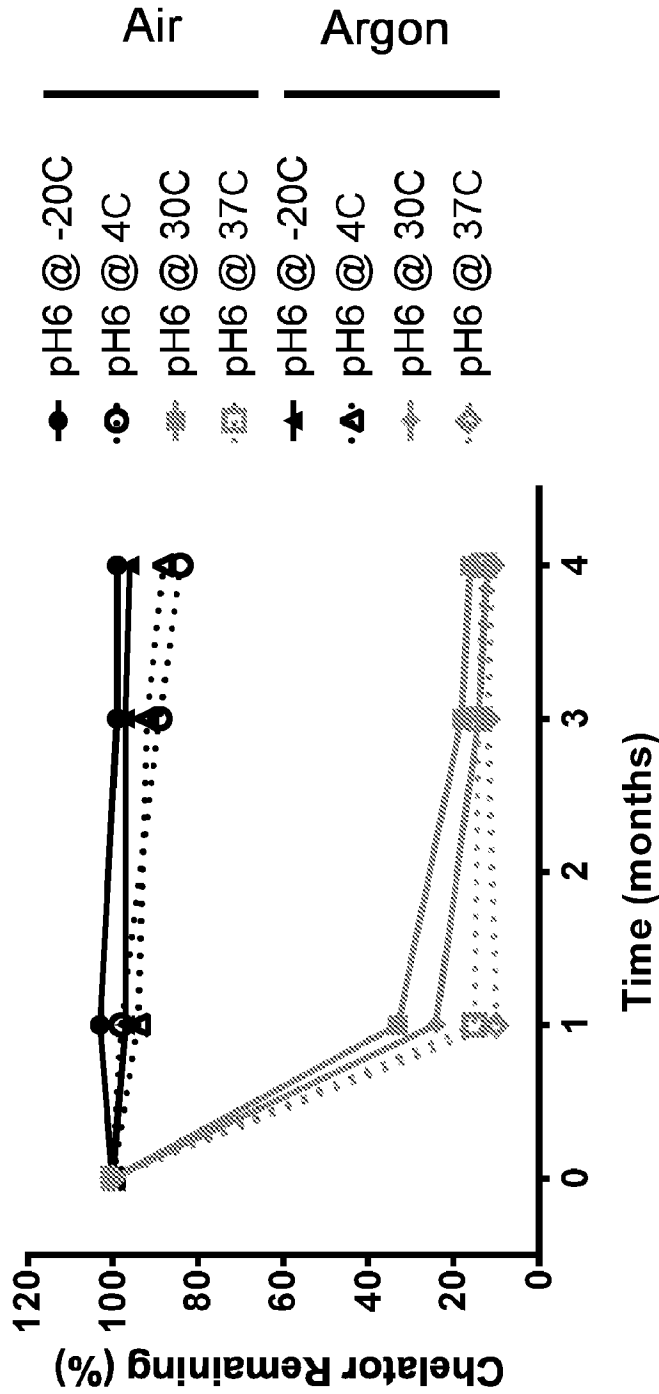
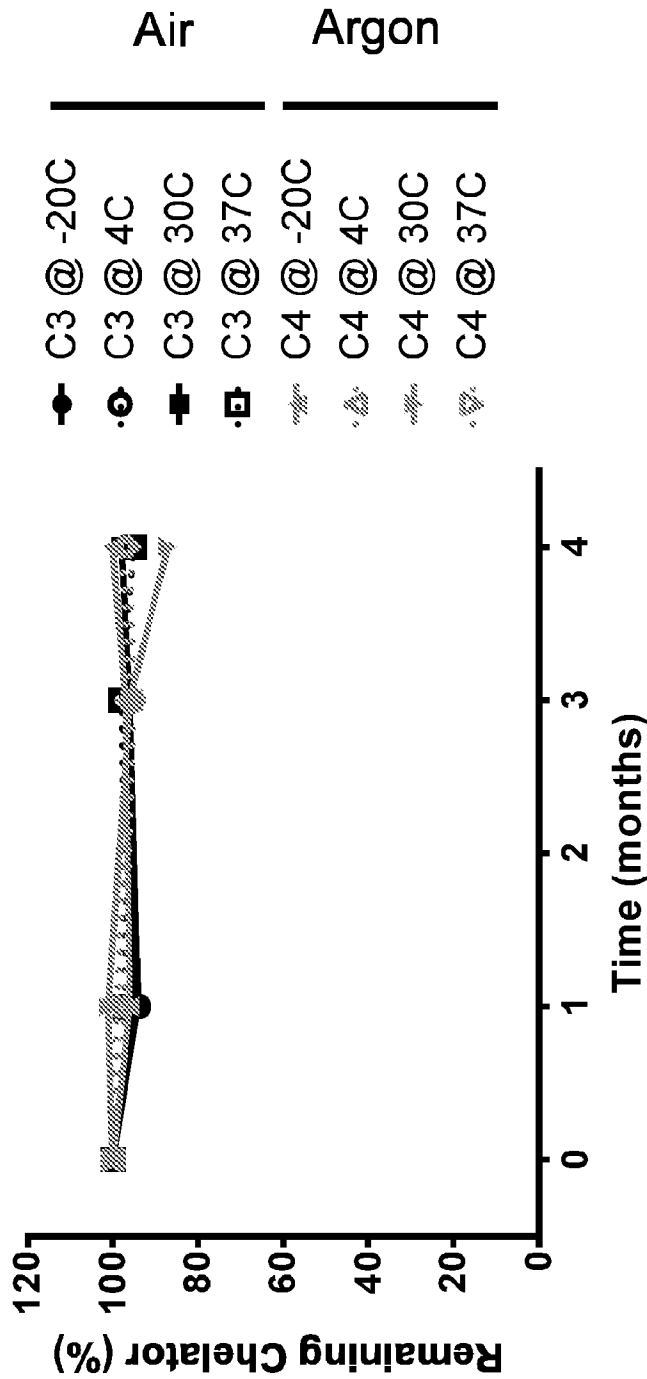
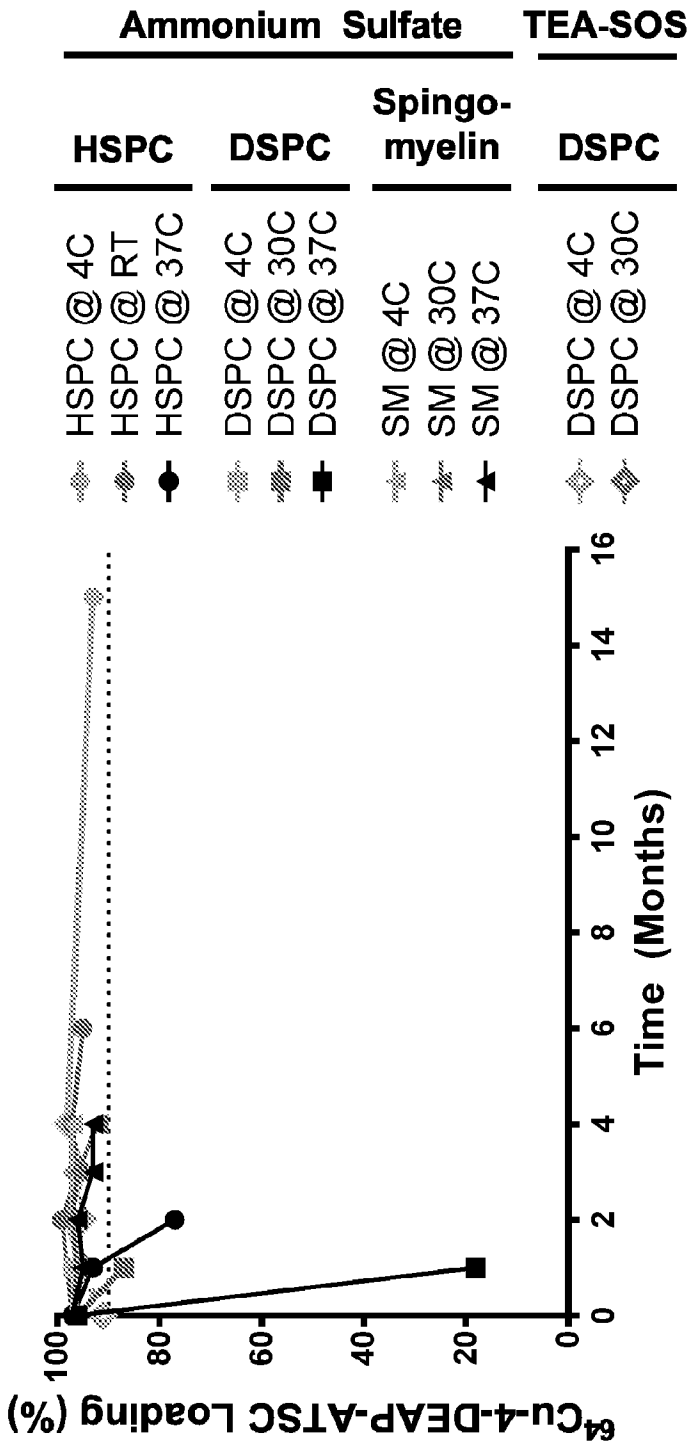


FIGURE 19E



**FIGURE 19F**



**FIGURE 20A**

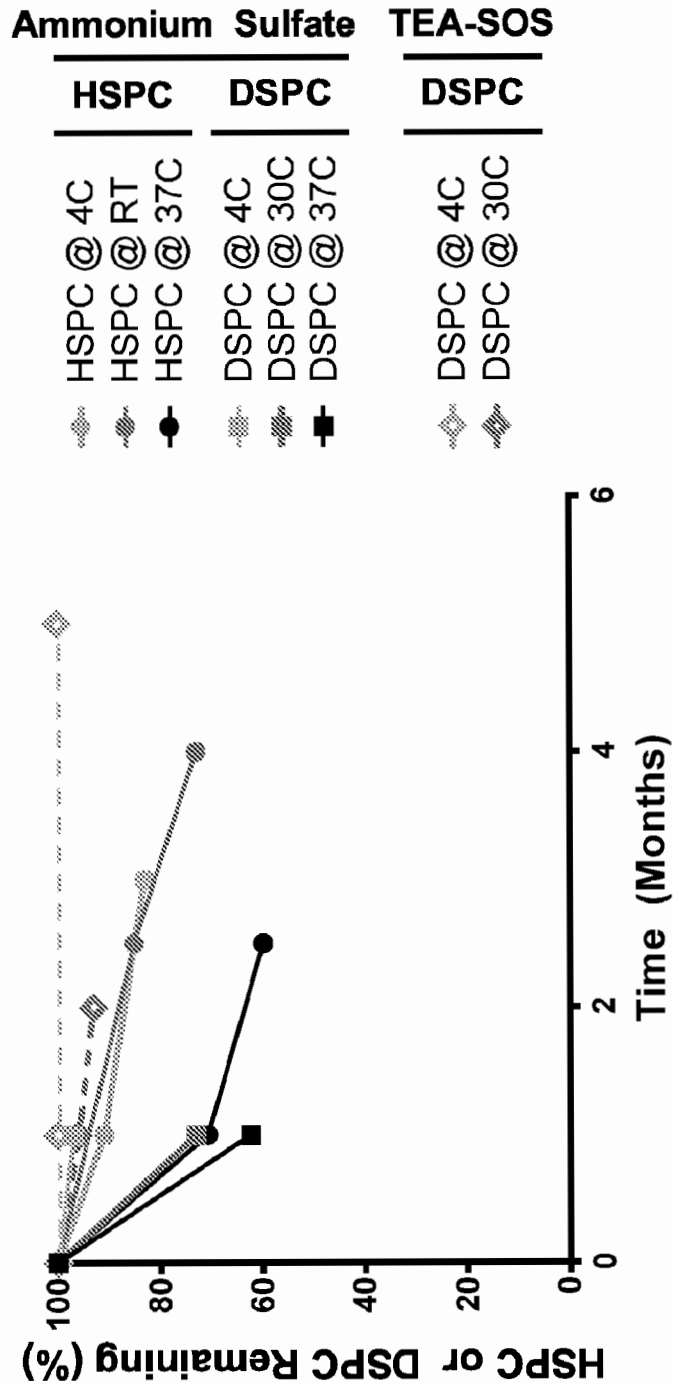


**FIGURE 20B**

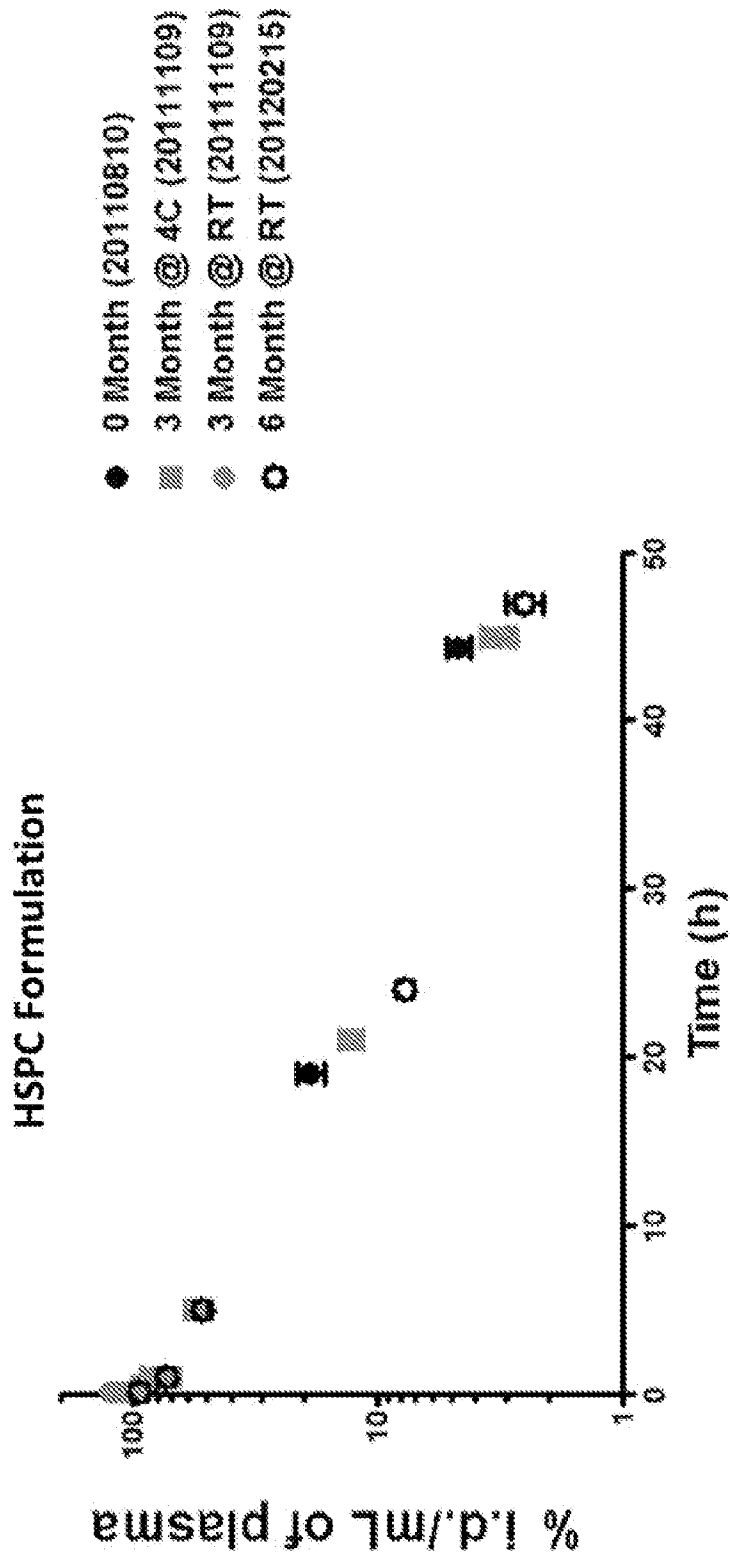


**FIGURE 20C**

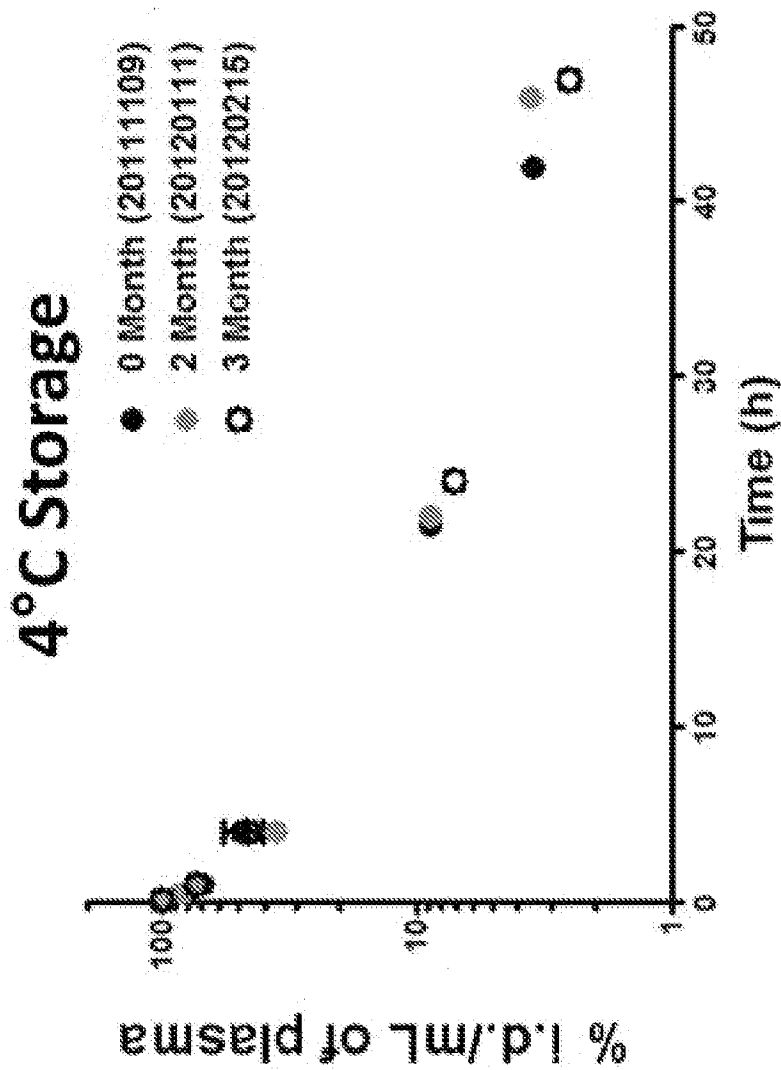


**FIGURE 20D**



# 30°C Storage

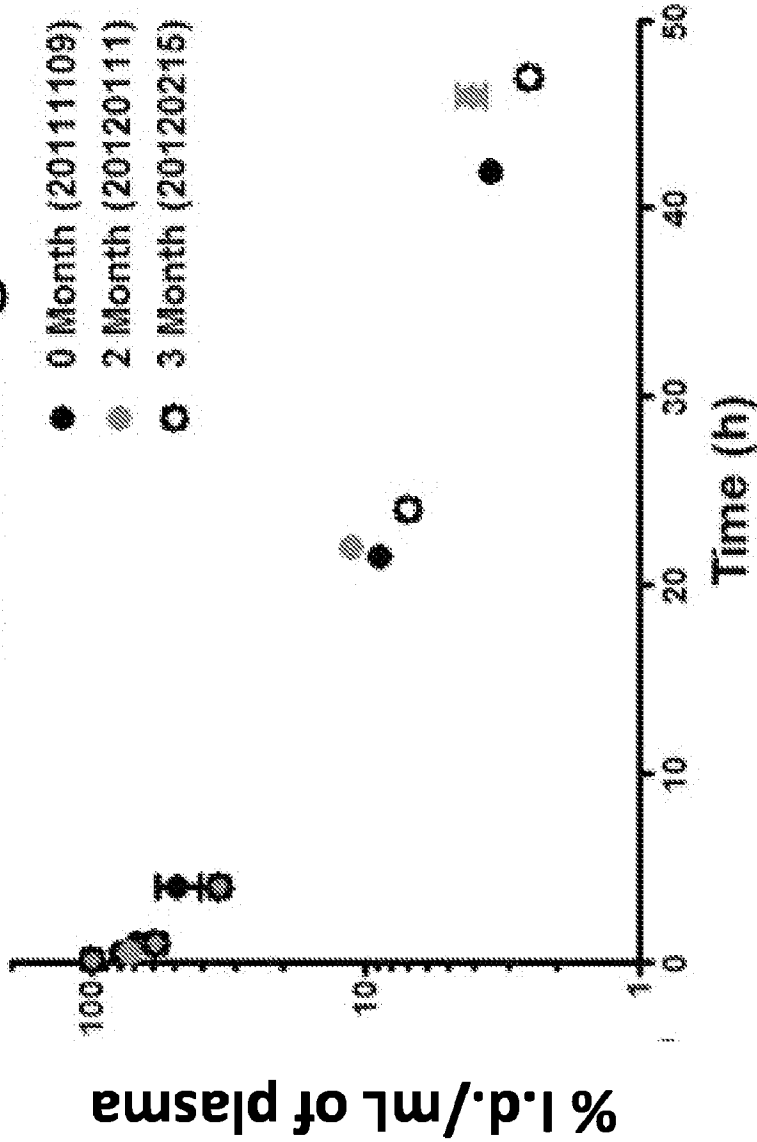


**FIGURE 20E**

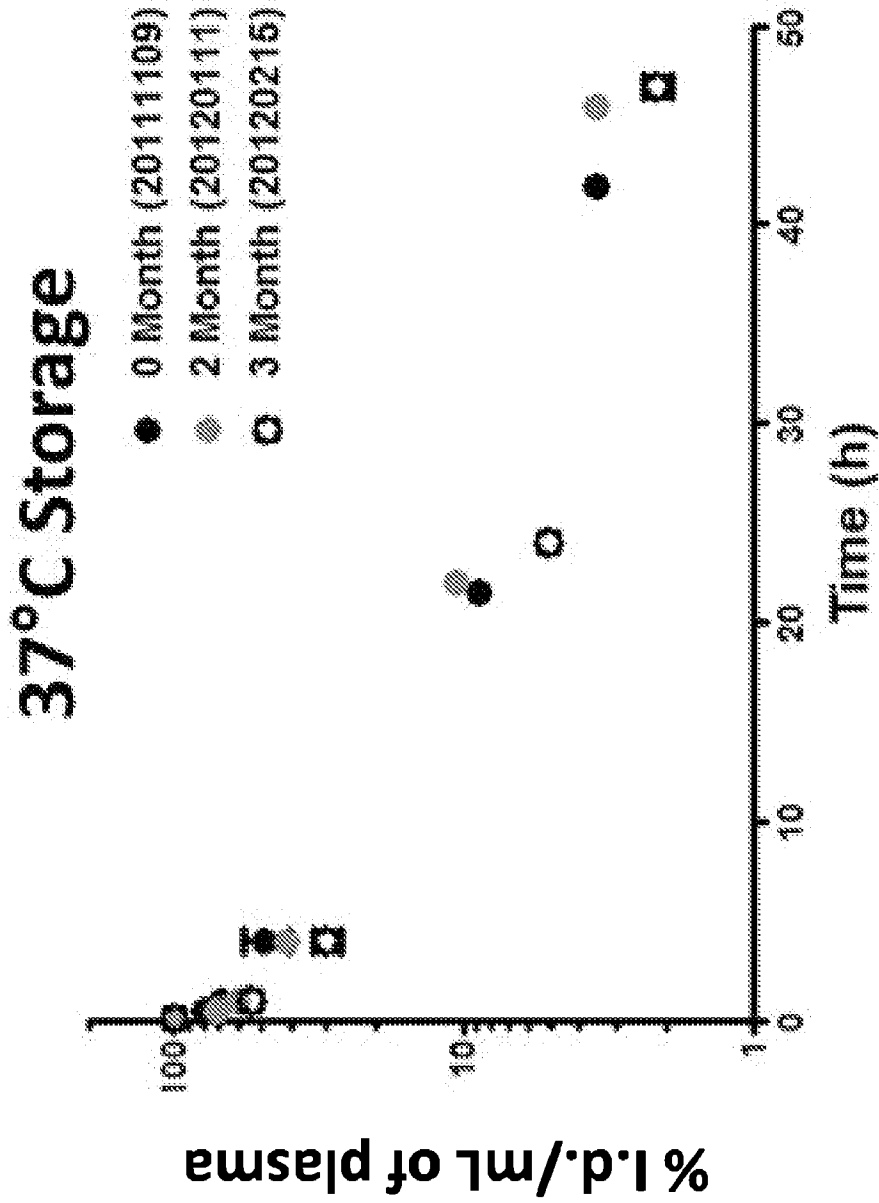


**FIGURE 20F**

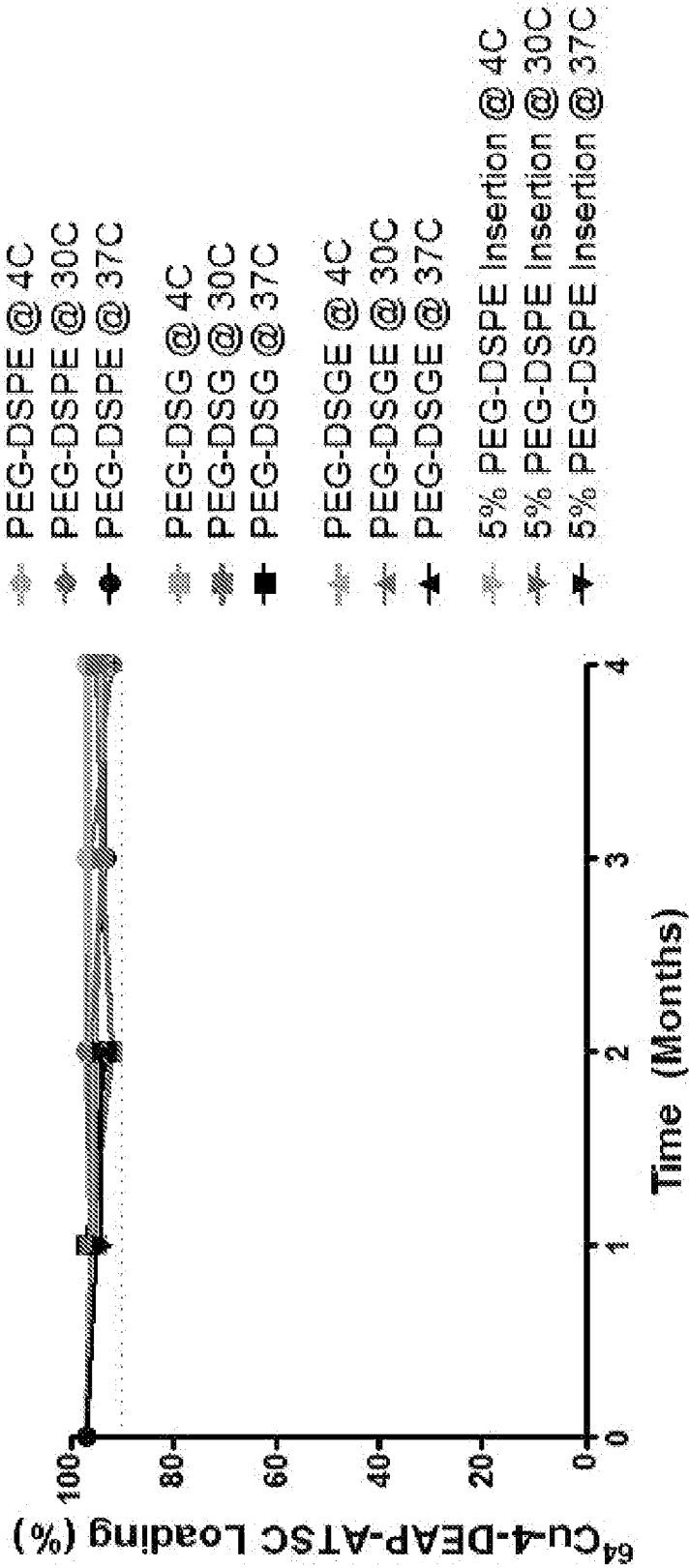


FIGURE 20G

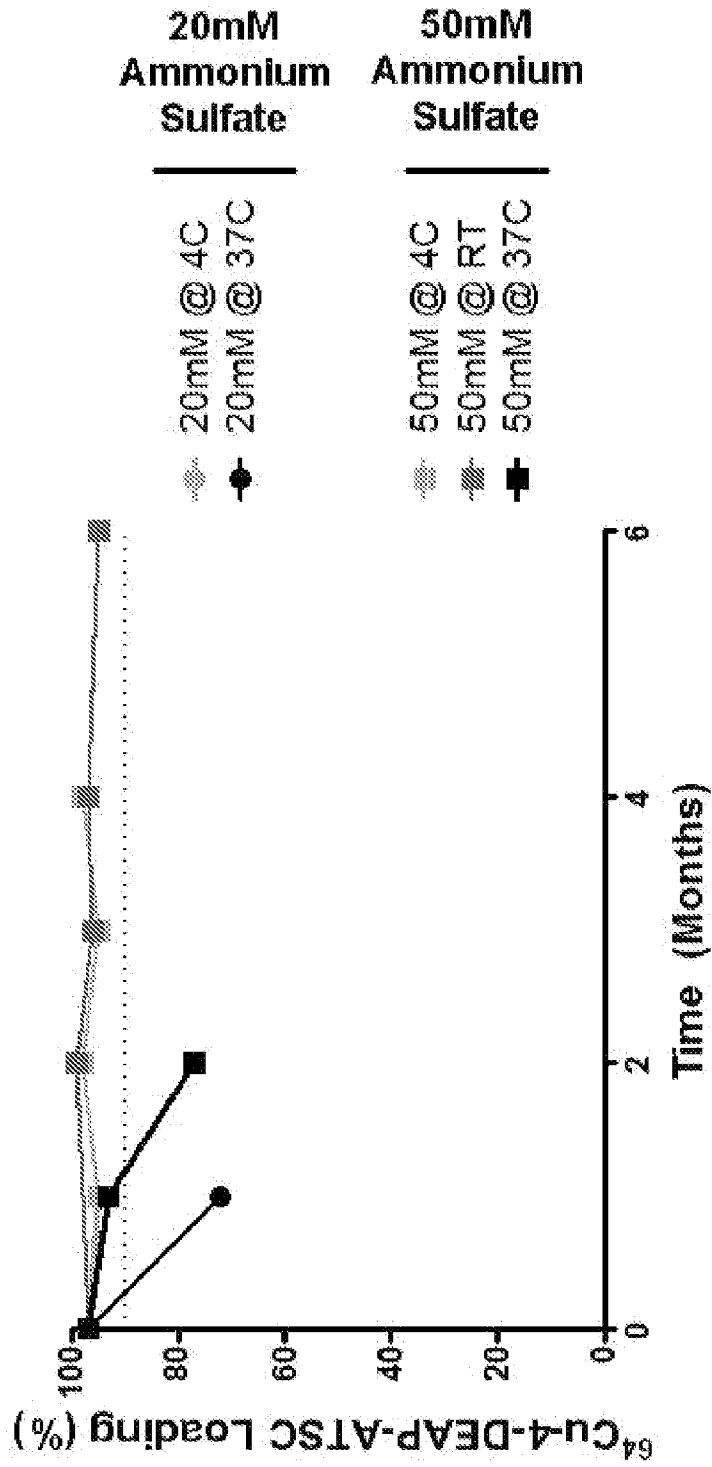


FIGURE 21A

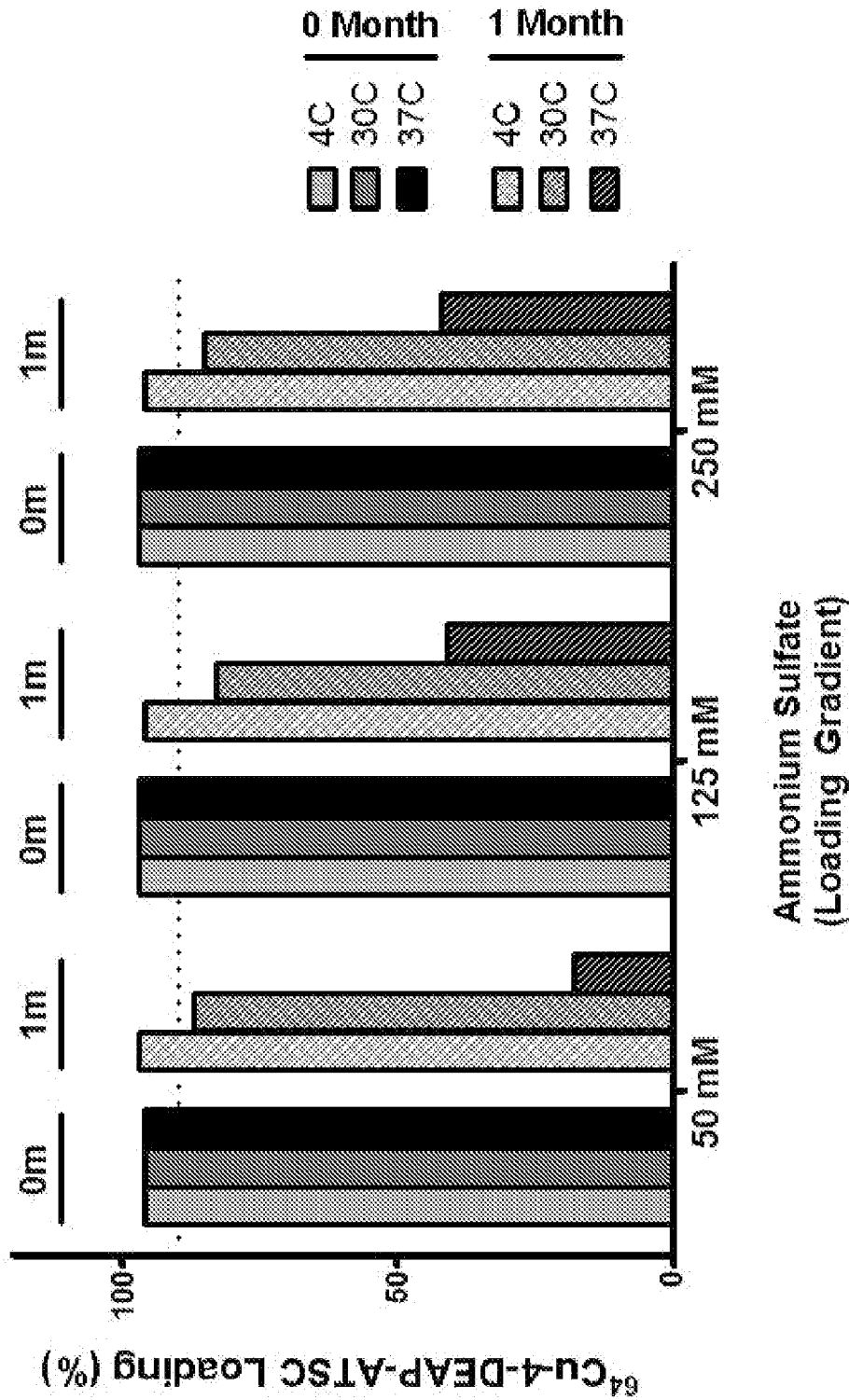
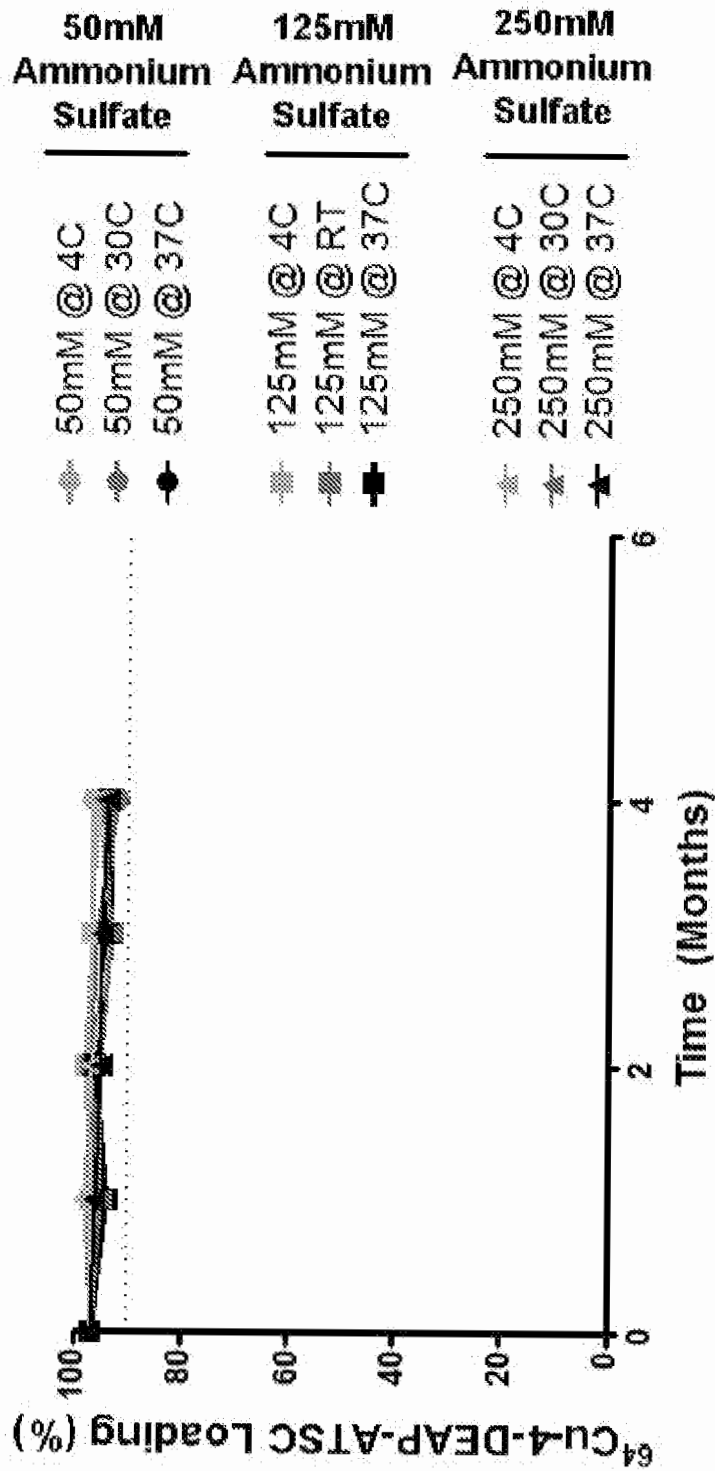


FIGURE 21B



**FIGURE 21C**

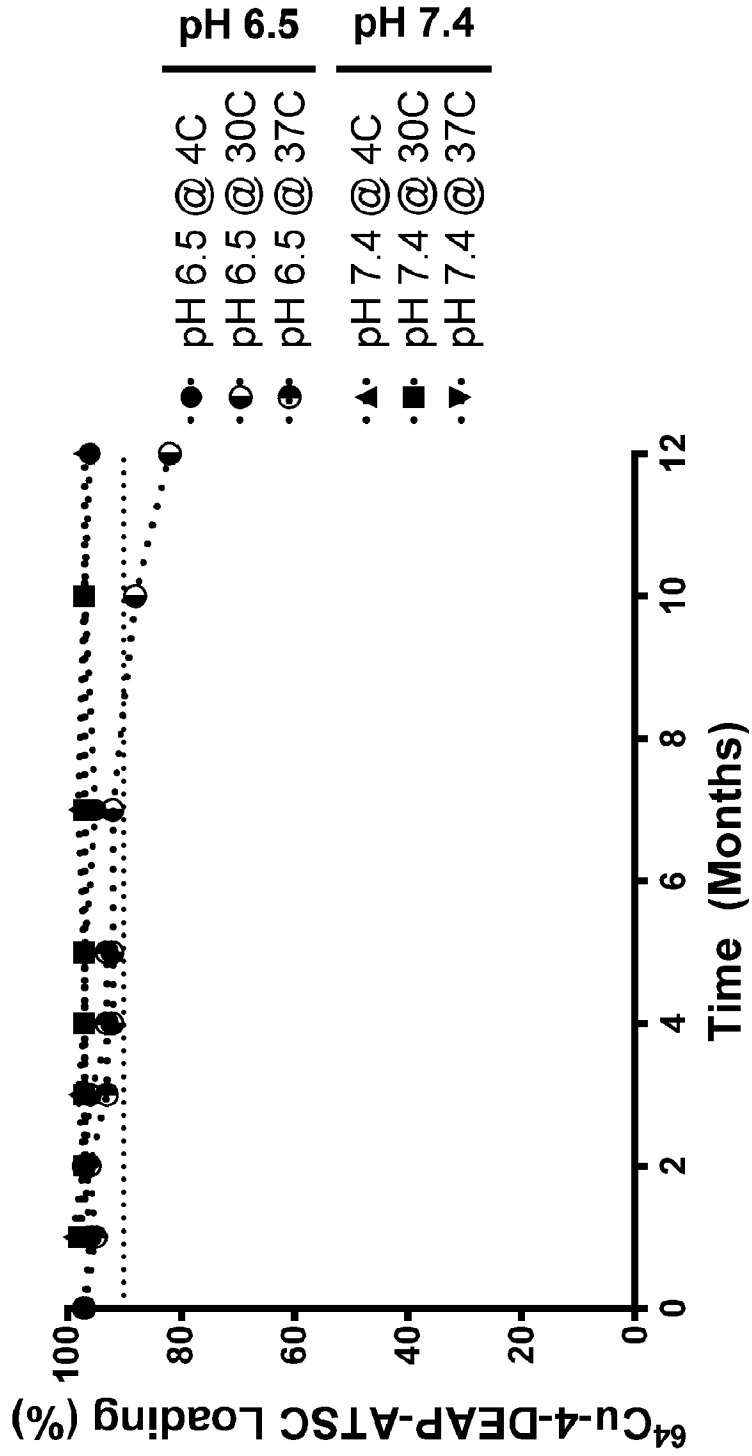
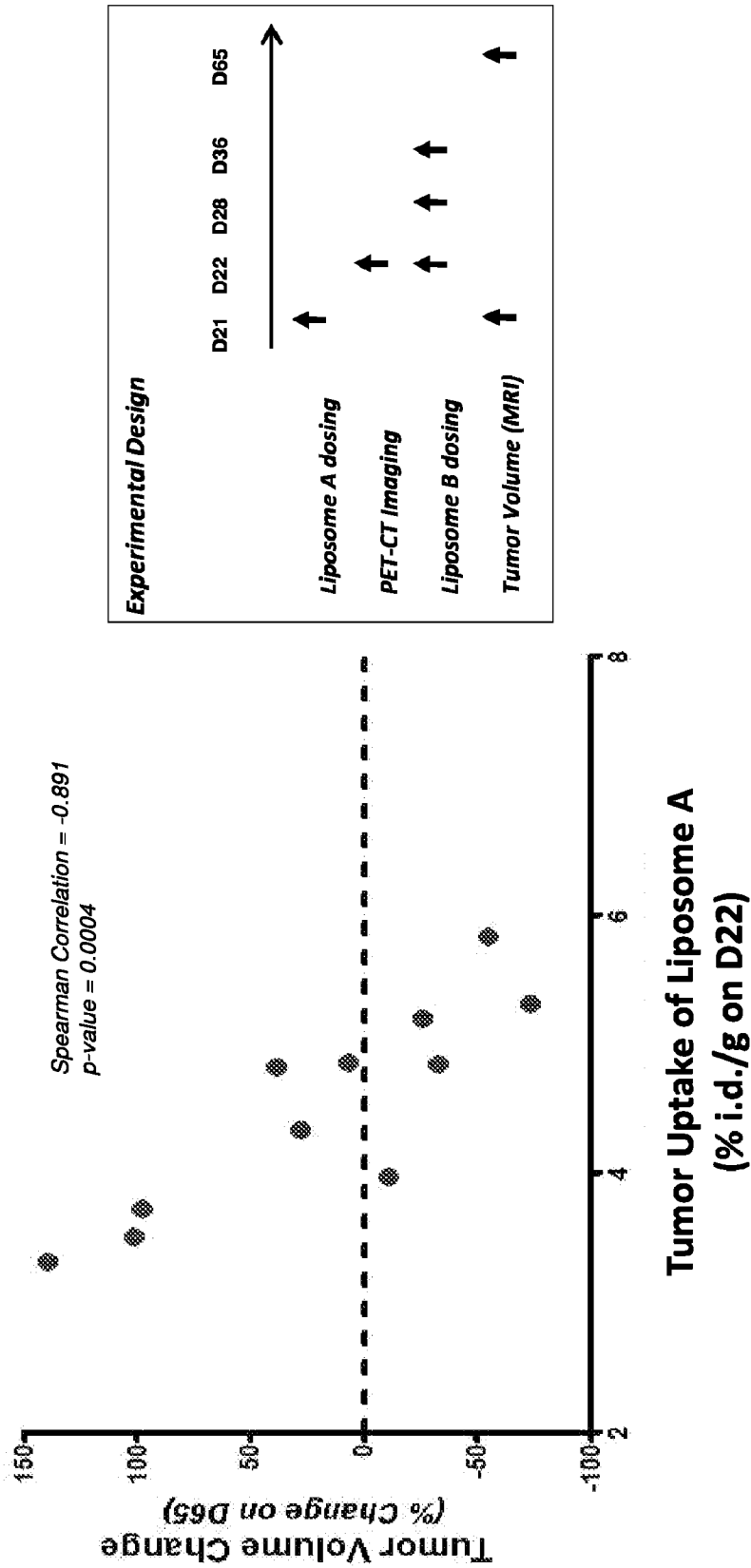
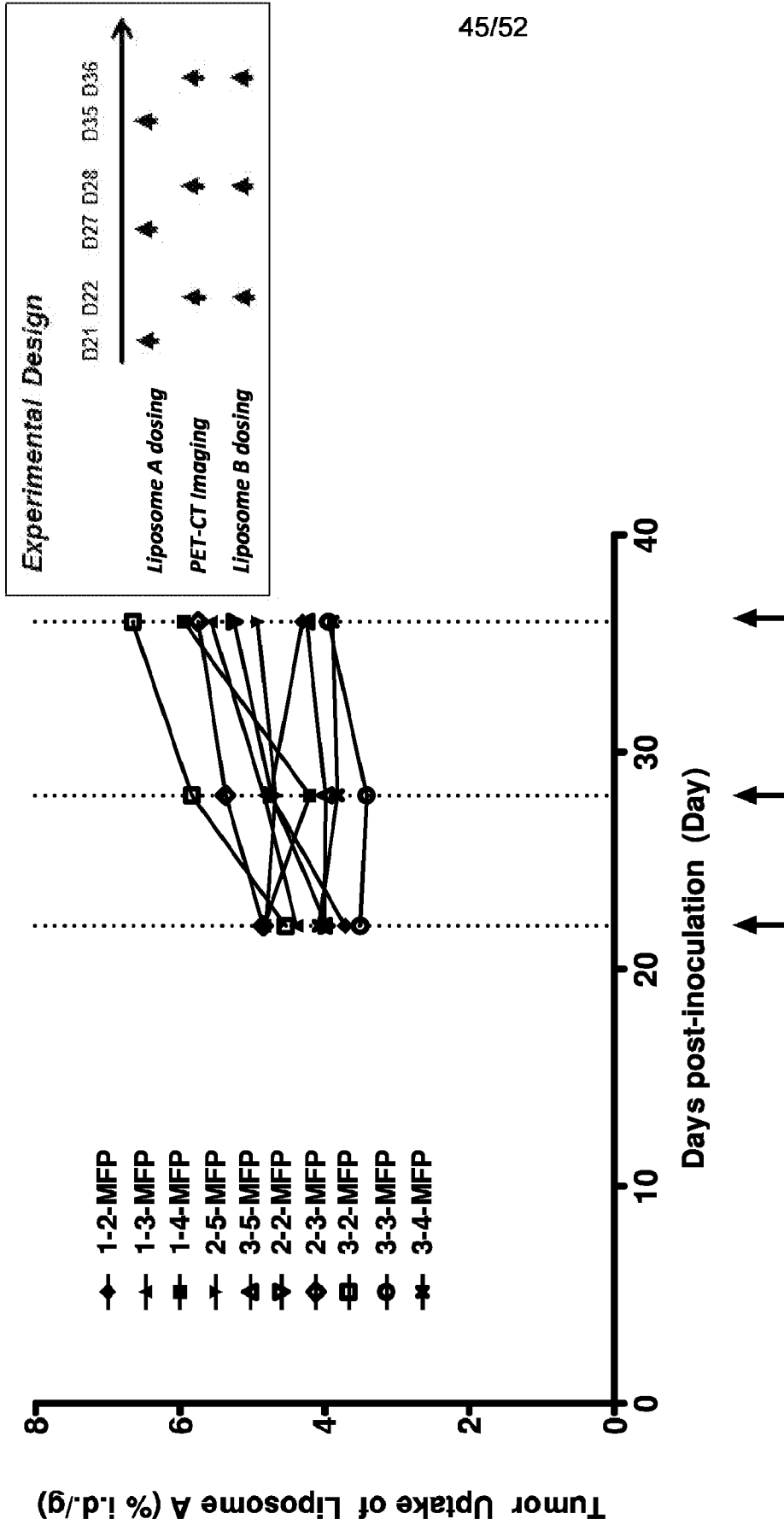


FIGURE 22



**FIGURE 23**





**FIGURE 24A**

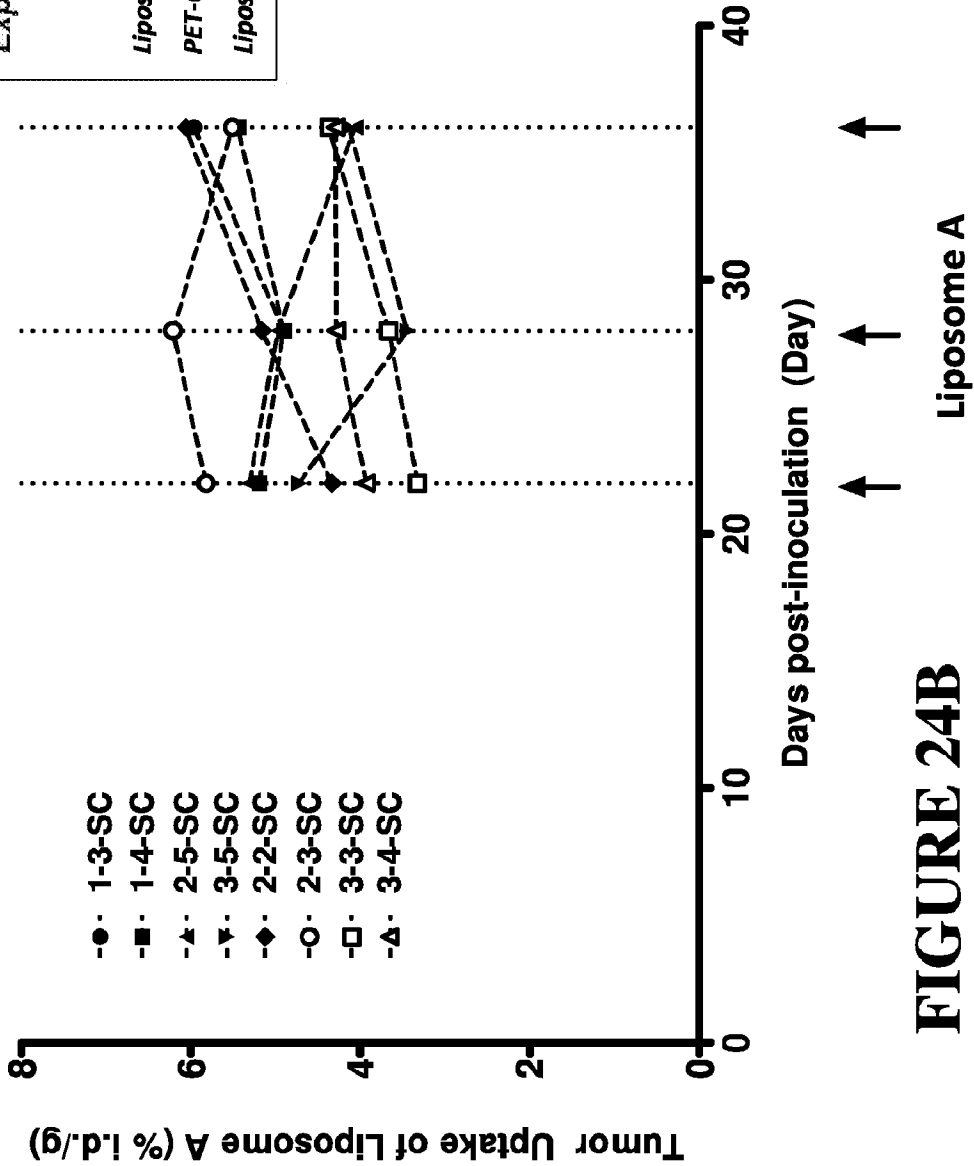
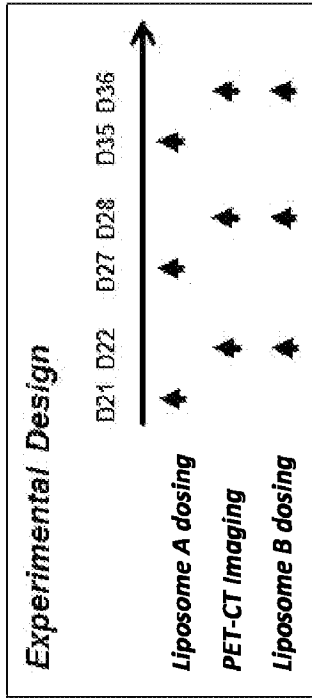


**FIGURE 24B**

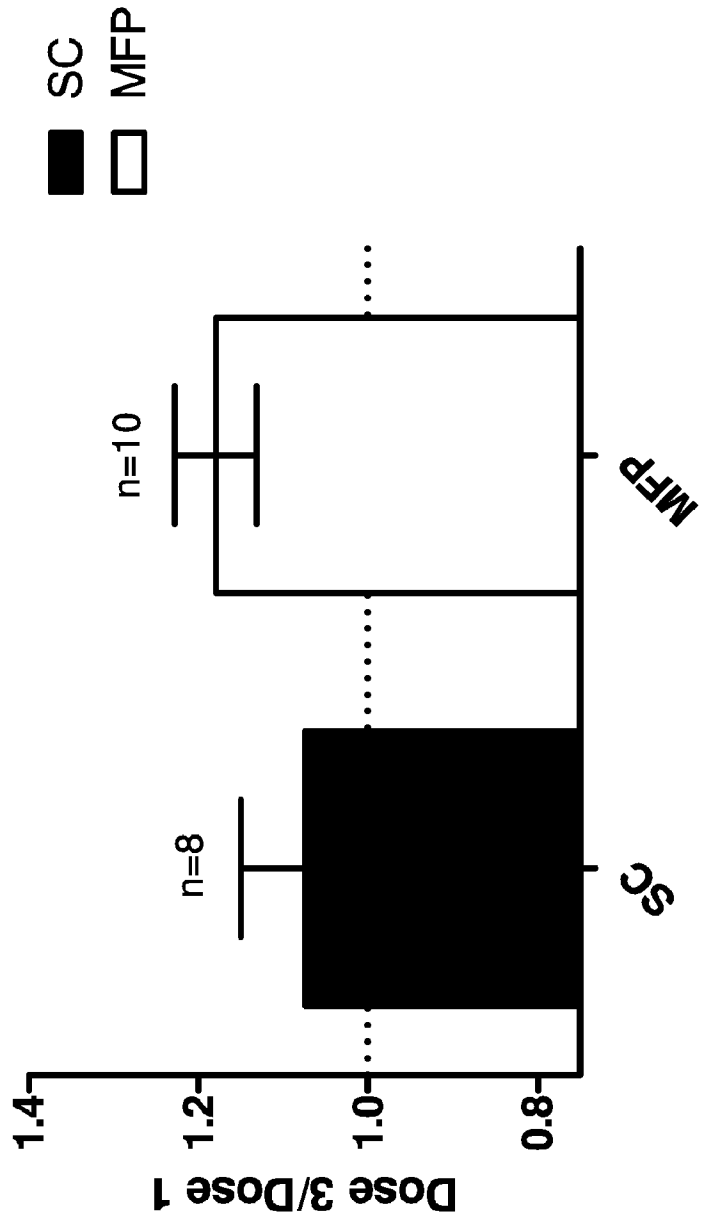


**FIGURE 24C**

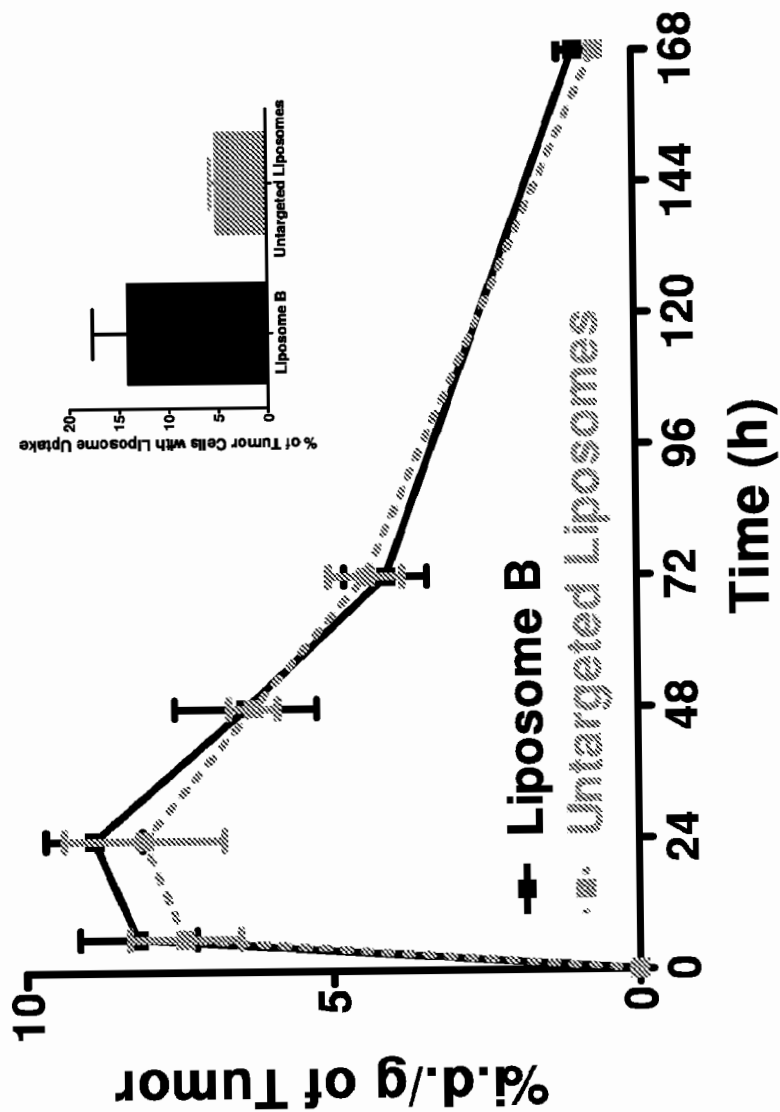


**FIGURE 25**

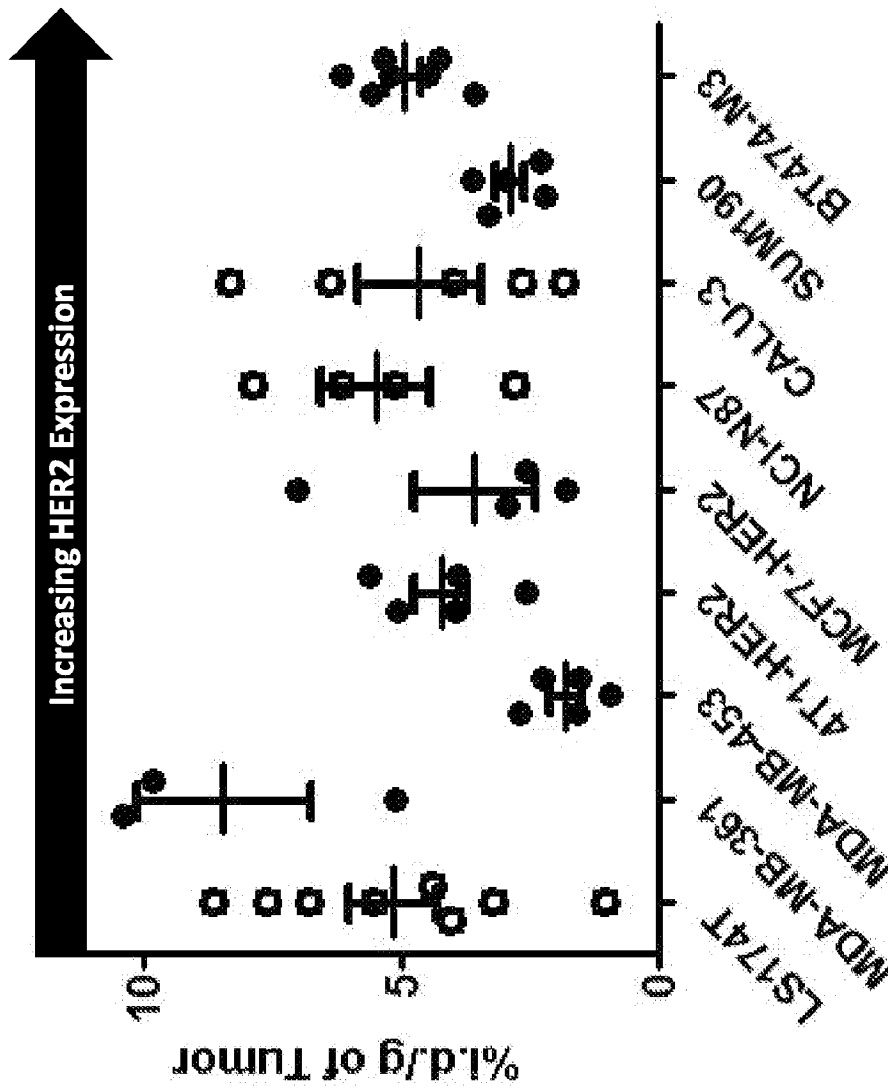
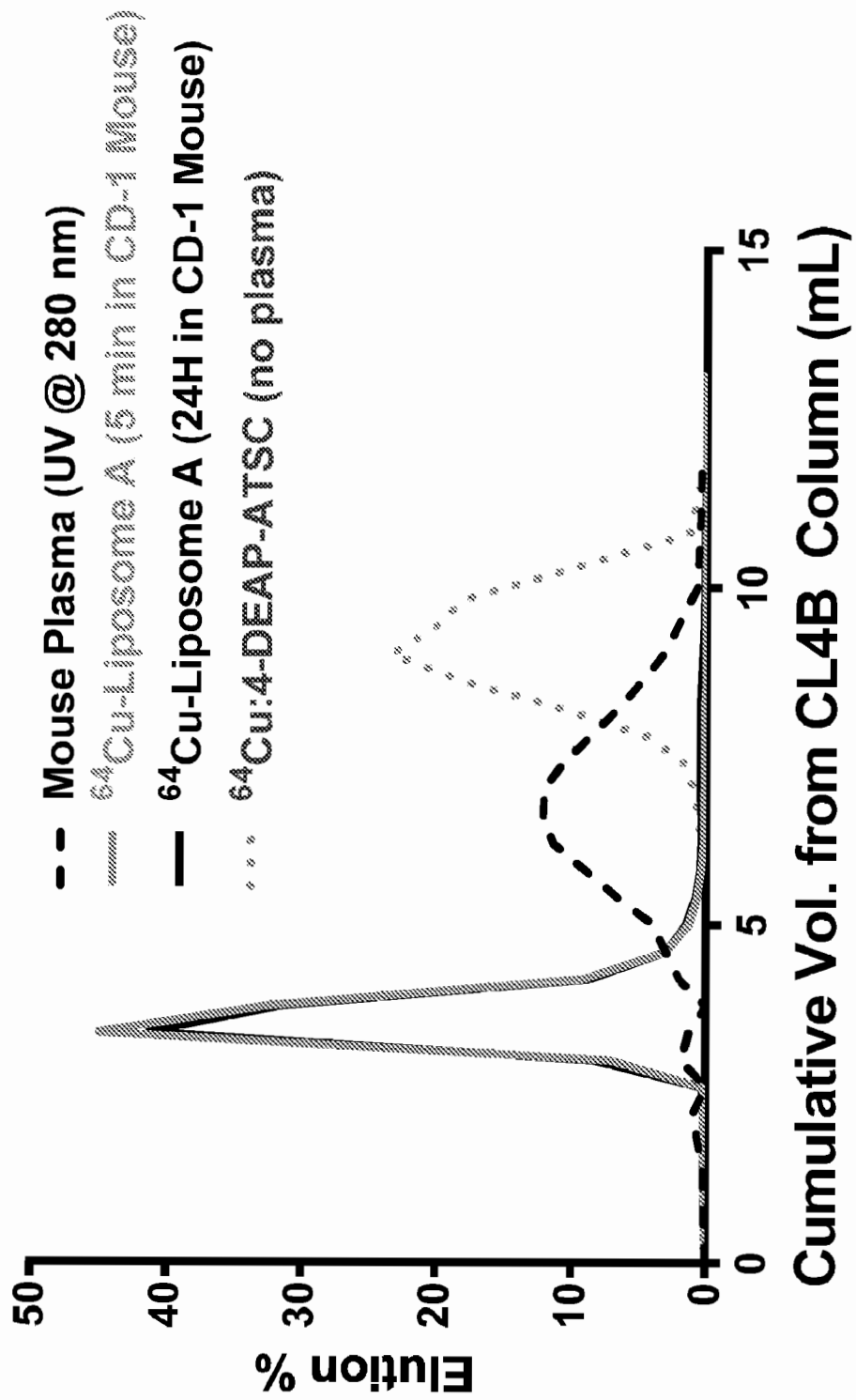
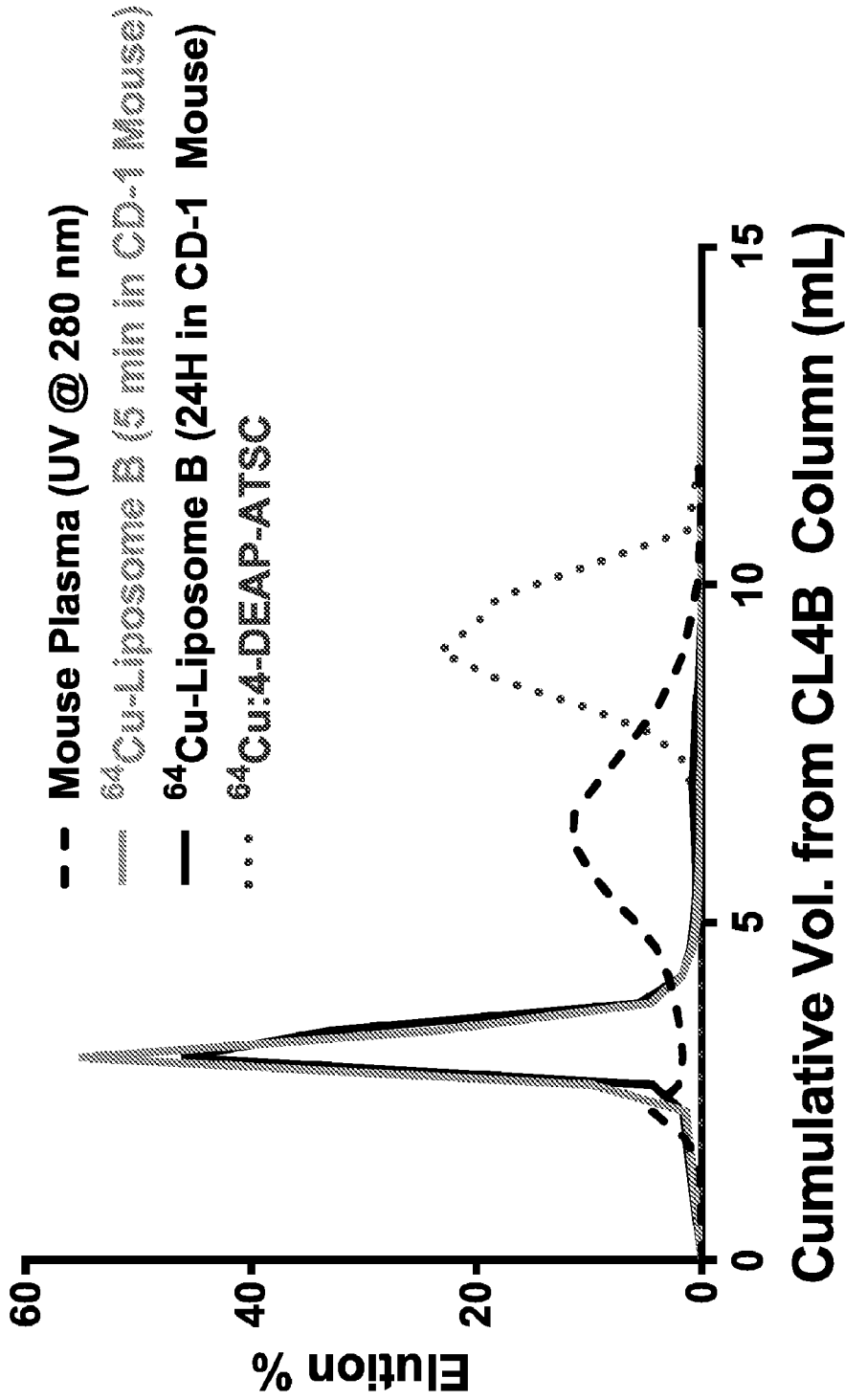


FIGURE 26



**FIGURE 27A**



**FIGURE 27B**

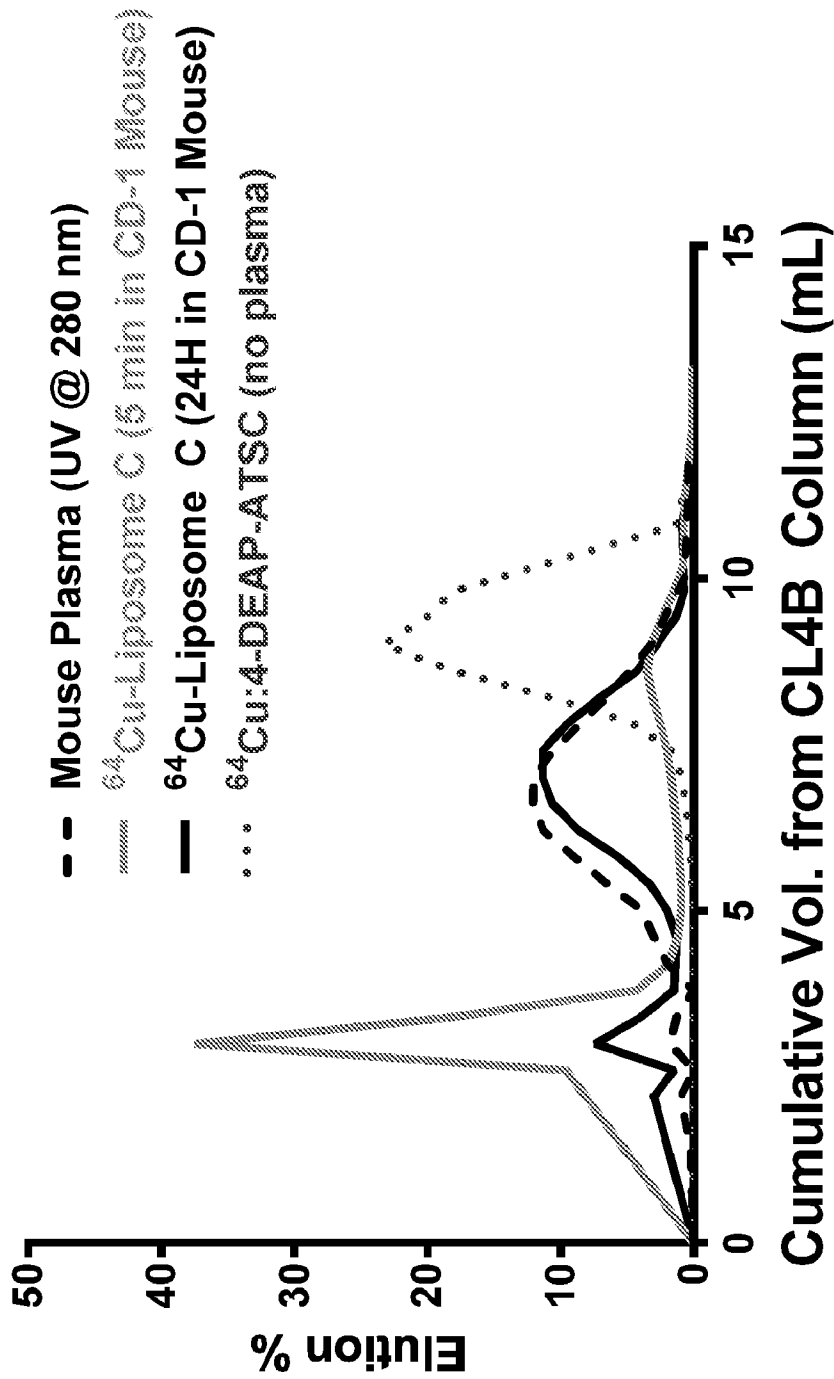


**FIGURE 27C**



**Box No. II Observations where certain claims were found unsearchable (Continuation of item 2 of first sheet)**

This international search report has not been established in respect of certain claims under Article 17(2)(a) for the following reasons:

1.  Claims Nos.:  
because they relate to subject matter not required to be searched by this Authority, namely:
  
2.  Claims Nos.:  
because they relate to parts of the international application that do not comply with the prescribed requirements to such an extent that no meaningful international search can be carried out, specifically:
  
3.  Claims Nos.: 8-10, 23-25, 32-36  
because they are dependent claims and are not drafted in accordance with the second and third sentences of Rule 6.4(a).

**Box No. III Observations where unity of invention is lacking (Continuation of item 3 of first sheet)**

This International Searching Authority found multiple inventions in this international application, as follows:

1.  As all required additional search fees were timely paid by the applicant, this international search report covers all searchable claims.
2.  As all searchable claims could be searched without effort justifying additional fees, this Authority did not invite payment of additional fees.
3.  As only some of the required additional search fees were timely paid by the applicant, this international search report covers only those claims for which fees were paid, specifically claims Nos.:
  
4.  No required additional search fees were timely paid by the applicant. Consequently, this international search report is restricted to the invention first mentioned in the claims; it is covered by claims Nos.:

**Remark on Protest**

- The additional search fees were accompanied by the applicant's protest and, where applicable, the payment of a protest fee.
- The additional search fees were accompanied by the applicant's protest but the applicable protest fee was not paid within the time limit specified in the invitation.
- No protest accompanied the payment of additional search fees.

<b>A. CLASSIFICATION OF SUBJECT MATTER</b> IPC(8) - C07C 337/08 (2013.01) USPC - 424/9.42 According to International Patent Classification (IPC) or to both national classification and IPC		
<b>B. FIELDS SEARCHED</b> Minimum documentation searched (classification system followed by classification symbols) IPC(8) - A61K 49/04, 49/18; C07C 335/08, 335/40, 337/06, 337/08 (2013.01) USPC - 424/9.321, 9.42; 558/4; 564/19 Documentation searched other than minimum documentation to the extent that such documents are included in the fields searched CPC - A61K 49/18; C07C 337/06, 337/08 (2013.01) Electronic data base consulted during the international search (name of data base and, where practicable, search terms used) PatBase, Orbit, STN, PubChem, Google Scholar		
<b>C. DOCUMENTS CONSIDERED TO BE RELEVANT</b>		
Category*	Citation of document, with indication, where appropriate, of the relevant passages	Relevant to claim No.
X — Y	US 2005/0112065 A1 (DRUMMOND et al) 26 May 2005 (26.05.2005) entire document	46 ----- 11, 13-15, 21, 26-31, 37-45
Y	US 2011/0305632 A1 (DONNELLY et al) 15 December 2011 (15.12.2011) entire document	11, 13-15, 21, 26-31, 37-45
Y	US 5,922,350 A (JANOFF et al) 13 July 1999 (13.07.1999) entire document	21
Y	WO 2011/006510 A1 (PETERSEN et al) 20 January 2011 (20.01.2011) entire document	27
A	US 2011/0098353 A1 (DILWORTH et al) 28 April 2011 (28.04.2011) entire document	1-7, 11-22, 26-31, 37-46
A	US 3,478,035 A (BARRETT) 11 November 1969 (11.11.1969) entire document	1-7, 11-22, 26-31, 37-46
<input type="checkbox"/> Further documents are listed in the continuation of Box C. <input type="checkbox"/>		
* Special categories of cited documents: "A" document defining the general state of the art which is not considered to be of particular relevance "E" earlier application or patent but published on or after the international filing date "L" document which may throw doubts on priority claim(s) or which is cited to establish the publication date of another citation or other special reason (as specified) "O" document referring to an oral disclosure, use, exhibition or other means "P" document published prior to the international filing date but later than the priority date claimed "T" later document published after the international filing date or priority date and not in conflict with the application but cited to understand the principle or theory underlying the invention "X" document of particular relevance; the claimed invention cannot be considered novel or cannot be considered to involve an inventive step when the document is taken alone "Y" document of particular relevance; the claimed invention cannot be considered to involve an inventive step when the document is combined with one or more other such documents, such combination being obvious to a person skilled in the art "&" document member of the same patent family		
Date of the actual completion of the international search 13 August 2013		Date of mailing of the international search report <b>28 AUG 2013</b>
Name and mailing address of the ISA/US Mail Stop PCT, Attn: ISA/US, Commissioner for Patents P.O. Box 1450, Alexandria, Virginia 22313-1450 Facsimile No. 571-273-3201		Authorized officer: Blaine R. Copenheaver PCT Helpdesk: 571-272-4300 PCT OSP: 571-272-7774



(51) International Patent Classification:

A61B 5/055 (2006.01) A61P 35/00 (2006.01)  
A61K 49/06 (2006.01)

(21) International Application Number:

PCT/US2013/075513

(22) International Filing Date:

17 December 2013 (17.12.2013)

(25) Filing Language:

English

(26) Publication Language:

English

(30) Priority Data:

61/737,563 14 December 2012 (14.12.2012) US  
61/863,497 8 August 2013 (08.08.2013) US

(71) Applicant: **MERRIMACK PHARMACEUTICALS, INC.** [US/US]; One Kendall Square, Suite B7201, Cambridge, MA 02139-1670 (US).

(72) Inventors: **DRUMMOND, Daryl, C.**; 1 Brooks Road, Lincoln, MA 01773 (US). **FITZGERALD, Jonathan, Basil**; 32 Magnolia St., Arlington, MA 02474 (US). **KAIRA, Ashish**; 9 Burnham St. Unit D2, Belmont, MA (US). **KAMOUN, Walid**; 7 Wollaston Ave., Arlington, MA 02476 (US). **KLINZ, Stephan**; 132 Wilson St., Norwood, MA 02062 (US).

(74) Agents: **RUSSETT, Mark, D.** et al.; Edwards Wildman Palmer LLP, P.O. Box 55874, Boston, MA 02205 (US).

(81) Designated States (unless otherwise indicated, for every kind of national protection available): AE, AG, AL, AM,

AO, AT, AU, AZ, BA, BB, BG, BH, BN, BR, BW, BY, BZ, CA, CH, CL, CN, CO, CR, CU, CZ, DE, DK, DM, DO, DZ, EC, EE, EG, ES, FI, GB, GD, GE, GH, GM, GT, HN, HR, HU, ID, IL, IN, IR, IS, JP, KE, KG, KN, KP, KR, KZ, LA, LC, LK, LR, LS, LT, LU, LY, MA, MD, ME, MG, MK, MN, MW, MX, MY, MZ, NA, NG, NI, NO, NZ, OM, PA, PE, PG, PH, PL, PT, QA, RO, RS, RU, RW, SA, SC, SD, SE, SG, SK, SL, SM, ST, SV, SY, TH, TJ, TM, TN, TR, TT, TZ, UA, UG, US, UZ, VC, VN, ZA, ZM, ZW.

(84) Designated States (unless otherwise indicated, for every kind of regional protection available): ARIPO (BW, GH, GM, KE, LR, LS, MW, MZ, NA, RW, SD, SL, SZ, TZ, UG, ZM, ZW), Eurasian (AM, AZ, BY, KG, KZ, RU, TJ, TM), European (AL, AT, BE, BG, CH, CY, CZ, DE, DK, EE, ES, FI, FR, GB, GR, HR, HU, IE, IS, IT, LT, LU, LV, MC, MK, MT, NL, NO, PL, PT, RO, RS, SE, SI, SK, SM, TR), OAPI (BF, BJ, CF, CG, CI, CM, GA, GN, GQ, GW, KM, ML, MR, NE, SN, TD, TG).

Published:

- with international search report (Art. 21(3))
- before the expiration of the time limit for amending the claims and to be republished in the event of receipt of amendments (Rule 48.2(h))
- the filing date of the international application is within two months from the date of expiration of the priority period (Rule 26bis.3)



WO 2014/113167 A1

(54) Title: NON-INVASIVE IMAGING METHODS FOR PATIENT SELECTION FOR TREATMENT WITH NANOPARTICULATE THERAPEUTIC AGENTS

(57) Abstract: Methods for providing treatment of pathologic conditions with nanoparticulate therapeutic agents are disclosed. Novel methods for determining liposomal deposition at sites of pathology using non-invasive imaging are also disclosed.

**NON-INVASIVE IMAGING METHODS FOR PATIENT SELECTION  
AND TREATMENT WITH NANOPARTICULATE THERAPEUTIC AGENTS**

**Cross-Reference to Related Applications**

5           This application claims the benefit of and priority to U.S. Provisional Patent Application Nos. 61/737,563, filed December 14, 2012 and 61/863,497, filed August 8, 2013. The entire contents of each of the foregoing applications are incorporated herein by reference in their entirety.

**Background**

10           Liposomal and other nanoparticulate therapeutic agents often exhibit long-circulating pharmacokinetics and will preferentially extravasate and accumulate in tissues perfused by hyper-permeable capillaries. Tumor blood vessels typically develop abnormally and have structural and physiologic defects leading to tumor capillary hyper-permeability. Capillaries at sites of pathologic inflammation (e.g., infection or inflammatory disease) may also exhibit  
15 hyper-permeability. As a result of the abnormal vasculature at sites of inflammation or tumor, the long-term presence of nanotherapeutics in the circulation may result in enhanced accumulation of nanoparticles such as liposomes at such sites of pathology. This preferential deposition of nanoparticulate therapeutic agents in tumors and sites of inflammation is referred to as the enhanced permeability and retention (EPR) effect. Different sites of  
20 pathology exhibit varying degrees of EPR.

          Nanoparticle breakdown at the site of pathology releases the drug encapsulated in the nanoparticles locally, providing site-specific bioavailability of the active drug. In this setting nanoparticle breakdown is often an active process requiring cellular uptake. In some nanoparticulate agents, a pro-drug is entrapped that requires enzymatic activation for optimal  
25 function, e.g., hydrolysis by esterases such as those localized preferentially in intracellular organelles such as endosomes and lysosomes. In tumors and at other sites of inflammation, liposomes are often actively taken up (e.g., via phagocytosis) by white blood cells such as monocytes and macrophages, where prodrug activation may take place.

          Liposomes or lipidic nanocarriers can be designed to exhibit a wide range of  
30 physicochemical properties that in turn impact their pharmacologic properties, including

circulation lifetimes and degree of tumor deposition. The majority of liposomes developed to date display either a fairly rapid clearance from the circulation or rapid release of their encapsulated payload while in circulation.

A recently developed class of liposomes, that represents a minority of liposomal drugs in clinical development, exhibit a combination of long circulation lifetimes ( $t_{1/2}$ >6-10 h in mice, >12-24 h in humans) and highly stable retention of encapsulated drug while in the circulation ( $T_{1/2}$  of release >18-24h). These included a pegylated liposomal doxorubicin (PLD) prepared from mPEG-DSPE, hydrogenated soyphosphatidylcholine (HSPC) and cholesterol and stabilized with intraliposomal ammonium sulfate, and similar formulations decorated on their surface with antibody-fragments specific for ErbB2 or EGFR cell surface receptors (Park et al., Clin Cancer Res. 2002; 8(4):1172-1181; Drummond et al., Pharmacol Rev. 1999; Dec;51(4):691-743; Mamot et al., Cancer Res. 2005; 65(24):11631-11638). These also include liposomal formulations of irinotecan, topotecan, vincristine, and vinorelbine that have been stabilized through association (e.g., gelation) with an (optionally high density) sulfated sugar or polyol, e.g., with sucroseoctasulfate to form the sucrosolate salt, in the liposome interior (see US Pat. Nos. 8,147,867 and 8,329,213). Other members of this class of liposomes are nucleic acid formulations stabilized with mPEG-DSPE and a unique solvent condensation protocol (Hayes et al., 2006; Biochim Biophys Acta. 2006 Apr;1758(4):429-442, also see US Pat. No. 8,496,961 and US Application No. 13/967,664, filed 15-Aug-2013). This class of liposomes or lipidic nanocarriers will benefit from prediction of liposome deposition at sites of inflammation, infection, and/or high macrophage concentration.

An exemplary liposomal anti-neoplastic agent, MM-398, also known as PEP02 and as irinotecan (sucrosolate) liposome injection, comprises the pro-drug irinotecan encapsulated in a liposomal drug delivery system. MM-398 is prepared as described, e.g., in US Patent No. 8, 147,867. This stable nanoliposomal formulation of irinotecan has long-circulating pharmacokinetics. MM-398 liposomes accumulate in tumor-associated macrophages (TAMs). Once internalized by TAMs, irinotecan is believed to be released from within the liposomes and activated by cellular carboxyl esterase activity to yield SN-38, which is generally 100-1000x more active as an inhibitor of cancer cell proliferation than is irinotecan. In this fashion, TAMs are believed to play an essential role in establishing high concentrations of SN-38 in an MM-398 treated tumor, an outcome designed to improve

clinical outcomes in treated cancer patients. Thus, tumor deposition and accumulation, liposome breakdown, and conversion of irinotecan into SN-38 are all believed to be critical and rate-limiting elements of MM-398 trafficking and disease modification.

Other exemplary liposomal anti-neoplastic agents include doxorubicin liposome injection (DOXIL or CAELYX) and MM-302 - HER2-targeted immunoliposomal doxorubicin. Immunoliposomes are antibody (typically antibody fragment) targeted liposomes that can provide advantages over non-immunoliposomal preparations because they are selectively internalized by cells bearing cell surface antigens targeted by the antibody. Details of antibodies and immunoliposomes are described, for example, in the following US patents: US 7,871,620, 6,214,388, 7,135,177, and 7,507,407 (“Immunoliposomes that optimize internalization into target cells”); US 6,210,707 (“Methods of forming protein-linked lipidic microparticles and compositions thereof”); US 7,022,336 (“Methods for attaching protein to lipidic microparticles with high efficiency”) and US 7,892,554 and 7,244,826 (“Internalizing ErbB2 antibodies.”).

Ferumoxytol (Feraheme®, AMAG Pharmaceuticals, Inc., referred to herein as “FMX”) is a preparation of polyglucose sorbitol carboxymethylether coated magnetite (superparamagnetic iron oxide) nanoparticles (17-31 nm average diameter). Marketed for the treatment of iron deficiency anemia in patients with chronic renal failure, FMX is administered to adult patients at a dosage of 510 mg by intravenous injection followed by a second 510 mg intravenous injection 3 to 8 days later. FMX exhibits a prolonged residence time in the bloodstream (i.e., within the intravascular space). When performing MRI studies in subjects given this agent for the treatment of their anemia, exquisite angiographic images can be obtained up to 24 hours post injection. Contrast enhancement of the intravascular space following FMX administration has provided a novel approach to imaging pathologic conditions that involve the vascular tree such as stroke, vascular malformations, and chronic renal disease. In addition, this agent has been used in patients with CNS malignancies to measure tumor vascularity and the response to chemotherapy. Currently, the FDA has designated this agent as an orphan drug for brain tumor imaging.

FMX is significantly smaller than most liposomal therapies, which have an average size of 70-200 (more commonly 80-120) nm. Size dependence for clearance rates of liposomes from the blood stream and with respect to tumor deposition has been well

characterized. Generally liposomes smaller than 50 nm are cleared significantly more slowly than liposomes with a size of 100 nm or greater. In addition, many smaller nanoparticles accumulate less efficiently in tissues due to an apparently high efflux rate from tissues of smaller particles.

- 5           Because liposomes and other nanoparticulate therapeutic agents can vary in size, and nanoparticle size may impact EPR levels, it would be desirable to be able to predict EPR-mediated accumulation of nanoparticles of particular sizes at sites of pathology in patients. Furthermore, some imaging agents may saturate the reticuloendothelial system, resulting in a significant decrease in the clearance rate of subsequently administered nanotherapeutics.
- 10          This may dramatically increase the systemic exposure of the nanotherapeutics, creating a significant safety risk to the patient. Waiting for treatment until the effect on clearance has diminished is impractical for cancer patients, whose fast growing cancers require rapid implementation of new treatment options.

- There is thus a need for safe and effective methods of screening patients to identify  
15          those patients with sites of pathology that are predicted to exhibit nanoparticle accumulation or not to do so, which methods do not themselves alter nanoparticle accumulation. Patients identified as having sites of pathology that are predicted to exhibit nanoparticle accumulation would be considered more likely to respond to nanoparticulate therapeutic agents. Patients identified as having sites of pathology that are predicted not to exhibit nanoparticle  
20          accumulation would be considered less likely to respond to nanoparticulate therapeutic agents. Treating patients in accordance with such identifications would avoid the administration of sub-optimal therapeutic treatments to patients in need of therapy. The following disclosure addresses these needs and provides additional benefits.

### **Summary of the Invention**

The present invention provides methods for selecting and providing liposomal therapy for pathologic conditions based on novel methods for determining liposomal deposition at sites of pathology using non-invasive imaging. Such methods are useful in the selection of treatment for various conditions including localized infectious, inflammatory and proliferative diseases.

In certain aspects, a method is provided for selecting and providing pharmaceutical treatment to a patient for a localized infectious, inflammatory, or neoplastic condition, the method comprising identifying one or more locations of infection, inflammation or neoplasia in a patient, and subsequently, obtaining at least one contrast-enhanced MRI image of a first location of the one or more locations, and subsequently, selecting an anti-infective, anti-inflammatory, or anti-neoplastic pharmaceutical agent and treating the patient with the selected pharmaceutical agent, wherein, the contrast-enhanced MRI image is obtained following administration of an MRI contrast agent comprising an MRI contrast-enhancing amount of superparamagnetic iron oxide nanoparticles of about 15-30 nm in diameter, and if the contrast-enhanced MRI image shows contrast enhancement within at least one of the one or more locations, the selected pharmaceutical agent is a liposomal therapeutic agent that is formulated as nanoparticles or nanoliposomes of about 70 to about 200 nm in diameter, but if the contrast-enhanced MRI image does not show contrast enhancement at first location, the selected pharmaceutical agent is not formulated as nanoparticles or nanoliposomes of about 70 to about 200 nm in diameter, or, in another embodiment, the selected pharmaceutical agent is not formulated as nanoparticles or nanoliposomes of any size. In certain embodiments, the method comprises diagnosing a localized infectious, inflammatory, or neoplastic condition in the patient.

In certain embodiments, the MRI contrast agent is ferumoxytol. In certain embodiments, the ferumoxytol is administered at 5 mg iron per kg. In certain embodiments, the patient is an adult and 100 - 1000 milligrams (iron) of ferumoxytol are administered to the patient. In certain embodiments, the patient is an adult and 510 milligrams of ferumoxytol are administered to the patient. In certain embodiments, the contrast-enhanced MRI image is obtained no more than 72, 96, 120, 144 or 168 hours after administration of the superparamagnetic iron oxide nanoparticles. In certain embodiments, the contrast-enhanced



MRI image is obtained from 72-96, 96-120, 120-144, or 144 to 168 hours after administration of the superparamagnetic iron oxide nanoparticles.

In other aspects, a method is provided for selecting and providing pharmaceutical treatment to a patient for a localized infectious, inflammatory, or neoplastic condition, the method comprising identifying two or more locations of infection, inflammation or neoplasia in the patient, and subsequently, obtaining a first contrast-enhanced MRI image of a first location of the one or more locations, obtaining a second contrast-enhanced MRI image of a second location of the two or more locations, and subsequently, selecting an anti-infective, anti-inflammatory, or anti-neoplastic pharmaceutical agent and treating the patient with the selected pharmaceutical agent; wherein, the first and second contrast-enhanced MRI images are obtained following administration of an MRI contrast agent comprising an MRI contrast-enhancing amount of superparamagnetic iron oxide nanoparticles of about 15-30 nm in diameter, and if both the first and the second contrast-enhanced MRI images show contrast enhancement within both the first location and second location, the selected pharmaceutical agent is an agent that is formulated as nanoparticles or nanoliposomes of about 70 to about 200 nm in diameter (a liposomal therapeutic agent), but if both the first and the second contrast-enhanced MRI images do not show contrast enhancement within both the first location and second location, the selected pharmaceutical agent is an agent that is not formulated as nanoparticles or nanoliposomes of about 70 to about 200 nm in diameter.

In one embodiment of either of the above aspects, the method comprises identifying at least one region of interest in a patient (e.g., a region having a localized infection, inflammation, or neoplasm) and obtaining a contrast-enhanced MRI image of a region of interest predictive of the deposition of a liposomal anti-infective, anti-inflammatory, or antineoplastic therapeutic agent in the region of interest in the patient, e.g., a region of localized infection, inflammation, or a solid tumor in a cancer patient, and then for determining whether or not such a liposomal anti-infective, anti-inflammatory, or antineoplastic liposomal therapeutic agent will accumulate in the region of localized infection, inflammation, or solid tumor in the patient, and subsequently, selecting an anti-infective, anti-inflammatory, or anti-neoplastic liposomal therapeutic agent and treating the patient with the selected pharmaceutical agent. These methods comprise obtaining an MRI image of the tumor in the patient where, between 24 hours and 72 hours prior to MRI imaging, an MRI contrast agent consisting of an ultra-small superparamagnetic iron oxide

particle (USIOP) preparation comprising particles with an average size of about 15 to about 30 nm in diameter is administered, e.g., via a parenteral route, to the patient in an amount sufficient to provide MRI contrast and the MRI imaging is performed no more than 168 hours after administration of the contrast agent whereby the MRI image obtained is contrast-  
5 enhanced. In certain aspects, if the MRI image of the site of pathology or region of interest shows areas of enhanced contrast (e.g., as compared to images obtained of normal muscle, of other tissues where the contrast agent does not accumulate, or as compared to images obtained without pretreatment with an MRI contrast agent), the patient is identified as being suitable for treatment with the liposomal therapeutic agent. In certain aspects the patient so  
10 identified is so treated.

In some embodiments of either of the aspects above, the liposomal anti-infective, anti-inflammatory, or antineoplastic pharmaceutical agent comprises liposomes with an average diameter of, e.g., 70-200, or 75-160, or 80-200 nm, or e.g., about 80 nm to about 120 nm (e.g., an average size of about 100 nm in diameter with an average range of about 80 nm to  
15 about 120 nm). In one embodiment, the liposomal therapeutic comprises irinotecan or doxorubicin. In another embodiment, the liposomal therapeutic comprises a targeting antibody. In one embodiment, the liposomal therapeutic agent is MM-398 (irinotecan sucrosfate liposome injection). In another embodiment, the liposomal therapeutic agent is MM-302 (Her2-targeted liposomal doxorubicin). In one embodiment, the first contrast-  
20 enhanced MRI image shows contrast enhancement within the first location, the neoplastic condition comprises at least one tumor and the pharmaceutical agent is a liposomal anti-neoplastic agent. In another embodiment, the tumor is a non-small cell lung cancer (NSCLC) tumor, a triple negative breast cancer (TNBC) tumor, a colorectal cancer (CRC) tumor, an ER/PR positive breast cancer tumor, a pancreatic cancer tumor, an ovarian cancer tumor, a  
25 small cell lung cancer tumor, a gastric cancer tumor, a GEJ adenocarcinoma, a head and neck cancer tumor, a cervical cancer tumor, or Ewing's sarcoma and the selected pharmaceutical agent is a liposomal formulation of irinotecan.

In one embodiment of either of the aspects above, the contrast-enhanced MRI image is obtained no more than 72, 96, 120, 144 or 168 hours after administration of the  
30 superparamagnetic iron oxide nanoparticles. In another embodiment, the contrast-enhanced MRI image is obtained from 72-96, 96-120, 120-144, or 144 to 168 hours after administration of the superparamagnetic iron oxide nanoparticles.

In one embodiment of either of the aspects above, the MRI image is obtained using a magnetic field strength of 1-10 Tesla, e.g., 1.5 Tesla or 3 Tesla. An exemplary USIOP preparation is FMX (ferumoxytol). In some embodiments, the MRI contrast agent is ferumoxytol. In one embodiment, the ferumoxytol is administered at 5 mg/kg. In another  
5 embodiment, the patient is an adult and 100 - 1000 milligrams of ferumoxytol are administered to the patient. In yet another embodiment, the patient is an adult and 510 milligrams of ferumoxytol are administered to the patient.

In certain embodiments of either of the aspects above, the liposomal therapeutic agent is an anti-neoplastic agent. An exemplary anti-neoplastic agent is liposomal irinotecan, e.g.,  
10 irinotecan sucrosolate liposome injection. Another exemplary liposomal anti-neoplastic agent is liposomal doxorubicin, e.g., doxorubicin lipid complex injection or antibody-targeted doxorubicin liposomes (e.g., with anti-HER2 antibody attached to liposome surface).

In one embodiment, the tumor exhibits (e.g., in biopsy sections) an elevated level of tumor associated macrophages (TAMs). Tumors with 3 or more, or 4 or more, or 5 or more  
15 macrophage-marker (e.g., CD68) positive cells per high power field (hpf) are considered to exhibit elevated levels of TAMs. In some embodiments the elevated level of TAMs corresponds to 3 or more, or 4 or more, or 5 or more cells that are both CD68 positive and PCNA (proliferating cell nuclear antigen) positive per hpf. Macrophage marker and (optionally) PCNA positive TAMs in tumor sections may be identified and numbers per hpf  
20 determined as described, e.g., per Mukhtar, et al., *Cancer Res. Breast Cancer Research and Treatment*; 2011;130(2):635-644. The tumor may be any tumor, e.g., a tumor of a non-small cell lung cancer (NSCLC), a triple negative breast cancer (TNBC), a colorectal cancer (CRC), an ER/PR (estrogen receptor and/or progesterone receptor) positive breast cancer, a pancreatic cancer, an ovarian cancer, a small cell lung cancer, a gastric cancer, a GEJ (gastro-  
25 esophageal junction) adenocarcinoma, a head and neck cancer, a cervical cancer, or a Ewing's sarcoma.

In various embodiments the imaging is performed (about) 24, 48, or 72 hours after the administration of the contrast agent.

Other features and advantages will be apparent from the following disclosure and the  
30 claims.

### Brief Description of the Drawings

Figure 1. As described in Example 1, below, Figs. 1A and 1B show areas of ferumoxytol signal in two primary models of pancreatic tumors, while Figs. 1C, 1D, and 1E are images showing the spatial distribution of DiI5 liposomes (1C), FMX (1D), and F4/80 (1E).

Figures 2A and 2B. As described in Example 2, below, Fig. 2 shows the results of a treatment of HT-29 tumor-bearing mice injected with FMX followed by injection of DiI5 liposomes. The amounts of FMX injected are indicated on the X-axis as Fe\_0 (no FMX), Fe\_20 (20 mg/kg FMX) and Fe\_50 (50 mg/kg FMX). Overall DiI5 liposome uptake is indicated as the percent of the total population of cells that are DiI5 positive (Fig. 2A – no effect of FMX pre-treatment was observed) in either EpCAM+ tumor cells or CD11b+ myeloid cells. The mean fluorescence intensity (MFI) of DiI5 liposomes was higher in CD11b+ myeloid cells as compared to MFI in EpCAM+ tumor cells (Fig. 2B – no effect of FMX pre-treatment was observed).

Figure 3. As described in Example 3, below, Fig. 3 indicates the degree of accumulation of SN-38 in tumors after MM-398 administration following either no pretreatment, or pretreatment with 20 or 50 mg/kg of FMX. No effect of FMX pre-treatment was observed.

Figure 4 (see Example 4, below) shows the pharmacokinetics of MM-302 either without pre-dose, or following 72 hours pre-dose with iodine-loaded liposomes at 3, 10, and 30 times the lipid dose of the F5-ILs-Dox. “%i.d.” indicates the percentage of the initial dose remaining. A large effect of iodine-loaded liposome pretreatment was observed.

Figure 5 (see Example 5 below) shows the uptake of FMX 24hr after FMX (20mg/kg) intravenous injection by human HT29, A549 and A2780 tumors grown subcutaneously in SCID mice as measured by MRI and T2\* analysis. The FMX levels are plotted on the x-axis relative to the irinotecan (CPT-11) concentration in ng/g (as displayed on the y-axis) measured by HPLC in total tumor lysates from the imaged tumors harvested 72hrs after the injection of MM-398 (10mg/kg) into the same mice.

Figure 6 (see Example 7 below) describes typical FMX measurements in patient plasma, tumor lesions and the behavior of modeling parameters derived from such measurements. Figure 6A shows the FMX pharmacokinetics in patient plasma after injection of 5mg/kg FMX. Figure 6B shows the FMX signals in both plasma and four different tumor lesions of a single patient. Figure 6C shows the output of a pharmacokinetic model that can describe the measured FMX plasma and tumor lesion data through two parameters, a tissue permeability parameter and a tissue binding parameter that together describe lesion-specific FMX levels.

Figure 7 (see Example 8 below) describes IHC results from tissue sections derived from patient biopsies after treatment with FMX. Macrophages are stained with an anti-CD68 antibody (clone PG-M1, DAKO), while iron detection in an adjacent tissue section is by Prussian Blue staining.

Figure 8 (see Example 9 below) shows the relationship between the FMX signal in select regions-of-interest of tumor lesions measured at 24hr and the corresponding irinotecan (CPT-11) levels (ng/g) measured in biopsies from the vicinity of those regions.

Figure 9 is an image of an MRI standard curve or “phantom”, which shows a T2\* weighted MRI with TE of 13.2ms with phantom tubes from 0-200µg/ml ferumoxytol.

### **Detailed Description**

Provided herein are methods for obtaining images indicating whether or not a liposomal therapeutic agent will accumulate at a site of malignancy or inflammation, as well as methods of patient selection and treatment informed by such images.

A method is provided in which nanoparticulate MRI contrast agents are used to obtain contrast-enhanced MRI images of a site of pathology in a patient and the images are used to predict whether the site of pathology in the patient will have low or high deposition of liposomal drugs, with the prediction allowing a determination of whether or not a liposomal drug should be administered to the patient.

Because FMX particles are much smaller than therapeutic liposomes, it was surprising to find that FMX particle deposition in pathologic tissues is predictive of the deposition in such tissues of a much larger therapeutic agent (e.g., a liposomal agent). It is demonstrated

herein that tissues that display FMX contrast enhancement upon MRI are more likely to accumulate deposition of liposomal therapeutics (comprising liposomes averaging, e.g., 70-200, or 75-160, or 80-200 nm in diameter) than those that do not exhibit FMX MRI contrast enhancement.

5           As FMX has been demonstrated to be safe for intravenous administration to patients and is shown herein not to interfere with nanoliposome therapies if used as an imaging agent, even within 1-4 hours prior to administration of nanoliposomal therapeutics, these results indicate that FMX MRI allows for selection patients who will (or will not) benefit from nanoliposomal therapy.

10           Contrast enhancement is detected, typically by a radiologist, in a patient undergoing imaging. Contrast enhancement is detected when a region of interest (such as a region comprising or within a tumor or site of infection or inflammation) shows greater contrast than one or more regions not expected to show enhanced contrast (such as a tumor-free region in a tissue that does not typically comprise high levels of macrophages, such as liver and spleen  
15 do). For example, if a region of interest in such an imaging patient shows an observable enhancement over a tumor, infection and inflammation-free region in a tissue that is not expected to show enhanced contrast, the patient is identified as a candidate for treatment with a liposomal therapeutic. In some embodiments, contrast enhancement is detected for a region of interest as compared to the contrast enhancement observed in a similar region in at least  
20 one other patient, e.g., a comparator patient (i.e., a patient with a similar, per type and location, tumor, infection or inflammation) or a population of comparator patients, which patient or patients have also undergone the ferumoxytol imaging procedure. For example, for a given time point (e.g., 20, 24, 30, 36, 48, 72, 96, 120, 144, or 168 hours) after an imaging patient is injected with ferumoxytol, if the MRI contrast enhancement of the region of interest  
25 in the imaging patient is greater than the mean (or median) contrast enhancement observed for one or more regions of interest in the comparator patient or the comparator patient population, then the imaging patient is identified as a candidate for treatment with a liposomal therapeutic. In another embodiment, in a patient having more than one region of interest, an image is taken of a plurality of, or of all, regions of interest. If the plurality or all  
30 regions of interest show contrast enhancement, then the patient is identified as a candidate for treatment with a liposomal therapeutic. In certain embodiments, the patient so identified as a candidate is treated with an effective amount of a liposomal therapeutic.

The liposomal therapeutic agent to be administered in accordance with the methods disclosed herein retains the encapsulated drug in the bloodstream with a T1/2 of release of at least 18 hours, 24 hours, or 48 hours following injection. The average particle size (diameter) of the nanotherapeutic to be delivered is between 70-200 nm, e.g., 80-120 nm or 75-200 nm.

For an imaging agent to be used to be safely used to predict the deposition of a subsequently delivered nanotherapeutic, such as a nanoliposome, the imaging agent must not significantly alter the pharmacokinetics or pharmacodynamics of the nanotherapeutic with which the patient is to be treated.

10

**Example 1. FMX and nanoliposomes deposit within the same areas of tumors.**

In order to analyze the microdistribution of FMX as it compares to distribution of liposomes, two primary human pancreatic cancer tumor samples were passaged as flank xenografts through nu/nu mice. A tumor thus passaged 10 times produced xenograft tumor model 254, while another passaged 6 times produced xenograft tumor model 269. Tumor fragments thus prepared were implanted in the experimental mice (n=4 for model 254 and n=6 for model 269) and allowed to grow to ~200-300mm<sup>3</sup>.

Tumor-bearing mice thus prepared were injected with FMX at 25 mg/kg followed by an injection of DiI5-labeled liposomes 24 hours later at 40 micromoles of phospholipid per kg of body weight. Mice were sacrificed at 48 hours post-FMX injection (24 hours post DiI5-liposome injection) and tumor sections were prepared and assessed by Prussian Blue staining (Aperio<sup>®</sup> ScanScope AT<sup>®</sup> whole slide scanner) for FMX and by fluorescence microscopy (Aperio<sup>®</sup> ScanScope FL<sup>®</sup> whole slide scanner) for DiI5 liposomes. Each resulting scan measured fluorescence intensity (fi) and was segmented and fraction of area that was FMX or DiI5 positive was calculated using MatLab<sup>®</sup>. The fraction of liposome-positive area was calculated from the images using simple thresholding (fi>5000 for areas of high liposome deposition and fi>100 for areas of low liposomal deposition). Model 269 showed statistically significantly higher levels of tumoral deposition of the liposomes when compared to animals in model 254. Deposition of FMX followed the same trend and correlated well with the deposition of the liposomes (Fig. 1A). In order to analyze the spatial distribution of the

liposome and FMX, corresponding areas were identified in serial sections of the same mouse stained for FMX, imaged for liposomes, or immunohistochemically stained for F4/80, a murine macrophage marker. Liposomal spatial distribution showed microdistribution with hot spots (areas of high liposomal deposition) scattered throughout the tumor. FMX showed a similar pattern and co-localized with the hot spots of liposomes. Macrophages were present at relatively high levels within these tumors and spatially correlated with the liposomes and the FMX (Fig. 1B). Microscopy confirmed the co-localization of liposomes (Fig. 1C), FMX (Fig. 1D) and F4/80 IHC-detected myeloid cells (e.g., macrophages - Fig. 1E).

## 10 **Example 2. Effects of FMX on phagocytosis by macrophages**

HT-29 tumor-bearing mice were injected with FMX followed by injection of liposomes pre-labeled with DiI5 (a fluorescent dye). HT-29 xenografts were developed by inoculating 10 million HT-29 colorectal adenocarcinoma cells (ATCC) per mouse in SCID mice. Once tumors were well established (~200-300mm<sup>3</sup>) treatment was initiated. Mice were administered a single dose of ferumoxytol (20mg/kg or 50 mg/kg) followed by an i.v. dose of MM-398 equivalent to 20 mg irinotecan HCL/kg, or DiI18(5)-DS (DiI5) labeled liposomes at 40 μmol phospholipid/kg, for HPLC and FACS analysis respectively. HT-29 tumors were collected at end of the study for IHC and HPLC analysis. Flow cytometry was performed on a BD FACSCalibur<sup>®</sup> instrument. Analysis of irinotecan levels in tumor tissues was as described by Noble, et al, *Cancer Res.* 2006;66:2801-2806. Water was added to tissues at a 20% (w/v) ratio, and tissues then homogenized with a mechanical homogenizer in an ice bath. Homogenates were extracted for the lactone form of irinotecan with an acidic methanol solution by vortexing and centrifugation at 13,000 rpm for 10 minutes, with the supernatants then transferred to autosampler vials for Dionex<sup>™</sup> (Thermo Scientific) high-pressure liquid chromatography (HPLC) analysis.

FACS analysis indicated that there was no effect of FMX (Fe) on overall DiI5 liposome uptake (Fig. 2A) in either EpCAM+ (tumor) cells or CD11b+ (myeloid) cells (e.g., macrophages). The mean fluorescence intensity (MFI) of DiI5 liposomes (Fig. 2B) was higher in CD11b+ myeloid cells and remained unaltered by FMX as compared to MFI in EpCAM+ tumor cells.



**Example 3. Effects of FMX on pharmacology of subsequently administered liposomal irinotecan**

HT-29 tumor-bearing mice were injected with imaging agent (FMX) followed by injection of therapeutic liposomes as described in the preceding Example. The liposomes  
5 were MM-398 liposomes and were administered at 20 mg/kg and at 50 mg/kg with tumor samples being taken at 2, 24 and 72 hours after liposome injection. Analysis of SN-38 levels in tumor tissues was as described by Noble, et al, *Cancer Res.* 2006;66:2801-2806. Results (Fig. 3) show no differences in tumor SN-38 levels between FMX untreated controls and FMX pre-treated animals, demonstrating that FMX has no effect on the pharmacodynamics  
10 of liposomal irinotecan, particularly MM-398.

**Example 4. Effects of liposomal iodine on pharmacology of subsequently administered antibody targeted liposomal doxorubicin**

HT-29 tumor-bearing mice were injected with imaging agent followed by injection of liposomes as described in the preceding Example, except that the imaging agent was  
15 nanoliposomal iodine and the therapeutic liposomes were MM-302 liposomal doxorubicin at a dosage of 3 mg/kg. The liposomal iodine was prepared by encapsulating iodixanol (LGM Pharma) in cholesterol, HSPC, PEG-DSPE (55:40:5) liposomes with an average diameter of from 110 to 170 nm and a final iodine concentration of  $6.3 \times 10^5$  to  $2.1 \times 10^6$  iodine molecules per liposome and was administered at levels indicated in Fig. 4. Results obtained  
20 indicate that pretreatment of mice with an iodine-loaded liposomal contrast agent dramatically reduced the clearance of a subsequent dose of HER2-targeted liposomal doxorubicin (MM-302) even three days after administration of a liposomal iodine contrast agent (Fig. 4). The 30x concentration is the concentration of liposomal iodine contrast agent required to give a low level of contrast for CT imaging.

**Example 5. FMX measurement by MRI and drug deposition in different tumor models**

In order to correlate MRI-based measurements of FMX deposition with irinotecan drug levels in tumor tissues after deposition of liposomes, three human tumor cell lines (HT29, A2780 and A549) were used to establish subcutaneous flank tumor xenografts growing bilaterally in SCID mice (n=4 for each model). Tumor-bearing mice thus prepared  
30 were injected intravenously with FMX at 20 mg/kg.

Mice were imaged at baseline with a T2/T2\* MRI just before the FMX injection and again at 24h and 72h after the injection. The average T2 rate was determined for each tumor volume. The FMX concentration at each time point was determined from the difference relative to the baseline of the relaxation rates divided by the known relaxivity parameter  $r_2$ .

5 Mice were then administered a single dose of MM-398 equivalent to 10 mg irinotecan HCL/kg. Tumor samples were taken after 24h or 72hr of that injection and analyzed for irinotecan levels by HPLC as described above in Example 3.

Results (Figure 5) show that especially for individual A2780-derived tumors the FMX concentration measured at 24hr after FMX injection correlated well with the irinotecan (CPT-  
10 11) drug levels measured at 72h in the lysates of the same tumors. The FMX concentrations in the A549 and HT29-derived tumors established a lower signal threshold for FMX-based MRI that correlated with lower irinotecan concentrations.

#### **Example 6. Non-invasive Imaging with Ultrasmall Superparamagnetic Iron Oxide Particles (USIOPs) in Patients**

##### 15 **Materials and methods**

###### *Administration of FMX*

As disclosed herein, FMX can robustly and accurately predict delivery, and thus activity, of nanotherapeutics that have a  $t_{1/2}$  of clearance of greater than 6 hours, greater than 10 hours, and greater than 18 hours in mice (or 12, 24, and 48 hours in humans).

20 The nanotherapeutic may be, e.g., a liposome-encapsulated small molecule drug or prodrug, e.g., a ligand-targeted liposome-encapsulated drug. The prodrug may be an ester, e.g., an ester that requires conversion by one or more esterases for activation. The encapsulated drug or prodrug may be, e.g., a taxane, a tyrosine kinase inhibitor (TKI), or a camptothecin. An exemplary camptothecin prodrug is irinotecan.

##### 25 *USIOPs*

USIOPs having particles ranging from 10-50 nm in size and exhibiting a half-life of clearance from the bloodstream of at least 10 hours are suitable for use in the imaging

techniques disclosed herein. An exemplary USIOP for use in the disclosed methods is ferumoxytol (FMX).

#### *Dosage*

A minimum dosage in humans of USIOPs for the imaging methods disclosed herein  
5 comprises 3 mg/kg of iron. In some embodiments, the dose is at least 5 mg/kg. In other  
embodiments, the dose is at least 10, at least 15, or up to 20 mg/kg of iron. In one  
embodiment, the patient is an adult, the USIOP is FMX, and the dose is a 510 mg dose.

#### *Prescreening prior to FMX Treatment*

A patient's iron levels are measured in the blood prior to ferumoxytol administration.  
10 Iron overload is diagnosed by measuring a fasting morning transferrin saturation  $\geq 45\%$  (ratio  
of serum iron divided by the serum total iron binding capacity and expressed as a  
percentage). A ferritin level of 1000 ng/ml is likely to be also associated with organ  
damaging levels of iron. Blood is collected from each patient and the plasma is analyzed for  
transferrin according to standard Clinical Laboratory protocols. Administration of USIOPs is  
15 contraindicated in patients with iron overload and such patients should not be imaged in  
accordance with the methods disclosed herein. For all patients, ferumoxytol is used in  
accordance with the manufacturer's label warnings.

#### *Dosage and Administration of FMX*

Ferumoxytol (30 mg/mL) is available for intravenous injection in single use vials.  
20 Each vial contains 510 mg of elemental iron in 17 mL.

A single dose of ferumoxytol will be administered at Day 1 by intravenous injection.  
Dosing is calculated according to patient weight at 5 mg/kg. The total single dose does not  
exceed 510 mg, the maximum approved single dose of ferumoxytol. Ferumoxytol is  
administered as an undiluted IV injection at a rate of up to 1 ml (30 mg) per second with  
25 monitoring of vital signs.

#### *Magnetic Resonance Imaging (MRI)*

The MRI image is obtained using a magnetic field strength of 1-10 Tesla. For example, a  
magnetic field strength of 1.5 or 3 Tesla is used. Basic MRI scan sequences for the

acquisition of T1-weighted, T2-weighted and T2\*-weighted images are used to measure FMX-dependent T1 hyper-enhancement or T2/T2\*-signal hypoenhancement (contrast enhancement due to the excellent relaxivity properties of this USPIO). The  $r_2$  relaxivity for FMX at 1.5T, 37°C in water or plasma is reported to be  $r_2 = 89 \text{ mM}^{-1} \text{ sec}^{-1}$ . The relaxivity parameter can be used to quantify the signal contrast in FMX images by either T2(\*) or R2(\*) (R2=1/T2) analysis methods. The relationship between the R2(\*) relaxation rates, the  $r_2$ (\*) relaxivity parameter and the FMX concentration is given by the following equation [1].

$$R_{2*} = \frac{1}{T_{2*}} = (R_{2*})_0 + (r_{2*}) \cdot [FMX] \quad [1]$$

#### *Imaging timepoints*

For prediction of liposomal deposition and activity in humans, imaging is typically performed initially pre-FMX administration to establish a background level of contrast and then subsequently between 1 and 168 hours (0-7 days) following FMX administration. For prediction of activity by nanocarriers that are dependent on macrophage uptake (e.g., non-targeted and/or prodrug-containing nanocarriers), the imaging will be performed between 1-7 days post-FMX dosing. Finally, for targeted nanotherapeutics that do not rely primarily on macrophage uptake for uptake, processing and/or conversion, the imaging may beneficially be carried out earlier, e.g., between 20 and 48, or 24 and 72 hours post-FMX dosing.

#### *Imaging procedure*

In an exemplary embodiment, FMX is administered to a patient being considered for nanoliposomal therapy for a tumor. First a pre-dose MRI (MRI1) is performed to established baseline. Following FMX administration one or more additional MRIs is performed.

A second MRI (MRI2) is (optionally) performed (1.5-4 hours after FMX administration) to record tumor blood volume.

A third MRI (MRI3) is (optionally) performed approximately 24 hours after FMX administration. Liposome tumor deposition peaks around 24 hours after administration and FMX signal should be also predominately tumor-based (as FMX should have been at least partially cleared from the blood). Therefore, MRI3 results (corrected for MRI1 and MRI2) are correlated with liposome deposition potential.

A fourth MRI (MRI4) is (optionally) performed approximately 72 hours after FMX administration. FMX accumulation in macrophages follows deposition, and is expected to peak between 24 and 72 hours; therefore, MRI4 signal enhancement should correlate with USIOP uptake by TAMs.

5           The difference in contrast between MRI3 and MRI1 is calculated to provide an estimate of the amount of deposition that occurred and therefore what can be expected for a liposome therapy. If deposition is undetectable, or is lower than a preset threshold (e.g., at least 5%, 10%, 15%, 20%, or 25% over MRI1) a patient should be excluded from nanoliposomal therapy.

10           The difference in contrast between MRI2, MRI3, or MRI4 and MRI1 is calculated to provide an estimate of the USIOP uptake by TAMs, which is believed to correlate with the liposome drug release potential for a liposome therapy at the location of USIOP uptake. If the liposome drug release potential is lower than a preset threshold (e.g., at least 5%, 10%, 15%, 20%, or 25% over MRI1) a patient is excluded from receiving nanoliposomal therapy.

15           As shown with equation [1] above, the difference in contrast can be related to FMX concentrations at a specific site or sample location.

Standards (“phantoms”) of different concentrations of FMX ranging from 0 – 200 µg/ml with the FMX being suspended in 2% agarose or similar gels may be included within the MR imaging cavity (e.g., in tubes or vials), so that image acquisition of the standards can occur while imaging a patient. These imaging data can provide reference points for the  
20           quantitation of FMX. An exemplary image of such “phantoms” is shown in Figure 9, which shows a T2\* weighted MRI with TE of 13.2ms with phantom tubes from 0-200µg/ml ferumoxytol.

25           **Example 7. MRI imaging of FMX in patient plasma and tumor lesions and use of MRI-derived FMX data in a pharmacokinetic model**

In a human clinical trial (ClinicalTrials.gov Identifier: NCT01770353) patients with advanced solid tumors and multiple metastases were injected with FMX at 5mg/kg and imaged in an MRI scanner as described in Example 6. Blood was drawn before and at about 30min, 2hr, 24hr and 72hr after the injection of FMX. Plasma was prepared according to

published protocols. Plasma FMX concentrations for each patient were determined from MRI images of plasma imaged together with an FMX “phantom” standard. Analysis of T2\*-weighted images in comparison to an external “phantom” standard as described in Example 6 allowed the extrapolation of FMX concentrations in tumor lesions. Plasma and tissue FMX concentrations from individual lesions were input into a pharmacokinetic model of both compartments (MATLAB) that considers a mixed model of FMX deposition and allows estimation of tissue-specific parameters of FMX-dependent tissue permeability and signal retention/tissue binding. These two parameters can thus characterize individual lesions.

Results (Figure 6A) show that plasma levels of FMX decline consistent with published data in healthy volunteers (Landry et al., Am. J. Nephrol. 2005;25(4):400–10). In some patients FMX clearance was low resulting in higher FMX levels in both plasma and tumor lesions. As shown in Figure 6B the FMX signal in lesions from a representative patient show an immediate perfusion-dependent uptake of FMX, but levels are maintained or even increase at the 24h MRI measurement. FMX clearance was slower in tumor lesions than in the plasma. A pharmacokinetic model (see Figure 6C) identifies lesion-characteristic tissue permeability and tissue binding parameters that together allow a fit to the measured FMX levels in individual lesions. The permeability parameter contributes to early FMX signals, while the binding parameter contributes to later FMX signals.

#### **Example 8. Deposition of FMX in patient tumor lesions and co-localization with macrophages**

Tumor biopsies from the NCT01770353 clinical trial outlined in Example 7 were obtained 72h and 168hrs after FMX injection at 5mg/kg and immediately fixed in formalin. Serial tumor sections from formalin fixed paraffin embedded (FFPE) tissue were prepared and assessed by Prussian Blue staining for FMX and by staining with anti-CD68 antibody (clone PG-M1, DAKO) for macrophages. Sections were imaged with an Aperio® ScanScope AT® whole slide scanner.

Results (Figure 7) show that FMX deposition was detectable primarily in stromal areas around tumor nests. The staining pattern suggests intracellular FMX accumulation that is highly co-localized with macrophages stained in adjacent sections. This association was

observed in biopsies obtained at 72h and 168h and suggests that FMX deposition can identify vascular-accessible macrophages within tumor lesions.

**Example 9. Drug levels in biopsies targeted towards lesion areas with different levels of FMX signal hypoenhancement**

5            In the NCT01770353 clinical trial described above, patients with advanced solid tumors and multiple metastases were injected with FMX at 5mg/kg and imaged in an MRI scanner. The T2\*-weighted images from all time-points were used to outline lesion-specific regions of interest (ROI) with higher or lower levels of FMX-dependent signal hypoenhancement. MRI image analysis extrapolated FMX levels from these ROI within the  
10            lesions. CT-guided needle core biopsies were directed towards the same ROI, and the localization of the percutaneous sampling site was projected back onto the FMX MRI images by multimodality image fusion for optimization of the ROI outline. This percutaneous sampling was done using manual control. Tissue collection was performed 72hr after the  
15            infusion of 80mg/m<sup>2</sup> MM-398, which coincided with 168hr after the injection of FMX. Core biopsies were frozen. For measurements of the irinotecan metabolites SN-38 and SN-38G, samples were weighted and homogenized in a 50% methanol/water mixture in a bullet blender. After extraction with acidified methanol, the supernatant was collected, dried down, reconstituted in mobile phase solution and analyzed on an LC/MS/MS TSQ Vantage (Thermo Scientific) system.

20            Results (Figure 8) show the tumor FMX signal measured at 24hr in ROI with higher or lower levels of FMX-dependent signal hypoenhancement (prior to ROI outline optimization) and the irinotecan levels measured in biopsies from the vicinity of the same ROI. For a majority of biopsy samples there is a correlation between the level of the 24h FMX signal and the irinotecan level.

25            **Example 10. MRI imaging of FMX in patient lesions and comparison to treatment-dependent changes in lesion volume**

              In the NCT01770353 clinical trial described above, patients with advanced solid tumors and multiple metastases were injected with FMX at 5mg/kg and imaged in an MRI scanner as described in Example 6. Patient lesions were also imaged by X-ray Computed

Tomography at the beginning of treatment (“Screening”) and after four weeks (“EOC2”). The individual lesion volumes were calculated at both time points.

Results summarized in the table below show the measured FMX levels at day 2 (24h) and day 4 (72h) after FMX injection together with the calculated volumes of four liver lesions at treatment start (“Screening”) and after four weeks or two treatment cycles (“EOC2”). All four lesions showed a decrease in measurable lesion size. Compared to the median FMX levels in 26 lesions of seven patients the 24h FMX levels are all elevated, but the levels in lesion 2 are lower than in the other three lesions. The 72h FMX levels for lesions 2-4 are above the median FMX levels, but have dropped below the median in lesion 1. Lesion 1 was the smallest lesion at treatment start, lesion 2 was the largest lesion at treatment start.

Lesion	Day 2 Fe-MRI (µg/ml)	Day 4 Fe-MRI (µg/ml)	Screening CT (cc)	EOC2 (cc)	Vol change
1	38.98	6.11	3.7	1.0	-73%
2	28.04	12.8	44.3	30.3	-32%
3	39.94	14.37	9.2	1.6	-83%
4	37.35	13.09	10.3	2.0	-81%
Median all lesions*	22.93	10.84			

\*Patients 0001 – 0009 (26 lesions)

### **Incorporation by Reference**

Each and every issued patent, patent application and publication specifically referred to herein is hereby incorporated herein by reference in its entirety.



What is claimed is:

1. A method for selecting and providing pharmaceutical treatment to a patient for a localized infectious, inflammatory, or neoplastic condition, the method comprising:

5           diagnosing a localized infectious, inflammatory, or neoplastic condition in a patient and  
              identifying one or more locations of infection, inflammation or neoplasia in the patient,  
              and subsequently,  
10           obtaining a contrast-enhanced MRI image of a first location of the one or more locations,  
              and subsequently,  
              selecting an anti-infective, anti-inflammatory, or anti-neoplastic pharmaceutical agent and treating the patient with the selected pharmaceutical  
15           agent;

wherein,

              the contrast-enhanced MRI image is obtained following administration of an MRI contrast agent comprising an MRI contrast-enhancing amount of superparamagnetic iron oxide nanoparticles of about 15-30 nm in diameter,  
20           and  
              if the contrast-enhanced MRI image shows contrast enhancement within the first location, the selected pharmaceutical agent is an agent that is formulated as nanoparticles or nanoliposomes of about 70 to about 200 nm in diameter, but  
25           if the contrast-enhanced MRI image does not show contrast enhancement at first location, the selected pharmaceutical agent is an agent that is not

formulated as nanoparticles or nanoliposomes of about 70 to about 200 nm in diameter.

2. The method of claim 1, wherein the MRI contrast agent is ferumoxytol.
- 5 3. The method of claim 2, wherein the ferumoxytol is administered at 5 mg iron per kg.
4. The method of claim 2, wherein the patient is an adult and 100 - 1000 milligrams (iron) of ferumoxytol are administered to the patient.
- 10 5. The method of claim 2, wherein the patient is an adult and 510 milligrams of ferumoxytol are administered to the patient.
6. The method of claim 1, wherein the contrast-enhanced MRI image is obtained no more than 72, 96, 120, 144 or 168 hours after administration of the superparamagnetic  
15 iron oxide nanoparticles.
7. The method of claim 1, wherein the contrast-enhanced MRI image is obtained from 72-96, 96-120, 120-144, or 144 to 168 hours after administration of the superparamagnetic iron oxide nanoparticles.  
20
8. A method for selecting and providing pharmaceutical treatment to a patient for a localized infectious, inflammatory, or neoplastic condition, the method comprising:  
  
diagnosing a localized infectious, inflammatory, or neoplastic condition in a patient and  
  
25 identifying one or more locations of infection, inflammation or neoplasia in the patient,  
  
and subsequently,  
  
obtaining a first contrast-enhanced MRI image of a first location of the one or more locations,

obtaining a second contrast-enhanced MRI image of a second location of the one or more locations,

and subsequently,

selecting an anti-infective, anti-inflammatory, or anti-neoplastic

5 pharmaceutical agent and treating the patient with the selected pharmaceutical agent;

wherein,

10 the first and second contrast-enhanced MRI images are obtained following administration of an MRI contrast agent comprising an MRI contrast-enhancing amount of superparamagnetic iron oxide nanoparticles of about 15-30 nm in diameter, and

15 if both the first and the second contrast-enhanced MRI images show contrast enhancement within both the first location and second location, the selected pharmaceutical agent is an agent that is formulated as nanoparticles or nanoliposomes of about 70 to about 200 nm in diameter, but

if both the first and the second contrast-enhanced MRI images do not show contrast enhancement within both the first location and second location, the selected pharmaceutical agent is an agent that is not formulated as nanoparticles or nanoliposomes of about 70 to about 200 nm in diameter.

20 9. The method of claim 8, wherein the contrast agent is ferumoxytol and 1) is administered at 5 mg/kg, or 2) is administered to an adult patient at a dosage of 100 - 1000 milligrams, or 3) is administered to an adult patient at a dosage of 510 milligrams.

25 10. The method of any one of claims 1 - 9, wherein the MRI image is obtained using a magnetic field strength of 1-10 Tesla or about 1.5 Tesla, or about 3 Tesla.

11. The method of any one of claims 1 - 9, wherein the liposomal therapeutic agent comprises liposomes of an average size of about 100 nm in diameter with an average

range of about 75 to about 200 nm or of about 80 to about 120 nm.

12. The method of any one of claims 1 – 9, wherein the liposomal therapeutic agent is MM-398.

5

13. The method of any one of claims 1 – 9, wherein the liposomal therapeutic agent is MM-302.

14. The method of any one of claims 1 – 9, wherein the first contrast-enhanced MRI image shows contrast enhancement within the first location, the neoplastic condition comprises at least one tumor and the pharmaceutical agent is a liposomal anti-neoplastic agent.

10

15. The method of claim 14 wherein the tumor is a non-small cell lung cancer (NSCLC) tumor, a triple negative breast cancer (TNBC) tumor, a colorectal cancer (CRC) tumor, an ER/PR positive breast cancer tumor, a pancreatic cancer tumor, an ovarian cancer tumor, a small cell lung cancer tumor, a gastric cancer tumor, a GEJ adenocarcinoma, a head and neck cancer tumor, a cervical cancer tumor, or Ewing's sarcoma and the selected pharmaceutical agent is a liposomal formulation of irinotecan.

15

20

16. The method of claim 15 wherein the liposomal formulation of irinotecan is MM-398 (irinotecan sucrosfate liposome injection).

25

17. The method of claim 14 wherein the liposomal anti-neoplastic agent is liposomal doxorubicin.

18. The method of claim 17 wherein the liposomal doxorubicin comprises antibody-targeted doxorubicin liposomes.

30

19. The method of claim 18 wherein the antibody-targeted doxorubicin liposomes are targeted with an anti-HER2 antibody.

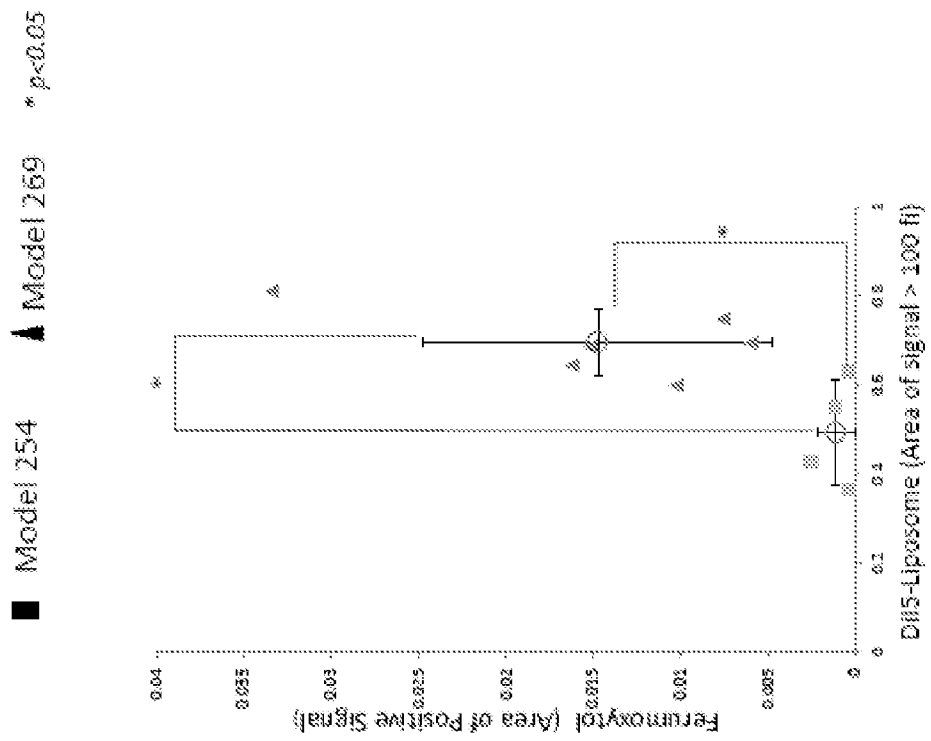


Figure 1A

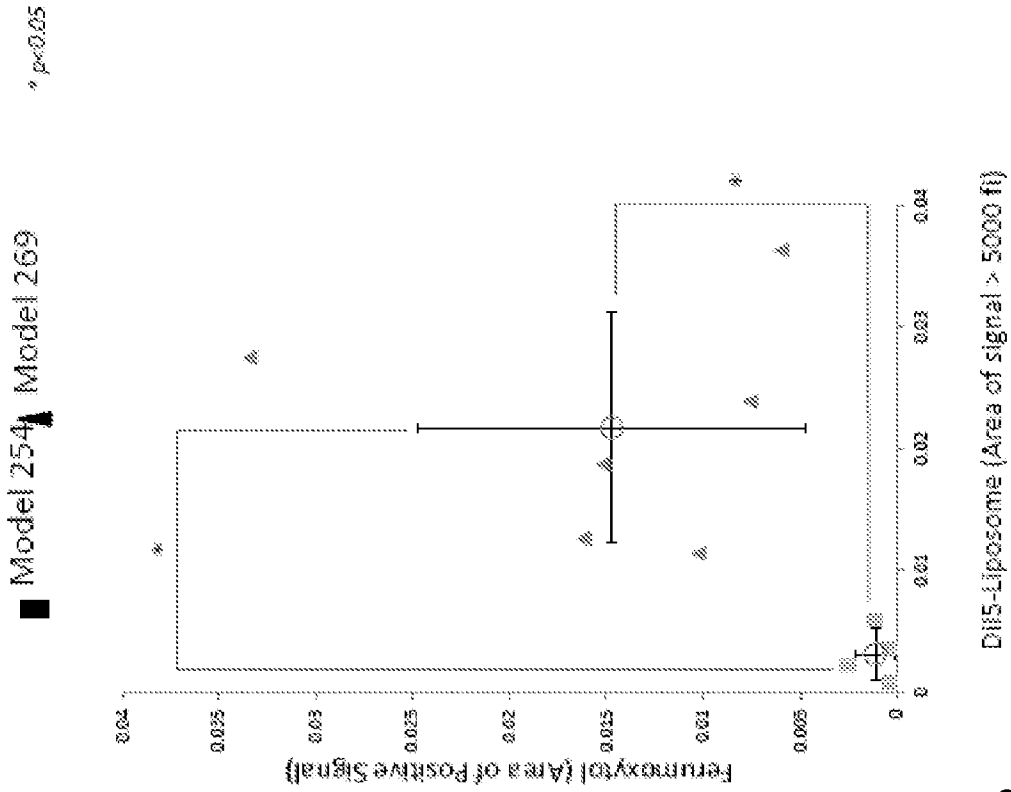


Figure 1B

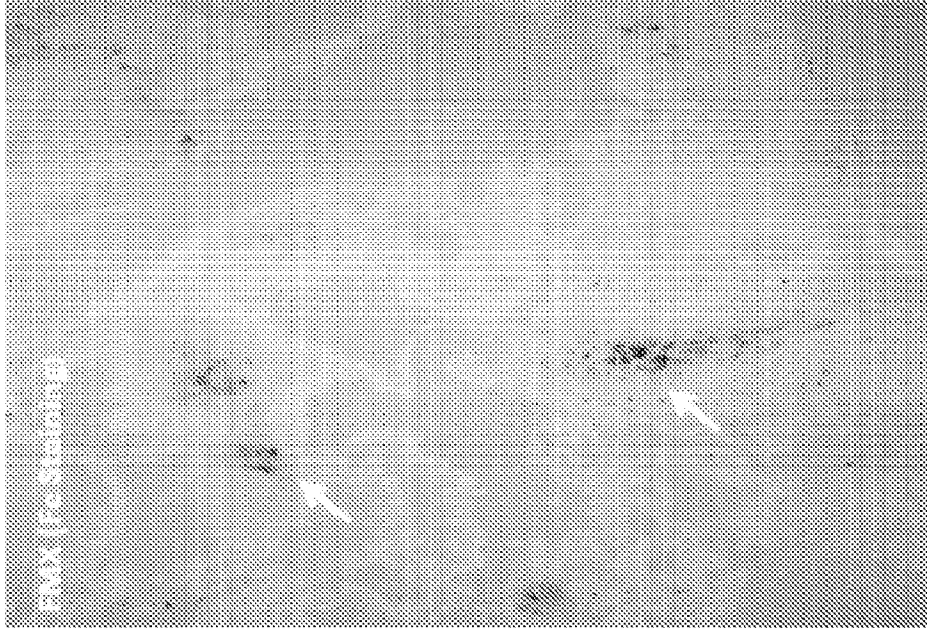


Figure 1D

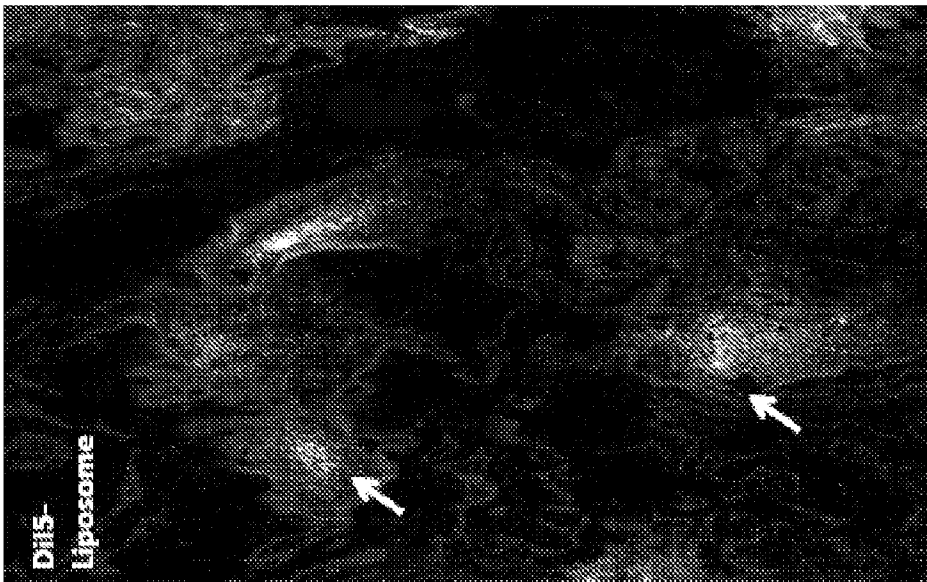
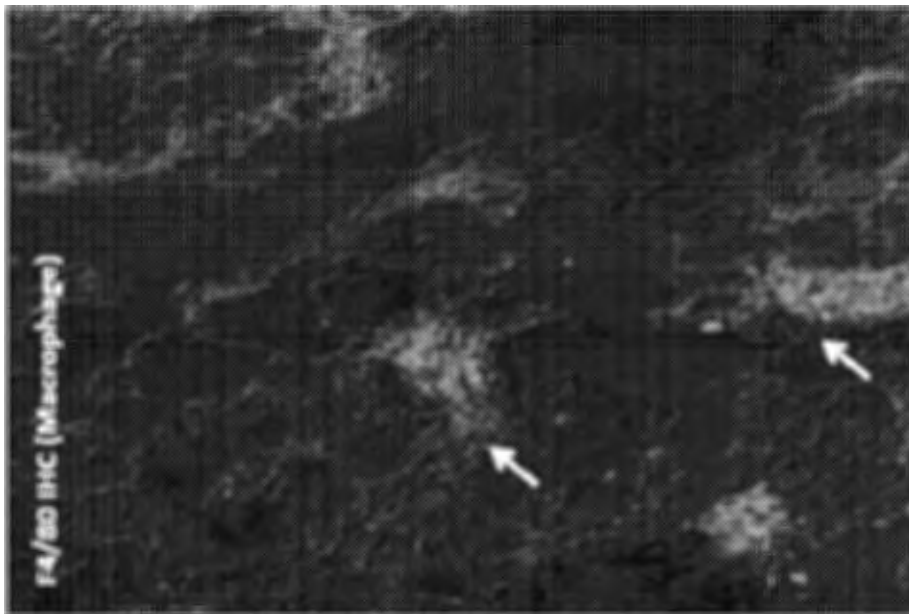


Figure 1C



**Figure 1E**



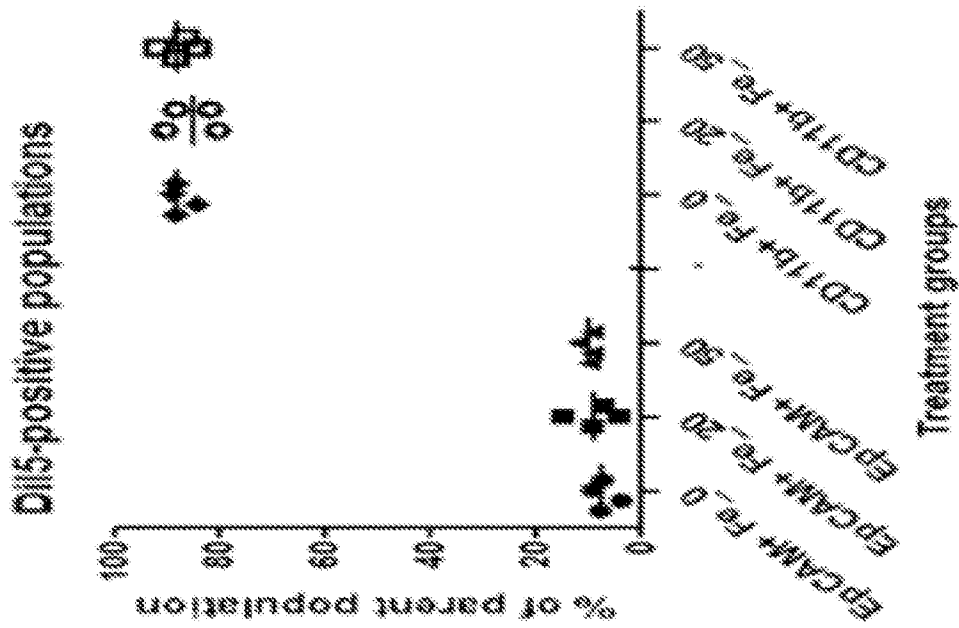


Figure 2A

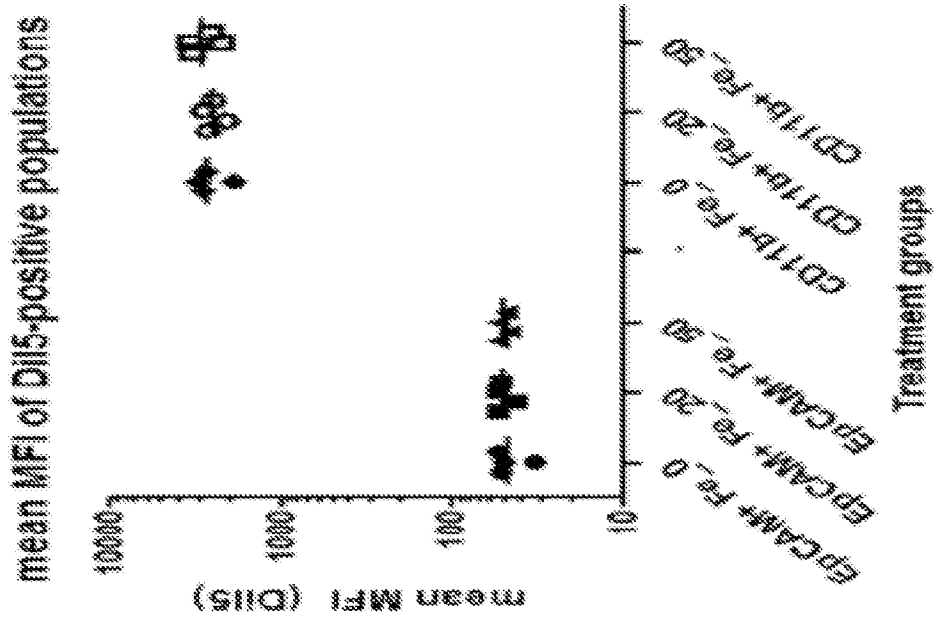


Figure 2B

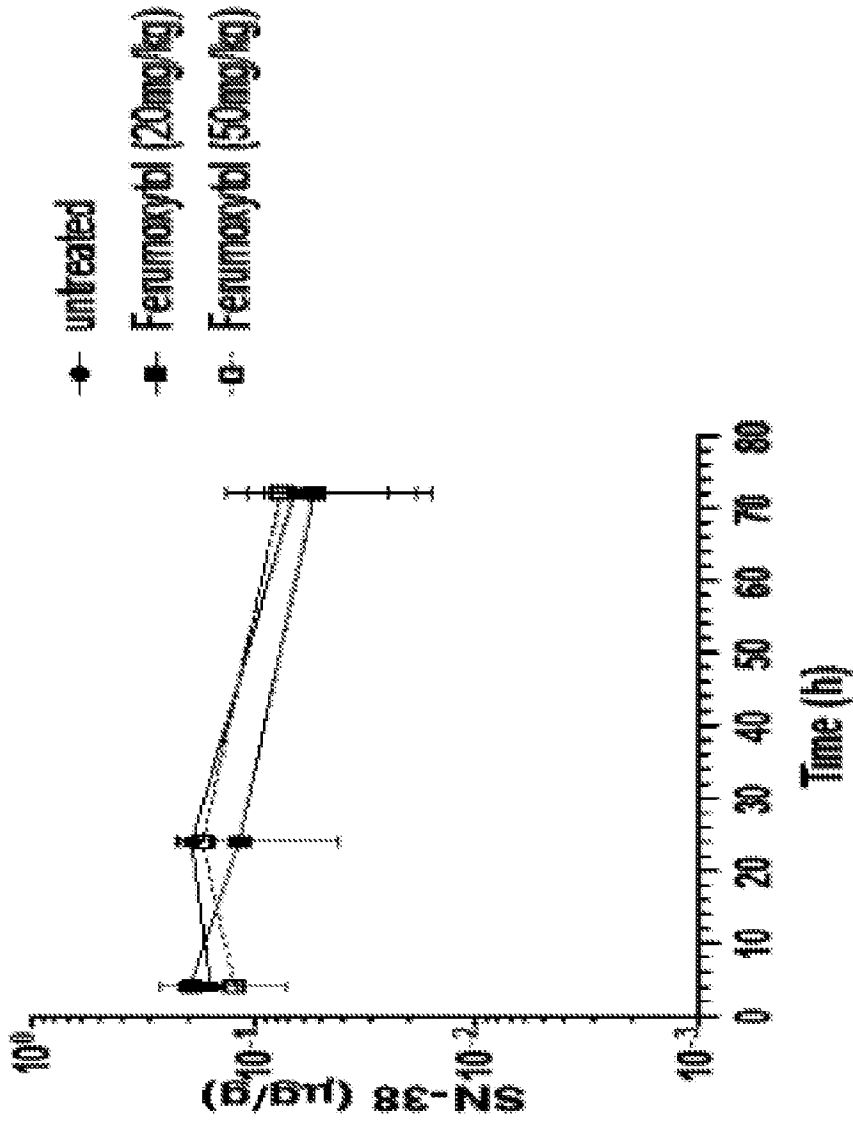
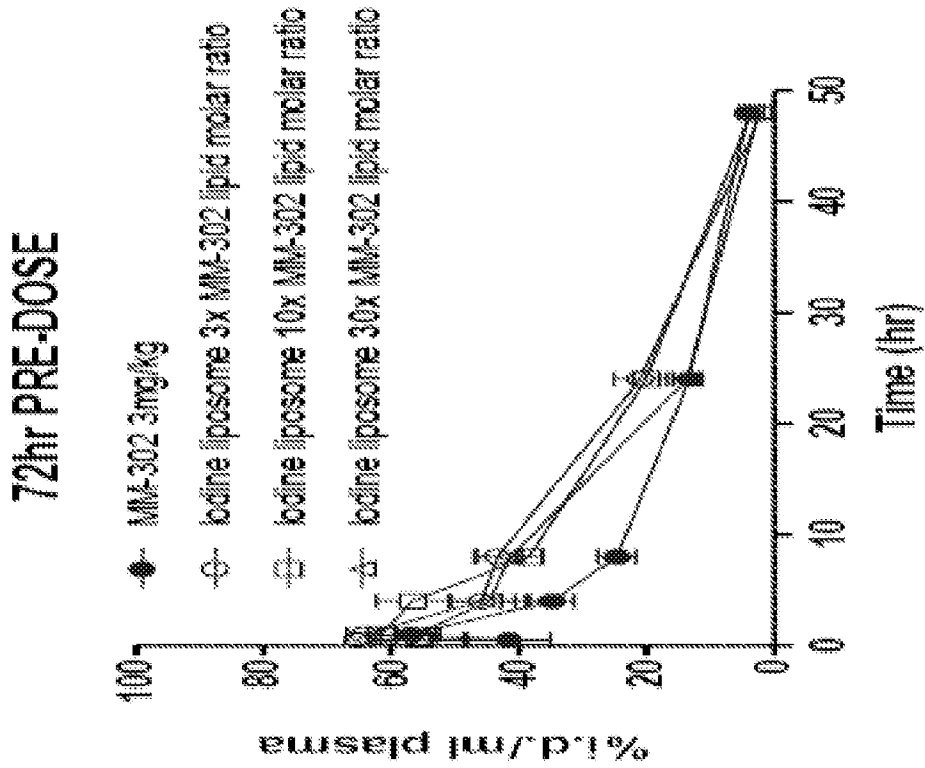


Figure 3



**Figure 4**

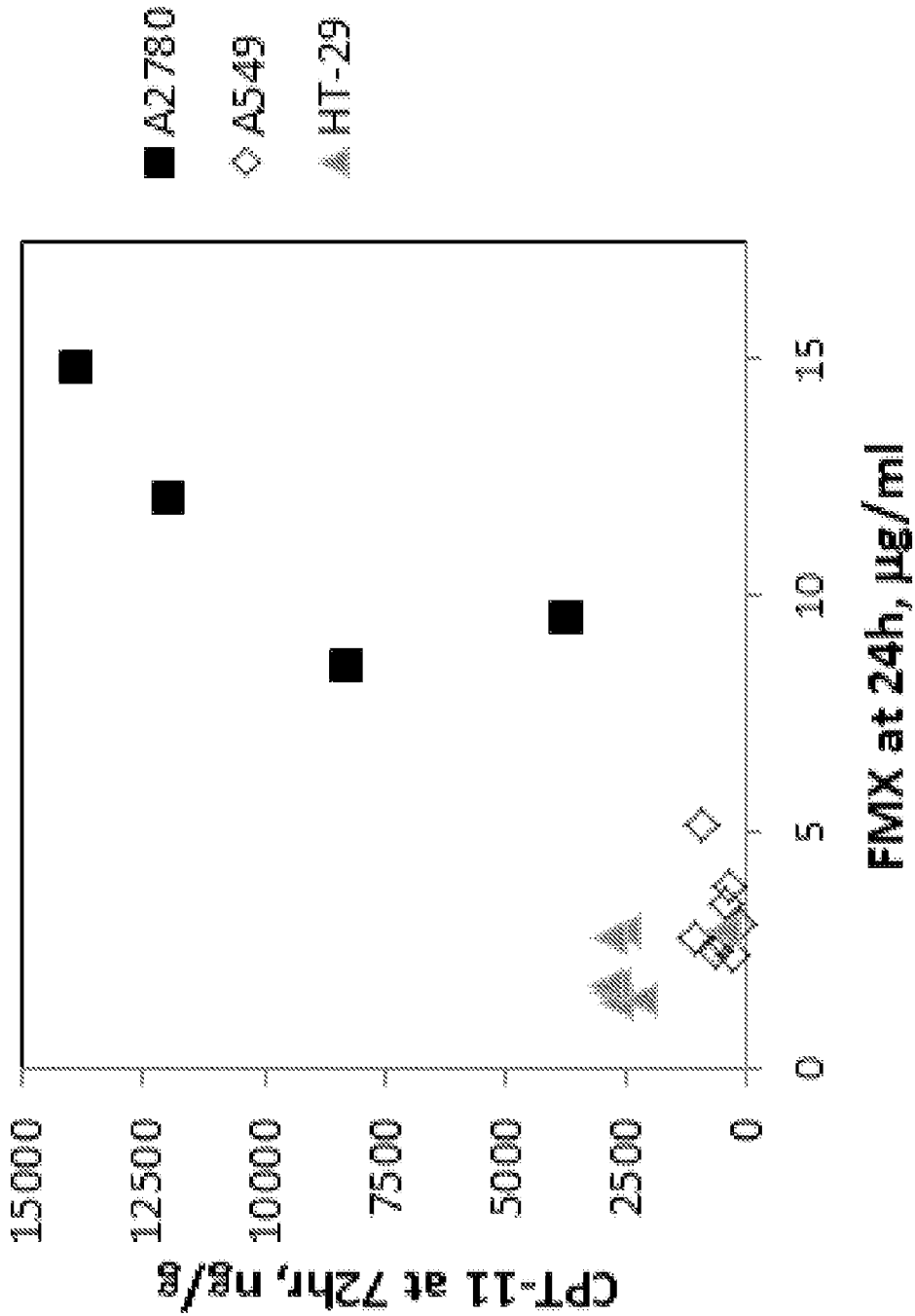


Figure 5

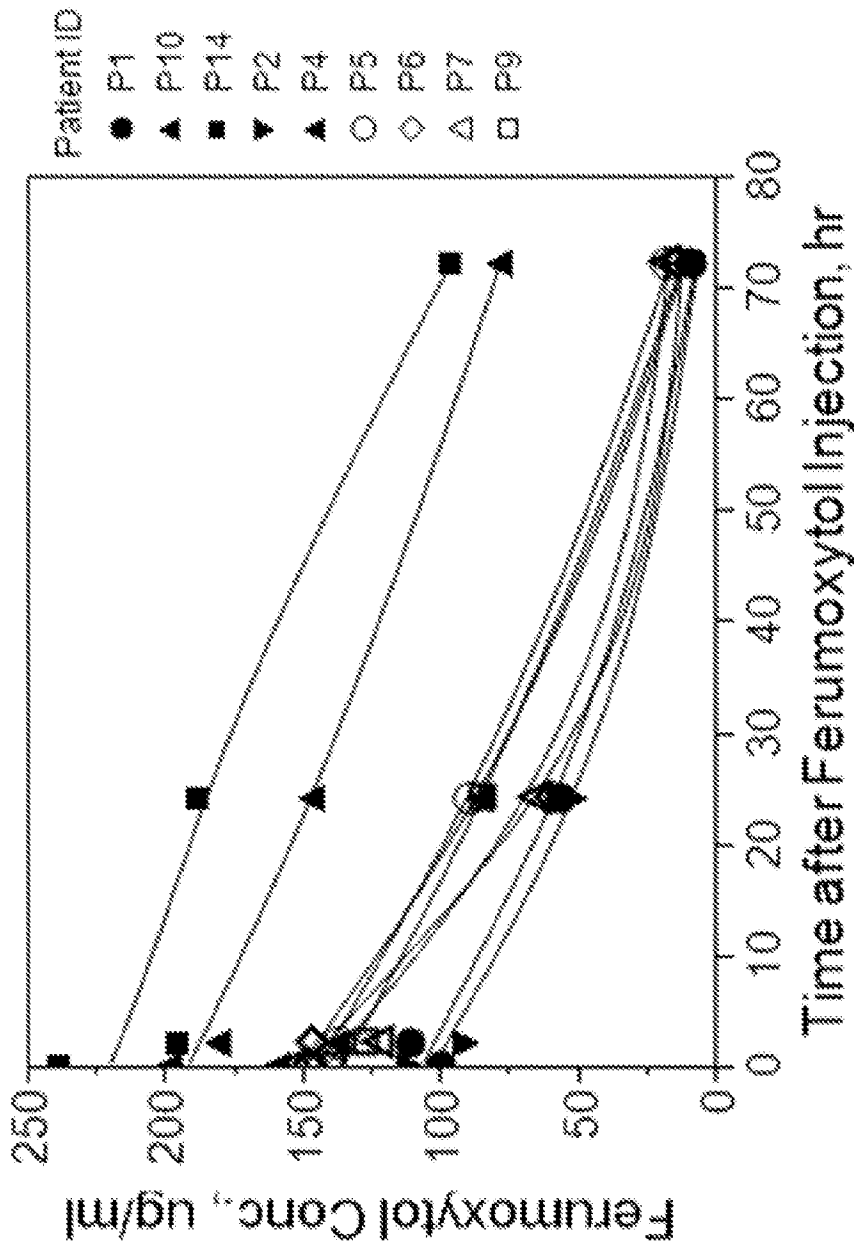


Figure 6A

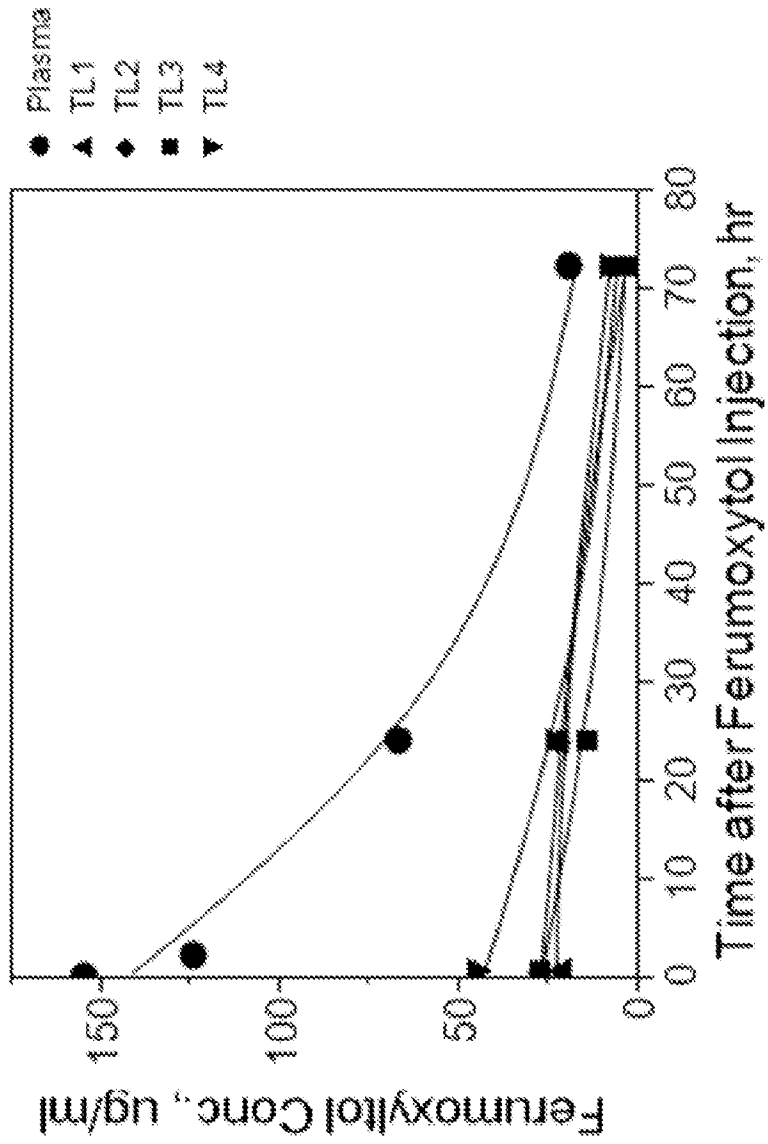


Figure 6B

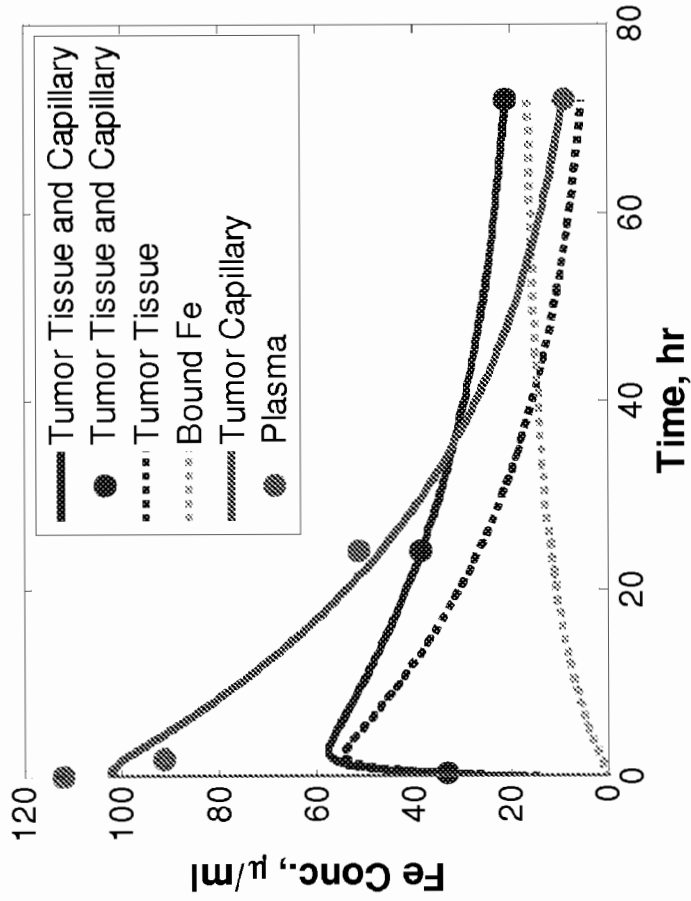


Fig. 6C



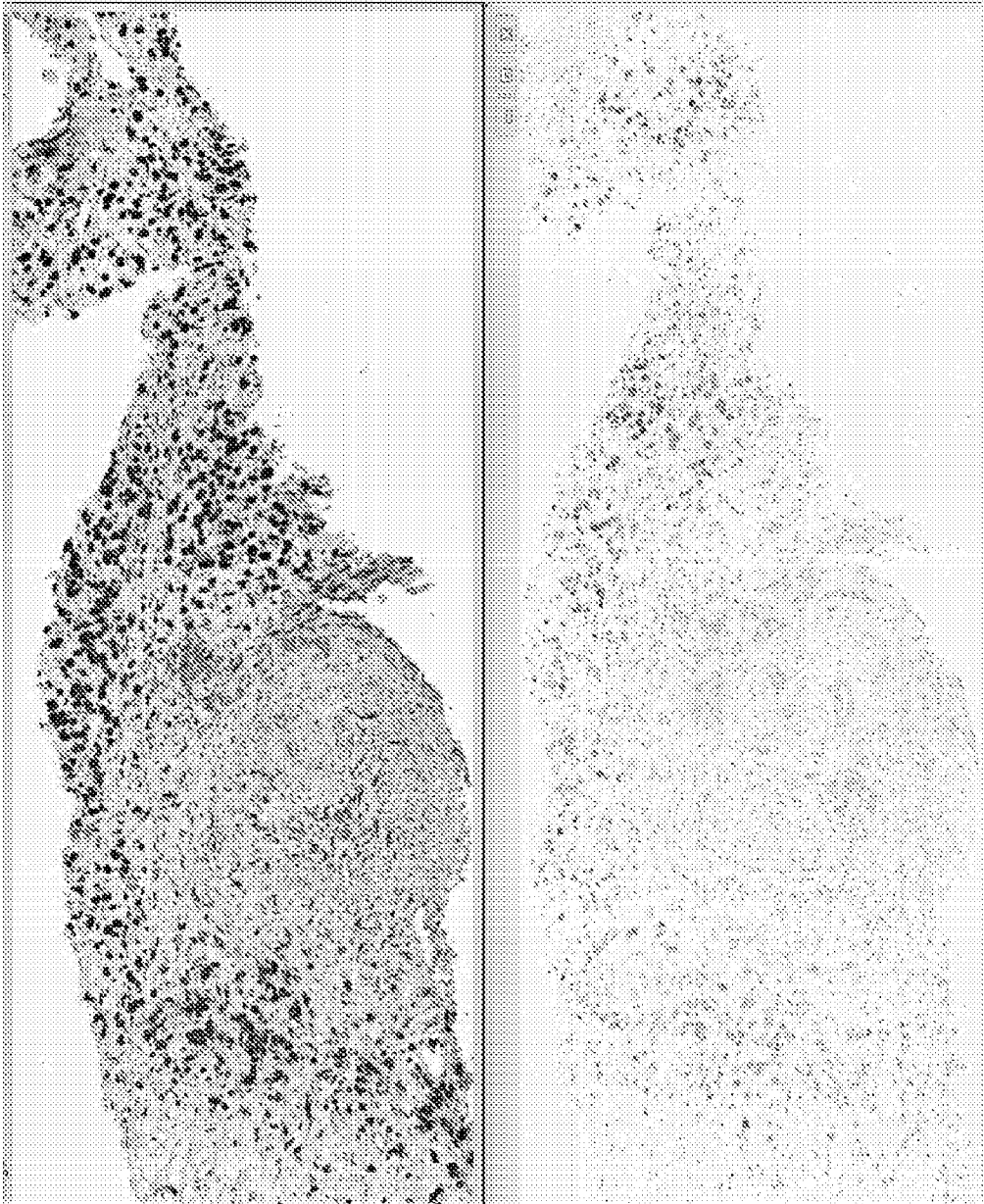


Fig. 7

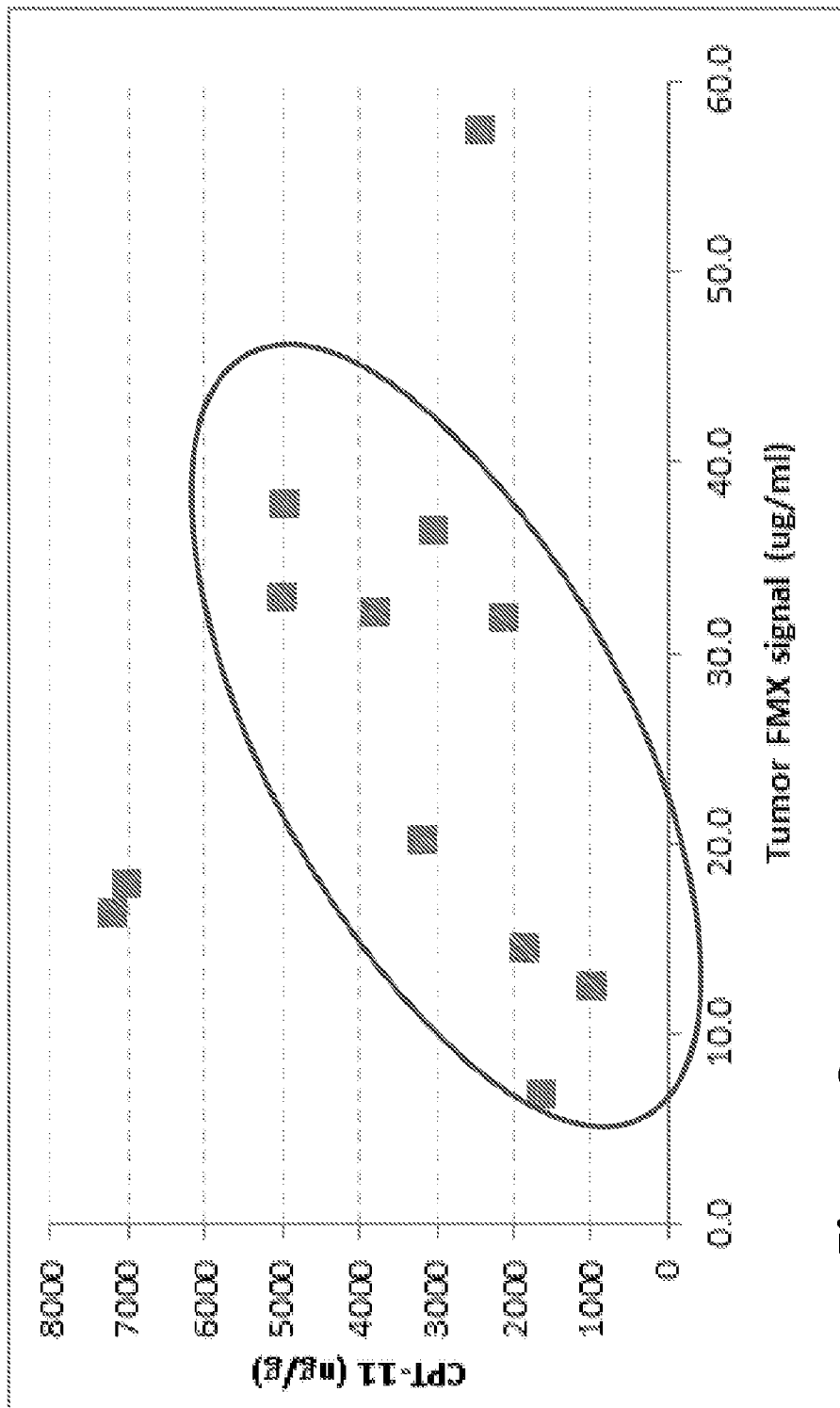


Figure 8

Fig. 8

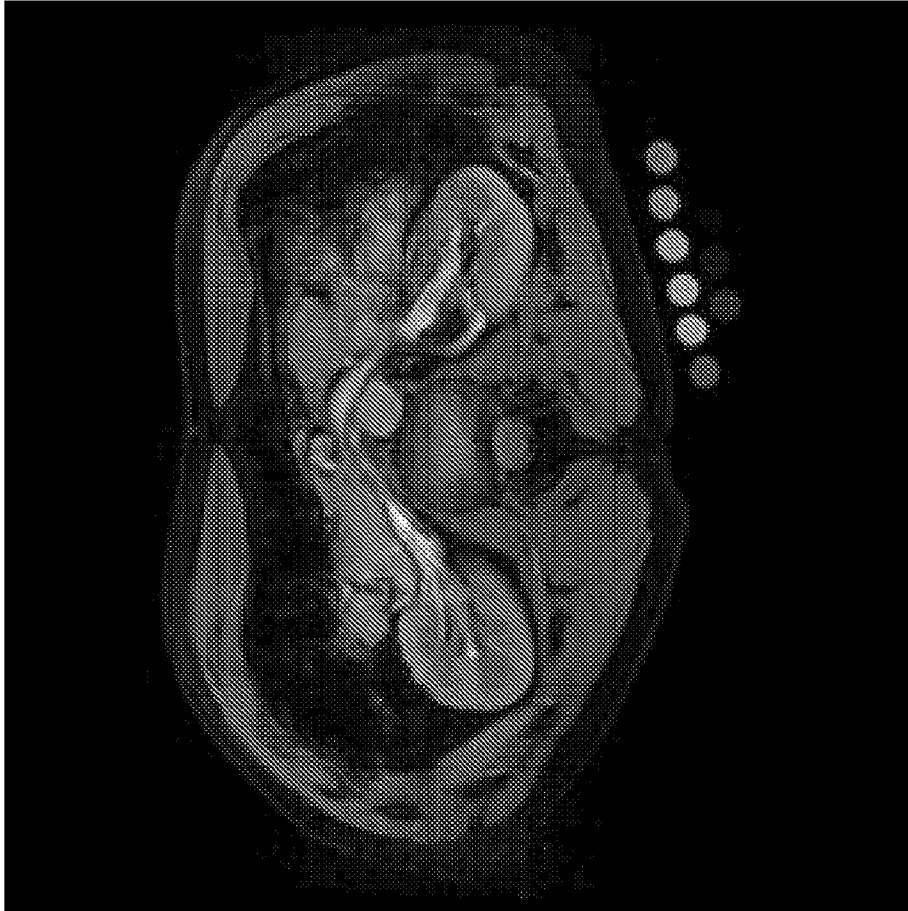


Fig. 9

## INTERNATIONAL SEARCH REPORT

13/07/2014 08:00:00.2014  
International application No.

PCT/US 13/75513

## A. CLASSIFICATION OF SUBJECT MATTER

IPC(8) - A61B 5/055, A61K 49/06, A61P 35/00 (2014.01)

USPC - 424/9.321, 514/19.3, 600/410

According to International Patent Classification (IPC) or to both national classification and IPC

## B. FIELDS SEARCHED

Minimum documentation searched (classification system followed by classification symbols)

IPC(8) - A61B 5/055, A61K 49/06, A61P 35/00 (2014.01)

USPC - 424/9.321, 514/19.3, 600/410

Documentation searched other than minimum documentation to the extent that such documents are included in the fields searched

USPC - 424/9.3, 424/9.32, 424/9.323, 424/450, 514/19.2, 600/411

(keyword limited; terms below)

Electronic data base consulted during the international search (name of data base and, where practicable, search terms used)

PatBase, PubWEST(USPT,PGPB,EPAB,JPAB), Google Scholar, Google Web

Search terms: MRI, magnetic resonance imaging, ferumoxylol, cancer, tumor, neoplasm, malignancy, contrast enhancement, liposome, nanoliposome, nanoparticle, MM-398, irinotecan, sucrosfate, MM-302, doxorubicin, Her2, tumor-associated macrophages, TAM

## C. DOCUMENTS CONSIDERED TO BE RELEVANT

Category*	Citation of document, with indication, where appropriate, of the relevant passages	Relevant to claim No.
Y	US 2012/0003160 A1 (WOLF et al.) 5 January 2012 (05.01.2012) para [0020], [0042], [0050], [0051], [0059], [0062], [0075], [0115], [0122], [0129], [0139]	1-19
Y	KLINZ et al., Identifying differential mechanisms of action for MM-398/PEP02, a novel nanotherapeutic encapsulation of irinotecan. AACR/EORTC 2011, Abstract C207, 2011 [online]. [Retrieved on 16 May 2014]. Retrieved from the Internet <URL: <a href="http://www.merrimackpharma.com/sites/default/files/documents/AACR%20EORTC%20MM-398%20MOA%20SKlinz%20November%202011%20FINAL.pdf">http://www.merrimackpharma.com/sites/default/files/documents/AACR%20EORTC%20MM-398%20MOA%20SKlinz%20November%202011%20FINAL.pdf</a> > Especially box entitled "Abstract"	1-19
Y	KLINZ et al., MM-302, a HER2-targeted liposomal doxorubicin, shows binding/uptake and efficacy in HER2 2+ cells and xenograft models. AACR 2011, Abstract 3637, 2011 [online]. [Retrieved on 16 May 2014]. Retrieved from the Internet <URL: <a href="http://www.merrimackpharma.com/sites/default/files/documents/10.%20AACR%202011%20MM-302%20HER2%20Threshold%20Klinz.pdf">http://www.merrimackpharma.com/sites/default/files/documents/10.%20AACR%202011%20MM-302%20HER2%20Threshold%20Klinz.pdf</a> > Especially box entitled "Abstract"	13, 17-19

 Further documents are listed in the continuation of Box C.

\* Special categories of cited documents:

"A" document defining the general state of the art which is not considered to be of particular relevance

"E" earlier application or patent but published on or after the international filing date

"L" document which may throw doubts on priority claim(s) or which is cited to establish the publication date of another citation or other special reason (as specified)

"O" document referring to an oral disclosure, use, exhibition or other means

"P" document published prior to the international filing date but later than the priority date claimed

"T" later document published after the international filing date or priority date and not in conflict with the application but cited to understand the principle or theory underlying the invention

"X" document of particular relevance; the claimed invention cannot be considered novel or cannot be considered to involve an inventive step when the document is taken alone

"Y" document of particular relevance; the claimed invention cannot be considered to involve an inventive step when the document is combined with one or more other such documents, such combination being obvious to a person skilled in the art

"&amp;" document member of the same patent family

Date of the actual completion of the international search

19 May 2014 (19.05.2014)

Date of mailing of the international search report

06 JUN 2014

Name and mailing address of the ISA/US

Mail Stop PCT, Attn: ISA/US, Commissioner for Patents

P.O. Box 1450, Alexandria, Virginia 22313-1450

Facsimile No. 571-273-3201

Authorized officer:

Lee W. Young

PCT Helpdesk: 571-272-4300  
PCT OSP: 571-272-7774

CSPC Exhibit 1093



(51) International Patent Classification:

A61K 31/04 (2006.01) A61K 31/475 (2006.01)  
A61K 31/166 (2006.01) A61K 31/502 (2006.01)  
A61K 31/416 (2006.01) A61K 31/55 (2006.01)  
A61K 31/4184 (2006.01) A61K 9/127 (2006.01)  
A61K 31/436 (2006.01) A61K 47/06 (2006.01)  
A61K 31/4745 (2006.01) A61P 35/00 (2006.01)

(21) International Application Number:

PCT/US2016/047814

(22) International Filing Date:

19 August 2016 (19.08.2016)

(25) Filing Language:

English

(26) Publication Language:

English

(30) Priority Data:

62/207,709 20 August 2015 (20.08.2015) US  
62/207,760 20 August 2015 (20.08.2015) US  
62/269,756 18 December 2015 (18.12.2015) US  
62/269,511 18 December 2015 (18.12.2015) US  
62/308,924 16 March 2016 (16.03.2016) US  
62/323,422 15 April 2016 (15.04.2016) US

(71) Applicant: MERRIMACK PHARMACEUTICALS, INC. [US/US]; One Kendall Square, Suite B7201, Cambridge, MA 02139-1670 (US).

(72) Inventors: BLANCHETTE, Sarah, F.; 24 Edgemere Road, Lynnfield, MA 01940 (US). DRUMMOND, Daryl, C.; 1 Brooks Road, Lincoln, MA 01773 (US). FITZGERALD, Jonathan, Basil; 32 Magnolia Street, Arlington,

MA 02474 (US). MOYO, Victor; 2 Neshanic Drive, Ringoes, NJ 08551 (US).

(74) Agent: BOTT, Cynthia, M.; Honigman Miller Schwartz and Cohn, LLP, 350 East Michigan Avenue, Suite 300, Kalamazoo, MI 49007-3800 (US).

(81) Designated States (unless otherwise indicated, for every kind of national protection available): AE, AG, AL, AM, AO, AT, AU, AZ, BA, BB, BG, BH, BN, BR, BW, BY, BZ, CA, CH, CL, CN, CO, CR, CU, CZ, DE, DK, DM, DO, DZ, EC, EE, EG, ES, FI, GB, GD, GE, GH, GM, GT, HN, HR, HU, ID, IL, IN, IR, IS, JP, KE, KG, KN, KP, KR, KZ, LA, LC, LK, LR, LS, LU, LY, MA, MD, ME, MG, MK, MN, MW, MX, MY, MZ, NA, NG, NI, NO, NZ, OM, PA, PE, PG, PH, PL, PT, QA, RO, RS, RU, RW, SA, SC, SD, SE, SG, SK, SL, SM, ST, SV, SY, TH, TJ, TM, TN, TR, TT, TZ, UA, UG, US, UZ, VC, VN, ZA, ZM, ZW.

(84) Designated States (unless otherwise indicated, for every kind of regional protection available): ARIPO (BW, GH, GM, KE, LR, LS, MW, MZ, NA, RW, SD, SL, ST, SZ, TZ, UG, ZM, ZW), Eurasian (AM, AZ, BY, KG, KZ, RU, TJ, TM), European (AL, AT, BE, BG, CH, CY, CZ, DE, DK, EE, ES, FI, FR, GB, GR, HR, HU, IE, IS, IT, LT, LU, LV, MC, MK, MT, NL, NO, PL, PT, RO, RS, SE, SI, SK, SM, TR), OAPI (BF, BJ, CF, CG, CI, CM, GA, GN, GQ, GW, KM, ML, MR, NE, SN, TD, TG).

Published:

— with international search report (Art. 21(3))

(54) Title: COMBINATION THERAPY USING LIPOSOMAL IRINOTECAN AND A PARP INHIBITOR FOR CANCER TREATMENT

(57) Abstract: Combination therapies for treating cancer comprising administration of a topoisomerase-1 inhibitor and a PARP inhibitor are provided. The topoisomerase-1 inhibitor can be delivered as a liposomal formulation that provides for prolonged accumulation of the topoisomerase-1 inhibitor within a tumor relative to outside of the tumor. Therapeutic benefit can thereby be obtained by delaying the administration of the PARP inhibitor after each administration of a liposomal irinotecan formulation until the accumulation of the topoisomerase inhibitor in the tumor is sufficiently greater than outside the tumor to result in increased efficacy of the PARP inhibitor and topoisomerase inhibitor within the tumor, while reducing the peripheral toxicity of the combination therapy. The therapies disclosed herein are useful in the treatment of human cancers with solid tumors, including cervical cancer. For example, methods of treating a patient having cancer with a combination of a liposomal Topi inhibitor, e.g., MM-398, and veliparib.



WO 2017/031442 A1

### **Cross-Reference of Related Applications**

[0001] This application claims the benefit of U.S. Provisional Application No(s): 62/207,709, filed on August 20, 2016; 62/207,760, filed on August 20, 2015; 62/269,756, filed on December 18, 2015; 62/269,511, filed on December 18, 2015; 62/323,422, filed on April 15, 2016, and 62/308,924, filed on March 16, 2016, the disclosures of which are hereby incorporated by reference in their entireties.

### **Field of Invention**

[0002] This invention relates to the treatment of cancer with a Poly(ADP-ribose) polymerase (PARP) inhibitor and a topoisomerase inhibitor, for example: the combination of an irinotecan liposomal formulation (MM-398) and a PARP inhibitor, such as veliparib, to treat cancer.

### **Background of the Invention**

[0003] Topoisomerase I (Top1) inhibitors have proven valuable as anticancer agents, with regulatory approvals for topotecan in cervical, ovarian, and small cell lung cancer, and for irinotecan in colorectal cancer. Type 1 topoisomerases are enzymes that cut one strand of DNA to allow relaxation during DNA replication and repair. The inhibitors create a stable complex of DNA and Top1 that induces DNA damage. Preclinical strategies to improve the activity of Top1 inhibitors are aimed at increasing the level of DNA damage to promote cell death.

[0004] Nanoliposomal irinotecan (nal-IRI) is a highly stabilized liposomal formulation of irinotecan that provides for sustained exposure of irinotecan, and the active metabolite SN-38, in the tumor to a higher proportion of cells during the more sensitive S-phase of the cell cycle. Nal-IRI has shown promising preclinical and clinical activity in a range of cancer types, and was recently approved in the United States in combination with 5-FU/LV for patients with metastatic adenocarcinoma of the pancreas after disease progression following gemcitabine-based therapy.

[0005] Poly(ADP-ribose) polymerase (PARP) inhibitors are a new class of chemotherapeutic agents currently in development for the treatment of various cancer types. PARPs are a family of enzymes involved in DNA repair. Inhibition of the repair pathway results in cell death.

[0006] Combinations of PARP and Top1 inhibitors have shown to be synergistic in *in vitro* assays. However, the clinical development of PARP inhibitor and Top1 inhibitor combinations has been limited due to increased toxicities and resultant dose reductions, thereby limiting the potential clinical utility of the combination. For example, significant myelosuppression was seen in a dose-escalation study of veliparib and topotecan, wherein the maximum tolerated dose was exceeded at the first planned dose level. Most PARP inhibitors are being developed to date solely as monotherapies.

**[0007]** As a result, there is a need for methods to safely and effectively combine a PARP inhibitor with a Top1 inhibitor to treat cancer. The present disclosure addresses this need and provides additional benefits.

### Summary

**[0008]** The present disclosure provides for methods of administering with reduced peripheral toxicity a combination of a Top1 inhibitor and a PARP inhibitor to a tumor. In one aspect, a method of treating a cancer, e.g., a malignant tumor, is provided, the method comprising a treatment regimen comprising one or more instances of co-administration of the Top1 inhibitor and the PARP inhibitor, each instance of co-administration comprising: (a) administering to a patient in need thereof an effective amount of an irinotecan liposomal formulation; and (b) after completion of the administration of the Top1 inhibitor, administering to the patient an effective amount of a PARP inhibitor, wherein the PARP inhibitor is administered to the patient following an interval that allows for a reduction in peripheral toxicity as compared to simultaneous administration of the Top1 inhibitor and the PARP inhibitor.

**[0009]** The present disclosure provides methods of treating cancer by administering a topoisomerase inhibitor and a PARP inhibitor with reduced peripheral toxicity. This can be accomplished by administering the topoisomerase inhibitor in a form (e.g., liposomal irinotecan) that prolongs accumulation of the topoisomerase inhibitor in a tumor relative to sites outside the tumor, and then subsequently administering the PARP inhibitor(s) to the patient after an interval between the administration of the topoisomerase inhibitor and the PARP inhibitor. The interval can be selected to provide enough time for the topoisomerase inhibitor (e.g., irinotecan and/or its metabolite SN-38) to clear plasma or tissue outside of the tumor to a greater extent than inside the tumor. Preferably, the interval is an effective topoisomerase-1 inhibitor plasma clearing interval. As used herein, the term “effective topoisomerase-1 inhibitor plasma clearing interval” (e.g., irinotecan plasma clearing interval) is that interval between concluding the administration of a topoisomerase-1 inhibitor formulation (e.g., liposomal irinotecan) and initiating the administration of one or more PARP inhibitors, where the time interval is selected to allow sufficient clearance of the topoisomerase-1 inhibitor (e.g., irinotecan or its active metabolite SN-38) from the blood plasma (or peripheral tissue) but allows an effective quantity of the topoisomerase-1 inhibitor (e.g., irinotecan and/or SN38) to remain in one or more tumors within the patient during the subsequent administration of the PARP inhibitor in an amount effective to provide a desired effect on the tumor (e.g., heightened combined toxicity localized within the tumor). Preferably, the PARP inhibitor is administered after an irinotecan plasma clearing interval of 3-5 days (e.g., 3, 4 or 5 days) after completing the administration of liposomal irinotecan on days 1 and 15 during each of one or more 28-day treatment cycles.

**[0010]** Methods of treating cancer disclosed herein include the treatment of solid tumors. In certain examples, the cancer treated can be selected from the group consisting of cervical cancer, ovarian cancer, triple negative breast cancer, non-small cell lung cancer, small cell lung cancer, gastrointestinal stromal tumors gastric cancer, pancreatic cancer, colorectal cancer, and a neuroendocrine cancer. Preferably, the cancer is cervical cancer.

**[0011]** The topoisomerase inhibitor can be provided as a liposome formulation. Preferably, the topoisomerase inhibitor is a liposomal irinotecan. The liposomal irinotecan can provide an irinotecan terminal elimination half-life of 26.8 hours and a maximal irinotecan plasma concentration of 38.0 micrograms/ml. In some examples, the liposomal irinotecan can include irinotecan sucrose octasulfate encapsulated within phospholipid vesicles having a size of about 110 nm. For example, the liposomal irinotecan can be the product ONIVYDE® (irinotecan liposome injection) (Merrimack Pharmaceuticals, Inc., Cambridge, MA), previously designated “MM-398.” The PARP inhibitor can include one or more compounds selected from the group consisting of niraparib, olaparib, veliparib, and rucaparib, preferably veliparib or olaparib.

**[0012]** The topoisomerase-1 inhibitor is preferably a liposomal irinotecan (e.g., MM-398), which can be administered at dose of 80 mg/m<sup>2</sup> (salt) irinotecan once every 2 weeks in combination with a PARP inhibitor (e.g., veliparib, olaparib, niraparib or rucaparib) administered daily during each two week cycle starting 3-5 days after administration of liposomal irinotecan without administering the PARP inhibitor on days when the liposomal irinotecan is administered (e.g., without administering the PARP inhibitor 1, 2 or 3 days before the next liposomal irinotecan administration). Preferably, the PARP inhibitor is not administered within 3 days of (i.e., neither 3 days after nor 3 days before) the administration of liposomal irinotecan.

**[0013]** Specific methods of treating a cancer provided herein include administering an antineoplastic therapy consisting of the administration of liposomal irinotecan every 2 weeks (e.g., on days 1 and 15 of a 28-day treatment cycle), and the administration of a PARP inhibitor one or more times per day (e.g., twice per day) for one or more days (e.g., 7-9 days) starting at least 3 days (e.g., 3, 4 or 5 days) after each administration of the liposomal irinotecan, without administering other antineoplastic agents during the antineoplastic therapy. For example, one antineoplastic therapy is a 28-day treatment cycle consisting of: administering 70 mg/m<sup>2</sup> ONIVYDE/MM-398 liposomal irinotecan (free base) on days 1 and 15, and administering a therapeutically effective amount of the PARP inhibitor (e.g., 50-400 mg twice per day for veliparib) on each of days 5-12 and days 19-25 of the treatment cycle, where no other antineoplastic agent is administered during the treatment cycle. Another antineoplastic therapy is a 28-day treatment cycle consisting of: administering 70 mg/m<sup>2</sup> ONIVYDE/MM-398 liposomal irinotecan (free base) on days 1 and 15, and administering a therapeutically effective amount of



the PARP inhibitor (e.g., 50-400 mg twice per day for veliparib) on each of days 3-12 and days 17-25 of the treatment cycle, where no other antineoplastic agent is administered during the treatment cycle.

**[0014]** In some embodiments, liposomal irinotecan and a PARP inhibitor can be combined in an antineoplastic therapy for the treatment of a solid tumor, comprising a 28-day antineoplastic therapy treatment cycle consisting of: administering the liposomal irinotecan on days 1 and 15 of the treatment cycle, and administering the PARP inhibitor on one or more days starting at least 3 days after the liposomal irinotecan and ending at least 1 day prior to administration of additional liposomal irinotecan. In some embodiments, the PARP inhibitor is not administered for at least 3 days after the administration of liposomal irinotecan. For example, the PARP inhibitor can be administered on one or more of days 5-12 of the antineoplastic therapy treatment cycle, and administered on one or more of days 19-25 of the antineoplastic therapy treatment cycle. In some embodiments, the PARP inhibitor is administered on one or more of days 3-12 of the antineoplastic therapy treatment cycle, and administered on one or more of days 17-25 of the antineoplastic therapy treatment cycle. In some embodiments, the PARP inhibitor is not administered within 3 days before or after the administration of the liposomal irinotecan. In addition, therapeutically effective doses of the topoisomerase inhibitor and PARP inhibitor compounds are provided herein. In some embodiments, each administration of liposomal irinotecan is administered at a dose of 80 mg/m<sup>2</sup> (salt) of ONIVYDE/MM-398. In some embodiments, each administration of the PARP inhibitor is administered at a dose of from about 20 mg/day to about 800 mg/day. Each administration of the PARP inhibitor can be administered once or twice daily at a dose of from about 20 mg/day to about 400 mg/day.

**[0015]** Without wishing to be bound by any particular theory of operation, it is believed that such an interval allows time for sufficient clearance of the Top1 inhibitor (e.g., either or both of irinotecan and SN-38) from the blood plasma to avoid peripheral toxicity due to the synergistic toxic effects of the combination of Top1 inhibitor and PARP inhibitor, while allowing an effective quantity of Top1 inhibitor to remain in one or more tumors within the patient for the subsequent administration of the PARP inhibitor to have a desired synergistic therapeutic effect.

**[0016]** This treatment regimen provides one or more attributes, which may include increased efficacy of the combination as compared to single agent treatment; reduced side effects, dosing the drugs at a higher dose compared with administration of the combination of a PARP inhibitor and a non-liposomal Top1 inhibitor.

**[0017]** Further aspects include providing an existing standard of care therapy to the patients, which may or may not include treatment with appropriate single agents. In some instances, the standard of care may include administration of a PARP inhibitor compound.

[0018] Thus, in one aspect, the present disclosure provides a method of treating a patient with cancer and having a tumor, the method comprising:

- i. parenterally (e.g., intravenously) administering to the patient an effective amount of an irinotecan liposomal formulation; and
- ii. administering to the patient an effective amount of a PARP inhibitor wherein the PARP inhibitor is administered after an effective irinotecan plasma clearing interval.

[0019] As disclosed herein, the administration of a PARP inhibitor can be delayed after administration of liposomal irinotecan for a period of time after administering liposomal irinotecan to allow for the treatment of cancerous tumors.

#### **Brief Description of the Drawings**

[0020] Figure 1A is a graph showing the results of a cell viability *in vitro* measurement of ME-180 human cervical cancer cells treated with the topoisomerase 1 inhibitor SN-38 and various PARP inhibitors.

[0021] Figure 1B is a graph showing the results of a cell viability *in vitro* measurement of MS-751 human cervical cancer cells treated with the topoisomerase 1 inhibitor SN-38 and various PARP inhibitors.

[0022] Figure 1C is a graph showing the results of a cell viability *in vitro* measurement of C-33A human cervical cancer cells treated with the topoisomerase 1 inhibitor SN-38 and various PARP inhibitors.

[0023] Figure 1D is a graph showing the results of a cell viability *in vitro* measurement of SW756 human cervical cancer cells treated with the topoisomerase 1 inhibitor SN-38 and various PARP inhibitors.

[0024] Figure 1E is a graph showing the results of a cell viability *in vitro* measurement of SiHa human cervical cancer cells treated with the topoisomerase 1 inhibitor SN-38 and various PARP inhibitors.

[0025] Figure 2A is a graph showing the results of *in vitro* measurement of % cell number over time for DMS-114 small cell lung cancer cells treated with the topoisomerase inhibitor SN-38 and the PARP inhibitor rucaparib.

[0026] Figure 2B is a graph showing the results of *in vitro* measurement of % cell number over time for NCI-H1048 small cell lung cancer cells treated with the topoisomerase inhibitor SN-38 and the PARP inhibitor rucaparib.

[0027] Figure 2C is a graph showing the results of *in vitro* measurement of % cell number over time for CFPAC-1 pancreatic cancer cells treated with the topoisomerase inhibitor SN-38 and the PARP inhibitor rucaparib.

**[0028]** Figure 2D is a graph showing the results of *in vitro* measurement of % cell number over time for BxPC-3 pancreatic cancer cells treated with the topoisomerase inhibitor SN-38 and the PARP inhibitor rucaparib.

**[0029]** Figure 2E is a graph showing the results of *in vitro* measurement of % cell number over time for MDA-MB-231 triple negative breast cancer (TNBC) cancer cells treated with the topoisomerase inhibitor SN-38 and the PARP inhibitor rucaparib.

**[0030]** Figure 3A is a graph showing the results of *in vitro* measurement of cell survival for BT-20 triple negative breast cancer (TNBC) cancer cells treated with the topoisomerase inhibitor SN-38 and the PARP inhibitor talazoparib.

**[0031]** Figure 3B is a graph showing the results of *in vitro* measurement of cell survival for HCC38 triple negative breast cancer (TNBC) cancer cells treated with the topoisomerase inhibitor SN-38 and the PARP inhibitor talazoparib.

**[0032]** Figures 4A and 4B are graphs depicting the prolonged accumulation of SN-38 seen in tumor after MM-398 administration compared to other organs. (A) HT-29 colorectal cancer (CRC) tumor xenograft-bearing mice were injected intravenously (IV) with MM-398 at a dose of 20 mg/kg and following a single injection, tissue samples were collected at various time points (1, 4, 8, 24, 48, 72, 168 hours). HPLC analysis was used to measure the levels of SN-38 in these samples. (B) Time of SN-38 duration over a threshold of 120 nmol/L was computed from the pharmacokinetic profiles of SN-38 in tumor and normal tissues following 20 mg/kg of MM-398.

**[0033]** Figures. 5A-5D are graphs showing the MM-398 PK parameters in a murine HT-29 colorectal cancer (CRC) xenograft study. Plasma CPT-11 levels (A) or SN-38 levels (B) following IV injections of various doses of MM-398 or free irinotecan. Tumor CPT-11 levels (C) or SN-38 levels (D) were calculated at various time points following dosing with equivalent doses of either free irinotecan (red) or MM-398 (blue). HPLC analysis was used to measure the levels of the CPT-11 and its metabolite SN-38 in these samples.

**[0034]** Figures. 6A-6D are graphs showing the efficacy of MM-398 in various cancer models. Cancer cells were implanted subcutaneously in mice; when tumors were well established and had reached mean volumes of 200 mm<sup>3</sup>, IV treatment with free irinotecan, MM-398 or control was initiated. The doses of free and nanoliposomal irinotecan used in each study are indicated above, with dose time points indicated by arrows. (A) BT474 breast cancer model treated with control (○), drug- and liposome-free vehicle only; free CPT-11 (●); or nanoliposomal CPT-11 (■). (B) OVCAR8 ovarian cancer model treated with control (black) or MM-398 (blue). (C) HT-29 CRC model treated with control (black), free irinotecan (red) or MM-398 (blue). (D) An orthotopic pancreatic tumor xenograft model dosed with control (PBS, black), free irinotecan (red), or MM-398 (blue).

**[0035]** Figures 7A and 7B are graphs depicting PK analysis from a Phase II clinical study. Gastric cancer patients received either MM-398 at a dose of 120 mg/m<sup>2</sup> (dark grey line) or free irinotecan at a dose of 300 mg/m<sup>2</sup> (lighter grey line) every 3 weeks. CPT-11 (A) and its active metabolite, SN-38 (B) were measured during Cycle 1. Figures 7C-7E depicts clinical evidence for local activation and accumulation of SN-38 in tumor tissue. (C) The mechanistic tumor PK model of nal-IRI predicted higher SN-38 levels in tumor compared to plasma. The range of actual data, collected from a Phase I study of patients (n=12) with advanced solid tumors, is indicated by the black (tumor) or grey (plasma) vertical bars. (D) CPT-11 levels and (E) SN-38 levels, as measured from patient tumor (black) and plasma (grey) samples collected 72h post-MM-398 infusion.

**[0036]** Figure 8 depicts a dose tolerability study of MM-398 + veliparib combination in mice. All mice were dosed chronically once weekly on day 1, with veliparib subsequently dosed for 3 consecutive days either on days 2-4 (A), days 3-5 (B), or days 4-6 (C). Mice were weighed daily and % bodyweight gain is indicated on the Y-axis. Weight loss is indicative of intolerability of the combination. In more detail Figure 8A is a graph showing the results of a murine tolerability study measuring % change in bodyweight after administration of liposomal irinotecan (15 mg/kg, 28 mg/kg, or 50- mg/kg of MM398 (salt) once weekly) followed by administration of 50 mg/kg veliparib daily on days 2, 3 and 4 after MM-398 administration.

**[0037]** Figure 8B is a graph showing the results of a murine tolerability study measuring % change in bodyweight after administration of different doses of liposomal irinotecan (15 mg/kg, 28 mg/kg, or 50 mg/kg of MM398 (salt) once weekly) followed by administration of 50 mg/kg veliparib daily on days 3, 4 and 5 after MM-398 administration.

**[0038]** Figure 8C is a graph showing the results of a murine tolerability study measuring % change in bodyweight after administration of different doses of liposomal irinotecan (15 mg/kg, 28 mg/kg, or 50- mg/kg of MM398 (salt) once weekly) followed by administration of 50 mg/kg veliparib daily on days 4, 5 and 6 after MM-398 administration.

**[0039]** Figure 9 depicts a graphical representation of a murine tolerability study design comparing MM-398 and olaparib as a monotherapy or in combination using a fixed dose of MM-398 and varying doses of olaparib, with various dosing schedules for different groups.

**[0040]** Figure 10A-D is a series of graphs graph showing the results of a murine tolerability study measuring % change in bodyweight after administration of liposomal irinotecan (10mg/kg), olaparib alone, and combinations of MM-398 with different dosing schedules of olaparib.

**[0041]** Figure 11 shows that the combination of MM-398 + veliparib is synergistic. Two different cervical cancer xenograft models were utilized to study the efficacy of MM-398 dosed

once weekly on Day 1 (blue arrows), veliparib dosed at 50 mg/kg orally once daily for 3 consecutive days on Days 4-6 of each week, or the combination dosed on the same schedule as the single agent treatments combined. (A) MS751 cervical cancer xenograft model using MM-398 dosed at 5 mg/kg and (B) C33A cervical cancer xenograft model using MM-398 dosed at 2 mg/kg.

**[0042]** Figure 12A depicts the *in vivo* tolerability of MM-398 in combination with veliparib results, with an adjusted lower limit, bar is SEM. In particular it depicts the *in vivo* tolerability of 50 mg/kg dose of MM-398 in combination with 50 mg/kg veliparib given on days 1, 2 3 or 2, 3, 4 or 3, 4, 5 after administration of the MM-398.

**[0043]** Figure 12B depicts the *in vivo* tolerability of MM-398 in combination with veliparib results. In particular it depicts the *in vivo* tolerability of 28 mg/kg dose of MM-398 in combination with 50 mg/kg veliparib given on days 1, 2 3 or 2, 3, 4 or 3, 4, 5 after administration of the MM-398.

**[0044]** Figure 13A shows antitumor efficacy of MM-398 in combinations with veliparib in MS751 xenograft model where veliparib was dosed 72 h following MM-398 (nal-IRI) administration. In particular, the graph shows data from a mouse xenograft study using MS751 cervical cancer cells in a murine model treated with liposomal irinotecan (5 mg/kg MM398) and/or the PARP inhibitor veliparib (50 mpk) on days 3-5 starting after administration of MM398.

**[0045]** Figure 13B depicts the effect of MM-398 in combinations with veliparib in MS751 xenograft model on the animal's survival. In particular, the graph shows survival data from a mouse xenograft study using MS751 cervical cancer cells in a murine model treated with liposomal irinotecan (5 mg/kg MM398) and/or the PARP inhibitor veliparib (50 mpk) on days 3-5 starting after administration of MM398.

**[0046]** Figure 13C depicts the effect of MM-398 in combinations with veliparib in MS751 xenograft model and on body weight, where veliparib was dosed 72 h following MM-398 (nal-IRI) administration. In particular, the graph depicts the effect of MM-398 in combinations with veliparib in MS751 xenograft murine model treated with liposomal irinotecan (5 mg/kg MM398) and/or the PARP inhibitor veliparib (50 mpk) on days 3-5 starting after administration of MM398.

**[0047]** Figure 14 depicts the antitumor efficacy of MM-398 in combinations with veliparib in C33A xenograft model, where veliparib was dosed 72 h following MM-398 (nal-IRI) administration. The mouse xenograft study using C33 cervical cancer cells is in a murine model treated with liposomal irinotecan (2 mg/kg MM398) and/or the PARP inhibitor veliparib (50 mpk) on days 3-5 starting after administration of MM398.

**[0048]** Figure 15 depicts the effect of MM-398 in combinations with veliparib in C33A xenograft model an animal's survival. In the mouse xenograft study using C33 cervical cancer cells the murine model is treated with liposomal irinotecan (5 mg/kg MM398) and/or the PARP inhibitor veliparib (50 mpk) on days 3-5 starting after administration of MM398.

**[0049]** Figure 16 depicts the effect of MM-398 in combination with veliparib in C33A xenograft model and body weight, where veliparib was dosed 72 h following MM-398 (nal-IRI) administration. (5 mg/kg MM398) and/or the PARP inhibitor veliparib (50 mpk) on days 3-5 starting after administration of MM398.

**[0050]** Figures 17A and 17B depict the *in vitro* activity (A) and tumor content (B) of SN-38 in cervical models. (A) Cervical cells lines were treated with veliparib and SN-38 at either the same time or with scheduling with veliparib being added 24 h after SN-38, and cell viability was measured using CTG assay. The *in vitro* activity (IC50) is measured for multiple cervical cancer cell lines. (B) Nude mice bearing cervical tumors were injected with a single dose of nal-IRI at 10 mg/kg and tumor content of CPT-11 and SN-38 were measured by LC-MS.

**[0051]** Figure 18 is a graphical representation of a phase I study design employing the combinations of MM-398 (nal-IRI) and veliparib. The primary endpoint readout is to identify MTD / RP2D, and the secondary endpoint readouts is AE profile, PK parameters, and biomarker analysis that includes pre-treatment MRI to measure nanoparticle tumor delivery and efficacy.

**[0052]** Figure 19 shows that FMX MRI may be a predictive tool for tumor response to MM-398. (A) MM-398 and FMX have similar properties, including 1) extended PK, 2) the ability to deposit in tumor tissues through the EPR effect (i.e. leaky vasculature), and 3) uptake by macrophages. Therefore, visualization of FMX on MRI may be able to predict MM-398 deposition. Figure 19A is a schematic showing a use of ferumoxytol (FMX) as a predictive biomarker for cancer treatment with liposomal irinotecan (e.g., MM-398) (B) FMX concentration of individual patient lesions was calculated using a standard curve from MR images obtained 24h post-FMX injection. (C) graph showing FMX signal from lesions at 24h are grouped relative to the median value observed in the FMX MRI evaluable lesions and compared to the best change in lesion size based on CT scans (data available from 9 patients; total of 31 lesions).

**[0053]** Figure 20A is a graph showing the tumor SN-38 (nmol/L) measured in tumors after administration of free (non-liposomal) irinotecan (CPT-11) at 50mg/kg or 100 mg/kg, compared to the administration of MM-398 (5 mg/kg, 10 mg/kg or 20 mg/kg).

**[0054]** Figure 20B is a graph showing levels of tumor growth inhibition as a function of time of SN-38 concentration required to yield tumor response.

**[0055]** Figure 21 shows line graphs that depict cell viability following treatment with SN-38 or olaparib as single agents or in combination. C-33A (cervical carcinoma, ATCC®HTB-31™;

A) or OVCAR-8 (ovarian carcinoma, from NCI-60 panel; B) SK-OV-3 (ovarian carcinoma, ATCC® HTB-77™; C) or OVCAR-3 (ovarian adenocarcinoma, ATCC® HTB-161™, D) cells were plated at 1000 cells/well in a 348-well plate and treated with SN-38 and olaparib, each alone or in combination, for 24h, washed, and then incubated for an additional 72h with fresh media, following which cell viability was assessed. Treatment of the cells with a combination of SN-38 and olaparib decreased the IC50 as compared to treatment with single agents in all cell lines tested.

### Detailed Description

**[0056]** The present disclosure provides a method of treating a patient with cancer and having a tumor, the method comprising a treatment regimen that may be repeated at weekly or longer intervals (e.g., Q2W, Q3W, or Q4W), each instance of the treatment comprising:

- i. intravenously administering to the patient an effective amount of an irinotecan liposomal formulation of a Top1 inhibitor such as irinotecan, topotecan, lurtotecan, indotecan, and indimitecan; and
- ii. administering to the patient an effective amount of a PARP inhibitor wherein the PARP inhibitor is administered after an interval following completion of the administration of the Top1 inhibitor, e.g., an effective irinotecan plasma clearing interval.

**[0057]** In a further embodiment, the method comprises:

- i. intravenously administering to the patient an effective amount of an irinotecan liposomal formulation having a terminal elimination half-life of about 26.8 hours and a maximal irinotecan plasma concentration of about 38.0 micrograms/ml; and
- ii. administering to the patient an effective amount of a PARP inhibitor wherein the PARP inhibitor is administered after an interval of 24 hours or up to three days following completion of the administration of the irinotecan.

**[0058]** In some embodiments of the above two methods, the effective plasma clearing interval is from about 24 to about 240 hours such as, the effective plasma clearing interval is from about 48 to about 168 hours, for example, about 48 to about 90 hours. In some embodiments of the above two methods, above embodiment or as disclosed elsewhere herein, the effective plasma clearing interval is 2, 3, 4 or 5 days. In some embodiments of the above two methods, above embodiments or as disclosed elsewhere herein, the effective amount of MM-398 is from about 60 mg/m<sup>2</sup> to about 120 mg/m<sup>2</sup>. In some embodiments of the above two methods, above embodiments or as disclosed elsewhere herein, the effective amount of MM-398 is about 80 mg/m<sup>2</sup>. In some embodiments of the above two methods, above embodiments or as disclosed elsewhere herein, the PARP inhibitor is administered at a dose of from about 20 mg/day to about 800 mg/day. In some embodiments of the above two methods, above embodiments or as

disclosed elsewhere herein, the PARP inhibitor is administered at a dose of from about 10 percent to 100 percent of its maximum tolerated dose. In some embodiments of the above two methods, above embodiments or as disclosed elsewhere herein, the PARP inhibitor is administered once or twice daily at a dose of from about 20 mg to about 400 mg. In some embodiments the PARP inhibitor is selected from the group consisting of talazoparib, niraparib, olaparib, veliparib, iniparib, rucaparib, CEP 9722, talazoparib and BGB-290 for example is veliparib. In some embodiments of the above two methods, above embodiments or as disclosed elsewhere herein, the cancer is cervical cancer, ovarian cancer, triple negative breast cancer, non-small cell lung cancer, small cell lung cancer, gastrointestinal stromal tumors gastric cancer, pancreatic cancer, colorectal cancer, or a neuroendocrine cancer.

**[0059]** The invention also provides use of liposomal irinotecan in combination with a Poly(ADP-ribose) Polymerase (PARP) inhibitor in an antineoplastic therapy for the treatment of a solid tumor, wherein the liposomal irinotecan is repeatedly administered once every two weeks and the PARP inhibitor is administered daily for 3 to 10 days between consecutive administrations of the liposomal irinotecan, without administering the PARP inhibitor within 3 days of the liposomal irinotecan. The PARP inhibitor can be administered on each of consecutive days 3 to 10 between the days when the liposomal irinotecan is administered.

**[0060]** The invention also provides use of liposomal irinotecan and a Poly(ADP-ribose) Polymerase (PARP) inhibitor in an antineoplastic therapy for the treatment of a solid tumor, the use comprising a 28-day antineoplastic therapy treatment cycle consisting of: administering the liposomal irinotecan on days 1 and 15 of the treatment cycle, and administering the PARP inhibitor on one or more days starting at least 3 days after the liposomal irinotecan and ending at least 1 day prior to administration of additional liposomal irinotecan. In some embodiments, the PARP inhibitor is not administered for at least 3 days after the administration of liposomal irinotecan, such as wherein the PARP inhibitor is not administered for at least 3 days prior to the next administration of liposomal irinotecan.

**[0061]** In some embodiments of any of the uses or methods set out herein, the PARP inhibitor is administered on one or more of days 5-12 of the antineoplastic therapy treatment cycle. In some embodiments of any of the uses or methods set out above, the PARP inhibitor is administered on one or more of days 19-25 of the antineoplastic therapy treatment cycle. In some embodiments of any of the uses or methods set out above, the PARP inhibitor is administered on one or more of days 3-12 of the antineoplastic therapy treatment cycle. In some embodiments of any of the uses or methods set out above, the PARP inhibitor is administered on one or more of days 17-25 of the antineoplastic therapy treatment cycle.



**[0062]** As already noted, in some embodiments, such as of the methods or uses described within this section, the liposomal irinotecan has an irinotecan terminal elimination half-life of 26.8 hours and a maximal irinotecan plasma concentration of 38.0 micrograms/ml. In some embodiments of any of the uses or methods set out above, wherein the PARP inhibitor is not administered within 3 days before or after the administration of the liposomal irinotecan.

**[0063]** In some embodiments of any of the uses or methods set out herein, liposomal irinotecan is administered at a dose of 80 mg/m<sup>2</sup> (salt) or 70 mg/m<sup>2</sup> (free base). In some embodiments of any of the uses or methods set out herein, each administration of the PARP inhibitor is administered at a dose of from about 20 mg/day to about 800 mg/day. In some embodiments of any of the uses or methods set out herein, each administration of the PARP inhibitor is administered once or twice daily at a dose of from about 20 mg/day to about 400 mg/day.

**[0064]** In some embodiments of any of the uses or methods set out herein, liposomal irinotecan is administered at a dose of 80 mg/m<sup>2</sup> (salt) or 70 mg/m<sup>2</sup> (free base), and the PARP inhibitor is administered at a dose of from about 20 mg/day to about 800 mg/day.

**[0065]** In some embodiments of any of the uses or methods set out herein, liposomal irinotecan is administered at a dose of 80 mg/m<sup>2</sup> (salt) or 70 mg/m<sup>2</sup> (free base), and the PARP inhibitor is administered once or twice daily at a dose of from about 20 mg/day to about 400 mg/day.

**[0066]** In some embodiments of any of the uses or methods set out herein, wherein the PARP inhibitor is selected from the group consisting of niraparib, olaparib, veliparib, rucaparib and talazoparib. In some embodiments of any of the uses or methods set out herein, the cancer is cervical cancer, ovarian cancer, triple negative breast cancer, non-small cell lung cancer, small cell lung cancer, gastrointestinal stromal tumors gastric cancer, pancreatic cancer, colorectal cancer, or a neuroendocrine cancer.

**[0067]** In some embodiments of any of the uses or methods set out herein, the cancer is cervical cancer and the PARP inhibitor is veliparib. In some embodiments of any of the uses or methods set out herein, the cancer is cervical cancer and the PARP inhibitor is olaparib.

**[0068]** In some embodiments of any of the uses or methods set out herein, the cancer is cervical cancer and the PARP inhibitor is veliparib, liposomal irinotecan is administered at a dose of 80 mg/m<sup>2</sup> (salt) or 70 mg/m<sup>2</sup> (free base), and the PARP inhibitor is administered at a dose of from about 20 mg/day to about 800 mg/day. In some embodiments of any of the uses or methods set out herein, the cancer is cervical cancer and the PARP inhibitor is olaparib, liposomal irinotecan is administered at a dose of 80 mg/m<sup>2</sup> (salt) or 70 mg/m<sup>2</sup> (free base), and the PARP inhibitor is administered at a dose of from about 20 mg/day to about 800 mg/day. In some

embodiments of any of the uses or methods set out herein, the cancer is cervical cancer and the PARP inhibitor is veliparib, liposomal irinotecan is administered at a dose of  $80 \text{ mg/m}^2$  (salt) or  $70 \text{ mg/m}^2$  (free base), and the PARP inhibitor is administered once or twice daily at a dose of from about 20 mg/day to about 400 mg/day. In some embodiments of any of the uses or methods set out herein, the cancer is cervical cancer and the PARP inhibitor is olaparib, liposomal irinotecan is administered at a dose of  $80 \text{ mg/m}^2$  (salt) or  $70 \text{ mg/m}^2$  (free base), and the PARP inhibitor is administered once or twice daily at a dose of from about 20 mg/day to about 400 mg/day.

**[0069]** In some embodiments of any of the uses or methods set out herein, the cancer is cervical cancer and the PARP inhibitor is veliparib, liposomal irinotecan is administered at a dose of  $80 \text{ mg/m}^2$  (salt) or  $70 \text{ mg/m}^2$  (free base), and the PARP inhibitor is administered at a dose of from about 20 mg/day to about 800 mg/day, wherein the liposomal irinotecan is repeatedly administered once every two weeks and the PARP inhibitor is administered daily for 3 to 10 days between consecutive administrations of the liposomal irinotecan, without administering the PARP inhibitor within 3 days of the liposomal irinotecan. In some embodiments of any of the uses or methods set out herein, the cancer is cervical cancer and the PARP inhibitor is olaparib, liposomal irinotecan is administered at a dose of  $80 \text{ mg/m}^2$  (salt) or  $70 \text{ mg/m}^2$  (free base), and the PARP inhibitor is administered at a dose of from about 20 mg/day to about 800 mg/day, wherein the liposomal irinotecan is repeatedly administered once every two weeks and the PARP inhibitor is administered daily for 3 to 10 days between consecutive administrations of the liposomal irinotecan, without administering the PARP inhibitor within 3 days of the liposomal irinotecan. In some embodiments of any of the uses or methods set out herein, the cancer is cervical cancer and the PARP inhibitor is veliparib, liposomal irinotecan is administered at a dose of  $80 \text{ mg/m}^2$  (salt) or  $70 \text{ mg/m}^2$  (free base), and the PARP inhibitor is administered once or twice daily at a dose of from about 20 mg/day to about 400 mg/day, wherein the liposomal irinotecan is repeatedly administered once every two weeks and the PARP inhibitor is administered daily for 3 to 10 days between consecutive administrations of the liposomal irinotecan, without administering the PARP inhibitor within 3 days of the liposomal irinotecan. In some embodiments of any of the uses or methods set out herein, the cancer is cervical cancer and the PARP inhibitor is olaparib, liposomal irinotecan is administered at a dose of  $80 \text{ mg/m}^2$  (salt) or  $70 \text{ mg/m}^2$  (free base), and the PARP inhibitor is administered once or twice daily at a dose of from about 20 mg/day to about 400 mg/day, wherein the liposomal irinotecan is repeatedly administered once every two weeks and the PARP inhibitor is administered daily for 3 to 10 days between consecutive administrations of the liposomal irinotecan, without administering the PARP inhibitor within 3 days of the liposomal irinotecan.

**[0070]** In one embodiment, the cancer is a breast cancer, e.g., metastatic breast cancer, comprising a mutation in one of the breast cancer associated genes, BRCA1 or BRCA2. In another embodiment, the cancer is ovarian cancer comprising a mutation in BRCA1 and BRCA2. Mutations in the tumor suppressor genes BRCA1 and BRCA2 are associated with increased risk of breast cancer (about 5X the risk of a person without a BRCA mutation) and/or increased risk of ovarian cancer (about 10-30 times the risk of a person without a BRCA mutation). Statistics for BRCA-related ovarian cancer typically encompass not only cancer of the ovaries themselves, but also peritoneal cancer and cancer of the Fallopian tubes; women with a BRCA mutation have more than 100 times the normal rate of Fallopian tube cancer. BRCA mutations are also with increased risk of prostate cancer risk in men. Cancer cells lacking normal BRCA1 or BRCA2 (or other DNA-repair enzymes such as ATM) depend instead on PARP-regulated DNA repair, and thus are hypersensitive to PARP inhibition.

**[0071]** In some embodiments of any of the uses or methods set out herein, the use of method further comprising the use of ferumoxytol as an imaging agent to select patients to receive the liposomal irinotecan and PARP inhibitor, for example wherein the method further comprises administering ferumoxytol and then obtaining a MRI image of the patient 24 hours after ferumoxytol administration.

**[0072]** Irinotecan is a Top1 inhibitor. The chemical name of irinotecan is (S)-4,11-diethyl-3,4,12,14-tetrahydro-4-hydroxy-3,14-dioxo1*H*-pyrano[3',4':6,7]-indolizino[1,2-b]quinolin-9-yl-[1,4'bipiperidine]-1'-carboxylate. Irinotecan is also referred to by the name CPT-11 and by the trade name CAMPTOSAR. Irinotecan acts as a prodrug, and is converted by esterase enzymes into the more active metabolite, SN-38.

**[0073]** The present disclosure also provides for methods of administering a combination of a topoisomerase-1 (Top1) inhibitor (e.g., irinotecan and/or its metabolite SN-38) and a PARP inhibitor to a tumor with reduced peripheral toxicity. The Top1 inhibitor can be administered in a liposome formulation resulting in the prolonged accumulation of the Top1 inhibitor in a solid tumor compared to peripheral plasma and/or healthy organs. Subsequently, a PARP inhibitor can be administered after a period of time permitting a reduction in the amount of the Top1 inhibitor outside the tumor relative to the amount of Top1 inhibitor within the tumor. Preferably, the Top1 inhibitor is administered as a liposomal irinotecan that provides SN-38 to a solid tumor.

**[0074]** Methods of treating a cancer are provided, as well as therapeutic uses of PARP inhibitor compounds in combination with liposomal irinotecan formulations for the treatment of cancer, particularly cancer comprising solid tumors.

The uses and methods disclosed herein are based in part on experiments evaluating the combination of a topoisomerase 1 inhibitor (e.g., liposomal irinotecan or SN-38) and a PARP

inhibitor in both pre-clinical and human clinical studies. The topoisomerase 1 inhibitor was administered in certain *in vitro* animal models using a formulation delivering a more prolonged exposure of the topoisomerase 1 inhibitor (e.g., irinotecan and/or the irinotecan active metabolite designated SN-38) within solid tumors than in peripheral tissue and plasma outside the tumor. Combinations of the topoisomerase 1 inhibitor SN38 and/or irinotecan and PARP inhibitor compounds were tested in various *in vitro* experiments. As detailed in Example 2, the *in vitro* testing of multiple combinations of a topoisomerase 1 inhibitor (SN38) and various PARP inhibitors in more than 20 different cancer cell lines (including cervical, breast, ovarian, colorectal, pancreatic, and small cell lung cancer cell lines) all demonstrated decreased cancer cell line viability (Figures 1A, 1B, 1C, 1D, 1E, 2A, 2B, 2C, 2D, 2E, and 17A). The liposomal irinotecan (MM398) demonstrated greater tumor volume reduction than non-liposomal (free) irinotecan (CPT11) in mouse xenograft studies across multiple types of cancer cell lines (including breast, ovarian, colorectal and pancreatic cancer cell lines).

**[0075]** As detailed in Example 3, the tolerability of a topoisomerase 1 inhibitor (liposomal irinotecan) administered in combination with various PARP inhibitors was evaluated by measuring the change in animal (mouse) body weight in multiple murine models by comparing various dosing schedules. In some experiments, both liposomal irinotecan and a PARP inhibitor were administered together on the same day (day 1). In other experiments, the PARP inhibitor was first administered daily starting 2, 3 or 4 days after each administration of the liposomal irinotecan. The PARP inhibitor was administered for multiple consecutive days (e.g., 3 consecutive days), and not administered on the same day as the topoisomerase 1 inhibitor. As detailed in multiple experiments herein, administration of the PARP inhibitor at least one day after the liposomal irinotecan resulted in improved tolerability of comparable combined doses of the PARP inhibitor and liposomal irinotecan (MM-398) as measured by change in percent bodyweight in the animal (e.g., Figures 10A-10D, 8A, 8B, 8C, 12A, and 12B). Delaying the administration of the PARP inhibitor 2, 3 or 4 days after administration of the liposomal irinotecan led to greater overall tolerability of a combined administration of the liposomal irinotecan and the PARP inhibitor, compared to the administration of the liposomal irinotecan and the PARP inhibitor on the same day. For example, administration of veliparib on days 2, 3 and 4 after administration of liposomal irinotecan on day 1 resulted in successively increased tolerability (measured as higher percent mouse bodyweight) of the combination of these two drugs (observed at 15 mg/kg liposomal irinotecan dose on day 1 followed by veliparib dosing on days 2, 3 and 4; at 28 mg/kg liposomal irinotecan dosage on day 1 followed by veliparib dosing on days 3, 4, and 5 in Figure 12B, or followed by veliparib dosing on days 2, 3 and 4 in Figure 12B; and at 50 mg/kg liposomal irinotecan dose on day 1 followed by veliparib dosing on days 4,

5 and 6, or followed by veliparib dosing on days 2, 3 and 4 or followed by veliparib dosing on days 3, 4, and 5 in Figure 12A). Similarly, administering olaparib starting on days 2 or 3 after MM398 resulted in comparable or improved tolerability compared to administration of both agents on day 1. For example, administering a 200 mg/kg dose of olaparib to mice on days 2, 3, 4 and 5 after administration of 10 mg/kg MM398 liposomal irinotecan on day 1 resulted in a lower reduction in bodyweight than administering the same doses of both MM398 and olaparib on days 1, 2, 3 and 4.

**[0076]** Combinations of a topoisomerase 1 inhibitor (SN38 and/or irinotecan) and PARP inhibitor compounds were tested in various preclinical *in vivo* experiments to evaluate the effectiveness of the administration of various PARP inhibitors starting 3 or 4 days after administration of the liposomal topoisomerase 1 inhibitor MM398. As detailed in Example 4, the administration of liposomal irinotecan (MM398) on day 1 followed by the PARP inhibitor veliparib on either days 3, 4 and 5 or days 4, 5, and 6, resulted in decreased tumor volume and extended percent survival in mouse xenograft models of cervical cancer using two different cell lines (MS751 and C33A) (Figures 11A, 11B, 13A, 13B, 14 and 15).

**[0077]** Based in part on these experiments, methods of treating human cancer include the administration of a PARP inhibitor one or more days (preferably 2, 3, 4, 5 or 6 days) after the administration of liposomal topoisomerase inhibitor such as liposomal irinotecan. Preferably, the PARP inhibitor and the liposomal irinotecan are not administered on the same day. Example 6 provides preferred embodiments for the use of liposomal irinotecan and one or more PARP inhibitors for the treatment of human cancer, such as cervical cancer, while other embodiments (e.g., Table 3) are also provided.

*Topoisomerase Inhibitors, Including Liposomal Irinotecan and Camptothecin Conjugates*

**[0078]** The topoisomerase inhibitor can be administered in any form that provides for the prolonged retention of a topoisomerase-1 inhibitor activity within a tumor compared to outside the tumor, after administration of the topoisomerase inhibitor. For example, the topoisomerase inhibitor can be a formulation that delivers SN-38 to a tumor cell *in vivo*, administered in an amount and manner providing a higher concentration of the SN-38 within the tumor than outside the tumor for a period of time after administration of the topoisomerase inhibitor. Suitable formulations of topoisomerase inhibitors include conjugate molecules of a topoisomerase inhibitor (e.g., camptothecin conjugated to a polymer or antibody), liposomes containing a topoisomerase inhibitor or other targeted release formulation technologies. The Top1 inhibitor is preferably formulated to provide prolonged accumulation in a tumor site, compared to accumulation in healthy (non-cancer) tissue outside the tumor site (e.g., in the plasma and/or healthy organs such as colon, duodenum, kidney, liver, lung and spleen). Various Top1 inhibitor

liposomal formulations are described in U.S. Patent No. 8,147,867 and U.S. Patent Application Publication No. 2015/0005354, both of which are incorporated herein by reference.

**[0079]** In one embodiment, the topoisomerase inhibitor is SN-38, camptothecin or a compound that is converted to SN-38 within the body, such as irinotecan. Irinotecan and SN-38 are examples of Top1 inhibitors. Irinotecan is converted by esterase enzymes into the more active metabolite, SN-3

**[0080]** The topoisomerase inhibitor can be camptothecin conjugated to a biocompatible polymer such as a cyclodextrin or cyclodextrin analog (e.g., sulfonated cyclodextrins). For example, the topoisomerase inhibitor can be a cyclodextrin-containing polymer chemically bound to a camptothecin, irinotecan, SN-38 or other topoisomerase 1 inhibitor compound. A cyclodextrin-camptothecin conjugated topoisomerase 1 inhibitor can be administered at a pharmaceutically acceptable dose including 6, 12, or 18 mg/m<sup>2</sup> weekly administration, or 12, 15 or 18 mg/m<sup>2</sup> biweekly administration. Examples of camptothecin-cyclodextrin conjugate topoisomerase 1 inhibitors (e.g., the cyclodextrin-containing polymer conjugate with camptothecin designated “CRLX101”), and related intermediates for preparing the same, are disclosed, for example, in Greenwald et al., *Bioorg. Med. Chem.*, 1998, 6, 551-562, as well as United States Patent Application 2010/0247668, United States Patent Application 2011/0160159 and United States Patent Application 2011/0189092

**[0081]** The topoisomerase inhibitor can also be a liposomal formulation of a topoisomerase inhibitor such as irinotecan, camptothecin or topotecan. Liposomal irinotecan (e.g., MM-398, also called “nal-IRI”) is a highly stabilized liposomal formulation of irinotecan that provides for sustained exposure of irinotecan, and the active metabolite SN-38 in the tumor to a higher proportion of cells during the more sensitive S-phase of the cell cycle. MM-398 is a liposomal irinotecan that has shown promising preclinical and clinical activity in a range of cancer types, and was recently approved in the United States in combination with 5-FU/LV for patients with metastatic adenocarcinoma of the pancreas after disease progression following gemcitabine-based therapy. Compared with free irinotecan, nal-IRI has an extended PK profile with prolonged local tumor exposure of MM-398 and SN-38. Since SN-38 is cleared more quickly from normal tissues than from tumor, it is hypothesized that delayed dosing of veliparib relative to MM-398 will allow for the expected window of maximum irinotecan-induced toxicity to pass in the absence of concurrent veliparib toxicity. However, the tumor levels of SN-38 are predicted to be sustained upon subsequent veliparib dosing, therefore maintaining the ability of both drugs to act on tumor tissue simultaneously and maintain synergy.

**[0082]** One suitable liposomal Top1 inhibitor formulation is liposomal irinotecan available under the brand name ONIVYDE® (irinotecan liposome injection) (Merrimack Pharmaceuticals,

Inc, Cambridge, MA), previously designated “MM-398” prior to FDA approval, and liposomal irinotecan products that are bioequivalent to ONIVYDE.

**[0083]** As used herein, the term “MM-398” refers to a nanoliposomal irinotecan composition. The dose of MM-398 refers to the dose of irinotecan based on the molecular weight of irinotecan hydrochloride trihydrate unless clearly indicated otherwise.

**[0084]** As used herein, unless otherwise indicated, the dose of irinotecan in ONIVYDE/MM-398 refers to the dose of irinotecan based on the molecular weight of irinotecan hydrochloride trihydrate (i.e., “(salt)” dose), unless clearly indicated otherwise. The dose may also be expressed as the irinotecan free base (i.e., “(base)” dose). Converting a dose based on irinotecan hydrochloride trihydrate to a dose based on irinotecan free base is accomplished by multiplying the dose based on irinotecan hydrochloride trihydrate with the ratio of the molecular weight of irinotecan free base (586.68 g/mol) and the molecular weight of irinotecan hydrochloride trihydrate (677.19 g/mol). This ratio is 0.87 which can be used as a conversion factor. For example, the 80 mg/m<sup>2</sup> dose based on irinotecan hydrochloride trihydrate is equivalent to a 69.60 mg/m<sup>2</sup> dose based on irinotecan free base (80 x 0.87). In the clinic this is rounded to 70 mg/m<sup>2</sup> to minimize any potential dosing errors. Similarly, a 120 mg/m<sup>2</sup> dose of irinotecan hydrochloride trihydrate is equivalent to 100 mg/m<sup>2</sup> of irinotecan free base.

**[0085]** The MM-398 irinotecan liposome injection) includes an irinotecan sucrosolate salt, encapsulated in liposomes for intravenous use. The drug product liposome is a small unilamellar lipid bilayer vesicle, approximately 110 nm in diameter, which encapsulates an aqueous space which contains irinotecan in a gelated or precipitated state, as the sucrosolate salt. The liposome carriers are composed of 1,2-distearoyl-sn-glycero-3-phosphocholine (DSPC), 6.81 mg/mL; cholesterol, 2.22 mg/mL; and methoxy-terminated polyethylene glycol (MW 2000)-distearoylphosphatidylethanolamine (MPEG-2000-DSPE), 0.12 mg/mL. Each mL also contains 2-[4-(2-hydroxyethyl)piperazin-1-yl]ethanesulfonic acid (HEPES) as a buffer, 4.05 mg/mL; sodium chloride as isotonicity reagent, 8.42 mg/mL. The solution is buffered at pH 7.25.

**[0086]** ONIVYDE/MM-398 has been shown to improve the pharmacokinetic and safety profile of the free irinotecan, through high retention of the irinotecan molecules within the liposome, by extending the half-life of irinotecan in the plasma, and increased exposure of tumor cells to irinotecan compared with other organs. Table 1 below provides a summary of median (%IQR)\* total irinotecan and SN-38 pharmacokinetic parameters observed in patients with solid tumors after administration of ONIVYDE/MM-398 at a dose of 80 mg/m<sup>2</sup> irinotecan (salt) dose administered once every 2 weeks.

**[0087]** Summary of Median (%IQR)\* Total Irinotecan and SN-38 Pharmacokinetic Parameters in Patients with Solid Tumors.

Dose (mg/m <sup>2</sup> )	Total Irinotecan					SN-38		
	C <sub>max</sub> [µg/ml]	t <sub>1/2</sub> [h] <sup>†</sup>	AUC <sub>0-∞</sub> [h·µg/ml] <sup>†</sup>	V <sub>d</sub> [L/m <sup>2</sup> ] <sup>†</sup>	CL [L h/m <sup>2</sup> ] <sup>†</sup>	C <sub>max</sub> [ng/ml]	t <sub>1/2</sub> [h] <sup>†</sup>	AUC <sub>0-∞</sub> [h·ng/ml] <sup>†</sup>
80 (n=25)	38.0 (36%)	26.8 (110%)	1030 (169%)	2.2 (55%)	0.077 (143%)	4.7 (89%)	49.3 (103%)	587 (69%)

\* %IQR: % Interquartile Ratio =  $\frac{\text{Interquartile Range}}{\text{Mean}} \cdot 100\%$

<sup>†</sup> t<sub>1/2</sub>, AUC<sub>0-∞</sub> and V<sub>d</sub> were only calculated for a subset of patients with sufficient number of samples in the terminal phase: n=23 for total irinotecan; n=13 for SN-38.

C<sub>max</sub>: Maximum plasma concentration

t<sub>1/2</sub>: Terminal elimination half-life

AUC<sub>0-∞</sub>: Area under the plasma concentration curve extrapolated to time infinity

V<sub>d</sub>: Volume of distribution

**[0088]** For MM-398, over the dose range of 60 to 180 mg/m<sup>2</sup>, the maximum concentrations of both total irinotecan and SN-38 increase linearly with dose. The AUCs of total irinotecan increase linearly with dose; the AUCs of SN-38 increase less than proportionally with dose. The half-lives of both total irinotecan and SN-38 do not change with dose. In a pooled analysis from 353 patients, higher plasma SN-38 C<sub>max</sub> was associated with increased likelihood of experiencing neutropenia, and higher plasma total irinotecan C<sub>max</sub> was associated with increased likelihood of experiencing diarrhea. Direct measurement of liposomal irinotecan shows that 95% of irinotecan remains liposome-encapsulated during circulation. The volume of distribution of MM-398 80 mg/m<sup>2</sup> is 2.2 L/m<sup>2</sup>. The volume of distribution of Irinotecan HCl is between 110 L/m<sup>2</sup> (dose=125mg/m<sup>2</sup>) and 234 L/m<sup>2</sup> (dose=340 mg/m<sup>2</sup>). The plasma protein binding of MM-398 is <0.44% of the total irinotecan in MM-398. The plasma protein binding of irinotecan HCl is 30% to 68% and approximately 95% of SN-38 is bound to human plasma proteins. The plasma clearance of total irinotecan from MM-398 80 mg/m<sup>2</sup> is 0.077 L/h/m<sup>2</sup> with a terminal half live of 26.8 h. Following administration of irinotecan HCl 125 mg/m<sup>2</sup>, the plasma clearance of irinotecan is 13.3 L/h/m<sup>2</sup> with a terminal half live of 10.4 h. MM398 liposomal irinotecan can provide irinotecan and its active metabolite, SN-38, inside a patient, which are metabolically cleared by the human cytochrome P450 3A4 isoenzyme (CYP3A4) and uridine diphosphate-glucuronosyl transferase 1A1 (UGT1A1), respectively. The metabolic conversion of irinotecan to the active metabolite SN-38 is mediated by carboxylesterase enzymes. *In vitro* studies indicate that irinotecan, SN-38 and another metabolite, aminopentane carboxylic acid (APC), do not inhibit cytochrome P-450 isozymes. SN-38 is subsequently conjugated predominantly by the enzyme UGT1A1 to form a glucuronide metabolite. UGT1A1 activity is reduced in individuals with genetic polymorphisms that lead to reduced enzyme activity such as the UGT1A1\*28 polymorphism. Approximately 10% of the North American population is homozygous for the



UGT1A1\*28 allele (also referred to as UGT1A1 7/7 genotype). Based on the results of the population pharmacokinetic analysis, patients homozygous and non-homozygous for the UGT1A1\*28 allele (UGT1A1 7 / 7 genotype) have similar SN-38 exposure. The urinary excretion of irinotecan HCl is 11% to 20%; SN-38, <1%; and SN-38 glucuronide, 3%. The cumulative biliary and urinary excretion of irinotecan HCl and its metabolites (SN-38 and SN-38 glucuronide), over a period of 48 hours following administration of irinotecan HCl in two patients, ranged from approximately 25% (100 mg/m<sup>2</sup>) to 50% (300 mg/m<sup>2</sup>). A mass balance study in Sprague-Dawley rats, using liposomal encapsulated <sup>14</sup>C-irinotecan, showed that once irinotecan was released from the liposomes, it followed the same elimination pathway as unencapsulated irinotecan. Fecal excretion was the major route of excretion in male and female rats, accounting for 78.3% and 83.4%, respectively, of the total radioactivity dose administered of liposomal encapsulated <sup>14</sup>C-irinotecan over 168 hours.

**[0089]** Various irinotecan liposomal formulations are described in U.S. Patent No. 8,147,867 and U.S. Patent Application Publication No. 2015/0005354, both of which are incorporated herein by reference. MM-398 is believed to include about 80,000 molecules of irinotecan in a gelled or precipitated state as a sucrosolate salt encapsulated in a liposome of about 100 nm in diameter. MM-398 has been shown to improve the pharmacokinetic and safety profile of the free irinotecan, through high retention of the irinotecan molecules within the liposome, by extending the half-life of irinotecan in the plasma, and increased exposure of tumor cells to irinotecan compared with other organs.

**[0090]** In the methods of this disclosure, the effective amount of liposomal irinotecan is provided as MM-398 at from about 60 mg/m<sup>2</sup> to about 120 mg/m<sup>2</sup>. In a further embodiment, the effective amount of MM-398 is about 80 mg/m<sup>2</sup>, optionally administered in combination with 400 mg/m<sup>2</sup> of leucovorin over 30 minutes, followed by intravenous administration of 2400 mg/m<sup>2</sup> of 5-fluorouracil as an infusion over 46 hours. In some embodiments, the dose is 70, 80, 90, 100, 110 or 120 mg/m<sup>2</sup> (based on the weight of irinotecan hydrochloride trihydrate salt) and doses of 50, 60, 70, 80, 95, and 100 mg/m<sup>2</sup> (based on the weight of irinotecan free base), each given once every two (2) weeks (e.g., on days 1 and 15 of a 28 day antineoplastic treatment cycle). In some embodiments, the effective amount of MM-398 is about 90 mg/m<sup>2</sup> (free base).

**[0091]** Liposomal irinotecan MM-398 extends the tumor exposure of the topoisomerase 1 inhibitor SN-38. MM-398 liposomal irinotecan was found to be more active than irinotecan in multiple murine xenograph models. The duration of tumor exposure to the topoisomerase 1 inhibitor SN-38 above a threshold minimum concentration (e.g., 120 nM) correlated with anti-tumor activity of the liposomal irinotecan. In addition, MM-398 liposomal irinotecan can provide prolonged SN-38 tumor durations that exceed those provided by non-liposomal

irinotecan. For example, Figure 17B depicts tumor content of SN-38 in multiple murine cervical cancer models. Nude mice bearing cervical tumors were injected with a single dose of MM-398 at 10 mg/kg and tumor content of CPT-11 and SN-38 were measured by LC-MS. Figure 20A is a graph showing the tumor SN-38 (nmol/L) measured in tumors after administration of free (non-liposomal) irinotecan (CPT-11) at 50mg/kg or 100 mg/kg, compared to the administration of MM-398 (5 mg/kg, 10 mg/kg or 20 mg/kg). The graph depicts the prolonged accumulation of SN-38 (concentration) measured in a tumor after liposomal irinotecan (MM-398) administration compared to other organs, obtained using a using HT-29 colorectal cancer (CRC) tumor xenograft-bearing mice. Figure 20B is a graph showing levels of tumor growth inhibition as a function of time of SN-38 concentration required to yield tumor response. Levels of SN-38 of 120 nM was identified as the SN-38 tumor concentration required to yield tumor response. The in vitro IC50 for SN-38 effect on cell line can be used as an in vivo threshold (GI50 for HT-29 was observed to be about 60 nM). MM-398 liposomal irinotecan was observed to prolong the duration of SN-38 exposure at doses of 10 mg/kg and 20 mg/kg.

**[0092]** *PARP inhibitors*

**[0093]** In the methods of this disclosure, the PARP inhibitor is selected from the group consisting of talazoparib, niraparib, olaparib, veliparib, iniparib, rucaparib, CEP 9722 or BGB-290. In a further embodiment, the PARP inhibitor is veliparib.

**[0094]** PARPs are a family of enzymes involved in DNA repair that act via two mechanisms: catalytic inhibition and trapping of PARP-DNA complexes, and inhibition of this repair pathway can result in cell death following DNA damage. In preferred embodiments, combining PARP inhibitors with Top1 inhibitors results in increased efficacy in the clinic compared to either agent alone. While it has been demonstrated that synergism between PARP inhibitors and Top1 inhibitors is due to PARP catalytic inhibition, and does not involve PARP trapping, this promising preclinical activity has given rise to unacceptable toxicity in the clinic for these combinations.

**[0095]** The PARP inhibitor can be selected from compounds that inhibit Poly(ADP-ribose) polymerase (PARP), a family of enzymes involved in DNA repair. Preferably, the PARP inhibitor is a compound that acts via two mechanisms: catalytic inhibition and trapping of PARP-DNA complexes. The PARP inhibitor can be one or more clinically available PARP inhibitor compounds (e.g. talazoparib, niraparib, olaparib, and veliparib, among others), including compounds that can act via both mechanisms, although to different degrees. For example, niraparib is much more potent at PARP trapping than veliparib, whereas they both exhibit similar PARP catalytic activity.

**[0096]** In a further embodiment, the PARP inhibitor is veliparib, olaparib, rucaparib or

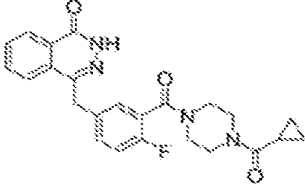
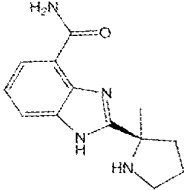
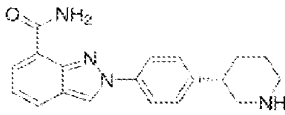
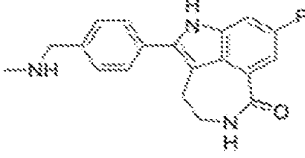
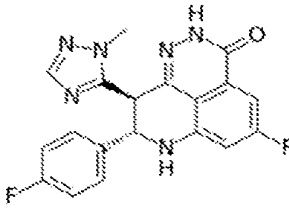
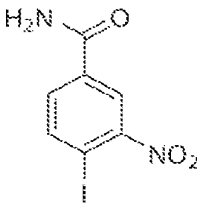
niraparib. In another embodiment, the PARP inhibitor is veliparib, or olaparib. The PARP inhibitor can be veliparib administered after liposomal irinotecan. The PARP inhibitor can be olaparib administered after liposomal irinotecan

**[0097]** Olaparib is indicated as monotherapy in patients with deleterious or suspected deleterious germline BRCA mutated (as detected by an FDA-approved test) advanced ovarian cancer who have been treated with three or more prior lines of chemotherapy. The recommended dose of olaparib for this indication is 400 mg (eight 50 mg capsules) taken twice daily, for a total daily dose of 800 mg. Patients taking olaparib are instructed to avoid concomitant use of strong and moderate CYP3A inhibitors and consider alternative agents with less CYP3A inhibition. If the inhibitor cannot be avoided, reduce the Lynparza dose to 150 mg (three 50 mg capsules) taken twice daily for a strong CYP3A inhibitor or 200 mg (four 50 mg capsules) taken twice daily for a moderate CYP3A inhibitor.

**[0098]** The PARP inhibitor can inhibit PARP 1 and/or PARP 2. For example, the PARP inhibitor can be a PARP  $\frac{1}{2}$  inhibitor with IC<sub>50</sub> of 5nM/1nM in cell-free assays and 300-times less effective against tankyrase-1 (e.g., olaparib). The PARP inhibitor can be an inhibitor of PARP 1 and PARP2 with Ki of 5.2 nM and 2.9 nM respectively in cell-free assays, and inactive to SIRT2 (e.g., veliparib). The PARP inhibitor can be an inhibitor of PARP1 with a Ki of 1.4 nM in a cell-free assay, and can also show binding affinity for other PARP domains (e.g., rucaparib). The PARP inhibitor can be effective against triple negative breast cancer (TNBC) alone or in combination with other agents. The PARP inhibitor can be a PARP1 inhibitor with an IC<sub>50</sub> of 0.58 nM in a cell free assay that does not inhibit PARG and is sensitive to a PTEN mutation (e.g., talazoparib). The PARP inhibitor can be a potent and selective tankyrase inhibitor with an IC<sub>50</sub> of 46 nM and 25 nM for TNKS 1/2, respectively (e.g., G007-LK). The PARP inhibitor can be a potent inhibitor of PARP 1 with a Ki of less than about 5nM in a cell free assay (e.g., AG-14361). The PARP inhibitor can be a selective inhibitor of PARP 2 with an IC<sub>50</sub> of 0.3 micromolar, and can be about 27-fold selective against PARP 1 (e.g., UPF-1069). The PARP inhibitor can be a potent and selective inhibitor with an IC<sub>50</sub> for PARP 3 of about 0.89 micromolar, and about 7-fold selectivity over PARP 1 (e.g., ME0328). The PARP inhibitor can be an inhibitor of PARP 1 and PARP2 with Ki values of 1 nM and 1.5 nM, respectively.

**[0099]** Preferred examples of PARP inhibitors are provided in the table 2A below, as well as pharmaceutically acceptable prodrugs, salts (e.g., tosylates) and esters thereof.

Table 2A: Examples of PARP inhibitors

Olaparib (AZD-2281)	
Veliparib (ABT-888)	
Niraparib (MK04827)	
Rucaparib (AG 014699)	
Talazoparib (BMN-673)	
Iniparib (BSI-201)	

[00100] The dose of the PARP inhibitor and the frequency of dosing can be selected based on various characteristics of the PARP inhibitor, including the pharmacokinetic properties of the compound (e.g., half-life), prior dosing regimens and patient characteristics. Parameters that can be used in selecting the PARP inhibitor dose include those listed in Table 2B below.

**[00101]** In addition, patients can be selected to receive treatment combining a topoisomerase inhibitor and a PARP inhibitor. For example, patients can be selected based on their status in BRCA (e.g. BRCA1, BRCA2), Homologous Recombination Deficiency (HRD), BROCA-HR or other genetic risk panel analysis of a patient.

**Table 2B Characteristics of Some PARP inhibitors**

Characteristic	Veliparib	Olaparib	Rucaparib	Niraparib	Talazoparib
Molecular Weight	244.3	434.5	323.4	320.4	380.4
PARP1 IC50	4.73-5.2	1.94-5	1.4-1.98	2.1-3.8	0.57-1.2
PAR EC50	5.9	3.6	4.7		2.5
Monotherapy dosing	200-400 mg BID	300 mg BID	240-600 mg BID	300 mg QD	1 mg QD
CDx	BRCA	BRCA, HRD	HRD	BRCA, HR	HRD, HR

**[00102]** In the methods of this disclosure, the PARP inhibitor is administered at a therapeutically effective dose (e.g., a dose selected for the PARP inhibitor monotherapy, such as from about 200 mg/day to about 800 mg/day for veliparib). In a further embodiment, the PARP inhibitor is administered twice daily at a dose of from about 100 to about 400 mg. In some embodiments veliparib, rucaparib or olaparib is administered twice daily at a dose of from about 100 to about 400 mg. In some embodiments, 200 mg BID dose of veliparib is administered to patients after (e.g., 3-5 days after) each administration of liposomal irinotecan

**[00103]** In the methods of this disclosure, the PARP inhibitor is administered after an "effective irinotecan plasma clearing interval." "Effective irinotecan plasma clearing interval" is that interval between the administration of the liposomal irinotecan and the PARP inhibitor that allows sufficient clearance of irinotecan and SN-38 from the blood plasma and allows an effective quantity of irinotecan and/or SN38 to remain in one or more tumors within the patient for the subsequent administration of the PARP inhibitor to have a desired therapeutic effect. The effective plasma clearing interval in the methods of this disclosure is from about 24 to about 168 hours, including 48 hours to about 168 hours. In a further embodiment, the effective plasma clearing interval is from about 48 to about 96 hours. In a further embodiment, the effective plasma clearing interval is 24 hours or 2, 3, 4 or 5 days.

**[00104]** In the methods of this disclosure, the cancer is cervical cancer, ovarian cancer, triple negative breast cancer (TNBC), non-small cell lung cancer (NSCLC), small cell lung cancer (SCLC), gastric cancer, pancreatic cancer, colorectal cancer, or neuroendocrine tumor.

**[00105]** In one embodiment, a method of treating a patient according to the present invention results in a pathologic complete response (pCR), complete response (CR), partial response (PR) or stable disease (SD).

**[00106]** The methods of this disclosure can further comprise administering to the patient one or more additional agents including, but not limited, to anti-emetics such as a 5-HT3 antagonist; agents for treating of diarrhea, such as loperamide; dexamethasone; or other chemotherapeutic agents.

**[00107]** In one embodiment, the methods of the present disclosure result in a pathologic complete response (pCR), complete response (CR), partial response (PR) or stable disease (SD). In another embodiment the combination therapy with MM-398 and a PARP inhibitor, e.g., veliparib, results in therapeutic synergy.

**[00108]** In certain embodiments, the MM-398 and the PARP inhibitor are administered in at least one cycle. A cycle comprises the administration of a first agent (e.g., a first prophylactic or therapeutic agents) for a period of time, followed by the administration of a second agent (e.g., a second prophylactic or therapeutic agents) for a period of time, optionally followed by the administration of a third agent (e.g., a third prophylactic or therapeutic agents) for a period of time and so forth, and repeating this sequential administration, i.e., the cycle. In one embodiment, the combination of MM-398 and a PARP inhibitor is administered for at least one cycle. In one embodiment the cycle is a 2 week cycle. In another embodiment, the cycle is a 3 week cycle. In another embodiment, the cycle is a 4 week cycle. In one embodiment MM-398 is administered at the beginning of the cycle and administration of a PARP inhibitor (e.g., veliparib) is delayed until at least about 12, 24, 48, 72, 96, or 120 hours, after the administration of MM-398. In one embodiment MM-398 is administered at the beginning of the cycle and administration of a PARP inhibitor (e.g., veliparib) is delayed until at least about 24, 48, 72, 96, or 120 hours, after the administration of MM-398. In one embodiment, MM-398 is administered as part of a 28 day cycle on days 1 and 15 and the PARP inhibitor is administered on days 3-12 and on days 17-25. In another embodiment, MM-398 is administered as part of a 28 day cycle on days 1 and 15 and the PARP inhibitor is administered on days 5-12 and days 19-25.

**[00109]** In some examples, including the protocols in Table 3, the PARP inhibitor is not administered within 3 days of the administration of liposomal topoisomerase 1 inhibitor such as MM-398 liposomal irinotecan (i.e., the PARP inhibitor is only administered on days that are both at least 2, 3, 4 or 5 days after the administration of the liposomal topoisomerase 1 inhibitor, and 2, 3, 4 or 5 days prior to the next administration of the liposomal topoisomerase 1 inhibitor). Table 3 shows dose timing protocols for administering a therapeutically effective amount of a

PARP inhibitor and liposomal irinotecan on certain days of a 28-day antineoplastic treatment cycle.

**Table 3: Examples of 28-day Treatment Cycles**

Protocol	PARP inhibitor given on days	Liposomal Irinotecan given on days
1	3-12; 17-25	1, 15
2	4-12; 17-25	1, 15
3	5-12; 17-25	1, 15
4	6-12; 17-25	1, 15
5	3-12; 18-25	1, 15
6	4-12; 18-25	1, 15
7	5-12; 18-25	1, 15
8	6-12; 18-25	1, 15
9	3-12; 19-25	1, 15
10	4-12; 19-25	1, 15
11	5-12; 19-25	1, 15
12	6-12; 19-25	1, 15

**[00110]** In some examples, the PARP inhibitor is administered on one or more of days of a 28-day antineoplastic treatment cycle. For example, the PARP inhibitor can be administered on one or more of days 3, 4, 5, 6, 7, 8, 9, 10, 11 and 12 and 19, 20, 21, 22, 23, 24 and 25 of the 28-day antineoplastic treatment cycle when the liposomal irinotecan (e.g., MM-398) is administered once every two weeks, or on days 1 and 15 of the 28-day antineoplastic treatment cycle.

**[00111]** Methods of treatment and therapeutic uses of PARP inhibitors and topoisomerase inhibitors.

### Examples

**[00112]** The following non-limiting examples illustrate the methods of the present disclosure.

#### Example 1:

#### Phase I Study of a Combination of MM-398 and Veliparib in Solid Tumors

#### Background--PARP inhibitors and Top1 inhibitors

**[00113]** Poly(ADP-ribose) polymerase (PARP) inhibitors are a new class of chemotherapeutic agents currently in development for the treatment of various cancer types. PARPs are a family of enzymes involved in DNA repair, and inhibition of this repair pathway results in cell death. PARP inhibitors, therefore, have been investigated in tumor types with other known DNA repair pathway deficiencies, such as breast and ovarian tumors with BRCA1 or BRCA2 mutations, which results in synthetic lethality. PARP inhibitors act via two mechanisms: catalytic inhibition and trapping of PARP-DNA complexes. Clinically available PARP inhibitors (e.g. talazoparib, niraparib, olaparib, and veliparib, among others) act via both mechanisms, although to different degrees. For example, niraparib is much more potent at PARP trapping than veliparib, whereas

they both exhibit similar PARP catalytic activity. It is hypothesized that this translates into the decreased toxicity observed with veliparib compared with either niraparib or olaparib. Decreased toxicity does not preclude efficacy, however, as veliparib has demonstrated clinical activity in a Phase I study of 88 patients (60 BRCA+ and 28 BRCA-wt) receiving veliparib monotherapy, where the overall response rate (ORR; CR+PR) was 23% with a clinical benefit rate (CBR; CR + PR + stable disease) of 58% in BRCA+ patients, and an ORR of 40% with a CBR of 68% at the MTD and RP2D. The ORR in BRCA-wt patients evaluable for response was 4% with a CBR of 38% [5].

**[00114]** In BRCA-wt patients, where monotherapy treatment does not demonstrate synthetic lethality, the ability to improve tumor response may be achieved with combination therapy. As such, pre-treatment of tumor cells with other anticancer agents that damage DNA is thought to sensitize tumor cells to PARP inhibitors. Top1 inhibitors are a class of chemotherapeutic agents aimed at inhibiting DNA replication and are known to induce DNA strand breaks that involve PARP for their repair. It is hypothesized that combining PARP inhibitors with Top1 inhibitors will result in increased efficacy in the clinic compared to either agent alone. While PARP inhibitors are still being developed, Top1 inhibitors have already demonstrated successful clinical activity in various tumor types, as noted above. Recently, it has been demonstrated that synergism between PARP inhibitors and Top1 inhibitors is due to PARP catalytic inhibition, and does not involve PARP trapping. Therefore, when combining the two classes of drugs, using veliparib, a less potent PARP trapper, in combination with a Top1 inhibitor is predicted to allow for optimal synergy while minimizing dose-limiting toxicity, and was selected for this study (Figure 1). When combining the two classes of drugs using olaparib, a more potent PARP trapper as compared to veliparib, in combination with a Top1 inhibitor is predicted to allow for optimal synergy (Figure 21). Toxicity related to olaparib dosing was decreased by staggering the administration of olaparib and Top1 inhibitor. Additionally, Top1-induced DNA damage can also be repaired through alternate endonuclease repair pathways, such as the XPF-ERCC1 pathway. Therefore, tumors deficient in endonuclease repair pathways are also predicted to be more sensitive to cell death with irinotecan (CPT-11). Pre-clinically, the cytotoxicity of veliparib plus CPT-11 was further enhanced in XPF-deficient cells. In the clinic, irinotecan plus veliparib is expected to result in increased efficacy when targeting tumors with deficiencies in various DNA damage response pathways.

#### **Clinical experience of veliparib in combination with Top1 inhibitors**

**[00115]** PARP inhibitors and Top1 inhibitor combinations have been tested in phase I clinical trials. However, the development of these chemotherapy combination regimens has been limited by the increased toxicities that are observed, resulting in dose reductions that may limit efficacy.



In particular, significant myelosuppression was seen in a dose-escalation study of veliparib and topotecan, where the maximum tolerated dose was exceeded at the first planned dose level. The result was decreased doses of topotecan, and no escalation of veliparib, with a final veliparib dosage of 10 mg BID, a 40-fold decrease compared to the established monotherapy dose of 400 mg BID. In a Phase I trial of veliparib in combination with irinotecan, dose-limiting toxicities (DLTs) included febrile neutropenia (grade 3), leukopenia and neutropenia (grade 4), and resulted in a 10-fold lower dose of veliparib compared with veliparib monotherapy. Another phase 1 dose-escalation study combined veliparib with bimonthly FOLFIRI in patients with advanced solid tumors. Importantly, three out of four DLTs on this study were neutropenia events, and the grade 3/4 neutropenia rate was 47%. Yet, in these Phase 1 trials, some efficacy in individual patients has been observed. For example, 5 PR were observed among the 32 treated patients in the veliparib plus irinotecan trial, while 12 PR and 1 CR were observed in a study enrolling 96 total patients receiving veliparib in combination with FOLFIRI. Table 1 below provides a summary of available clinical data for trials that combined veliparib with a Top1 inhibitor, illustrating the dose reductions of one or more drugs with combination treatment, as well as considerable toxicity. The challenge, therefore, is to determine how to safely combine these two classes of drugs, as the potential efficacy of the combination remains promising.

## Summary of clinical trials combining veliparib with a Top1 inhibitor.

Trial	Top1 inhibitor	MTD / RP2D	DLTs	Most common G3/4 AEs	Most common AEs	Reference
Phase 1 dose-escalation study of veliparib (V) with bimonthly FOLFIRI in patients with advanced solid tumors	Irinotecan (as part of a FOLFIRI regimen with 5-FU)	V: 200 mg bid, Days 1-5 and 15-19 every 28 days Irinotecan: 150 (reduced) or 180 (standard) mg/m <sup>2</sup> bi-weekly	neutropenia (n=3; P1, 160 mg and 270 mg BID V; P2, 100 mg BID V); and gastritis and vomiting (P1, 270 mg BID V)	>30 patients each: neutropenia (47%), nausea (38%), and diarrhea (34%)	diarrhea (61%), nausea (60%), neutropenia (59%), vomiting (48%), fatigue (47%), anemia and alopecia (each, 41%)	J Clin Oncol 32, 2014 (suppl 15S; abstr 2574)
Phase I study of the safety, pharmacokinetics (PK), and pharmacodynamics (PD) of the poly(ADP-ribose) polymerase (PARP) inhibitor veliparib (ABT-888; V) in combination with irinotecan (CPT-11; Ir) in patients (pts) with advanced solid tumors.	Irinotecan	V: 40 mg BID 15 days on/6 days off (21 day cycle) Irinotecan: 100 mg/m <sup>2</sup> on Days 1 and 8 of a 21-day cycle	fatigue, diarrhea, febrile neutropenia (gr 3), leukopenia and, neutropenia (gr 4)	Not provided	diarrhea (59%), nausea (56%), leucopenia (50%), fatigue (47%), neutropenia (47%), anemia (34%), and vomiting (31%)	J Clin Oncol 29: 2011 (suppl; abstr 3000)
Phase I study of PARP inhibitor ABT-888 (veliparib) in combination with topotecan in adults with refractory solid tumors and lymphomas	Topotecan	V: 10 mg BID on days 1-5 of 21-day cycles Topotecan: 0.6 (reduced) mg/m <sup>2</sup> /day on days 1-5 of a 21-day cycle	grade 4 neutropenia and thrombocytopenia (1 pt), grade 4 neutropenia lasting longer than 5 days (2 pts), febrile neutropenia (2 pts), grade 4 thrombocytopenia (2 pts)	Not provided	Not provided	Cancer Res 2011;71:562 6-5634.

**MM-398 Mechanism of Action**

[00116] MM-398 is a nanoliposomal formulation of irinotecan (nal-IRI), consisting of approximately 80,000 molecules of irinotecan encapsulated in a liposome of ~100 nm in diameter. This stable formulation is designed to improve the pharmacokinetic and safety profile of the free drug, by extending exposure and protecting the irinotecan molecules within the liposome. Liposomes are also known to preferentially deposit in tumor tissue through the enhanced permeability and retention (EPR) effect, which results from abnormal tumor vasculature permitting extravasation of macromolecules, as well as impaired lymphatic drainage that promotes the retention of these molecules within the tumor microenvironment. The EPR effect allows for prolonged tumor tissue exposure to MM-398 which in turn allows MM-398 exposure to a higher proportion of cells during the more sensitive S-phase of the cell cycle. In a murine biodistribution study, the active metabolite of irinotecan, SN-38, was measured in various tissues following MM-398 dosing and it was determined that SN-38 persisted in the tumor tissue longer than normal tissues, including kidney and liver (Figure 4). Additional pre-clinical pharmacokinetic (PK) studies show both extended plasma PK, as well as extended tumor PK, following dosing with MM-398 relative to dosing with free irinotecan (Figure 5). Both irinotecan and SN-38 are cleared very rapidly (within 8 hours) from the plasma following free irinotecan administration. However, MM-398 clearance is considerably slower with a half-life of approximately 48 hours as shown in Figure 5A; as >90% of irinotecan is encapsulated throughout in the plasma, irinotecan levels are reflective of MM-398 concentration. SN-38 plasma exposure is also greater, though  $C_{max}$  levels are reduced, following MM-398 administration, suggesting the advantage of the liposomal formulation in prolonging exposure and half-life (Figure 5B). In tumor tissue, CPT-11 and SN-38 are cleared in approximately 2 days following dosing with free irinotecan, however both CPT-11 and SN-38 persist in the tumor tissue for at least 1 week following an equivalent dose of MM-398.

[00117] Tumor permeability as well as tumor tissue carboxylesterase (CES) activity, which is responsible for the enzymatic conversion of CPT-11 to SN-38, are predicted to be critical factors for local tumor exposure of SN-38 following MM-398 dosing. *In vivo* tumor xenograft studies have demonstrated that efficacy of MM-398 is related to high CES activity and/or high tumor levels of CPT-11 following dosing with MM-398. Additionally, MM-398 has demonstrated superior activity compared to equivalent dosing of free irinotecan in several pre-clinical models including breast, colon, ovarian, and pancreatic tumor xenograft models (Figure 6).

**Clinical Experience with MM-398 and Ferumoxytol MRI**

[00118] Clinically, MM-398 has also demonstrated prolonged exposure of SN-38. PK results from a Phase II study of gastric cancer patients demonstrated extended plasma PK of both CPT-

11 and SN-38 upon treatment with MM-398 compared to treatment with free irinotecan (Figure 7A/B). Further, a Phase I study (protocol #MM-398-01-01-02) investigated tumor levels of both CPT-11 and SN-38 following treatment with MM-398 using post-treatment biopsies. Based on model predictions, SN-38 levels in tumor were expected to be higher than in plasma, suggesting local conversion of CPT-11 to SN-38 in the tumor microenvironment with MM-398 (Figure 7C). Predictions were confirmed by measuring levels of CPT-11 and SN-38 in tumor biopsy samples collected from patients 72 hours post-dose, demonstrating 5-fold higher levels of SN-38 in the tumor than the plasma (Figure 7D-E).

**[00119]** Collectively, the evidence suggests that the prolonged exposure to SN-38 will lead to prolonged DNA damage. SN-38 binds reversibly to the topoisomerase 1 cleavage complex ("Top1cc"). Therefore, the cleavage complex- "trapped" SN-38 is in equilibrium with free SN-38. The binding affinity is relatively low (but compensated by total selectivity) due to the IC<sub>50</sub> being in the high nanomolar range. In short, intracellularly, free SN-38 is a reliable reflection of Top1cc-bound SN-38. SN-38 metabolism relies on glucuronidation by UGT1A1 and excretion from the liver via ABCC2. UGT1A1 is found at much higher levels in normal liver than in other tissues and tumors (except for hepatocellular cancers). SN-38 in the tumor tissue will therefore not be metabolized to any significant extent. Figure 7 shows clinical data suggesting sustained circulating levels and more striking, sustained tumor levels. Thus, it has now been discovered that continuing DNA damage is occurring with MM-398 (as opposed rapidly cleared free irinotecan, which would cause initial DNA damage which was then rapidly repaired).

**[00120]** The phase I study of MM-398 also examined the feasibility of magnetic resonance (MR) imaging to predict tumor-associated macrophage (TAM) content and MM-398 deposition. TAMs appear to play a key role in the deposition, retention and activation of MM-398 within the tumor microenvironment. In this clinical study, ferumoxytol (FMX) a microparticulate preparation of a superparamagnetic iron oxide coated with polyglucose sorbitol carboxymethylether) was used as an imaging contrast agent and MR images were obtained at 1h, 24h, and 72h following FMX injection. FMX is an approved therapy that is indicated for the treatment of iron deficiency anemia in adult patients with chronic kidney disease; however a growing number of cancer patients without iron deficiency are being administered FMX as an imaging agent to visualize macrophage content and vasculature. Like MM-398, FMX is also a nanoparticle with a diameter of approximately 17-31 nm. As tumor permeability was predicted to be an important factor in MM-398 efficacy, FMX was also investigated for use as a surrogate for liposome deposition (Figure 19A). A benefit of FMX is that this agent helps to identify patients that are less likely to respond to MM-398 because of poor drug uptake. Ferumoxytol as a

diagnostic test enables the detection of a patient population that would significantly benefit from MM-398 that would otherwise be uncategorized.

**[00121]** With respect to risks associated with FMX infusion, as per the Feraheme<sup>®</sup> package insert, the following warnings and precautions are indicated for FMX: hypersensitivity reactions, hypotension, iron overload and ability to affect the diagnostic capability of MRI. Across three randomized clinical trials that enrolled 605 patients treated with FMX, the following adverse events were reported by  $\geq 1\%$  of patients treated with ferumoxytol: nausea, dizziness, hypotension, peripheral edema, headache, edema, vomiting, abdominal pain, chest pain, cough, pruritus, pyrexia, back pain, muscle spasms, dyspnea and rash. All IV iron products carry a risk of potentially life-threatening allergic reactions. In the initial clinical trials of Feraheme<sup>®</sup>, conducted predominantly in patients with chronic kidney disease, serious hypersensitivity reactions were reported in 0.2 percent (3/1,726) of patients receiving Feraheme<sup>®</sup>. Other adverse reactions potentially associated with hypersensitivity (e.g., pruritus, rash, urticaria or wheezing) were reported in 3.7 percent (63/1,726) of these patients. In other trials that did not include patients with chronic kidney disease, moderate to severe hypersensitivity reactions, including anaphylaxis, were reported in 2.6 percent (26/1,014) of patients treated with Feraheme<sup>®</sup>. Since the approval of Feraheme<sup>®</sup> on June 30, 2009, cases of serious hypersensitivity, including death, have occurred. In study MM-398-01-01-02, a total of 15 patients have received ferumoxytol to-date and 13/15 patients continued on study to receive MM-398. No hypersensitivity reactions or adverse events related to ferumoxytol were reported for these 15 patients. Patients with advanced incurable cancers being treated with investigational agents such as MM-398 have end stage cancer with very limited treatment options and a very high risk of dying from their underlying disease. The incremental risk of treating patients with FMX followed by MM-398 appears to be small relative to overall risks associated with MM-398 treatment of metastatic cancer patients. Precautions are taken to ensure FMX is administered according to the label instructions, including careful monitoring of patients during and for 30 minutes following ferumoxytol infusion, when administered as part of an MM-398 clinical trial. Additional precautions are taken not to administer FMX to patients with any of the following conditions: evidence of iron overload, a known hypersensitivity to ferumoxytol or any other IV iron product, a documented history of multiple drug allergies, or those for whom MRI is otherwise contraindicated.

**[00122]** The MRI results from study MM-398-01-01-02 demonstrated that the amount of FMX depositing in tumor lesions was able to be quantified (Figure 19B), and it was subsequently shown that a correlation existed between tumor lesion ferumoxytol uptake by MRI and response to MM-398 (Figure 19C). This correlation is now being studied further in an expansion of the Phase 1 study, and is included as a correlative imaging study for a trial of MM-398 + veliparib.

**[00123]** Ultimately, the development of FMX as a companion diagnostic agent has the potential to both spare non-responder patients unnecessary exposure to treatment-related toxicity while also serving as an enrichment tool to increase the proportion of treated patients that may respond.

#### **Treatment Plan**

**[00124]** MM-398 will be administered by intravenous (IV) infusion over 90 minutes at a dose of 80 mg/m<sup>2</sup> every two weeks. The starting dose of MM-398 at 80 mg/m<sup>2</sup> was chosen as a dose that was successfully used in the NAPOLI trial in pancreatic cancer in combination with 5-FU and leucovorin, therefore the MM-398 dose will be held constant and will not be escalated. Veliparib will be administered orally twice daily by the patient at home; a diary will be kept to document the dosage and time of day the drug was dosed. The number of dosing days of veliparib will be explored through the dose escalation scheme in the table below. The starting dose of veliparib at 100 mg bid is one-half the dose administered in combination with irinotecan as part of FOLFIRI and recently reported at the ASCO annual meeting (J Clin Oncol 32, 2014 (suppl 15S; abstr 2574)). Safety at the starting dose level is ensured by initiation of veliparib beginning day 5 after MM-398 dosing. Data obtained to date suggest SN-38 will be cleared from plasma by this point, but still accumulated in tumor tissue (see Figure 7C). Dose level 2, 200 mg BID of veliparib, was the MTD of veliparib used in the FOLFIRI regimen; therefore if Dose Level 2 is deemed safe following the evaluation period, increasing the number of dosing days of veliparib is the planned dose escalation step for the next dose level (Dose Level 3). If the dose and schedule of veliparib at Dose Level 3 is deemed safe, then escalation of the veliparib dose will proceed. If Dose Level 3 is not deemed safe, an alternate dosing schedule may be explored, where the number of dose days of veliparib is de-escalated.

**[00125]** MM-398 is administered by intravenous (IV) infusion over 90 minutes at a dose of 80 mg/m<sup>2</sup> every two weeks. Veliparib is co-administered orally twice daily by the patient at home according to the following schedule:

Dose Level <sup>1</sup>	Veliparib Dose (mg BID)	Veliparib Dose Days	MM-398 Dose (mg/m <sup>2</sup> q2w)
1	100	Day 2, 3, 4, or 5-12; 16, 17, 18, or 19-25	80, Day 1, 15
2	200	Day 2, 3, 4, or 5-12; 16, 17, 18, or 19-25	80, Day 1, 15
3	200	Day 2, 3, 4, or 5-12; 16 or 17-25	80, Day 1, 15
4	300	Day 2, 3, 4, or 5-12; 16, 17, 18, or 19-25	80, Day 1, 15
5	400	Day 2, 3, 4, or 5-12; 16, 17, 18, or 19-25	80, Day 1, 15

<sup>1</sup>Additional dose levels and alternate dosing schedules may be explored upon agreement of Sponsor, Medical Monitor and Investigators.

\*\* After the MTD is reached, and for the first cycle only, we plan to enroll approximately 18 patients obtain tumor biopsies according to the schema outlined in the correlates section below.

#### Example 2: In Vitro Studies

**[00126]** *In vitro* studies were performed testing combinations of various PARP inhibitors and topoisomerase inhibitors liposomal irinotecan and SN-38.

**[00127]** Figures 1A-1D show line graphs that depict cervical cancer cell viability following treatment with SN-38 and/or various PARP inhibitors. Unless otherwise indicated, the data in each of these figures was obtained by measuring cell viability of 5 different cervical cancer cells (ME-180 in Figure 1A, MS-751 in Figure 1B, C-33A in Figure 1C, SW756 in Figure 1D and SiHa in Figure 1E) with 1000 cells/well in a 384 well plate treated with SN-38 (topoisomerase 1 inhibitor) and/or one of 3 different PARP inhibitors (veliparib, niraparib, or olaparib) at 0.33 micrograms/mL) for 24 hours, followed by washing and incubation for an additional 72 hours with fresh media.

**[00128]** The combination of the topoisomerase 1 inhibitor SN-38 and various PARP inhibitors (veliparib, olaparib and rucaparib) were tested in vitro with various small cell lung cancer (SCLC), pancreatic cancer and breast cancer cell lines. At 2nM SN-38 concentration, an additive/synergistic growth inhibition of the cancer cells was observed in combination with olaparib, veliparib and rucaparib (with veliparib observed to be slightly less potent in the combination with SN-38 than olaparib and rucaparib). At all concentrations tested, the static growth of the cancer cell population was achieved. Figures 2A-2E are graphs showing the results of in vitro experiments evaluating combinations of the topoisomerase 1 inhibitor SN38 with various PARP inhibitors, formatted according to the tables 4-5 below (plates of 5,000

cells/well, 100 microliters per well; drugs added with 20x at 10 microliters per drug, top up to 100 microliters total with DMEM; then initiate scan every 4 hours up to 68 hours).

**Table 4**

	Small Cell Lung Cancer		Pancreatic Cancer		TNBC
Treatment	DMS-114	NCI-H1048	CFPAC-1	BxPC-3	MDA-MB-231
SN-38 & Olaparib	Plate 1	Plate 2	Plate 3	Plate 4	Plate 5
SN-38 & Rucaparib	Plate 1	Plate 2	Plate 3	Plate 4	Plate 5
SN-38 & Veliparib	Plate 1	Plate 2	Plate 3	Plate 4	Plate 5

**Table 5**

Target Concentrations				
Drug	Active Range based on XTC008	Estimated tumor range (nM)	Dose Level	Conc' (nM)
SN-38	1-50 nM	3-163 nM (398); IRI < 200nM	S1	2
			S2	5
			S3	10
			S4	20
			S5	50
Olaparib	1000-10000 nM	8000nM	O1	2000
			O2	4000
			O3	8000
Veliparib	1000-10000 nM	> 2000 nM	V1	2000
			V2	4000
			V3	8000
Rucaparib	1-100 nM (Panc)	< 6000 nM	R1	2000
			R2	4000
			R3	8000

**[00129]** Additive/synergistic effects were observed between SN-38 at 2nM combined with the tested PARP inhibitors olaparib, veliparib and rucaparib with DMS-114 SCLC cells. Figure 2A is a graph showing the results of *in vitro* measurement of % cell number over time for DMS-114 small cell lung cancer cells treated with the topoisomerase inhibitor SN-38 and the PARP inhibitor rucaparib.

**[00130]** The NCI-H1048 SCLC cells were slow-growing and very sensitive to combinations of olaparib and rucaparib with SN-38 at 2nM. Figure 2B is a graph showing the results of *in vitro* measurement of % cell number over time for NCI-H1048 small cell lung cancer cells treated with the topoisomerase inhibitor SN-38 and the PARP inhibitor rucaparib.



[00131] Additive/synergistic effects were observed between SN-38 at 2nM combined with the tested PARP inhibitors olaparib, veliparib and rucaparib with CFPAC-1 pancreatic cancer cells. Figure 2C is a graph showing the results of *in vitro* measurement of % cell number over time for CFPAC-1 pancreatic cancer cells treated with the topoisomerase inhibitor SN-38 and the PARP inhibitor rucaparib.

[00132] Figure 2D is a graph showing the results of *in vitro* measurement of % cell number over time for BxPC-3 pancreatic cancer cells treated with the topoisomerase inhibitor SN-38 and the PARP inhibitor rucaparib. Figure 2E is a graph showing the results of *in vitro* measurement of % cell number over time for MDA-MB-231 triple negative breast cancer (TNBC) cancer cells treated with the topoisomerase inhibitor SN-38 and the PARP inhibitor rucaparib.

[00133] Figure 17A depicts the *in vitro* activity of SN-38 in cervical models. Cervical cells lines were treated with veliparib and SN-38 at either the same time or with scheduling with Veliparib being added 24 h after SN-38, and cell viability was measured using CTG assay.

### Example 3: Pre-Clinical Dose Tolerability Studies

[00134] Various pre-clinical *in vivo* experiments were conducted to evaluate delayed dosing of veliparib relative to liposomal irinotecan can alleviate systemic toxicity, including a pre-clinical dose tolerability study. The combination of veliparib and irinotecan has been plagued by dose-limiting toxicities that have prevented this combination from being dosed at high (effective) doses of each drug, thereby limiting its clinical utility. To address this problem, pre-clinical studies evaluated administering a liposomal preparation of a topoisomerase 1 inhibitor, followed by the administration of a PARP inhibitor at least 1 day (preferably 2-3 days) after the day on which the liposomal topoisomerase 1 inhibitor was administered.

[00135] The advantage of dosing with MM-398 compared to free irinotecan is the extended PK profile and prolonged local tumor exposure of MM-398. Since SN-38 is cleared more quickly from normal tissues than from tumor, delayed dosing of veliparib (e.g. starting veliparib dosing a few days after MM-398 administration) allows for the window of maximum irinotecan-induced toxicity to pass in the absence of concurrent veliparib toxicity. However, the tumor levels of SN-38 are sustained longer than in healthy tissue, such that upon PARP inhibitor dosing subsequent to liposomal Top1 inhibitor (e.g., MM-398) administration, both drugs will act on tumor tissue simultaneously.

[00136] To demonstrate that delayed dosing of veliparib relative to nal-IRI can alleviate systemic toxicity, a pre-clinical dose tolerability study was performed. Mice were dosed chronically with nal-IRI once weekly at various doses on Day 1, while veliparib was dosed once daily at a fixed dose for 3 consecutive days each week (either on Days 2-4, Days 3-5, or Days 4-

6), and body weight was followed as a gross measure of toxicity. All mice were dosed chronically once weekly on day 1, with veliparib subsequently dosed for 3 consecutive days either on days 2-4 (8A), days 3-5 (8B), or days 4-6 (8C). Mice were weighed daily and % bodyweight gain is indicated on the Y-axis. Weight loss is indicative of intolerability of the combination. Notably, the highest (50 mg/kg) dose of MM-398 liposomal irinotecan was best tolerated (i.e., lowest measured reduction in % bodyweight observed over the experiment) when the veliparib was administered on days 4, 5 and 6 (Figure 8C). Similarly, the combination of veliparib and MM-398 was best tolerated at lower MM-398 liposomal irinotecan doses when the veliparib was only administered on days 4, 5, and 6 after MM-398 administration. Toxicity of the combination was seen at the highest doses of MM-398 when given in close proximity to the veliparib doses (Figure 8A). However, this toxicity could be alleviated either by dose reducing MM-398 or delaying the start of veliparib dosing, whereby the highest dose of MM-398 could be successfully dosed with veliparib if given on Days 4-6 following Day 1 dosing of MM-398 (Figures 8A-8C). The Day 4-6 veliparib dosing schedule (following day 1 dosing of MM398) was followed in subsequent efficacy studies which demonstrated synergy of the combination in two cervical cancer tumor xenograft models, in which veliparib alone was not efficacious (Figure 11A) and a second model in which neither MM-398 or veliparib were efficacious as single agents (Figure 11B), however the combination demonstrated tumor growth inhibition (Figure 11B).

**[00137]** To exemplify an embodiment demonstrating that delayed dosing of olaparib relative to MM-398 can alleviate systemic toxicity, a pre-clinical dose tolerability study was performed. Figure 9 depicts a graphical representation of a murine tolerability study design comparing MM-398 and olaparib as a monotherapy or in combination using a fixed dose of MM-398 and varying doses of olaparib, with various dosing schedules for different groups: Group 1: MM-398 alone IV (10mg/kg); Group 2: olaparib alone oral (200mg/kg); Group 3: MM-398 (d1) + olaparib (200mg/kg, d1-5); Group 4: MM-398 (d1) + olaparib (150mg/kg, d1-5); Group 5: MM-398 (d1) + olaparib (200mg/kg, d1-4); Group 6: MM-398 (d1) + olaparib (200mg/kg, d2-5); Group 7: MM-398 (d1) + olaparib (200mg/kg, d3-5); group 8: DMSO alone oral. Figures 10A-10D are line graphs demonstrating the toxicities associated with MM-398 and olaparib given as monotherapy or combined therapy at varying doses of olaparib and varying schedule of PARP inhibitor administration following MM-398 in a murine model. Mice that received monotherapy of MM-398, olaparib were dosed 5x weekly. Mice that received a combination of a constant concentration of MM-398 (10mg/kg) and varying concentration of olaparib were dosed in varying schedules: Group 3: MM-398 (d1) + olaparib (200mg/kg, d1-5); Group 4: MM-398 (d1) + olaparib (150mg/kg, d1-5); Group 5: MM-398 (d1) + olaparib (200mg/kg, d1-4); Group 6:

MM-398 (d1) + olaparib (200mg/kg, d2-5); Group 7: MM-398 (d1) + olaparib (200mg/kg, d3-5). Mice were monitored for treatment dependent toxicities by charting (A) body weight and (B) percent survival. Addition of olaparib seemed to be more toxic as compared to monotherapy, however delaying start of olaparib administration to d3 seemed to decrease olaparib specific toxicity as compared to concurrent therapy. Mice were dosed chronically with MM-398 once weekly at various doses on Day 1, while olaparib was dosed once daily at a weekly fixed dose for 5, 4 or 3 consecutive days each week (either on Days 1-5, Days 1-4, Days 2-5 or Days 3-5), and body weight and percent survival were followed as a gross measure of toxicity. Toxicity of the combination was seen at the highest doses of MM-398 when given in close proximity to the olaparib doses (Figure 8). However, this toxicity could be alleviated either by delaying the start of olaparib dosing, whereby the highest dose of MM-398 could be successfully dosed with olaparib if given on Days 3-5 following Day 1 dosing of MM-398 (Figures 10A-10D).

**[00138]** Mice were dosed chronically with MM-398 once weekly at various doses on Day 1, while veliparib was dosed once daily at a fixed dose for 3 consecutive days each week (either on Days 2-4, Days 3-5, or Days 4-6) and body weight was followed as a gross measure of toxicity. Toxicity of the combination was seen at the highest doses of nal-IRI when given in close proximity to the veliparib doses. However, this toxicity could be alleviated either by dose reducing nal-IRI or delaying the start of veliparib dosing. This dosing schedule was followed in subsequent mouse efficacy studies which demonstrated synergy of the combination in two cervical cancer tumor xenograft models, in which veliparib alone was not efficacious, and a second model in which neither nal-IRI or veliparib were efficacious as single agents, however the combination demonstrated tumor growth inhibition.

**[00139]** The tolerability of the combination of MM398 in a mouse model on day 1 was evaluated in combination with the administration of veliparib on days 1-3, days 2-4 and days 3-5. The tolerability of the combined regimen in mice (measured by change in percent bodyweight over 20 days) increased as the first administration of the veliparib occurred on day 2 and day 3, with day 3 initial veliparib dosing providing the most tolerated dosing schedule. Figure 12A is a graph that further depicts the *in vivo* tolerability of the 50 milligrams/kilogram (mpk) dose of MM-398 on day 1 in combination with 50 mg/kg veliparib given on days 1, 2 3 or 2, 3, 4 or 3, 4, 5 after administration of the MM-398, as reflected in percent change in body weight with an adjusted lower limit. Figure 12B is a graph that further depicts the *in vivo* tolerability of the 28 mpk dose of MM-398 on day 1 in combination with 50 mg/kg veliparib given on days 1, 2 3 or 2, 3, 4 or 3, 4,5 after administration of the MM-398, as reflected in percent change in body weight with an adjusted lower limit.

[00140] Figure 16 is a graph showing that treatment of mice with the combination of MM-398 with veliparib in C33A xenograft model described in Example 5 also lead to decreases in body weight as compared to administration of either drug alone.

[00141] These studies demonstrated that this toxicity could be alleviated by delaying the start of PARP inhibitor dosing, preferably by 2-3 days after the day on which liposomal irinotecan was administered. A dosing schedule where the PARP inhibitor was only administered on days subsequent to administration of liposomal irinotecan was followed in mouse efficacy studies (Example 4) demonstrating therapeutic synergy of the combination of a PARP inhibitor and liposomal irinotecan in two cervical cancer tumor xenograft models (in which veliparib alone was not efficacious, and a second model in which neither MM-398 or veliparib were efficacious as single agents, however the combination demonstrated tumor growth inhibition).

#### **Example 4: Pre-Clinical Efficacy of Liposomal Irinotecan**

[00142] *In vivo* tumor xenograft studies demonstrated that the efficacy of liposomal irinotecan is greater than free irinotecan. In addition, *in vivo* tumor xenograft studies demonstrated MM-398 is related to high CES activity and/or high tumor levels of CPT-11 following dosing with MM-398. Additionally, MM-398 has demonstrated superior activity compared to equivalent dosing of free irinotecan in several pre-clinical models including breast, colon, ovarian, and pancreatic tumor xenograft models.

[00143] Liposomal irinotecan (MM-398) has greater efficacy in various cancer models, compared to non-liposomal irinotecan. Cancer cells were implanted subcutaneously in mice; when tumors were well established and had reached mean volumes of 200 mm<sup>3</sup>, IV treatment with free irinotecan, MM-398 or control was initiated. The doses of free and nanoliposomal irinotecan used in each study are indicated above, with dose time points indicated by arrows. Tumor permeability as well as tumor tissue carboxylesterase (CES) activity, which is responsible for the enzymatic conversion of CPT-11 to SN-38, are predicted to be critical factors for local tumor exposure of SN-38 following MM-398 dosing. *In vivo* tumor xenograft studies have demonstrated that efficacy of MM-398 is related to high CES activity and/or high tumor levels of CPT-11 following dosing with MM-398. Additionally, MM-398 has demonstrated superior activity compared to equivalent dosing of free irinotecan in several pre-clinical models including breast, colon, ovarian, and pancreatic tumor xenograft models.

**Example 5: Pre-Clinical Activity of Liposomal Irinotecan and PARP inhibitors**

**[00144]** Referring to Figure 11A and Figure 11B, the antitumor activity of MM-398 was studied in combinations with veliparib (PARPi) in multiple cervical xenograft models. In this study, MS-751 and C33A xenograft models of cervical cancer were employed to probe the effect of administering suboptimal doses of MM-398 in combination with the PARP inhibitor veliparib. Differential tissue levels of MM-398 at 24 and 72 hours indicated that MM-398 and the active metabolite SN-38 cleared faster from the liver, spleen, colon, and plasma, than from tumors. The combination of veliparib and MM-398 gave improvements in key PD biomarkers (cleaved caspase and  $\gamma$ H2AX) when compared to veliparib or MM-398 alone. Figures 11A and 11B show that the combination of MM-398 + veliparib is synergistic. Two different cervical cancer xenograft models were utilized to study the efficacy of MM-398 dosed once weekly on Day 1 (arrows), veliparib dosed at 50 mg/kg orally once daily for 3 consecutive days on Days 4-6 of each week, or the combination dosed on the same schedule as the single agent treatments combined. (A) MS751 cervical cancer xenograft model using MM-398 dosed at 5 mg/kg and (B) C33A cervical cancer xenograft model using MM-398 dosed at 2 mg/kg. In the study, control mice were the same strain, and were harvested prior to tested mice (slightly younger). Data is not presented for mice removed from study for weight loss or for mice removed unintentionally before end date.

*Cervical MS-751 Xenograft Model*

**[00145]** The MS-751 Xenograft Model details are summarized in Table 6.

**Table 6**

Mouse strain:	Nude (Tacoma)			
Tumor	Cervical MS-751, C33A			
Inoculation:	$5 \times 10^6$ (s.c.) in 30% MG			
Drug:	MM-398 (iv) + Veliparib (oral)			
Groups:		Animal per group:	Dose (mpk)	
1	Saline	10		
2	MM-398	10	5	
3	veliparib/oral	10	50	3/4/5th day
4	MM-398 +veliparib	10	5+50	3/4/5th day

**[00146]** Figure 13A shows that tumor volume decreased when MM-398 (5 mpk dose) was administered in combinations with veliparib in the MS751 xenograft model ( $p = 0.03$ ) as compared to administration of either drug alone. Figure 13B shows that percent survival was better for mice treated with MM-398 (5 mpk dose) in combinations with veliparib in MS751

xenograft model as compared to treatment with either drug alone either drug administered alone. Figure 13C shows that treatment with the combination of MM-398 with veliparib in MS751 xenograft model lead to decreases in body weight as compared to administration of either drug alone.

*C33A Cervical Xenograft Model*

[00147] The C33A Xenograft Model details are summarized in Table 7.

**Table 7**

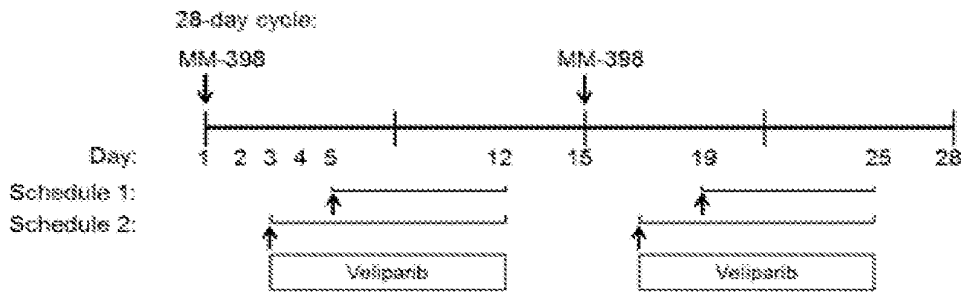
Mice:	Female, Ncr Nudes (Taconic), 5-6 weeks.	
Cell Lines:	C33 A	
Tumor Inoculation: $5 \times 10^6$ in 100 $\mu$ l Matrigel (30 vol%) sc		
15 mice per a cell line		
<u>Groups:</u>	<u>Dose, mpk:</u>	
MM-398 alone	2	
Veliparib alone	50	
MM-398 + Veliparib (3-4-5 d)	2+60	
<u>End-life Collection: 72 h after first injection</u>		
Frozen (Tumor, Liver, Spleen, Plasma)		
FFPA (Tumor)		
<u>Analysis:</u>		
gamma H2AX and cleaved caspase/Tunnel in FFPE (Lia)		
CPT-11 and SN-38 in all tissues for MM-398 flash frozen only (Roswell)		

[00148] Figure 14 shows that the combination of MM-398 with veliparib in the C33A xenograft model leads to decreases in tumor volume as compared to either drug alone administered alone. Figure 15 shows that percent survival was better for mice MM-398 (5 mpk dose) in combinations with veliparib in C33A xenograft model as compared to either drug administered alone.

**Example 6: Clinical Use of Liposomal Irinotecan and PARP inhibitors**

*Clinical Use of Liposomal Irinotecan and Veliparib*

[00149] This is a Phase 1 human dose escalation study to characterize the safety, tolerability, MTD and PK of MM-398 in combination with veliparib in order to determine an optimal combination dose and schedule that will be identified as the recommended Phase 2 dose. The following schematic outlines two different schedules of veliparib dosing that will be explored in combination with MM-398 bi-weekly dosing:



**[00150]** MM-398 will be administered by intravenous (IV) infusion over 90 minutes at a dose of 80 mg/m<sup>2</sup> every two weeks. MM-398 is administered by intravenous (IV) infusion over 90 minutes at a dose of 80 mg/m<sup>2</sup> (salt) irinotecan once every two weeks (days 1 and 15 of each 28-day treatment cycle). Veliparib is co-administered orally twice daily by the patient at home according to the following schedule:

**Table 8**

Dose Level <sup>1</sup>	Veliparib Dose (mg BID)	Veliparib Dose Days	MM-398 Dose (salt) (mg/m <sup>2</sup> q2w)
1	100	Day 5-12; 19-25	80, Day 1, 15
2	200	Day 5-12; 19-25	80, Day 1, 15
3	200	Day 5-12; 17-25	80, Day 1, 15
4	300	Day 5-12; 19-25	80, Day 1, 15
5	400	Day 5-12; 19-25	80, Day 1, 15

<sup>1</sup>Additional dose levels and alternate dosing schedules may be explored upon agreement of Sponsor, Medical Monitor and Investigators.

\*\* After the MTD is reached, and for the first cycle only, we plan to enroll approximately 18 patients obtain tumor biopsies according to the schema outlined in the correlates section below.

**[00151]** The study will enroll 3 patients per dose cohort following a traditional 3 + 3 dose escalation design. Dose limiting toxicities (DLTs) will be evaluated during the first cycle of treatment (28 days) in order to determine the MTD. If there are no DLTs within the safety evaluation period, then the next cohort can be initiated following agreement between the Investigators and Medical Monitor. If a DLT occurs, then the cohort will be expanded to 6 patients. If 2 or more patients have DLTs within a given dose level, then the dose will not be escalated further; however, lower doses may be explored. Additional dosing schedules may also be explored depending on the safety, tolerability, and PK observed.

**[00152]** Given that these individual therapies have been studied in previous clinical trials, it is important that the safety assessment takes into account the expected safety profile of the standard dose regimens. For all treatment regimens, any toxicity that is related to disease progression will

not be considered a DLT. The following events, occurring during cycle 1 of the study combination, will be considered DLTs if deemed drug-related:

- grade 3 or 4 neutropenia complicated by fever  $\geq 38.5$  °C (i.e. febrile neutropenia) and/or documented infection;
- grade 4 neutropenia that does not resolve within 7 days despite optimal therapy (withholding study drug and GCSF administration);
- grade 4 thrombocytopenia that does not resolve within 7 days or any grade 3-4 thrombocytopenia complicated with hemorrhage;
- grade 4 anemia that does not resolve within 7 days despite optimal therapy (withholding study drug and red blood cell transfusions);
- inability to begin subsequent treatment course within 14 days of the scheduled date, due to study drug toxicity;
- any grade 3-4 non-hematologic toxicity (except fatigue/asthenia < 2 weeks in duration; vomiting or diarrhea lasting less than 72 hours whether treated with an optimal anti-emetic or anti-diarrheal regimen or not; or alkaline phosphatase changes).
- $\geq$  grade 2 seizure

**[00153]** Patients will be treated until disease progression as determined by RECIST v1.1 criteria evaluated by CT scan every 8 weeks from first dose of study drug. The inclusion and exclusion criteria for the clinical trial are summarized in the table 9 below.

**Table 9**

<u>Inclusion Criteria</u>	<u>Exclusion Criteria</u>
<ul style="list-style-type: none"> <li>• Patients must have histologic or cytologic confirmation of cancer for which there is no known standard therapy capable of extending life expectancy.</li> <li>• ECOG Performance Status 0 or 1</li> <li>• Tumor lesion(s) amenable to multiple pass percutaneous biopsies and patient willing to undergo required pre- and post-treatment biopsies</li> <li>• Must have adequate:</li> <li>• Bone marrow function                             <ul style="list-style-type: none"> <li>○ ANC &gt; 1,500 cells/<math>\mu</math>l without the use of hematopoietic growth factors</li> <li>○ Platelet count &gt; 100,000 cells/<math>\mu</math>l</li> <li>○ Hemoglobin &gt; 9 g/dL</li> </ul> </li> <li>• Hepatic function                             <ul style="list-style-type: none"> <li>○ Normal serum total bilirubin</li> <li>○ AST and ALT <math>\leq 2.5</math> x ULN (<math>\leq 5</math> x ULN is acceptable if liver metastases are present)</li> </ul> </li> <li>• Renal function                             <ul style="list-style-type: none"> <li>○ Serum creatinine <math>\leq 1.5</math> x ULN</li> </ul> </li> <li>• Normal ECG</li> </ul>	<ul style="list-style-type: none"> <li>• Active CNS metastasis</li> <li>• Clinically significant GI disorders, including history of small bowel obstruction unless the obstruction was a surgically treated remote episode</li> <li>• Prior irinotecan therapy; or topotecan therapy or bevacizumab therapy within 6 months of first dose of study treatment</li> <li>• Prior chemotherapy or biological therapy within 3 weeks, or within a time interval less than 5 half-lives of the agent, prior to first dose of study treatment</li> <li>• Prior radiotherapy within 4 weeks of first dose of study treatment</li> <li>• Patients who have had radiation to the pelvis or other bone marrow-bearing sites will be considered on a case by case basis and may be excluded if the bone marrow reserve is not considered adequate (i.e. radiation to &gt;25% of</li> </ul>



<u>Inclusion Criteria</u>	<u>Exclusion Criteria</u>
<ul style="list-style-type: none"> <li>• ≥18 years of age</li> <li>• Able to understand and sign informed consent</li> <li>• Prior PARP inhibitor therapy is allowed</li> <li>• Willing to undergo pre-treatment ferumoxytol MRI (patients will be excluded from undergoing ferumoxytol MRI if they have evidence of iron overload , a known hypersensitivity to ferumoxytol or any other IV iron product, a documented history of multiple drug allergies, or those for whom MRI is otherwise contraindicated, including claustrophobia or anxiety related to undergoing MRI)</li> </ul>	<ul style="list-style-type: none"> <li>bone marrow)</li> <li>• Known hypersensitivity to MM-398</li> <li>• Active infection</li> <li>• Pregnant or breast feeding</li> </ul>

**[00154]** The dose escalation portion of the trial may require up to 30 patients if 6 patients are required at each of 5 dose levels. An additional 18 patients may be used to explore the effect of veliparib on the biologic correlates. Thus, the accrual ceiling will be set at 48 patients.

**[00155]** The study is proposed to include all solid tumor types, however, particular indications that are of high interest for this study includes the following: cervical cancer, ovarian cancer, triple negative breast cancer (TNBC), non-small cell lung cancer (NSCLC), small cell lung cancer (SCLC), gastric cancer, pancreatic cancer, and neuroendocrine tumors.

**[00156]** The methods and uses herein can also be applied to other tumor suitable types including those noted for increased frequency of DNA damage response (DDR) pathway deficiencies (or ‘BRCAness’) found in sporadic tumors, which are predicted to be sensitive to PARP inhibitors. As mentioned previously, BRCA1 or BRCA2 deficiencies, found particularly in triple negative breast cancer and high-grade serous ovarian cancer, sensitize cells to PARP-inhibitors . Likewise, loss of function of other genes and proteins involved in DDR pathways, including the endonuclease XPF-ERCC1, the homologous recombination repair proteins meiotic recombination protein 11 (MRE11) and Fanconi anemia pathway (FANC) proteins, also sensitize cells to PARP inhibitors. Fanconi anemia pathway deficiencies have been demonstrated in lung, cervical, and breast and ovarian cancers. These and other DDR pathway deficiencies may be predictive biomarkers for PARP inhibitor therapy, and will be explored retrospectively in this study. Veliparib, specifically, has also demonstrated clinical activity in a number of indications, including BRCA-positive and BRCA wild-type breast and ovarian cancer, as well as gastric cancer in combination with FOLFIRI. For the proposed study, indications were chosen not only for their high unmet medical need, but for potential sensitivity to irinotecan and/or veliparib based on the afore-mentioned pre-clinical and/or clinical experience. While the PARP inhibitor olaparib has recently been FDA approved as a monotherapy in BRCA+ ovarian cancer, this study

will not limit treatment in the ovarian patient population to BRCA+ patients, as this is a phase I study of a combination therapy and may retrospectively identify patients with other DDR pathway deficiencies in addition to BRCA.

*Use of Liposomal Irinotecan and Olaparib*

**[00157]** MM-398 is administered by intravenous (IV) infusion over 90 minutes at a dose of 80 mg/m<sup>2</sup> (based on the corresponding amount of irinotecan hydrochloride trihydrate, equivalent to 70 mg/m<sup>2</sup> irinotecan free base) every two weeks. Olaparib is co-administered orally twice daily by the patient at home according to the following schedule (Table 10).

**Table 10**

Dose Level <sup>1</sup>	Olaparib Dose (mg BID)	Olaparib Dose Days	MM-398 Dose (mg/m <sup>2</sup> q2w)*
1	100	Day 5-12; 19-25	80, Day 1, 15
2	200	Day 5-12; 19-25	80, Day 1, 15
3	200	Day 5-12; 17-25	80, Day 1, 15
4	300	Day 5-12; 19-25	80, Day 1, 15
5	400	Day 5-12; 19-25	80, Day 1, 15

\*= The 80 mg/m<sup>2</sup> MM-398 dose is based on the corresponding amount of irinotecan hydrochloride trihydrate (equivalent to 70 mg/m<sup>2</sup> based on irinotecan free base).

**Example 7: Measuring phosphorylated H2AX in Tumor Biopsies**

**[00158]** Phosphorylated H2AX (γ-H2AX) plays an important role in the recruitment and/or retention of DNA repair and checkpoint proteins such as BRCA1, MRE11/RAD50/NBS1 complex, MDC1 and 53BP1. DNA damage has been shown to increase H2AX phosphorylation in cancer cells following exposure to camptothecins. If the PARP inhibitor compound(s) is/are able to increase the degree of DNA damage due to irinotecan from MM-398, it may be detectable by measurement of H2AX phosphorylation. An immunofluorescence assay was used in previous clinical studies. Patient peripheral blood mononuclear cells (PBMCs), hair follicles, and/or tumor biopsy samples will be collected if there is readily accessible disease. The association between the pharmacodynamic response measured by γ-H2AX level can be assessed by Fisher’s test or the Wilcoxon rank sum test, as appropriate; this evaluation will be done at the MTD +/- a maximum of 2 dose levels (Figure 18).

**Table 11. Schedule for biopsies and surrogate samples**

Dose Level	PARPi Dose (mg BID)	PARPi Dose Days	MM-398 Dose (mg/m <sup>2</sup> q2w)	Biopsy in am for PD marker
1	100	Day 5-12; 19-25	80, Day 1, 15	--

2		200	Day 5-12; 19-25	80, Day 1, 15	--
3		200	Day 3-12; 17-25	80, Day 1, 15	Days 1, 5, 19
4		300	Day 3-12; 17-25	80, Day 1, 15	Days 1, 5, 19
5		400	Day 3-12; 17-25	80, Day 1, 15	Days 1, 5, 19
Confirm	A	MTD	Day 3-12; 19-25	80, Day 1, 15	Days 1, 5, 19
	B	MTD	Day 5-12; 17-25	80, Day 1, 15	Days 1, 5, 19

**Example 8: Administering and Detecting Ferumoxytol to Predict Deposition of Topoisomerase Inhibitor from Liposomal Irinotecan**

**[00159]** Figures 19A-19C show that FMX MRI may be a predictive tool for tumor response to MM-398. Figure 19A is a schematic showing that MM-398 and FMX have similar properties, including 1) extended PK, 2) the ability to deposit in tumor tissues through the EPR effect (i.e. leaky vasculature), and 3) uptake by macrophages. Therefore, visualization of FMX on MRI may be able to predict MM-398 deposition. (B) FMX concentration of individual patient lesions was calculated using a standard curve from MR images obtained 24h post-FMX injection. (C) FMX signal from lesions at 24h are grouped relative to the median value observed in the FMX MRI evaluable lesions and compared to the best change in lesion size based on CT scans (data available from 9 patients; total of 31 lesions).

**[00160]** The phase I study of MM-398 also examined the feasibility of magnetic resonance (MR) imaging to predict tumor-associated macrophage (TAM) content and MM-398 deposition. TAMs appear to play a key role in the deposition, retention and activation of MM-398 within the tumor microenvironment. In this clinical study, ferumoxytol (FMX) a microparticulate preparation of a superparamagnetic iron oxide coated with polyglucose sorbitol carboxymethylether) was used as an imaging contrast agent and MR images were obtained at 1h, 24h, and 72h following FMX injection. FMX is an approved therapy that is indicated for the treatment of iron deficiency anemia in adult patients with chronic kidney disease; however a growing number of cancer patients without iron deficiency are being administered FMX as an imaging agent to visualize macrophage content and vasculature. Like MM-398, FMX is also a nanoparticle with a diameter of approximately 17-31 nm. As tumor permeability was predicted to be an important factor in MM-398 efficacy, FMX was also investigated for use as a surrogate for liposome deposition (Figure 19A). A benefit of FMX is that this agent helps to identify patients that are less likely to respond to MM-398 because of poor drug uptake. Ferumoxytol as a diagnostic test enables the detection of a patient population that would significantly benefit from MM-398 that would otherwise be uncategorized.

**[00161]** The MRI results from a human clinical trial study demonstrated that the amount of FMX depositing in tumor lesions was able to be quantified (Figure 19B), and it was subsequently shown that a correlation existed between tumor lesion ferumoxytol uptake by MRI and response to MM-398 (Figure 19C). This correlation is now being studied further in an expansion of the Phase 1 study, and is included as a correlative imaging study for a trial of MM-398 + veliparib.

**[00162]** FMX is an iron replacement product indicated for the treatment of iron deficiency anemia in adult patients with chronic kidney disease. Although not approved as an indication, ferumoxytol has also been used as an imaging agent in cancer patients and will be utilized as such in this study. At least 2 days prior to Cycle 1 Day 1 (maximum of 8 days prior) a single dose of 5 mg/kg FMX will be administered by intravenous injection. The total single dose will not exceed 510 mg, the maximum approved single dose of FMX. This dosing schedule is less intense than the approved label, which recommends two doses of 510 mg 3 to 8 days apart; however since FMX is being used as imaging agent in this study as opposed to a replacement product for iron deficiency, a lower dose is more appropriate. Three MRIs will be performed for each patient over 2 days. All patients will have a baseline image acquired prior to the FMX infusion, and a second image acquired 1-4 h after the end of FMX administration. All patients will return the following day for a 24 h FMX-MRI using the same protocol and sequences as previously. Each patient will be required to complete their FMX-MRIs on the same scanner to reduce inter-scan variability. The body area to be scanned will be determined by the location of the patient’s disease. Each MRI study will be evaluated for image quality and signal characteristics of tumors and reference tissue on T1-, T2- and T2\*- weighted sequences. Once a completed set of images from each patient has been received, a qualitative review will be performed and sent to a quantitative lab for analysis. The data will be analyzed in a similar fashion as described above.

**Imaging Correlates Table 12**

<b>Correlative Objective</b>	<b>Imaging Technique</b>	<b>Organ(s) Scanned and Timing of Scans</b>
Ferumoxytol (FMX) uptake	MRI	Sites of disease; 3 scans completed approximately 2-6 days prior to Cycle 1 Day 1. Scan time points: -baseline (immediately prior to FMX infusion) -1h (post-FMX infusion) -24h (post-FMX infusion)
Histone gamma-H2AX (Pommier, DTB-CCR; Doroshow, Leidos)	Immunofluorescence microscopy ELISA (in development)	- Tumor biopsy before treatment, and during treatment. - Hair follicles during treatment. PBMC before treatment and during treatment

Imaging Correlate Study

**[00163]** Patients will be eligible to participate in the FMX imaging study if they do not meet any of the following criteria:

- Evidence of iron overload as determined by:
  - Fasting transferrin saturation of >45% and/or
  - Serum ferritin levels >1000 ng/ml
- A history of allergic reactions to any of the following:
  - compounds similar to ferumoxytol or any of its components as described in full prescribing information for ferumoxytol injection
  - any IV iron replacement product (e.g. parenteral iron, dextran, iron-dextran, or parenteral iron polysaccharide preparations)
  - multiple drugs
- Unable to undergo MRI or for whom MRI is otherwise contraindicated (e.g. presence of errant metal, cardiac pacemakers, pain pumps or other MRI incompatible devices; or history claustrophobia or anxiety related to undergoing MRI)

**[00164]** If a patient consents to FMX-MRI, the patient will receive ferumoxytol infusion and undergo the required FMX-MRI scans approximately 2-6 days prior to beginning MM-398 treatment (the FMX period). FMX will be administered at a dose of 5 mg/kg up to a maximum of 510 mg. All other aspects of administration will be consistent with the latest ferumoxytol prescribing information. A detailed FMX-MRI protocol will be included in the study imaging manual. Briefly, each patient will be required to complete their FMX-MRIs on the same scanner to reduce inter-scan variability. Each MRI study will be evaluated for image quality and signal characteristics of tumors and reference tissue on T1-, T2- and T2\*- weighted sequences. Once a completed set of images from each patient has been received, the images will be loaded onto the viewing workstation for qualitative review and then sent to a quantitative lab (handled by central imaging CRO) for analysis.

**[00165]** Multiple MR images will be collected on Day 1-Day 2 of the FMX period at various time points: a baseline image acquired prior to the FMX infusion, a second image occurring 1-4 h after the end of FMX administration, and a third image at approximately 24 h post-FMX, using the same protocol and sequences as on Day 1. The body areas to be scanned will be determined by the location of the patient's disease; detailed instructions will be described in the study imaging manual.

**[00166] Example 9: Clinical Use of Liposomal Irinotecan in Combination with 5-fluorouracil and leucovorin**

**[00167]** Clinical efficacy of MM-398 has also been demonstrated in gemcitabine-refractory metastatic pancreatic cancer patients: in a randomized, Phase 3, international study (NAPOLI-1), MM-398 was given in combination with 5-fluorouracil/leucovorin (5-FU/LV) and significantly prolonged overall survival (OS) compared to 5-FU/LV treatment alone. The median OS for the MM-398-containing arm was 6.1 months compared to 4.2 months for the control arm (HR=0.67, p=0.0122). Because the active pharmaceutical ingredient in MM-398 is irinotecan, the safety profile was, as anticipated, qualitatively similar to irinotecan, where the most common adverse events ( $\geq 30\%$ ) are nausea, vomiting, abdominal pain, diarrhea, constipation, anorexia, neutropenia, leukopenia (including lymphocytopenia), anemia, asthenia, fever, body weight decreasing, and alopecia (irinotecan package insert). Table 14 provides a summary of Grade 3 or higher safety data of patients treated with MM-398 plus 5-FU/LV from the NAPOLI-1 study. Table 13 provides toxicities observed in the Phase I monotherapy study, for comparison.

**Table 13. Summary of the most common (>10%) grade 3 or greater adverse events from the 13 patients treated with MM-398 monotherapy at a dose of 80 mg/m<sup>2</sup> every 2 weeks during the phase I study.**

Adverse Events $\geq$ Grade 3 in Study MM-398-01-01-02	
	n (%)
Diarrhea	4 (30.8)
Hypokalemia	3 (23.1)
Abdominal pain	2 (15.4)
Anemia	2 (15.4)
Nausea	2 (15.4)
Neutropenia	2 (15.4)

**Table 14. Summary of Grade 3 or higher AEs from the NAPOLI-1 phase III study.**

	MM-398 + 5-FU/LV <sup>1</sup> (N=117)	5-FU/LV <sup>2</sup> (N=134)
GRADE $\geq$ 3 NON-HEMATOLOGIC AEs IN $>$ 5% PATIENTS, % <sup>3</sup>	%	%
Fatigue	14	4
Diarrhea	13	5
Vomiting	11	3
Nausea	8	3
Asthenia	8	7
Abdominal pain	7	6
Decreased appetite	4	2
Hypokalemia	3	2
Hypernatremia	3	2
GRADE $\geq$ 3 HEMATOLOGIC AES BASED ON LABORATORY VALUES, % <sup>3,4</sup>		
Neutrophil count decreased	20	2
Hemoglobin decreased	6	5
Platelet count decreased	2	0

<sup>1</sup> Dose: 80 mg/m<sup>2</sup> MM-398 + 2400 mg/m<sup>2</sup> over 46 h/400 mg/m<sup>2</sup> 5-FU/LV q2w

<sup>2</sup> Dose: 2000 mg/m<sup>2</sup> over 24 h/200 mg/m<sup>2</sup> 5-FU/LV weekly x 4, q6w

<sup>3</sup> Per CTCAE Version 4

<sup>4</sup> Includes only patients who had at least one post-baseline assessment

**[00168] Example 10: Cell survival for various TNBC cell lines following SN-38 and PARP inhibitor combination treatment.**

**[00169]** Tables 15 and 16 provide the results of *in vitro* measurements of cell survival for various triple negative breast cancer (TNBC) cancer cell lines to determine the cell viability following treatment with SN-38 and/or a PARP inhibitor. Table 15 provides IC50 data and Table 16 provides Maximum Kill data.

**[00170]** The experiments that generated these data were performed in 384 well format. Cells were plated at 1000 cells/well and then incubated for 24 hours. Then SN-38 and/or one of four different PARP inhibitors (talazoparib niraparib, olaparib or rucaparib) was added and incubated for an additional 24 hours then the wells were washed with PBS to remove the drug and fresh media was added back into the wells. The plates were then allowed to incubate for 72 hours period. After the 72 hour incubation period the media was removed and cell viability was determined using the CellTiter-Glo® cell viability assay (Promega, Madison WI) according to the product instructions. Figures 3A and 3B are line graphs that depict cell viability in BT20 and HCC38 breast cancer cell lines, respectively, following treatment with SN-38 and/or talazoparib.

Table 15 IC50 log10(uM)

Exp. 1	Treatment	Cell Line					
		BT20	SUM159PT	HCC38	HCC1187	HCC1806	BT549
	SN38	-0.18	-2.35	-2.80	-0.68	-2.08	-0.10
	Niraparib	2.14	0.35	1.23	2.11	1.27	2.03
	SN38 & Niraparib (3ug/ml)	-0.67	-3.99	-0.12	-1.58	-2.80	-0.39
	SN38 & Niraparib (1ug/ml)	-0.70	-3.42	-4.09	-1.45	-2.62	-0.64
	SN38 & Niraparib (0.3ug/ml)	-0.71	-2.85	-4.23	-1.61	-2.55	-0.74
	SN38 & Niraparib (0.1ug/ml)	-0.61	-2.87	-4.05	-1.41	-2.52	-0.55
Exp. 2	Treatment	Cell Line					
		BT20	SUM149PT	SUM159PT	HCC70	HCC1187	BT549
	SN38	-0.69	0.24	-2.39	-0.07	-0.64	-0.04
	Olaparib	1.24	2.40	0.18	-4.2 x10 <sup>7</sup>	2.41	2.04
	SN38 & Olaparib (3ug/ml)	-1.48	-0.19	-3.70	-0.58	-1.77	-0.55
	SN38 & Olaparib (1ug/ml)	-1.49	-0.34	-3.31	-0.49	-1.67	-0.48
	SN38 & Olaparib (0.3ug/ml)	-1.44	-0.18	-2.92	-0.50	-1.35	-0.35
	SN38 & Olaparib (0.1ug/ml)	-1.29	-0.11	-2.92	-0.48	-1.56	-0.04
Exp. 3	Treatment	Cell Line					
		BT20	SUM149PT	SUM159PT	HCC38	HCC1954	BT549
	SN38	-0.37	0.27	-2.66	-2.89	-0.97	-0.05
	Rucaparib	1.27	1.68	-0.07	-0.07	1.60	1.75
	SN38 & Rucaparib (3ug/ml)	-1.33	-0.16	-3.64	4.93	-1.22	-0.48
	SN38 & Rucaparib (1ug/ml)	-1.47	-0.23	-3.28	-3.88	-1.33	-0.57
	SN38 & Rucaparib (0.3ug/ml)	-1.48	-0.49	-3.23	-4.01	-1.51	-0.49
	SN38 & Rucaparib (0.1ug/ml)	-1.24	-0.10	-3.11	-3.29	-1.57	-0.52
Exp. 4	Treatment	Cell Line					
		BT20	SUM159PT	HCC38	HCC1187	HCC1954	SKBR3
	SN38	-0.24	-2.33	-2.75	-0.98	-0.65	-1.38
	Talazoparib	1.45	-1.03	-1.23	2.28	3.64	-2.8 x 10 <sup>4</sup>
	SN38 & Talazoparib (3ug/ml)	-1.88	-4.01	-3.41	-1.79	-1.64	-2.05



Exp. 1	Treatment	Cell Line					
	SN38 & Talazoparib (1ug/ml)	-1.70	-4.01	-4.01	-1.79	-1.51	-2.65
	SN38 & Talazoparib (0.3ug/ml)	-1.10	-4.01	-5.46	-1.94	-1.45	-2.23
	SN38 & Talazoparib (0.1ug/ml)	-1.36	-4.01	-2.87	-1.92	-1.29	-2.41

**Table 16 Maximum Kill**

Exp. 1	Treatment	Cell Line					
		BT20	SUM159PT	HCC38	HCC118 7	HCC1806	BT549
	SN38	100	97	96	90	93	95
	Niraparib	100	97	100	98	100	100
	SN38 & Niraparib (3ug/ml)	100	100		89	91	94
	SN38 & Niraparib (1ug/ml)	100	100	93	93	92	92
	SN38 & Niraparib (0.3ug/ml)	100	99	100	89	92	92
	SN38 & Niraparib (0.1ug/ml)	100	100	100	89	93	94
Exp. 2	Treatment	Cell Line					
		BT20	SUM149PT	SUM159P T	HCC70	HCC1187	BT549
	SN38	100	96	97	97	100	93
	Olaparib	98	100	94	50	87	100
	SN38 & Olaparib (3ug/ml)	98	97	100	98	100	
	SN38 & Olaparib (1ug/ml)	99	96	97	100	91	96
	SN38 & Olaparib (0.3ug/ml)	100	98	99	100	99	94
	SN38 & Olaparib (0.1ug/ml)	100	96	99	100	99	96
Exp. 3	Treatment	Cell Line					
		BT20	SUM149PT	SUM159P T	HCC38	HCC1954	BT549
	SN38	100	95	99	92	94	94
	Rucaparib	100	99	97	87	100	100
	SN38 & Rucaparib (3ug/ml)	92	97	99		96	93
	SN38 & Rucaparib (1ug/ml)	100	97	99	98	94	92
	SN38 & Rucaparib (0.3ug/ml)	94	95	100	98	95	93
	SN38 & Rucaparib (0.1ug/ml)	96	100	97	97	93	94
Exp. 4	Treatment	Cell Line					
		BT20	SUM159PT	HCC38	HCC118 7	HCC1954	SKBR 3

	SN38	100	96	92	88	100	88
	Talazoparib	100	94	92		100	
	SN38 & Talazoparib (3ug/ml)	100			89	93	90
	SN38 & Talazoparib (1ug/ml)	90			89	94	89
	SN38 & Talazoparib (0.3ug/ml)	93			89	94	100
	SN38 & Talazoparib (0.1ug/ml)	93			100	96	87

**[00171]** While the invention has been described in connection with specific embodiments thereof, it will be understood that it is capable of further modifications and this application is intended to cover any variations, uses, or adaptations of the invention following, in general, the principles of the invention and including such departures from the present disclosure that come within known or customary practice within the art to which the invention pertains and may be applied to the essential features set forth herein. The disclosure of each and every U.S., international or other patent or patent application or publication referred to herein is hereby incorporated herein by reference in its entirety.

## CLAIMS

1. Use of liposomal irinotecan in combination with a Poly(ADP-ribose) Polymerase (PARP) inhibitor in an antineoplastic therapy for the treatment of a solid tumor, wherein the liposomal irinotecan is repeatedly administered once every two weeks and the PARP inhibitor is administered daily for 3 to 10 days between consecutive administrations of the liposomal irinotecan, without administering the PARP inhibitor within 3 days of the liposomal irinotecan.
2. The use of claim 1, wherein the PARP inhibitor is administered on each of consecutive days 3 to 10 between the days when the liposomal irinotecan is administered.
3. Use of liposomal irinotecan and a Poly(ADP-ribose) Polymerase (PARP) inhibitor in an antineoplastic therapy for the treatment of a solid tumor, the use comprising a 28-day antineoplastic therapy treatment cycle consisting of: administering the liposomal irinotecan on days 1 and 15 of the treatment cycle, and administering the PARP inhibitor on one or more days starting at least 3 days after the liposomal irinotecan and ending at least 1 day prior to administration of additional liposomal irinotecan.
4. The use of claim 3, wherein the PARP inhibitor is not administered for at least 3 days after the administration of liposomal irinotecan.
5. The use of any one of claims 3-4, wherein the PARP inhibitor is not administered for at least 3 days prior to the next administration of liposomal irinotecan.
6. The use of any one of claims 1-5, wherein the PARP inhibitor is administered on one or more of days 5-12 of the antineoplastic therapy treatment cycle.
7. The use of any one of claims 1-6, wherein the PARP inhibitor is administered on one or more of days 19-25 of the antineoplastic therapy treatment cycle.
8. The use of any one of claims 1-7, wherein the PARP inhibitor is administered on one or more of days 3-12 of the antineoplastic therapy treatment cycle.
9. The use of any one of claims 1-8, wherein the PARP inhibitor is administered on one or more of days 17-25 of the antineoplastic therapy treatment cycle.
10. The use of any one of claims 1-9, wherein the liposomal irinotecan has an irinotecan terminal elimination half-life of 26.8 hours and a maximal irinotecan plasma concentration of 38.0 micrograms/ml.
11. The use of any one of claims 1-10, wherein the PARP inhibitor is not administered within 3 days before or after the administration of the liposomal irinotecan.
12. The use of any one of claims 1-11, wherein each administration of liposomal irinotecan is administered at a dose of 80 mg/m<sup>2</sup> (salt) or 70(salt) or 70 mg/m<sup>2</sup> (free base).

13. The use of any one of claims 1-12, wherein each administration of the PARP inhibitor is administered at a dose of from about 20 mg/day to about 800 mg/day.
14. The use of any one of claims 1-13, wherein each administration of the PARP inhibitor is administered once or twice daily at a dose of from about 20 mg/day to about 400 mg/day.
15. The use of any one of claims 1-14, wherein the PARP inhibitor is selected from the group consisting of niraparib, olaparib, veliparib, rucaparib and talazoparib.
16. The use of any one of claims 1-15, wherein the cancer is cervical cancer, ovarian cancer, triple negative breast cancer, non-small cell lung cancer, small cell lung cancer, gastrointestinal stromal tumors gastric cancer, pancreatic cancer, colorectal cancer, or a neuroendocrine cancer.
17. The use of any one of claims 1-16, wherein the cancer is cervical cancer and the PARP inhibitor is veliparib.
18. The use of any one of claims 1-17, wherein the cancer is cervical cancer and the PARP inhibitor is olaparib.
19. The use of any one of claims 1-18, further comprising the use of ferumoxytol as an imaging agent to select patients to receive the liposomal irinotecan and PARP inhibitor.
20. The use of claim 19, further comprising administering ferumoxytol and then obtaining a MRI image of the patient 24 hours after ferumoxytol administration.

ME-180 cells viability (1000cells/well in 384-well plate) treated with SN-38 and with different PARP inhibitors (0.33 ug/ml) for 24hrs, washed and incubated for additional 72hrs with fresh media

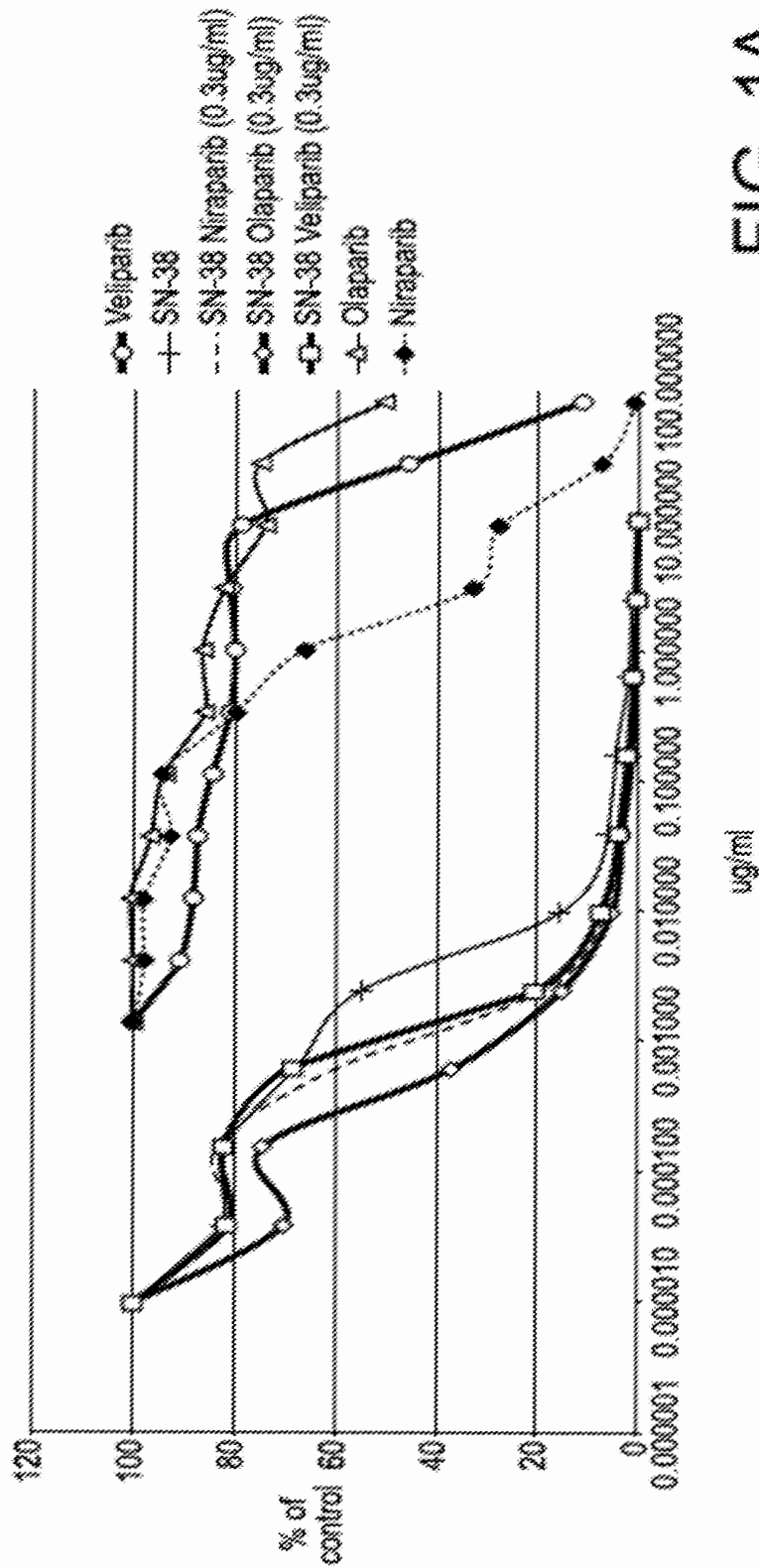


FIG. 1A

MS-751 cells viability (1000cells/well in 384-well plate) treated with SN-38 and with different PARP inhibitors (0.33 ug/ml) for 24hrs, washed and incubated for additional 72hrs with fresh media

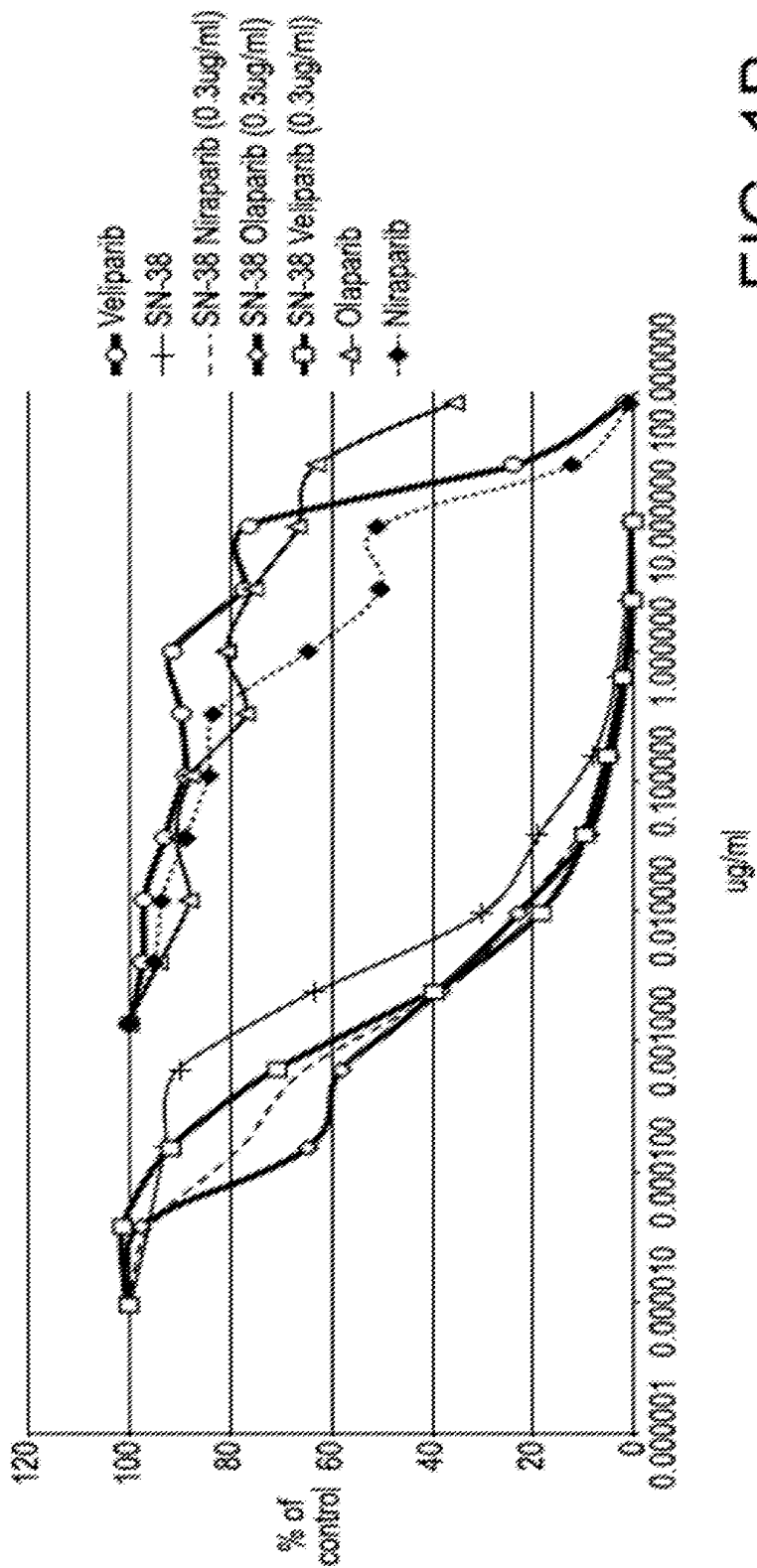


FIG. 1B

C-33A cells viability (1000cells/well in 384-well plate) treated with SN-38 and with different PARP inhibitors (0.33 ug/ml) for 24hrs, washed and incubated for additional 72hrs with fresh media

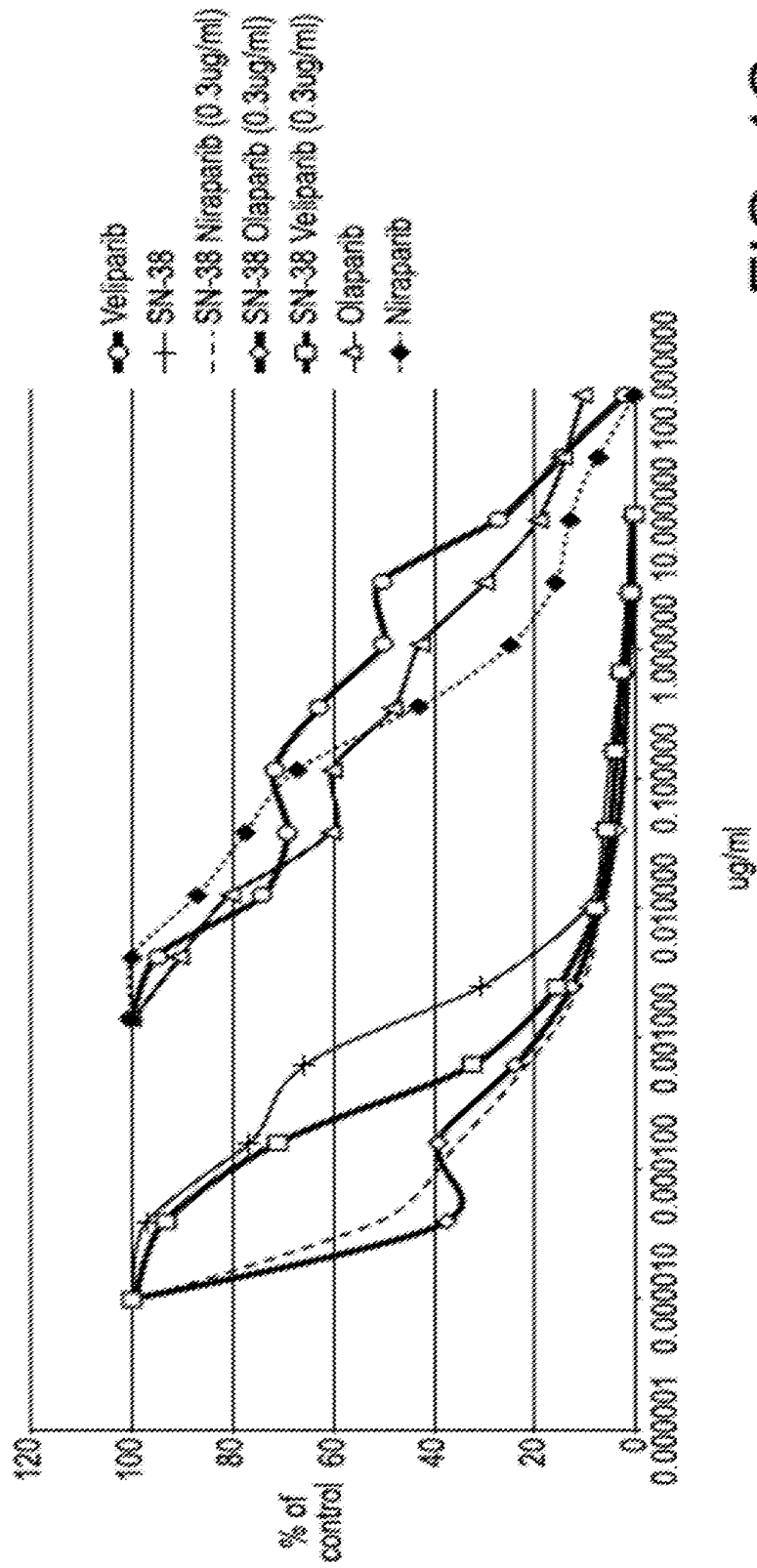


FIG. 1C

SW756 cells viability (1000cells/well in 384-well plate) treated with SN-38 and with different PARP inhibitors (0.33 ug/ml) for 24hrs, washed and incubated for additional 72hrs with fresh media

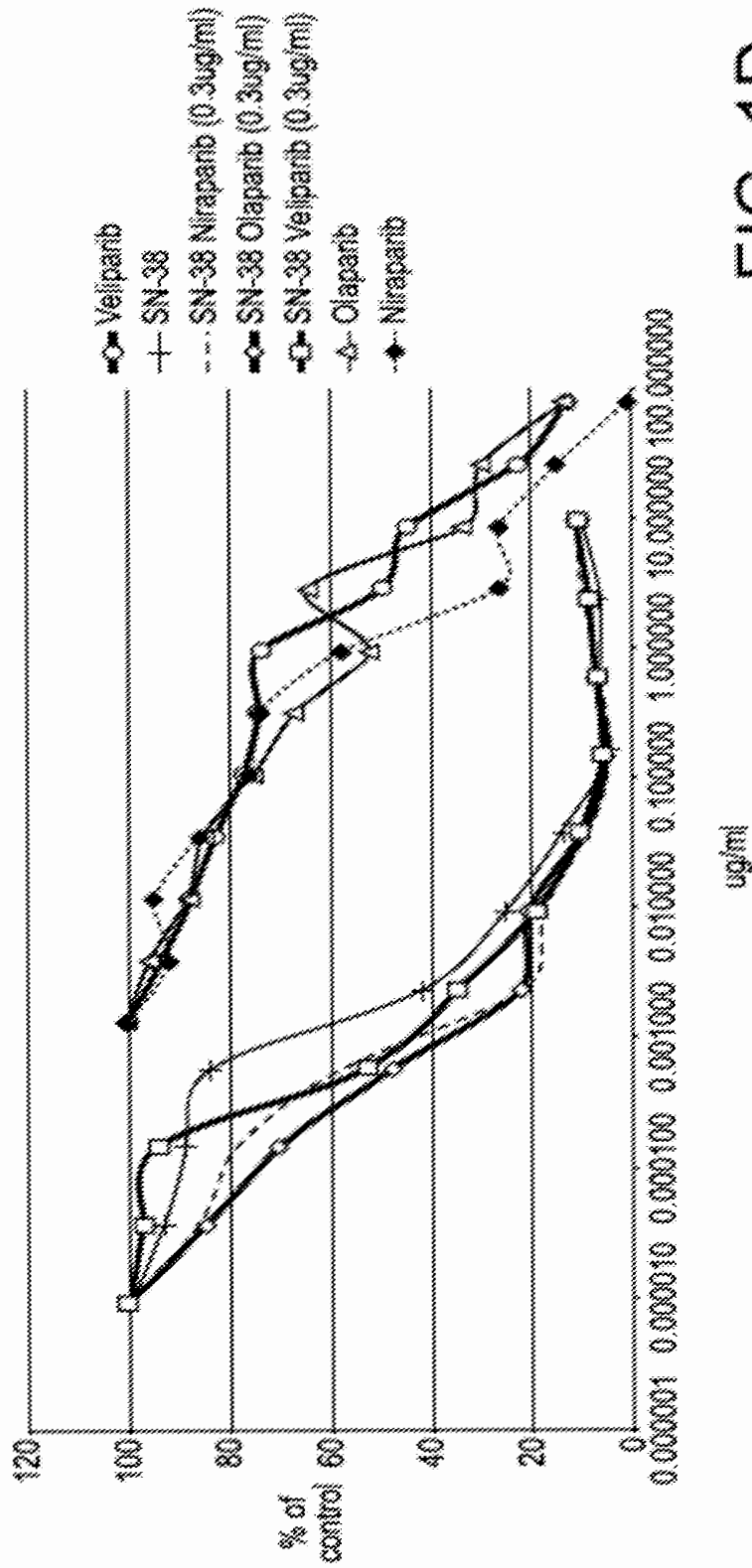


FIG. 1D



SiHa cells viability (1000cells/well in 384-well plate) treated with SN-38 and with different PARP inhibitors (0.33 ug/ml) for 24hrs, washed and incubated for additional 72hrs with fresh media

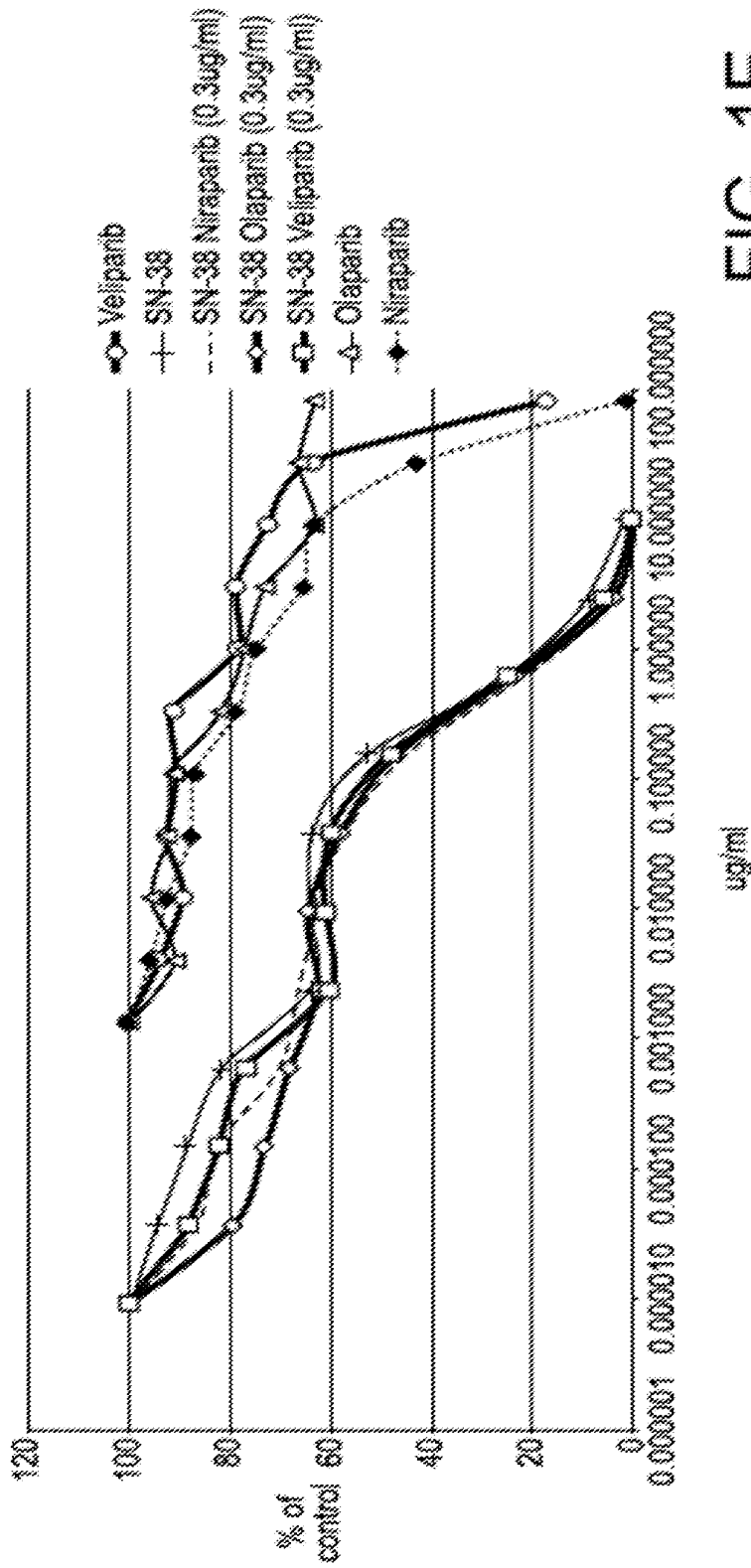


FIG. 1E

DMS-114\_Rucaparib: SN-38 (2nM)

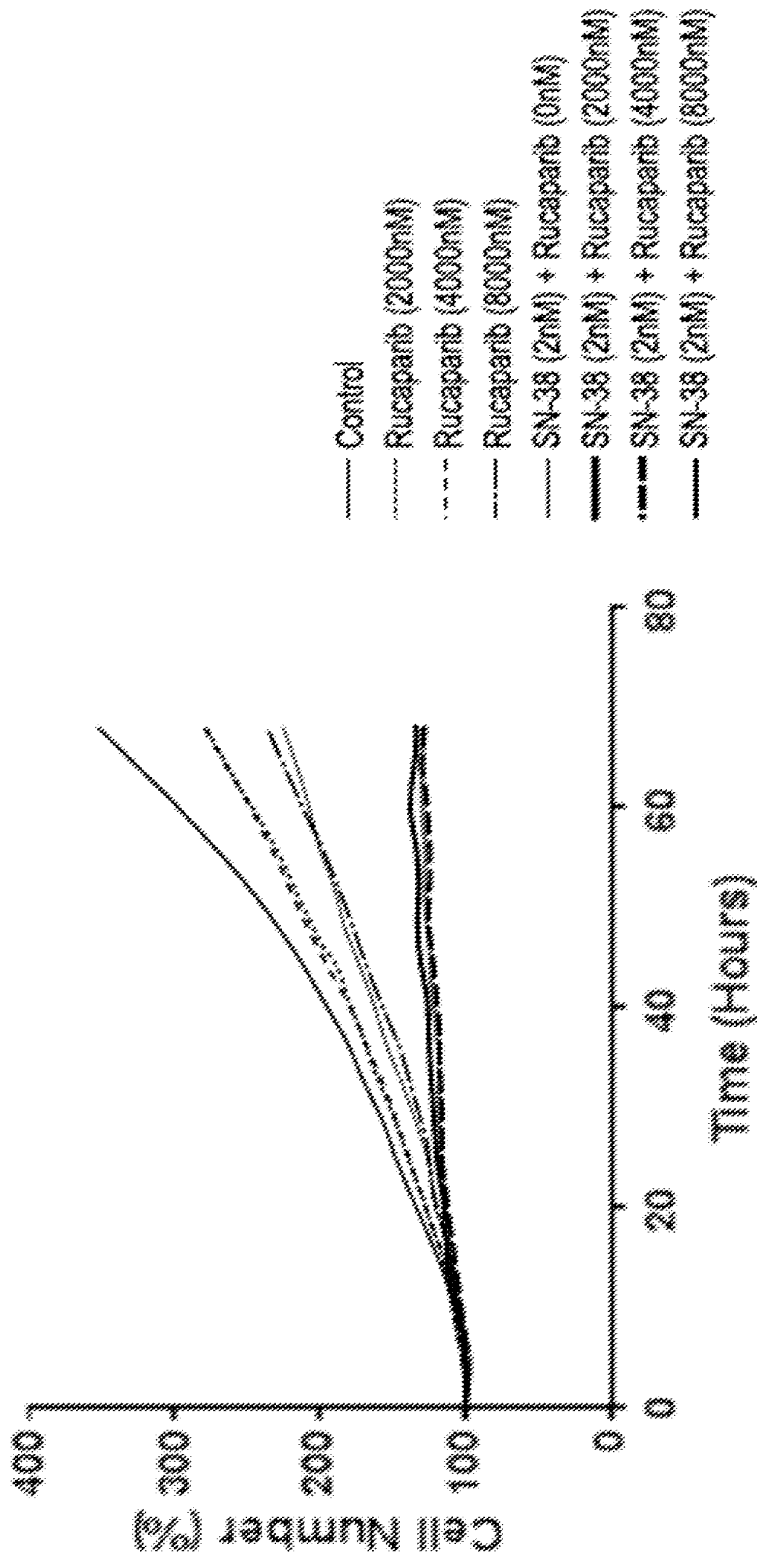


FIG. 2A

NCI-H1048\_Rucaparib: SN-38 (2nM)

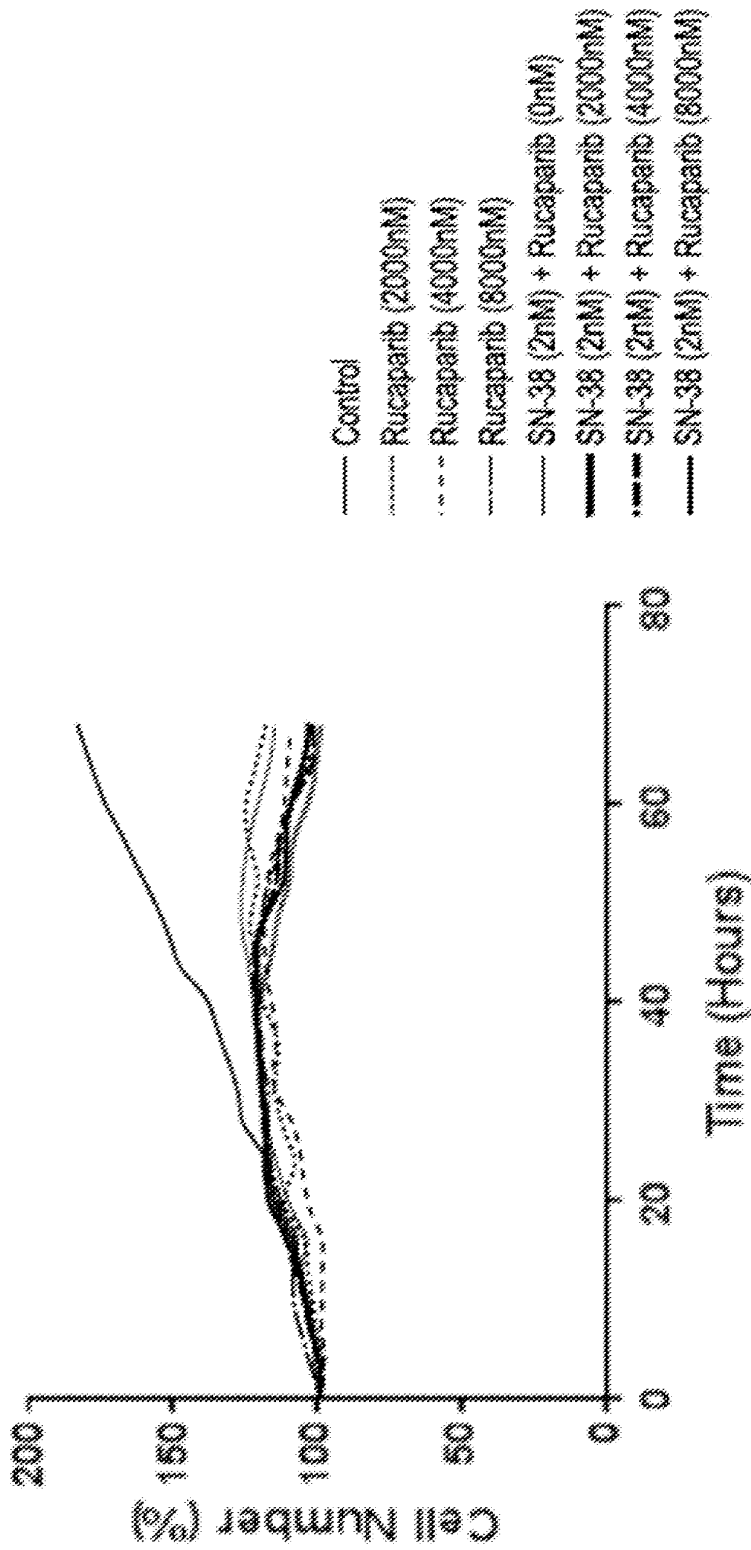
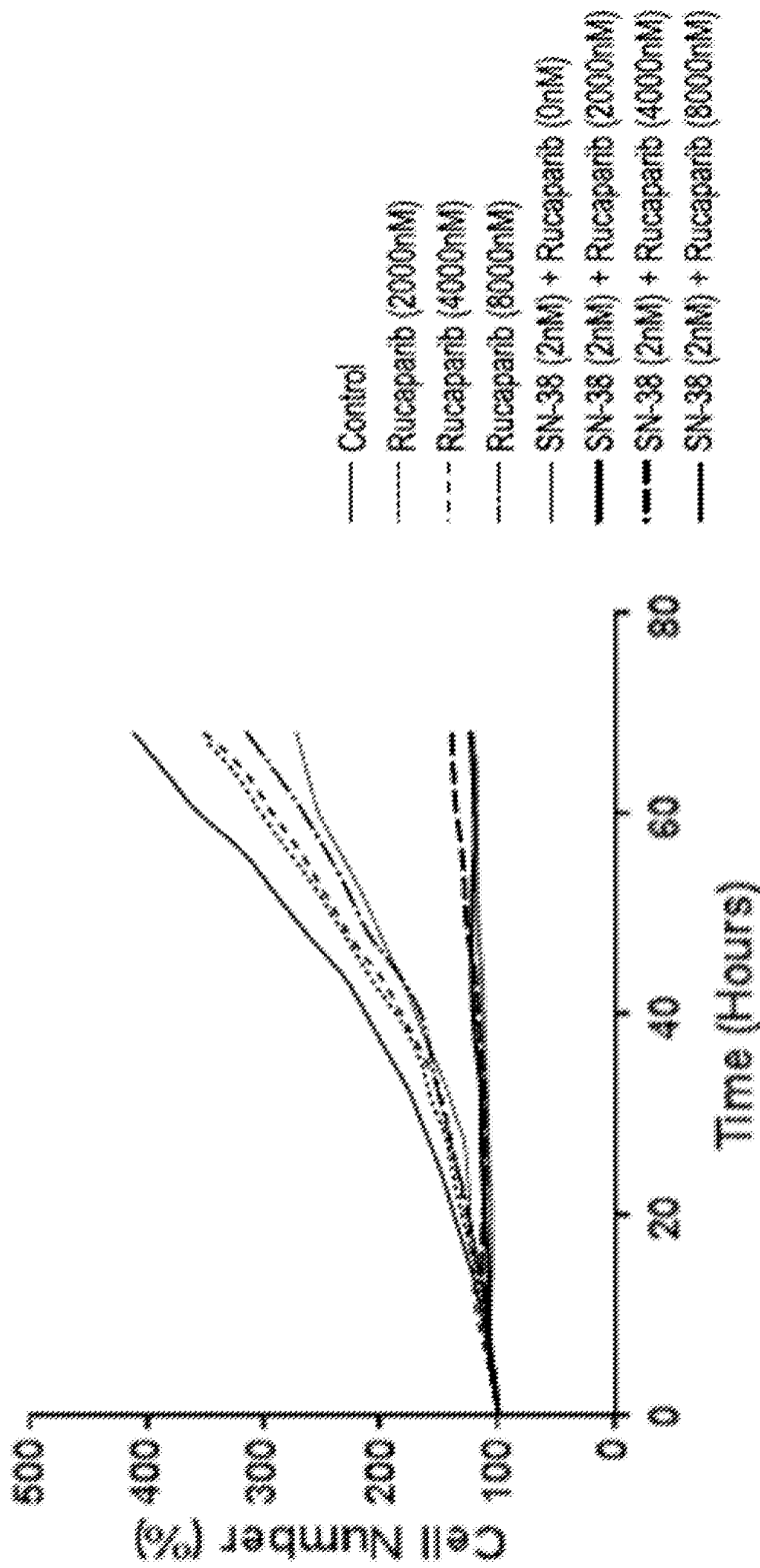


FIG. 2B

**CFPAC-1\_Rucaparib: SN-38 (2nM)**



**FIG. 2C**

**BxPC-3\_Rucaparib: SN-38 (2nM)**

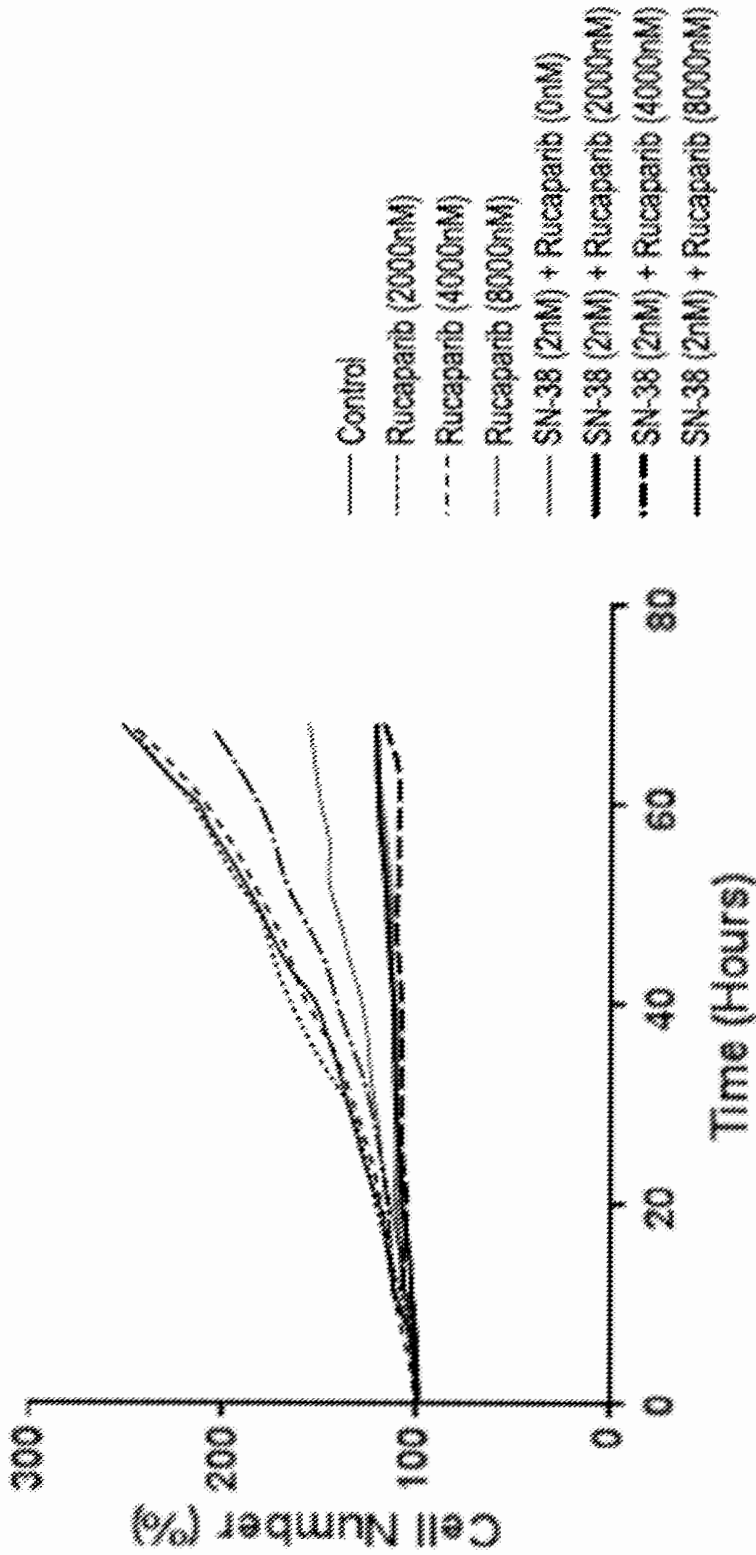


**FIG. 2D**

**MDA-MB-231\_Rucaparib: SN-38 (2nM)**

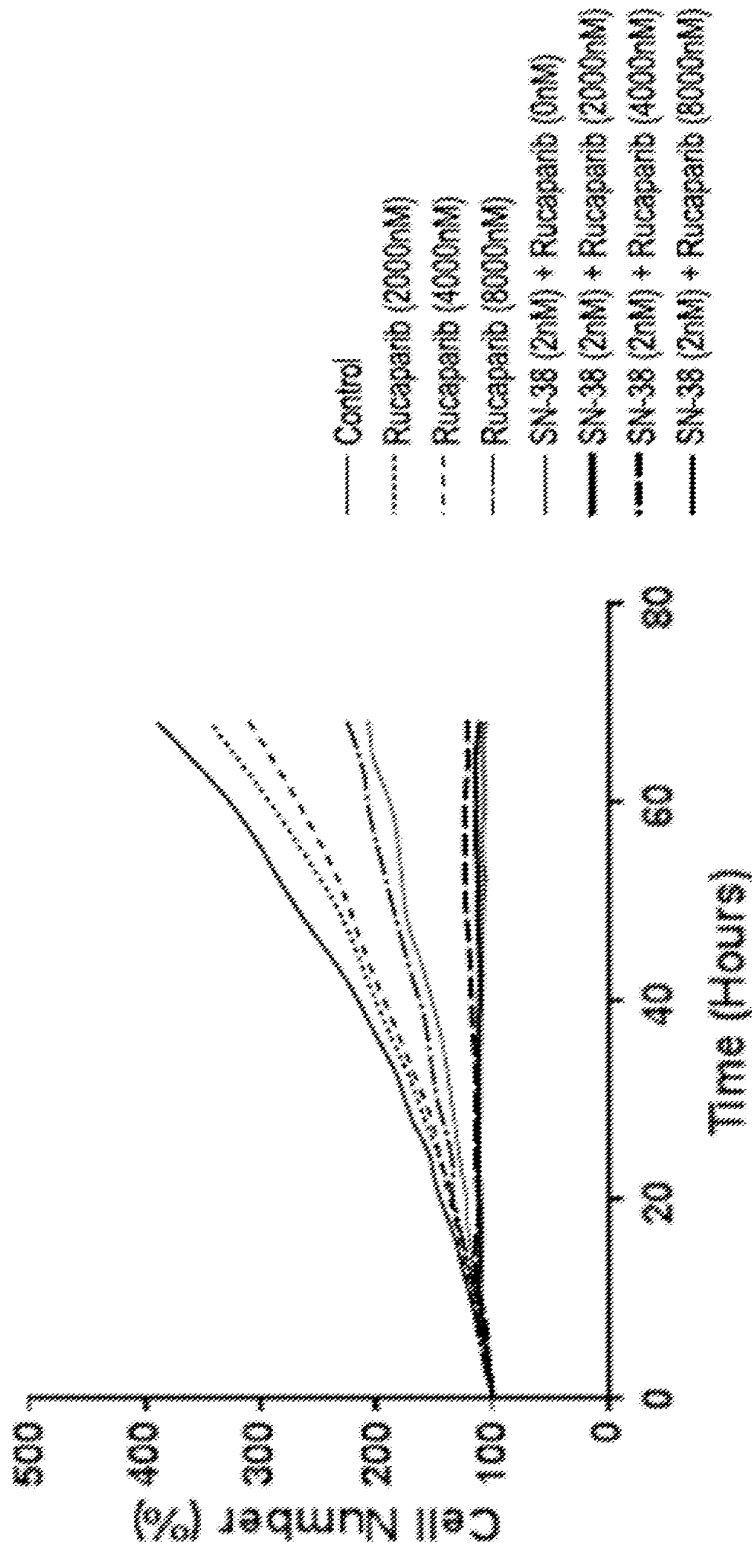
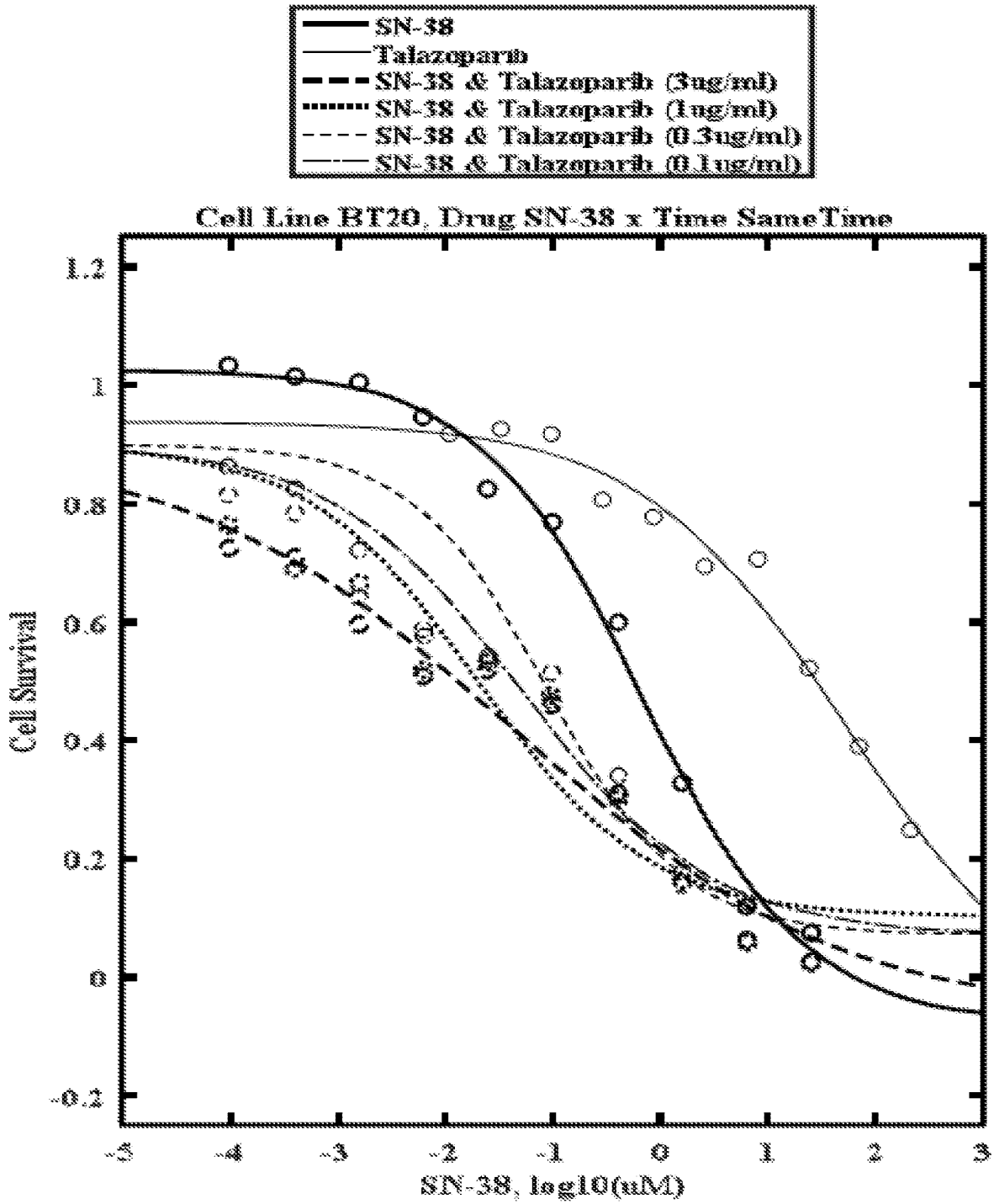


**FIG. 2E**

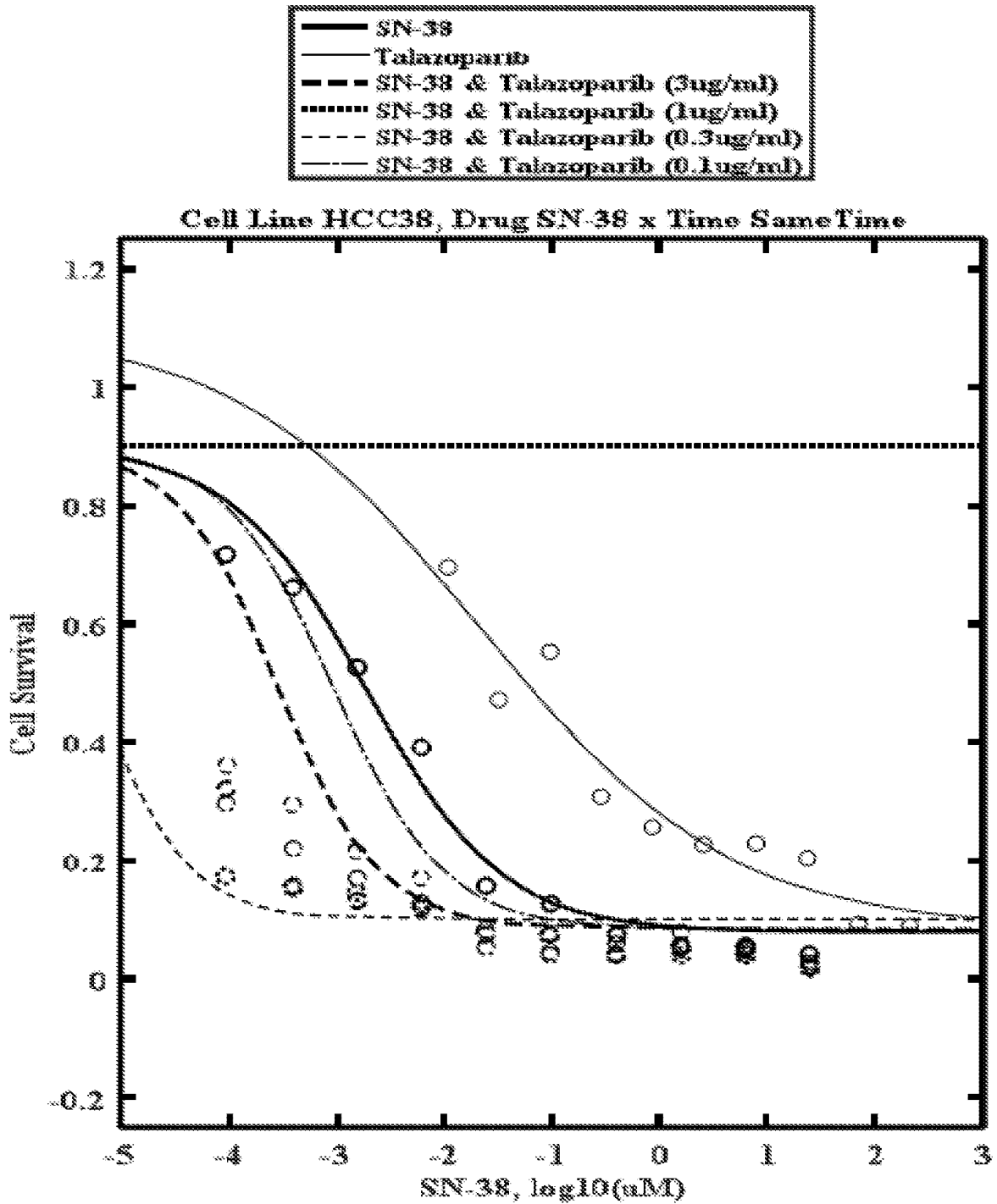
### BT20 cell survival treated with SN-38 and Talazoparib

## FIG. 3A



### HCC38 cell survival treated with SN-38 and Talazoparib

## FIG. 3B





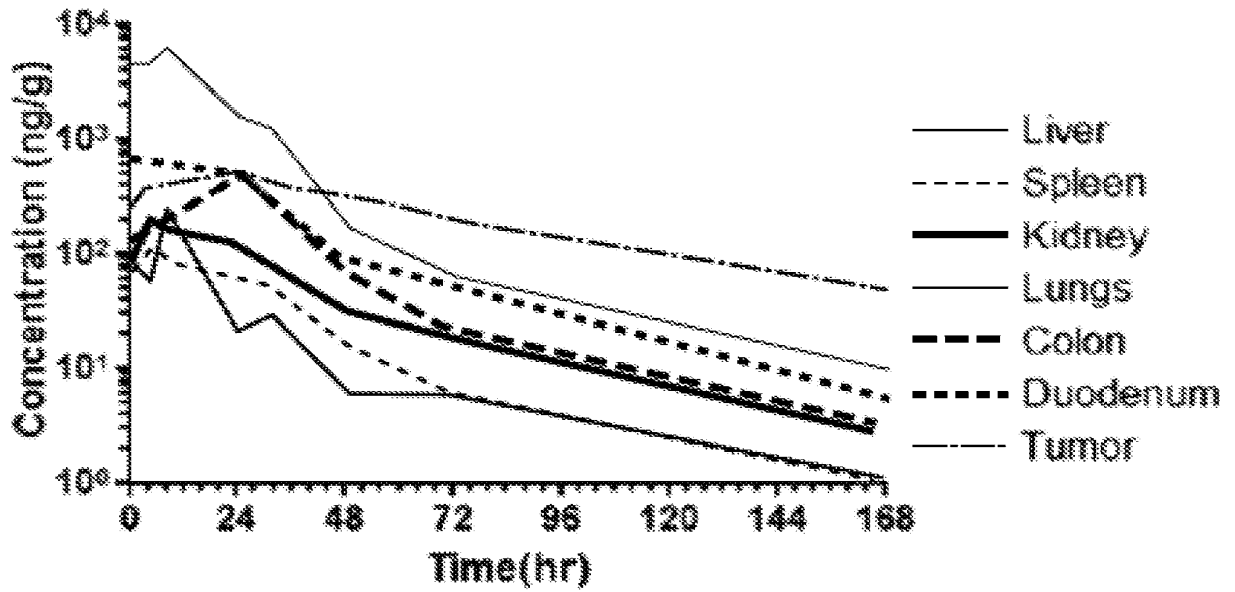


FIG. 4A

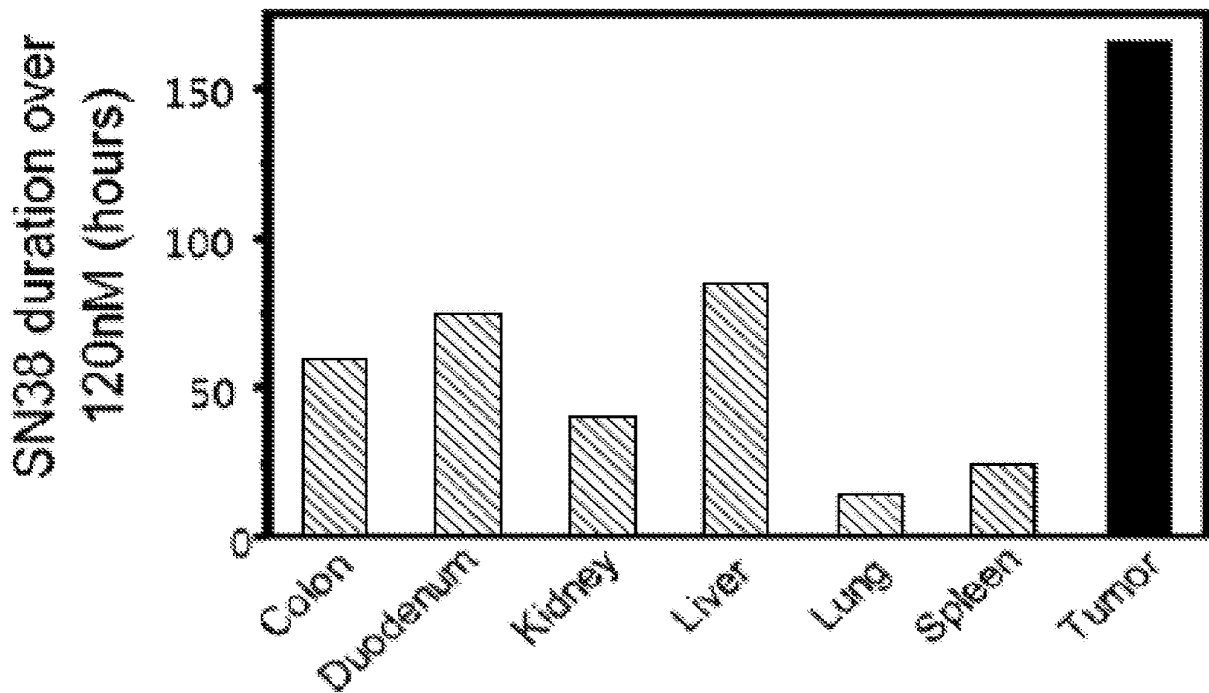


FIG. 4B

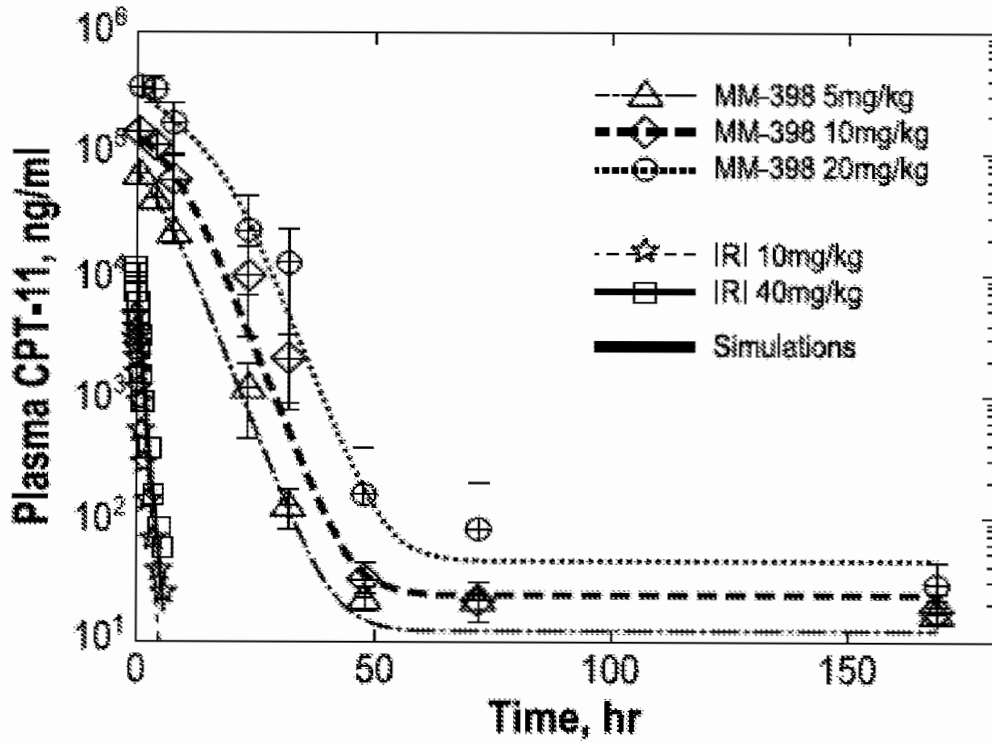


FIG. 5A

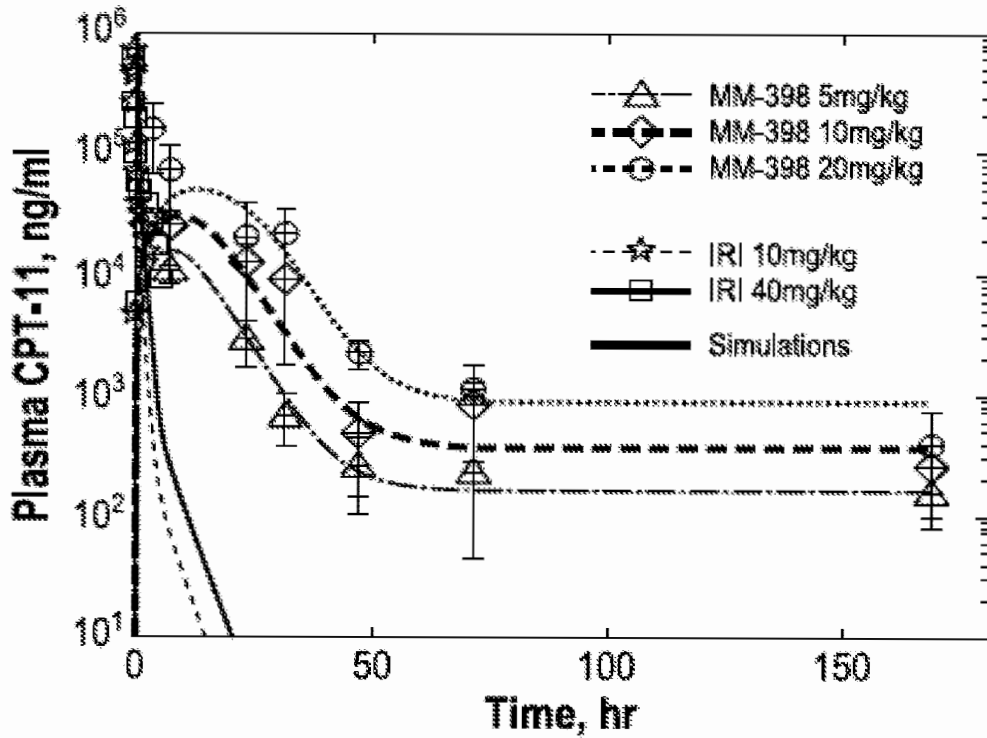


FIG. 5B

### HT29 CRC tumor levels of irinotecan (CPT-11)

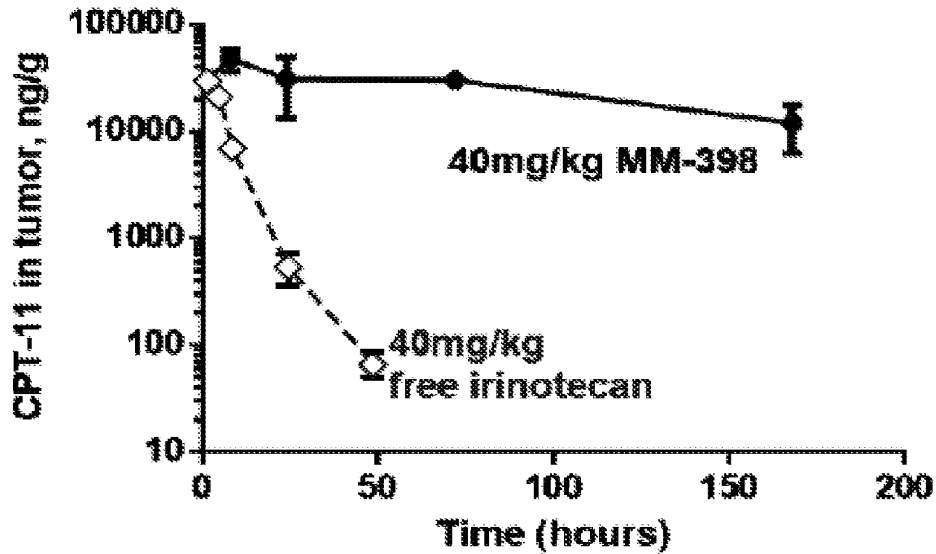


FIG. 5C

### HT29 CRC tumor levels of SN-38

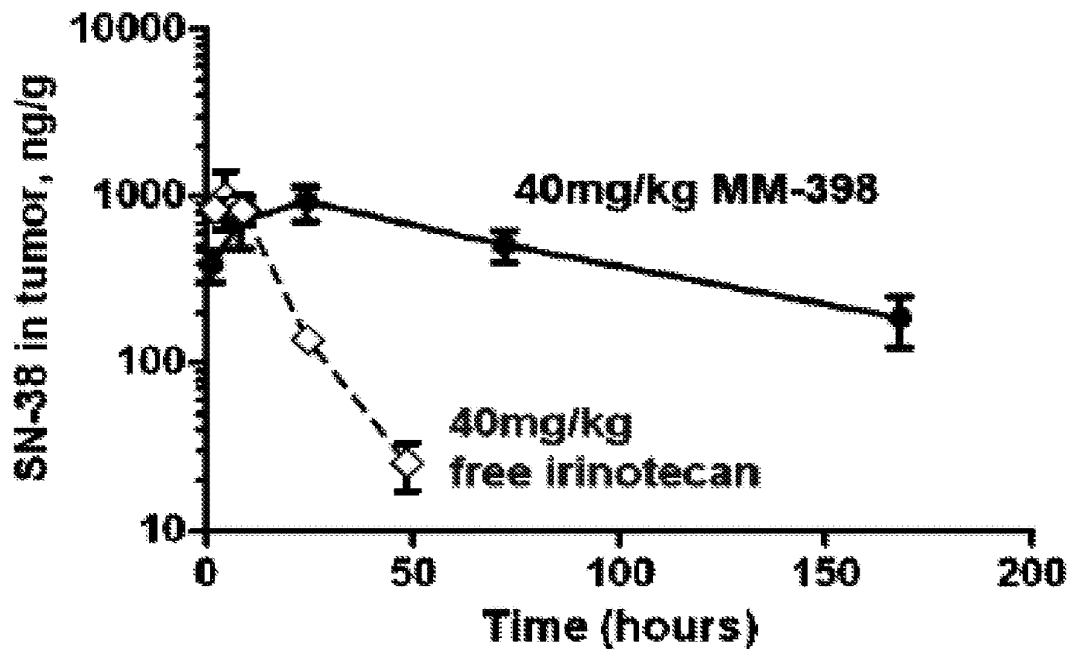


FIG. 5D

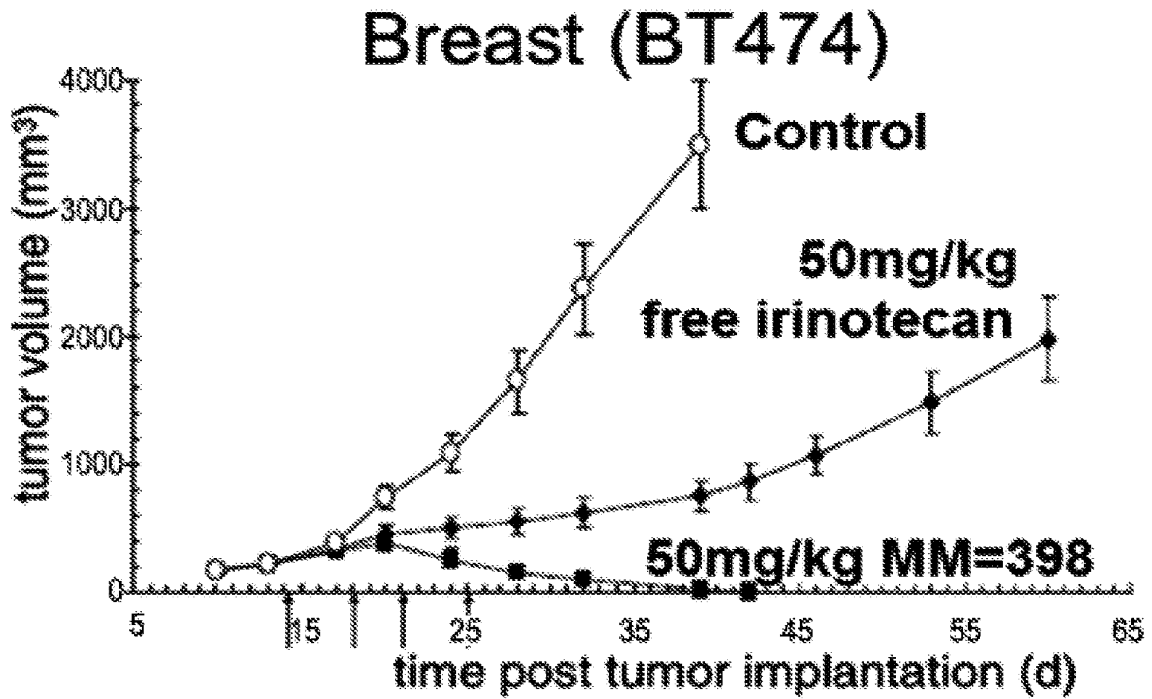


FIG. 6A

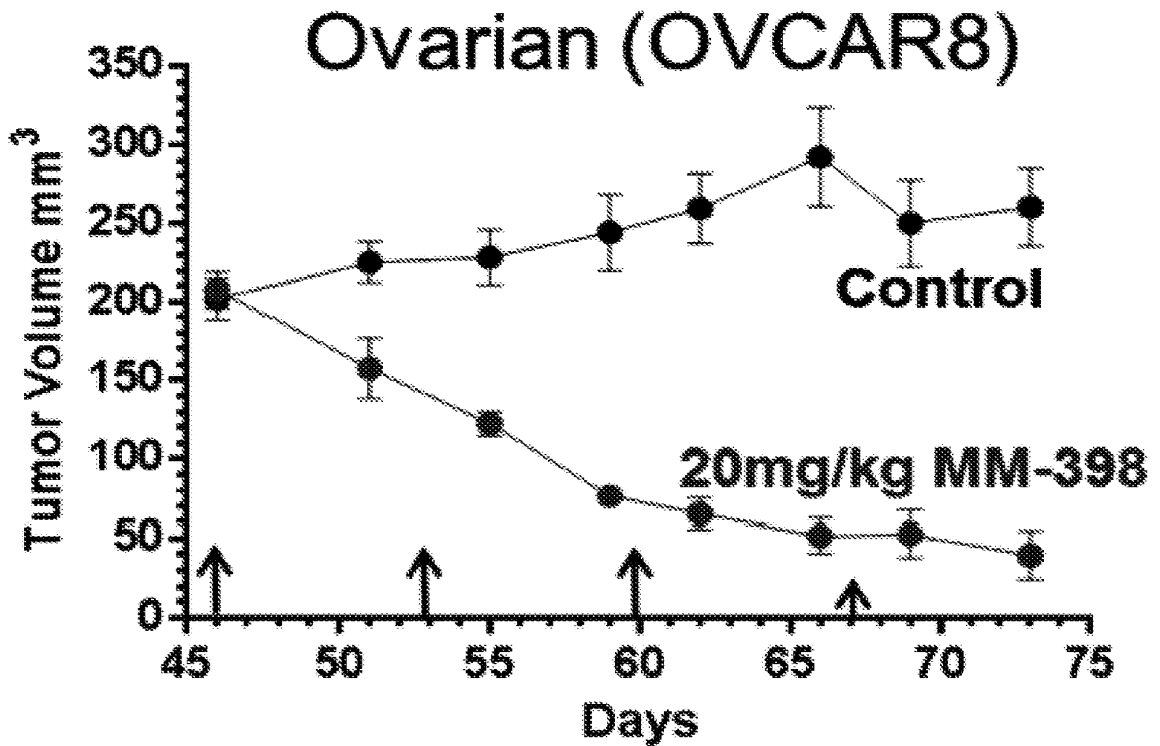


FIG. 6B

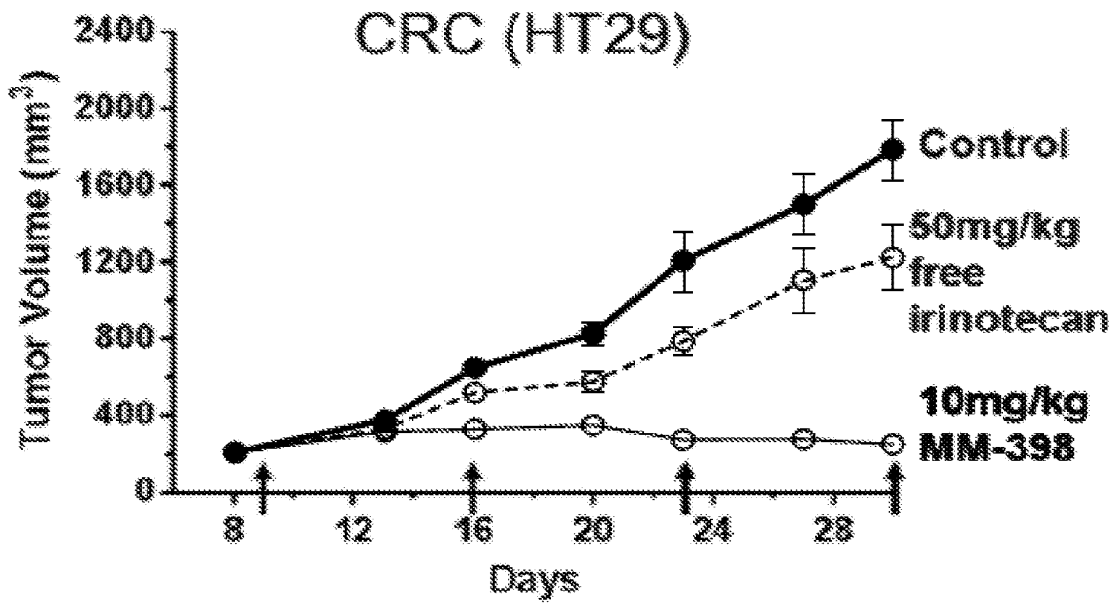


FIG. 6C

Orthotopic, hypoxic, L3.6pl pancreatic xenograft

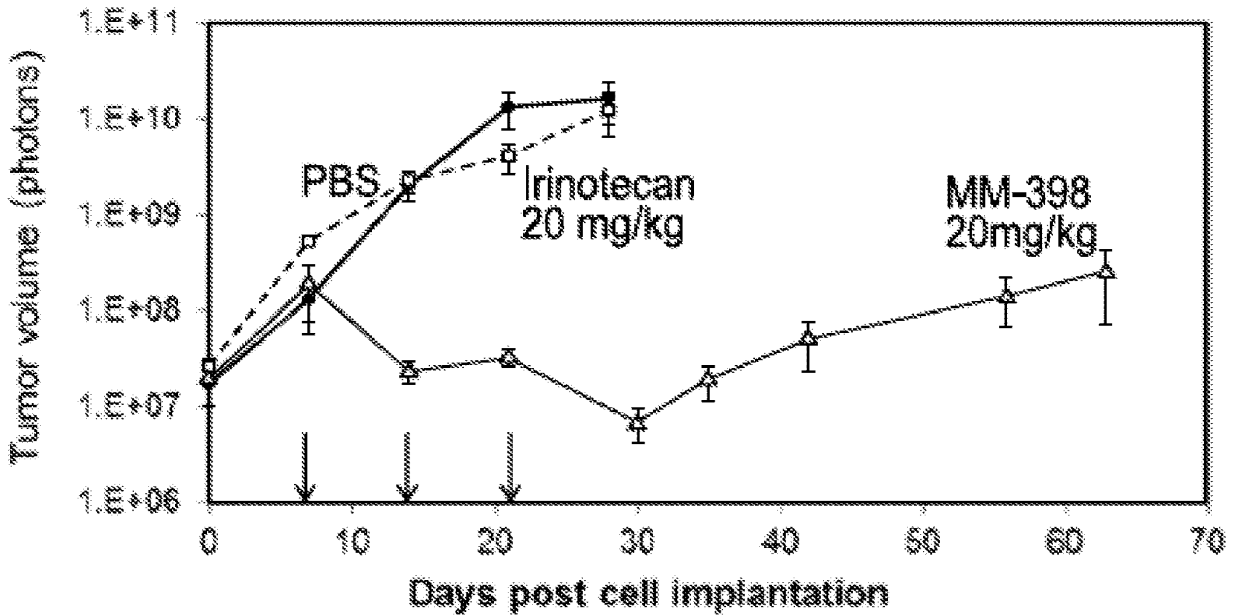


FIG. 6D

### Irinotecan (CPT-11)

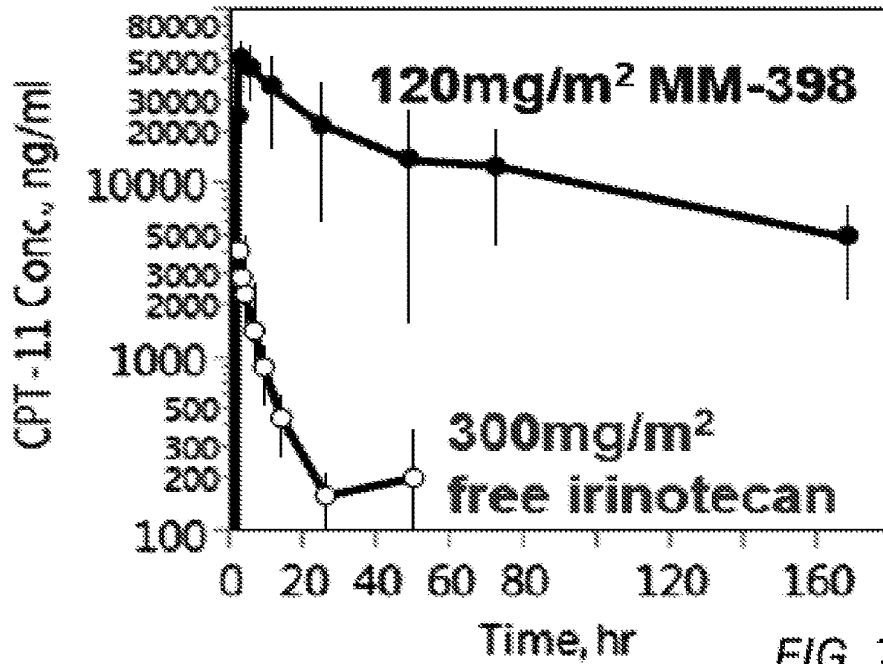


FIG. 7A

### SN-38

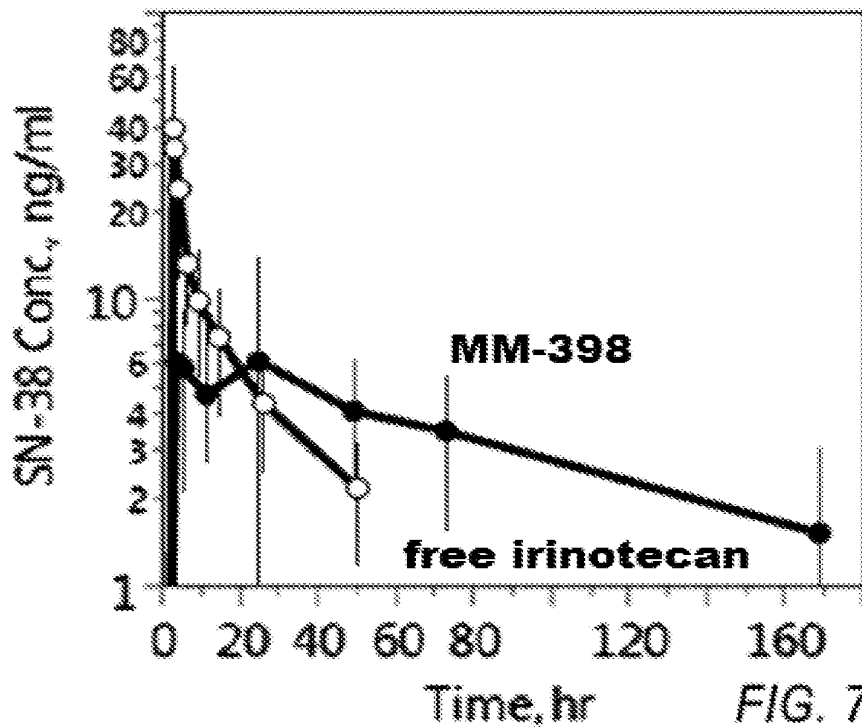


FIG. 7B

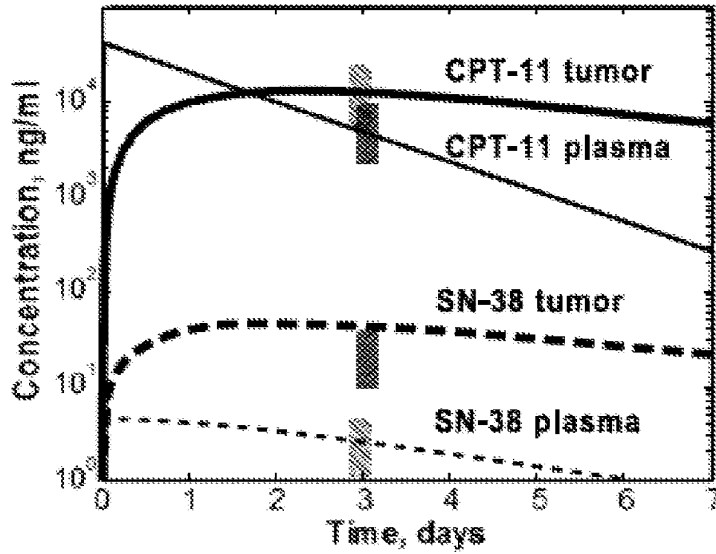


FIG. 7C

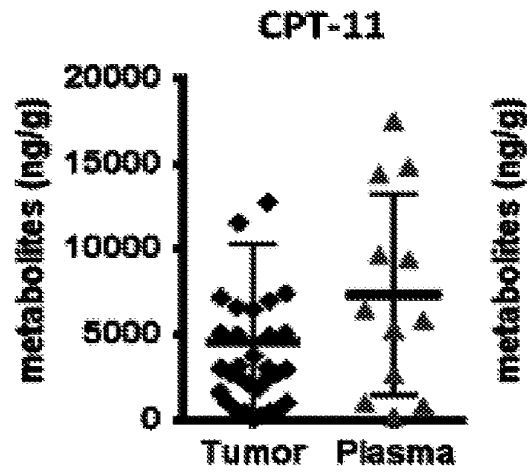


FIG. 7D

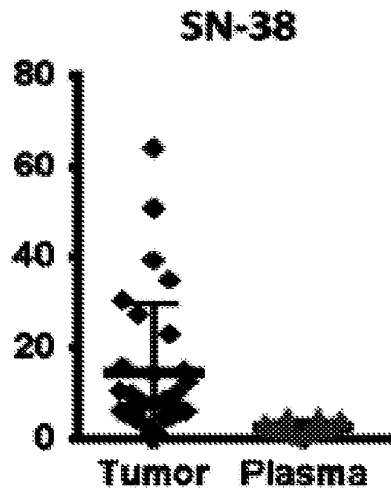


FIG. 7E

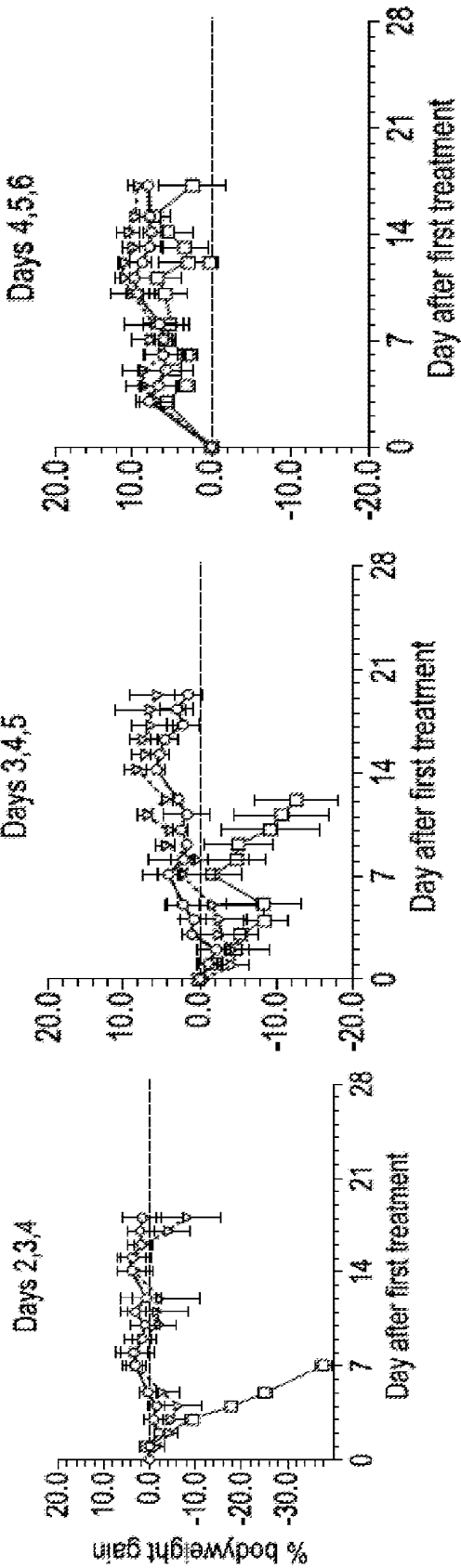


FIG. 8A

FIG. 8B

FIG. 8C



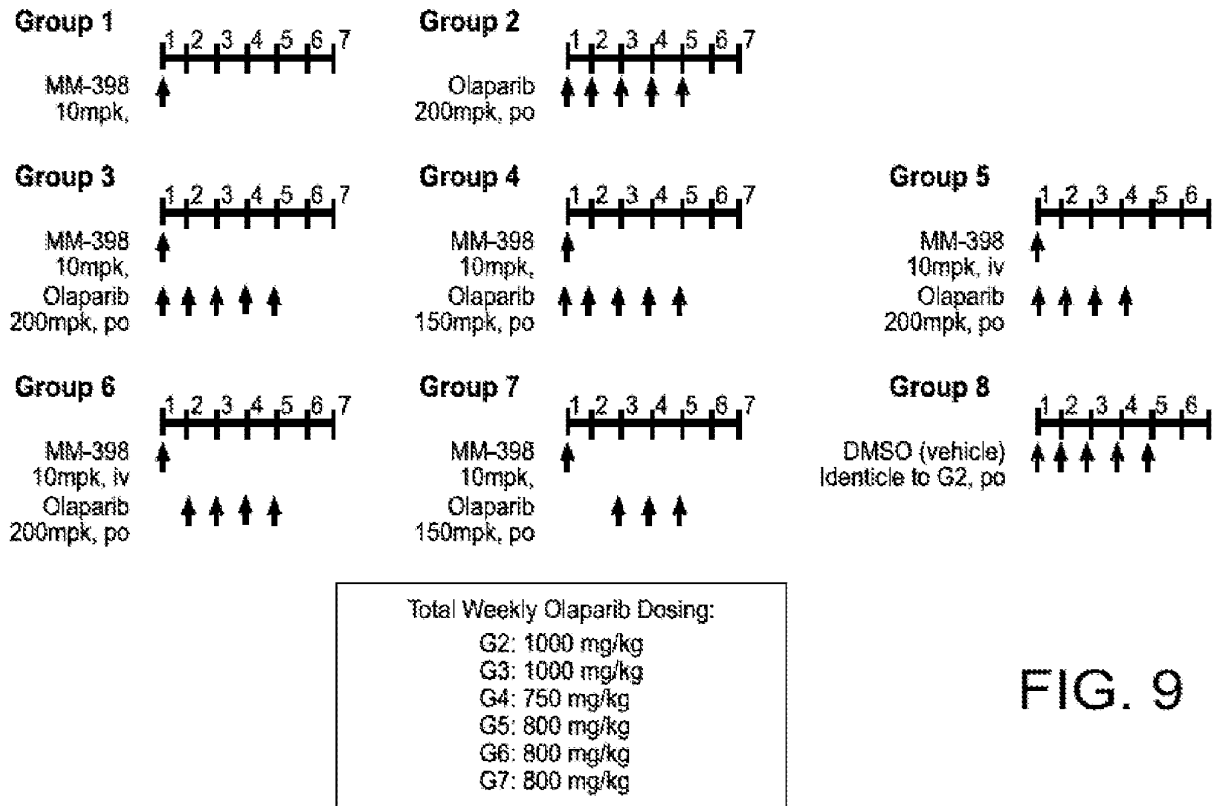
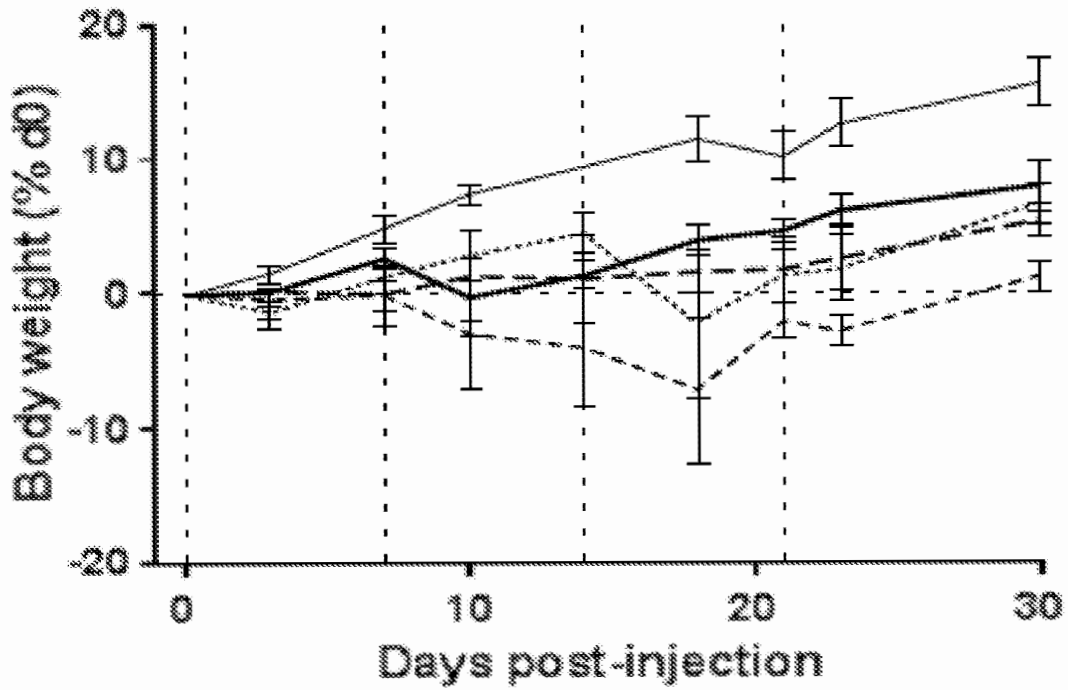


FIG. 9

22/39

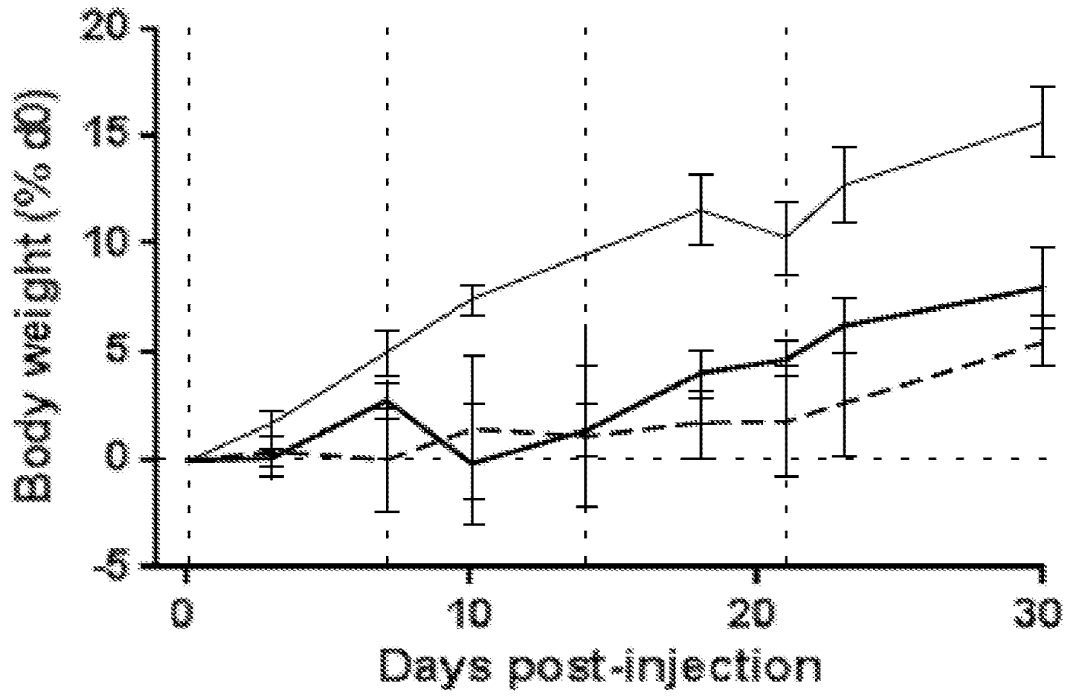
### Weight (% of d0)



- Vehicle (DMSO, 1-5)
- MM-398 (10mg/kg) (+PBS)
- Olaparib (200mg/kg/day)
- MM398 (10) + Olaparib (200, 1-4)
- ..... MM398 (10) + Olaparib (200, 2-5)

## FIG. 10A

23/39  
**Weight (% of d0)**



- Vehicle (DMSO, 1-5)
- - - MM-398 (10mg/kg) (+PBS)
- ..... Olaparib (200mg/kg/day)

**FIG. 10B**

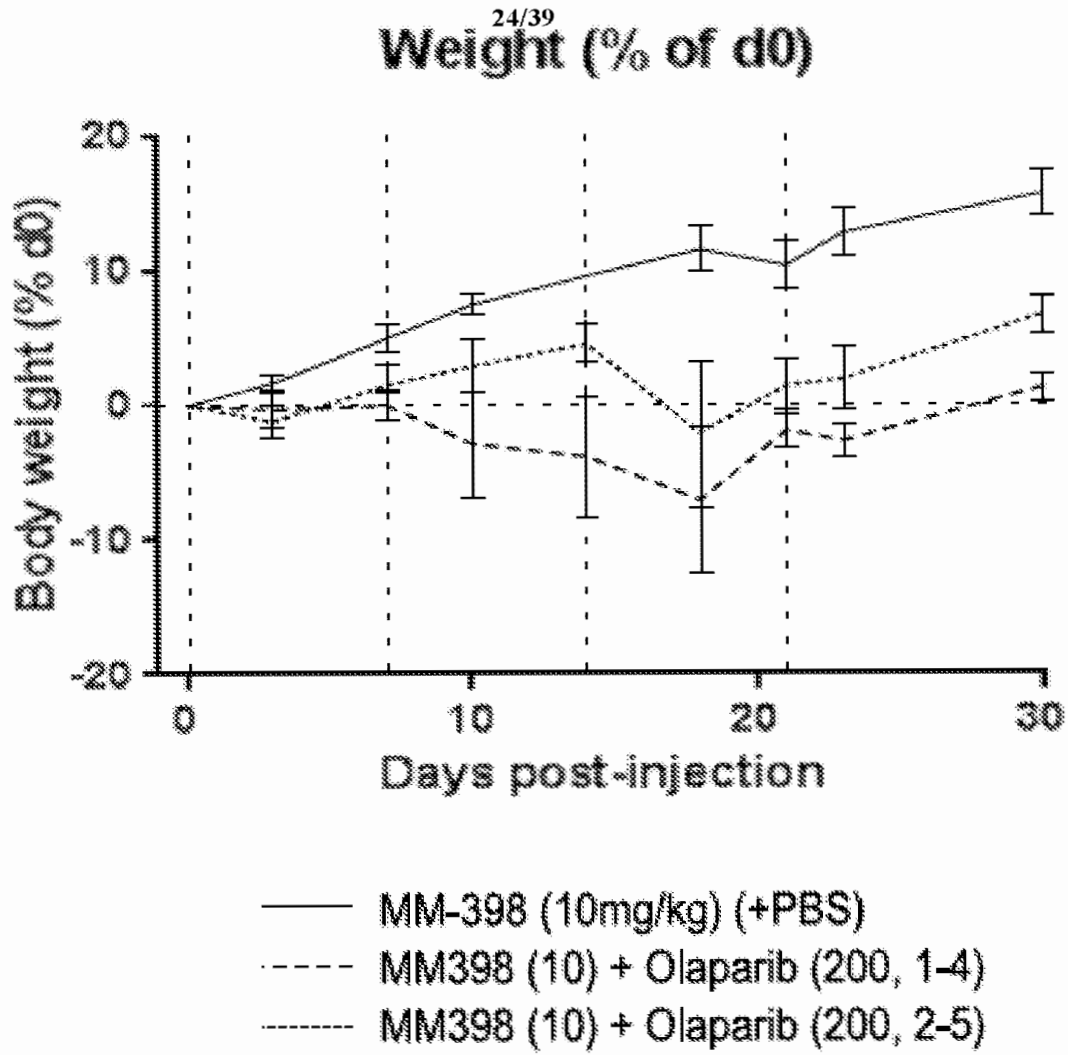


**FIG. 10C**

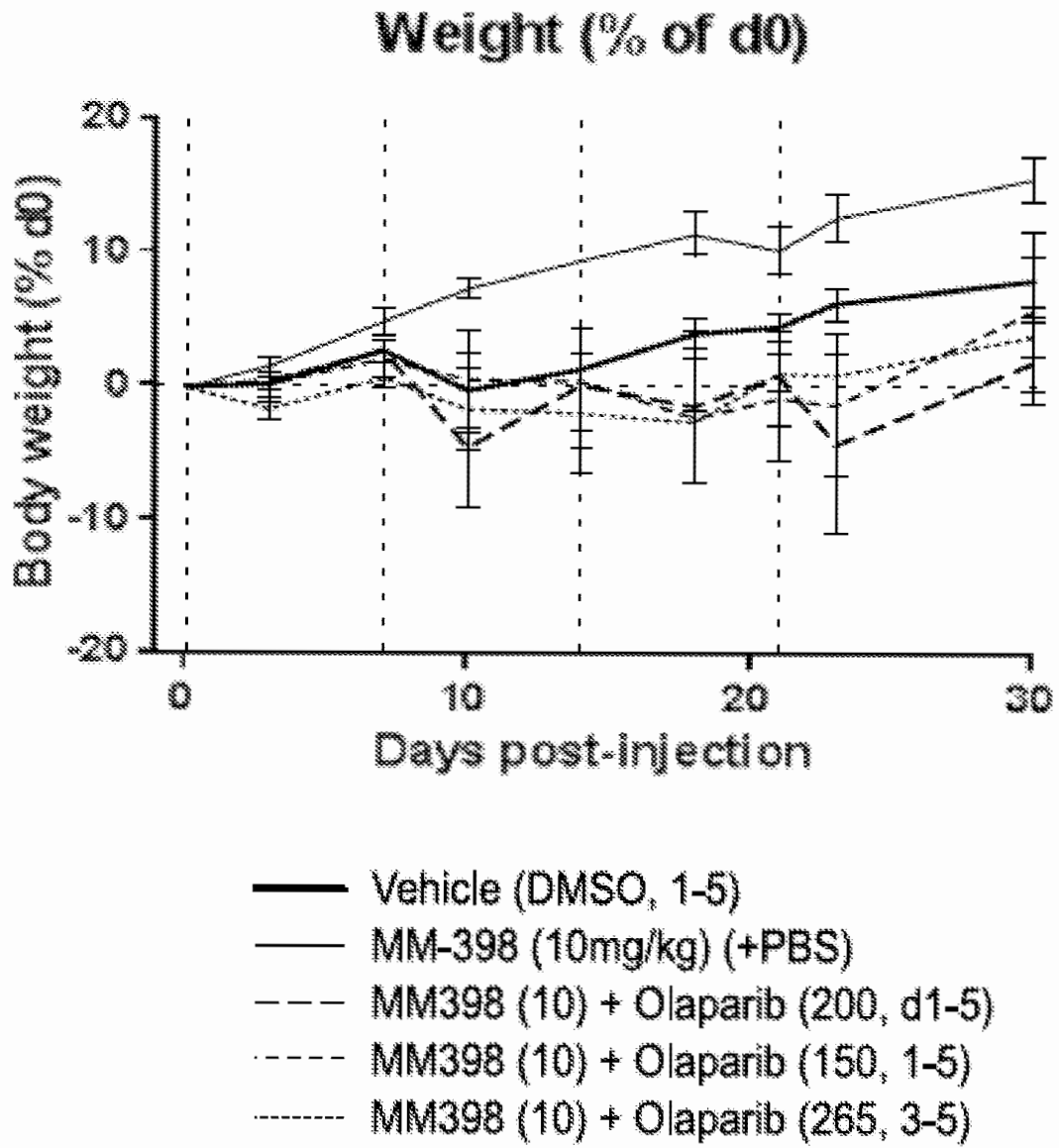


FIG. 10D

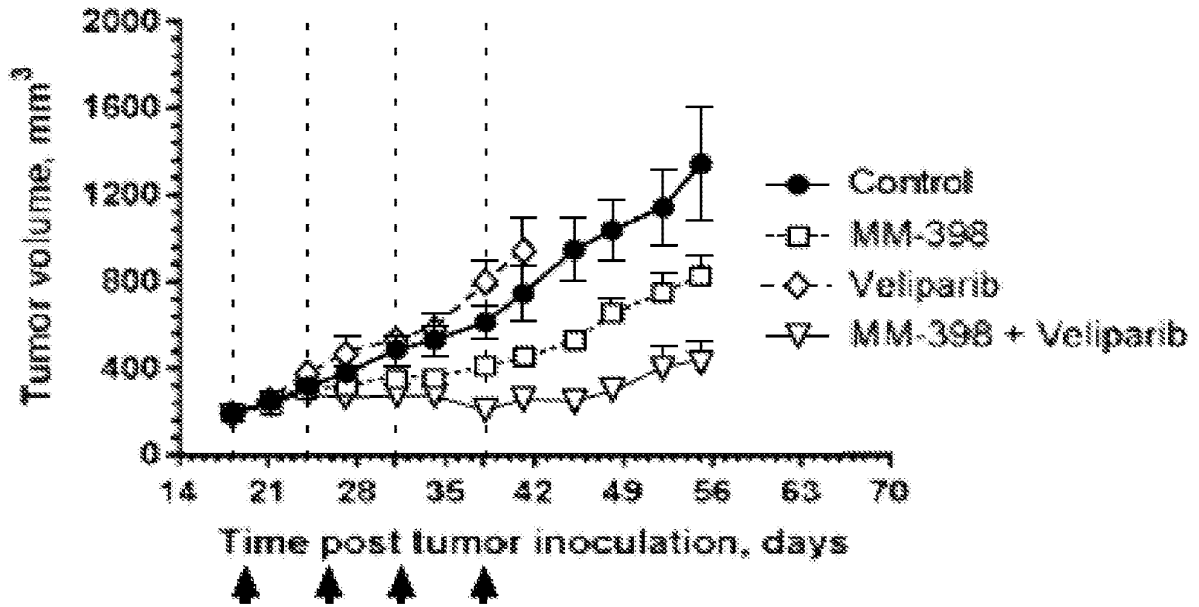


FIG. 11A

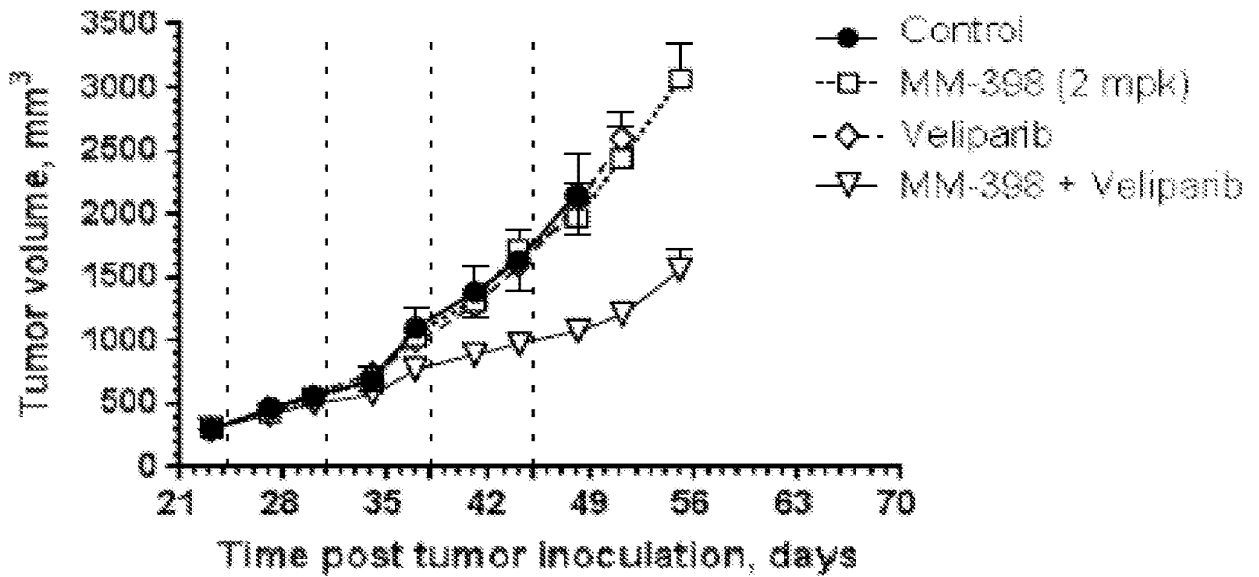
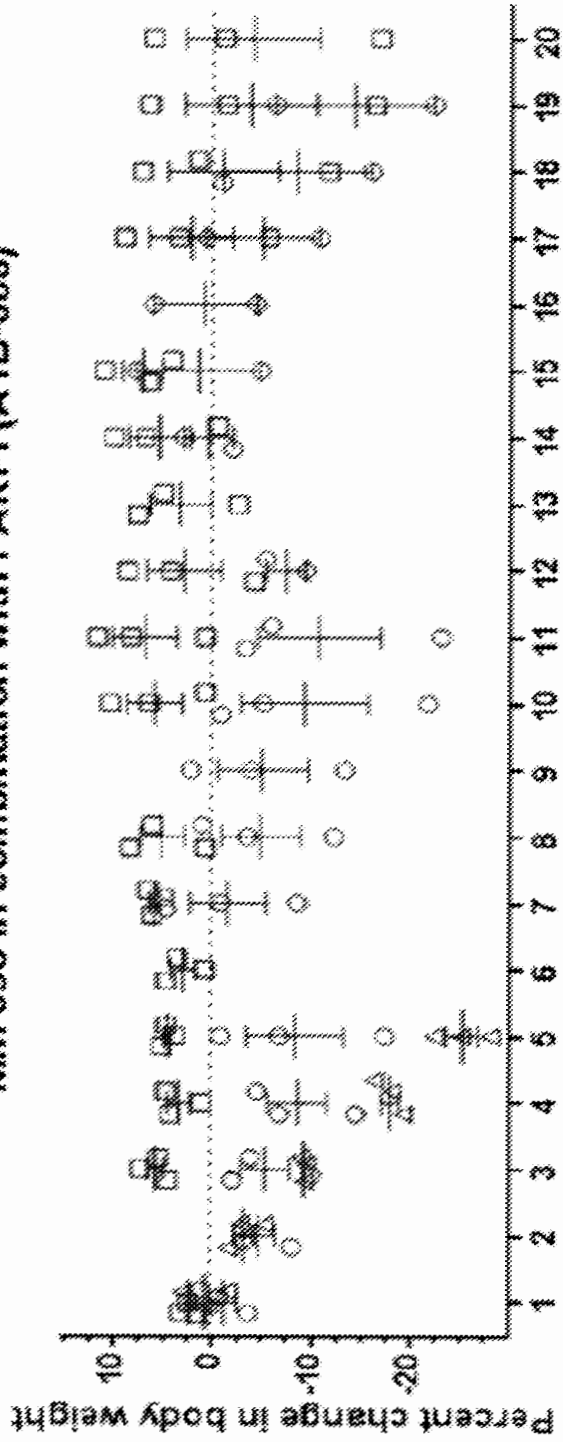


FIG. 11B

MM-398 in combination with PARPi (A TB-888)



Day

□ MM-398/50 mpk + PARPV345  
○ MM-398/50 mpk + PARPV234  
△ MM-398/50 mpk + PARPV123

FIG. 12A

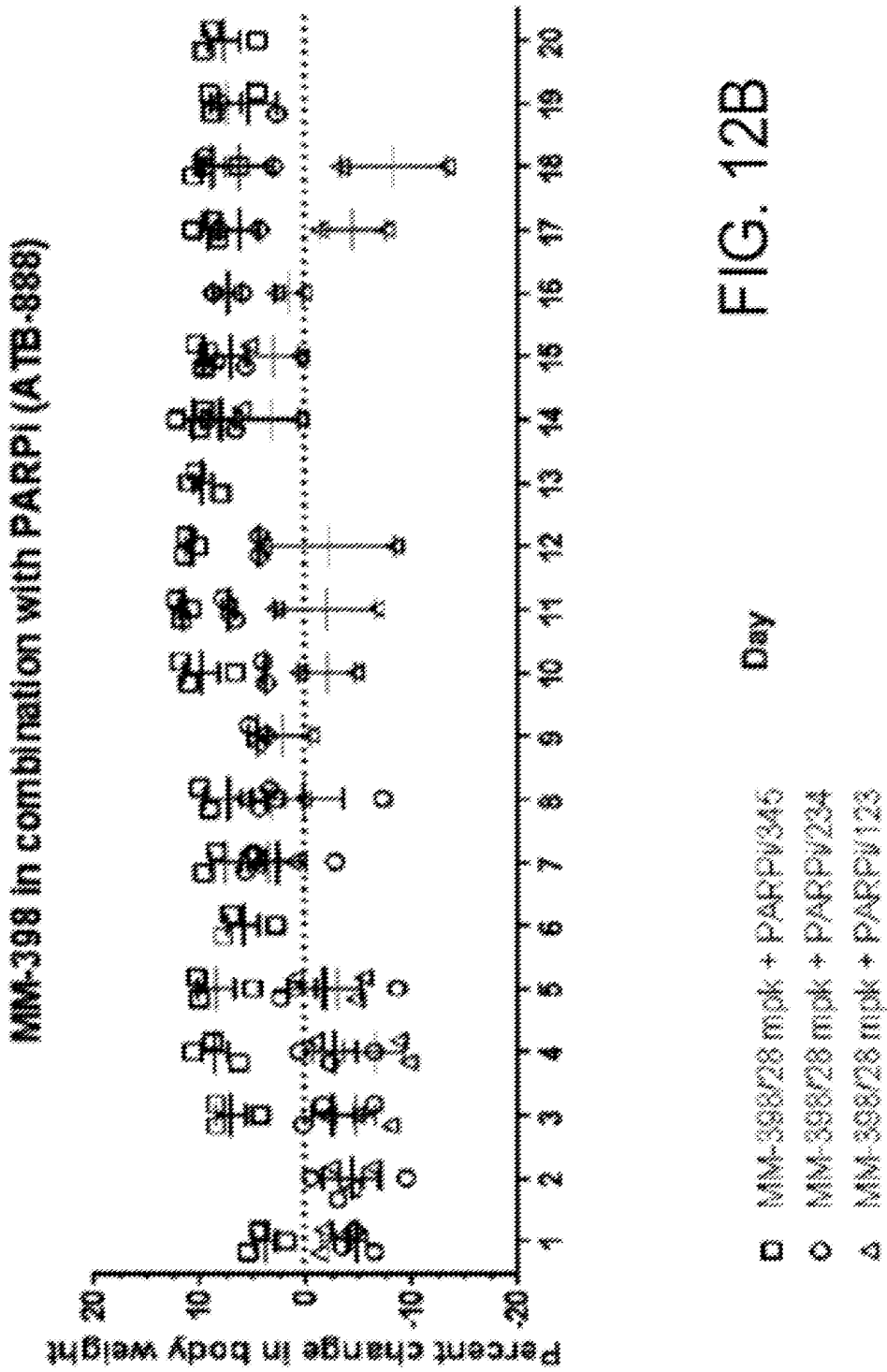


FIG. 12B



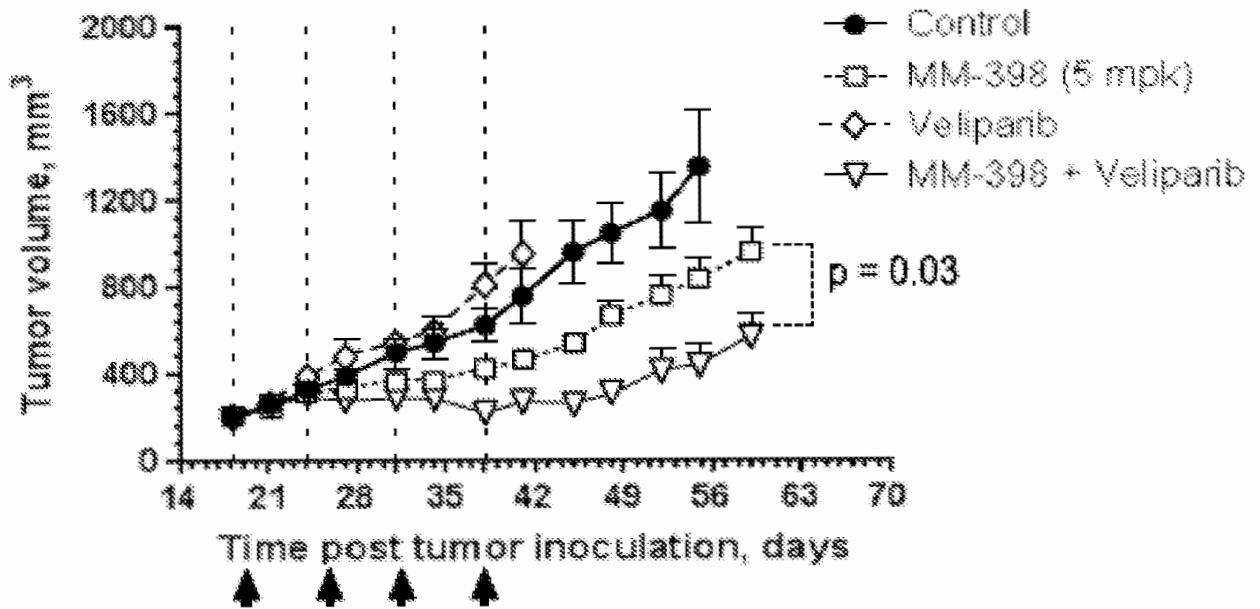


FIG. 13A

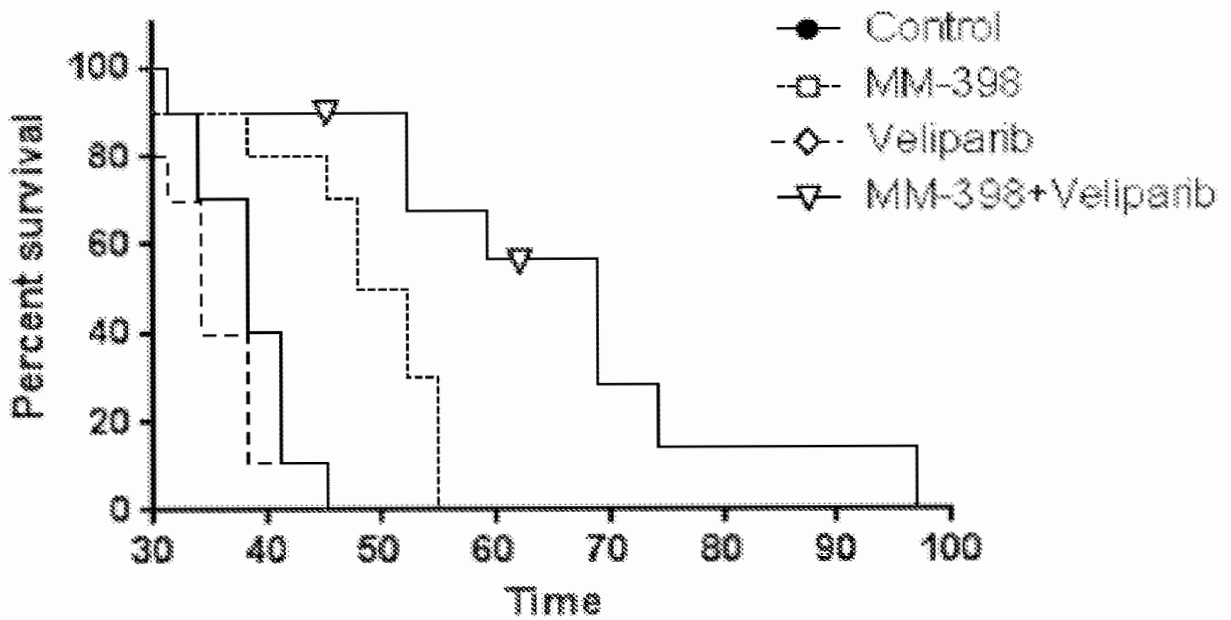


FIG. 13B

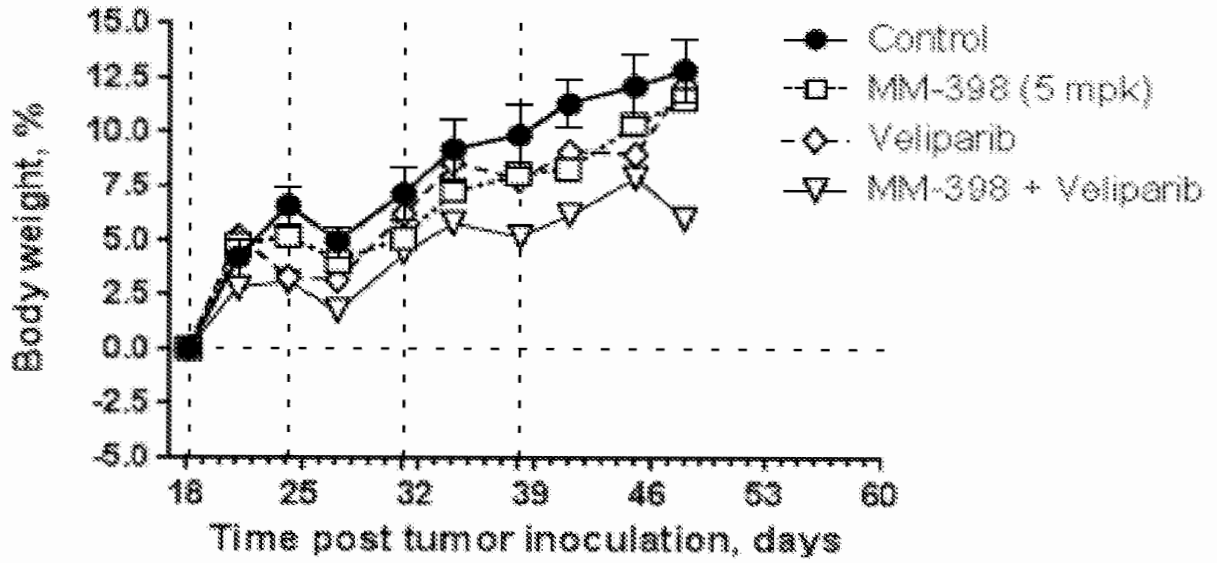


FIG. 13C

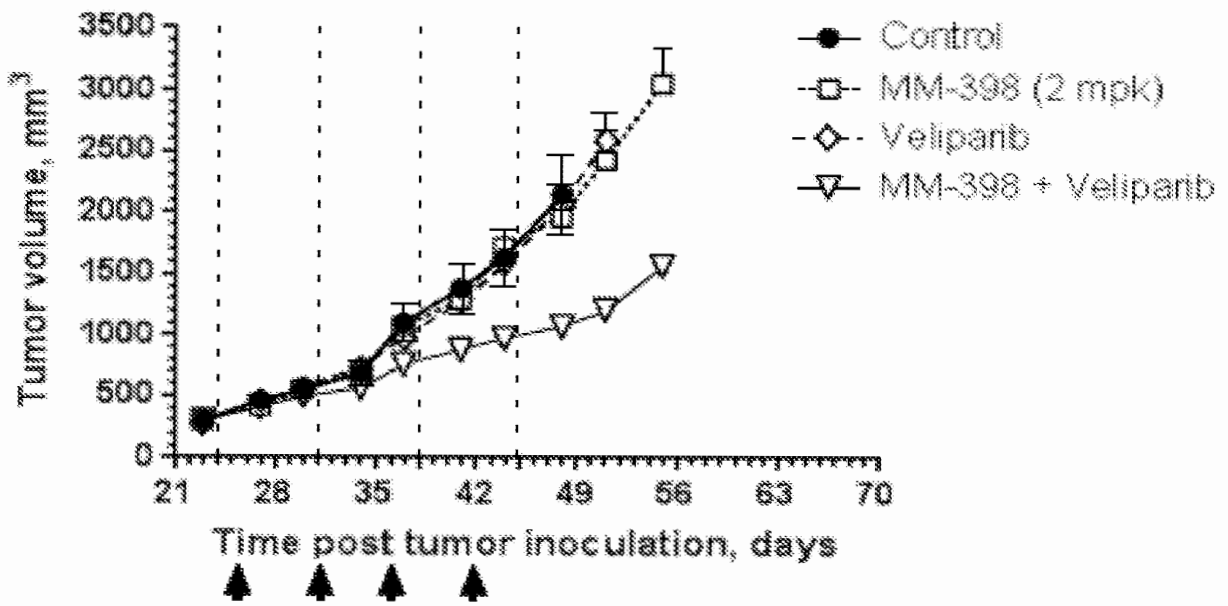


FIG. 14

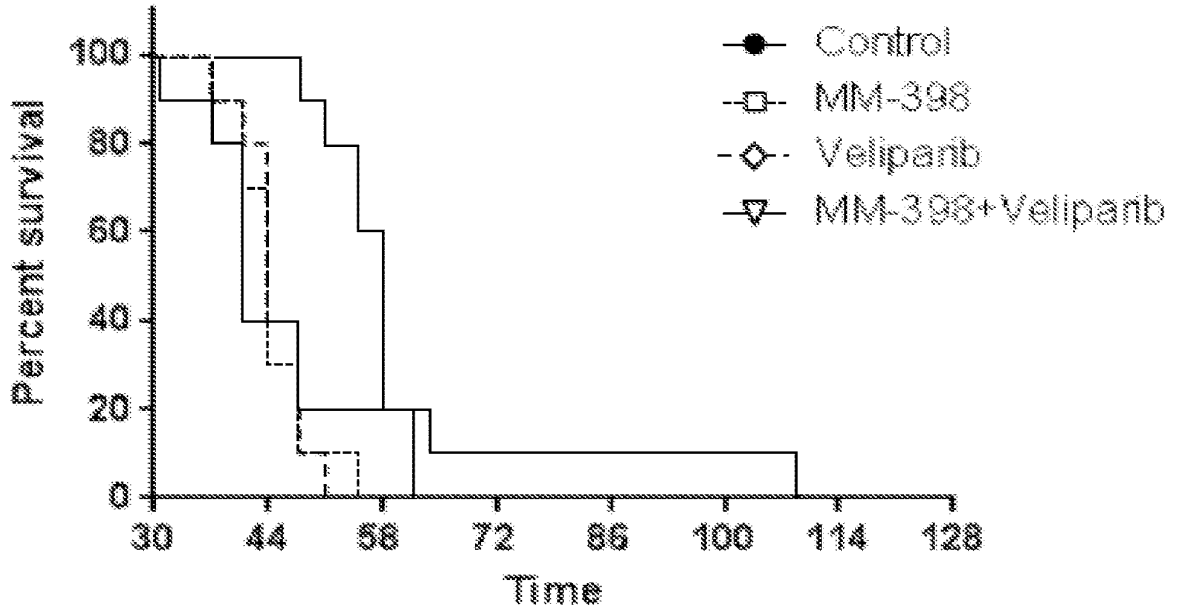


FIG. 15

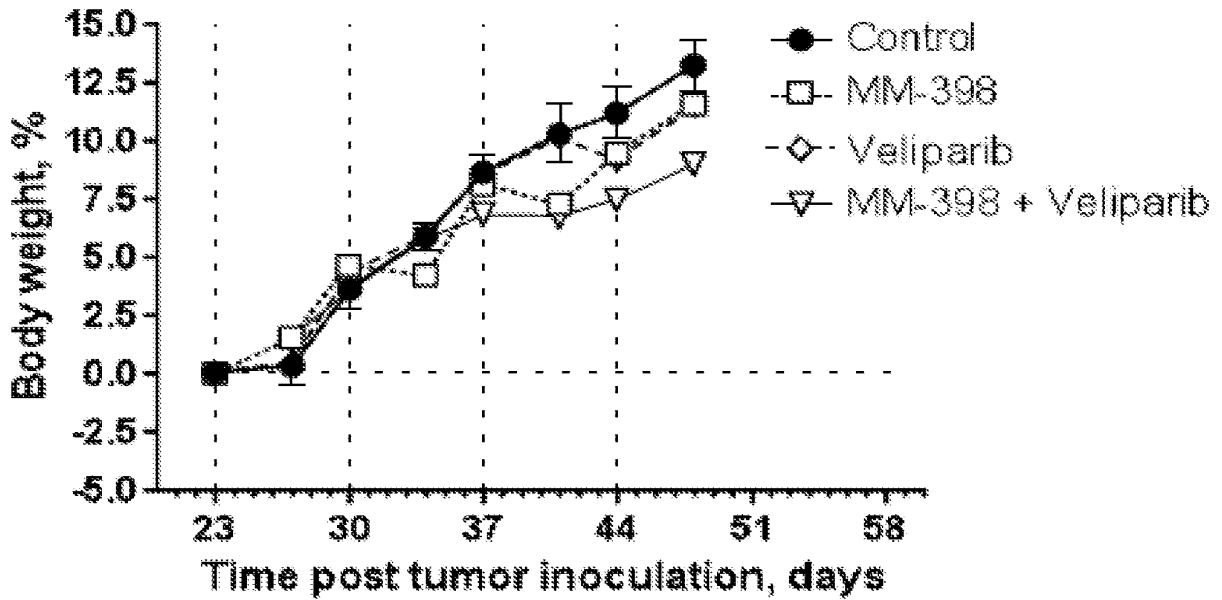


FIG. 16

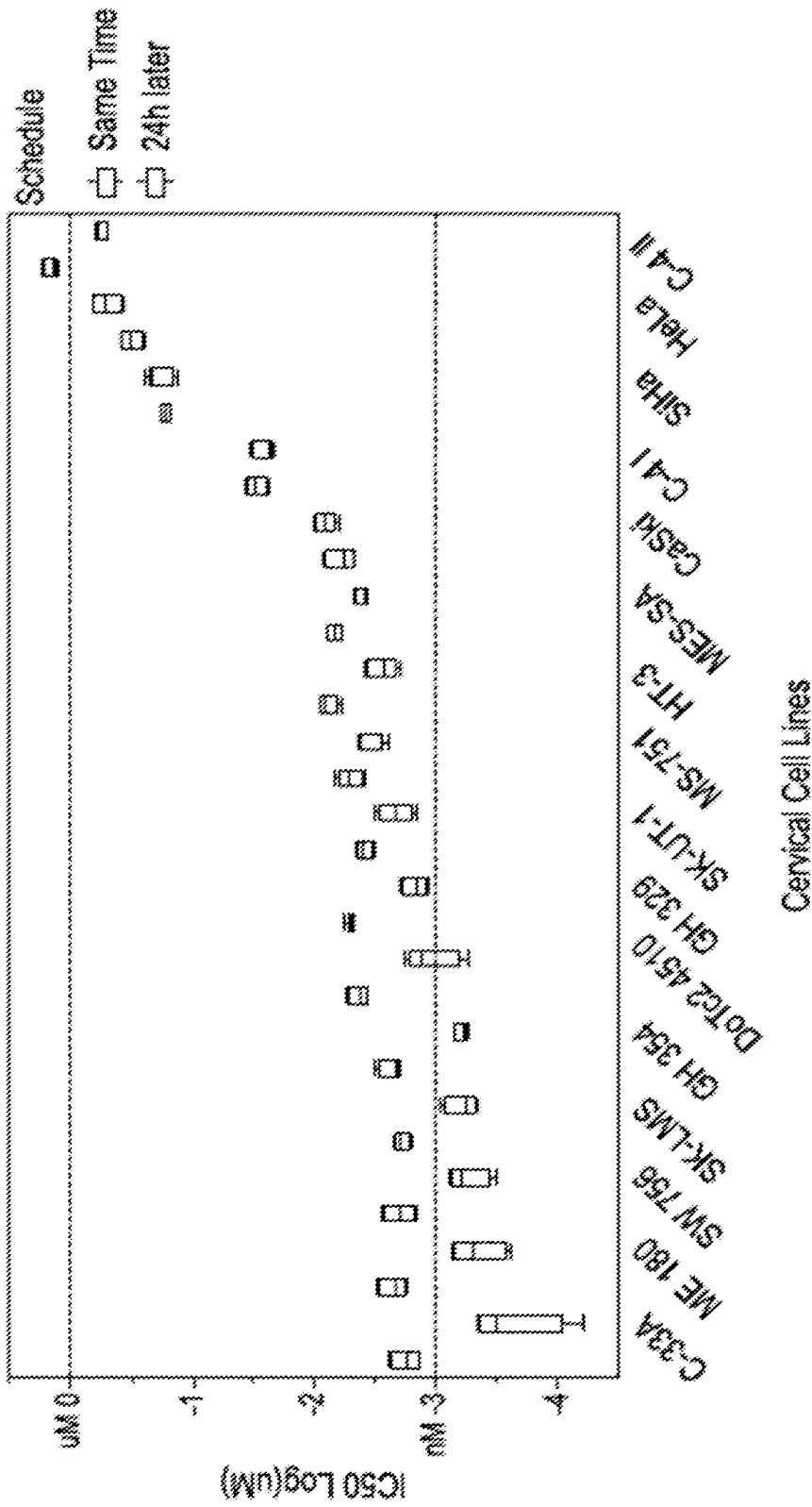


FIG. 17A

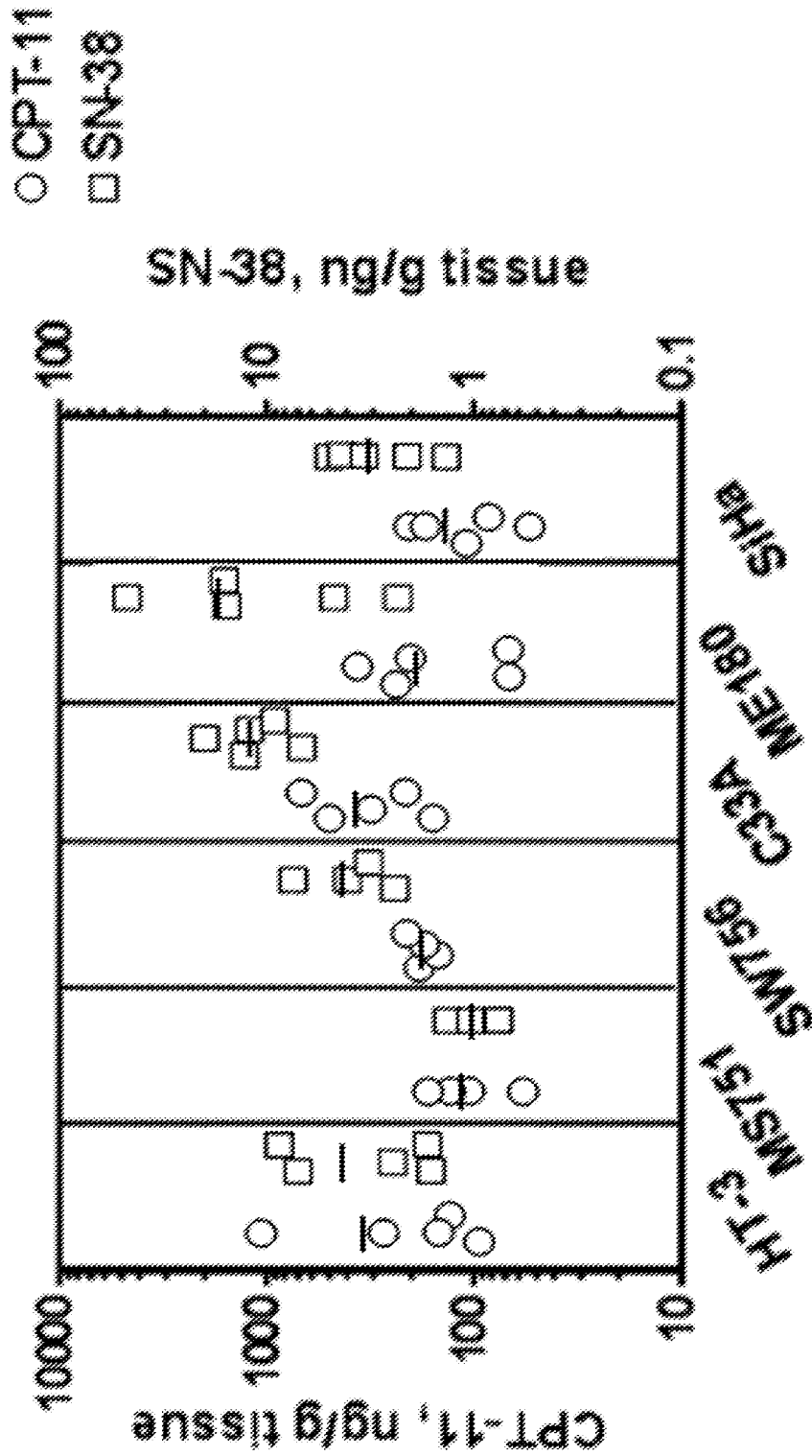
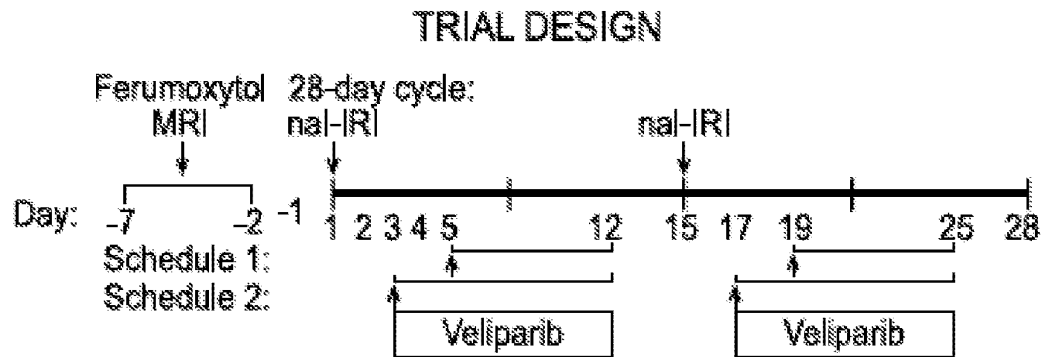


FIG. 17B



Dose Escalation Cohorts			
Dose Level	Veliparib Dose (mg BID)	Veliparib Start Day	naI-IRI Dose (salt) (mg/m <sup>2</sup> q2w)
1	100	Day 5	80
2	200	Day 5	80
3	200	Day 3	80
4	300	Day 3	80
5	400	Day 3	80

FIG. 18

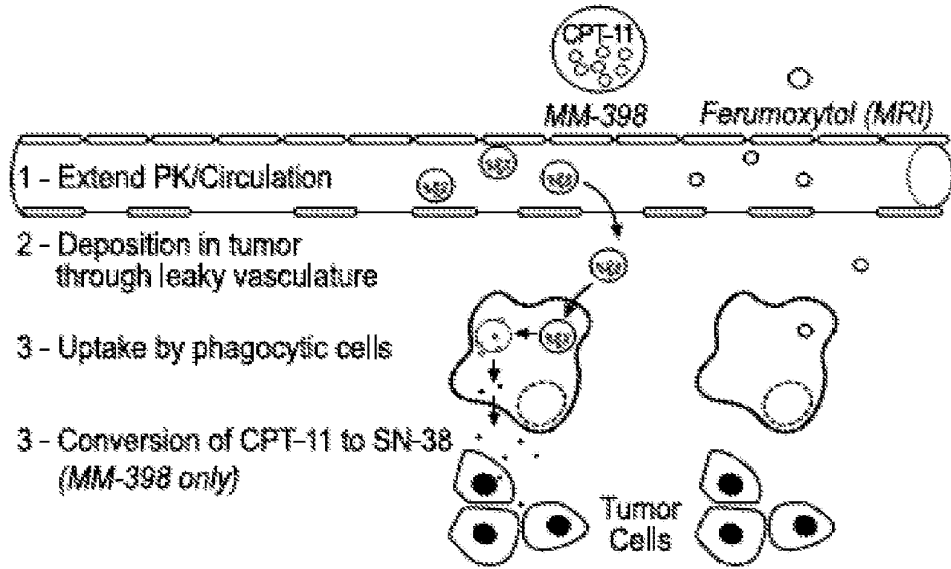


FIG. 19A

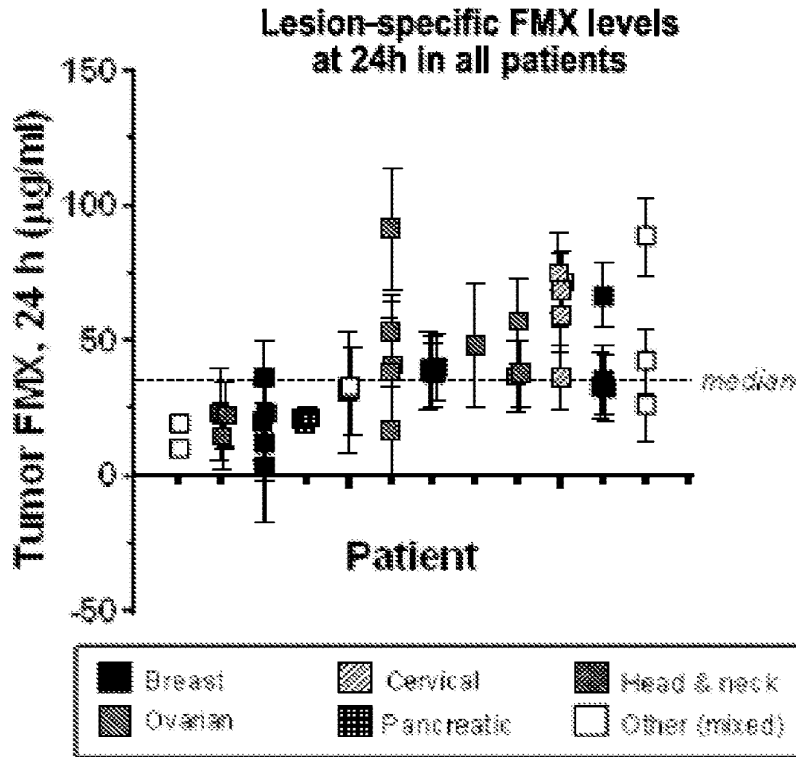


FIG. 19B

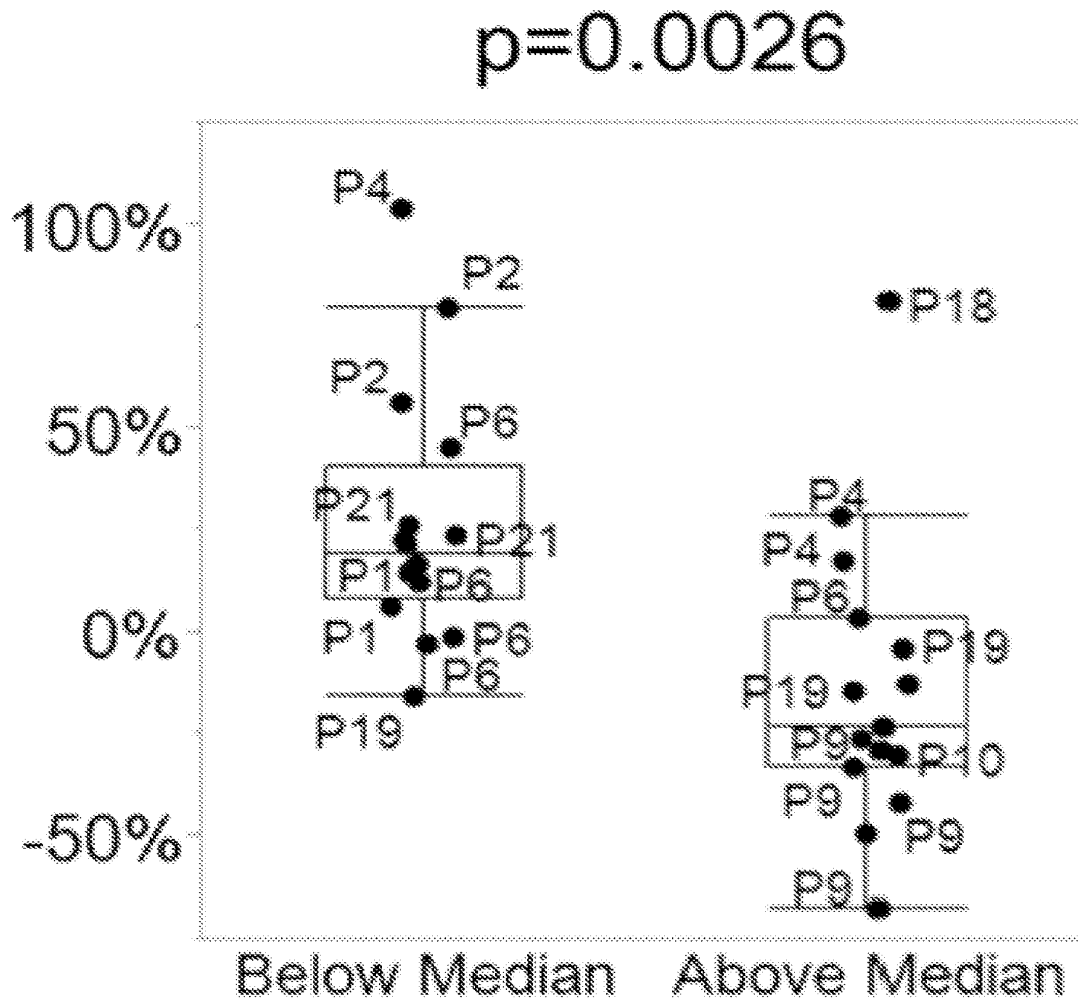


FIG. 19C



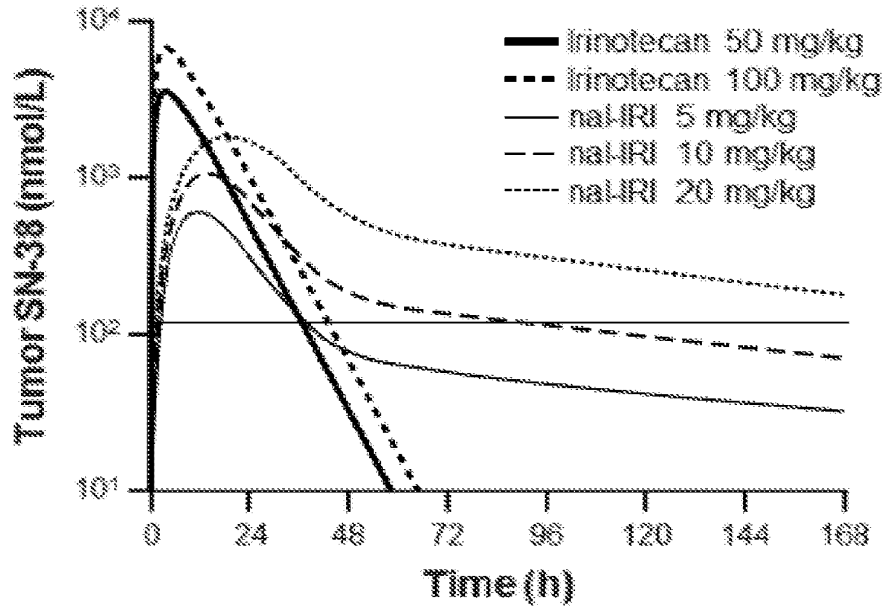


FIG. 20A

**SN-38 duration above threshold**

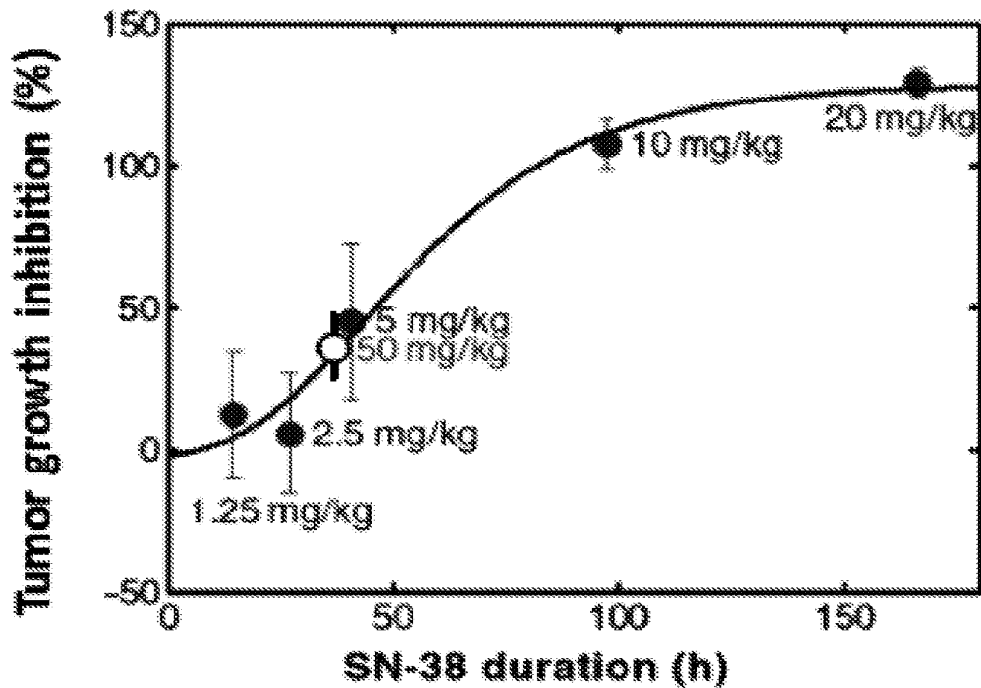


FIG. 20B

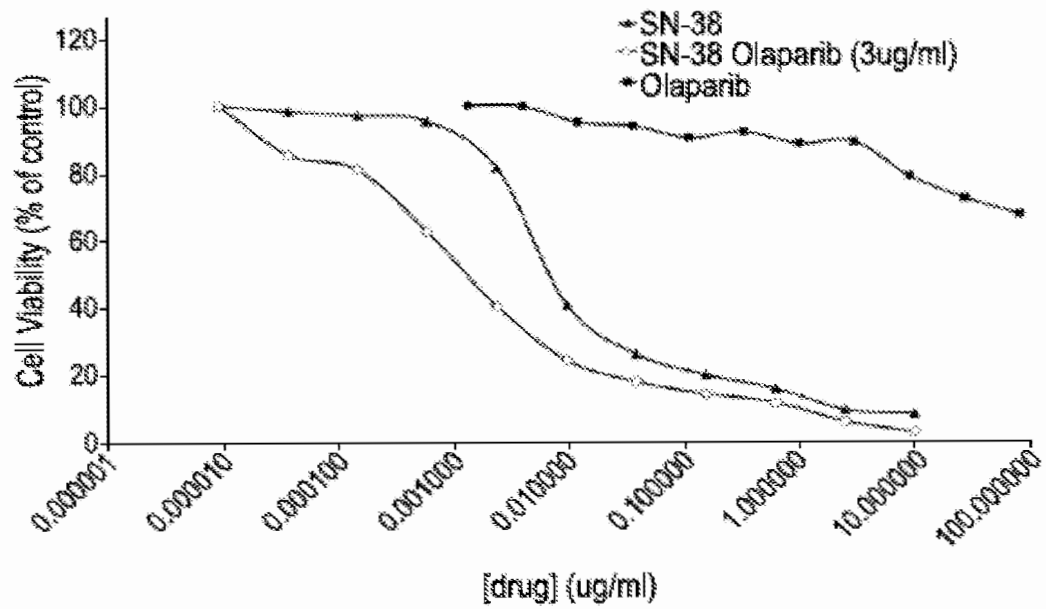


FIG. 21A

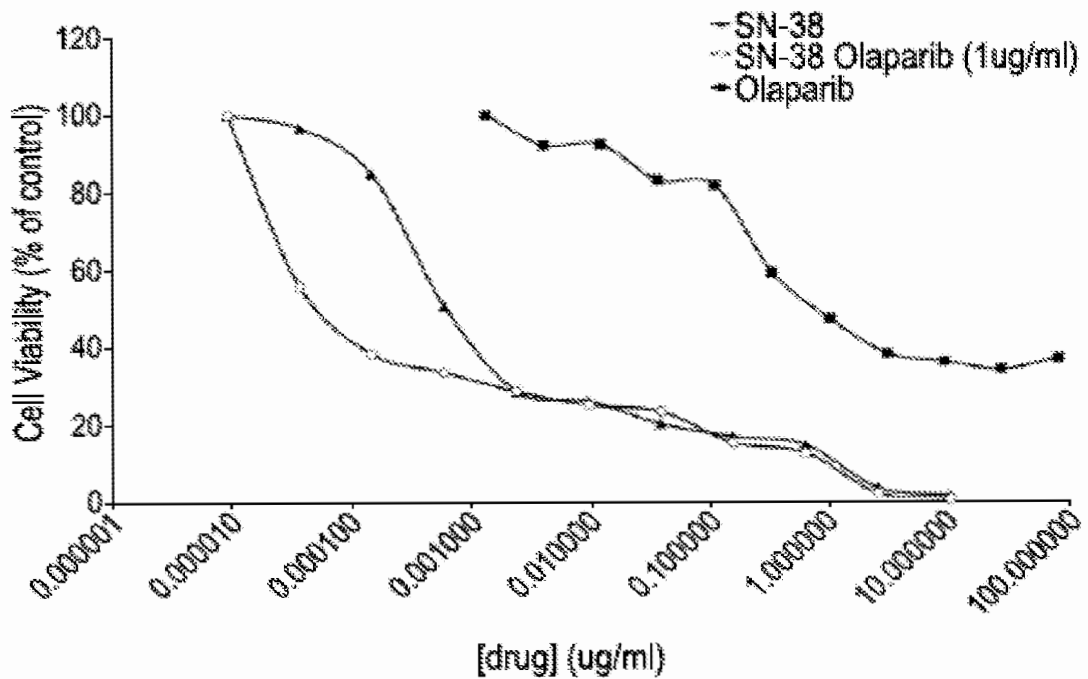
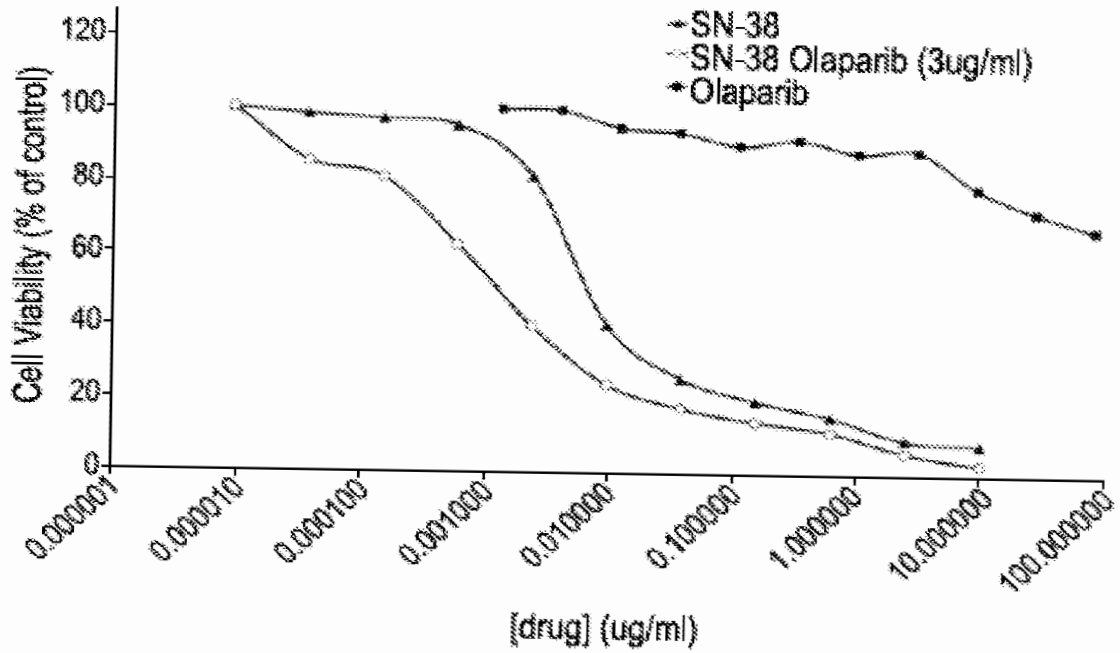
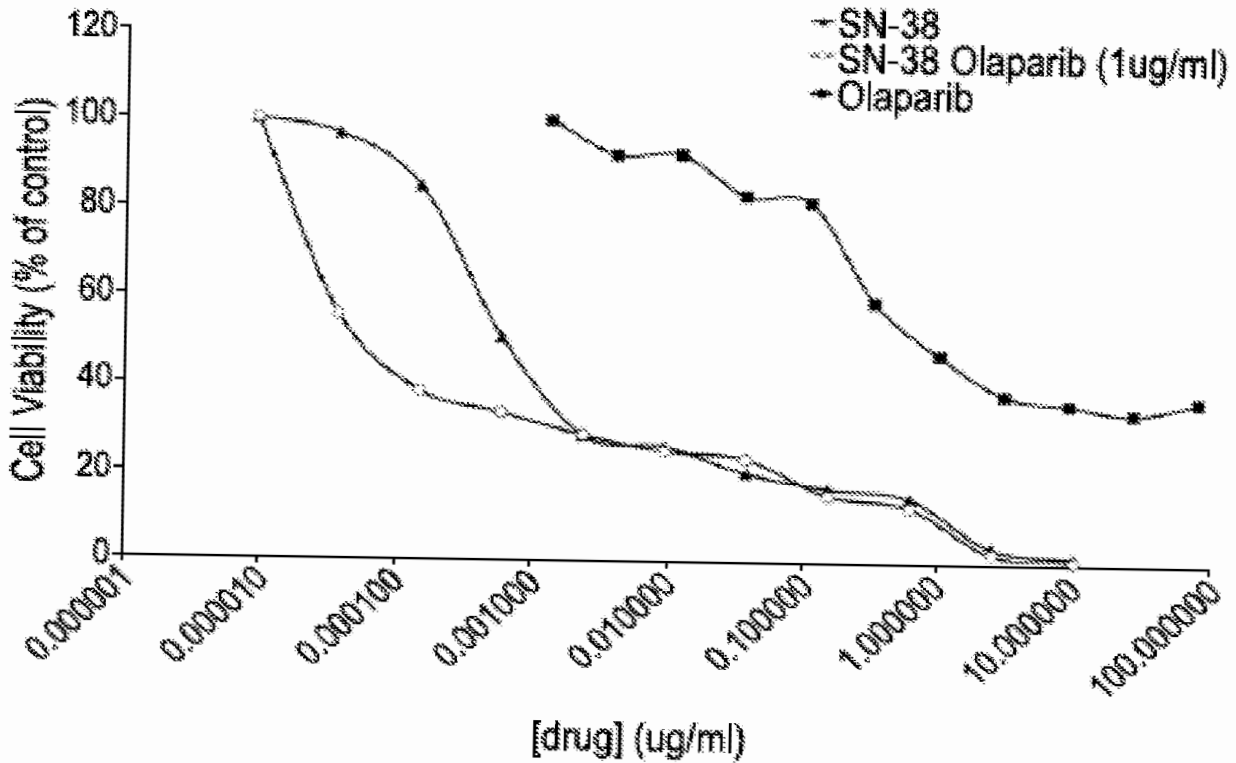


FIG. 21B



**FIG. 21C**



**FIG. 21D**

INTERNATIONAL SEARCH REPORT

International application No  
PCT/US2016/047814

A. CLASSIFICATION OF SUBJECT MATTER

INV. A61K31/04 A61K31/166 A61K31/416 A61K31/4184 A61K31/436  
A61K31/4745 A61K31/475 A61K31/502 A61K31/55 A61K9/127  
A61K47/06 A61P35/00

According to International Patent Classification (IPC) or to both national classification and IPC

B. FIELDS SEARCHED

Minimum documentation searched (classification system followed by classification symbols)

A61K

Documentation searched other than minimum documentation to the extent that such documents are included in the fields searched

Electronic data base consulted during the international search (name of data base and, where practicable, search terms used)

EPO-Internal

C. DOCUMENTS CONSIDERED TO BE RELEVANT

Category*	Citation of document, with indication, where appropriate, of the relevant passages	Relevant to claim No.
Y	<p>MESSERER CORRIE LYNN ET AL: "Liposomal irinotecan: formulation development and therapeutic assessment in murine xenograft models of colorectal cancer", CLINICAL CANCER RESEARCH : AN OFFICIAL JOURNAL OF THE AMERICAN ASSOCIATION FOR CANCER RESEARCH, vol. 10, no. 19, 1 October 2004 (2004-10-01), pages 6638-6649, XP002763354, ISSN: 1078-0432 the whole document</p> <p style="text-align: center;">----- -/--</p>	1-20

Further documents are listed in the continuation of Box C.

See patent family annex.

\* Special categories of cited documents :

"A" document defining the general state of the art which is not considered to be of particular relevance

"E" earlier application or patent but published on or after the international filing date

"L" document which may throw doubts on priority claim(s) or which is cited to establish the publication date of another citation or other special reason (as specified)

"O" document referring to an oral disclosure, use, exhibition or other means

"P" document published prior to the international filing date but later than the priority date claimed

"T" later document published after the international filing date or priority date and not in conflict with the application but cited to understand the principle or theory underlying the invention

"X" document of particular relevance; the claimed invention cannot be considered novel or cannot be considered to involve an inventive step when the document is taken alone

"Y" document of particular relevance; the claimed invention cannot be considered to involve an inventive step when the document is combined with one or more other such documents, such combination being obvious to a person skilled in the art

"&" document member of the same patent family

Date of the actual completion of the international search

27 October 2016

Date of mailing of the international search report

17/11/2016

Name and mailing address of the ISA/

European Patent Office, P.B. 5818 Patentlaan 2  
NL - 2280 HV Rijswijk  
Tel. (+31-70) 340-2040,  
Fax: (+31-70) 340-3016

Authorized officer

Engl, Brigitte

## INTERNATIONAL SEARCH REPORT

International application No

PCT/US2016/047814

C(Continuation). DOCUMENTS CONSIDERED TO BE RELEVANT

Category*	Citation of document, with indication, where appropriate, of the relevant passages	Relevant to claim No.
Y	SYBIL M GENTHER WILLIAMS ET AL: "Treatment with the PARP inhibitor, niraparib, sensitizes colorectal cancer cell lines to irinotecan regardless of MSI/MSS status", CANCER CELL INTERNATIONAL, vol. 15, no. 1, 4 February 2015 (2015-02-04), page 14, XP021213062, BIOMED CENTRAL, LONDON, GB ISSN: 1475-2867, DOI: 10.1186/S12935-015-0162-8 the whole document	1-20
Y	----- DAVIDSON DAVID ET AL: "The PARP inhibitor ABT-888 synergizes irinotecan treatment of colon cancer cell lines", INVESTIGATIONAL NEW DRUGS, vol. 31, no. 2, April 2013 (2013-04), pages 461-468, XP002763355, ISSN: 1573-0646 the whole document	1-20
Y	----- DOUILLARD J ET AL: "Irinotecan combined with fluorouracil compared with fluorouracil alone as first-line treatment for metastatic colorectal cancer: a multicentre randomised trial", THE LANCET, vol. 355, no. 9209, 25 March 2000 (2000-03-25), pages 1041-1047, XP004814762, THE LANCET PUBLISHING GROUP, GB ISSN: 0140-6736, DOI: 10.1016/S0140-6736(00)02034-1 the whole document	1-20
Y	----- HARE JENNIFER I ET AL: "Treatment of colorectal cancer using a combination of liposomal irinotecan (Irinophore C(TM)) and 5-fluorouracil", PLOS ONE, vol. 8, no. 4, E623491, 23 April 2013 (2013-04-23), pages 1-12, XP002763356, ISSN: 1932-6203, DOI: 10.1371/journal.pone.0062349 the whole document -----	1-20



(51) International Patent Classification:

A61K 31/04 (2006.01) A61K 31/475 (2006.01)  
A61K 31/166 (2006.01) A61K 31/502 (2006.01)  
A61K 31/416 (2006.01) A61K 31/55 (2006.01)  
A61K 31/4184 (2006.01) A61K 9/127 (2006.01)  
A61K 31/436 (2006.01) A61K 47/06 (2006.01)  
A61K 31/4745 (2006.01) A61P 35/00 (2006.01)

(21) International Application Number:

PCT/US2016/047827

(22) International Filing Date:

19 August 2016 (19.08.2016)

(25) Filing Language:

English

(26) Publication Language:

English

(30) Priority Data:

62/207,760 20 August 2015 (20.08.2015) US  
62/207,709 20 August 2015 (20.08.2015) US  
62/269,756 18 December 2015 (18.12.2015) US  
62/269,511 18 December 2015 (18.12.2015) US  
62/308,924 16 March 2016 (16.03.2016) US  
62/323,422 15 April 2016 (15.04.2016) US

(71) Applicant: **MERRIMACK PHARMACEUTICALS, INC.** [US/US]; One Kendall Square, Suite B7201, Cambridge, MA 02139-1970 (US).

(72) Inventors: **BLANCHETTE, Sarah, F.**; 24 Edgemere Road, Lynnfield, MA 01940 (US). **DRUMMOND, Daryl, C.**; 1 Brooks Road, Lincoln, MA 01773 (US). **FITZGERALD, Jonathan, Basil**; 32 Magnolia Street, Arlington,

MA 02474 (US). **MOYO, Victor**; 2 Neshanic Drive, Ringoes, NJ 08551 (US).

(74) Agent: **FORBES, Christopher, C.**; Honigman Miller Schwartz and Cohn LLP, 350 East Michigan Avenue, Suite 300, Kalamazoo, MI 49007 (US).

(81) Designated States (unless otherwise indicated, for every kind of national protection available): AE, AG, AL, AM, AO, AT, AU, AZ, BA, BB, BG, BH, BN, BR, BW, BY, BZ, CA, CH, CL, CN, CO, CR, CU, CZ, DE, DK, DM, DO, DZ, EC, EE, EG, ES, FI, GB, GD, GE, GH, GM, GT, HN, HR, HU, ID, IL, IN, IR, IS, JP, KE, KG, KN, KP, KR, KZ, LA, LC, LK, LR, LS, LU, LY, MA, MD, ME, MG, MK, MN, MW, MX, MY, MZ, NA, NG, NI, NO, NZ, OM, PA, PE, PG, PH, PL, PT, QA, RO, RS, RU, RW, SA, SC, SD, SE, SG, SK, SL, SM, ST, SV, SY, TH, TJ, TM, TN, TR, TT, TZ, UA, UG, US, UZ, VC, VN, ZA, ZM, ZW.

(84) Designated States (unless otherwise indicated, for every kind of regional protection available): ARIPO (BW, GH, GM, KE, LR, LS, MW, MZ, NA, RW, SD, SL, ST, SZ, TZ, UG, ZM, ZW), Eurasian (AM, AZ, BY, KG, KZ, RU, TJ, TM), European (AL, AT, BE, BG, CH, CY, CZ, DE, DK, EE, ES, FI, FR, GB, GR, HR, HU, IE, IS, IT, LT, LU, LV, MC, MK, MT, NL, NO, PL, PT, RO, RS, SE, SI, SK, SM, TR), OAPI (BF, BJ, CF, CG, CI, CM, GA, GN, GQ, GW, KM, ML, MR, NE, SN, TD, TG).

Published:

— with international search report (Art. 21(3))

(54) Title: COMBINATION THERAPY FOR CANCER TREATMENT

(57) Abstract: Combination therapies for treating cancer comprising administration of a topoisomerase-1 inhibitor and a PARP inhibitor are provided. The topoisomerase-1 inhibitor can be delivered as a liposomal formulation that provides for prolonged accumulation of the topoisomerase-1 inhibitor within a tumor relative to outside of the tumor. Therapeutic benefit can thereby be obtained by delaying the administration of the PARP inhibitor after each administration of a liposomal irinotecan formulation until the accumulation of the topoisomerase inhibitor in the tumor is sufficiently greater than outside the tumor to result in increased efficacy of the PARP inhibitor and topoisomerase inhibitor within the tumor, while reducing the peripheral toxicity of the combination therapy. The therapies disclosed herein are useful in the treatment of human cancers with solid tumors, including cervical cancer.

